
C

CAD

- ▶ [Computer-Aided Design](#)

Caliber Rolling

- ▶ [Rolling](#)

Calibration

Simone Carmignato
Department of Management and Engineering,
University of Padua, Vicenza, Italy

Definition

Operation that, under specified conditions, in a first step, establishes a relation between the **quantity values** with **measurement uncertainties** provided by **measurement standards** and corresponding **indications** with associated measurement uncertainties and, in a second step, uses this information to establish a relation for obtaining a **measurement result** from an indication.

Note 1: A calibration may be expressed by a statement, calibration function, **calibration diagram**, **calibration curve**, or calibration

table. In some cases, it may consist of an additive or multiplicative **correction** of the indication with associated measurement uncertainty. Note 2: Calibration should not be confused with **adjustment of a measuring system**, often mistakenly called “self-calibration,” nor with **verification** of calibration.

Note 3: Often, the first step alone in the above definition is perceived as being calibration (JCGM 200:2012, Definition 2.39).

Theory and Application

Basic Concepts

According to the definition given in the *International Vocabulary of Metrology* (JCGM 200:2012, Definition 2.39), calibration establishes a relation between the quantity value provided by a measurement standard and the corresponding indication provided by a measuring instrument or system. Calibration also requires determination of the uncertainties associated with the measurements performed. A calibration can be executed either on a measuring instrument (or system) or on a measurement standard.

The **calibration of a measuring instrument** allows determining the deviation of the indication of the measuring instrument from a known value of the measurand provided by the measurement standard, with associated measurement uncertainty. In other words, the deviation of the indication of an instrument from the conventional “true

value” of the measurand is established and documented. For example, this is the case of calibrating micrometers or other dimensional measuring instruments using gauge blocks.

The **calibration of a measurement standard** can be performed by comparing its quantity value and associated measurement uncertainty to a reference indication (with associated measurement uncertainty) obtained by a calibrated measuring system. For instance, a measuring system calibrated by a primary reference standard can be used to calibrate a secondary measurement standard. Also a comparison between two measurement standards can be viewed as a calibration if the comparison is used to check (and, if necessary, to correct) the quantity value and measurement uncertainty attributed to one of the two measurement standards. This is, for example, the case of the calibration of gauge blocks through comparison with other previously calibrated gauge blocks.

In certain fields, such as measurement of quantities in biological samples and medical applications, a measurement standard used for calibration can be called “calibrator” (see JCGM 200:2012, Definition 5.12).

As explicitly stated in the *International Vocabulary of Metrology*, calibration should not be confused with verification nor with adjustment. Verification in fact is the “provision of objective evidence that a given item fulfils specified requirements” (JCGM 200:2012, Definition 2.44). For example, this is the case of checking if a measuring system achieves the performance properties stated by the manufacturer. Adjustment, on the other hand, is “the set of operations carried out on a measuring system so that it provides prescribed indications corresponding to given values of a quantity to be measured” (JCGM 200:2012, Definition 3.11). Calibration is a prerequisite for adjustment, and after the measuring system has been adjusted, a recalibration must usually be performed.

Calibration is typically performed in metrological laboratories under controlled environmental conditions. The relation established by a calibration maintains its validity under the specified operating conditions in which the calibration is performed.

In general, for daily operation of a measuring system in a company, a global calibration is usually not needed. A task-related calibration can be performed, which is a calibration of only those metrological characteristics that influence the measurement uncertainty for the intended use (see ISO 14978:2006).

Why Are Calibrations Necessary?

There are technical and legal reasons why calibration is performed. Four main reasons for having an instrument calibrated are, e.g., outlined in the EURAMET handbook “Metrology – in short” (2008):

1. To establish and demonstrate metrological traceability
2. To ensure readings from the instrument are consistent with other measurements
3. To determine the accuracy of the instrument readings
4. To establish the reliability of the instrument, i.e., that it can be trusted

To guarantee interchangeability of parts, it is fundamental to establish traceability of measurements to national standards by means of calibration. In particular, suppliers and customers producing and assembling parts with other components must ensure valid measurement results and need to measure parts with the “same measure.” For organizations with quality management systems, calibration is also a requirement of ISO 9001, which states that “when necessary to ensure valid results, measuring equipment shall be calibrated, or verified, or both, at specified intervals, or prior to use, against measurements standards traceable to international or national measurements standards” (ISO 9001:2008).

Documentation of Calibration Results

The results obtained by a calibration are documented in a calibration certificate or calibration report. The associated measurement uncertainty must be stated.

Information gained with calibration may be expressed by a statement, a function, an additive or multiplicative correction of the indication, a

calibration diagram, or a **calibration curve**. For the latter ones, the *International Vocabulary of Metrology* gives the following definitions.

Calibration diagram: graphical expression of the relation between **indication** and corresponding **measurement result**.

Note 1: A calibration diagram is the strip of the plane defined by the axis of the indication and the axis of measurement result that represents the relation between an indication and a set of **measured quantity values**. A one-to-many relation is given, and the width of the strip for a given indication provides the **instrumental measurement uncertainty**.

Note 2: Alternative expressions of the relation include a **calibration curve** and associated **measurement uncertainty**, a calibration table, or a set of functions.

Note 3: This concept pertains to a **calibration** when the instrumental measurement uncertainty is large in comparison with the measurement uncertainties associated with the **quantity values of measurement standards** (JCGM 200:2012, Definition 4.30).

Calibration curve: expression of the relation between **indication** and corresponding **measured quantity value**.

Note: A calibration curve expresses a one-to-one relation that does not supply a **measurement result** as it bears no information about the **measurement uncertainty** (JCGM 200:2012, Definition 4.31).

While a calibration curve needs a separate statement for measurement uncertainty, a calibration diagram delivers a complete statement of the information obtained with calibration, including the measured value and the associated measurement uncertainty.

Calibration Hierarchy

To ensure metrological traceability, a calibration made at a local level, such as an industrial internal calibration (also called in-house calibration), must be linked to a national standard by an unbroken chain of calibrations, with each step explicitly supported by appropriate documentation (ILAC P10:01/2013). The measurement uncertainty necessarily increases along the sequence of calibrations, starting from the national level down to the local level. Therefore, the prerequisite of metrological traceability is the establishment of a calibration hierarchy as shown in Fig. 1.

The calibration hierarchy is defined in the *International Vocabulary of Metrology* as follows.

Calibration,

Fig. 1 Illustration of a calibration hierarchy



Calibration hierarchy: sequence of **calibrations** from a reference to the final **measuring system**, where the outcome of each calibration depends on the outcome of the previous calibration.

Note 1: **Measurement uncertainty** necessarily increases along the sequence of calibrations.

Note 2: The elements of a calibration hierarchy are one or more **measurement standards** and measuring systems operated according to **measurement procedures**.

Note 3: For this definition, the “reference” can be a definition of a **measurement unit** through its practical realization or a measurement procedure or a measurement standard.

Note 4: A comparison between two measurement standards may be viewed as a calibration if the comparison is used to check and, if necessary, correct the **quantity value** and measurement uncertainty attributed to one of the measurement standards (JCGM 200:2012, Definition 2.40).

Organizations Performing Calibration

Different organizations perform calibrations (Fig. 1): national metrology institutes, accredited calibration laboratories, and in-house calibration laboratories (ILAC P10:01/2013). In each step of the calibration chain, measurement standards are used to calibrate measuring equipment of the next step. For example, an accredited laboratory can calibrate a company’s working standard against a reference standard. Accredited laboratories must fulfill the requirements of (ISO 17025:2005).

Above the national organizations, at the international level, decisions concerning the International System of Units (SI) and the realization of the primary standards are taken by the Conférence Générale des Poids et Mesures (CGPM). The development and maintenance of primary standards is coordinated by the Bureau International des Poids et Mesures (BIPM), which also organizes intercomparisons on the highest level. The International Laboratory Accreditation Cooperation (ILAC) promotes laboratory accreditation and the recognition of competent calibration and test facilities around the world.

Calibration Interval

Calibrations must be repeated at appropriate intervals (ILAC G24:2007). A measurement instrument, for example, should be periodically recalibrated because changes in its characteristics can occur during its use and after some time. Recalibration on appropriate intervals ensures detection of these possible changes. The length of these intervals will depend on a number of variables, such as:

- Uncertainty required
- Frequency of use
- Way of use
- Environmental conditions at use
- Stability of the equipment

Cross-References

- ▶ Accuracy
- ▶ Measurement Uncertainty
- ▶ Traceability

References

- European Association of National Metrology Institutes (EURAMET) (2008) Metrology – in short, 3rd edn. http://www.euramet.org/fileadmin/docs/Publications/Metrology_in_short_3rd_ed.pdf. Accessed 15 Apr 2014
- ILAC G24:2007 (2007) Guidelines for the determination of calibration intervals of measuring instruments. International Laboratory Accreditation Cooperation. <http://ilac.org/?ddownload=818>. Accessed 15 April 2014.
- ILAC P10:01/2013 (2013) ILAC policy on traceability of measurement results. International Laboratory Accreditation Cooperation. <http://ilac.org/?ddownload=840>. Accessed 15 Apr 2014
- ISO 14978:2006 (2006) Geometrical product specifications (GPS) – general concepts and requirements for GPS measuring equipment. International Organization for Standardization, Geneva
- ISO 17025:2005 (2005) General requirements for the competence of testing and calibration laboratories. International Organization for Standardization, Geneva
- ISO 9001:2008 (2008) Quality management systems – requirements. International Organization for Standardization, Geneva
- JCGM 200:2012 (2012) International vocabulary of metrology – basic and general concepts and associated terms (VIM), 3rd edn. Joint Committee for Guides in Metrology. www.bipm.org/utls/common/documents/jcgm/JCGM_200_2012.pdf. Accessed 15 Apr 2014

CAM

► [Computer-Aided Manufacturing](#)

Capacity Planning

Hoda A. ElMaraghy^{1,2} and Ahmed M. Deif³

¹Intelligent Manufacturing Systems Center,
University of Windsor, Windsor, ON, Canada

²Canada Research Chair in Manufacturing Systems,
Intelligent Manufacturing Systems Centre,
University of Windsor, Windsor, ON, Canada

³Orfalea College of Business, California
Polytechnic State University (CAL POLY), San
Luis Obispo, CA, USA

Synonyms

[Productive volume planning](#)

Definition

Capacity is defined, in the context of manufacturing, as the maximum rate of production and the ability to yield production. Capacity planning is concerned with defining all resources and factors that affect the ability of a manufacturer to produce including equipment, labor, space, and time (i.e., number of shifts). The outcome of capacity planning is an investment strategy and resource utilization plan defined based on optimal policies that try to fulfill demand and its variation while considering various system's operational objectives and constraints.

Theory and Application

History

Capacity planning is motivated by manufacturers' desire to meet customers' demand. Uncertainty of the customer's demand increases the complexity of capacity planning. Capacity planning is often confused with scheduling since both deal with

managing production to meet demand. However, a major distinction between both activities is that capacity planning is focused on meeting the anticipated demand on the strategic and tactical level, while scheduling focuses on how to meet demand on the shop floor operational level. This distinction brings about different scope, strategies, models, and tools used in meeting the capacity and resource scheduling demands. A classic example of how a scheduling is addressed as a capacity problem is the typical formulation to solve an allocation problem of a set of unrelated machines which process a group of products by trying to determine the optimal values of the allocation variables which assign portion of each of the machine's time to each of the considered products to improve a specific performance metric (a typical example can be found in Leachman and Carmon 1992).

Capacity planning was classically addressed as a problem of capacity expansion. However, modern planning is concerned with both the reduction and expansion of capacity given the turbulence in markets today. Another major difference between classical and modern capacity planning is their enabling technologies. The techniques used for planning capacity expansion are classical techniques such as adding work shifts, manpower, new production facilities, and subcontracting, whereas for modern capacity planning technologies such as modular design, reconfiguration, open control architectures, and changeability strategies are used, in addition to classical approaches, to implement more scalable, flexible, and successful capacity planning policies.

Theory

About the Capacity Planning Problem

The major decisions in any capacity planning activity are:

- What is the best *magnitude* of capacity expansion/reduction?
- When is the best *time* to expand/reduce production capacity?
- What is the best *type* of capacity expansion/reduction?
- What is the best *location* for expansion/reduction?

The word “best” (sometimes called optimal) in the previous questions means satisfying the market demand at a minimum cost, effort, and/or time. A capacity planning policy should answer the previous questions. However, in practice it is difficult to devise a capacity planning policy that satisfies all questions at the same time in an optimal manner.

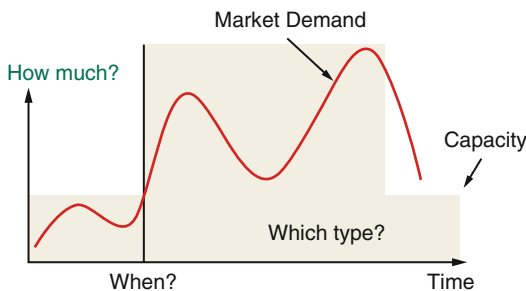
The main inputs required to answer the previous questions are (a) the planning horizon, (b) the costs of capacity expansion and/or reduction, (c) the different system constraints and time parameters, (d) the production strategic policies, and (e) the demand forecast.

The demand pattern is a very important parameter in developing any capacity planning policy or plan. It describes the demand over a certain time horizon which is usually the capacity planning period indicated by management. The demand patterns can take deterministic or stochastic forms depending on the desired accuracy in capturing uncertainty-associated demand as well as availability of information. Figure 1 illustrates the main dimensions of the capacity planning problem.

Capacity Planning in Various Manufacturing Systems

Dedicated Mass Production Systems

Capacity planning for dedicated manufacturing lines and mass production systems is carefully optimized a priori to define the best size of manufacturing facilities and resources given the expected steady and large production volume.



Capacity Planning, Fig. 1 Capacity planning problem’s questions

These systems sometimes face the need to expand or shrink production capacity due to changes in market conditions. Such changes beyond the initial design are not easy to implement in dedicated production systems and may require duplication of the lines or of certain machines in the line or even the expansion of the whole facility into multiple facilities if justifiable. It can be said that capacity planning in these dedicated systems is normally done on a macroscale at the system level and without considering potential capacity reduction/expansion (except in very few cases). This is understandable since these dedicated mass production systems were economically justified and designed for production of a specific part/product at high volume without dealing with variety or mix of products. Typically capacity expansion methods in dedicated systems have the objective of minimizing the discounted costs associated with expansion. These include expansion cost, congestion, idle capacity, shortages, maintenance, and inventory (examples include Kalotay (1973) and Erlenkotter 1977). Figure 2 shows the capacity planning approach in dedicated production systems.

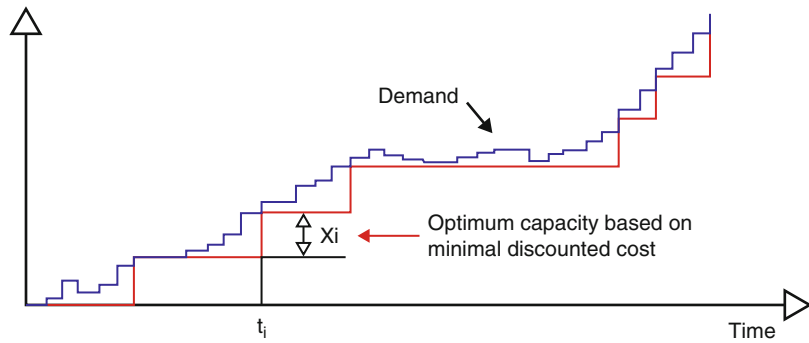
Flexible Manufacturing Systems

Capacity planning for flexible manufacturing systems (FMS) is considered a complicated task. Functionality planning usually receives much more attention in FMS than capacity planning, and it is mainly accomplished by using multipurpose, multiaxes CNC programmable machines. The problem of capacity planning in FMS arises from the great alternatives of identical and nonidentical machines available in the system with multiple functionalities. Capacity planning is very expensive in flexible manufacturing systems since these systems are planned for producing a product family defined a priori in the mid-volume and mid-variety range of products.

Capacity planning in these systems is viewed as optimally satisfying the demand for multiple products within the existing family boundary using existing built-in capacity change alternatives (programmable machines). The capacity

Capacity Planning,

Fig. 2 Capacity planning approach in dedicated production systems (Reprinted with author's permission from "Capacity management via feedback control in reconfigurable manufacturing systems", by Asl and Ulsoy (2002))



planner will aim to find the optimal control of production flow (alternatives) within the FMS systems to balance between investment cost and lost sales cost (Kimemia and Gershwin 1983).

Reconfigurable Manufacturing Systems

Capacity planning in advanced manufacturing systems such as reconfigurable manufacturing systems (RMS) and changeable manufacturing systems is usually referred to as "capacity scalability." ElMaraghy (2005) explains the dimensions of capacity scalability in RMS by identifying and classifying the scalability characteristics into "physical scalability" and "logical scalability" attributes. Examples of physical capacity scalability enablers include the adding or removing of material handling equipment, machines, machine modules, such as axes of motions or heads, as well as tools or other components. Examples of logical capacity scalability enablers include increasing or decreasing the number of shifts or the number of workers as well as outsourcing. Modular components' design and interfaces as well as open control architecture are basic enabling technologies required for "plug-and-play" cost-effective way of achieving physical capacity scalability in RMS (Koren et al. 1999). A good reference on capacity scalability definitions, approaches, and examples can be found in Putnik et al. (2013).

Modeling Capacity Planning Problems

The interest in modeling the capacity planning problem goes back to the middle of the nineteenth century. A capacity planning model typically uses

deterministic demand that grows linearly with time and balances between the cost of installing capacity before it is needed and the economies of scale savings of capacity expansion/reduction.

The model determines the type and sizes of facilities to be added/removed and when so that the present worth of all capacity changes is minimized while meeting forecasted demand. Examples of such classical and static models can be found in Manne (1967) and Freidenfelds (1981), while a good review on classical capacity expansion models can be found in Luss (1982).

Various researchers attempted to enhance such basic notion and models by considering stochastic demands and dynamic lot sizes, accounting for various expansion costs, considering inventory along with capacity, and finally implementing different classical optimization techniques.

Modeling and formulating capacity planning problems were further considered from a more dynamic perspective due to the increased level of uncertainty as well as the fast advancements in manufacturing systems technologies. Dynamic modeling approaches included the application of control theoretic methods and feedback loops to control capacity under uncertainty with real-time information of both the market and production system. Examples of this approach include the work of Wiendahl and Breithaupt (2000), Duffie and Falu (2002), and Deif and ElMaraghy (2006). System dynamics was used to capture the dynamics associated with the capacity planning or scalability problem and the various parameters influencing it. An example of this approach for capacity planning includes the work of Deif and

ElMaraghy (2009). Other approaches to understand the dynamic nature of capacity planning were through the application of nonlinear dynamic analysis, chaos theory, dynamic optimization, simulation, and stochastic analysis (examples include Radons and Neugebauer 2005 and Scholz-Reiter et al. 2002). More recently, the dynamic capacity problem was modeled in the emerging cloud-based manufacturing using stochastic petri nets (Wu et al. 2015).

The common objective of all such methods and models is to determine the best capacity planning policies which advise manufacturers on which, when, where, and how to expand/reduce capacity in response to varying and often uncertain demand.

Importance of Capacity Planning

Sound capacity planning models and strategies are essential to maximize the potential of satisfying demands while minimizing cost and remaining profitable. Any unmet demand is a lost opportunity, and any unused production capacity is a waste of money and resources. Effective capacity planning is needed more than ever today to match demands to ability to produce and to rationalize outsourcing and subcontracting.

Cross-References

- ▶ [Manufacturing System](#)
- ▶ [Production Capacity](#)
- ▶ [Production Planning and Control](#)

References

Asl FM, Ulsoy AG (2002) Capacity management via feedback control in reconfigurable manufacturing systems. In: Mitsubishi M, Kurfess TR (eds) Proceedings 2002 Japan-USA symposium on flexible automation: International conference on new technological innovation for the 21st century, July 14–19, 2002 Hiroshima, Japan. The Institute of Systems, Control and Information Engineers (ISCIE), Kyoto, Japan

Deif A, ElMaraghy W (2006) A control approach to explore the dynamics of capacity scalability in reconfigurable manufacturing systems. *J Manuf Syst* 25(1):12–24

Deif A, ElMaraghy H (2009) Modeling and analysis of dynamic capacity complexity in multi-stage production. *Prod Plan Control* 20(8):737–749

Duffie N, Falu I (2002) Control-theoretic analysis of a closed-loop PPC system. *Ann CIRP* 51(1):379–382

ElMaraghy H (2005) Flexible and reconfigurable manufacturing systems paradigms. *Int J Flex Manuf Syst* 17(4):261–276 (Special issue on reconfigurable manufacturing systems)

Erlenkotter D (1977) Capacity expansion with imports and inventories. *Manag Sci* 23(7):694–702

Freidenfelds J (1981) Capacity expansion: analysis of simple models with applications. Elsevier North Holland, New York

Kalotay AJ (1973) Capacity expansion and specialization. *Manag Sci* 20(1):56–64

Kimemia J, Gershwin SB (1983) An algorithm for the computer control of a flexible manufacturing system. *IIE Trans* 15(4):353–362

Koren Y, Heisel U, Jovane F, Moriwaki T, Pritschow G, Ulsoy G, Van Brussel H (1999) Reconfigurable manufacturing systems (Keynote paper). *CIRP Ann Manuf Technol* 48(2):527–540

Leachman R, Carmon T (1992) On capacity modeling for production planning with alternative machine types. *IIE Trans* 24(4):62–72

Luss H (1982) Operation research and capacity expansion problems: a survey. *Oper Res* 30(5):907–947

Manne AS (ed) (1967) Investments for capacity expansion: size, location, and time-phasing. MIT Press, Cambridge, MA

Putnik C, Sluga A, ElMaraghy H, Teti R, Koren Y, Tolio T, Hon B (2013) Scalability in manufacturing systems design and operation: state-of-the-art and future developments roadmap. *CIRP Ann* 62(2):751–774

Radons G, Neugebauer R (eds) (2005) Nonlinear dynamics of production systems. Wiley-VCH, Weinheim

Scholz-Reiter B, Freitag M, Schmieder F (2002) Modeling and control of production systems based on nonlinear dynamics theory. *Ann CIRP* 51(1):375–378

Wiendahl H, Breithaupt J (2000) Automatic production control applying control theory. *Int J Prod Econ* 63(1):33–46

Wu D, Rosen DW, Schaefer D (2015) Scalability planning for cloud-based manufacturing systems. *J Manuf Sci Eng* 137(4):041007–1–041007–13

CAPP

- ▶ [Computer-Aided Process Planning](#)

Carbide

- ▶ [Cemented Carbides](#)

Cavitation Peening

► Peening

Cemented Carbides

Markus Groppe
Sandvik Coromant GmbH, Düsseldorf, Germany

Synonyms

Carbide; Hard metal; Tungsten carbide

Definition

The cemented carbides are a range of powder-metallurgical composite materials, which consist of hard carbide particles bonded together by a metallic binder (Sandvik Hard Materials 2012). The proportion of carbide phase is generally between 70% and 97% of the total weight of the composite and its grain size averages between 0.4 and 10 μm . In cemented carbides, these hard

particles are mainly tungsten carbides (WC) compared to cermets (TiC, TaC, NiC) or ceramics where metal oxides or nitrides are used.

Theory and Application

Cemented carbide is one of the most successful composite engineered materials. Its unique combination of strength, hardness, and toughness satisfies the most demanding applications.

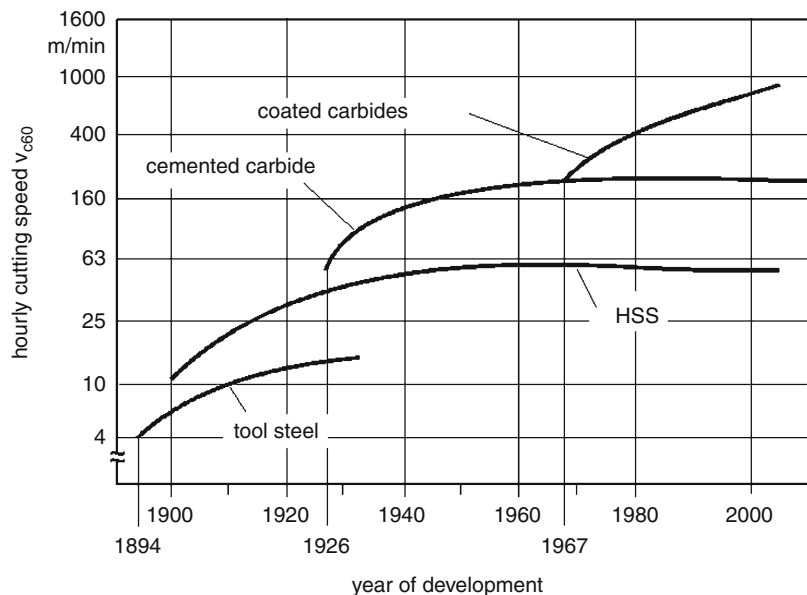
History

The development of this highly optimized cutting material is strongly connected to the history of the industrial manufacturing. First important invention which had very practical impact on the cutting technology was the invention of high-speed steel (HSS). With the new cutting material 3 \times , higher cutting speeds could be applied. High-speed steel has even today importance as a material for applications where tools with sharp cutting edges are needed, e.g., in reaming or fine finishing (Fig. 1).

The second important step was the invention of the cemented carbides. This material was a by-product of an entirely different technology. William D. Coolidge had invented the so-called

Cemented Carbides,

Fig. 1 Development of cutting materials (Toenshoff and Denkena 2013)



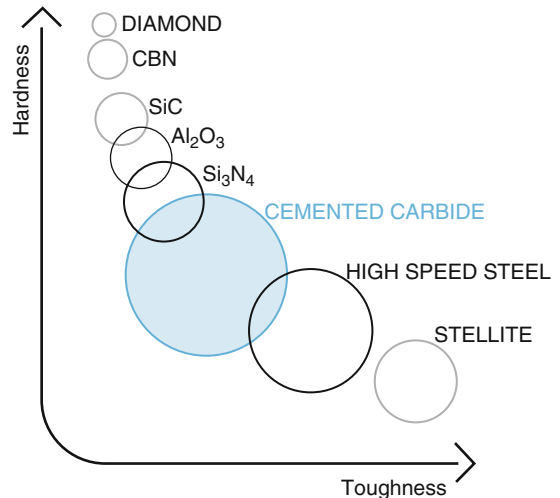
ductile tungsten, applied to manufacture the filaments for the incandescent light bulbs. To form these filaments, diamond drawing dies were used which were very expensive. A research institute in Germany “Osram Studiengesellschaft” got the order to find a replacement material for the diamond tools. The idea was to take the material cemented carbide and a binding material and have it sintered. In 1923, a young scientist, Karl Schroeter, was given patent no. 498349A for “the process to manufacture a hard, melting alloy for working tools especially drawing dies.” This material was not a melting alloy; it was sintered. The patent started a new age of tool material (Schröter 1923). It was soon sold to a company who was very interested in cutting materials, namely, to the Krupp Company in Essen in 1926. They introduced it under the trademark WIDIA (*wie Diamant*, like diamond). One year after, in 1927, the new cutting material was displayed at the Leipzig Exhibition. While this was not primarily a material innovation, it was, however, a great step forward in productivity with 4× higher cutting speeds than HSS, which is connected to a five times higher productivity (Toenshoff and Denkena 2013).

Engineering Cemented Carbide

To fulfill the requirements of a high productive cutting material, the tool must (Sandvik Coromant and Society of Manufacturing Engineers 1996):

- Be hard to resist flank wear and deformation
- Have a high toughness to resist fracture
- Be chemically inert to workpiece
- Be chemically stable to resist oxidation and dissolution
- Have good resistance to thermal shocks

The most commonly used materials are shown schematically relative to their hardness and toughness properties in Fig. 2. Diamond (PCD) is the hardest, of all, followed by cubic boron nitride (CBN) and ceramics (Al₂O₃, SiC, SIALON, etc). The super hard materials all suffer from lower toughness and poor resistance to sudden fracture; the cemented carbides have a unique



Cemented Carbides, Fig. 2 Application area of cemented carbides. (Source: <http://www.allaboutcementcarbide.com/01.html> [Date of access: 16.5.2013])

combination of high hardness and good toughness within a wide range and thus constitute the most versatile hard materials group for engineering and tooling applications.

A key feature of the cemented carbide is the potential to vary its composition so that the resulting physical and chemical properties ensure maximum resistance to above-listed wear mechanism. In addition, the wide variety of shapes and sizes that can be produced using modern powder-metallurgical processing offers tremendous scope to design cost-effective cutting solutions (Toenshoff and Denkena 2013).

The unique property of cemented carbide is that it offers a safer and more dependable solution than any other known material to one of the toughest problems which engineers have to contend with – reliability.

Reliability is often a problem of wear. Wear resistance is the most outstanding feature of cemented carbide. Cemented carbide can also withstand deformation, impact, heavy load, high pressure, corrosion, and high temperature – often the only material that can fulfill these requirements satisfactorily. One restriction is the limited capacity to withstand tensile stresses which has to be considered for the application. Over the years, cemented carbides have also proven their

superiority in a great number of other tooling and engineering applications than cutting.

Tungsten carbide (WC), the hard phase, together with cobalt (Co), the binder phase, forms the basic cemented carbide structure from which other types of cemented carbide have been developed. In addition to the straight tungsten carbide – cobalt compositions – cemented carbide may contain varying proportions of titanium carbide (TiC), tantalum carbide (TaC), and niobium carbide (NbC). These carbides are mutually soluble and can also dissolve a high proportion of tungsten carbide. Also, cemented carbides are produced which have the cobalt binder phase alloyed with, or completely replaced by, other metals such as iron (Fe), chromium (Cr), nickel (Ni), molybdenum (Mo), or alloys of these elements.

There are three individual phases which make up cemented carbide. In metallurgical terms, the tungsten carbide phase (WC) is referred to as the α -phase (alpha), the binder phase (i.e., Co, Ni) as the β -phase (beta), and any other single or combination of carbide phases (TiC, Ta/NbC, etc.) as the γ -phase (gamma). Other than for metal cutting applications, there is no internationally accepted classification of cemented carbides (please see section “Classification DIN ISO 513”) (Fig. 3).

The group of WC-Co grades contains WC and Co only (i.e., two phases) and a few trace elements. These grades are classified according to their cobalt content and WC grain size (Fig. 4).

Grades of Cemented Carbide

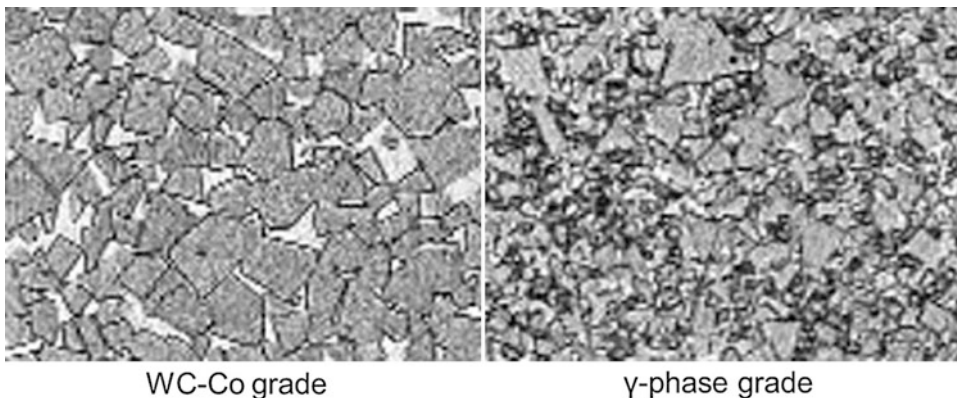
The grades of cemented carbides in this group contain WC and Co as the main elements, although small additions or trace levels of other elements are often added to optimize properties. These grades are classified according to their cobalt content and WC grain size and are often called the “straight grades.” They have the widest range of strength and toughness of all the cemented carbide types and this is in combination with excellent wear resistance.

There is no “official” grain size classification. Figure 5 shows an industrial standard.

Nano, Ultrafine, and Submicron Grades

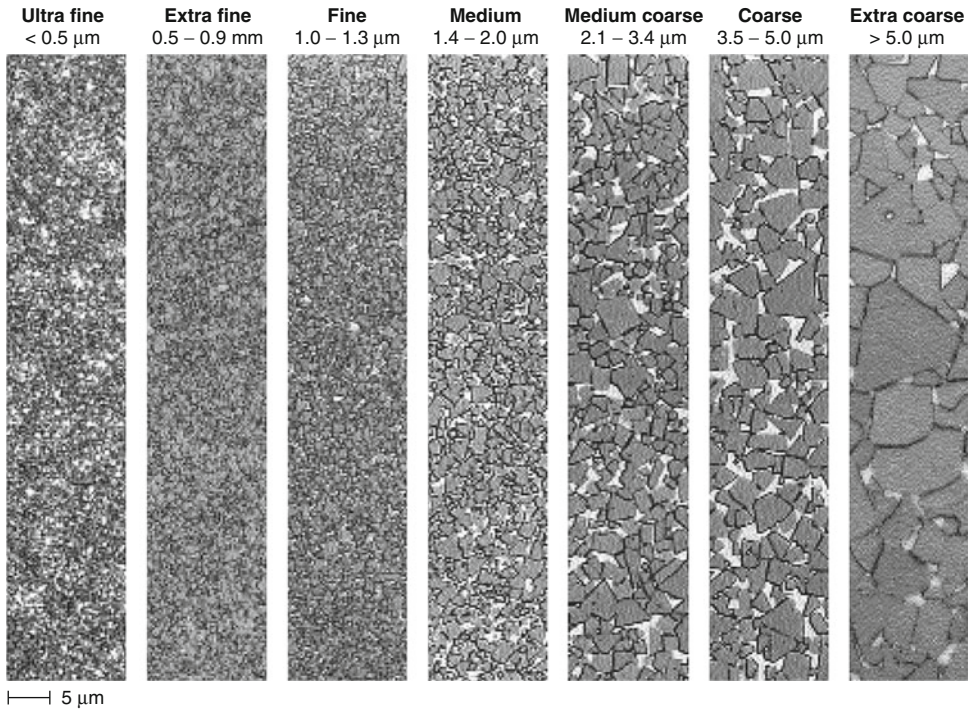
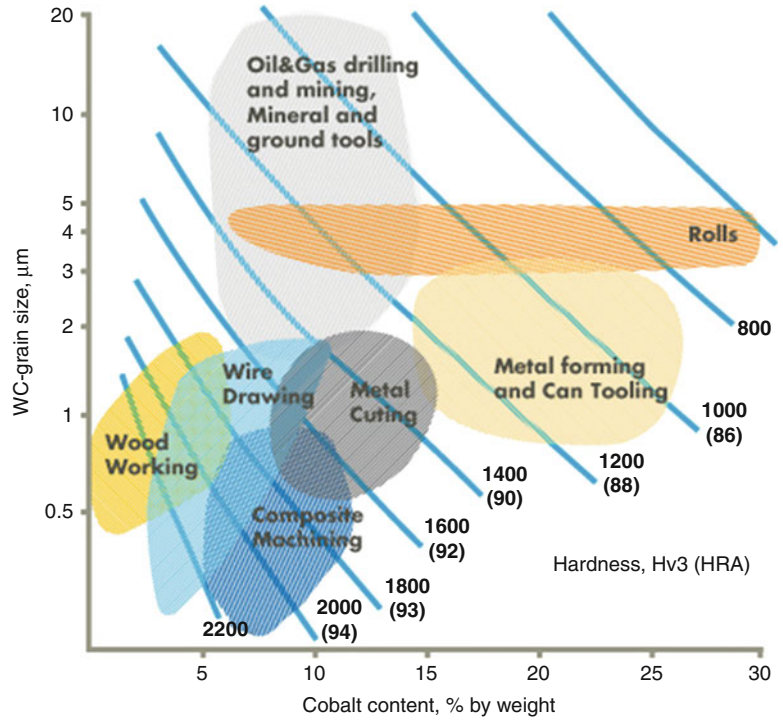
Grades with binder content in the range of 3–10 wt% and grain sizes below 1 μm have the highest hardness and compressive strengths, combined with exceptionally high wear resistance and high reliability against breakage. These grades are used in a wide range of wear parts applications and in cutting tools and carbide drill bits designed for metallic and nonmetallic machining for which a combination of high strength, high wear resistance, and sharp cutting edges are essential (Fig. 6).

Today the trend is towards miniaturization: digital cameras, laptops, and mobile phones are becoming even smaller and are expected to include more features. This has resulted in more complex printed circuit boards with a greater



Cemented Carbides, Fig. 3 Microstructure of cemented carbides. (Source: <http://www.allaboutcementedcarbide.com/02.html> [Date of access: 16.5.2013])

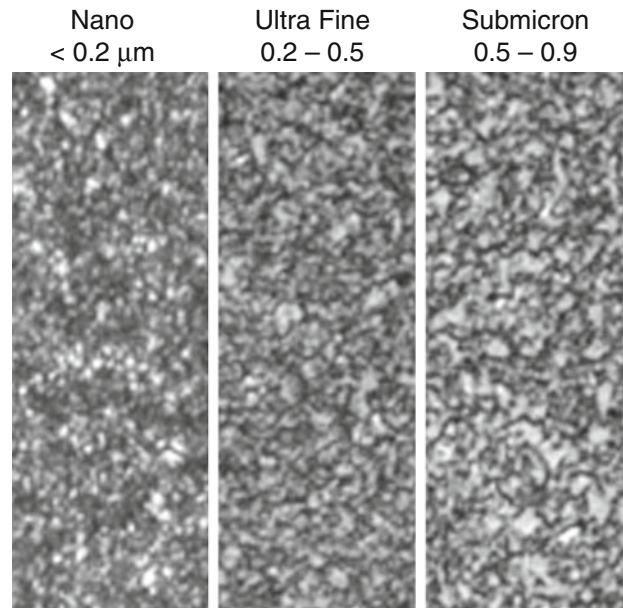
Cemented Carbides, Fig. 4 The application range of straight grade cemented carbide. (Source: <http://www.allaboutcementedcarbide.com/02.html> [Date of access: 16.5.2013])



Cemented Carbides, Fig. 5 Grain size classification (Sandvik Hard Materials 1997)

Cemented Carbides,

Fig. 6 Nano, ultrafine, and submicron grades. (Source: http://www.allaboutcementedcarbide.com/02_01.html [Date of access: 16.5.2013])



C

number of components per surface area. To meet this demand, PCB manufacturers are compelled to drill more and smaller holes with smaller carbide drill bits. This shift in drill size has increased the demands on tool material. The smallest drill diameter in carbide drill bits today is only 10–20 μm . To realize those small diameters, the grain sizes on cemented carbides have to be even smaller. To facilitate the use of tiny carbide drill bits and raise productivity, spindles with increasing rpm are being developed. It is now possible to machine with a standard NC machine with a maximum speed of 300,000 rpm (Fig. 7).

Fine and Medium Grades

The grades with binder content in the range 10–20% by weight and WC grain sizes between 1 and 5 μm have high strength and toughness, combined with good wear resistance.

The grades with binder contents in the range 3–15% and grain sizes below 1 μm have high hardness and compressive strength, combined with exceptionally high wear resistance.

Cubic and Cermet Grades

Cubic and cermet grades are one of the latest developments of cemented carbide. This group consists of grades containing a significant



Cemented Carbides, Fig. 7 Micro drills. (Source: http://www.allaboutcementedcarbide.com/02_01.html [Date of access: 16.5.2013])

proportion of γ -phase, (i.e., TiC, TaC, NbC) together with WC and Co.

The main features of the γ -phase are good thermal stability, resistance to oxidation, and

high temperature wear. These grades are designed to provide a favorable balance of wear resistance and toughness, e.g., for high-speed cutting (HSC) application or in can tooling applications that generate high temperatures and have close contact with ferrous materials.

If these grades are designed without any WC phase, they are named cermets which give a unique combination of high temperature hardness, chemical wear resistance, and low density. Cermets are traditionally avoided for wear parts because of being more brittle than standard WC-Co grades. New developments have allowed toughness to be improved significantly and cermets are now applied in a number of demanding applications from advanced engineering components to high-performance metal sawing blades (Fig. 8).

Dual Property (DP) Grades

This group contains grades which have had the distribution of their binder phase modified in such a way as to create a material with different properties in the surface zone compared with the bulk.

This entirely new concept enables components to be produced which contain distinct microstructural zones, each with different binder content. Thus, each zone has different properties – hence the term “Dual Property.”

For conventional cemented carbides, wear resistance and toughness are related in such a

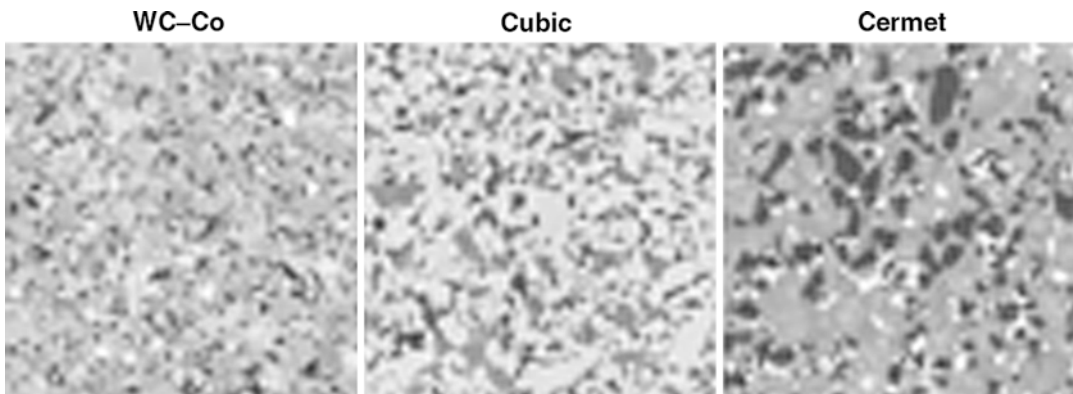
manner that an improvement in one property results in a deterioration in the other.

The company Sandvik has developed an entirely new type of WC-Co cemented carbide in which wear resistance and toughness can be improved independently of each other. By means of a controlled redistribution of the cobalt binder phase, cemented carbide components can now be made which contain three distinct microstructural zones, each of which has different properties. These gradients, together with the differences in thermal expansion, redistribute the internal stresses. For example, it is possible to create a very hard and wear-resistant surface layer which is simultaneously preloaded with compressive stresses to prevent the initiation and propagation of cracks.

Carbide having such a distribution of properties has high wear resistance at the surface combined with a tough core. These materials have therefore been given the designation DP – Dual Property.

The Manufacturing Process

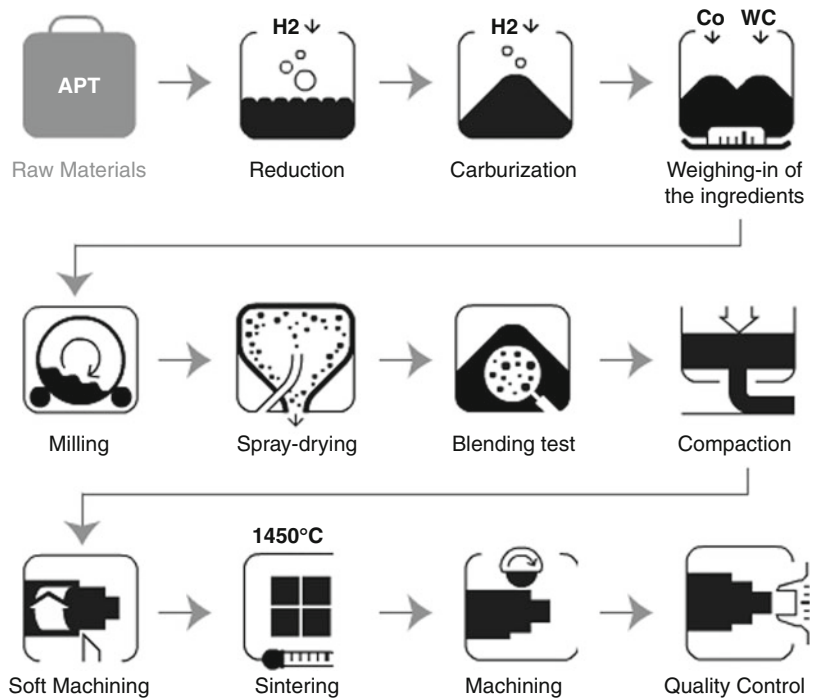
The manufacturing process begins with the composition of a specific Cemented carbide powder mixture – tailored for the application. Scheelite or wolframite are the tungsten-containing minerals. Ammonium-Para Tungstate (APT) is the starting raw material of the production. The first step is a wet process involving a sequence of stepwise dissolutions, precipitations, and separations (Fig. 9).



Cemented Carbides, Fig. 8 Microstructure of cubic and cermet grades. (Source: http://www.allaboutcementedcarbide.com/02_05.html [Date of access: 16.5.2013])

Cemented Carbides,

Fig. 9 Manufacturing process. (Source: <http://www.allaboutcementcarbide.com/03.html> [Date of access: 16.5.2013])



After a hot reduction of the APT in hydrogen, pure tungsten powder is obtained. By varying the reduction process, the grain size of the tungsten powder can be controlled within 1–20 μm .

Tungsten and carbon (soot) is mixed in exact proportions. The mixture is heated at high temperature in hydrogen under formation of Cemented carbide powder (WC).

Different WC powder types and binder cobalt (Co) powder are the raw material for the manufacturing of cemented carbide. After weighing-in of WC, Co and several additives to prescribed composition, and cemented carbide grade, the mixture is wet milled. The milling has effect on both carbide grain size and homogeneity of the slurry. The milling procedure is important for achieving homogeneous cemented carbide after sintering.

After milling, the slurry must be dried, e.g., by spray drying to powder form. This “ready-to-press” (RTP) powder consists of spherical agglomerates of the constituents.

The pressing properties and the composition of the powder are measured. Furthermore the powder must have a good flow behavior in order to uniformly fill the cavities of a press tool.

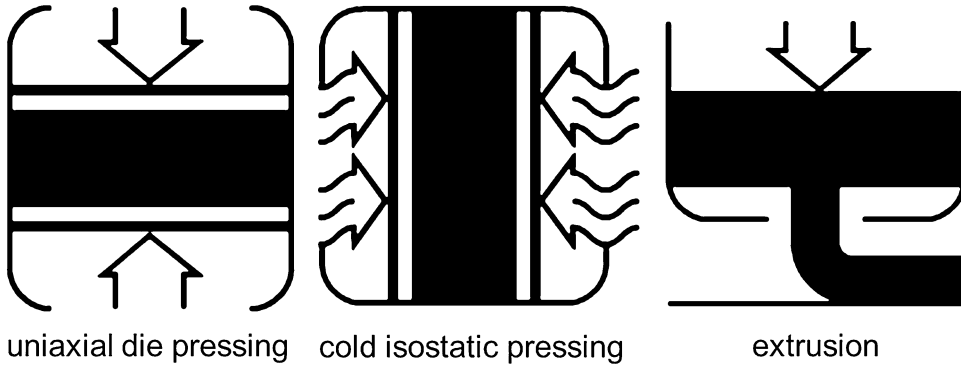
The production of cemented carbide starts by pressing the compacts. Different methods of compaction of the powder (Fig. 10) are:

- Uniaxial die pressing (high fixed and low variable costs)
- Cold isostatic pressing for products with shapes unsuited for uniaxial die pressing (low fixed and high variable costs)
- Extrusion: for cemented carbide rods (high fixed and low variable costs)

In some cases the compacts are soft machined or green shaped into a proper shape prior to sintering.

The sintering is the final process step in which the cemented carbide gets its properties as a high-strength engineering material. The sintering process is performed at such high temperatures so the molten binder could combine with the WC. The sintering could be done with or without high isostatic gas pressure (HIG).

After the sintering the compact has undergone shrinkage of about 50 vol.%. The cemented carbide blanks are ready for dispatch after sintering or they are machined by further processes like EDM or grinding.



Cemented Carbides, Fig. 10 Compaction methods. (Source: <http://www.allaboutcementedcarbide.com/03.html> [Date of access: 16.5.2013])

Cemented Carbides, Fig. 11 Cutting application groups acc (DIN ISO 513)

- P-group (plastic): long chip building ferrous materials, steel
- K-group: nonferrous metals, cast iron, AlSi alloys, plastics, wood
- M-group (mixed): alloyed austenitic and ferritic steels, alloyed cast iron
- further classification

01	↑	increasing	↑	increasing wear
10		toughness,		resistance,
20		higher feed		higher cutting speed
40				
50	↓			

typical marking: HW – P10; HC – K20

A quality control in the end ensures the approval of dimensions, shape, and physical properties.

Classification DIN ISO 513

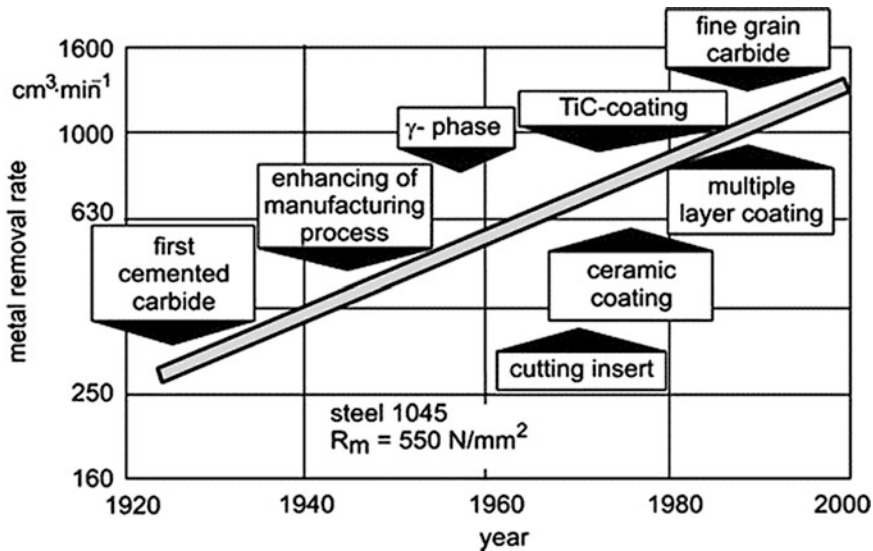
There are 3 main application groups: P for steel, K for nonferrous metals and cast iron, and the M group as a mixed group for alloyed ferritic and austenitic steels and for alloyed cast iron. Further classification is given by the toughness and wear resistance described by numbers. With higher numbers the toughness is increasing and the hardness will be lower (DIN ISO 513 2005). Please see Fig. 11.

Each manufacturer of carbide grades is free to sort his product in any of the groups. Different from common material standards, the classification is not based on the material composition. The content

and the ingredients of the cutting material are not described. In addition the coating of cemented carbide is not taken in consideration.

Coating of Cemented Carbide

There is a dualism of cemented carbides; the substrate can be either tough or wear resistant. In the late 1960s, a remarkable enhancement was gained by combining both positive effects. This was reached by a kind of functional separation: Toughness is necessary to bear mechanical loads particularly dynamic loads. Wear resistance is necessary to withstand tribological loading, but that is mainly required in the surface of a cutting tool. This consideration leads to hard coatings like titanium carbide (TiC), titanium nitride (TiN), or aluminum oxide (Al_2O_3) in combination with tough substrates (Toenshoff and Denkena 2013) (Fig. 12).



Cemented Carbides, Fig. 12 Developments of cemented carbides and coatings (Toenshoff and Denkena 2013)

Cross-References

- ▶ [Cermets](#)
- ▶ [Coated Tools](#)
- ▶ [Cutting of Inconel and Nickel Base Materials](#)
- ▶ [Cutting, Fundamentals](#)
- ▶ [Superhard Tools](#)

insbesondere Ziehsteine [A hard fusible alloys production technique for craft-tools in particular drawing dies]. Deutsches Reichspatent [German Imperial Patent] No 498349A

Toenshoff HK, Denkena B (2013) Basics of cutting and abrasive processes. Springer, Heidelberg/Berlin

References

- DIN ISO 513:2005-11 (2005) Classification and application of hard cutting materials for metal removal with defined cutting edges: designation of the main groups and groups of application (ISO 513:2004). Beuth, Berlin
- Sandvik Coromant, Society of Manufacturing Engineers (1996) Modern metal cutting: a practical handbook. Sandvik Coromant, Sandviken
- Sandvik Hard Materials (1997) Understanding cemented carbide. Retrieved from [http://www2.sandvik.com/sandvik/0130/Hi/SE03411.nsf/a0de78d35676d88d412567d900294747/4c7827530abfa4e1c1256b0a0034cc36/\\$FILE/ATTYN87R/9100%20eng.pdf](http://www2.sandvik.com/sandvik/0130/Hi/SE03411.nsf/a0de78d35676d88d412567d900294747/4c7827530abfa4e1c1256b0a0034cc36/$FILE/ATTYN87R/9100%20eng.pdf). Accessed 26 May 2013
- Sandvik Hard Materials (2012) Understanding cemented carbide. www.allaboutCementedcarbide.com. Accessed 6 May 2013
- Schröter K (1923) Verfahren zur Herstellung einer harten Schmelzlegierung für Arbeitswerkzeuge,

Centerless Grinding

Barbara Linke

Mechanical and Aerospace Engineering,
University of California Davis, Davis, CA, USA

Definition

Centerless grinding is a cylindrical grinding process variant without fixing the workpiece along its axis between centers.

In external centerless grinding, the workpiece lies between grinding wheel, workrest plate, and control wheel which regulates the speed of the workpiece. In internal centerless grinding, the workpiece lies between rolls or shoes and is driven by a control wheel or a faceplate.

Theory and Application

Basic Principles

In 1853, Schleicher developed the first centerless grinding machine for needle grinding. In 1917, Heim introduced workrest plate and control wheel, which improved the performance and enlarged the field of application (Hashimoto et al. 2012). Since then, centerless grinding is highly applicable for large batch and mass production. No clamping steps and no center holes on the workpiece faces are required, which eliminates process steps, reduces time, and diminishes possible form errors (Marinescu et al. 2007). Workpiece loading can be easily automated. Moreover, the linear workpiece support through workrest plate and control wheel enables machining of thin components or machining with high removal rates and minimal deformations (Klocke 2009). Besides the advantages in process performance, machine setup in centerless grinding is complex and needs experienced and skilled workers for highest efficiency.

The control wheel, also known as regulating wheel, is a conventional grinding wheel or a steel body with a cemented carbide coating. It slows the workpiece down during grinding through friction. Ideally tangential slipping is negligible, and workpiece speed, v_w , depends only on control wheel speed, v_{cw} , and control wheel tilt angle, α_{cw} (see Fig. 1). Centerless grinding commonly works in down grinding, i.e., grinding wheel speed and

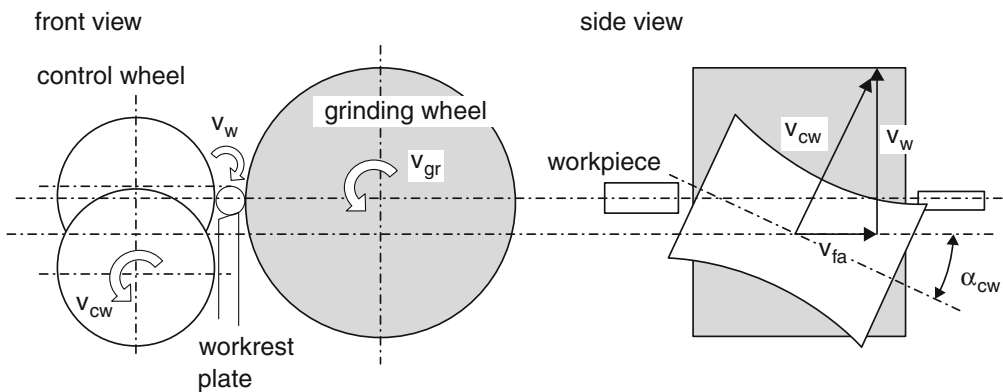
workpiece speed are same directional in the contact zone:

$$v_w = v_{cw} \cdot \cos \alpha_{cw} \quad (1)$$

The workrest plate, also known as workrest blade, work blade, or workplate, needs to be highly wear-resistant and consists of tool steel or cast iron with hardened surfaces, cemented carbide inserts or coatings of PCD, or other hard material. Workrest plate angle is important for grinding force directions and process stability.

A large workrest plate angle, β , results in comparatively high horizontal forces on the workrest plate which can lead to deflection or resonance vibrations (Meyer 2011). Small workrest plate angles are therefore preferred for large grinding forces, e.g., in the case of high material removal rates. For too small workrest plate angles, however, the normal force between control wheel and workpiece can get too small to controllably decelerate the workpiece (Meyer 2011). A typical value for the workrest plate angle is $\beta = 30^\circ$ (Marinescu et al. 2007).

If possible, control wheel and workrest plate support the workpiece on the machined circumferential area to avoid bending. However, this three-point support can induce self-regenerative roundness errors as explained in the next section. In centerless grinding, the depth of cut is half of that in grinding between centers, because the feed



Centerless Grinding, Fig. 1 Centerless throughfeed grinding, after (Klocke 2009)

is relative to the workpiece diameter and the workpiece center moves away from the grinding wheel during centerless grinding (Marinescu et al. 2007). Therefore, the depth of cut, a_e , per workpiece revolution can be calculated as

$$a_e = \frac{v_{fr}}{2n_w} \quad (2)$$

with radial feed rate, v_{fr} , and number of workpiece revolutions, n_w .

Roundness Errors

In centerless grinding, the workpiece is machined and supported on its circumferential area, which can lead to roundness errors. If an error on the workpiece comes into contact with the control wheel or workrest plate, the workpiece center will move, and the depth of cut at the grinding wheel will change. The error regenerates itself at another position on the workpiece circumference. Therefore, this phenomenon is called “regenerative effect.”

Several causes of roundness errors in centerless grinding can be identified (Rowe et al. 1989; Marinescu et al. 2007; Klocke 2009):

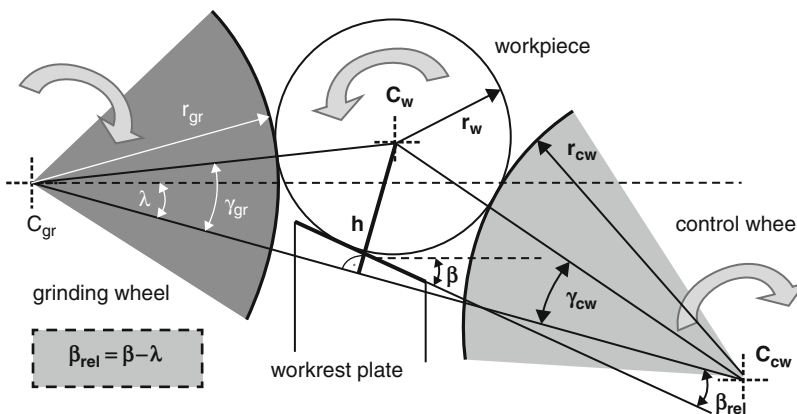
- Geometric stability, also known as lobing stability (Dall 1946; Rowe 1964; Reeka 1967; etc.)
- Dynamic stability (Furukawa et al. 1971; Hashimoto et al. 2000; Miyashita et al. 1982; etc.)
- External disturbances, excited vibrations

However, these mechanisms are interrelated and were analyzed by several researchers. A lot of work has been done on workpiece rounding mechanisms in centerless grinding and possible implementation in software systems (Bhateja and Levi 1984; Hashimoto et al. 2000; Friedrich 2004; Zeppenfeld et al. 2008; Barrenetxea et al. 2009; etc.).

Geometric Stability

The geometric position of the workpiece in the grinding gap is crucial for the geometric form of the workpieces. The connection between the grinding wheel center, C_{gr} , and control wheel center, C_{cw} , might be tilted with the angle, λ , to the horizon (Fig. 2). The distance of the workpiece center, C_w , from the center connection is defined as workpiece center height, h . Above-center grinding, i.e., centerless grinding with positive center heights, is generally advantageous against below-center grinding with more theoretical areas for geometric process stability. Workpiece change is easier for above-center grinding, but it allows workpieces to jump so that covers are necessary. In below-center grinding, the workpiece is enclosed from all sides, and more force can be applied, but geometric stability is worse than above-center.

The tangent angles, γ_{gr} and γ_{cw} , affect geometric stability strongly and, therefore, the likeliness of wave formation on the workpiece circumference (Dall 1946; Reeka 1967). Cloud diagrams or



Centerless Grinding, Fig. 2 Grinding gap, after (Zeppenfeld et al. 2008)

software programs help to choose stable grinding conditions (Fig. 3).

Dynamic Stability

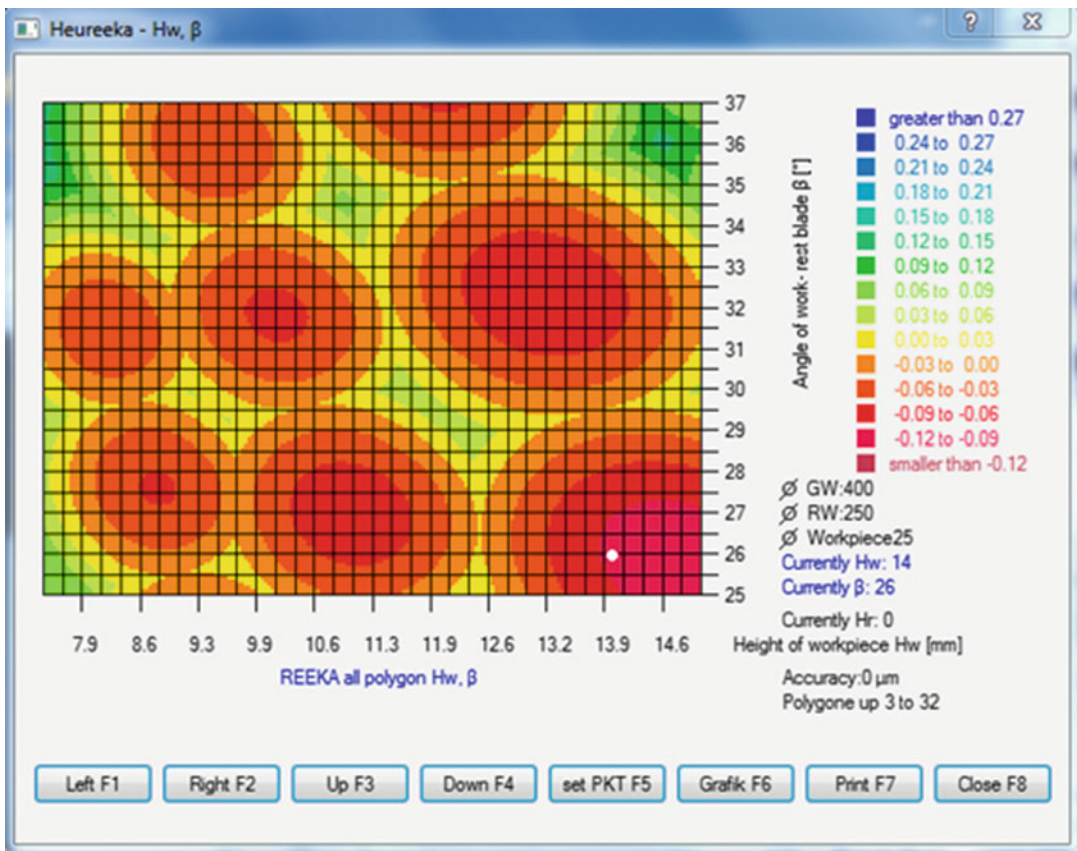
Chatter occurs at frequencies near the machine structural resonant frequencies. If it occurs, chatter is typically more severe than geometric instability. Models on dynamic instability include the contact deformation between grinding wheel, control wheel, and workpiece (Hashimoto et al. 2000).

Most research on stability focuses on centerless plunge grinding as a two-dimensional setup. However, Meis, Barrenextra, and others deduced stability conditions for throughfeed grinding adding a third dimension to the stability conditions (Meis 1981; Barrenetxea et al. 2009; etc.).

Both geometric and dynamic stability are superimposed during centerless grinding and should be modeled together (Brecher and Hannig 2008).

External Centerless Plunge Grinding

In centerless plunge grinding, the grinding wheel moves with radial feed towards the workpiece. This process produces cylindrical steps, profiles, or tapers with a single grinding wheel or a set of wheels (Fig. 4). To ensure the axial position of the workpiece, the control wheel is tilted at a small angle, α_{cw} (often below 0.5°), and a stop is installed at the face of the workpiece. Centerless plunge grinding includes roughing, finishing, and a spark-out phase similar to cylindrical grinding between centers. The control wheel is commonly



Centerless Grinding, Fig. 3 Stability charts (Source: Schaudt Mikrosa GmbH, reprinted with permission)



Centerless Grinding, Fig. 4 Parts manufactured by centerless plunge and throughfeed grinding (Source: Schaudt Mikrosa GmbH, reprinted with permission)

dressed with a stationary diamond dressing tool, whereas the grinding wheel is either dressed with a stationary or rotating tool depending on the grit type.

External Centerless Throughfeed Grinding

In centerless throughfeed grinding, the workpieces move along the grinding wheel with axial feed. Cylindrical, slightly conical, or slightly convex form elements on the workpiece are generated (Fig. 4). The control wheel is inclined along workpiece feed direction with the control wheel angle, α_{gw} (often between 1° and 3°) (Fig. 1). Without axial slip, the control wheel generates a force on the workpiece in axial direction. Therefore, workpiece feed rate, v_{fa} , results from control wheel speed, v_{cw} , and control wheel tilt angle, α_{cw} :

$$v_{fa} = v_{cw} \cdot \sin \alpha_{cw} \quad (3)$$

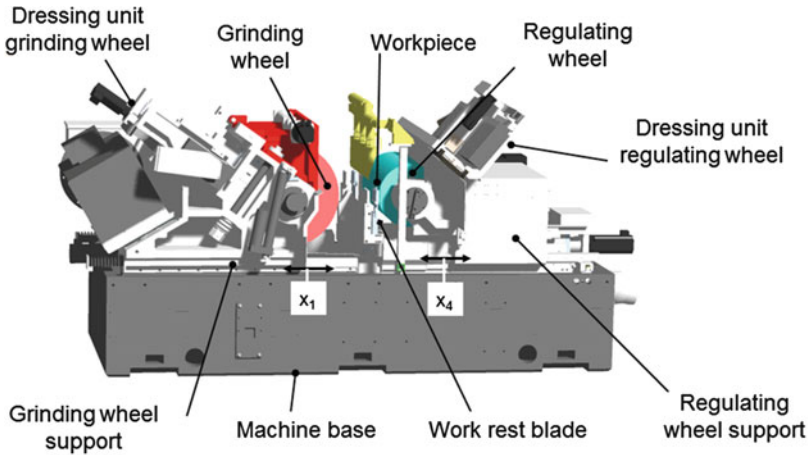
The control wheel has a complex shape to realize line support of the workpiece. The control wheel profile is influenced by control wheel inclination

angle, workpiece center height, and workpiece diameter. Dressing rulers or NC programs with corresponding calculations help to profile the control wheel accordingly to the actual process setup, commonly with a single-point diamond dresser (Fig. 5). The control wheel profile affects the workpiece speeds and can be optimized for maximum speed control and longevity of the control wheel (Meyer 2011).

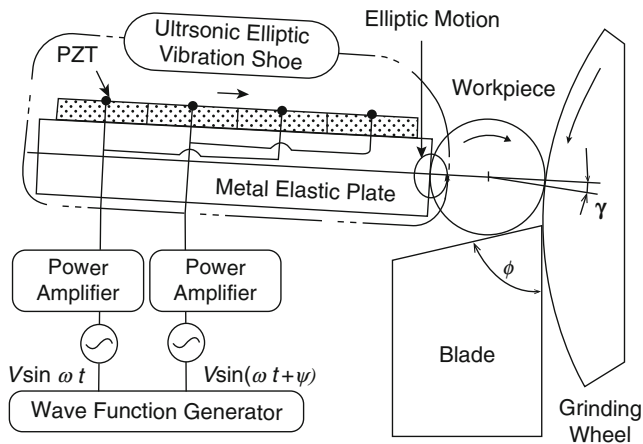
Moreover, the grinding gap must narrow in axial feed direction to decrease the workpiece diameter. This is achieved by profiling grinding wheel into corresponding zones or pivoting the control wheel. The grinding wheel is commonly profiled and sharpened by stationary or rotating diamond dressing tools. Dressing can happen intermittently or during grinding, but in the latter case, the respective parts will need to be scrapped.

Other Process Variants

Internal centerless grinding works with grinding wheel, control wheel, support roll, and pressure roll to fix the workpiece. The external workpiece



Centerless Grinding, Fig. 5 Centerless throughfeed grinding machine (Source: Schaudt Mikrosa GmbH, reprinted with permission)



Centerless Grinding, Fig. 6 Principle of ultrasonic shoe centerless grinding (Reprinted from Journal of Materials Processing Technology, Volumes 155–156, Wu Y, Fan Y,

Kato M, Kuriyagawa T, Syoji K, Tachibana T, Development of an ultrasonic elliptic-vibration shoe centerless grinding technique, ©2004 with permission from Elsevier)

surface provides the reference for concentricity and roundness of the inner diameter (Marinescu et al. 2007).

Shoe centerless grinding can be applied to external and internal cylindrical surfaces and is especially important for small length-to-diameter ratio. In shoe grinding, the component is positioned by metal plates, which are called shoes, instead of control wheel and workrest plate (Marinescu et al. 2007). This allows to apply

additional vibrations through the shoe (Fig. 6) (Wu et al. 2004).

References

- Barrenetxea D, Marquinez JI, Bediaga I, Uriarte L (2009) Continuous workpiece speed variation (CWSV): model based practical application to avoid chatter in grinding. *CIRP Ann Manuf Technol* 58(1):319–322

- Bhateja CP, Levi R (1984) Current state of the Art of workpiece roundness control in precision centerless grinding. *CIRP Ann Manuf Technol* 33(1):199–203
- Brecher C, Hannig S (2008) Simulation of plunge centerless grinding processes. *Prod Eng* 2(1):91–95
- Dall AH (1946) Rounding effect in centerless grinding. *Mech Eng* 68(4):325–329
- Friedrich D (2004) Prozessbegleitende Beeinflussung des geometrischen Rundungseffektes beim spitzenlosen Aussenrundeinstechschleifen [Process-accompanying manipulation of geometric rounding in centerless infeed grinding], PhD thesis, RWTH Aachen University (in German)
- Furukawa Y, Miyashita M, Shiozaki S (1971) Vibration analysis and work-rounding mechanism in centerless grinding. *Int J Mach Tool Des Res* 11:145–175
- Hashimoto F, Zhou SS, Lahoti GD, Miyashita M (2000) Stability diagram for chatter free centerless grinding and its application in machine development. *Ann CIRP* 49(1):225–230
- Hashimoto F, Gallego I, Oliveira JFG, Barrenetxea D, Takahashi M, Sakakibara K, Stalfelt H-O, Stadt G, Ogawa K (2012) Advances in centerless grinding technology. *Ann CIRP* 61(2):747–770
- Klocke F (2009) Manufacturing processes 2 - grinding, honing, lapping (RWTH edition). (Kuchle A, Trans). Springer, Berlin
- Marinescu ID, Hitchiner M, Uhlmann E, Rowe WB, Inasaki I (2007) Handbook of machining with grinding wheels. CRC Press, Boca Raton
- Meis, FU (1981) Geometrische und kinematische Grundlagen für das spitzenlose Durchlaufschleifen [Geometrical and Kinematical Fundamentals for Throughfeed Centerless Grinding]. PhD-thesis at RWTH Aachen University, Westdt. Verlag, EAN (in German)
- Meyer, B (2011) Prozesskräfte und Werkstückgeschwindigkeiten beim Spitzenlosschleifen [Process forces and workpiece speeds in centerless grinding], PhD thesis, RWTh Aachen. Apprimus Verlag, Aachen (in German)
- Miyashita M, Hashimoto F, Kanai F (1982) Diagram for selecting chatter free conditions of centerless grinding. *CIRP Ann Manuf Technol* 31(1):221–223
- Reeka D (1967) Zusammenhang zwischen Schleifspaltgeometrie, Bearbeitungsbedingungen und Rundheitsfehlern beim spitzenlosen Schleifen [The Interdependence of Grinding-Gap Geometry, Process-Parameter and Roundness Error in Centerless Grinding]. PhD-thesis at RWTH Aachen University (in German)
- Rowe WB (1964) Some studies of the centerless grinding with particular reference to the roundness accuracy. PhD-thesis at University of Manchester
- Rowe WB, Miyashita M, Koenig W (1989) Centerless grinding research and its application in advanced manufacturing technology. *Ann CIRP* 38(2):617–624
- Wu Y, Fan Y, Kato M, Kuriyagawa T, Syoji K, Tachibana T (2004) Development of an ultrasonic elliptic-vibration shoe centerless grinding technique, *J Mater Process Technol*, volumes 155–156, Proceedings of the International Conference on Advances in Materials and Processing Technologies: Part 2, pp. 1780–1787. <http://www.sciencedirect.com/science/article/pii/S0924013604005011>. [Date of access: 10/25/2016]
- Zeppenfeld C, Meyer B, Klocke F, Krajnik P (2008) Rundheitsfehler beim Spitzenlosschleifen [Roundness error in centerless grinding]. *wt-online* 6–2008, pp. 446–451 (in German)

Ceramic Cutting Tools

Raouf Ben Amor¹ and Dev Banerjee²

¹Kennametal Shared Services GmbH, Fürth, Germany

²Kennametal Inc., Latrobe, PA, USA

Synonyms

Advanced ceramic; Ceramic machining tool; Engineering ceramic; Fine ceramic (Japan); Superhard cutting material; Technical ceramic

Definition

Ceramics are inorganic, nonmetallic materials. The structure of ceramics may be crystalline or partly crystalline (having intergranular amorphous phases). The definition of ceramic is often restricted to inorganic crystalline materials.

Ceramics are primarily divided into two classes: whiteware ceramic and technical ceramic (refer to section “**Synonyms**”). Whiteware ceramics typically possess poor mechanical properties. Technical ceramic materials are of high purity and are designed for specific application and use. Ceramics used in wear applications are harder compared to metallic materials, maintain strength and hardness, and are chemically inert at high temperatures. The combination of hardness, high-temperature strength, and chemical resistivity makes ceramics important cutting tool materials.

Theory and Application

Introduction

Ceramic cutting tools are becoming more and more popular with rise in demand for higher productivity, improvement in machine capabilities, and growth of automotive, energy, and aerospace markets. Also, recent developments in machine technology leading to higher power as well as higher cutting speed have enabled a wider use of ceramic-based cutting materials.

There have been some excellent reviews of ceramic cutting tools in the past (North 1987; Kamanduri and Samanta 1989; Krishnamurthy and Sivashankaran 1994; Casto et al. 1996). The types of materials available today have not changed significantly since then, even though variations of the basic types that improve performance have become available. Most significant advancements have been made in processing techniques enabling new geometries, cutting edge quality, and lower cost.

Selection of a tool material for a machining application depends on:

- Productivity demand
- Machine capabilities, such as spindle power, spindle speed, and rigidity
- Type of material to be machined
- Tooling cost and tool reliability

Factors that positively affect performance of a tool material are:

- High hardness, enhancing abrasive wear resistance to maximize tool life
- Edge strength and toughness to prevent edge chipping
- Absence of plastic deformation at cutting temperature to prevent a dull edge
- Absence of chemical reactivity with workpiece

The popularity of ceramics is due to their high hardness and abrasion resistance, ability to maintain hardness at high temperature, chemical stability at high temperature, and lower friction. These enable ceramic tools to be run at much higher speed than carbide tools, often without

any need of coolant. With new environmental regulations, use of coolant may become an issue in the future, making ceramics more attractive. Higher cutting speed and feed enable higher material removal rates resulting in lower overall machining cost.

One significant development in the last couple of decades has been increasing use of superhard (PCD, PcBN) in machining. Even though cBN is a ceramic material, it will be discussed in the “superhard” section. In some applications cemented carbide, which used to be benchmark of performance, is now replaced by superhard to define productivity. This dynamics will play an important role in determining the role of ceramics in the future.

Tool Materials

Ceramic tool materials can be broadly categorized in the following classes:

Oxides and Oxide Composites

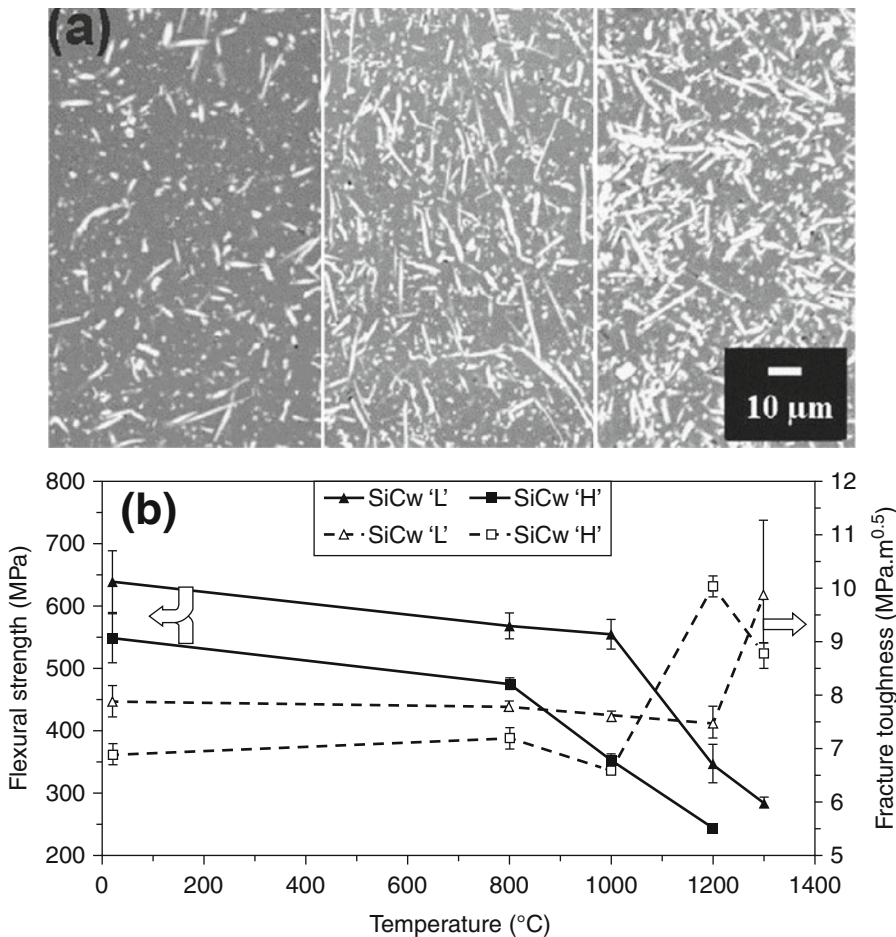
One of the earliest classes of materials to be used for industrial machining was alumina (Al_2O_3). Alumina has high abrasion resistance and chemical resistivity toward materials being machined but is also one of the most brittle cutting materials available. Combined with its low thermal conductivity, a poor thermal shock resistance is ensured. Today pure alumina occupies a relatively small percentage of the cutting tool material market. Improvements have been made in formulations and processing to increase toughness and hardness and reduce cost. Primary methods of improvement have been:

1. Finer grain size and higher purity raw material
2. Additives and reinforcement (Osayande et al. 2008): SiC whisker, SiC particles, zirconia, ZrO_2 , YAG, TiC, TiCN, ZrCN, TiB₂ (Jianxin et al. 2005), etc.
3. Better densification at lower cost

Today, majority of the oxide-based cutting tools are composites. In spite of the development of materials such as Si_3N_4 and Sialon, and the inherent brittleness of oxide-based materials, the popularity of these materials remained due to their high abrasion and chemical resistance.

Among the oxide composites, SiC whisker-reinforced alumina deserves some discussion. It was first introduced in the 1980s, and there was high level of enthusiasm for whisker composites. In addition to SiC whiskers, work had been done with whiskers of TiC, TiCN, and TiB₂ showing improved performance in laboratory (Pettersson and Johnsson 2003) (Fig. 1a), but these did not get much commercial success due to lack of significant differentiation in performance and lack of whisker availability. Commercially available composites have used SiC as whisker for the last two decades. Improvements have been made in understanding the whisker-matrix relationship. Whisker is the cost driver and is a health

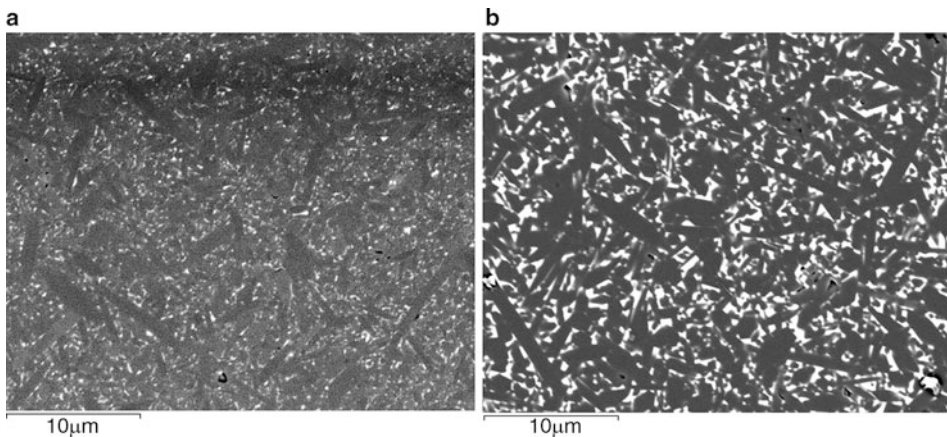
hazard, and therefore, minimizing whisker content while maximizing performance has been the goal. It was found that the optimum whisker level is 20–30% by weight in alumina matrix. Above this limit the whiskers form cluster, degrading properties. Surface quality of whiskers in terms of roughness and impurities such as oxygen also have been the subject of investigation, aiming at creating a weak interface. A weak interface between matrix and whiskers leads to a different fracture mechanism that enhances toughness (Belcher et al. 1988; Garnier et al. 2005) (Fig. 1b). Today most major ceramic cutting tool manufacturers offer alumina-SiC whisker tools, some with coating.



Ceramic Cutting Tools, Fig. 1 (a) Alumina-Ti(C,N) whisker composites with various volume fractions of whisker (Pettersson and Johnsson 2003), (b) effect of oxygen on whisker surface *L* low oxygen, *H* high oxygen (Garnier et al. 2005)

Ceramic Cutting Tools, Table 1 Summarizes the benefits and drawbacks of various ceramic tool materials

Table 1 Relative behavior of various ceramic cutting tool materials		
Material	Pro	Con
Alumina	Chemically inert, good abrasion resistance	Brittle, poor thermal shock resistance
Alumina-zirconia	Greater toughness than pure alumina	Lower hardness
Alumina-TiC	Higher hardness. Some reported increase in thermal conductivity and toughness	Relatively brittle
Alumina-TiCN		
Alumina-SiC whisker	Higher toughness from crack bridging by whiskers, higher thermal shock resistance	Chemical affinity of SiC for Fe
Alumina-TiB ₂	Higher hardness and lubricity	Chemical reactivity
Silicon nitride	High toughness, high thermal shock resistance, and high T strength	Interaction with Fe and Co alloys
Sialon	Combines high T properties with chemical stability	Inferior thermal shock resistance to Si ₃ N ₄
	Wear resistance can be tailored	

**Ceramic Cutting Tools, Fig. 2** Structure of (a) low additive, (b) high additive Si₃N₄ showing *elongate* β grains

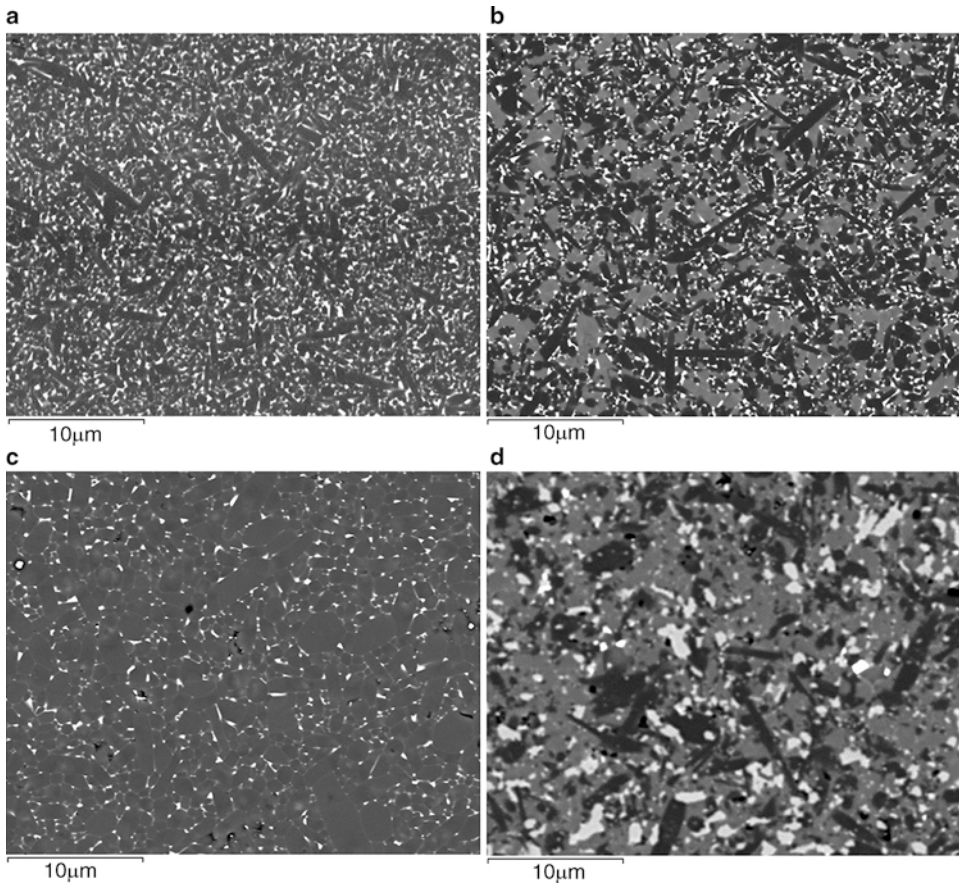
Silicon Nitride (Si₃N₄)

Superior high-temperature properties of Si₃N₄ brought a lot of promise in the world of machining. One particular advantage of silicon nitride is its high thermal shock resistance due to low coefficient of thermal expansion, high thermal conductivity, and toughness. Pure Si₃N₄ is very difficult to sinter. Additives such as MgO and Y₂O₃ are added to silicon nitride to make it sinterable. The additives form a glassy phase with the SiO₂ present on Si₃N₄ grains, which facilitates sintering. However, the glassy phase that becomes intergranular also reduces high-temperature strength. The best silicon nitride grades used in machining have a small amount of additives (Kamanduri and Samanta 1989;

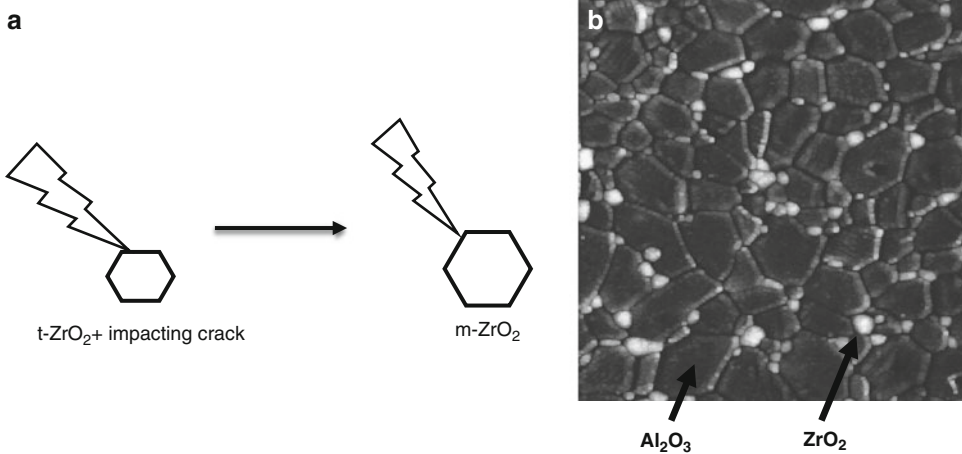
Krishnamurthy 1994), and the final product is a beta-Si₃N₄ with a small amount of glassy phase and free silicon. Various other sintering aids, including rare-earth oxides, have been tried to tailor the grain morphology and improve toughness (Becher et al. 2006; Belcher et al. 1998; Kitayama et al. 2001; Kleebe et al. 1999; Park et al. 1998; Santos et al. 2008; Satet et al. 2005; Wang et al. 1996). Figure 2 shows microstructures of a typical Si₃N₄ cutting tool materials.

Sialon

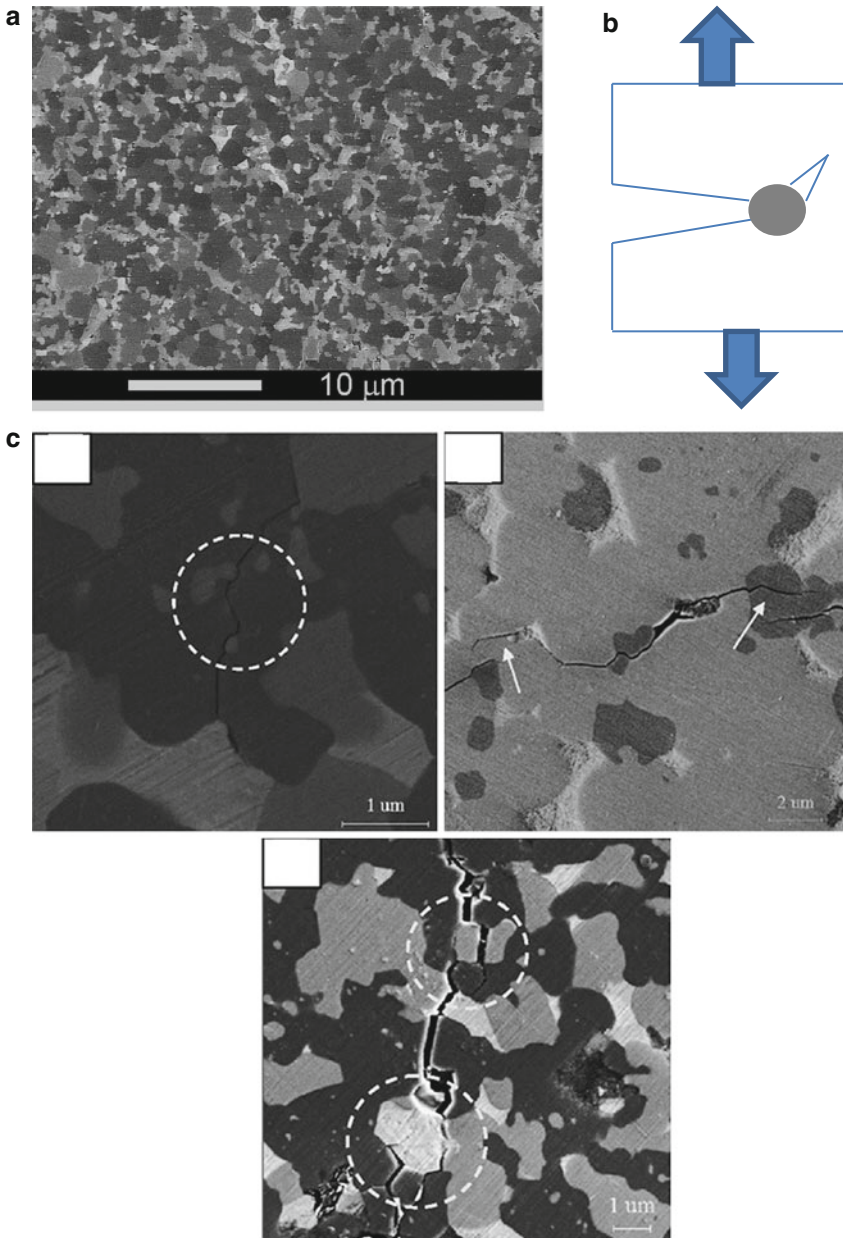
This class of materials was developed to combine the chemical stability of alumina and properties of Si₃N₄ with ease of sintering. A beta-Sialon is formed by substitution of Al and O ions for Si



Ceramic Cutting Tools, Fig. 3 Structure of (a) 100% β -Sialon, (b) α -/ β -Sialon, (c) 100% α -Sialon, and (d) Sialon with electrical conductivity (Sialon-SiC-TiN composite)



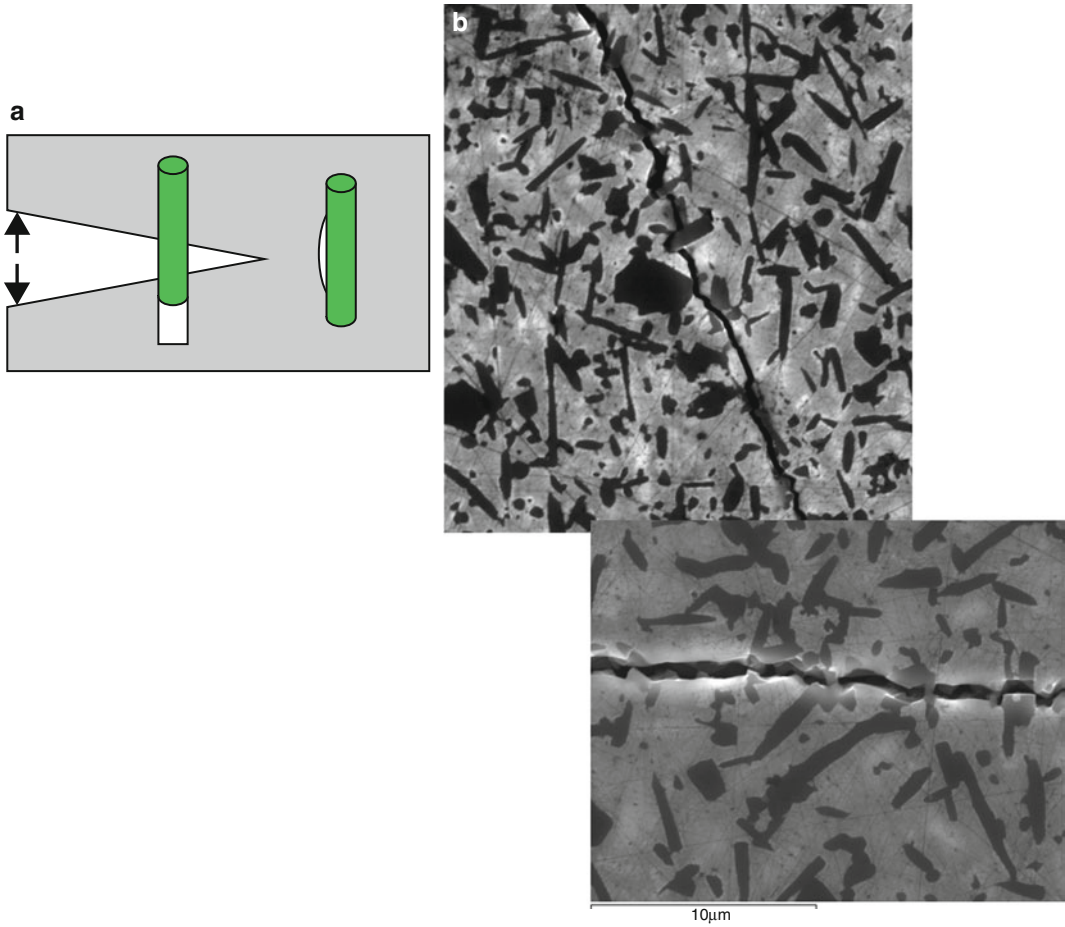
Ceramic Cutting Tools, Fig. 4 (a) Schematic of transformation toughening, (b) structure of zirconia-reinforced alumina



Ceramic Cutting Tools, Fig. 5 (a) Structure of alumina-TiCN composite, (b) schematic of crack deflection by a hard particle, and (c) crack deflection in alumina matrix by TiC particle (Yin et al. 2013)

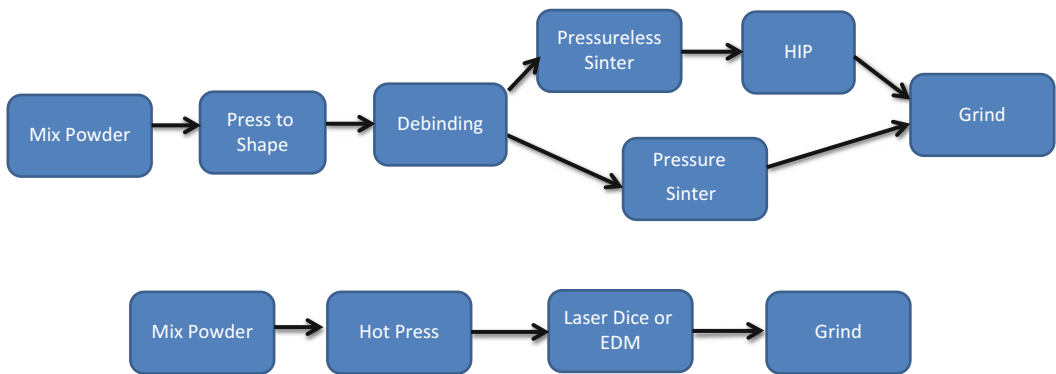
and N in Si_3N_4 lattice, as $\text{Si}_{6-z}\text{Al}_z\text{O}_z\text{N}_{8-z}$. The resultant structure contains elongated beta-Sialon grains, typically with some intergranular phase, which could be amorphous or crystalline. Substitution of alumina adds to the chemical stability over pure silicon nitride. The structure can be further altered by addition of a cation (m) with

valence v to form alpha-Sialon ($\text{M}_{m/v}\text{Si}_{12-(m+n)}\text{Al}_{(m+n)}\text{O}_n\text{N}_{16-n}$) in a beta-Sialon matrix. The alpha-Sialon grains are typically equiaxed but are more wear resistant. Changing alpha to beta ratio, various wear-toughness combinations can be achieved. Formation of alpha-Sialon also consumes the intergranular phase and improves



C

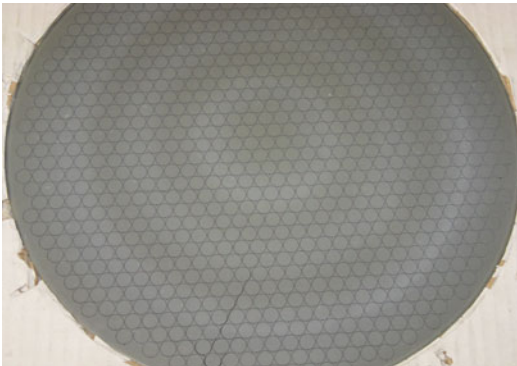
Ceramic Cutting Tools, Fig. 6 (a) Schematic of crack bridging and (b) crack deflection and bridging in an Alumina-SiC whisker composite



Ceramic Cutting Tools, Fig. 7 Common processing routes for ceramic tools

Ceramic Cutting Tools, Table 2 Processing routes of ceramic tool materials

Material	Green shaping	Densification			Post sintering
		Process	T (°C)	P (MPa)	
Alumina	Press	Air sintering	1,400–1,500	Ambient	Grinding
SiC _W -alumina	–	Hot press	1,800–1,900	35–45	Laser dicing, grinding
TiCN-alumina	Press	Gas pressure sintering	1,800	10–15	Grinding
		Hot press			35–45
Zirconia-toughened alumina	Press	Air sintering	1,400–1,500	Ambient	Grinding
Si ₃ N ₄	Press	1. Gas pressure sintering	1,750–1,900	Gas pressure: 10–15 HIP: 175–225	Grinding
		2. Inert sintering + HIP			
Sialon	Press	1. Gas pressure sintering	1,750–1,900	Gas pressure: 10–15 HIP: 175–225	Grinding
		2. Inert sintering + HIP			

**Ceramic Cutting Tools, Fig. 8** An alumina-SiC_W hot-pressed billet, laser diced in circular shapes to make RNG inserts

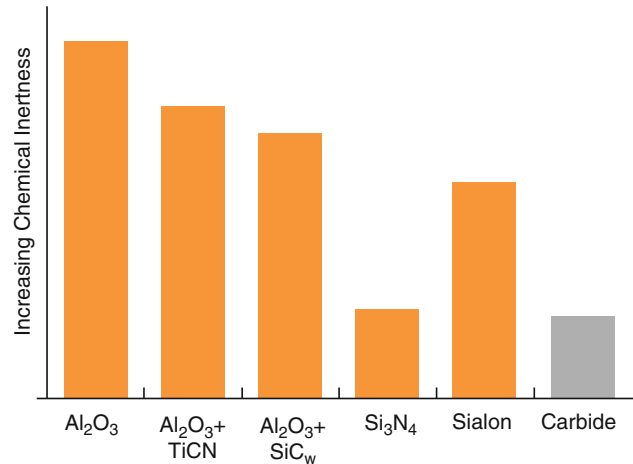
high-temperature behavior. However, the Sialons have inferior thermal shock resistance to Si₃N₄, and presence of alpha phase has a stronger negative effect on thermal shock resistance. Work has been done to create 100% alpha-Sialon while trying to elongate the grain morphology to improve toughness. Addition of rare-earth oxides increases tendency to alpha formation, whereas larger RE ions tend to elongate the alpha grains (Chen et al. 2003; Liu et al. 2008; Hoffman and Holzer 2003; Mandal et al. 1999). The alpha-beta ratio and morphology of the grains can also be

optimized by heat treatment (Carman et al. 2009; Huang et al. 2012; Ye et al. 2003, 2004). However, a higher aspect ratio of grains does not always translate to higher toughness due to strong interfacial bond, which prevents effective debonding and crack bridging. Very high alpha-Sialons have found limited traction due to processing difficulties and/or poor performance. Figure 3 shows microstructure of various Sialon materials developed for cutting applications.

Si₃N₄ Composites

Efforts have been made to combine the toughness and high-temperature strength of Si₃N₄ with improved abrasion resistance and electrical conductivity by making composites with SiC particles (Kodama et al. 1990; Sajgalik et al. 2006), SiC whisker (Kodama et al. 1990; Bradley et al. 1989), TiN (Blugan et al. 2005), zirconia (Markys et al. 1993; Feng et al. 2006), etc. Distinct benefit of these materials in machining is still not clear, and these have found a relatively low level of acceptance.

The toughening mechanisms in ceramics have been reviewed by various authors (Hutchison 1989; Ighodaro et al. 2008). This section describes the toughening mechanism utilized particularly for development of cutting tool materials:

Ceramic Cutting Tools,**Fig. 9** Relative chemical resistance of various tool materials, mostly against Fe- or Co-based alloys

1. Phase transformation toughening: This mechanism utilizes a phase transformation-induced volume change. The most common method is to incorporate tetragonal zirconia particles in a brittle matrix, such as alumina. As a crack approaches a t-zirconia particle, the stress at the crack tip induces a phase transformation to monoclinic form accompanied by an increase in the volume of the particle. This puts the surrounding matrix under compression and helps stop the crack from propagating (Fig. 4). Associated microcracking may also contribute to increased toughness.
2. Crack pinning, deflection, and bowing: These mechanisms are utilized by incorporating harder particles, such as WC, TiC, and TiCN in a brittle matrix. The reinforcing particles could create a stress field around them from thermal expansion mismatch and may be weakly bonded to the matrix. An approaching crack is either pinned by the particle or is deflected in a different direction through interfacial debonding (Fig. 5).
3. Crack bridging and pullout: This mechanism utilizes high aspect ratio of a phase in the structure (whisker, beta- Si_3N_4 , etc.). A required condition for this mechanism to be activated is a weak interface between the matrix and the high aspect ratio phase. When a crack approaches the elongated phase, the interface debonds, and the crack goes around the phase, instead of through it. In order for the

crack to extend, the crack faces must open up against the needlelike phase, which consumes energy, and for some period of time, the unbroken needle bridges the crack preventing catastrophic failure, as shown in Fig. 6.

Processing

Processing of ceramic inserts traditionally has taken one of the paths shown in Fig. 7. Table 2 summarizes typical processing conditions. Figure 8 shows a hot-pressed alumina- SiC_w billet laser cut to circular insert shape.

The primary component of cost of an insert manufacturing could be the post-sintering finishing. This is particularly critical for inserts with complex geometries. The trends in processing have been to find ways to reduce cost and exploring new techniques to create new microstructure. Some avenues explored are:

- Near net shaping to eliminate post-sintering grinding. This is achieved by exercising control during pressing and sintering, minimizing distortion.
- Hot isostatic pressing (HIP) to substitute for hot press.
- Substitute HIP with pressure sintering, using new sintering techniques such as micro wave sintering (Chockalingam et al. 2009) and spark plasma sintering (Belmonte et al. 2010; Nishimura et al. 1995).

Ceramic Cutting Tools,

Fig. 10 High temperature strength of various ceramics (North 1987)

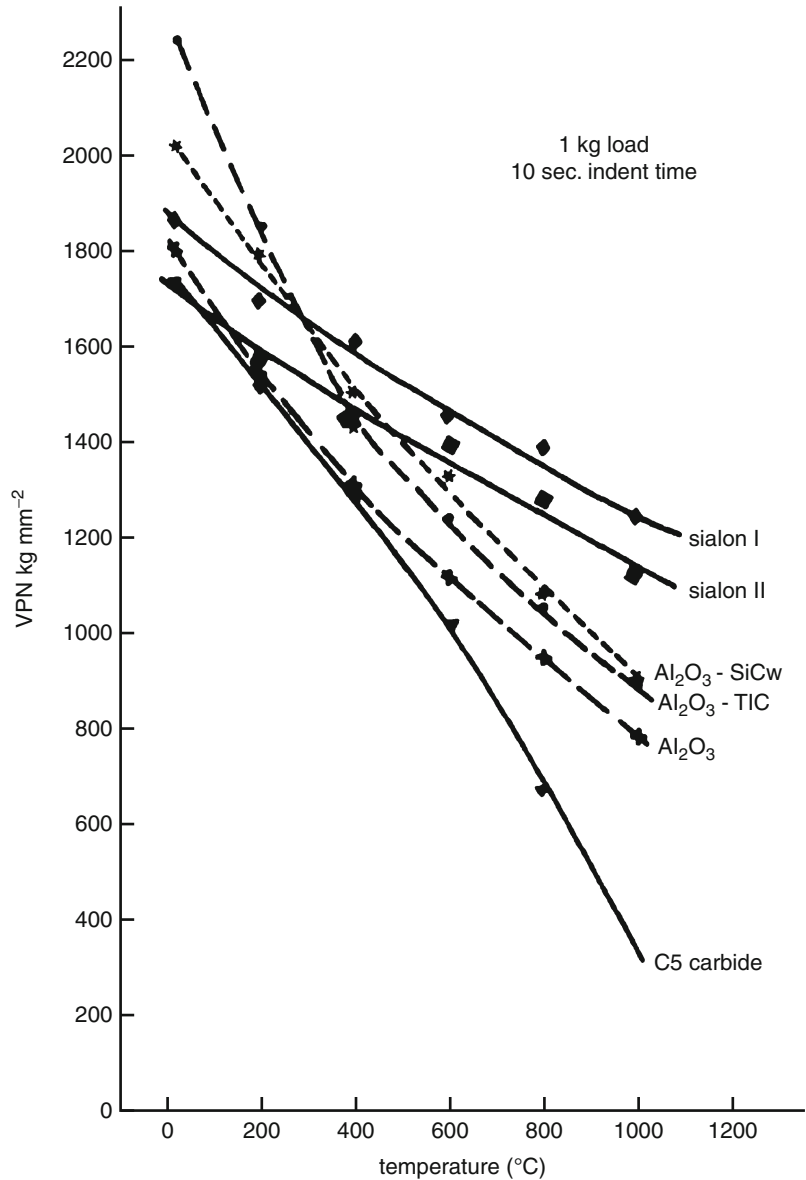
**Properties of Ceramics**

Table 1 summarizes relative attributes of various ceramic materials used in metal cutting. Figures 9, 10, 11, and 12 show the behavior of various ceramics used in cutting in relation to cemented carbide. In general, the primary advantage of ceramics comes from higher chemical stability and ability to maintain strength and hardness at high temperature. Si₃N₄ and Sialon also possess higher

thermal shock resistance which enables use in interrupted cutting.

Coating

Both PVD and CVD coatings are applied on ceramics, even though CVD is more common. PVD coating application requires electrical conductivity of the substrates, which limits the application range, particularly for oxide ceramics. New PVD

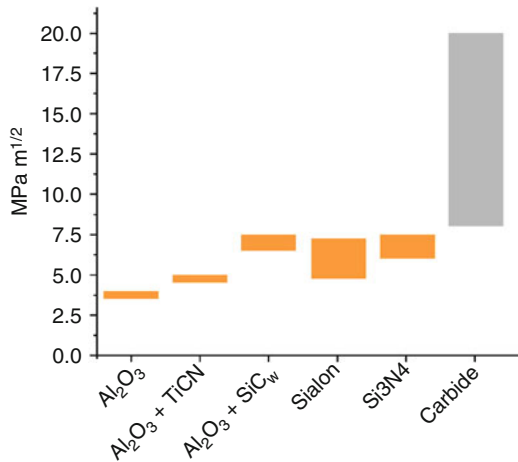
coating materials and technologies are overcoming this limitation. Single or multilayer CVD coatings on the other hand are quite common. Thickness of CVD coating is generally higher than PVD. Since ceramic inserts are typically honed, a thicker coating is not a concern. However, for applications requiring a sharp edge, PVD is preferred. The most common PVD coating is TiN. CVD coatings include TiN, TiAlN, alumina, TiB₂, and multiple layers of these.

Coatings over ceramic substrates serve the following purposes:

- Reduce chemical reactivity with workpiece material

- Reduce friction resulting in lower cutting force and lower heat buildup
- May facilitate as wear indicator
- Increase microhardness and abrasion resistance

The benefits of coatings have been verified in the field, and coated tools today are state of the art. Figure 13 shows a double-layer coating on Sialon substrate.



Ceramic Cutting Tools, Fig. 11 Relative fracture toughness (median crack method) of various ceramic tool materials

Geometries

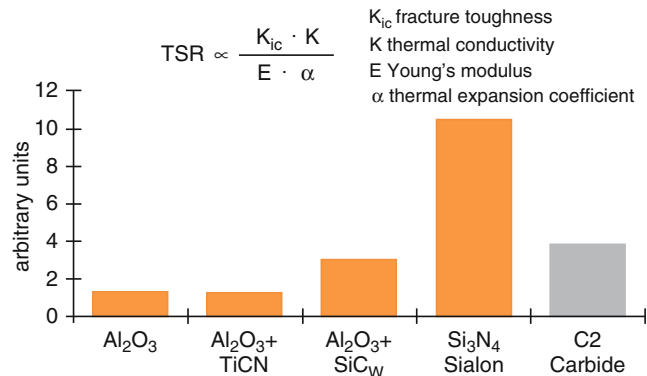
Due to low strength and toughness of ceramics compared to cemented carbide, simpler shapes and negative geometries have been common. Processing cost of inserts also plays a significant role as some materials can only be made by hot pressing, and cost of grinding chip breaker forms becomes prohibitive. Figure 14 shows the most common geometries conforming to ISO/ANSI norm used in ceramics with their relative edge strength. Figure 15 shows various edge preparation methods and an actual insert with honed and chamfered edge.

Mostly recommended ceramic inserts are of negative style due to better force distribution resulting in better edge retention. Negative style edges require higher cutting forces and generate higher temperature. Some of this heat is transferred to the workpiece, softening it and making it easier to cut.

Honing and chamfering of the edge is almost always recommended to minimize chipping tendency. Some of these treatments may reduce

Ceramic Cutting Tools,

Fig. 12 Relative thermal shock resistance of ceramic tool materials ($\Delta T = 800\text{ }^\circ\text{C}$)



$$TSR \propto \frac{K_{ic} \cdot K}{E \cdot \alpha}$$

K_{ic} fracture toughness
 K thermal conductivity
 E Young's modulus
 α thermal expansion coefficient

sharpness of cutting edge and cutting efficiency but is a good compromise.

Applications and Guidelines

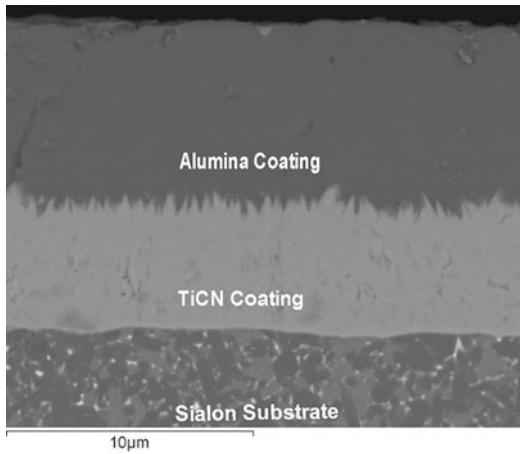
Three machining parameters generally describe the cutting process – cutting speed, feed rate, and depth of cut. Ceramics are typically chosen for high speed. For interrupted cuts with higher feed, such as in rough turning or milling, high strength and toughness are required from the tool material. For high-speed finishing (low DOC), high hot hardness is critical. Silicon-bearing materials, such as SiC, Si3N4, or Sialons, have reactivity with Fe- and Co-based alloys. This can be

mitigated by using alumina additive (as in Sialon) or a coating.

Figures 16 and 17 display some general tool selection guidelines for a particular workpiece or machining type. Development of coatings is enabling wider application ranges for the tool materials.

Some general guidelines for cutting speed are shown in Table 3. Actual speed of operation depends on the tool material characteristics, tool holder, and machine rigidity as well as degree of interruption.

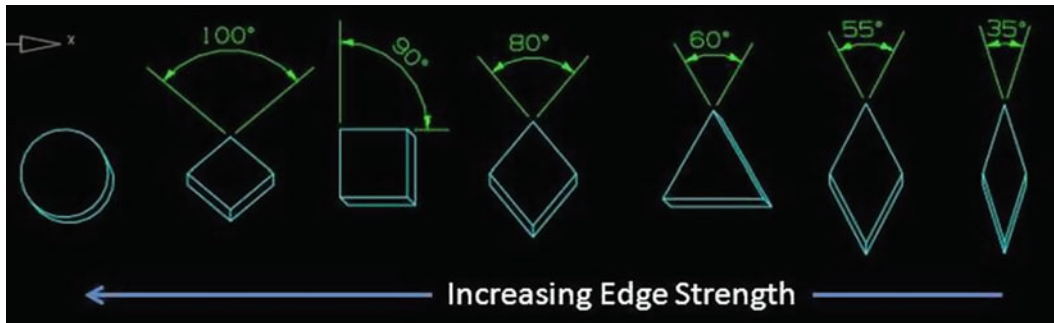
Si3N4 offers a good balance of toughness and hardness. For years silicon nitride has remained the first choice of high-performance machining of gray cast iron. Composite ceramics made of alumina and TiN/TiCN are characterized by high thermal stability and high hardness and are frequently used in machining hardened steels or chilled cast iron. Whisker composites are widely used in cutting materials for aerospace and defense applications. High-temperature hardness and toughness have made whisker composites a unique solution in machining high-temperature alloys. Alumina is still the most economical solution in certain niche areas, such as heavy machining of large components (e.g., train wheels).



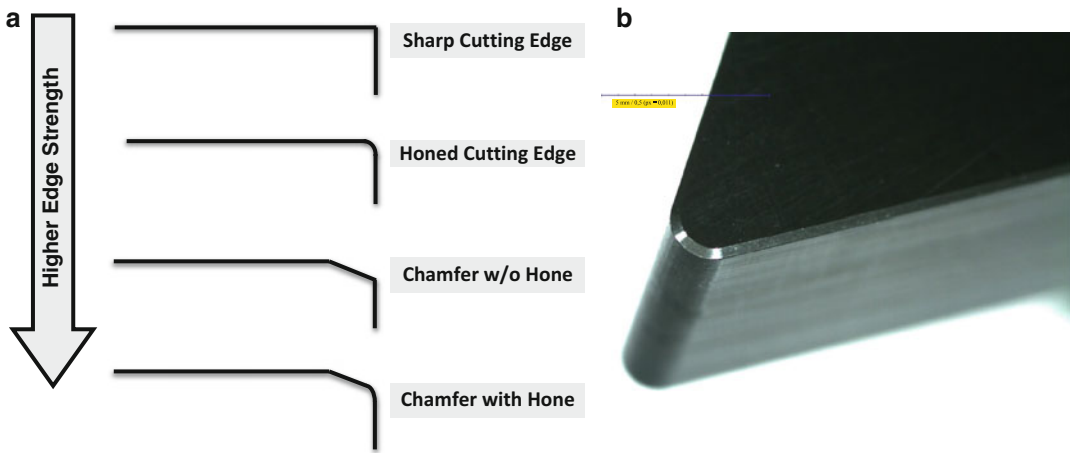
Ceramic Cutting Tools, Fig. 13 Multilayer CVD coating on a Sialon cutting tool

Machining Ti

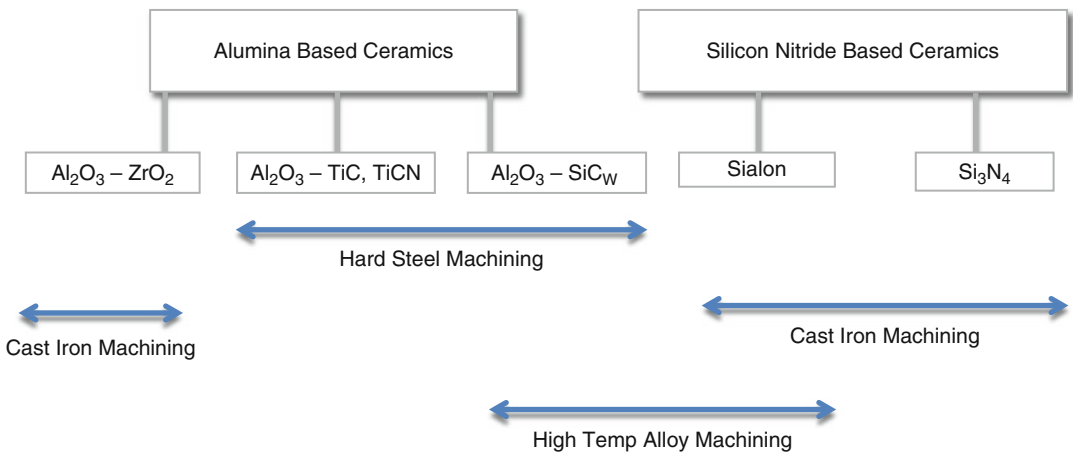
Ceramics have not found much success in machining Ti alloys yet. Machining Ti and its alloys involve high localized heat generation due to poor thermal conductivity, chatter due to high shear stress in chip formation, and chemical



Ceramic Cutting Tools, Fig. 14 Common geometries for ceramic tools



Ceramic Cutting Tools, Fig. 15 (a) Examples of edge preparation in ceramic tools and (b) actual edge of a cutting insert with hone and chamfer



Ceramic Cutting Tools, Fig. 16 Workpiece-dependent choice of ceramic tool

reactivity with Ti. The characteristics of Ti demands very sharp and high positive cutting edges, requiring high toughness and rigidity from tool material. Compared to cemented carbide, ceramics show insufficient toughness and are therefore not applicable for Ti alloy machining. In addition, poor thermal conductivity of ceramics and high temperature result in temperature gradient in the subsurface area of the tool, leading to thermal cracks.

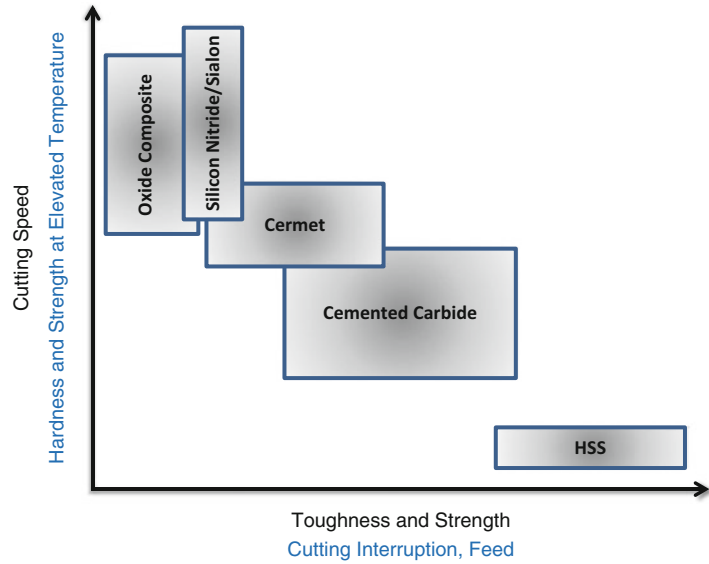
Case Studies

Following are a couple of case studies done in the field. Results from similar tests may vary depending on tool materials, geometry, cutting conditions, etc.

Case Study I

Challenge: Improve tool life of silicon nitride inserts machining ductile cast iron

Ceramic Cutting Tools,
Fig. 17 Choice of cutting tool materials for various types of machining jobs



Ceramic Cutting Tools, Table 3 Speed recommendation for ceramic tools in turning

Workpiece material	Speed (m/min)
Gray cast iron	500–1200
Ductile cast iron	150–500
High T alloy	120–300
Hard steel	60–180

Material	Uncoated Si ₃ N ₄	Coated Si ₃ N ₄
Coolant	Dry	Dry
Pieces/edge	5.00	12.00
Tool life/edge	4.90	11.77
Primary failure mode	Flank wear	Flank wear

Tool materials: Low additive silicon nitride and same silicon nitride coated with multilayer CVD (alumina-TiCN/TiN)
 Insert geometry: CNGA
 Workpiece: Ductile cast iron with BHN 180–230, with casting scale on surface
 Operation type: External face turning, heavily interrupted
 Machine: Rigid lathe

Case Study II

Challenge: Improve productivity in turning Inconel 718
 Tool materials: SiC whisker-reinforced alumina and CVD-coated α -/ β -Sialon
 Insert geometry: RPG45
 Workpiece: Inconel 718
 Operation type: External facing, continuous
 Machine: Rigid lathe

Results

Material	Uncoated Si ₃ N ₄	Coated Si ₃ N ₄
Speed	167 m/min	167 m/min
Rpm	1146	1146
Feed	0.2032 mm	0.2032 mm
Depth of cut	1.27 mm	1.27 mm
Length	228.3460 mm	228.3460 mm
No of passes	1	1

(continued)

Results

Tool material	SiC _w -alumina	Coated Sialon
Speed	230 m/min	230 m/min
Rpm	1146	1146
Feed	0.23 mm	0.23 mm
Depth of cut	1.5 mm	1.5 mm
Length	76.2 mm	76.2 mm
Coolant	Wet	Wet

(continued)

Tool material	SiC _w -alumina	Coated Sialon
Pieces/edge	1	1
Tool life/edge	3 min	43 min
Primary failure mode	Flank wear	Flank wear

Cross-References

- ▶ [Cutting Edge Geometry](#)
- ▶ [Cutting, Fundamentals](#)
- ▶ [Cutting Temperature](#)
- ▶ [Coated Tools](#)

References

- Becher et al (1998) Microstructural design of silicon nitride with improved fracture toughness: I, effects of grain shape and size. *Am Ceram Soc* 81(11):2821–2830
- Becher et al (2006) Influence of additives on anisotropic grain growth in silicon nitride ceramics. *Mater Sci Eng A* 422:85–91
- Belcher et al (1988) Toughening behavior in whisker-reinforced ceramic matrix composites. *J Am Ceram Soc* 71:1050–1061
- Belmonte et al (2010) Spark plasma sintering: a powerful tool to develop new silicon nitride-based materials. *J Eur Ceram Soc* 30(14):2937–2946
- Blugan et al (2005) Fractography, mechanical properties, and microstructure of commercial silicon nitride–titanium nitride composites. *J Am Ceram Soc* 88(4):926–933
- Bradley et al (1989) Silicon carbide whisker stability during processing of silicon nitride matrix composites. *J Am Ceram Soc* 12:628–636
- Carman et al (2009) Grain boundary evolution in sm- and nd-sialons during post-sintering heat treatment. *J Aus Ceram Soc* 45(1):27–34
- Casto et al (1996) Machining of steel with advanced ceramic cutting tools. *Key Eng Mater* 114:105–134
- Chen et al (2003) Development of tough alpha sialon. *Key Eng Mater* 237:65–78
- Chockalingam S et al (2009) Phase transformation and densification behavior of microwave sintered Si₃N₄–Y₂O₃–MgO–ZrO₂ system. *Int J Appl Ceram Technol* 6(1):102–110
- Feng et al (2003) Effect of amount of additives and post-heat treatment on the microstructure and mechanical properties of yttrium- α -sialon ceramics. *J Am Ceram Soc* 86(12):2136–2142
- Feng et al (2006) Microstructures of microwave-sintered silicon nitride with zirconia as secondary particulates. *J Am Ceram Soc* 89(12):3770–3777
- Garnier et al (2005) Influence of sic whisker morphology and nature of sic/al₂o₃ interface on thermomechanical properties of sic reinforced Al₂O₃ composites. *J Eur Ceram Soc* 25:3485–3493
- Hoffman MJ, Holzer S (2003) Processing and microstructural evolution of rare earth containing sialons. *Key Eng Mater* 237:141–148
- Huang et al (2012) Effect of Y- α -Sialon seeding and holding time on the formation of elongated (Ca, Dy)- α -Sialon crystals prepared via carbothermal reduction and nitridation. *J Am Ceram Soc* 95(9):2777–2781
- Hutchison JW (1989) Theoretical and applied mechanics. In: Germain P, Piau M, Caillerie D (eds). Elsevier, p 139
- Ighodaro et al (2008) Fracture toughness enhancement for alumina systems: a review. *J Appl Ceram Technol* 5(3):313–323
- Jianxin et al (2005) Self-lubricating behaviors of al₂o₃/tib₂ ceramic tools in dry high-speed machining of hardened steel. *J Eur Ceram Soc* 25:1073–1079
- Kamanduri R, Samanta SK (1989) ASM handbook, vol 16. ASM International, Materials Park, pp 98–104
- Kitayama et al (2001) Thermal conductivity of β -Si₃N₄: III, effect of rare-earth (RE 5 La, Nd, Gd, Y, Yb, and Sc) oxide additives. *J Am Ceram Soc* 84(2):353–358
- Kleebe et al (1999) Microstructure and fracture toughness of Si₃N₄ ceramics. *J Am Ceram Soc* 82(7):1857–1867
- Kodama et al (1990) Toughening of silicon nitride matrix composites by the addition of both silicon carbide whiskers and silicon carbide particles. *J Am Ceram Soc* 73(3):78–83
- Krishnamurthy S, Sivashankaran V (1994) Machining of cast iron with advanced ceramic tools. *Key Eng Mater* 96:221–0
- Liu et al (2008) Effect of different rare-earth on microstructure and properties of α -sialon ceramics. *J Mater Sci Technol* 24(6):878–882
- Mandal H (1999) Preparation of multiple-cation α -sialon ceramics containing lanthanum. *J Am Ceram Soc* 82(1):229–232
- Markys et al (1993) Microstructure and fracture toughness of hot pressed zirconia toughened sialon. *J Am Ceram Soc* 76(6):1401–1408
- Nishimura et al (1995) Fabrication of silicon nitride nanoceramics by spark plasma sintering. *J Mater Sci Lett* 14(15):1046–1047
- North B (1987) Ceramic cutting tools, a review. *Int J High Technol Ceram* 3:113–127
- Osayande L et al (2008) Fracture toughness enhancement for alumina systems: a review. *Int J Appl Ceram Technol* 5(3):313–323
- Park et al (1998) Extra-large grains in the silicon nitride ceramics doped with yttria and hafnia. *J Am Ceram Soc* 81(7):1876–1880
- Pettersson P, Johnsson M (2003) Thermal shock properties of alumina reinforced with Ti(C,N) whiskers. *J Eur Ceram Soc* 23:309–313
- Sajgalik et al (2006) In situ preparation of Si₃N₄/SiC nanocomposites for cutting tools application. *Int J Appl Ceram Technol* 3(1):41–46

- Santos et al (2008) High temperature properties of silicon nitride with neodymium oxide additions. *Mater Sci Forum* 591–593:560–564
- Satet et al (2005) Influence of the rare-earth element on the mechanical properties of RE–Mg-Bearing Silicon Nitride. *J Am Ceram Soc* 88(9):2485–2490
- Wang et al (1996) Grain boundary films in rare earth glass based silicon nitride. *J Am Ceram Soc* 79(3):788–792
- Ye et al (2003) Effect of amount of additives and post-heat treatment on the microstructure and mechanical properties of yttrium- α -sialon ceramics, *J Am Ceram Soc* 86(12):2136–2142
- Ye et al (2004) Microstructural development of Y-A/(B)-sialons after post heat-treatment and its effect on mechanical properties. *Ceram Int* 30:229–238
- Yin et al (2013) Preparation and characterization of Al₂O₃/Tic micro-nano-composite ceramic tool materials. *Ceram Int* 39:4253–4262

Ceramic Machining Tool

- ▶ [Ceramic Cutting Tools](#)

Ceramic/Metal Mixture

- ▶ [Cermets](#)

Ceramic-and-Metal Composite

- ▶ [Cermets](#)

Ceramic-Metal Bond

- ▶ [Cermets](#)

Ceramics

- ▶ [Cutting of Inconel and Nickel Base Materials](#)

Cermets

Toshiyuki Enomoto
Department of Engineering, Osaka University,
Osaka, Japan

Synonyms

[Ceramic/metal mixture](#); [Ceramic-and-metal composite](#); [Ceramic-metal bond](#)

Definition

A cermet is a composite material composed of ceramic particles including titanium carbide (TiC), titanium nitride (TiN), and titanium carbonitride (TiCN) bonded with metal. The name “cermet” combines the words ceramic (cer) and metal (met). They are most successfully used for finishing and light roughing applications.

Theory and Application

History

During the 1950s, cutting tool manufacturers began to develop a new TiC/nickel alloy cermet that contained molybdenum and carbon. Although the cutting tool material was able to perform well at high speed and high temperature, the lack of toughness restricted the applications to light finishing cuts with light feed rate. In addition, machinists inevitably compared the cermet tools to the tougher tungsten-carbide tools that were available then, and they saw that tungsten carbide performs satisfactorily for use in rough cutting or interrupted cutting applications.

On the other hand, Japanese tool manufacturers such as Sumitomo, Mitsubishi, and Toshiba saw cermet had important advantages as a cutting tool material because of its strength at high temperature and began to sell cermet inserts in the 1960s. Such acceptance of cermet

cutting tools spurred manufacturers to develop cermet inserts with improved toughness with the addition of tungsten carbide (WC) and tantalum carbide (TaC). The additional elements were not able to make a cermet as tough as traditional tungsten carbide, however, and so the use of cermet inserts remained limited to light finishing applications.

Other advances in cermet properties came in the 1970s, Japanese producers found that a cermet with a considerably finer microstructure could be created with the addition of titanium nitride (TiN). This modification significantly improved its oxidation resistance and high-temperature strength.

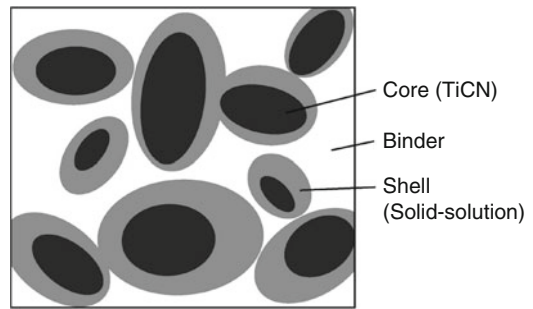
These improvements enable cermet tools to offer various advantages and spread into a broad range of applications, and cermet manufacturers are still actively pursuing further evolution. Moreover, a cermet is expected to serve as an alternative to tungsten carbide out of concern for the steady supply of tungsten.

Characteristic Properties of Cermets

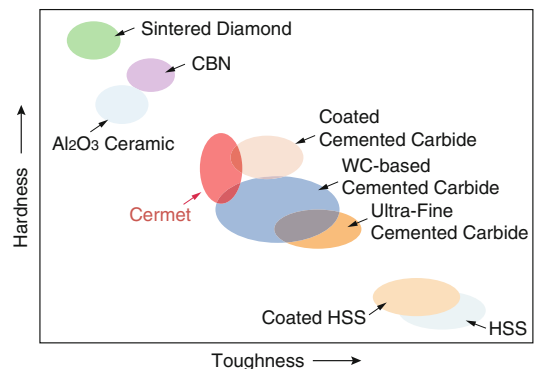
Typical cermet material is generally composed of titanium carbide (TiC), titanium nitride (TiN), titanium carbonitride (TiCN), tantalum (Ta), nickel (Ni), cobalt (Co), tungsten carbide (WC), molybdenum (Mo), and vanadium (V) (Byrne et al. 2003).

The technology for producing cermets corresponds closely to that of conventional WC-based cemented carbides. Cermets are produced by sintering the hard particles mixed with powders for the binder phase. Figure 1 shows schematic diagram of structure of the sintered TiCN-based cermet. As can be seen in the diagram, the microstructure of cermets features structured grains of a hard phase embedded in a binder phase, often with a core-rim structure. The black core is rich in titanium carbonitride (TiCN) and is covered by a shell composed of carbonitride solid solutions including Ti, W, and Nb, with a binder phase composed of Ni and/or Co.

Figure 2 compares the hardness and toughness of TiCN-based cermet to other cutting tool



Cermets, Fig. 1 Microstructure of TiCN-based cermet



Cermets, Fig. 2 Relationship between toughness and hardness of various cutting tool materials

materials. It is found from its position near the center of group of materials that cermet offers a balance between hardness and toughness; it is harder than WC-based cemented carbide and HSS cutting tool and tougher than diamond and ceramic tools.

In order to meet requirements of the cutting task, the physical and mechanical properties of cermets should be adjusted by considering the relationship between the composition and its properties as follows:

TiCN

- Increasing hardness
- Increasing high resistance to diffusion and adhesive wear

TaC/NbC

- Increasing hot hardness and thermal shock resistance
- Increasing the resistance against plastic deformation

Mo_xC

- Increasing the volume of the shell
- Decreasing the volume of the binder
- Increasing wettability of the carbides and carbonitrides
- Increasing toughness

WC

- Increasing wettability between the binder and the core
- Working as a binder element between TaC/NbC and TiC

VC

- Increasing the shearing strength of the TiC by creating a mixed crystal of TiC-VC
- Increasing fatigue strength

Ni/Co

- Creating a binder in a solid solution
- Increasing the resistance against plastic deformation

In addition, the Ni/Co ratio (weight ratio of Ni/(Ni + Co)) also affects the mechanical properties of cermets. With increasing cobalt content, the hardness increases slightly, while fracture toughness values tend to decrease (see Fig. 3). When both Ni and Co are added as the binder phase, the ratio is preferably within 0.3–0.8 considering the miscibility or affinity with a hard phase (Zhang 1993).

Through above-mentioned knowledge, a few rules of thumb for cutting application have been developed. For example, cermets usually have high TiC contents with modest TiN additions and low binder contents in the case that abrasion and wear resistances are required; for milling applications that requires high thermal and shock-stress levels, the compositions feature higher binder contents as well as higher nitrogen and Ta/Nb levels in the hard phase (Ettmayer et al. 1995).

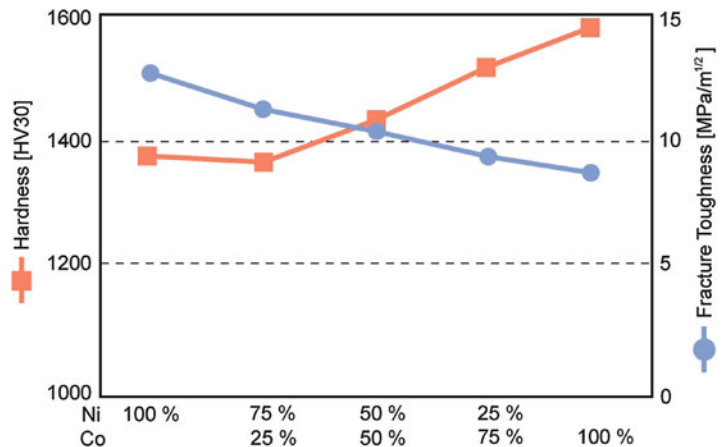
Key Applications

Users must understand that cermets are not general-purpose cutting tool, although cermet manufacturers have greatly improved their properties, which has enabled them to be used for interrupted cutting. However, cermets show excellent performances in particular applications as below

High-Speed Machining

All of cermet’s characteristics have led to a cutting tool that is ideal for users who want to realize

Cermets, Fig. 3 Hardness and toughness of cermet cutting tools versus binder composition



high-speed machining (Schulz and Moriwaki 1992). When the cutting speed is increased, the temperature at the cutting edge of cutting tool increases; the friction between the cutting tool surface and workpiece can raise the temperature at the cutting edge to more than 1,000 °C. For such applications, WC-based cemented carbide cutting tools provide insufficient cutting performances because such heat can quickly degrade their mechanical properties. However, high temperatures have less effect on a cermet's hardness, transverse rupture strength, and oxidation resistance.

It is reported that, for instance, commercial cermet insert (ISO IC-30) showed a great advantage of lower wear than conventional WC-based cemented carbide insert (ISO K-25) with TiCN coating in the cutting of chromium molybdenum steel (AISI 4140) for the speed range up to 250 m/min, while both tools were almost identical in their performance at lower cutting speed (Porat and Ber 1990).

Finishing Machining

The cermet inserts can be used to produce mirror-like finishes that can replace an additional grinding process in the cutting of steel and cast iron, due to their unique properties such as high wear resistance, resistance to high-temperature

oxidation, and a low rate of interaction with iron-based materials (Weinert et al. 2004).

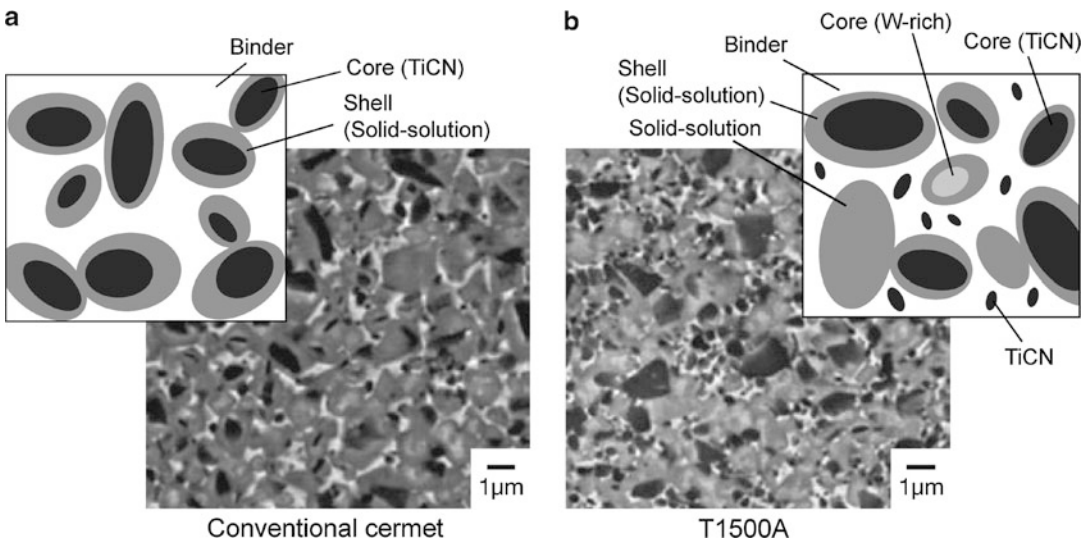
There oxidation resistance reduces notching at the cutting edge in finishing application, leading to minimized damage to the workpiece surface. Moreover, cermets are also able to resist built-up edge with iron-based material cutting, because of their low affinity with such materials, compared to the WC-based cemented carbide cutting tools. In finishing operation, this enables close tolerances and results in shiny finished surfaces.

Near-Net-Shape Manufacturing

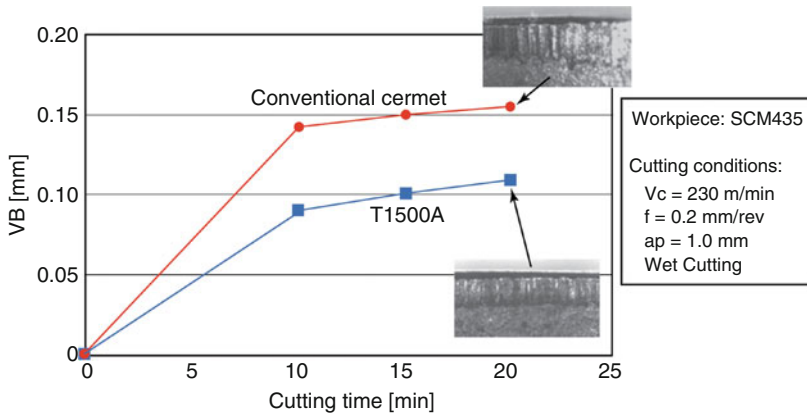
Light depth of cut applications with close tolerance requirements, such as near-net-shape parts, are well suited for cermets because of their unique performance characteristics. Technological advances in the forging and casting industries permit production of raw products that require minimal material removal during machining operation. Near-net-shape manufacturing can benefit from the capabilities including longer tool life and higher-machining speeds of cermet cutting tools.

Outlook of the Cermet Development

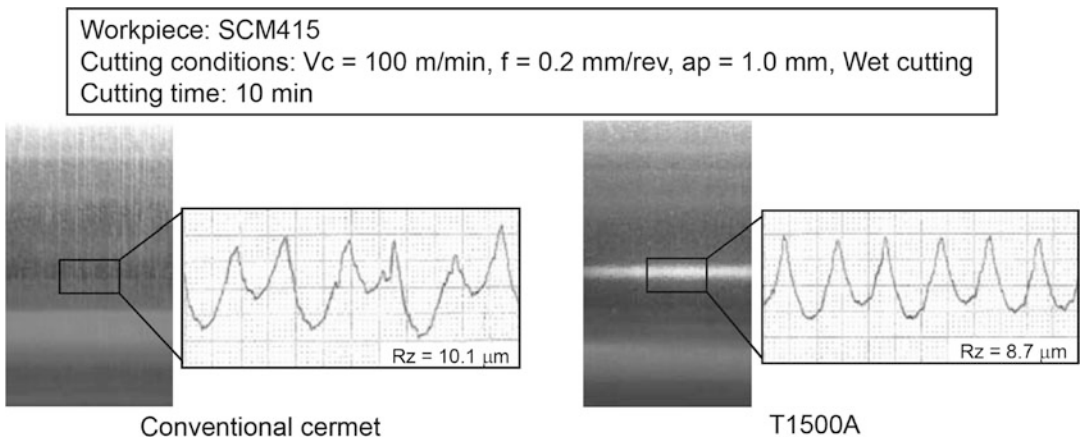
Cermet tool manufacturers continue to modify the structure and components of cermet materials, in order to enhance their merits and eliminate their weakness.



Cermets, Fig. 4 Structure of conventional cermet and T1500A



Cermets, Fig. 5 Wear resistance of T1500A



Cermets, Fig. 6 Finished surface roughness

A good example of recent advances is a new cermet “T1500A” developed by Sumitomo Electric Hardmetal Corporation (Hirose et al. 2011). T1500A was developed for steel turning tool, which has been improved in stability of finishing and the balance wear resistance and toughness while utilizing the characteristics of the cermet materials.

T1500A is characterized by its structure with the following four types of hard phase with different particle size and compositions: (a) core-rim structure with TiCN core, as observed in the conventional cermet, (b) fine TiCN particle, (c) solid solution carbonitride, and (d) core-rim structure with W-rich core (see Fig. 4).

In the conventional cermet, the binder phase region composed of Co and Ni existing around hard phases is obvious and thick in some regions. On the other hand, there is no region with a thick binder phase in T1500A, because (b) fine TiCN particles are scattered in the binder phase, which enable the material to have higher wear resistance and as well as higher toughness, owing to the suppression of cracks. In addition, (c) solid solution phase and (d) core-rim structure with W-rich core phase further improve the toughness. As a result, T1500A achieves longer tool life and excellent finished surface quality (see Figs. 5 and 6).

Cermet tools account for 15–20% of all materials used for the tools, and it is expected that this

ratio will remain unchanged in the future; cermet tools that can realize high-quality finishing and high-speed turning will hold a leading position among the turning tools. These advances would enable cermets to cover a wide range of metal cutting applications and increase their market penetration.

Cross-References

- ▶ [Ceramic Cutting Tools](#)
- ▶ [Composite Materials](#)
- ▶ [Cutting, Fundamentals](#)
- ▶ [High Speed Cutting](#)

References

- Byrne G, Dornfeld D, Denkena B (2003) Advanced cutting technology. *CIRP Ann* 52(2):483–507
- Ettmayer P, Kolaska H, Lengauer W, Dreyer K (1995) Ti (C, N) cermets: metallurgy and properties. *Int J Refract Met Hard Mater* 13:343–351
- Hirose K, Tsuda K, Fukuyasu Y, Sakamoto A, Yonekura H, Nishi K, Yamagata K, Moriguchi H (2011) Development of cermet “T1500A” for steel turning. *SEI Tech Rev* 72:107–111
- Porat R, Ber A (1990) New approach of cutting tool materials: CERMET (Titanium carbonitride-based material) for machining steels. *Ann CIRP* 39(1):71–75
- Schulz H, Moriwaki T (1992) High-speed machining. *CIRP Ann* 41(2):511–537
- Weinert K, Inasaki I, Sutherland JW, Wakabayashi T (2004) Dry machining and minimum quantity lubrication. *CIRP Ann* 53(2):511–537
- Zhang S (1993) Titanium carbonitride-based cermet: processes and properties. *Mater Sci Eng A* 163:141–148

Chamfer

- ▶ [Cutting Edge Geometry](#)

Change of Elemental and Functional Characteristics of the Surface

- ▶ [Corrosion](#)

Changeable Manufacturing

Hoda A. ElMaraghy^{1,2} and Hans-Peter Wiendahl³

¹Intelligent Manufacturing Systems Center, University of Windsor, Windsor, ON, Canada

²Canada Research Chair in Manufacturing Systems, Intelligent Manufacturing Systems Centre, University of Windsor, Windsor, ON, Canada

³Institut für Fabrikanlagen und Logistik, University of Hannover, Hannover, Germany

Synonyms

[Adaptable manufacturing/production](#); [Adjustable manufacturing/production](#)

Definition

Changeable manufacturing is defined as the ability of a manufacturing system to economically accomplish early and foresighted adjustments of the factory’s structures and processes on all levels in response to change impulses. It is closely related to “flexible” and “reconfigurable” manufacturing which apply to the manufacturing equipment and systems on the shop floor respectively – the difference being the level, degree, and scope of change.

Theory and Application

History

In the past, a steady production volume increase is observed after releasing a new product and followed by long stable production phases and finally a slow ramp down. Nowadays, production volume climbs much faster to the first peak then drops; it reaches a second peak after promotion activities and often a product face lift in subsequent releases.

Furthermore, the product life cycle was usually within the range of the life cycle of the technological processes and production machines. With decreasing market life of the products and fast changing technologies, the equipment is now expected to produce more than one product generation. The factory buildings have to be

adaptable to these product changes and the plant site must also follow new requirements regarding logistics and lean supply chains, etc.

In addition, increasing outsourcing, manufacturing at different sites, and the multi-cooperation in networks increase the complexity of the production processes particularly as the operation of global supply becomes reality for more and more manufacturing companies. The reliable delivery of customized products nowadays has the highest priority in globally distributed markets.

Therefore, the ability of production processes, resources, structures, and layouts as well as their logistical and organizational concepts to adapt quickly and with minimum effort is a prerequisite for success in local and global production networks. This “ability” is necessary to cope with the continuous change and the turbulence surrounding production companies and is described as “changeability.”

Theory

Objects of Changeability

It is important to define the objects, which have to be changeable and the appropriate degree of changeability. Figure 1 summarizes the main influential factors (see also, ElMaraghy 2005; Dashchenko 2006).

The impulse for a change is triggered by *change drivers*, whose first category is the demand volatility measured by volume

fluctuation over time. Variety is the span width of the product variants. A major change driver is introducing a new business strategy such as the decision to enter a new market, to sell or buy a product line, or to start a turnaround program.

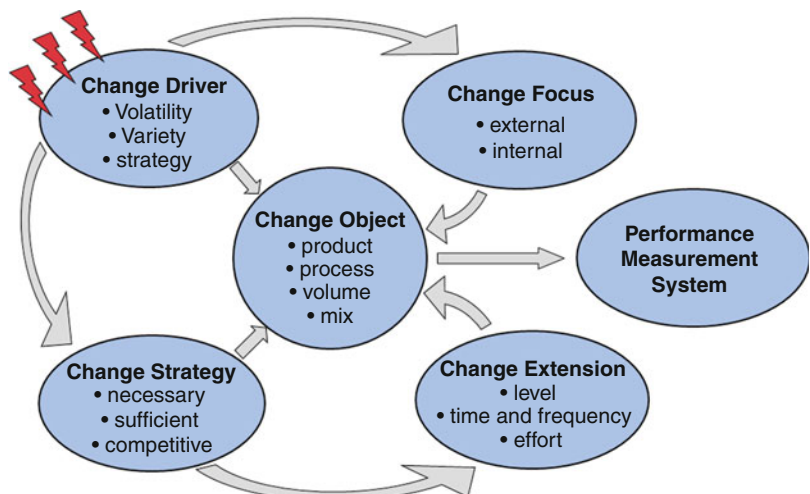
The *change focus* can be external or internal. The external focus targets the added customer’s value for instance by offering a product with lower life cycle cost or faster delivery. The internal focus is typically addressed if the performance of the firm is not satisfactory mainly with respect to profit loss caused by badly organized business processes.

A *change strategy* should be devised on the operational, tactical, and/or strategic levels as appropriate. Operational change strategies are more defensive in nature to target immediate needs. They are typically performed within existing production structures and procedures such as installing or replacing machinery. Tactical change strategies are aimed to fulfill needs in the foreseeable future. These change strategies are more proactive and occur typically in business processes such as order fulfillment or service. Strategic change strategies involve investments in changeability enablers to be prepared for a future optional position.

Obviously the selected change potential determines very much the *change extent*. First, the level of the factory on which the changeability has to be ensured must be determined. The levels are station, cell/segment, sector, factory, and network (s. Sect. C). Secondly, the expected change

Changeable Manufacturing,

Fig. 1 Factors affecting the change objects



frequency and the time allowed for each change has to be estimated. Thirdly, the necessary effort in equipment, manpower, knowledge, and time are determined as the cost of a change. Typically changeability beyond the immediate necessity requires additional investment. Therefore, there is always a trade-off between the effort and cost of achieving the desired level of changeability and the expected benefits.

The change object(s) can be a product or product family both of which can change with respect to type, volume or mix, technological or logistical processes, the part of the manufacturing facilities, or the firm organization to be affected.

Finally a *performance measurement system* has to be installed in order to measure the impact of the implemented changeability on the factory output performance. Typical performance indicators are delivery time, due date performance, turnaround rate, inventory, days of supply, and overhead cost.

Changeability Classes

If the five levels of a factory are combined with the associated product levels, a hierarchy emerges that allows the definition of five types of changeability (Wiendahl and Hernández 2001; ElMaraghy 2009a, Chapter 2) as shown in Fig. 3.

The hierarchy of product levels starts from the top with the product portfolio a company offers to the market. Then the product or a product family

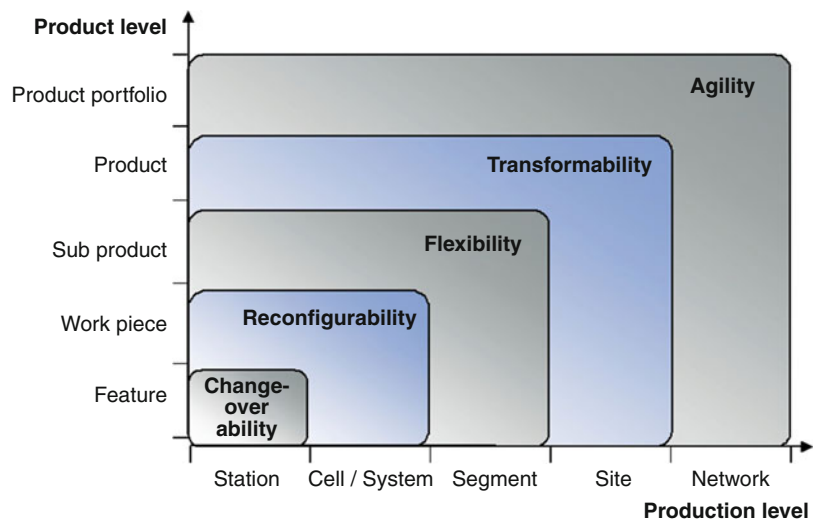
follows downwards. The product is usually structured into subproducts or assembly groups that contain workpieces. The workpieces themselves consist of features.

The hierarchy of a factory starts with a station, which is performing a manufacturing task with the result of one or more features of a workpiece. One or more stations form a cell or manufacturing system to produce complete workpieces. On the next level not only machines and workplaces but also storage and transportation devices are arranged in a layout to form a section. Sectors produce subproducts like assemblies or subassemblies, which fulfill subfunctions of a product. The site (or factory) delivers whole products and includes not only the manufacturing and assembly equipment but also the buildings with their technical infrastructure. At the highest level the production network supplies a product portfolio from different locations to various markets.

Five classes of changeability evolve from this matrix where any changeability type at a higher level subsumes those below it (Wiendahl and Heger 2004) (Fig. 2).

- Changeover ability is the operative ability of a single machine or work station to perform particular operations on a known workpiece or subassembly at any desired time with minimal effort and delay.

Changeable Manufacturing,
Fig. 2 Classes of factory changeability



- Reconfigurability is the operative ability of a manufacturing or assembly system to switch with minimal effort and delay to a particular family of workpieces or subassemblies through the addition or removal of functional elements.
- Flexibility refers to the tactical ability of an entire production and logistics area to switch within reasonably little time and effort to new, albeit similar, families of components by changing manufacturing processes, material flows, and logistical functions.
- Transformability indicates the tactical ability of an entire factory structure to switch to another product family. This calls for structural intervention in the production and logistics systems, the structure and facilities of the buildings, the organization structure and process, as well as in personnel.
- Agility means the strategic ability of an entire company to open up new markets, to develop the requisite products and services, and to build up necessary manufacturing capacity.

In the context of this definition, the changeover ability needs no special attention for changeable manufacturing since this aspect is an ongoing concern of machine tool and assembly systems design. Agility is beyond the factory level and is treated as a strategic setting for the design of a

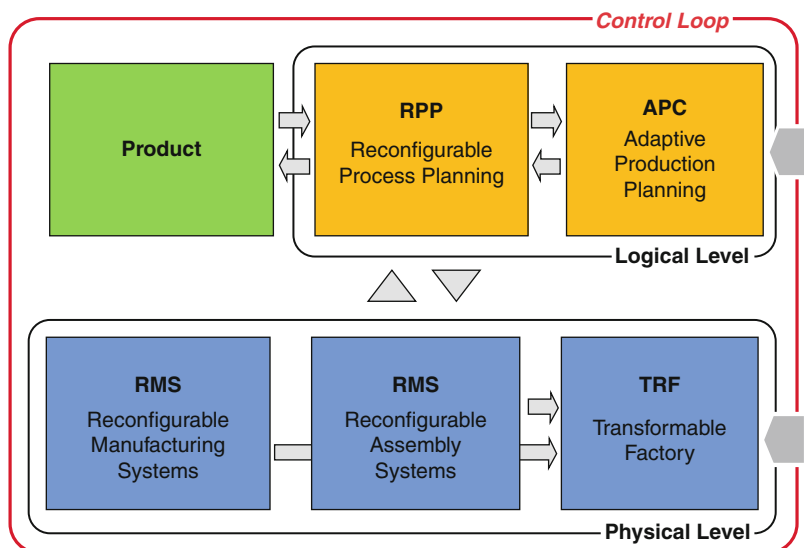
changeable factory. Different types of flexibility have been defined and are relevant to the various levels in the changeability in Fig. 2 (ElMaraghy 2005; Chryssolouris 2006).

Scope of Changeable Manufacturing

Changeability serves as an umbrella concept applicable to all levels of manufacturing (Wiendahl et al. 2007). Figure 3 depicts the constituents of such a changeable manufacturing and their specific properties. Product design may be influenced by the requirements of the physical and logical manufacturing changeability level.

On the physical level, the manufacturing and assembly systems have to be reconfigurable (RMS and RAS), and the factory with its technical infrastructure including building should be transformable (TRF). The logical level is necessary to operate a factory and calls for process planning systems able to react to changes in the product design or manufacturing resources from the physical level and is therefore called reconfigurable process planning (RPP) (ElMaraghy 2007). The production planning and control has to react to changes in product volume, mix or reconfigured process plans. Therefore, it is called adaptive production planning and control (APC). A specific additional component is a control loop to monitor external or internal change drivers and to trigger

Changeable Manufacturing,
Fig. 3 Scope of changeable manufacturing



change activities either on the physical or the logical level. Finally an evaluation procedure is necessary to justify additional expenses due to the changeability of the physical and logical objects.

Physical Changeability Enablers

A factory that is designed to be changeable must have certain inherent features or properties called changeability enablers. They enable the physical and logical objects of a factory to change their capability towards a predefined objective within a predefined time and are not to be confused with the flexibility types or its objectives. Figure 4 provides an overview of the enablers of the physical and logical subsystems of changeable manufacturing.

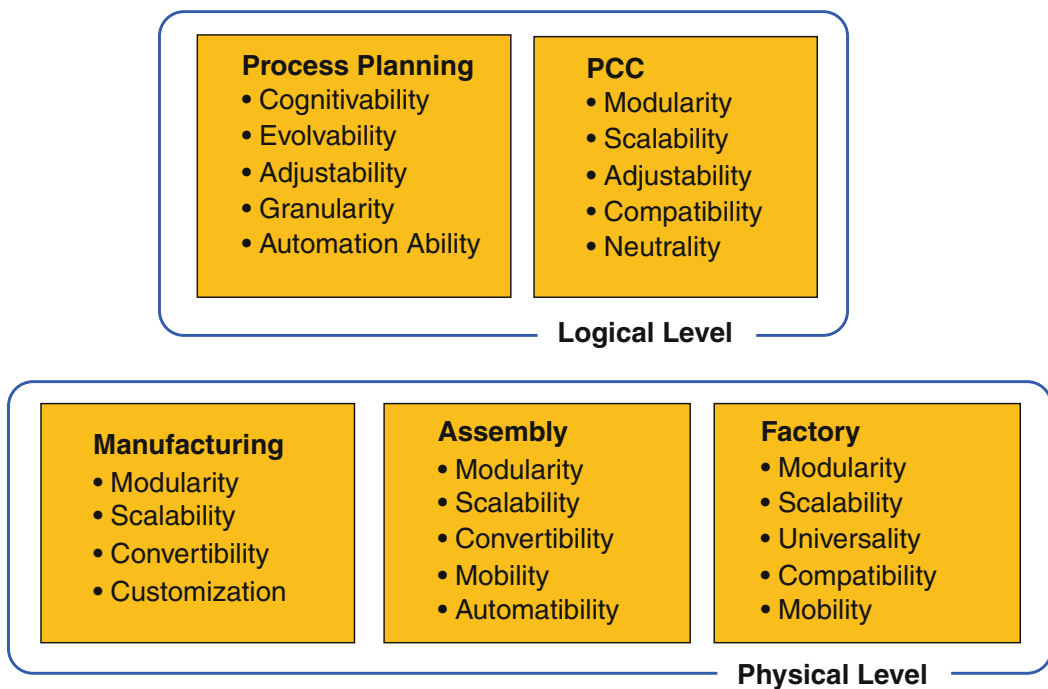
Manufacturing Level

On this level reconfigurable manufacturing systems are assumed to be the appropriate answer to changeability. Koren states that in order to achieve exact flexibility in response to fluctuation in demands, an RMS must be designed considering certain qualitative and quantitative properties, the so-called key RMS characteristics:

modularity, integrability, customization, scalability, convertibility, and diagnosability (Koren 2005; ElMaraghy 2007). They can be interpreted as enablers of reconfigurability. These characteristics can be divided into essential and supporting RMS characteristics. Therefore, customization, scalability, and convertibility are seen as essential RMS characteristics, while modularity, integrability, and diagnosability constitute supporting RMS characteristics.

Assembly Level

On the assembly level mainly the same enablers for reconfigurable manufacturing systems are applicable. Two specific enablers should be added. The first is mobility, which is important to reconfigure single stations or modules of an assembly system or even to move these modules or the whole system to another location. The second is the ability to upgrade or downgrade the degree of automation. For assembly operations, in contrast to machining operations, assembly can be performed manually, automatically, or in a hybrid combination depending on various factors like production rate



Changeable Manufacturing, Fig. 4 Enablers of changeable manufacturing

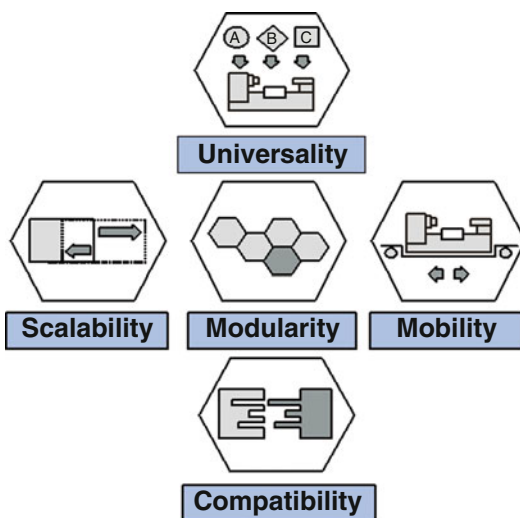
and wages level. Hence, automatability allows for adapting the ratio of manual and automated work content in an assembly system.

Factory Level

On the factory level the change of objects itself can mainly take place through five transformation enablers which contribute to the fulfillment of a transformation process. Furthermore, the enablers characterize the potential of the ability to transform and become active only when needed. The characteristics of an enabler influence positively or negatively the ability of a factory to adapt. Figure 5 illustrates the main five enablers that may be used for purposes of attaining changeability by design.

Universality represents the characteristic of factory objects to be dimensioned and designed to be capable of carrying out diverse tasks, demands, purposes, and functions. This enabler stipulates an over-dimensioning of objects to guarantee independence of function and use.

Scalability provides technical, spatial, and personnel extensibility. In particular this enabler provides for spatial degrees of freedom, regarding expansion, growth, and shrinkage of the factory layout.



Changeable Manufacturing, Fig. 5 Enablers of factory changeability

Modularity follows the idea of standardized, pre-tested units and elements with standardized interfaces and also concerns the technical facilities of the factory (e.g., buildings, production facilities, and information systems) as well as the organizational structures (e.g., segments or function units). Modules are autonomously working units or elements that ensure a high interchangeability with little cost or effort (i.e., plug and produce modules).

Mobility ensures the unimpeded mobility of objects in a factory. It abolishes the classical division between immobile and mobile objects and covers all production and auxiliary facilities including buildings and building elements, which can be placed, as required, in different locations with the least effort.

Compatibility allows various interactions within and outside the factory. It especially concerns all kinds of supply systems for production facilities, materials, and media. It also facilitates diverse materials, information, and personal relationships. Besides the ability to detach and to integrate facilitates, this enabler allows incorporating or disconnecting products, product groups and workpieces, components, manufacturing processes, or production facilities in existing production structures and processes with little effort, by using uniform interfaces.

Logical Changeability Enablers

Process Planning Level

As shown in Fig. 4, there are certain key logical enablers for achieving and supporting changeability including (1) reconfigurable process plans and (2) reconfigurable production plans and commensurate techniques for their efficient regeneration when needed. Enablers of reconfigurable process plans are:

Cognitability: the ability to recognize the need for and initiate reconfiguration when prerequisite conditions exist.

Evolvability: the ability to utilize the multi-directional relationships and associations

between the product features, process plan elements, and all manufacturing system modules capable of producing them.

Adjustability: the ability and representation characteristics that allow implementing optimally determined feasible and economical alterations in process plans to reflect the needed reconfiguration.

Granularity: the ability to model process plans at varying levels of detail to readily and appropriately respond to changes at different levels (e.g., in products, processes, technologies, and systems).

Automation ability: the availability of complete knowledge bases and rules for process planning reconfiguration, accurate mathematical models of the various manufacturing process at macro- and microlevels, as well as meta-knowledge rules for using this knowledge.

Production Planning and Control Level

There are five enablers of PPC changeability (Fig. 4):

Modularity: workable functions and methods or clearly defined objects, e.g., “plug and produce” modules, exist.

Scalability: applicability is independent of product, process, and customer and supplier relationship complexity.

Adjustability: design for different demands of the functional logic of order processing, e.g., order generation or release algorithm, and/or weight of the PPC targets.

Compatibility: networkability regarding object, method, and process, e.g., different IT tools use the same object “resource” to plan maintenance and production.

Neutrality: design of the workflow of order processing for different requirements making the definition of the process status independent of the structural and process organization and the enterprise size.

With these basic definitions the implementation of changeability on the various levels of a factory can be started. Implementation examples can be found in Wiendahl et al. (2007) and ElMaraghy (2009b).

Cross-References

- ▶ [Factory](#)
- ▶ [Flexible Manufacturing System](#)
- ▶ [Machine Tool](#)
- ▶ [Manufacturing](#)
- ▶ [Manufacturing System](#)
- ▶ [Production](#)
- ▶ [System](#)

References

- Chryssolouris G (2006) Manufacturing systems: theory and practice, 2nd edn. Springer, New York
- Dashchenko O (2006) Analysis of modern factory structures and their transformability. In: Dashchenko AI (ed) Reconfigurable manufacturing systems and transformable factories. Springer, Berlin/Heidelberg, pp 395–422
- ElMaraghy HA (2005) Flexible and reconfigurable manufacturing systems paradigms. *Int J Flex Manuf Syst* 17(4):261–276 (Special issue: Reconfigurable manufacturing systems)
- ElMaraghy HA (2007) Reconfigurable process plans for responsive manufacturing systems. In: Cunha PF, Maropoulos PG (eds) Digital enterprise technology: perspectives & future challenges. Springer Science, Berlin, pp 35–44
- ElMaraghy H (2009) Chapter 2: Changing and evolving products and systems – models and enablers. In: ElMaraghy HA (ed) Changeable and reconfigurable manufacturing systems. Springer, London, pp 25–45
- ElMaraghy HA (ed & contributor) (2009b) Changeable and reconfigurable manufacturing systems. Springer, London
- ElMaraghy HA, Wiendahl H-P (2009) Chapter 1: Changeability—an introduction. In: ElMaraghy HA (ed) Changeable and reconfigurable manufacturing systems. Springer, London, pp 3–23
- Koren Y (2005) Reconfigurable manufacturing and beyond (Keynote paper). In: Proceedings of the CIRP 3rd international conference on reconfigurable manufacturing, Ann Arbor, Michigan, 11–12 May 2005, pp 1–6
- Wiendahl H-P, Heger CL (2004) Changeability of factories – a prerequisite for global competitiveness. In: 37th CIRP international seminar on manufacturing systems, Budapest, 19–21 May 2004
- Wiendahl H-P, Hernández R (2001) The transformable factory – strategies, methods and examples. In: 1st international conference on agile, reconfigurable manufacturing, Ann Arbor, 20–21 May 2001
- Wiendahl H-P, ElMaraghy HA, Nyhuis P, Zäh MF, Wiendahl H-H, Duffie N, Brieke M (2007) Changeable manufacturing – classification, design and operation. Keynote paper. *Ann CIRP* 56(2):783–809

Wiendahl H-P, Reichardt J, Nyhuis P (2009) Handbuch Fabrikplanung: Konzept, Gestaltung und Umsetzung wandlungsfähiger Produktionsstätten [Handbook factory planning: concept, design and realization of changeable production sites] Hanser München (in German)

Changeable Manufacturing System

► [Reconfigurable Manufacturing System](#)

Charge

► [Cost](#)

Chatter

Erhan Budak
Manufacturing Research Laboratory, Faculty of Engineering and Natural Sciences, Sabanci University, Istanbul, Turkey

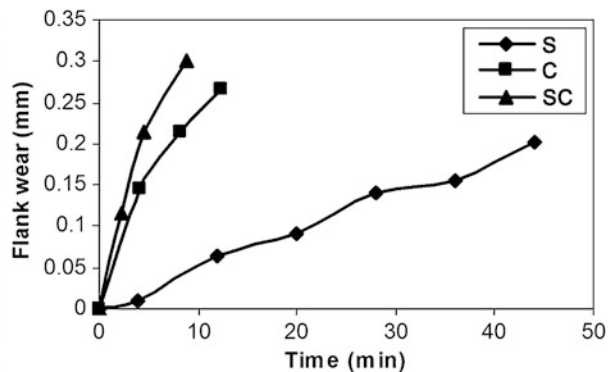
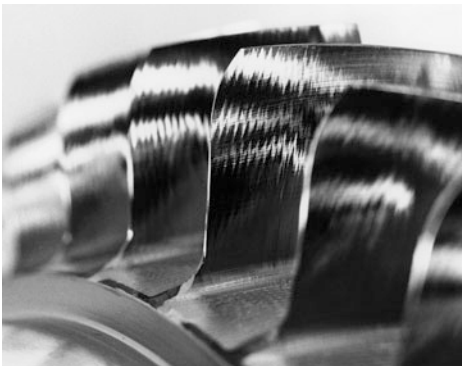
Synonyms

[Machine tool vibrations](#); [Self-excited vibrations in metal cutting](#)

Definition

Chatter is one of the most important limitations in machining processes causing poor surface finish, decreased tool life, and damage to the machine tool. Additional operations are required to clean the marks left on the surface; however this may not be possible in cases of severe chatter. In short, chatter vibrations result in reduced productivity, increased cost, and inconsistent product quality.

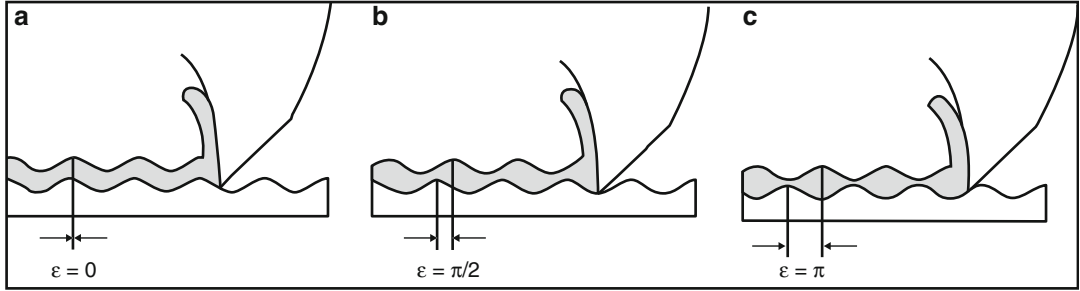
Chatter is a self-excited vibration type resulting from the dynamic interaction between the cutting tool and the work material (Tobias 1965; Koenigsberger and Tlustý 1967). For forced vibrations arising in mechanical systems, the excitation is independent of the response, i.e., the vibrations do not affect the forces. In self-excited chatter vibrations, on the other hand, the chip thickness becomes modulated due to the vibration marks left on the surface in a previous pass and the present vibrations causing oscillatory cutting forces which vary at the same frequency with the vibrations. This process is called regeneration of waviness or chip thickness (or simply regeneration) and is responsible for instability and chatter as shown in Fig. 1. Thus, in regenerative chatter, vibrations and cutting forces are coupled through the process where increase in one of them causes the other to increase resulting in instability. For a stable cutting process, on the other hand, vibrations, and thus the dynamic part of the forces, will diminish in a short time although the process



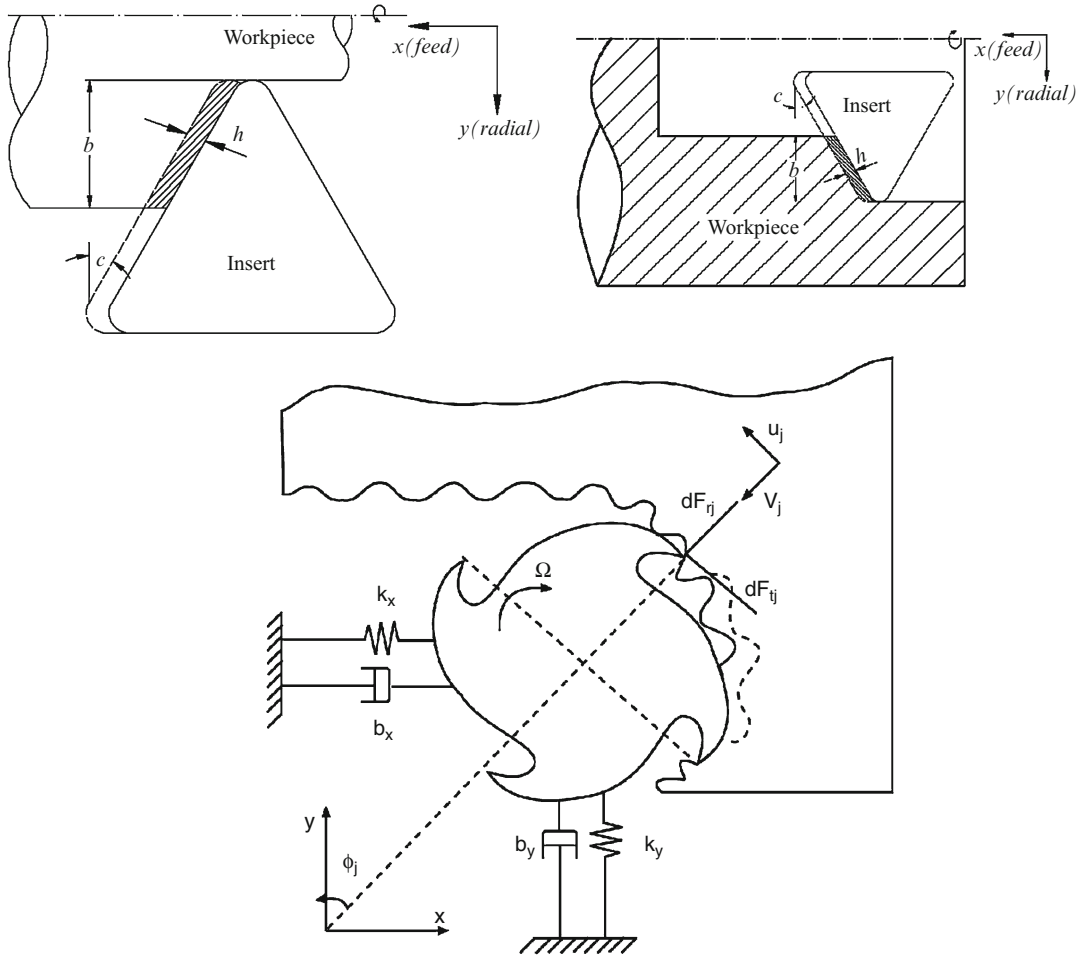
Chatter, Fig. 1 Chatter marks left on a machined surface and effect of chatter on tool wear (*S* stable, *C* chatter, *SC* severe chatter)

may start with the existence of vibrations due to impacts, step forces, and transients. Modulation in the chip thickness depends on the phase between

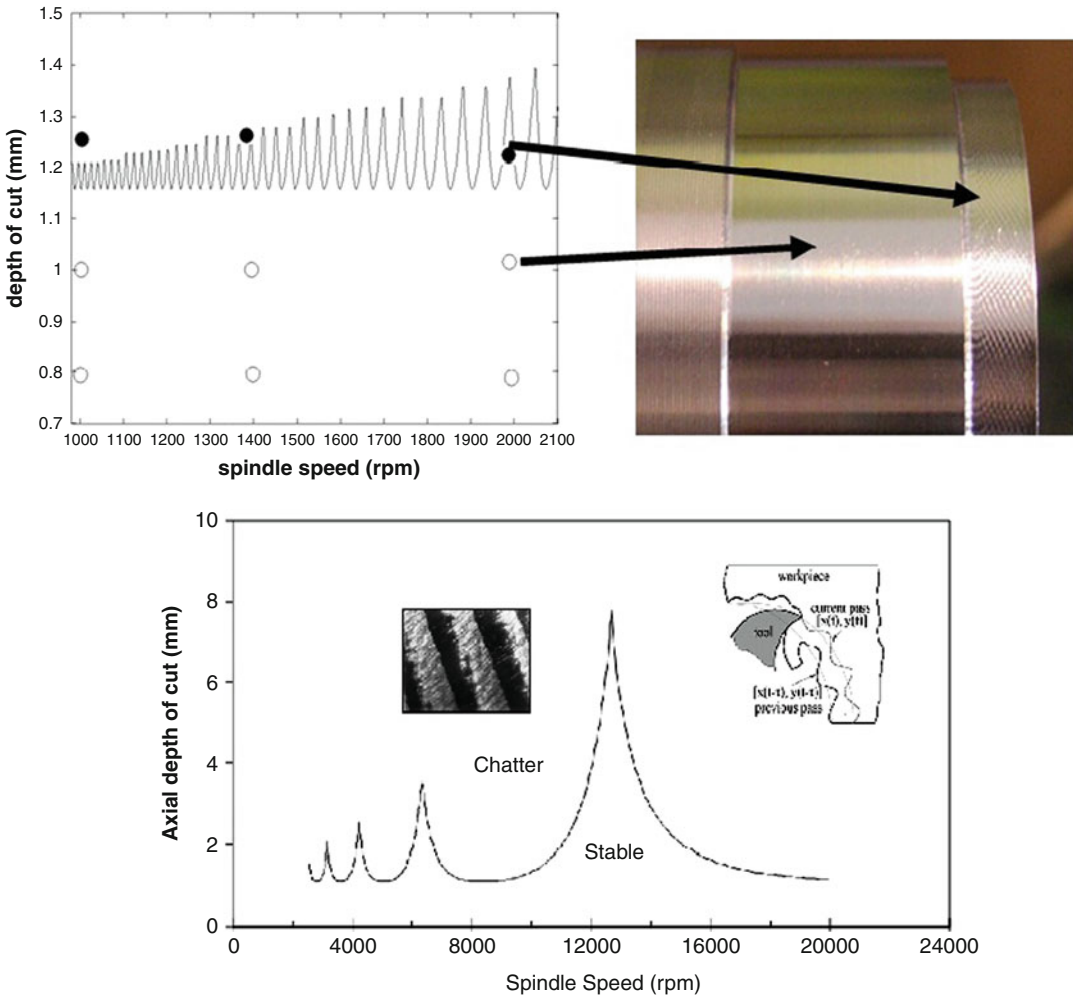
two successive vibration waves shown with ϵ in Fig. 2. The phase depends on the dynamic properties of the cutting system and the cutting speed.



Chatter, Fig. 2 Modulated chip thickness in dynamic cutting (regeneration of waviness). (a) stable, (b) and (c) show unstable cases



Chatter, Fig. 3 Chip thickness in turning, boring, and milling under the effect of vibrations



Chatter, Fig. 4 Stability diagrams for turning and milling

The modulation in the chip thickness disappears if the phase angle ϵ is zero in which case the vibrations diminish and the system becomes stable.

Plusty 1967), the stable depth of cut, b_{lim} , is obtained as follows:

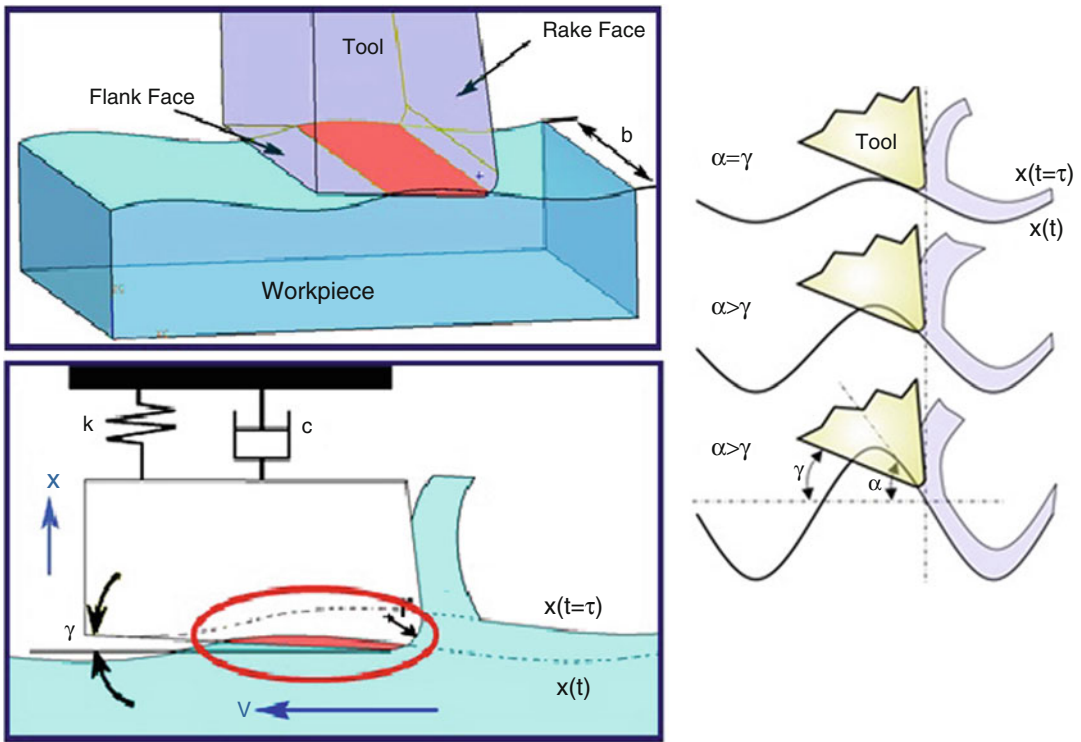
$$b_{lim} = \frac{-1}{2K_f G_R(j\omega)}$$

Theory and Application

Chatter Stability

Experimental and theoretical studies performed on machining chatter have shown that structural dynamics, tool geometry, and cutting conditions play important roles on stability of the process (Plusty 1978; Altintas and Weck 2004). In orthogonal chatter stability theory developed by Plusty (Plusty and Polacek 1963; Koenigsberger and

In the above equation, K_f and $G_R(j\omega)$ are the cutting force coefficient and the real part of the transfer function in the chip thickness direction, respectively. When the maximum (algebraic minimum) value of G_R is substituted, the minimum or absolute stability limit is obtained. Absolute stability is the minimum stable depth of cut which can be removed without chatter regardless of the cutting speed. However, since the chatter



Chatter, Fig. 5 Process damping due to flank contact under vibratory cutting

frequency, and thus the transfer function, varies with the cutting speed, so does the stable depth of cut. This can be observed in stability diagrams which show variation of the stability limit with cutting speed.

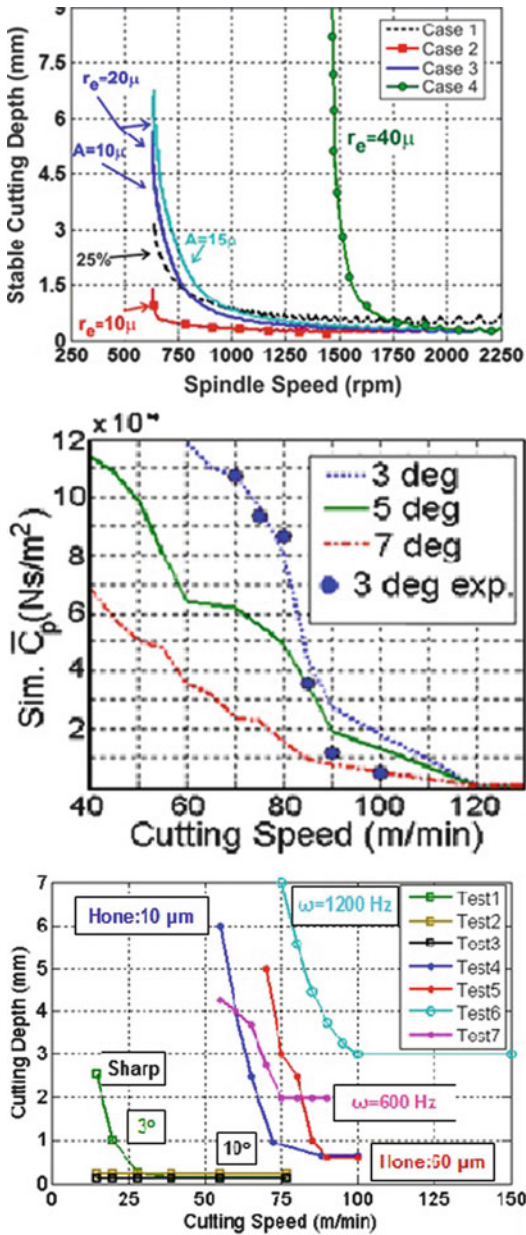
Although orthogonal theory demonstrates fundamentals and basic relations of chatter, dynamic cutting and chatter stability of industrial machining operations require multidimensional analysis due to their complex geometry. Figure 3 shows the chip thickness variation under the effect of vibrations in two directions. In these cases, components of each dynamic displacement in the chip thickness direction must be considered. These vibrations may come from the tool or workpiece side in more than one direction. The stability analysis must take the total dynamic variation of the chip thickness into account. Thus, the transfer functions of the tool and workpiece are added in respective directions, and then they are oriented in the chip thickness direction. In some practical cases, however, one of the component's flexibility

may be much higher than the others. For example, in boring processes, the tool is much more flexible in the radial direction compared to its high axial rigidity. In those cases the formulation and the solution may become one-dimensional.

In two- or three-dimensional turning chatter analysis, the characteristic equation of the system results in an eigenvalue problem solution of which provides the stability limit (Budak and Ozlu 2007). In case of milling, the solution becomes more complicated due to rotary tool which results in a time-varying dynamics system. The solution is obtained by using Fourier series expansion of the periodically varying directional coefficients matrix (Altintas and Budak 1995). The solution includes the effects of radial depth of cut and number of cutting teeth in addition to the parameters involved in turning stability.

Stability Diagrams

Stability limits can be solved for a range of chatter frequencies corresponding to different rotational



Chatter, Fig. 6 Effects of cutting conditions and tool geometry on process damping and stability limits at low cutting speeds

speeds to generate stability diagrams. Figure 4 shows examples of stability diagrams obtained for turning and milling. As it can be seen from the diagram, in milling, there are much wider and deeper stable pockets compared to turning. These pockets provide stable high material removal rates

in high-speed machining operations. At low cutting speeds, the vibration waves become shorter causing narrow and closely located lobes. As a result of this, high stability pockets, in general, cannot be obtained in turning operations, and the absolute stability limit is usually taken as the criteria.

Process Damping

Another important factor affecting chatter stability is the process damping which is generated due to the contact between the flank face of the tool and the material under vibratory cutting conditions as shown in Fig. 5. The contact volume and the indentation force, and thus the process damping, increase as the wavelength decreases resulting in higher stability at slower cutting speeds.

Stable depth of cuts obtained in chatter tests can be used to determine the process damping and the indentation force coefficients between the flank face of the tool and the material (Budak and Tunc 2010). In addition to the cutting speed and the vibration frequency, which determine the wavelength, clearance angle and edge hone radius also affect process damping, and thus the stability limits substantially, due to their impact on the interference volume. Figure 6 shows the effects of cutting conditions and tool geometry on stability limits and identified process damping coefficients for different cases (Budak and Tunc 2010). As it can be seen from this figure, chatter stability significantly increases due to process damping at low cutting speeds which are commonly used for low machinability materials such as titanium and nickel alloys. Therefore, for cases where higher speeds cannot be used due to material or machine tool limitations, stability of the process can be increased by utilizing process damping. For those cases tool edge and flank geometry become very important.

Cross-References

- ▶ Chatter Prediction
- ▶ Dynamics
- ▶ Stability
- ▶ Vibration

References

- Altintas Y, Budak E (1995) Analytical prediction of stability lobes in milling. *Ann CIRP* 44(1):357–362
- Altintas Y, Weck M (2004) Chatter stability of metal cutting and grinding. *CIRP Ann Manuf Technol* 53(2): 619–642
- Budak E, Ozlu E (2007) Analytical modeling of chatter stability in turning and boring operations: a multi-dimensional approach. *CIRP Ann Manuf Technol* 56(1):401–404
- Budak E, Tunc LT (2010) Identification and modeling of process damping in turning and milling using a new approach. *CIRP Ann Manuf Technol* 59(1):403–408
- Koenigsberger F, Tlustý J (1967) *Machine tool structures*. Pergamon Press, Oxford
- Tlustý J (1978) Analysis of the state of research in cutting dynamics. *Ann CIRP* 27(2):583–589
- Tlustý J, Polacek M (1963) The stability of machine tools against self excited vibrations in machining. In: *Proceedings of the ASME international research in production engineering conference*, Pittsburg, pp 465–474
- Tobias SA (1965) *Machine tool vibration* (trans: Burton AH). Blackie and Sons, Glasgow

Chatter Prediction

Michael F. Zaeh

iwb – Institut fuer Werkzeugmaschinen und Betriebswissenschaften, Technical University of Muenchen, Munich, Germany

Synonyms

[Process stability analysis](#)

Definition

The term *chatter prediction* describes a range of simulation methods, which are used to predict chatter vibrations (instabilities). These methods are based on the dynamic compliance of the machine tool structure as well as on the dynamics of the machining process. The whole machine behavior can be expressed in terms of mathematical descriptions (coupled structure-process models), from which stability lobe diagrams can be derived.

Theory and Application

Chatter

In the context of *chatter prediction*, chatter describes a self-excited vibration occurring during a metal-cutting machining process. Its vibration frequency is close to the eigenfrequency of the most compliant eigenmode of the excited machine structure. According to Totis (2009), chatter can be classified as primary or secondary. Primary chatter (e.g., friction on contact surfaces, stress distribution on the normal rake face, thermoplastic behavior of the chip material, and mode coupling) occurs at low spindle speeds and secondary chatter (e.g., regeneration of waviness) at higher spindle speeds. Tobias and Fishwick (1956) named the regeneration of waviness and the coupling of modes as the main sources of self-excited chatter vibrations.

Regeneration of Waviness

Starting with a small disturbance, which causes the machine to oscillate in its eigenfrequency, the cutting edge will leave a wavy surface behind. For some processes (e.g., turning, milling or boring) the tool cuts over these waves repeatedly, which results in an excitation of the machine tool in its eigenfrequency. Depending on the phase difference between the waves on both sides of the chip, regenerative chatter (or regeneration of waviness) occurs.

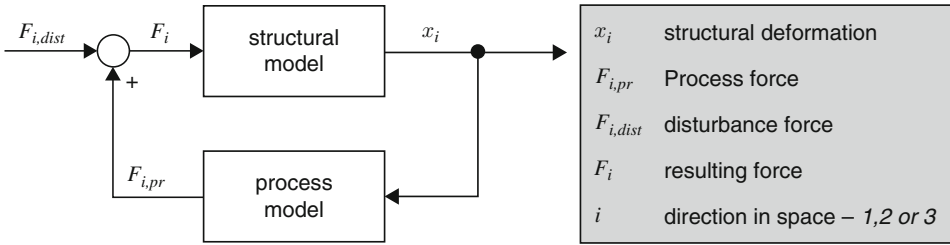
Mode Coupling

Mode coupling implies a high-order system with at least two degrees of freedom (DOF). If two of the eigenfrequencies with different directions of oscillation (different eigenvectors) are in the same frequency range, both can affect each other and mode-coupling chatter occurs.

Modeling of Chattering Systems

General

As shown above, the cause of chatter is associated to the machining process and its history as well. However, the intensity of chatter vibrations is characterized by all components within the force flux (tool, machine tool, and workpiece structure)



Chatter Prediction, Fig. 1 Control-oriented block diagram of the coupled overall system

respectively their compliance. To determine the stability of the coupled overall system (see Fig. 1), both subsystems have to be modeled.

Usually, such models are based on a mathematical description with ordinary differential equations (ODE). This kind of model will be used here.

For the purpose of simplification, an ideal rigid workpiece and fixture should be assumed. Consequently, the highest compliance is usually located on the tool-side of the machine tool.

Structural Model

The description of the machine tool structure is based on an approximation with a second-order ODE of motion (Eq. 1):

$$\mathbf{M} \cdot \ddot{\mathbf{x}}(t) + \mathbf{D} \cdot \dot{\mathbf{x}}(t) + \mathbf{C} \cdot \mathbf{x}(t) = \mathbf{0} \quad (1)$$

\mathbf{M} is the mass matrix, \mathbf{D} is the damping matrix, \mathbf{C} is the stiffness matrix, and $\mathbf{x}(t)$ is the displacement vector.

These three matrices (nodal matrices) can be obtained in two various ways in practice: with an experimental measurement or with a simulation (e.g., finite element or finite-difference method) of the tool center point's (TCP) compliance.

Experimental Measurement The experimental examination of the TCP's compliance is achieved by exciting the machine structure at this point with a defined force $F_i(\omega)$ (pulsed or continuously) and by recording its response signal $x_i(\omega)$. This procedure occurs analogously for all three directions in space 1, 2, and 3. From Eq. 2, the dynamic compliance $\alpha_{ij}(\omega)$ can be determined.

$$\alpha_{ij}(\omega) = x_i(\omega) / F_j(\omega) \quad (2)$$

By means of various methods (Ewins 1984), the respective frequency response $\alpha_{ij}(\omega)$ can be approximated by the superposition of several (n) adapted harmonic oscillators (so-called modal harmonic oscillators). Their parameters, the modal eigenfrequency ω_n , the associated eigenvector φ_n , as well as the modal damping θ_n , correspond to the modal matrices \mathbf{M}_m , \mathbf{D}_m , and \mathbf{C}_m (Gawronski 2004), but they are not comparable with a real mass, damping, or stiffness. Those modal harmonic oscillators only describe an arbitrary multi-degree-of-freedom (MDOF) system in modal space, whose frequency response complies with the measured one.

Modeling In this case, the matrices describing the system can be determined based on a model of the machine tool structure, which can be expressed as a numerical finite element model (FEM) or a finite-difference model (FDM).

FEM or FDM uses these nodal matrices in principle, but their dimension is highly correlated to the level of the model's discretization. With fine discretization, the dimension of the matrices becomes huge. Therefore, the calculation of stability will be very time-consuming. Furthermore, the determination of stability lobe diagrams only requires a fraction of all information within the FEM or FDM: the dynamic compliance of the TCP. Under this premise, the dimension of the model is usually reduced with a so-called modal reduction, which encompasses the following steps:

1. Transforming the ODE from nodal to modal space
2. Reducing the system of equations with a modal reduction

3. Calculating the system response within the modal space
4. Transforming the modal system response to the nodal space
5. Calculating the TCP's dynamic compliance by means of Eq. 2

Process Model

Normally, the machine structure gets excited by the machining process, in other words by occurring process forces $F(t)$ (Eq. 3):

$$\mathbf{M} \cdot \ddot{\mathbf{x}}(t) + \mathbf{D} \cdot \dot{\mathbf{x}}(t) + \mathbf{C} \cdot \mathbf{x}(t) = \mathbf{F}(t) \quad (3)$$

To model the regeneration of waviness inside the process model, history information about the cut is required. Generally, such relations are described by delayed differential equations (DDEs) in literature and within this article as well.

Altintas (2012) used an orthogonal turning process (see Fig. 2) to explain the modeling of process forces in consideration of the regeneration of a waviness. Mode coupling cannot be described by this model, because in this simple case, only a single-degree-of-freedom (SDOF) system is required to describe the machine tool's behavior.

In this example, h_0 is the intended chip thickness, which is defined by the machine's feed rate. Due to resonant vibrations, the process leaves a wavy surface on the workpiece. The resulting chip thickness $h(t)$ is now calculated from the

difference between the present and the previous tooth period (Eq. 4):

$$h(t) = h_0 - [x_1(t) - x_1(t - T)] \quad (4)$$

Within this equation, t represents the current time, whereas T defines the period of time, needed for one workpiece revolution.

One approach to model the radial cutting force $F_f(t)$ was proposed by Altintas (2012):

$$\begin{aligned} F_f(t) &= K_f \cdot a_e \cdot h(t) \\ &= K_f \cdot a_e \cdot [h_0 + x_1(t - T) - x_1(t)] \quad (5) \end{aligned}$$

K_f is the cutting coefficient, which should be assumed as a constant value (to consider, e.g., process damping, the cutting coefficient may also be variable), and a_e is the width of cut. Thus, the control-oriented block diagram considering the regeneration of waviness can be illustrated as shown in Fig. 3.

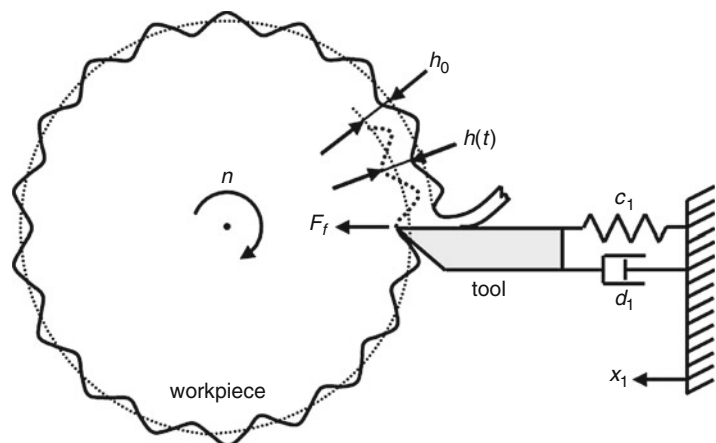
In this picture, μ specifies the degree of overlap between two consecutive cuts (e.g., groove turning: $\mu = 100\%$; thread turning: $\mu = 0\%$) (Weck and Brecher 2006).

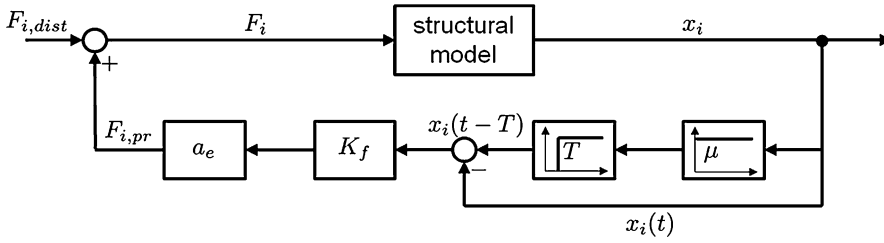
This approach, applied on the turning operation above, is freely transferable to other metal-cutting processes. A two-dimensional milling process (see Fig. 4) is explained below as a further example conducted by Altintas (2012).

Now, the intended chip thickness $h(\Phi_j)$ (Eq. 6) is depending on the instantaneous angular immersion Φ_j of the milling tool's tooth j and on the

Chatter Prediction,

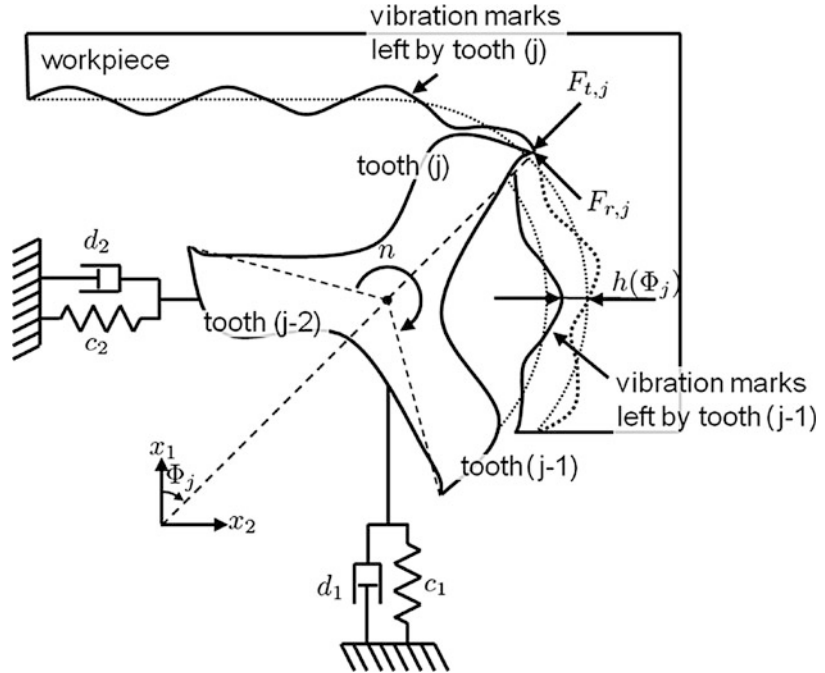
Fig. 2 Regenerative chatter vibrations occurring during an orthogonal cutting process with one SDOF x_1





Chatter Prediction, Fig. 3 Control-oriented block diagram of the coupled overall system considering the regeneration of waviness of waviness

Chatter Prediction, Fig. 4 Regenerative chatter vibrations occurring during a two-dimensional milling process with two DOF x_1 and x_2 . (Yusuf 2012, reprinted with permission)



dynamic displacements ($\Delta x_1, \Delta x_2$) of the whole structure at the present and previous tooth period:

$$h(\Phi_j) = [\Delta x_1 \cdot \cos(\Phi_j) + \Delta x_2 \cdot \sin(\Phi_j)] \cdot g(\Phi_j) \tag{6}$$

Since milling is not a continuous but an interrupted process, start (Φ_{st}) and exit (Φ_{ex}) immersion angles of each tooth must be considered within Eq. 6 by multiplying $h(\Phi_j)$ with the function $g(\Phi_j)$. The function $g(\Phi_j)$ is defined as a unit step function:

$$g(\Phi_j) = \begin{cases} 1 & \Phi_{st} < \Phi_j < \Phi_{ex} \\ 0 & \Phi_j < \Phi_{st}; \Phi_j > \Phi_{ex} \end{cases} \tag{7}$$

Analogously to Eq. 5, the tangential ($F_{t,j}$) and radial ($F_{r,j}$) cutting forces of tooth j are expressed by the cutting coefficients K_t and K_r as follows:

$$\begin{aligned} F_{t,j} &= K_t \cdot a_e \cdot h(\Phi_j) \\ F_{r,j} &= K_r \cdot a_e \cdot h(\Phi_j) \end{aligned} \tag{8}$$

The total milling forces F_{x1} and F_{x2} (Eq. 9) are resulted by transforming the cutting forces (Eq. 8)

into the global coordinate system x_1, x_2 and summing them up over all teeth:

$$\begin{Bmatrix} F_{x1} \\ F_{x2} \end{Bmatrix} = \frac{1}{2} \cdot a_e \cdot K_t \cdot \begin{bmatrix} a_{11} & a_{12} \\ a_{21} & a_{22} \end{bmatrix} \cdot \begin{Bmatrix} \Delta x_1 \\ \Delta x_2 \end{Bmatrix} \quad (9)$$

with a_{11}, a_{12}, a_{21} , and a_{22} as directional dynamic milling force coefficients.

Methods to Determine Chatter Stability

General

The stability of the system, in other words the solution of the ordinary differential equation (Eq. 3), can be calculated, based on the models of the machine tool's structure and the machining process. According to Altintas (2012), such problems are mainly solved with numerical methods, which could be time-domain, frequency-domain, or DDE-based methods (Totis 2009).

Time-Domain Methods

The time-domain methods enable a very realistic prediction of the behavior of the machine tool, since the effective kinematics of the machining process as well as nonlinear effects (e.g., tool jumping) are taken into account (Totis 2009). Adversely, such simulations cause a lot of

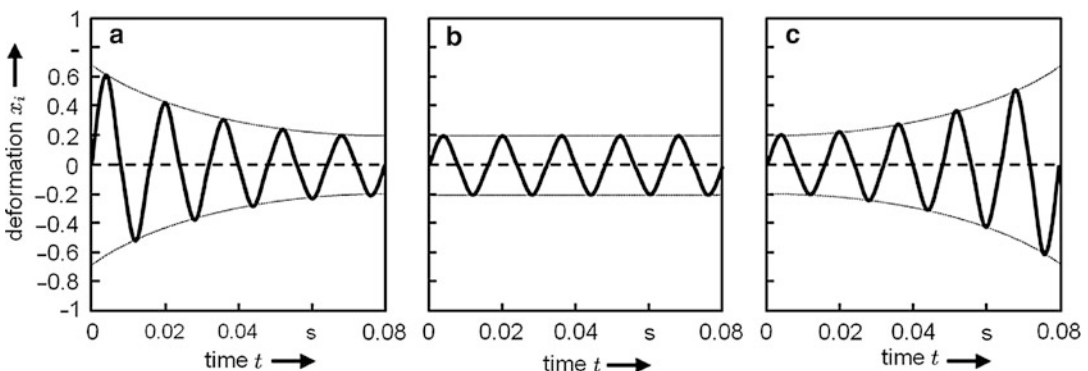
computation time, due to the high complexity. Furthermore, the identification of the whole stability lobe diagram requires its complete simulation for each combination of process parameters. To determine the limit of stability, changes of the vibration response or of the force amplitudes are detected during each run of simulation.

Sims (2005) uses a method, based on the theory of viscously damped systems. Depending on a damping ratio ζ , this method distinguishes between a still stable and an already unstable cases. Three different cases can be distinguished by examining the oscillation amplitude over time:

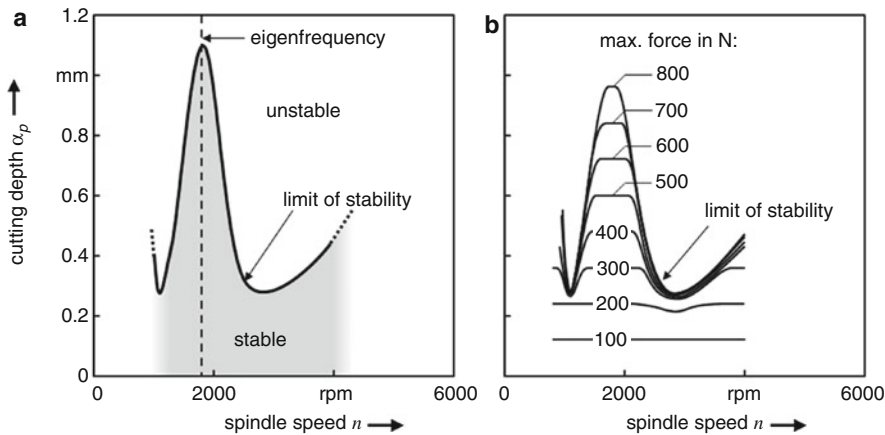
- $\zeta > 0$: stable (see Fig. 5a)
- $\zeta = 0$: marginally stable (see Fig. 5b)
- $\zeta < 0$: unstable (see Fig. 5c)

Especially the determination of the marginally stable vibration (system is close to the limit of stability in the stability lobe diagram) requires long simulation periods in order to register slow drifting into stable or unstable areas.

Another approach to estimate the limit of stability is to analyze the cutting forces. A diagram like Fig. 6b results by simulating these forces and plotting their maximum amplitudes for various combinations of the spindle speed n and the depth of cut a_p . In order to compare its characteristic with an ordinary stability lobe diagram, Fig. 6a shows a small part of that type of diagram.



Chatter Prediction, Fig. 5 Free vibrations of a linear, viscously damped system, where (a) represents the stable case, (b) the marginally stable case, and (c) the unstable case



Chatter Prediction, Fig. 6 Comparison between two stability lobe diagrams: (a) part of an ordinary stability lobe diagram; (b) stability lobe diagram estimated with PTP method. (Based on Smith and Tlustý 1990)

The previously explained method is called peak-to-peak (PTP) method. It was invented by Smith and Tlustý (1990) and is intended to be used for high-speed milling processes.

Within Fig. 6b, a sharp increase of the force level emerges, which corresponds to the stability limit shown in Fig. 6a. For stable regions, the PTP force is constant regardless of the spindle speed. Based on these criteria, a stability lobe diagram can be derived from the simulated forces.

Frequency-Domain Methods

The disadvantage of time-domain-based methods is the high computation time. To counteract this deficit, Altintas and Budak (1995) developed a frequency-based approach, which is called zeroth-order approximation (ZOA). Further approaches of frequency-domain methods are mainly based on it.

The ZOA provides a time-invariant formulation of the dynamic part of the cutting forces, which is time variant due to the rotation of the cutting tool. This is done by approximating the time varying part by means of a Fourier series, truncated at the zeroth-order constant term. Therefore, a single-frequency solution results, which is limited to slot milling processes. To determine the stability of milling processes with a lower width of cut, higher-order terms of the Fourier series are to be considered (Merdol and Altintas 2004). In addition, the cutting thickness modulation shows

a time-invariant part. This can be expressed according to the lowest eigenfrequency ω_c as well as to a constant time period T , which is defined as the time period between the present and the previous cut.

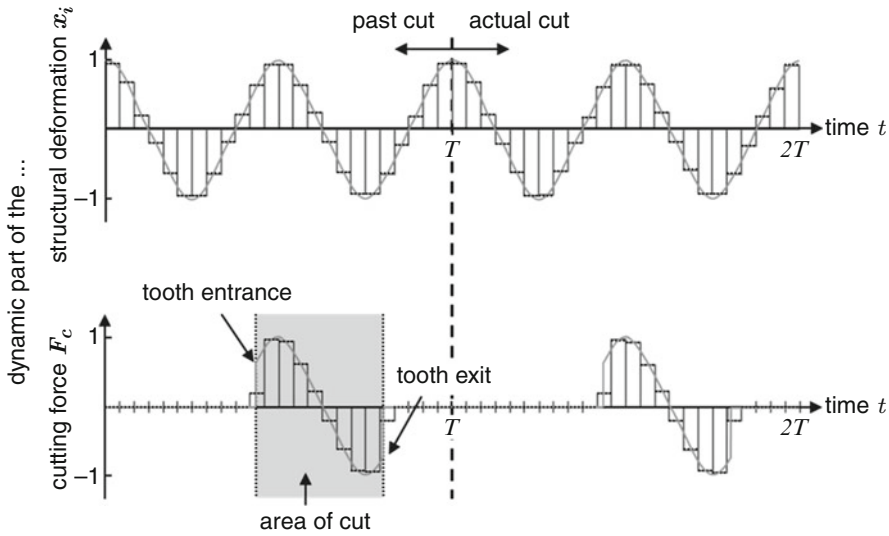
However, all time-variant terms of the coupled process-structure model are now formulated to be time invariant. By applying a stability criterion and by solving the characteristic equation, the stability lobe diagram can be determined.

DDE-Based Methods

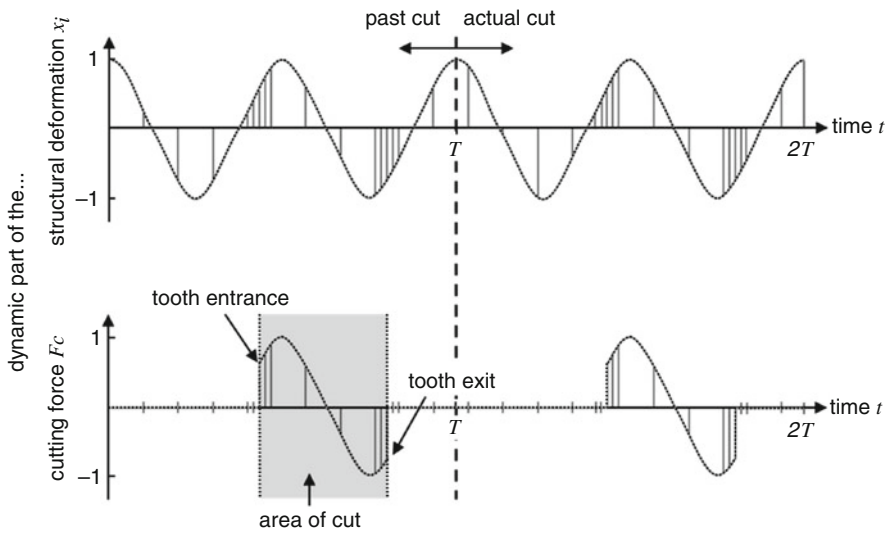
Beyond these previously mentioned methods to determine the stability lobe diagram, also analytical approaches are used to solve DDEs. By means of different forms of time discretization, the DDE is being transformed into an ODE. Two of these methods are explained within the following: the semi-discretization method (SDM) and the quick chatter prediction method (QCPM).

The SDM, which was developed by Insperger and Stépán (2004), provides an equally spaced time discretization. Within these time steps, the coefficients of the cutting force as well as the dynamic part of the cutting depth are assumed to be piecewise constant, comparable to Fig. 7.

The accuracy of this method is highly dependent on the length of the chosen time intervals: the finer the discretization, the better the prediction accuracy. But in terms of calculation speed, this approach is disadvantageous,



Chatter Prediction, Fig. 7 Principle of the semi-discretization method (SDM) according to Totis (2009) for a milling process



Chatter Prediction, Fig. 8 Principle of the quick chatter prediction method (QCPM) according to Totis (2009) for a milling process

because a fine discretization is not necessary at each time step.

Kuljanic et al. (2007) take up this deficit by adapting the time step size to signal changes of the cutting force coefficients or the cutting depth. Furthermore, these time steps were no longer

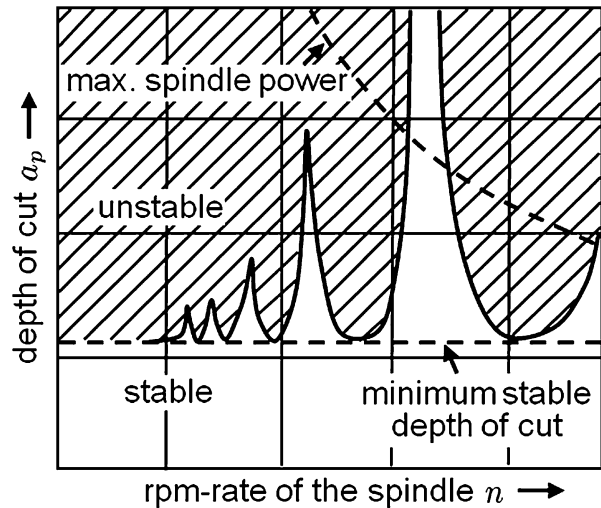
assumed to be constant but are interpolated by polynomials within their range (see Fig. 8).

Stability Lobe Diagram

Previous chapters mentioned the main methods to predict the stability of metal-cutting machining

Chatter Prediction,

Fig. 9 Qualitative stability lobe diagram of a milling process. (Weck and Brecher 2006. With permission of Springer)



processes. By varying the cutting parameters, like depth of cut a_p and spindle speed n , a classical stability lobe diagram (see Fig. 9) can be obtained. This can be used to configure a desired cutting process concerning a stable cut and a high productivity simultaneously.

Nevertheless, such a diagram is only valid for a specific milling tool, tool wear, radial immersion, and machine tool. To compare two milling tools, for example, two stability lobe diagrams have to be calculated in consequence.

Cross-References

- ▶ [Chatter](#)
- ▶ [Cutting Force Modeling](#)
- ▶ [Cutting, Fundamentals](#)
- ▶ [Dynamics](#)
- ▶ [Finite Element Method](#)
- ▶ [Stability](#)

References

- Altintas Y (2012) Manufacturing automation: metal cutting mechanics, machine tool vibrations, and CNC design, 2nd edn. Cambridge University Press, New York
- Altintas Y, Budak E (1995) Analytical prediction of stability lobes in milling. *Annals of the CIRP* 44(1):357–362
- Ewins DJ (1984) Modal testing: theory and practice. Research Studies Press, Taunton

- Gawronski WK (2004) Advanced structural dynamics and active control of structures. Springer, New York
- Inspurger T, Stépán G (2004) Updated semi-discretization method for periodic delay-differential equations with discrete delay. *Int J Numer Meth Eng* 61(1):117–141
- Kuljanic E, Sortino M, Totis G (2007) Quick chatter prediction method – QCPM, an innovative algorithm for quick chatter prediction in milling. In: 8th Convegno AITeM. Italy, Montecatini Terme 2007, pp 1–10
- Merdol SD, Altintas Y (2004) Multi frequency solution of chatter stability for low immersion milling. *J Manuf Sci Eng* 126(3):459–466
- Sims ND (2005) The self-excitation damping ratio: a chatter criterion for time-domain milling simulations. *J Manuf Sci Eng* 127(3):433–445
- Smith S, Thusty J (1990) Update on high-speed milling dynamics. *J Manuf Sci Eng* 112(2):142–149
- Tobias SA, Fishwick W (1956) Eine Theorie des regenerativen Ratterns an Werkzeugmaschinen. [A theory of regenerative chatter of machine tools]. *Maschinenmarkt* 60(17):183–190 (in German)
- Totis G (2009) RCPM – a new method for robust chatter prediction in milling. *Int J Mach Tools Manuf* 49(3–4):273–284
- Weck M, Brecher C (2006) *Werkzeugmaschinen 5: Messtechnische Untersuchung und Beurteilung, dynamische Stabilität* [Machine tools. Vol. 5: measurement investigations and evaluation, dynamic stability], 7th edn. Springer, Berlin/Heidelberg (in German)

Chemical Machining Processes

- ▶ [Etching](#)

Chemical Vapor Deposition (CVD)

Kurt Coppers¹ and Eleonora Ferraris²

¹KU Leuven – Campus De Nayer, Sint-Katelijne-Waver, Belgium

²Department of Mechanical Engineering, Production Engineering, Machine Design and Automation (PMA) Section, KU Leuven, Leuven, Belgium

Definition

Chemical vapor deposition (CVD) is a process whereby a solid material is deposited from the reaction of vapor-phase chemical reactants on or close to a substrate surface. The solid material is obtained as a coating, a powder, or single crystals. A reaction chamber is used for the process, into which the reactant gases are introduced to decompose and react. By varying the environmental conditions such as substrate material and temperature, composition of the reaction gas mixture, total pressure gas flows, etc., materials with different properties can be grown (Martin 2010).

Theory and Application

Process Description

Chemical vapor deposition (CVD) is a widely used materials-processing technology. It is a synthesis process capable of producing high-purity, high-performance solid materials through chemical reactions in vapor phase. CVD is commonly used to deposit conformal films to surfaces essential in the manufacture of semiconductors and other electronic components; in the coating of tools, bearings, and other wear-resistant parts; and in many optical, optoelectronic, and corrosion applications (Pierson 1999). CVD is also used to produce high-purity bulk materials and powders. With CVD it is possible to process most metals, many nonmetallic elements such as carbon and silicon, as well as a large number of compounds including carbides, nitrides, oxides, etc. Around

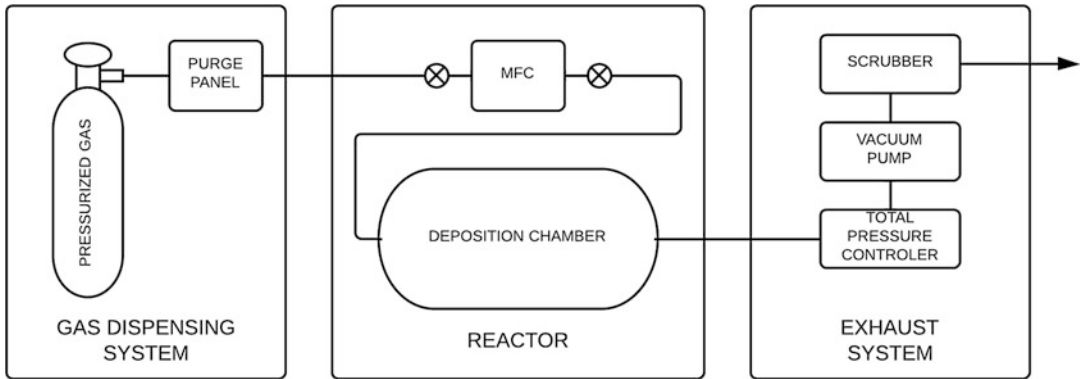
70 % of elements in the periodic table have been deposited by the CVD technique, either in the form of the pure element or the compound materials (Yan and Xu 2010).

The base of CVD involves in flowing a precursor gas or gases into a chamber containing one or more heated objects to be coated. On and near the hot surfaces chemical reactions occur in the vapor phase, resulting in the deposition of a thin film, while chemical by-products and unreacted precursor gases are exhausted out of the process chamber. Because of the large variety of materials deposited and the wide range of applications, many variants of CVD exist (Park and Sudarshan 2001).

Process Technology

A generic CVD reactor consists of three basic features: (1) the reaction gas dispensing system; (2) the reactor, including components for defining the gas flows; and (3) the exhaust system containing a total pressure controller, vacuum pump, scrubber, and/or reactant recycle system. Processes working at atmospheric pressures do not require vacuum pumps and total pressure control. Each CVD system can have additional or adapted features affected by a number of factors such as the reactants used in the process, the maximum acceptable leak rate for air into the system, purity of the deposit, size and shape of the substrate, process economy, etc. A schematic overview of a generic CVD reactor is shown in Fig. 1 (Dobkin and Zuraw 2003).

During the basic CVD process, a predefined mix of reactant gases and an inert carrier gas is introduced into the reaction chamber. A mass flow controller is used to keep a specified inward gas flow rate. While the gas flow moves over the substrate, the reactants get absorbed on or near the surface of the substrate where they undergo a chemical reaction to form a film. Reactions at the substrate surface itself are called heterogeneous reactions and are selectively occurring on the heated surface. Reactions that take place in the gas phase itself are known as homogeneous reactions and should be avoided since they form gas-phase aggregates of the depositing material which poorly adhere to the surface and could cause low-density films with lots of defects. The



Chemical Vapor Deposition (CVD), Fig. 1 Generic CVD reactor

Chemical Vapor Deposition (CVD), Table 1 Overview of CVD processes

Type	Description
Atmospheric pressure CVD <i>APCVD</i>	Processes at atmospheric pressure
Low-pressure CVD <i>LPCVD</i>	Processes at subatmospheric pressures
Ultrahigh vacuum CVD <i>UHVCD</i>	Processes at very low pressure
Aerosol-assisted CVD <i>AACVD</i>	Precursors are transported to the substrate by means of a liquid/gas aerosol, which can be generated ultrasonically
Direct liquid injection CVD <i>DLICVD</i>	Precursors are in liquid form (liquid or solid dissolved in a convenient solvent). Liquid solutions are injected in a vaporization chamber toward injectors (typically car injectors). Then the precursor's vapors are transported to the substrate as in classical
Remote plasma-enhanced CVD <i>RPECVD</i>	Utilizes a plasma to enhance chemical reaction rates of the precursors and allows deposition at lower temperatures
Atomic layer CVD <i>ALCVD</i>	Deposits successive layers of different substances to produce layered, crystalline films
Hot wire CVD <i>HWCVD</i>	Also known as catalytic CVD (Cat-CVD) or hot filament CVD (HFCVD). Uses a hot filament to chemically decompose the sources gases
Metal-organic CVD <i>MICVD</i>	Based on metal-organic precursors
Hybrid physical-CVD <i>HPCVD</i>	Vapor deposition processes that involve both chemical decomposition of precursor gas and vaporization of a solid source
Rapid thermal CVD <i>RTCVD</i>	Uses heating lamps or other methods to rapidly heat the wafer substrate

gaseous by-products are evacuated from the reaction chamber and often have to be neutralized. To remove them before exhaust, scrubbers are used.

Process Classification

There is a large variety in CVD processes, differentiated by their application, the process and reactor used, or the precursor and chemical reactions.

For that reason, different ways of classification are possible, such as classification by operating pressures, by excitation techniques, or by precursor type and feeding procedure. Table 1 gives an overview of a selection of CVD processes (Martin 2010).

Thermally activated CVD (TACVD) is the conventional process in which the chemical

reactions are initiated by thermal energy in a hot-wall or cold-wall reactor using inorganic chemical precursors. In a hot-wall reactor a heating system is used that heats up the walls of the reactor itself, an example of which is radiant heating from resistance-heated coils. A major downside of hot-wall reactors is that they need frequent wall cleaning, because films are deposited on the walls in much the same way as they are deposited on the substrate. With thicker films on the reactor walls, there is a risk that particles will break loose, fall down on the surface of the growing film, and introduce pinholes in it. The film growing on the reactor walls might also be a source of contamination because of the reaction between the material of the reactor wall and the vapor. Cold-wall reactors use heating systems that minimize the heating up of the reactor walls and only intent to heat the substrate, an example of which is heating via IR lamps inside the reactor. Using a cold-wall reactor reduces the risk of particles breaking loose from the walls and contaminating vapor/wall reactions, but the steep temperature gradients near the substrate surface may introduce severe natural convection resulting in a nonuniform film thickness and microstructure (Choy 2003).

The simplest reactors in design are atmospheric pressure CVD (APCVD) reactors, which operate at atmospheric pressure. Low-pressure CVD (LPCVD) reactors operate at medium vacuum (30–250 Pa) and at higher temperatures than APCVD reactors. Other types of CVD reactors operating under low pressure are, e.g., plasma-enhanced CVD (PECVD) reactors. PECVD reactors do not depend completely on thermal energy to accelerate the reaction processes, as thermal activated CVD (TACVD) reactors do, but also transfer energy to the reactant gases by using an RF-induced glow discharge. By applying an RF field to the low-pressure gas, free electrons are created within the discharge region. The electrons are sufficiently energized by the electric field that gas-phase dissociation and ionization of the reactant gases occur when the free electrons collide with them. Energetic species are then adsorbed on the film surface, where they are subjected to ion and electron bombardment, rearrangements,

reactions with other species, new bond formation, and film formation and growth. In photo-assisted CVD (PACVD) a light source, i.e., a lamp, CO₂ laser, Nd-YAG laser, excimer laser, or argon ion laser, is used to raise the surface temperature which causes thermal decomposition of the precursor in the gas phase and/or substrate surface. Flame-assisted CVD (FACVD) is another variant, whereas the combustion of liquid or gaseous precursors injected into diffused or premixed flames will decompose and undergo chemical reactions and/or combustions in the flame. This provides the required thermal environment for vaporization, decomposition, and chemical reaction and helps to heat the substrate to enhance the diffusion and surface mobility of the absorbed atoms on the substrate surface during deposition of the films (Choy 2003).

Other variants of CVD include metal-organic CVD (MOCVD) which uses metal-organic as the precursor, i.e., compounds containing metal atoms bonded to organic radicals, rather than the inorganic precursor used in conventional CVD processes. Variants such as pulsed injection MOCVD and aerosol-assisted CVD (AACVD) use special precursor generation and delivery systems unlike conventional CVD processes.

Advantages and Limitations of the Process

One of the primary advantages of CVD is that it is not restricted to a line-of-sight deposition which is a general characteristic of sputtering, evaporation, and other physical vapor deposition (PVD) processes. The deposited films are generally quite conformal, meaning that the film thickness on the walls of features is comparable to the thickness on the top. This means that films can also be applied to freeform objects, including the insides and undersides of features, and that high-aspect-ratio holes (10:1) and other features can be completely filled. Another advantage of CVD is, in addition to the wide variety of materials that can be deposited, they can be deposited with very high purity. This results from the relative ease with which impurities are removed from gaseous precursors using distillation techniques. Other advantages include relatively high deposition rates which make it possible to form thick coatings

(in some cases centimeters thick) and the fact that CVD often does not require as high a vacuum as PVD processes (Pierson 1999).

CVD also has a number of limitations. One of the primary disadvantages lies in the properties of the precursors. Ideally, the precursors need to be volatile at near room temperatures. This is non-trivial for a number of elements in the periodic table, although the use of metal-organic precursors and the development of plasma CVD have eased this situation (Park and Sudarshan 2001). Another limitation is the requirement of having chemical precursors with high vapor pressure which are often hazardous and at times extremely toxic. The by-products of the CVD reactions can also be toxic and corrosive and may need to be neutralized, which could be a costly and environmentally controversial operation. The other major disadvantage is the fact that the films are usually deposited at elevated temperatures. This puts some restrictions on the kind of substrates that can be coated. More importantly, it leads to stresses in films deposited on materials with different thermal expansion coefficients, which can cause mechanical instabilities in the deposited films.

Applications

CVD is a versatile and dynamic technology which is constantly expanding and improving. Many of the early applications involved refining or purification of metals and a limited number of non-metals from their carbonyl or halide precursors. Powders of TiO_2 , SiO_2 , carbon black, and other materials such as Al_2O_3 , Si_3N_4 , and BN have been routinely made by CVD. Most of the recent R&D effort is aimed at thin-film deposition (Park and Sudarshan 2001). Two major areas of application of CVD have rapidly developed, namely, in the semiconductor industry and in the so-called metallurgical-coating industry which includes the manufacture of coated cemented carbide cutting tools. The semiconductor industry is estimated to comprise three-quarters of all CVD production.

CVD has been a critical enabling technology in silicon-based microelectronics and is even used at

the earliest stage of refining and purification of elemental silicon. CVD techniques can be used for depositing thin films of the active semiconductor material (e.g., doped Si), conductive interconnects (e.g., tungsten), and/or insulating dielectrics (e.g., SiO_2).

In cutting tool fabrication a wear-resistant coating of a refractory compound is applied on tungsten carbide-cobalt alloys by CVD. Commonly used coatings include TiC, TiN, and Al_2O_3 and their combinations (Tracton 2005).

The communications revolution also relies on a diverse set of CVD technologies for the manufacturing of components such as solid-state diode lasers. Even fiber-optic cables are manufactured using CVD techniques to achieve the desired refractive index profile by coating the inside of a fused silica tube with oxides of silicon, germanium, boron, etc. After deposition the fused silica tube is collapsed to a rod and the rod is then drawn into a fiber. CVD techniques used to grow optoelectronic material also have many applications outside of the communications industry. One example is high-brightness blue and green LEDs based on group-III nitride alloys, e.g., InGaN, which are grown on sapphire substrates (Park and Sudarshan 2001).

CVD processes are also used in the production of microelectromechanical systems or MEMS. Most MEMS devices are manufactured from polycrystalline silicon (polysilicon) films deposited on silicon wafers, with intermediate sacrificial SiO_2 layers that are later removed by chemical etching. Both the polysilicon and oxide are deposited by CVD or PECVD. The CVD steps define the structure of the device perpendicular to the silicon substrate, while numerous lithographic and etching steps define the structure in the other two dimensions (Park and Sudarshan 2001).

Also powders of nuclear fuel materials from the fuel rods used in nuclear reactors have been coated in a fluidized bed with coatings of SiC, graphite, and ZrC for containment of fission products.

Another interesting application of the CVD technology is the deposition of whiskers of metals and refractory compounds. Whiskers are

needle-shaped single crystals of materials, typically 1 μm or less in diameter and several micrometers long. They are being used in the development of composites. Adding whiskers to ceramics, which are inherently brittle, significantly improves their fracture toughness. Today, composites have become a very important new class of engineering materials in, e.g., aerospace structural applications (Tracton 2005).

Cross-References

- ▶ [Coated Tools](#)
- ▶ [Physical Vapor Deposition \(PVD\)](#)

References

- Choy K (2003) Chemical vapour deposition of coatings. *Prog Mater Sci* 48(2):57–170
- Dobkin D, Zuraw M (2003) Principles of chemical vapor deposition. Kluwer, Dordrecht/Boston
- Martin P (2010) Handbook of deposition technologies for films and coatings science, applications and technology. Elsevier, Amsterdam/Boston
- Park J-H, Sudarshan TS (2001) Chemical vapor deposition. ASM International, Materials Park
- Pierson H (1999) Handbook of chemical vapor deposition: principles, technology, and applications, 2nd edn. Noyes, Norwich
- Tracton A (2005) Coatings technology handbook. Taylor & Francis, Boca Raton
- Yan X-T, Xu Y (2010) Chemical vapour deposition: an integrated engineering design for advanced materials. Springer, London

Chip Breakability

- ▶ [Chip-Forms, Chip Breakability, and Chip Control](#)

Chip Breaking

- ▶ [Chip-Forms, Chip Breakability, and Chip Control](#)

Chip Formation

- ▶ [Machinability of Aluminum and Magnesium Alloys](#)

Chip Formation (Abrasive Process)

Fritz Klocke¹ and Frederik Vits²

¹Laboratory for Machine Tools and Production Engineering (WZL), RWTH Aachen University, Aachen, Germany

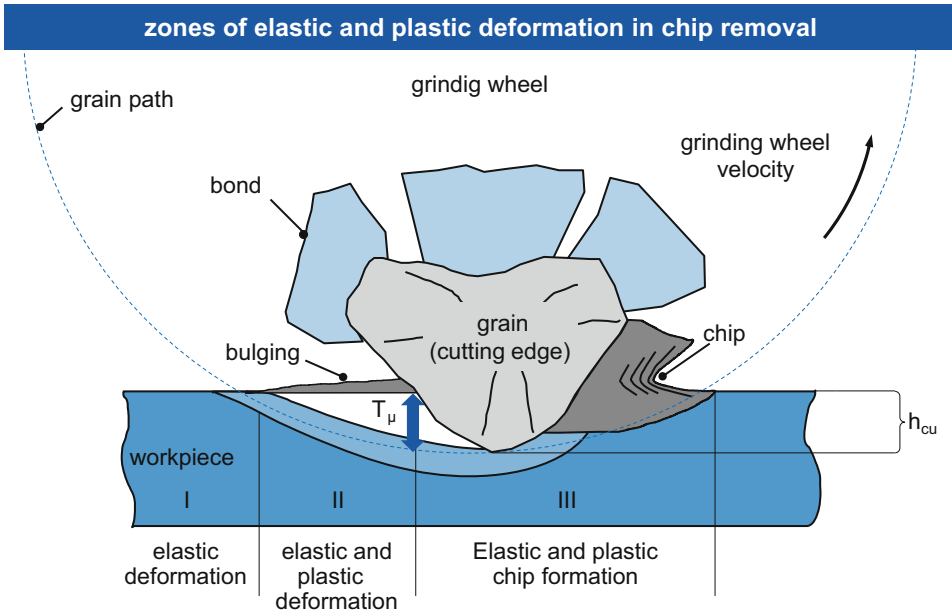
²Research Area Manufacturing Technology - Research Group Grinding, Laboratory for Machine Tools and Production Engineering (WZL) of RWTH Aachen University, Aachen, Germany

Definition

The chip formation in abrasive processes defines the local interaction between abrasive grains and workpiece material in combination with the surrounding fluid media (cooling lubricant or air). It can mainly be distinguished between brittle and ductile removal mechanisms.

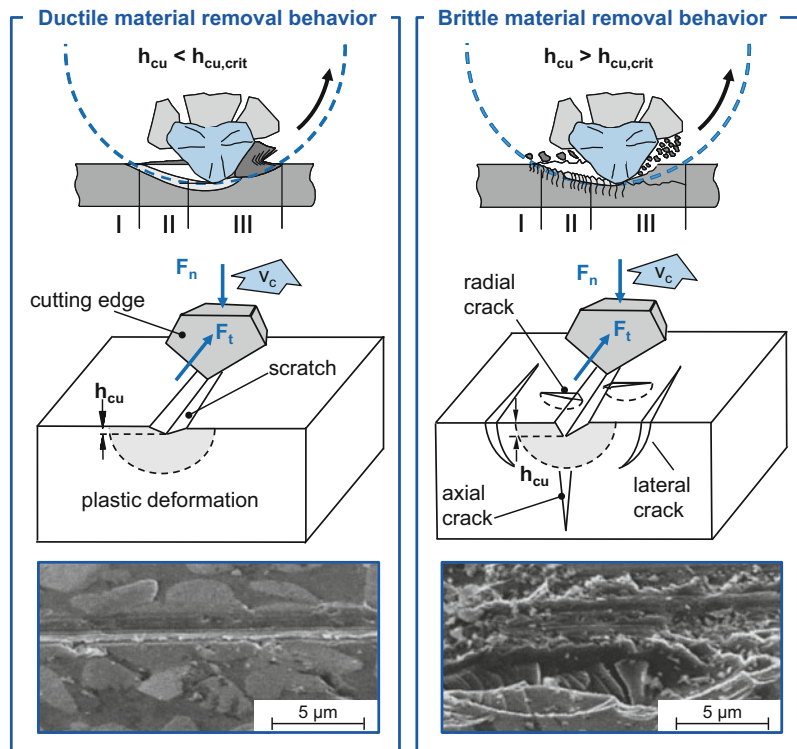
Theory and Application

The common removal mechanisms in grinding can be divided into ductile material removal and brittle material removal. For ductile materials, the chip formation can be distinguished in three zones beginning with zone one, where elastic deformation takes place (see Figs. 1 and 2 left). Because of the shape of the grain, the rake angle is very small at the beginning of the engagement. As the grain continues to penetrate the material, the stress exceeds the yield strength which results in a development of plastic strain. This is labeled as zone two on the left side of Fig. 1. In zone three, the grain penetrates deeper until the chipping thickness h_{cu} corresponds to the grain cutting depth T_{ls} where



Chip Formation (Abrasive Process), Fig. 1 Zones of elastic and plastic deformation and separation in chip removal (Klocke 2009)

Chip Formation (Abrasive Process), Fig. 2 Brittle material behavior versus ductile material behavior in grinding (Based on Saljé and Möhlen 1987; Klocke 2009)



material separation starts. The depth of cut T_μ might be considered as the minimal chip thickness. The value of T_μ is influenced by the applied coolant and the friction coefficient between the grain and the workpiece material (Klocke 2009).

The machinability of brittle materials (e.g., glasses, high-performance ceramics) significantly differs in contrast to the machining of metallic materials. When machining brittle materials with increasing penetration depths, material separation is dominated by the characteristic behavior of brittle materials. Elastic and plastic deformation is little. Chip formation is dominated by crack initiation and crack growth. As the grain cutting edge penetrates into the brittle material, radial and lateral cracks occur (see Fig. 2, right). In this case, the chip removal takes place by means of lateral cracks, which causes spalling of the material on the one hand. On the other hand, axial cracks lead to permanent damage to surface layer (see Marshall et al. 1983; Saljé and Möhlen 1987; Bifano et al. 1991; Klocke 2009).

For brittle materials, Bifano confirmed the hypothesis that even hard and brittle materials could be ground at a ductile regime as long as the chip thickness remains below the critical chip thickness $h_{cu,crit}$ (Fig. 2, left). His experiments showed a certain relation between the results and Eq. 1 (see Bifano 1988; Bifano et al. 1991).

$$h_{cu,crit} = b \cdot \left(\frac{E}{H}\right) \cdot \left(\frac{K_{IC}}{H}\right)^2 \quad (1)$$

where

$h_{cu,crit}$: critical undeformed chip thickness [μm]

b : tool-specific constant

E : elastic modulus [N/mm^2]

H : Vickers hardness [GPa]

K_{IC} : fracture toughness [$\text{MPa}\cdot\text{m}^{1/2}$]

Cross-References

- ▶ [Grinding](#)
- ▶ [Machinability](#)
- ▶ [Ploughing](#)
- ▶ [Ultraprecision Grinding](#)

References

- Bifano TG (1988) Ductile regime grinding of brittle materials. PhD-thesis, North Carolina State University
- Bifano TG, Dow TA, Scattergood RO (1991) Ductile regime grinding, a new technology for machining brittle materials. *J Eng Ind Trans ASME* 113(2):184–189
- Klocke F (2009) *Manufacturing processes 2: grinding, honing, lapping* (trans: Kuchle A). Springer, Berlin
- Marshall DB, Evans AG, Khuri Yakub BT, Tien JW, Kino GS (1983) The nature of machining damage in brittle materials. *Proc R Soc Lond A* 385:461–475
- Saljé E, Möhlen H (1987) Prozessoptimierung beim schleifen keramischer werkstoffe [Optimization of grinding processes for engineering ceramics]. *Ind Diam Rundsch* 21(4):243–247. (in German)

Chip-Forms

- ▶ [Chip-Forms, Chip Breakability, and Chip Control](#)

Chip-Forms, Chip Breakability, and Chip Control

I. S. Jawahir

Institute for Sustainable Manufacturing, College of Engineering, University of Kentucky, Lexington, KY, USA

Synonyms

[Chip breakability](#); [Chip breaking](#); [Chip-forms](#)

Definition

Chip control involves *efficient breaking* and *effective removal of chips*.

Theory and Application

Introduction

Significance

Chip control is an essential aspect of automated machining. The basic functional elements of chip

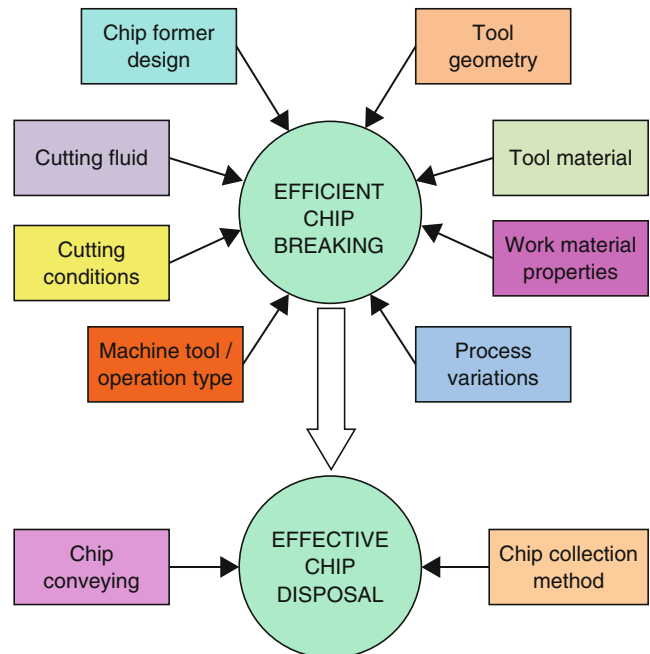
control are *efficient breaking* and *effective removal of chips*. The former helps to facilitate the latter; hence much of the fundamental work in the past has been on finding ways and means to break chips efficiently to enable effective removal from the machines and the subsequent recycling/disposal. Figure 1, which shows the most influencing factors on chip breaking, demonstrates the complex nature of the chip-breaking process. Each of the eight factors shown has a profound effect on chip breaking. Greater understanding of these influencing factors and their interactions would be essential for achieving efficient chip breaking and hence chip control.

The need for chip breaking is significant in continuous operations (such as turning and drilling). Unbroken chips can cause numerous problems in machining including damage to the machined surface, cutting tool, and machine tool itself and can be harmful to machine operators and shop floor workers. All of these effects may lead to added costs, due to scrap parts, lost machining time, and delay in the delivery of parts, in addition to the unplanned health-care costs. In general, it has been shown that efficient chip control in machining contributes to the following:

- Reliability of the machining process
- Production of high-quality machined surfaces
- Increased productivity
- Safety of operation, including operator’s safety, and protection of machine tool and the cutting tool

Chip-form and chip breakability, in combination, indicate the degree of chip control. Unfortunately, no single computer-aided process planning (CAPP) system currently can predict the level of achievable chip control adequately, even though the cutting tool industry continues to develop and promote “chip chart” methods for increased marketability of their cutting tools. In modern unattended machining applications, lack of chip control is a chronic source of unplanned interruptions and problems leading to (a) loss of production time, (b) out of specification sizes and finishes, (c) rapid tool wear, and even (d) catastrophic tool failure. Thus, a better understanding on the mechanisms of chip formation, chip curl, and breaking processes is essential for machining process planning operations. Also, the knowledge of the mechanics of the chip-breaking process and the

Chip-Forms, Chip Breakability, and Chip Control, Fig. 1 Most influencing factors on chip breaking and disposal. (Adapted from Jawahir and van Luttervelt 1993)



chip material properties are necessary to establish any meaningful chip breakability criterion.

Figure 2 shows typical 2D and 3D chip-breaking processes. The precursor to chip breaking is the most desirable chip flow and curl. While each of the eight factors identified in Fig. 1 would be expected to influence the chip flow and curl, their combined effect needs to be studied for designing the chip-forming process for optimal chip-breaking performance. There has also been considerable effort to understand the optimal level of chip breaking. In order to plan for the most desirable type of chip-forms in machining, it is essential to understand the categories of chips that are attainable from combinations of conditions.

Figure 3 shows a simplified, ISO-based chip-form classification chart, which can be used for quantitative evaluation of the size and shape of the chips being produced from machining operations. This chart shows that the most commonly produced chips can be classified into eight groups in terms of their size and shape (Jawahir 1986).

Chip-Forming Tool Inserts

For over the last several decades, the cutting tool industry has been developing and introducing a wide variety of chip-control devices, known as chip breakers (also known as chip formers) – namely, tool inserts with varying chip-groove designs and configurations. With the never-ending market competition, the cutting tool industry groups

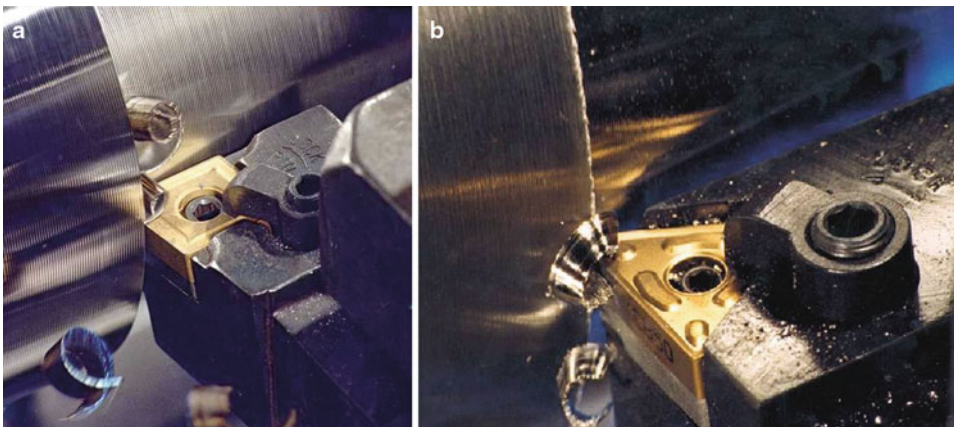
compete with each other in developing more and more functional chip-breaking tool inserts, largely using empirical methods, with little research involving fundamental studies to understand the basic mechanisms for chip-forms and chip-breaking modes. Figure 4 shows a representative sample of chip-forming tool inserts currently used in a variety of machining operations.

As seen, the complex 3D chip-groove geometry, coupled with advanced coatings, offers the functionality for these tool inserts. A closer look at the chip-forming tool geometry (Fig. 5) reveals the extremely complex geometric patterns including variable groove size and obstruction backwall configurations in a typical grooved tool insert.




















Figure 6 shows the variation of chip-forming mechanisms when machining of a given work material with the same tool insert but under different cutting conditions and on different geometric features of the workpiece. Unfortunately, predictive knowledge is still largely lacking for chip breaking due to the large number of complex variables involved in the machining process, including the complex tool geometry, tool material types (tool grade and coating), work material properties, and the interacting cutting conditions.

Cutting Edge Preparation and Chip-Groove Designs

The design of cutting edge and the chip-forming groove configurations play a significant role in

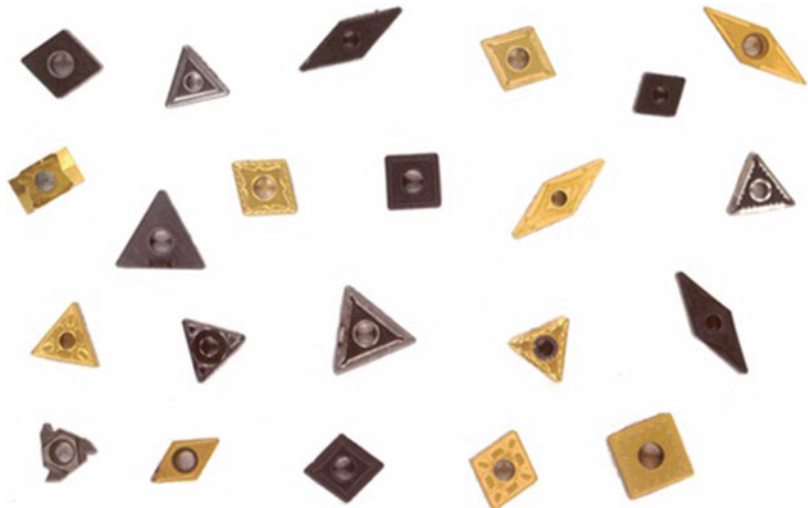


Chip-Forms, Chip Breakability, and Chip Control, Fig. 2 (a, b) Typical 2D and 3D chip-breaking mechanisms. (Courtesy: Kennametal, Inc.)

1	2	3	4	5	6	7	8
RIBBON CHIPS	TUBULAR CHIPS	CORK SCREW CHIPS	HELICAL CHIPS	SPIRAL CHIPS	ARC CHIPS	ELEMENTAL CHIPS	NEEDLE CHIPS
							
Short	Short	Short	Short	Flat	Loose		
							
Long	Long	Long	Long	Conical	Connected		
							
Snarled	Snarled	Snarled	Snarled	Short			

Chip-Forms, Chip Breakability, and Chip Control, Fig. 3 Simplified ISO-based chip-form chart (Jawahir 1986)

Chip-Forms, Chip Breakability, and Chip Control, Fig. 4 Representative sample of commercially available cutting tool inserts



developing chip-forms and the subsequent chip-breaking process in machining. While there are no universally acceptable standards as yet for these design features, the cutting tool industry continues to develop a large range of designs to suite specific

applications involving various work materials, tool materials, and cutting conditions. Figure 7 shows a range of cutting edge designs (straight, chamfered, and rounded edges), tool face designs for chip curling (obstruction type and narrow restricted contact configurations), conventional groove designs (standard and raised backwall designs), and complex groove designs with variable groove geometry for 3D chip-form (Jawahir and van Luttervelt 1993).

When a combination of these geometric configurations is incorporated into a tool insert design, the usual result is an ideally developed 3D chip-form with chip breaking as shown in Fig. 8.

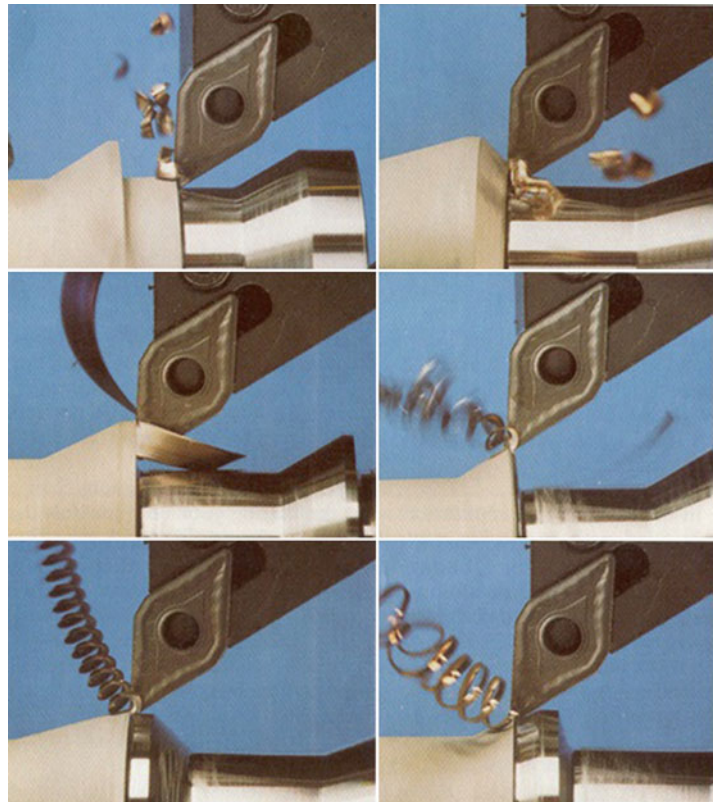
Commonly known geometric parameters in a typical 2D chip groove are shown in Fig. 9. Proper design of a chip groove for a given application would employ suitably selected combination of these geometric parameters.

With the growing emphasis on product quality, reliability, and cost-effectiveness, it has become even more important to develop a comprehensive

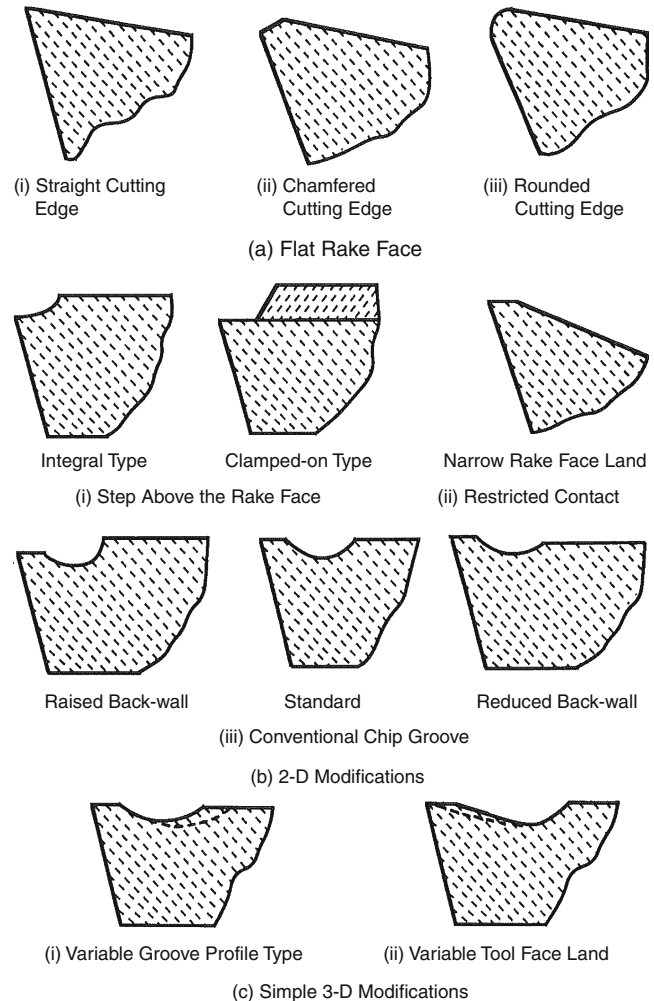


Chip-Forms, Chip Breakability, and Chip Control, Fig. 5 Complex chip-groove geometry in a cutting tool insert

Chip-Forms, Chip Breakability, and Chip Control, Fig. 6 Variation of chip-forming mechanisms in machining with the same tool insert (Sandvik 1996)



Chip-Forms, Chip Breakability, and Chip Control, Fig. 7 Variation of cutting edge designs and chip-forming groove design for tool inserts (Jawahir and van Luttervelt 1993)



understanding of the machining process to help process planners select the optimum cutting tool inserts and cutting conditions for given work materials for the most desirable chip-breaking levels. The wide range of empirically designed cutting tool inserts by the cutting tool industry demonstrates complex chip-groove geometries to attain an effective optimal level of chip control. However, in order to enable more effective design and selection of cutting tool inserts, a better understanding of the chip flow and chip curl mechanisms would be required. Nakayama and his colleagues (Nakayama 1962, 1984; Nakayama and Ogawa 1978) and Spaans (1971) made significant early contributions on chip flow, chip curl, and chip breaking. Results from the CIRP's international cooperative work on

chip control were also reported in two major CIRP keynote papers: Kluft et al. (1979) and Jawahir and van Luttervelt (1993).

Chip Morphology

The basic chip morphology results from chip flow and chip curl mechanisms. Three-dimensional chip-form can be characterized in terms of chip side-flow (chip motion from perpendicular to the feed direction), side-curl (chip curl in the plane of the cutting edge), and up-curl (chip curl out of the plane of the cutting edge) as illustrated in Fig. 10.

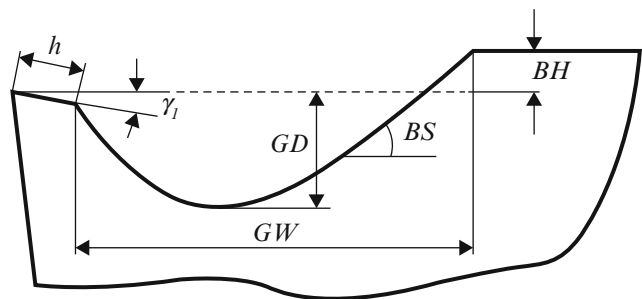
More general 3D chip flow and curl patterns were identified by Jawahir and Fang (1995). Chip flow in a grooved tool basically consists of

side-flow and *backflow* whereas chip curl consists of *up-curl* and *side-curl*. Figure 11 shows the combined effects of chip side-flow (η_s) and chip backflow (η_b) on 3D chip flow.



Chip-Forms, Chip Breakability, and Chip Control, Fig. 8 3D chip breaking from optimally designed cutting edge configuration and chip groove (Sandvik 1996)

Chip-Forms, Chip Breakability, and Chip Control, Fig. 9 Most common chip-groove geometric parameters



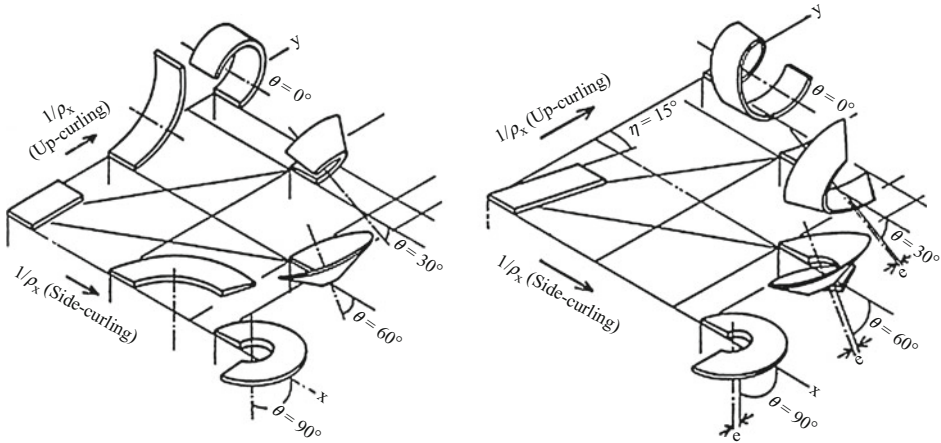
- h : primary land
- γ_1 : primary rake angle
- GW : groove width
- BH : backwall height
- BS : backwall slope angle
- GD : groove depth

These four parameters are needed for a comprehensive assessment of the 3D chip-form.

Slip-Line Models for Curled Chip Formation

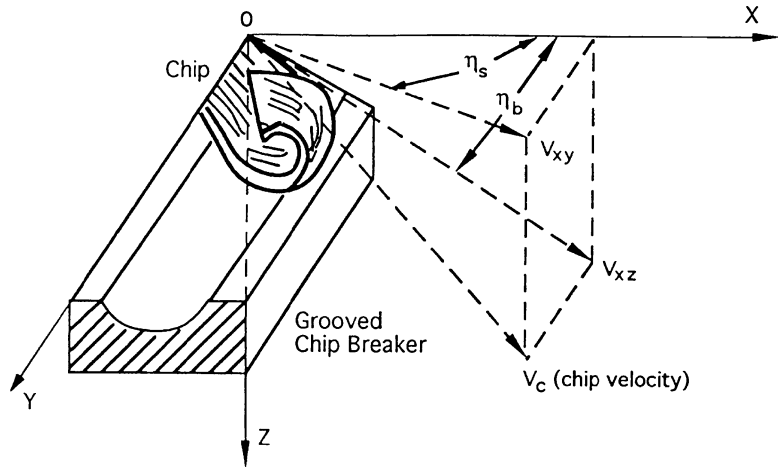
Dewhurst (1978) showed an inherent predictive capability of curled chip formation in orthogonal machining with flat-faced tools using slip-line field theory. He showed that the machining process is not uniquely defined by any given set of steady-state cutting conditions. A new universal slip-line model and the associated hodograph for machining with restricted contact tools, which take account of chip up-curl and backflow and provide nonunique solutions to machining processes, were recently proposed by Fang et al. (2001). With appropriate assumptions, this model can be decomposed to six slip-line models previously developed for machining by Shi and Ramalingam (1993), Dewhurst (1978), Kudo (1965), Usui and Hoshi (1963), Johnson (1962), Lee and Shaffer (1951), and Merchant (1944).

The universal slip-line field model offers a predictive capability for the following machining variables. The nondimensionalized cutting forces (F_c/kt_1w and F_t/kt_1w), where F_c and F_t are the cutting and thrust force components, k is the shear flow stress, t_1 is the undeformed chip thickness, and w is the width of cut, and chip up-curl radius (R_u), chip thickness (t_2), and the chip backflow angle (η_b) are determined using this model.



Chip-Forms, Chip Breakability, and Chip Control, Fig. 10 Variation of chip-form by up-curling and side-curling (Nakayama 1984)

Chip-Forms, Chip Breakability, and Chip Control, Fig. 11 Three-dimensional chip flow as a result of combined chip backflow and chip side-flow (Jawahir and Fang 1995)



Cutting forces:

$$\frac{F}{kt_1w} = \frac{F_{CA}}{kt_1w} + \frac{F_{CD}}{kt_1w} + \frac{F_{DB}}{kt_1w} \quad (1)$$

Chip up-curl radius:

$$R_u = \frac{1}{2} \times \sqrt{\left(\frac{V}{\omega}\right)^2 + \left(\frac{\rho}{\omega}\right)^2 + 2 \cdot \frac{\zeta}{\omega} \cdot \frac{\rho}{\omega} \cdot \cos \alpha_1} + \frac{V_{g'}}{2\omega} \quad (2)$$

where $\alpha_1 = \pi - \gamma_1 - \zeta + \theta + \psi - \eta_1 - \eta_2$

Chip thickness:

$$t_2 = 2 \left(\frac{V_{g'}}{\omega} - R_u \right) \quad (3)$$

Chip backflow angle:

$$\eta_b = \arctg \frac{V_{g'x}}{V_{g'y}} \quad (4)$$

This work has subsequently been extended to machining with a grooved tool to predict the effects of such groove parameters as the groove width and groove backwall height by Wang and Jawahir

(2002), and combined with Oxley's predictive model (Oxley 1989), the effects of strains, strain rates, and temperatures have been considered by Fang and Jawahir (2002). More recently, Wang and Jawahir (2007) extended this model to include machining with rounded cutting edge restricted contact grooved tools and developed an analytical predictive model for cutting forces, chip thickness, chip up-curl radius, stresses, strains, strain rates, and temperatures. Figure 12 shows this slip-line model and the associated hodograph.

Five nonlinear equations are established to solve for the five slip-line field angles, θ_1 , θ_2 , ψ , η_1 , and η_2 :

$$\begin{cases} f_1 = \mu_b \cdot F'_x - F'_y = 0 \\ f_2 = M' + F'_x \cdot CC_1 - F'_y \cdot CC_2 = 0 \\ f_3 = h^2 - (X_{f-gf} - Y_{f-bf})^2 + (X_{f-bf} + Y_{f-gf})^2 = 0 \\ f_4 = h^2 - (X_{l-hl} - Y_{l-hl})^2 + (X_{l-gl} + Y_{l-gl})^2 = 0 \\ f_5 = \left(R_u + \frac{t_2}{2}\right) \sin(\gamma_2 + \eta_g) - \frac{GW'}{2} = 0 \end{cases} \quad (5)$$

Based on this model, predictions can be made for the state of stresses in all contact regions, along with temperatures, chip backflow angle, chip up-curl radius, chip thickness, cutting forces, etc. (Wang and Jawahir 2007). The combined effects of cutting edge radius and the chip-groove parameters are also established, with predictions experimentally verified.

3D Chip Formation

A 3D chip-form is produced as a result of varying degrees of chip up-curl, chip backflow, chip side-curl, and chip side-flow. For classification of the chip-form, the twist angle in a chip (see Fig. 13) can be used to quantify the individual contributions of up-curl and side-curl. For a pure up-curved chip, the twist angle q is 0° , whereas for a pure side-curved chip, it is 90° .

Using the classic theories of mechanics, modeling the 3D chip-breaking process has been attempted as shown in Fig. 14 (Ghosh et al. 1998).

Cyclic Chip Formation

Cyclic chip formation refers to the periodic chip formation process of birth, growth, and final

breaking of chips. The study of cyclic chip formation is important because in practice chip formation is rarely a uniquely defined process that can be represented by a quasi-static condition but rather a cyclically repeated application of a time-dependent process involving chip formation, chip-form development, and chip fracture. Even if the cycles are not exactly repeatable, they indicate the history of chip formation and trace back important information to connect with the process mechanics. One of the earliest discoveries of cyclic chip formation in turning operations was reported by Jawahir (1986). This work was followed by an extensive experimental analysis which revealed cyclic chip formation in 2D and 3D modes (Jawahir 1990). Figure 15 shows a typical 2D chip-breaking cycle.

Chip Breakability

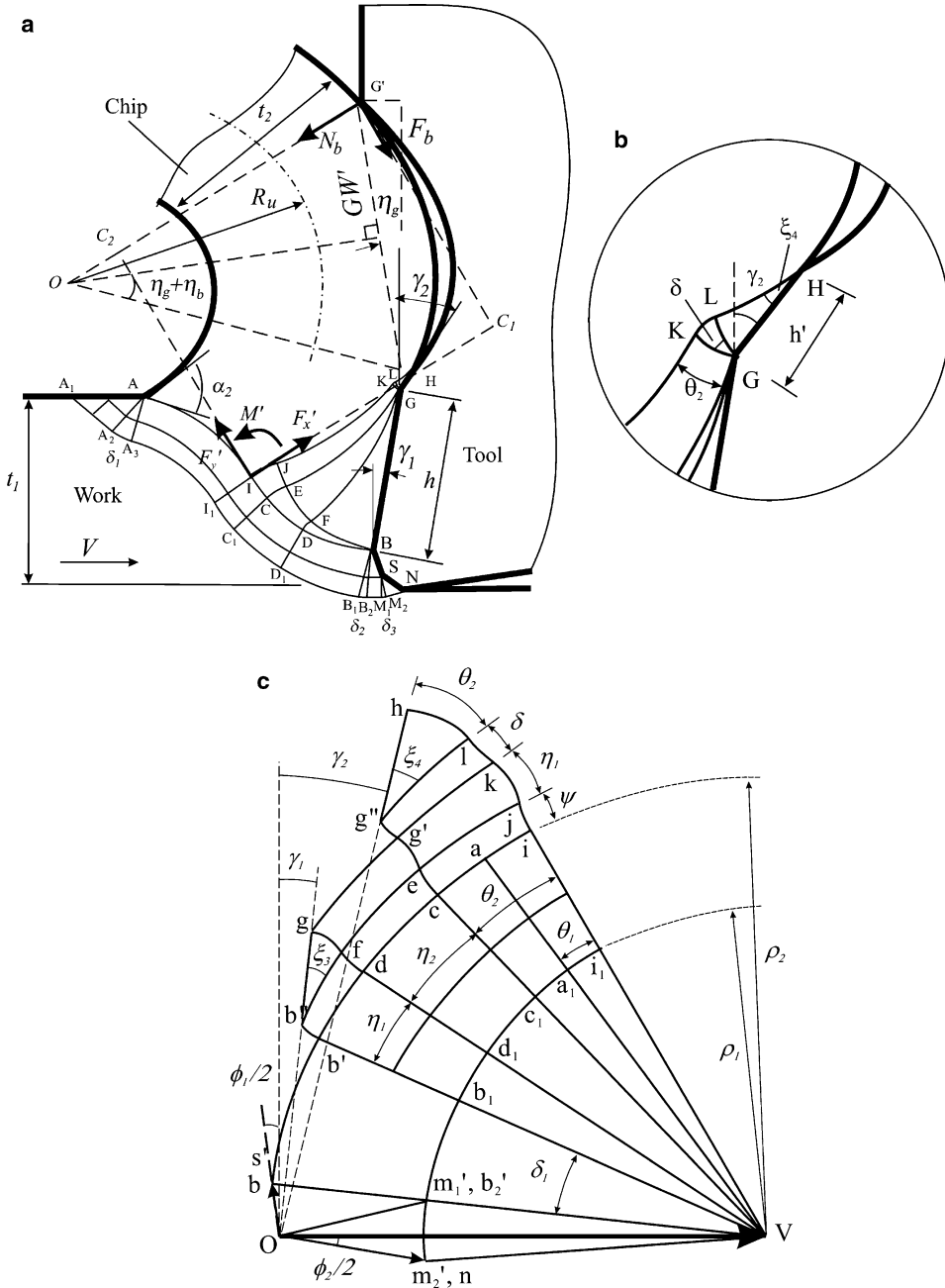
Based on the early work by Nakayama (1962), the chip breakability criterion is established (Fig. 16):

$$\varepsilon_{\max} \leq \frac{t_2}{2} \left[\frac{1}{r_{ui}} - \frac{1}{r_{uf}} \right] \quad (6)$$

where:

- r_{ui} is the initial chip up-curl radius.
- r_{uf} is the final chip up-curl radius.
- ε_{\max} is the ultimate tensile strain of the chip material.
- t_2 is the chip thickness.

In subsequent work by Ganapathy and Jawahir (1998), a force model was proposed for cyclic chip formation involving chip breaking. The additional force imposed on the machining process model due to the free-end of the chip contacting the workpiece results in a shift in the force equilibrium conditions, which requires a dynamic model to address the changes in the process mechanics with the birth, growth, and breaking of the chip. Fang and Jawahir (1996) presented an analytical model for 2D machining involving cyclic chip formation. The model provides a predictive



Chip-Forms, Chip Breakability, and Chip Control, Fig. 12 (a) Extended universal slip-line model for machining with rounded cutting edge restricted contact

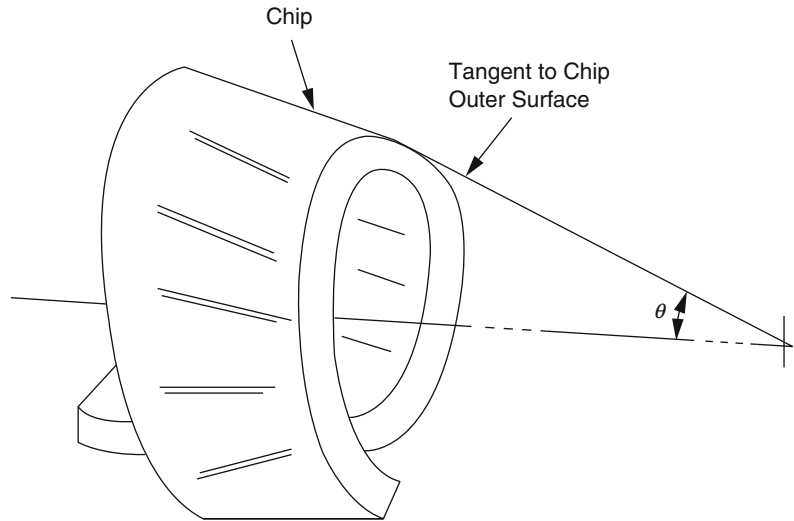
grooved tools: slip-line field. (b) Enlarged secondary rake region. (c) Hodograph (Wang and Jawahir 2007)

capability for forces acting on the chip, bending moment, chip thickness, chip velocity, tool-chip contact length, etc., for input conditions such as work material, cutting conditions, tool

geometry, and chip-work friction conditions at the free-end of the chip. Figure 17 shows an infrared thermal image of the curled chip formation (Wang et al. 1996).

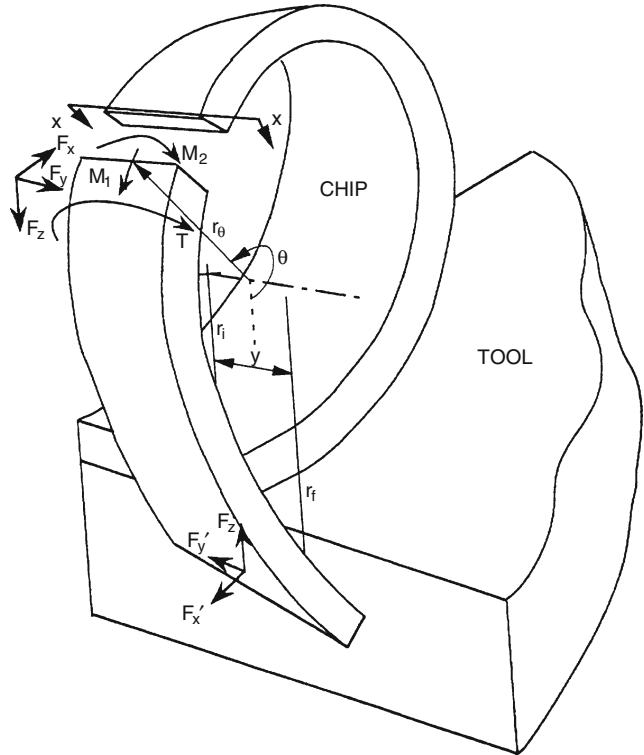
Chip-Forms, Chip Breakability, and Chip Control,

Fig. 13 Definition of twist angle, which would indicate the ratio of up-curl to side-curl in a 3D chip form



Chip-Forms, Chip Breakability, and Chip Control,

Fig. 14 Modeling of reaction forces in a 3D spiral chip-form (Ghosh et al. 1998)

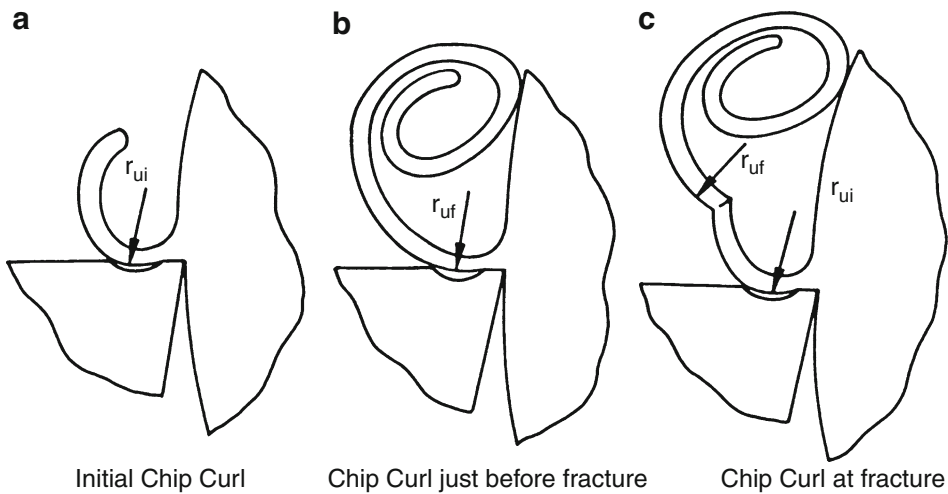
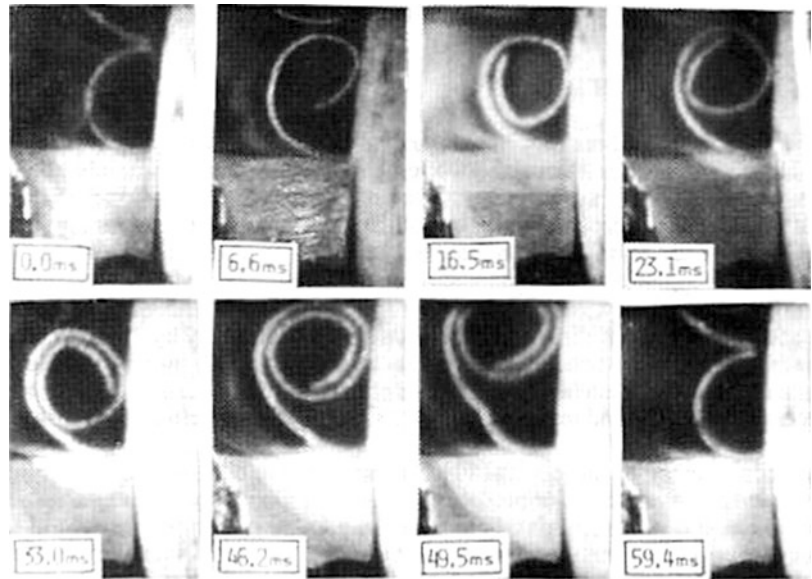


Predicting Chip Breakability

The advent of numerous cutting tool designs involving variations in chip-groove features and tool coatings has made the process planning for machining operations very tedious and complex. A very useful tool for ascertaining the

effectiveness of a cutting tool insert design is a chip chart which maps the size and shapes of chip-forms across a depth of cut-feed matrix as shown in Fig. 18. Detailed observations of the chip chart provide important visual information on the effective chip breakability.

Chip-Forms, Chip Breakability, and Chip Control, Fig. 15 A typical 2D chip-breaking cycle (Jawahir 1986)



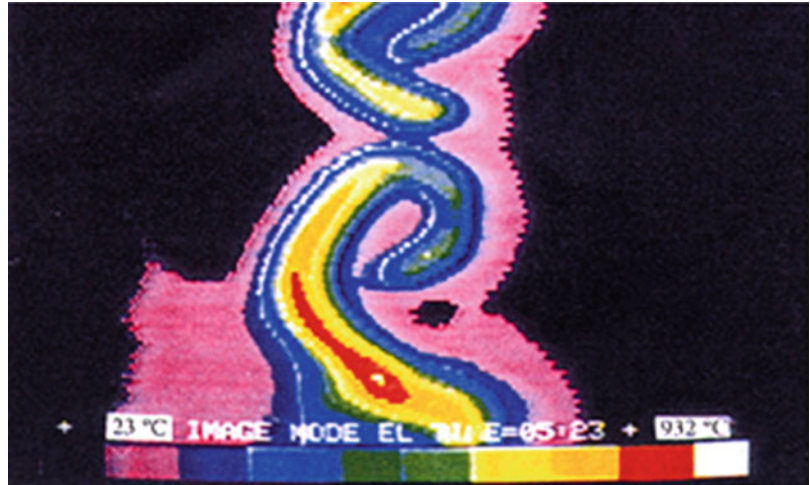
Chip-Forms, Chip Breakability, and Chip Control, Fig. 16 Three major stages of chip breaking (Jawahir 1986)

In an attempt to quantify the information presented visually, researchers have used fuzzy logic techniques to classify and predict chip breakability (Ghosh et al. 1995; Lin et al. 1998). In conjunction with this fuzzy logic approach, a new chip-groove classification system was proposed, and the most significant geometric chip-groove parameters were identified from chip-groove profiles. A fuzzy rule-based system was developed based on the composite profile of the tool insert and its chip breakability performance.

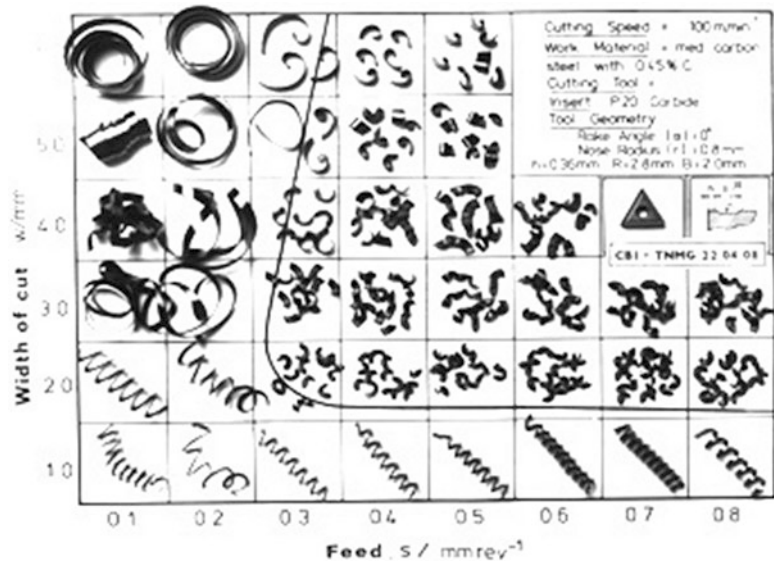
This new method for quantifying chip breakability was derived based on the fundamentals of fuzzy reasoning. It is assumed that the following three factors and the associated weighting factors determine the levels of chip breakability:

- *Size of chip* produced (60%): defined by the dimensional features such as length and other geometric parameters, e.g., diameter or curl radius of the chip or chip coil.

Chip-Forms, Chip Breakability, and Chip Control, Fig. 17 Typical cyclic chip formation sequence (Wang et al. 1996)



Chip-Forms, Chip Breakability, and Chip Control, Fig. 18 Typical chip chart showing wide variation of chip-forms over a feed depth of cut matrix



- *Shape of chip* produced (25%): defined by the geometric configurations of the chip such as helical form, spiral form, and arc shape.
- *Difficulty/easiness of chip producibility* (15%): defined by the characteristics of the produced chip, for example, smoothness of the chip surface, chip color, and any resulting burr formation. These characteristics are expected to reflect other performance measures such as cutting power, surface finish, and tool wear.

It is quite obvious that all three factors are fuzzy in nature owing to the “uncertainty” in

their definition levels, i.e., there are no well-defined boundaries. Chip breakability is classified into five fuzzy sets: Very Poor (VP), Poor (P), Fair (F), Good (G), and Excellent (E). In further analysis, a numerical rating system from 1 to 5 was used for representing these five levels of chip breakability. For example, chip-forms between Poor (P) and Fair (F) may be assigned a value, based on their relative sizes and shapes, e.g., 2, 2.3, 2.5, 2.7, and 3. This avoids the inaccuracy caused by having to classify a chip-form that is in between F and P to a discrete value of either F or P. A rule-based predictive system for

chip breakability was developed based on the analysis of effective chip-groove profile and is extended to include predictions for varying cutting conditions such as side-cutting edge angle, nose radius, and cutting speed with limited experiments.

The rule-based operation developed is of the following form:

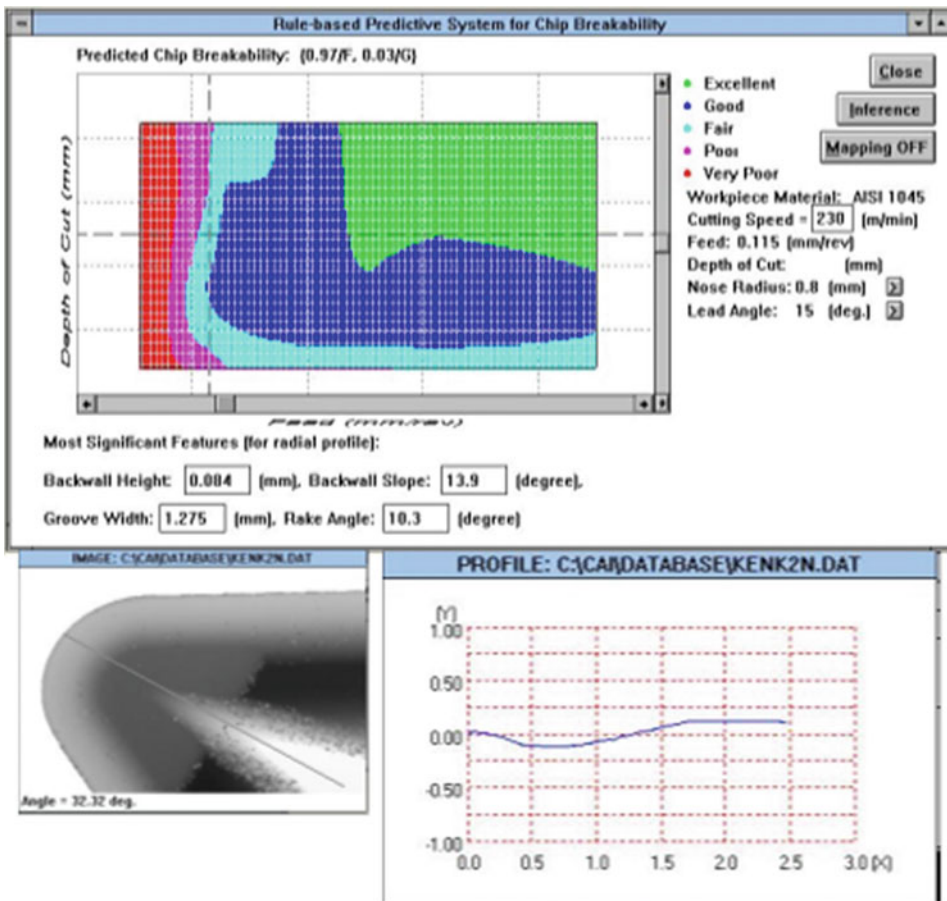
- **IF** Groove width is {GW} and backwall height is {BH} and backwall slope is {BS} and rake angle is {RA} ...
- **AND** Other conditions hold
- **THEN** Chip breakability is {CB}
- **AND** Chip breakability certainty level is {certainty}

The results of this rule-based operation are then post-processed using a fuzzy inference engine to obtain the final prediction.

Case Study 1: Predicting Chip Breakability in Turning Operation

Figure 19 shows the predicted chip breakability for a given cutting tool insert in machining of AISI 1045 steel, based on a 2D cross-sectional chip-groove profile obtained from a 3D image of the cutting tool insert.

This figure represents an interactive system developed for predicting the level of chip breakability, with statistical and probabilistic certainties, for a given set of cutting conditions



Chip-Forms, Chip Breakability, and Chip Control, Fig. 19 Predicted chip breakability for a specified grooved tool insert based on 2D chip-groove profile obtained from a 3D image of the tool insert (Jawahir et al. 2000)

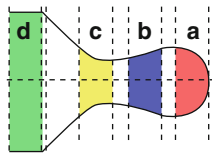
(cutting speed, feed, and depth of cut), tool insert material and geometry (tool grade, insert style, nose radius, groove parameter, etc.), and work material. This interactive predictive system uses predicted effective direction of chip flow. Figure 19 also shows that for a given tool insert with the effective chip-groove profile shown for the predicted chip flow angle of 32.32° , the following groove parameters are established: tool backwall height is 0.084 mm, backwall slope is 13.9° , tool groove width is 1.275 mm, and the effective tool rake angle is 10.3° . For this tool insert, in machining of AISI 1045 steel at a cutting speed of 230 m/min., the predicted chip chart is also shown in Fig. 19 with five different chip breakability ratings in color codes. The actual predicted chip breakability for the given set of

feed and depth of cut is 97% “Fair” and 3% “Good” chips. This predictive method has significant practical value for machining process planning applications, and this system has also been successfully used in automotive machining by a US automobile manufacturer.

Case Study 2: Improved Chip Breakability via Process Optimization in Contour Turning

In finish contour turning of AISI 1045 steel by a particular tool insert, at a feed of 0.10 mm/rev and the depth of cut 0.4 mm, the achievable chip breakability was very poor (see Fig. 20) (Hagiwara et al. 2009).

The unbroken, long, snarled chips obtained were detrimental to the machined surface and often caused tool breakage, consumed more



	d	c	b	a
$f = 0.10$ mm/rev (const.) $a_n = 0.4$ mm (const.)				
$f = 0.16$ mm/rev (const.) $a_n = 0.4$ mm (const.)				
Optimization Results for Case 2 $C_R = 0.2$, $C_{CR} = 0.8$ $a_n = 0.4518$	 $f = 0.1312$	 $f = 0.1338$	 $f = 0.1349$	 $f = 0.1600$

Chip-Forms, Chip Breakability, and Chip Control, Fig. 20 Improved chip breakability with increased feed and optimal cutting conditions (Hagiwara et al. 2009)

power during machining, and were sometimes harmful to the machine operators. High-speed filming results show that an increase in feed by 60% improves the chip breakability while imposing optimized cutting conditions, with a higher weighting applied to chip breaking, and produces almost ideal chip breaking and chip-forms.

Cross-References

- ▶ [Cutting, Fundamentals](#)
- ▶ [Machinability](#)

References

- Dewhurst P (1978) On the non-uniqueness of the machining process. *Proc Roy Soc Lond A* 360:587–610
- Fang XD, Jawahir IS (1996) An analytical model for cyclic chip formation in 2-D machining with chip breaking. *Ann CIRP* 45(1):53–58
- Fang N, Jawahir IS (2002) An analytical predictive model and experimental validation for machining with grooved tools incorporating the effects of strains, strain-rates and temperatures. *Ann CIRP* 51(1):83–86
- Fang N, Jawahir IS, Oxley PLB (2001) A universal slip-line field model with non-unique solutions for machining with curled chip formation and a restricted contact tool. *Int J Mech Sci* 43(2):557–580
- Ganapathy BK, Jawahir IS (1998) Modeling the chip-work contact force for chip breaking in orthogonal machining with a flat-faced tool. *J Manuf Sci Eng* 120(1):49–56
- Ghosh R, Lin M, Fei J, Jawahir IS, Khetan RP, Bandyopadhyay P (1995) A new feature-based chip-groove classification system for chip breakability assessment in finish turning. In: ASME WAM, San Francisco, Nov 1995, pp 679–701
- Ghosh R, Dillon OW Jr, Jawahir IS (1998) An investigation of 3-D chip curl in machining – part 1: a mechanics-based analytical model. *J Mach Sci Technol* 2(1):91–116
- Hagiwara M, Chen S, Jawahir IS (2009) Contour finish turning operations with coated grooved tools: optimization of machining performance. *J Mater Process Technol* 209(1):332–342
- Jawahir IS (1986) An theoretical and experimental study of the effects of tool restricted contact on chip breaking. PhD thesis. University of New South Wales, Sydney
- Jawahir IS (1990) On the controllability of chip breaking cycles and modes of chip breaking in metal machining. *Ann CIRP* 39(1):47–51
- Jawahir IS, Fang XD (1995) A knowledge-based approach for designing effective grooved chip breakers – 2D and 3D chip flow, chip curl and chip breaking. *Int J Adv Manuf Tech* 10:225–239
- Jawahir IS, van Luttervelt CA (1993) Recent developments in chip control research and applications. *Ann CIRP* 42(2):659–693
- Jawahir IS, Balaji AK, Rouch KE, Baker JR (2000) Towards integration of hybrid models for optimized machining performance in intelligent manufacturing systems. In: Proceedings of IMCC, Hong Kong
- Johnson W (1962) Some slip-line fields for swaging or expanding, indenting, extruding and machining for tools with curved dies. *Int J Mech Sci* 4:323–347
- Kluft W, Konig W, van Luttervelt CA, Nakayama K, Pekelharing AJ (1979) Present knowledge of chip control. *Ann CIRP* 28(2):441–455
- Kudo H (1965) Some new slip-line solutions for two-dimensional steady-state machining. *Int J Mech Sci* 7:43–52
- Lee EH, Shaffer BW (1951) The theory of plasticity applied to a problem of machining. *J Appl Mech* 18:405–413
- Lin M, Da ZJ, Jawahir IS (1998) Development and implementation of rule-base algorithms in CAPP systems for predicting chip breakability in machining. In: ICME 98, CIRP international seminar on intelligent computation in manufacturing engineering, 1–3 July, Capri, pp 517–522
- Merchant ME (1944) Basic mechanics of metal cutting process. *J Appl Mech* 11:A168–A175
- Nakayama K (1962) Chip curl in metal cutting process. *Bull Fac Eng Yokohama Natl Univ* 11:1–13
- Nakayama K (1984) Chip control in metal cutting. *Bull Jpn Soc Precis Eng* 18(2):97–103
- Nakayama K, Ogawa M (1978) Basic rules on the form of chip in metal cutting. *Ann CIRP* 27:17–21
- Oxley PLB (1989) Mechanics of machining: an analytical approach to assessing machinability. Ellis Horwood, Chichester
- Sandvik (1996) Modern metal cutting: a practical handbook. Sandvik Coromant, Fair Lawn
- Shi T, Ramalingam S (1993) Modeling chip formation with grooved tools. *Int J Mech Sci* 35(9):741–756
- Spaans C (1971) The fundamentals of three-dimensional chip curl, chip breaking and chip control. Doctoral dissertation. Department of Mechanical Engineering, TU Delft, Netherlands
- Usui E, Hoshi K (1963) Slip-line fields in metal machining which involve centered fans. In: Proceedings of the international production engineering research conference ASME, Pittsburgh, pp 61–71
- Wang X, Jawahir IS (2002) Prediction of tool-chip interface friction and chip-groove effects in machining with restricted contact grooved tools using the universal slip-line model. *Key Eng Mater* 233–236:469–476
- Wang X, Jawahir IS (2007) Recent advances in plasticity applications in metal machining: slip-line models for machining with rounded cutting edge restricted contact grooved tools. *Int J Mach Mach Mater* 2(1):347–360
- Wang L, Saito K, Jawahir IS (1996) Infrared temperature measurement of curled chip formation in metal machining. *Trans NAMRI* XXIV:87–92

CHM

- ▶ [Etching](#)

CIM

- ▶ [Computer-Integrated Manufacturing](#)

Cladistics

- ▶ [Cladistics for Products and Manufacturing](#)

Cladistics for Products and Manufacturing

Hoda A. ElMaraghy^{1,2} and Tarek AlGeddawy³

¹Intelligent Manufacturing Systems Center, University of Windsor, Windsor, ON, Canada

²Canada Research Chair in Manufacturing Systems, Intelligent Manufacturing Systems Centre, University of Windsor, Windsor, ON, Canada

³Department of Mechanical and Industrial Engineering, University of Minnesota, Duluth, MN, USA

Synonyms

[Cladistics](#); [Hierarchical classification](#); [Systematics](#)

Definition

Cladistics is a hierarchical classification technique which reveals evolution courses of organisms based on their shared characters. It was originally introduced and developed by Hennig (1966, republished in English in 1999). Cladistics generates phylogenetic trees (Fig. 1), which are acyclic tree graphs that show the

relationships between the studied entities and are called “cladograms.”

Cladistics Analysis

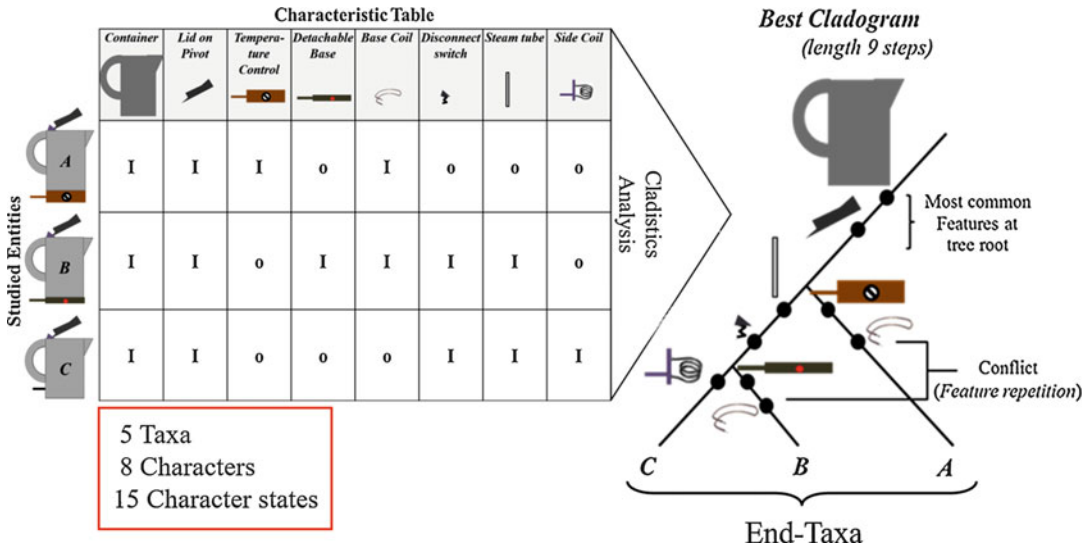
Cladogram Construction

The construction process of cladograms begins with choosing end taxa (singular: taxon), which are the entities to be investigated, placing them at the end of cladogram terminals and then determining the characters that provide relationship evidence. Next, character states inherited by each taxon are identified. A character refers to a feature, and character states represent its different values, ranges, shapes, phases, etc. There are two types of character states:

1. Primitive, where a feature does not exist (e.g., workpiece has no holes) or presents a low-profile state (e.g., workpiece has blind hole)
2. Derived, which represents the existence of a feature (e.g., part is drilled) or a more advanced state (e.g., part has through hole)

The objective of cladogram construction is to generate a minimum length tree, which is referred to as parsimony analysis to reduce information content. A cladogram length is the number of character changes (steps) appearing on a cladogram tree. Character states appear nine times on the cladogram in Fig. 1; consequently it has a nine-step length. Shorter cladogram length indicates a better cladogram with fewer assumptions and conflicts, which means that fewer character states are repeated on branches and also fewer character states are disappearing from evolutionary path after their emergence. Better parsimony suggests a better representative hypothesis of the taxa relationship, having the least information content. A handful of specialized software is dedicated for cladogram construction such as Hennig86, PAUP, NONA, PeeWee, and Phylip that can cluster large data sets very fast.

Using parsimony as an objective for cladogram construction leads to placing common character states at higher tree branches near the tree root, while unique character states would appear near



Cladistics for Products and Manufacturing, Fig. 1 Hierarchical classification using cladistics analysis. (Adapted from AlGeddawy et al. 2017)

tree terminals. Therefore, cladistics outperforms other classification criteria such as distance metrics or maximum likelihood, since many different taxa might have an equal level of overall similarity but do not share as much common characters. Hence, knowledge of the exact common and shared characters among different taxa has the potential for being used in engineering design, planning, and manufacturing, since shared characters can be used as product family platforms, product components and modules, manufacturing system modules, and machine clusters (ElMaraghy et al. 2008).

Reengineered Cladistics Analysis

AlGeddawy and ElMaraghy (2010) divided the parsimony analysis in cladograms construction into two subproblems (Fig. 2): (1) cladogram topological trees layout, where the number of topologies is $n - 1!$, and (2) the taxa arrangement decision at each tree terminal, where the number of arrangements is $n!$ and n is the number of studied taxa. This division provides more flexibility in adding constraints and modifying cost function to suite the criteria and objectives traditionally used in engineering applications. Combining a specific topology with a selected taxa arrangement generates a

cladogram tree which can be populated with characters accordingly.

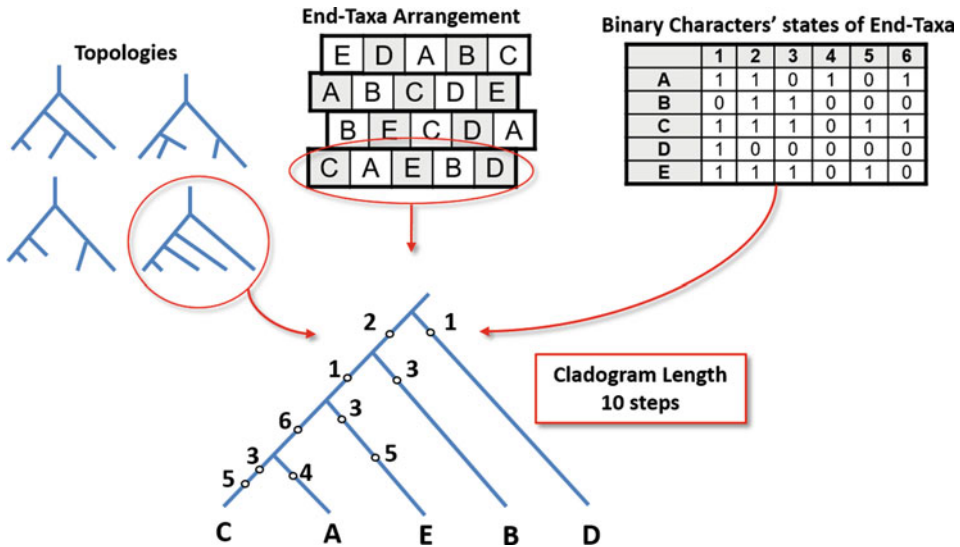
Cladistics Coevolution Analysis

Cladistics has been used extensively in the field of biological systematics. However, cladistics can be used to organize any comparative data. The resulting cladograms can be compared to infer coevolutionary relationships between different classes of species in biology and different sets of entities in any other field. Plotting pairs of cladograms results in “tanglegrams” as shown in Fig. 3. Tanglegrams are constructed to obtain the best untangled graphs without crossed relationships between associated entities. An untangled tanglegram with mirror-image cladograms infers a perfect coevolution of the compared sets of entities, which means reciprocal effects that lead to the emergence of new characters and entities on both sides (AlGeddawy and ElMaraghy 2011).

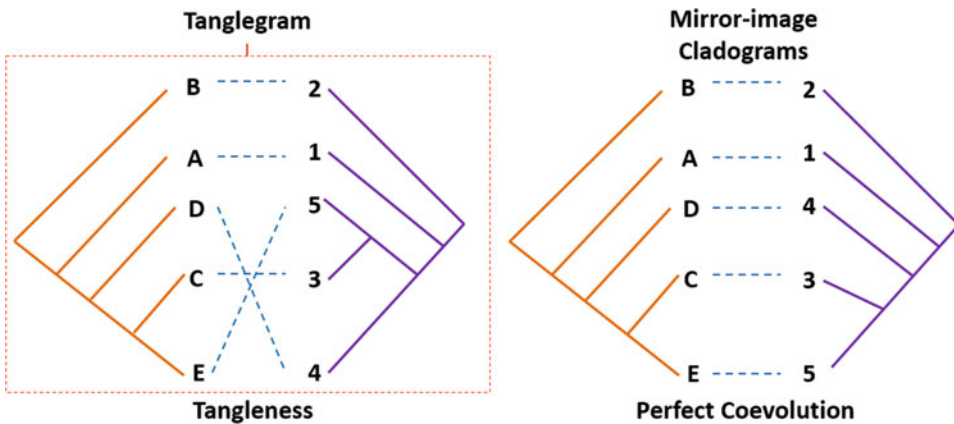
Engineering Applications

Design for Modularity

Cladograms, as a hierarchical classification tool, can be used to represent different ways of integrating and modularizing product architecture.



Cladistics for Products and Manufacturing, Fig. 2 Reengineered cladistics analysis by dividing cladistics analysis into cladogram topology generation and terminal arrangement (AlGeddawy and ElMaraghy 2010)



Cladistics for Products and Manufacturing, Fig. 3 Pair-wise cladogram comparison in a tanglegram for coevolution study (AlGeddawy and ElMaraghy 2011)

Cladogram tree nodes represent different granularity levels of the product, which is equivalent to the depth of its structure and bill of material (BOM). Modularity is evaluated at each granularity level to determine the best architecture and how product components should be integrated or modularized. Component relationships as described by component-based DSM (Fig. 4) are used as the character states that will populate resulting cladograms (AlGeddawy and ElMaraghy 2013a).

Design for Variety

A complete design process is performed when market domain and customer requirements are connected with product architecture. Customer requirements identify the main market segments that need to be addressed by a product variant. The planned variants will have product specifications that are satisfied by many variant structures. Cladistics is used to identify the best group of product variants which meet the product specifications for each

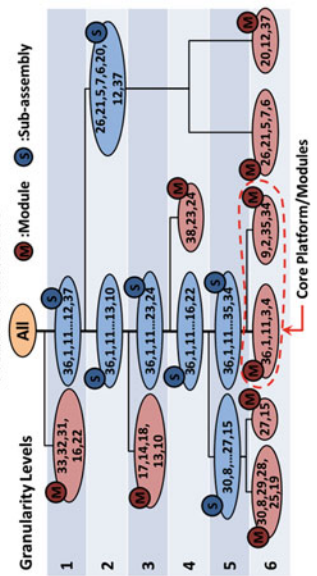


Body-in-White

Product Granularity Cladogram



Product Architecture



Component-DSM

	1	2	3	4	5	6	7	8	9	10	11	12	13	14	15	16	17	18	19	20	21	22	23	24	25	26	27	28	29	30	31	32	33	34	35	36	37	38	
Adapter A-pillar roof rail	1																																						
Adapter B-pillar roof rail	2																																						
Adapter C-pillar roof rail	3																																						
A-pillar reinforcement	4																																						
Back panel	5																																						
Back panel side	6																																						
Back panel upper	7																																						
Body side	8																																						
B-Pillar	9																																						
Channel	10																																						
Cowl	11																																						
Crosstrack rear floor	12																																						
Dash cross member	13																																						
Floor panel	14																																						
Floor panel	15																																						
Front header	16																																						
Front side rail	17																																						
Front suspension housing	18																																						
Hedlitch	19																																						
Rear floor panel	20																																						
Rear floor side	21																																						
Rear header	22																																						
Rear panel inner lower	23																																						
Rear panel inner upper	24																																						
Rear side floor	25																																						
Rear side rail	26																																						
Rear side rail center	27																																						
Rear side rail frt	28																																						
Reinforcement rocker rear	29																																						
Rocker	30																																						
Roof bow	31																																						
Roof panel	32																																						
Roof rail	33																																						
Seat crossmember front	34																																						
Seat crossmember rear	35																																						
Shortgun	36																																						
Shore wheel well	37																																						
Wheelhouse	38																																						

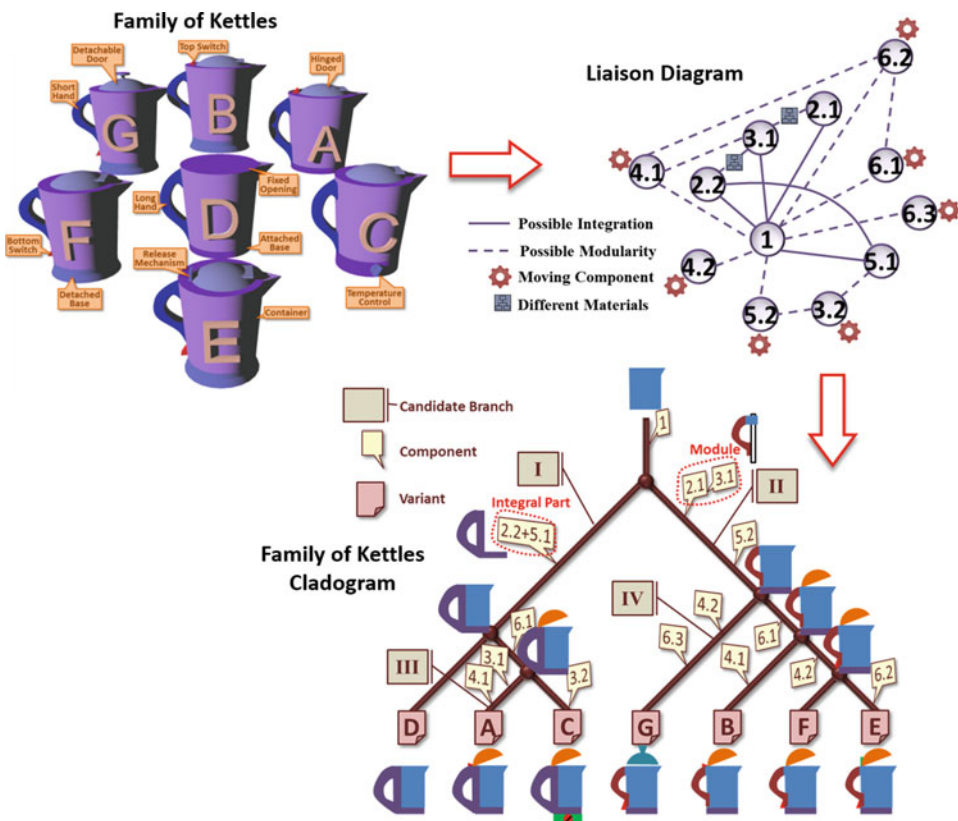
Cladistics for Products and Manufacturing, Fig. 4 Product architecture and granularity levels using cladistics. (Adapted from AlGedday and ElMaraghy 2013a)

market segment (Fig. 5) and at the same time maximize components commonality, modularity, and platforming ability (ElMaraghy and AlGeddawy 2012).

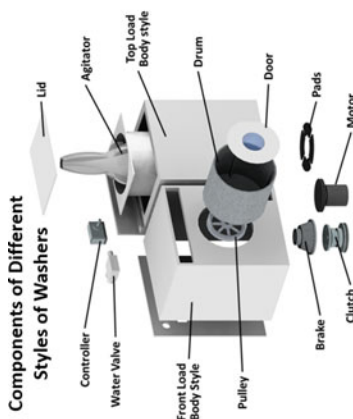
Redesign for Variety

For a set of already existing product variants, grouping based on their common parts and components is essential for assembly and production. Hierarchical classification using cladograms specifies groups of components and parts that are candidate for grouping into either a product platform, shared by all variants, or product modules shared by some variants. Introducing assembly relationships among components

using liaison diagrams (Fig. 6) would also identify components that are candidate for being integrated to reduce part count. A liaison graph is an assembly representation which characterizes an assembly by a network where nodes represent parts and lines between nodes that represent any of certain user-defined relations between assembled parts called “liaisons” which generally include physical contact between parts. This redesign process would result in a compromise between the guidelines of design for assembly (DFA) which aim to reduce number of parts and the guidelines of design for variety (DFV) that tend to divide integral architectures into smaller modules (AlGeddawy and ElMaraghy 2013b).

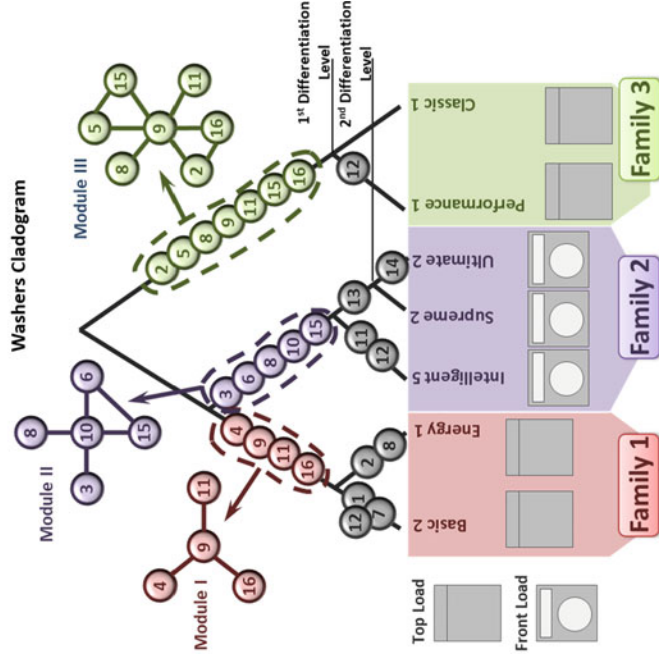


Cladistics for Products and Manufacturing, Fig. 5 Active product family design using cladistics and market segmentation. (Adapted from ElMaraghy and AlGeddawy 2012)



Components of Different Styles of Washers

Requirements	Market Segments & Requirements													
	Load Entrance	Load Capacity		Washing Cycles		Washing Parameters Control		Vibrations Damping		Steaming				
Market Segments	Top	Small 5K	Medium 7K	Large 9K	Basic	Regular	User Defined	No Control	Manual	Auto. Optimization	Normal	Quiet	Super Quiet	Advanced 6-Cycles Motion
Basic	•	•	•	•	•	•	•	•	•	•	•	•	•	•
Classic	•	•	•	•	•	•	•	•	•	•	•	•	•	•
Energy	•	•	•	•	•	•	•	•	•	•	•	•	•	•
Performance	•	•	•	•	•	•	•	•	•	•	•	•	•	•
Intelligent	•	•	•	•	•	•	•	•	•	•	•	•	•	•
Supreme	•	•	•	•	•	•	•	•	•	•	•	•	•	•
Ultimate	•	•	•	•	•	•	•	•	•	•	•	•	•	•



Feasible Product Variant Architectures

Components	Feasible Product Variant Architectures															
	1-Basic Timer	2-Digital	3-Digital	4-Low power	5-High power	6-Direct Drive	7-Water Inlet	8-Water mix control	9-Top Opening	10-Front Opening	11-Pads	12-Support Spring	13-Rod	14-Heater	15-Brake	16-Knobs
Variants	1	2	3	4	5	6	7	8	9	10	11	12	13	14	15	16
Basic	•	•	•	•	•	•	•	•	•	•	•	•	•	•	•	•
Classic	•	•	•	•	•	•	•	•	•	•	•	•	•	•	•	•
Energy	•	•	•	•	•	•	•	•	•	•	•	•	•	•	•	•
Performance	•	•	•	•	•	•	•	•	•	•	•	•	•	•	•	•
Intelligent	•	•	•	•	•	•	•	•	•	•	•	•	•	•	•	•
Supreme	•	•	•	•	•	•	•	•	•	•	•	•	•	•	•	•
Ultimate	•	•	•	•	•	•	•	•	•	•	•	•	•	•	•	•

Cladistics for Products and Manufacturing, Fig. 6 Reactive product family design using cladistics and liaison diagrams. (Adapted from AlGeddawy and ElMaraghy 2013b)

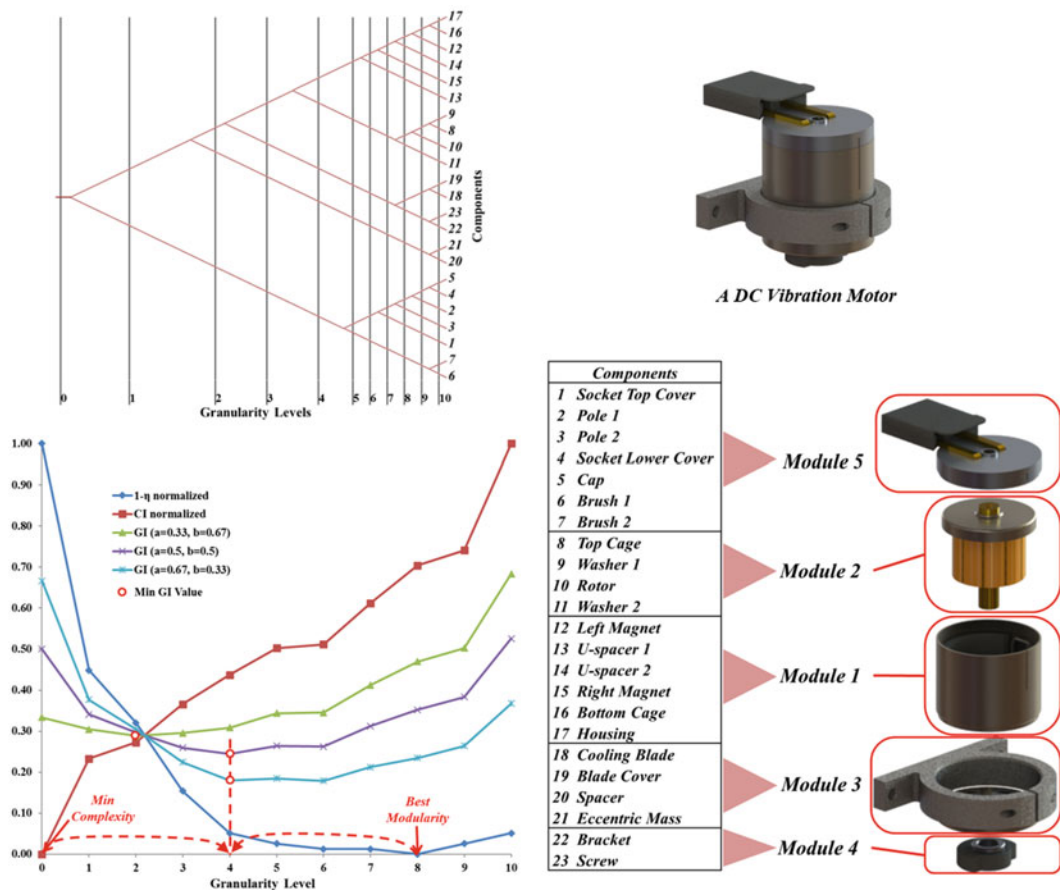
Design for Complexity

Maximizing product modularity helps design for variety (DFV), making it easier for designers and manufacturers to modify existing product family members and generate new product variants to meet market demands and consumers' expectations. Achieving this goal with the least additional cost depends on many factors including the relationships and interfaces between modules which in turn affect assembly complexity, time, and cost. The design for assembly (DFA) methods promote, among other objectives, integration of components when feasible to reduce assembly time, which conflicts increasing product modularity. Cladistics analysis can define product architectures which lie between extreme integration and extreme modularization

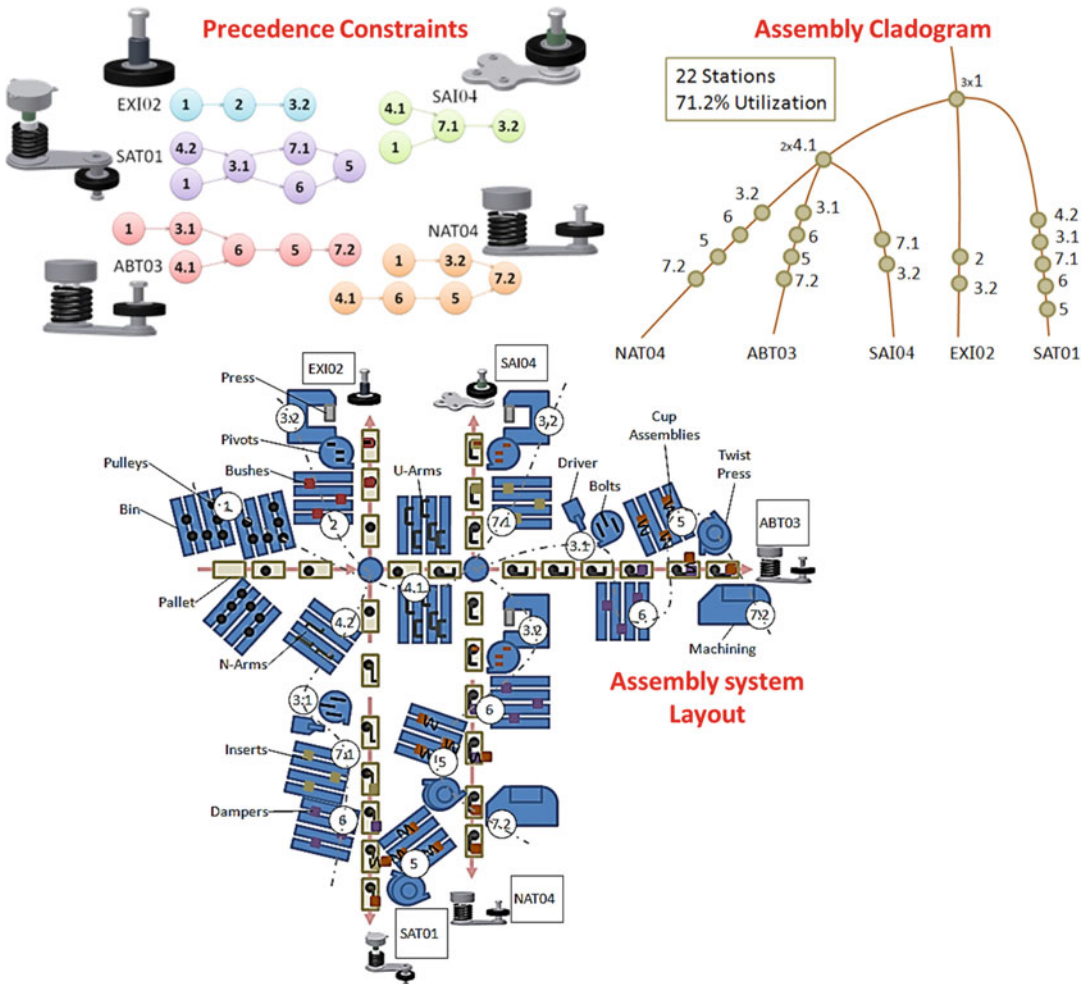
by finding the balance between integration and modularity (Fig. 7) and reducing complexity as a second guiding principle (AlGecddawy et al. 2017).

Design for Delayed Product Differentiation

Product delayed differentiation is a form postponement strategy used in mass customization and is very effective in production planning of product variants. It has been shown that cladistics is a useful tool for developing an assembly system layout which postpones product variants differentiation, defining the points of differentiation, while respecting product precedence constraints and balancing assembly stations for maximum utilization (AlGecddawy and ElMaraghy 2010) as illustrated in Fig. 8.



Cladistics for Products and Manufacturing, Fig. 7 The best granularity level for the optimum complexity and the generated modules. (Adapted from AlGecddawy et al. 2017)



Cladistics for Products and Manufacturing, Fig. 8 Assembly system layout using cladistics for delayed product differentiation. (Adapted from AlGeddawy and ElMaraghy 2010)

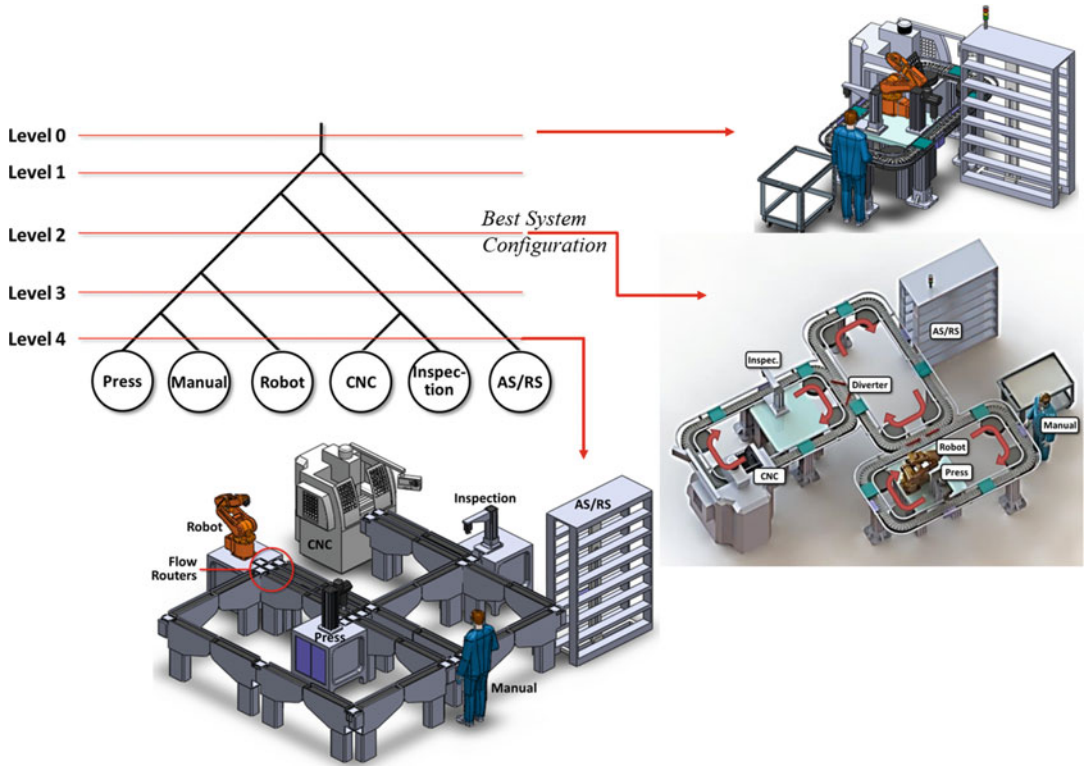
Design for System Complexity

System granularity has two direct effects on the structural complexity of manufacturing systems; it influences both system layout complexity and equipment complexity. Cladistics analysis showed that increasing the granularity level of manufacturing systems increases the complexity of its layout but also decreases the complexity of its equipment, while integrating pieces of equipment into a single integrated machine, line, or cell maximizes equipment complexity but also minimizes system layout complexity (Fig. 9). Each manufacturing system has a specific granularity level that represents a balance between

these two effects and reaches a point of equilibrium between system configuration decomposition vs. equipment integration (Samy et al. 2015).

Design for System Sustainability

Energy consumption throughout planning horizon of integrated or changeable manufacturing systems can be minimized by the right choice of system design structure and its degree of modularity. Changeable manufacturing system requires multiple system configurations at different time percentages during the planning horizon. A fine granularity high modularity system



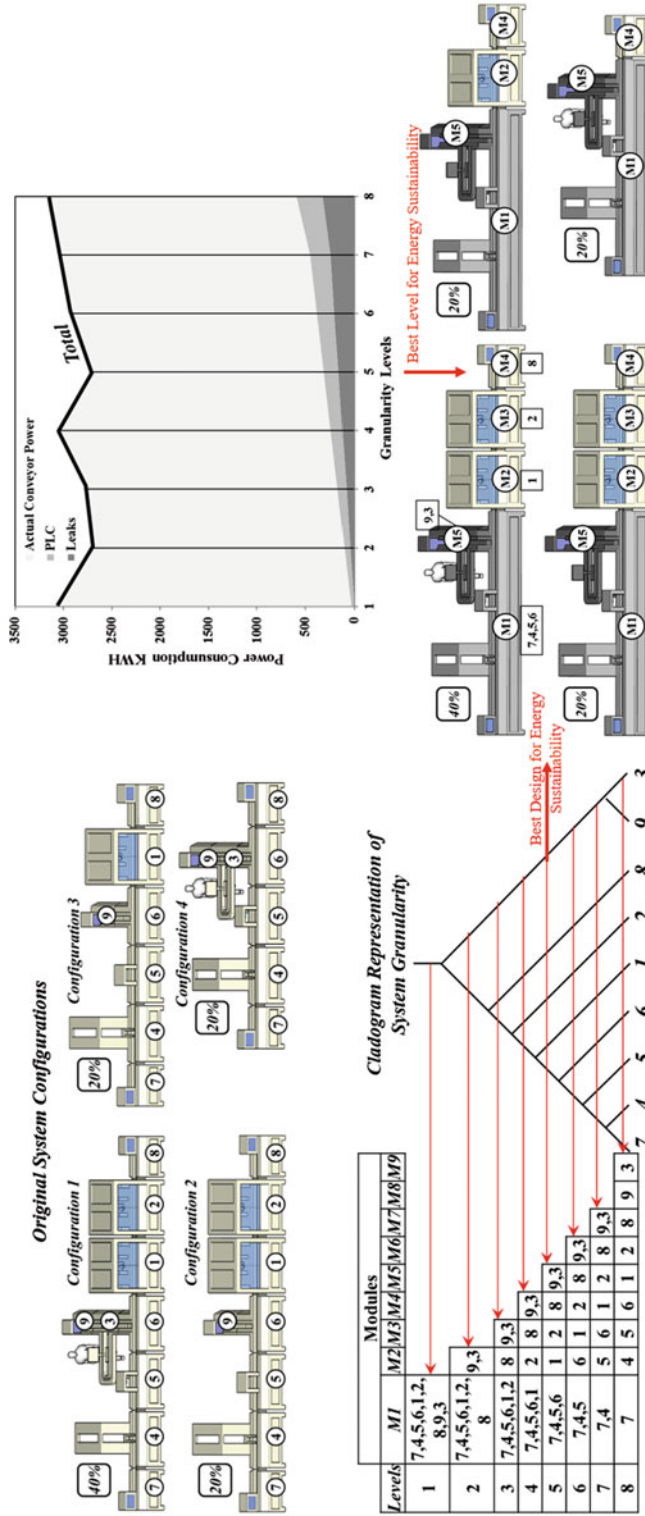
Cladistics for Products and Manufacturing, Fig. 9 The best granularity level for the least manufacturing system complexity. (Adapted from Samy et al. 2015)

structure would be the intuitive choice for such system to allow reconfiguration of system modules. However, using a cladistics model and augmented DSMs proved that individual energy characteristics of some modules might exceed the requirements of the specific process. The optimal system granularity level between the two extremes of maximum and minimum structure modularity optimizes energy consumption by combining some pieces of equipment (Fig. 10). This balances the load among processing modules and reduces wasted energy due to having many individual processes and interfaces while maintaining intended system functionality (AlGeddawy and ElMaraghy 2016).

Design for Systems and Products Coevolution

The synergy and dependency of manufacturing systems synthesis and product design are

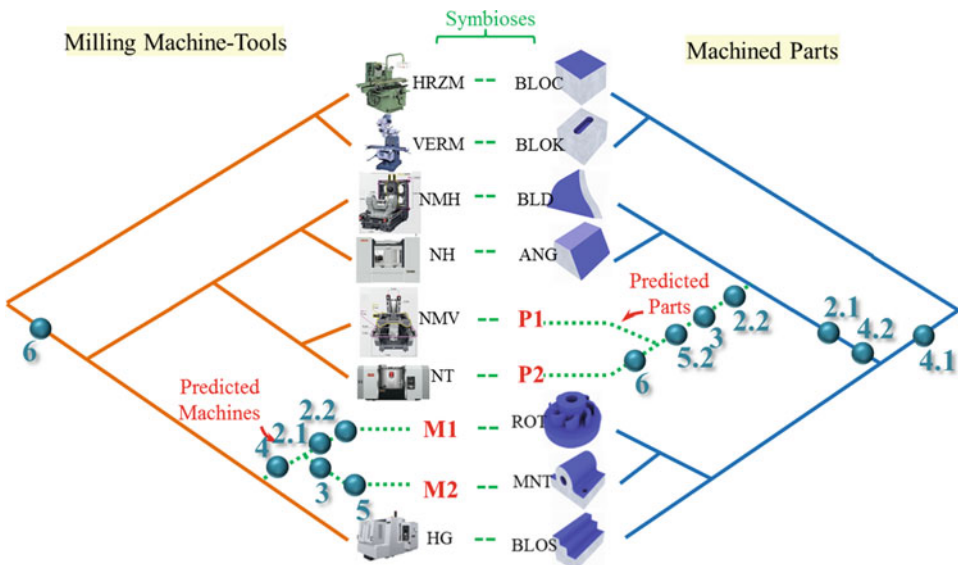
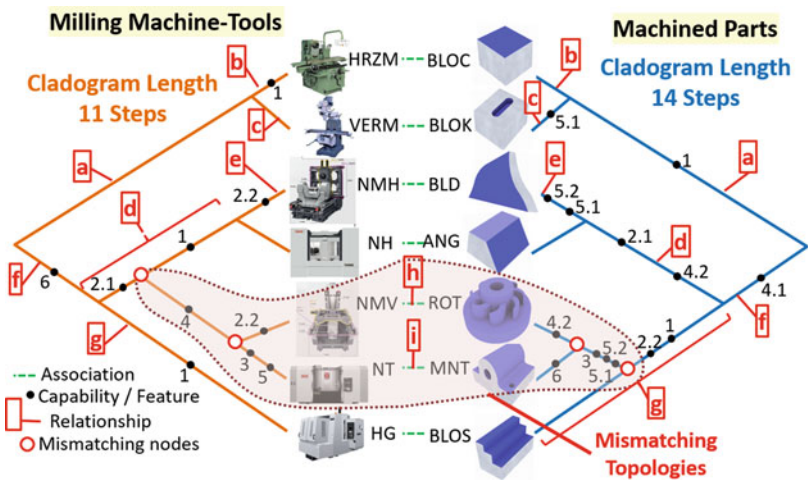
obvious and natural. Reciprocal changes affecting the design of both products and their manufacturing systems are most likely to take place after design or technology changes. Cladistic analysis represents a mathematical model to track codependence of manufacturing systems and products using cladistic analysis, and associate manufacturing capabilities with product features (Fig. 11) were developed (AlGeddawy and ElMaraghy 2012). If both system and product cladograms are not perfectly matching, the model suggests potential future development of the product and manufacturing resources to balance their imperfect coevolution and reach an equilibrium state, leading to a more economically sustainable manufacturing facility which can be used for more than one product generation or technological advance (AlGeddawy and ElMaraghy 2012) as illustrated in Fig. 12.



Cladistics for Products and Manufacturing, Fig. 10 Best system design for highest energy sustainability (AlGeddawy and ElMaraghy 2016)

Cladistics for Products and Manufacturing,

Fig. 11 Imperfect coevolution of products and manufacturing system causing mismatching branches (AlGeddawy and ElMaraghy 2012)



Cladistics for Products and Manufacturing, Fig. 12 Future manufacturing synthesis and product design by coevolution perfecting (AlGeddawy and ElMaraghy 2012)

Cross-References

- [Coevolution of Manufacturing Systems](#)

References

AlGeddawy T, ElMaraghy H (2010) Design of single assembly line for the delayed differentiation of product variants. *Flex Serv Manuf J* 22:163–182

AlGeddawy T, ElMaraghy H (2011) A model for co-evolution in manufacturing based on biological analogy. *Int J Prod Res* 49:4415–4435

AlGeddawy T, ElMaraghy H (2012) A co-evolution model for prediction and synthesis of new products and manufacturing systems. *J Mech Des* 134:051008

AlGeddawy T, ElMaraghy H (2013a) Optimum granularity level of modular product design architecture. *CIRP Ann Manuf Technol* 62:151–154

AlGeddawy T, ElMaraghy H (2013b) Reactive design methodology for product family platforms, modularity and parts integration. *CIRP J Manuf Sci Technol* 6:34–43

- AlGeddawy T, ElMaraghy H (2016) Design for energy sustainability in manufacturing systems. *CIRP Ann Manuf Technol* 65:409–412
- AlGeddawy T, Samy SN, ElMaraghy H (2017) Best design granularity to balance assembly complexity and product modularity. *J Eng Des*:1–24
- ElMaraghy H, AlGeddawy T (2012) New dependency model and biological analogy for integrating product design for variety with market requirements. *J Eng Des* 23:722–745
- ElMaraghy H, AlGeddawy T, Azab A (2008) Modelling evolution in manufacturing: a biological analogy. *CIRP Ann Manuf Technol* 57:467–472
- Hennig W (1966, republished in English in 1999) *Phylogenetic systematics*. University of Illinois Press, Urbana
- Samy SN, AlGeddawy T, ElMaraghy H (2015) A granularity model for balancing the structural complexity of manufacturing systems equipment and layout. *J Manuf Syst* 36:7–19

Clamping System

- ▶ [Tool Holder](#)

Clean Production

- ▶ [Sustainable Manufacturing](#)

Cleaner Production

Joost R. Dufflou and Karel Kellens
 Department of Mechanical Engineering, Centre for Industrial Management, KU Leuven, Leuven, Belgium

Synonyms

[Environmentally benign manufacturing](#); [Green manufacturing](#); [Sustainable manufacturing](#)

Definition

Cleaner production has been defined by the United Nations Environment Programme (UNEP) (UNEP 2012) as “the continuous

application of an integrated preventative environmental strategy to processes, products and services to increase efficiency and reduce risks to humans and the environment” (UNEP/DTIE/SCP 1990).

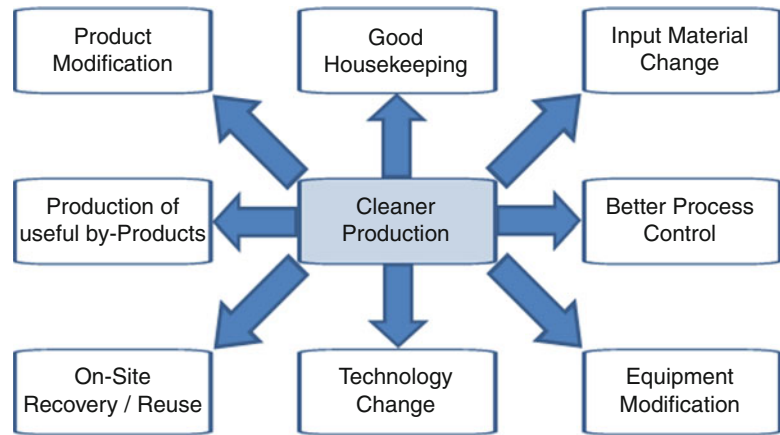
Theory and Application

Functional performance and purchase price have long been the key selection criteria for the purchase of new machine tools. Today, an evolution toward environmentally benign manufacturing can be observed that is stimulated by three drivers: more stringent regulatory mandates and standards (e.g., ISO 14955-1 2014; ISO 50001 2011), competitive economic advantage, and proactive green behavior (Gutowski et al. 2005).

Several complementary techniques and measures toward cleaner production can be applied, ranging from low- or even no-cost solutions to high-investment advanced technologies. A common classification of cleaner production strategies has been proposed by UNEP (Fig. 1) (UNIDO 2012). As described by Dufflou et al. (2012), these strategies can be implemented at different levels of the manufacturing chain: the process level, the multi-machine level, the factory level, the multiple factory level, and the supply chain level.

1. **Good Housekeeping:** appropriate provisions to prevent leaks and spills and to achieve proper, standardized operation and maintenance procedures and practices
 - Examples: Compressed air energy use, savings, and payback period of energy-efficient strategies are presented by Saidur et al. (2010). Local generation seems to be the best solution for cost consideration as well as energy efficiency (Yuan et al. 2006).
2. **Input Material Change:** replacement of hazardous or nonrenewable inputs by less hazardous or renewable materials or by materials with a longer service lifetime
 - Examples: Cutting fluids can be avoided or limited by applying *dry machining* or *minimum quantity lubrication* (e.g., Weinert et al. 2004; Aurich et al. 2008). Furthermore, environmentally benign fluids have

Cleaner Production,
Fig. 1 Classification of
 cleaner production
 strategies (UNIDO)



- been developed for operations which still require lubricants (Bay et al. 2010).
3. **Better Process Control:** modification of the working procedures, machine instructions, and process record keeping for operating the processes at higher efficiency and lower rates of waste and emission generation
 - Examples: Besides environmental optimization of process parameters (e.g., Mori et al. 2011), energy and resource efficiency measures are increasingly implemented in production planning software (e.g., Weinert et al. 2011; Herrmann et al. 2011; Thiede 2012).
 4. **Production Equipment Modification:** modification of the production equipment so as to run the processes at higher energy and resource efficiency and lower rates of waste and emission generation (e.g., Zein 2012; Kellens 2013)
 - Examples: Various research initiatives such as the CO₂PE!-Initiative (Kellens et al. 2012), the Self-Regulatory Initiative of CECIMO, and the eniPROD cluster of excellence focus on the documentation and improvement of the environmental footprint of discrete part manufacturing processes.
 5. **Technology Change:** replacement of the technology, processing sequence, and/or synthesis pathway in order to minimize the rates of waste and emission generation during production
 - Example: Solid freeform fabrication (SFF) techniques such as selective laser melting (SLM) and sintering (SLS) are often prized for being much cleaner than conventional machining processes and being able to fabricate products with minimum waste (e.g., Bourell et al. 2009; Chen et al. 2015).
 6. **On-Site Recovery/Reuse:** reuse of waste materials or energy streams in the same process or for another useful application within the company
 - Example: Wahl et al. (2011) describe a system to produce assist gasses for laser cutting machine tools using the heat losses of their own laser cooler system as input for a Stirling engine which drives a compressed air generator.
 7. **Production of Useful By-Products:** transformation of previously discarded waste into materials that can be reused or recycled for another application outside the company
 - Example: Solid state recycling of aluminum new process scrap (e.g., turning, millings, etc.) without need for reprocessing in a foundry via direct hot extrusion (Tekkaya et al. 2009) or spark plasma sintering processes (Paraskevas et al. 2014; Duflou et al. 2015).
 8. **Product Modification:** modification of product characteristics in order to minimize the environmental impacts of the product during or after its use (disposal) or to minimize the environmental impacts of its production. This implies the application of Life Cycle Engineering (Alting 1995; Hauschild et al. 2005) or eco-design (Brezet and Van Hemel 1997; Dewulf 2003; Wimmer et al. 2004) methodologies.

- Example: A recent industrial eco-design example is the Philips Econova ECO Smart LED TV, with a power consumption of just 56 watts in standard mode, which is 60 % less than conventional LCD TVs. In addition, it consists of recycled and recyclable materials and comprises a solar-powered remote control and a zero power switch.

- ▶ [Factory](#)
- ▶ [Life Cycle Engineering](#)
- ▶ [Manufacturing System](#)
- ▶ [Process](#)
- ▶ [Reuse](#)

Recommendations for Further Reading

- Research Initiatives
 - CO₂PE!-Initiative: <http://www.co2pe.org> (date of access: 28.01.2016)
 - Self-Regulatory Initiative of CECIMO: <http://www.cecimo.eu/site/publications/magazine/cecimo-self-regulatory-initiative/> (date of access: 28.01.2016)
 - eniPROD Cluster of Excellence: <http://www.eniprod.tu-chemnitz.de/index.php.en> (date of access: 28.01.2016)
- Journals
 - *Journal of Cleaner Production*: <http://www.journals.elsevier.com/journal-of-cleaner-production/> (date of access: 28.01.2016)
 - *International Journal of Sustainable Manufacturing*: <http://www.inderscience.com/jhome.php?jcode=IJSM> Accessed 4 Feb 2016
 - *Journal of Industrial Ecology*: <http://onlinelibrary.wiley.com/journal/10.1111/0%28ISSN%291530-9290>; <http://www.mitpressjournals.org/jie> (date of access: 28.01.2016)
 - *Environmental Science & Technology*: <http://pubs.acs.org/journal/esthag> (date of access: 28.01.2016)
- Books
 - Dornfeld D (2013) Green manufacturing: fundamentals and applications. Springer, New York. https://doi.org/10.1007/978-1-4419-6016-0_1

Cross-References

- ▶ [Energy Efficiency](#)
- ▶ [Environmental Impact](#)

References

- Alting L (1995) Life cycle engineering and design. *CIRP Ann Manuf Technol* 44(2):569–580
- Aurich JC, Herzenstiel P, Sudermann H, Magg T (2008) High-performance dry grinding using a grinding wheel with a defined grain pattern. *CIRP Ann Manuf Technol* 57(1):357–362
- Bay N, Azushima A, Groche P, Ishibashi I, Merklein M, Morishita M, Nakamura T, Schmid S, Yoshida M (2010) Environmentally benign tribo-systems for metal forming. *CIRP Ann Manuf Technol* 59(2):760–780
- Bourell D, Leu M, Rosen D (2009) Roadmap for additive manufacturing: identifying the future of freeform processing. University of Texas at Austin, Laboratory for Freeform Fabrication, Austin
- Brezet H, van Hemel C (1997) EcoDesign: a promising approach to sustainable production and consumption. UNEP, Paris
- Chen D, Heyer S, Ibbotson S, Salonitis K, Steingrimsson JG, Thiede S (2015) Direct digital manufacturing: definition, evolution, and sustainability implications. *J Cleaner Prod* 107:615–625
- Dewulf W (2003) A pro-active approach to eco-design: framework and tools. PhD Dissertation, K.U. Leuven
- Duflou JR, Sutherland JW, Dornfeld D, Herrmann C, Jeswiet J, Kara S, Hauschild M, Kellens K (2012) Towards energy and resource efficient manufacturing: a processes and systems approach. *CIRP Ann Manuf Technol* 61(2):587–609
- Duflou JR, Tekkaya AE, Haase M, Welo T, Vanmeensel K, Kellens K, Dewulf W, Paraskevas D (2015) Environmental assessment of solid state recycling routes for aluminium alloys: can solid state processes significantly reduce the environmental impact of aluminium recycling? *CIRP Annals – Manufacturing Technology* 64(1):37–40
- Gutowski T, Murphy C, Allen D, Bauer D, Bras B, Piwonka T, Sheng P, Sutherland JW, Thurston D, Wolff E (2005) Environmentally benign manufacturing: observations from Japan, Europe and the United States. *J Clean Prod* 13(1):1–17
- Hauschild M, Jeswiet J, Alting L (2005) From life cycle assessment to sustainable production: status and perspectives. *CIRP Ann Manuf Technol* 54(2):1–21
- Herrmann C, Thiede S, Kara S, Hesselbach J (2011) Energy oriented simulation of manufacturing systems: concept and application. *Manuf Technol* 60(1):45–48
- ISO 14955-1 (2014) Machine tools – environmental evaluation of machine tools. Part I: design methodology for energy efficient machine tools. International Organization for Standardization, Geneva

- ISO 50001 (2011) Energy management systems – requirements with guidance for use. International Organization for Standardization, Geneva
- Kellens K (2013) Energy and resource efficient manufacturing – unit process analysis and optimisation. PhD Dissertation, KU Leuven, ISBN: 978-94-6018-765-0
- Kellens K, Dewulf W, Overcash M, Hauschild M, Dufloy JR (2012) Methodology for systematic analysis and improvement of manufacturing unit process life cycle inventory (UPLCI). Part 1: methodology description. *Int J Life Cycle Assess* 17(1):69–78
- Mori M, Fujishima M, Inamasu Y, Oda Y (2011) A study on energy efficiency improvement for machine tools. *CIRP Ann Manuf Technol* 60(1):145–148
- Paraskevas D, Vanmeensel K, Vleugels J, Dewulf W, Deng Y, Dufloy JR (2014) Spark plasma sintering as a solid-state recycling technique: the case of aluminium alloy scrap consolidation. *Materials* 7(8):5664–5687
- Saidur R, Rahim NA, Hasanuzzaman M (2010) A review on compressed-air energy use and energy savings. *Renew Sustain Energy Rev* 14(4):1135–1153
- Tekkaya E, Schikorra M, Becker D, Biermann D, Hammer N, Pantke K (2009) Hot profile of AA-6060 aluminium chips. *J Mater Process Technol* 209(7):3343–3350
- Thiede S (2012) Energy efficiency in manufacturing systems. PhD Dissertation TU Braunschweig, Springer, Berlin
- United Nations Environment Programme (UNEP) (1990) Division of Technology, Industry, and Economics (DTIE), Sustainable Consumption & Production Branch (SCP), themes: resource efficient and cleaner production. <http://www.unep.fr/scp/cp/>. Accessed 13 Dec 2012
- United Nations Environment Programme (UNEP) www.unep.org. Accessed 13 Dec 2012
- United Nations Industrial Development Organization (UNIDO) (2012) Cleaner and sustainable production unit. <http://www.unido.org/index.php?id=o5152>. Accessed 13 Dec 2012
- Wahl E, Vincke K, Himmelsbach M (2011) Recovery of energy from a laser machining system. US patent application publication US2011/0024401
- Weinert K, Inasaki I, Sutherland J, Wakabayashi T (2004) Dry machining and minimum quantity lubrication. *CIRP Ann Manuf Technol* 53(2):511–537
- Weinert N, Chiotellis S, Seliger G (2011) Methodology for planning and operating energy-efficient production systems. *CIRP Ann Manuf Technol* 60(1):41–44
- Wimmer W, Züst R, Lee K-M (2004) Ecodesign implementation – a systematic guidance on integrating environmental considerations into product development. Springer, Dordrecht
- Yuan C, Zhang T, Rangarajan A, Dornfeld D, Ziemba B, Whitbeck R (2006) A decision-based analysis of compressed air usage patterns in automotive manufacturing. *J Manuf Syst* 25(4):293–300
- Zein A (2012) Transition towards energy efficient machine tools. PhD dissertation TU Braunschweig, Springer, Berlin

Closed-Die-Forging

- ▶ Hot Forging

CNC

- ▶ Adaptive Control
- ▶ Computer Numerical Control

Coated Tools

Konstantinos-Dionysios Bouzakis¹, Nikolaos Michailidis^{2,3}, Georgios Skordaris⁴ and Emmanouil Bouzakis⁵

¹Laboratory for Machine Tools and Manufacturing Engineering and Fraunhofer Project Center Coatings in Manufacturing (PCCM)/Mechanical Engineering Department, School of Mechanical Engineering, Aristoteles University of Thessaloniki, Thessaloniki, Greece

²Physical Metallurgy Laboratory (PML), Department of Mechanical Engineering, Aristotle University of Thessaloniki, Thessaloniki, Greece

³Center for Research and Development on Advanced Materials – CERDAM, Thessaloniki, Greece

⁴Laboratory for Machine Tools and Manufacturing Engineering and Fraunhofer Project Center Coatings in Manufacturing (PCCM)/Mechanical Engineering Department, Aristoteles University of Thessaloniki, Thessaloniki, Greece

⁵Department of Engineering, German University of Technology in Oman (GUtech), Muscat, Oman

Synonyms

Tools with thin hard protective surface films;
Tools with thin hard protective surface layers

Definition

Coatings deposited on cutting tools are ceramic layers of few micrometers in thickness which

exhibit high mechanical strength and hardness, chemical inertness, and low thermal conductivity. As such, a significant increase in performance is realized over uncoated tools.

Extended Definition

Coated tools have compound material structure, consisting of the substrate covered with a hard, antifriction, chemically inert, and thermal isolating layer, up to several micrometers thick. In this way, coated tools compared to uncoated ones offer better protection against mechanical and thermal loads, diminish friction and interactions between tool and chip, and improve wear resistance in a wide cutting temperature range. Coatings follow the topomorphy of the tool substrate surface. Depending on the deposition process, the film thickness may vary on the flank and rake faces of the tool. In addition to the inherent properties of the film, coating adhesion is also pivotal for the cutting performance. An electron micrograph of a cross section through a coated cemented carbide insert is presented in Fig. 1.

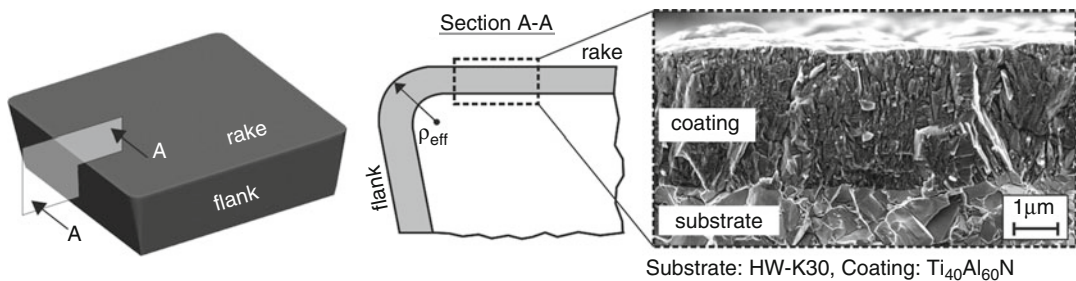
Theory and Application

History

Coatings produced by chemical vapor deposition (CVD) were already commercialized for carbide inserts in the 1960s. Physical vapor deposition (PVD) was developed almost 20 years later, and today both CVD and PVD are sharing the coating market of cutting tools.

TiN coatings were first applied industrially on cutting tools. The next generation of coatings was composed of chromium nitride (CrN) and titanium carbonitride (TiCN). The evolution of TiAlN, by adding aluminum to the TiN base composition, provided not only a higher hardness but also a remarkable improvement of high-temperature strength and inertness. The high hot hardness and oxidation resistance up to ca. 900 °C contributed to remarkable improvement in machining productivity. The next evolution of TiAlN coatings is usually known as AlTiN coatings, for their higher Al content, implying a better thermal resistance. The addition of silicon in the composition enabled further increases in cutting temperature (Flink et al. 2009). The hardness of AlCrN coating is similar to that of TiAlN, but what makes this coating outstanding is its high adhesion with the substrate material, due to Cr content and its high oxidation resistance, up to 1200 °C. AlCrN-based coating has been successfully applied in hobbing, drilling, and milling where both high temperature and oxidation resistance of the coating are required (Endrino and Derflinger 2005; Bouzakis et al. 2011a). From a materials perspective, alloying TiAlN coatings with different elements provides a large number of further possibilities: for example, TiAlCrN, TiAlCrSiN, and TiAlCrYSiN compositions are reported (Bohlmarm et al. 2011) and even more the addition of dopants like Zr, V, B, or O (Bouzakis et al. 2008a; López de Lacalle et al. 2010).

Alumina is uniquely suited for metal cutting tools due to its chemical inertness and high hot



Coated Tools, Fig. 1 Electron micrograph of a cross section through a coated carbide insert

hardness at the temperatures typically reached in these applications (Quinto 1988). In addition to sintered alumina-based ceramics, Al_2O_3 is also important as a coating material. Alumina-coated cemented carbide tools are used, for example, in turning and milling steel and cast iron. The Al_2O_3 coatings are typically manufactured by CVD. CVD has been used for about 30 years for industrial deposition of wear-resistant coatings and still dominates the market of Al_2O_3 coatings on cemented carbide tools. Crystalline alumina PVD coatings offer high potential for an application in cutting operations. Beneficial of these types of coatings are high chemical inertness, high hot hardness, and high oxidation resistance (Bouzakis et al. 2002). One promising candidate is $\gamma\text{-Al}_2\text{O}_3$, which can be deposited at lower temperatures and is more fine-grained than $\alpha\text{-Al}_2\text{O}_3$. At high temperatures, $\gamma\text{-Al}_2\text{O}_3$ transforms into $\alpha\text{-Al}_2\text{O}_3$, which could limit the application temperature (Erkens 2007; Bobzin et al. 2010).

CVD diamond thin films offer the hardness and wear resistance of diamond but on geometrically complex tools such as drills and end mills. The manufacturing chain of CVD diamond-coated cemented carbide tools commences with the identification of a suitable substrate as well as the substrate pretreatment to remove cobalt from the surface layer. This is necessary to prevent a catalytic reaction of cobalt with diamond and to provide a mechanical bond between substrate and diamond film. These manufacturing steps are followed by cleaning and diamond seeding measures before CVD diamond deposition is carried out (Uhlmann and Koenig 2009; Haubner and Kalss 2010). Residual stresses develop in a diamond film mainly due to epitaxial crystal differences and thermal expansion coefficients mismatch of the diamond coating and its cemented carbide substrate. The residual stresses usually enhance the diamond coating adhesion since they contribute to roughness peaks locking in the coating-substrate interface. However, they may overstress the substrate material in its interface region, thus deteriorating the coating adhesion (Skordaris et al. 2016). For selected applications, the extreme properties of diamond can be exploited.

Theory

Introduction

PVD covers a broad family of vacuum coating processes in which the metal comprising the film material is physically removed from a source or “target” by evaporation or sputtering. Then, they are transported in a vacuum or partial vacuum by the energy of the vapor particles and condensed as a film on the surfaces of appropriately positioned parts in the vacuum chamber. It is most common to deposit ceramic films, and these are formed by introducing a reactive gas (nitrogen, oxygen, or simple hydrocarbons) containing the desired chemical elements, which once reacted with the target materials form the required coating composition. PVD coatings can be deposited at temperatures lying in the range of 450–550 °C, which allows the film deposition on high-speed steel tools. Most of the PVD processes are known by various phrases or acronyms, and they are typically named for the physical vapor target, for example, diode or triode sputtering, planar or cylindrical magnetron sputtering, direct current (DC) or radio frequency (RF) sputtering, electron beam evaporation, activated reactive evaporation, and ARC evaporation (DC or alternate current (AC)) (Erkens 2007; Bobzin et al. 2009).

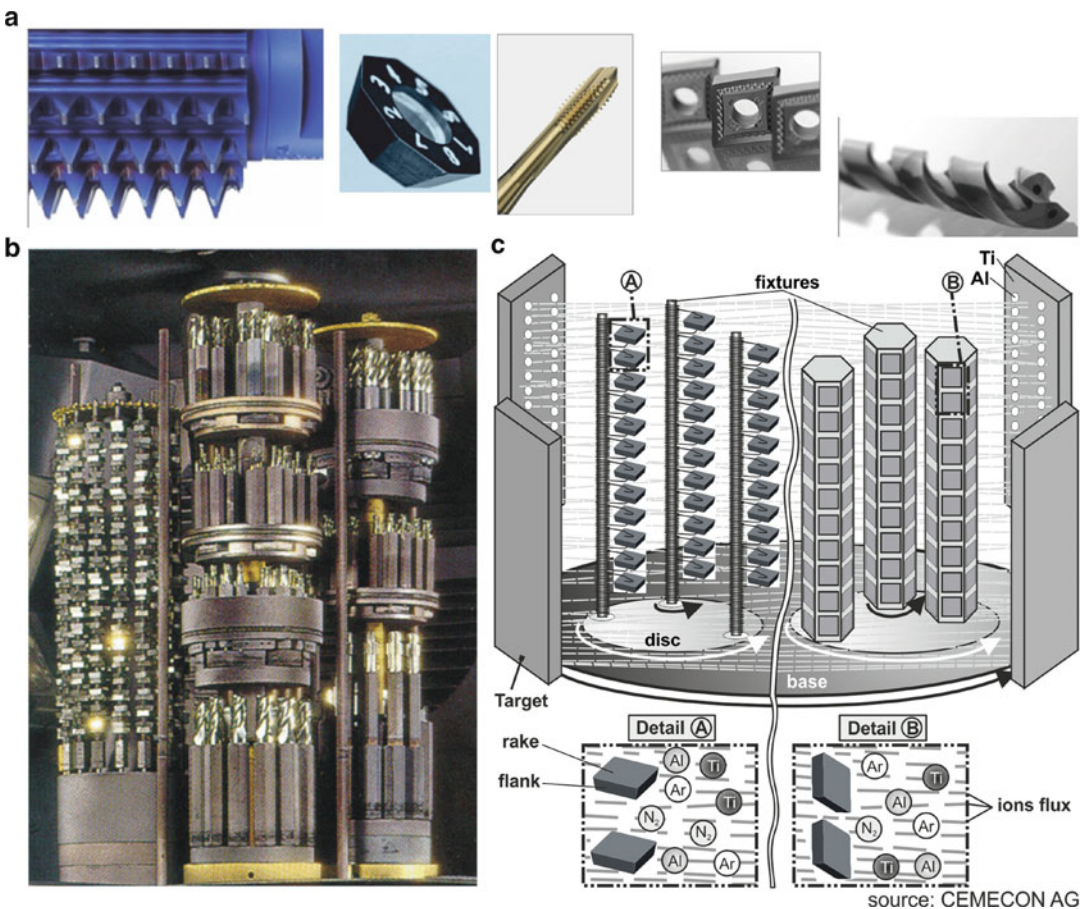
CVD, unlike to PVD vacuum processes, is a heat-activated process based on the reaction of gaseous chemical compounds within a reaction chamber containing the parts to be coated. It is possible to control the coating composition, crystal or lattice structure, and thickness by adjusting the reactor pressure, temperature, and/or reactant composition. Primary reactive vapors can be either metal halides or metal carbonyls, as well as hydrides and organometallic compounds. Typical deposition temperatures range from 800 to 1200 °C. The ability to provide uniformly thick coatings with refined grain is also influenced by the deposition temperature. Fewer CVD reactions are available for use at temperatures below 800 °C than above (moderate temperatures, MT-CVD). However, the temperature required for a given reaction can be lowered by exposing the substrate to an electrical plasma in the gas phase during deposition, referred to as plasma-assisted CVD

(PA-CVD) (Shimada et al. 2010). Metal-organic CVD (MO-CVD) has been reported for strengthening Al_2O_3 -based ceramic tools.

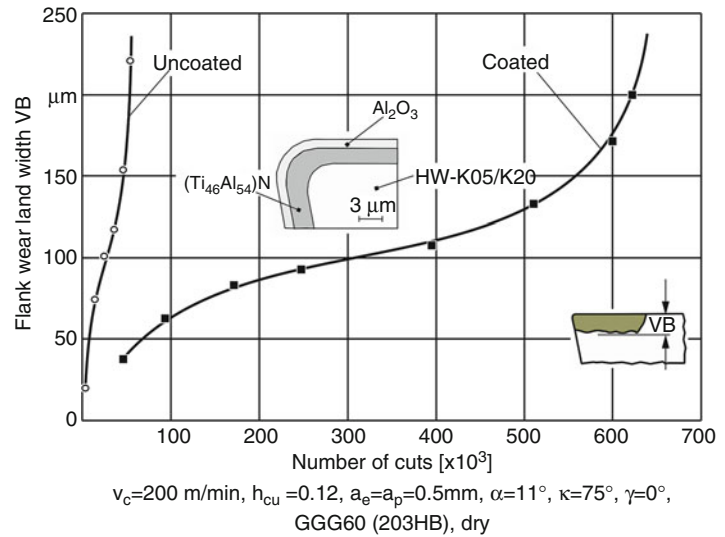
The ability to control thicknesses on the edges, when PVD is employed, guarantees a sharp-coated cutting edge. High intrinsic hardness and compressive stresses, inhibiting the crack growth in tool material, are among the beneficial properties of PVD films (Klocke and Krieg 1999). The possibility to produce thick layers by CVD at increased deposition rates renders the CVD-coated tools suitable for high material removal operations, whereas the PVD ones are selected in medium-finish and finish operations. PVD films can be produced without any chemical interaction with the substrate. CVD coatings easily interact with the substrates, occasionally producing brittle carbides at the

interfaces. The ease of decoating and resharping of PVD-coated tools opened a large industrial market highly sensitive to cost-reducing opportunities. Both coating processes contributed to significant enhancement of high-speed cutting (HSC) and high-performance cutting (HPC) (Toenshoff 2011).

Figure 2a illustrates a variety of coated cutting tools, from inserts to solid tools and hobs which can be industrially produced. Figure 2b exhibits characteristic fixtures for attaching cutting tools in the deposition chamber. Where the plasma flux during PVD is quasi-parallel to the insert rake (see Fig. 2c), a thicker coating is formed on the flank and vice versa. As a result, cutting inserts are coated with slightly variable film thickness on the rake and flank, depending on the incidence directions of the plasma flux. HPPMS technology



Coated Tools, Fig. 2 (a) Typical coated cutting tools produced, (b) characteristic fixtures for attaching the cutting tools in the deposition chamber, and (c) tool orientation against ion flux during PVD

Coated Tools,**Fig. 3** Flank wear development of uncoated and coated tools in milling cast iron

contributed to the elimination of this phenomenon (Bobzin et al. 2009).

The potential to increase tool life via the employment of coated tools is demonstrated in Fig. 3. In this figure a characteristic example in milling cast iron with coated and uncoated cemented carbide inserts is displayed. When an appropriate PVD film for this workpiece material is applied, an impressive number of cuts (tool life) can be attained compared to the uncoated tool. The used coating consists of a crystalline Al_2O_3 layer over a $(\text{Ti}_{46}\text{Al}_{54})\text{N}$ film. The substrate is a cemented carbide insert appropriate as coated or uncoated for milling cast iron. The coated tool managed to cut 650×10^3 cuts up to a flank wear of 0.2 mm (Bouzakis et al. 2002). The uncoated insert achieved only 50×10^3 cuts up to the same flank wear width. This superior performance of coated tools has resulted in their wide application in cutting processes, rendering the employment of uncoated ones as an exception.

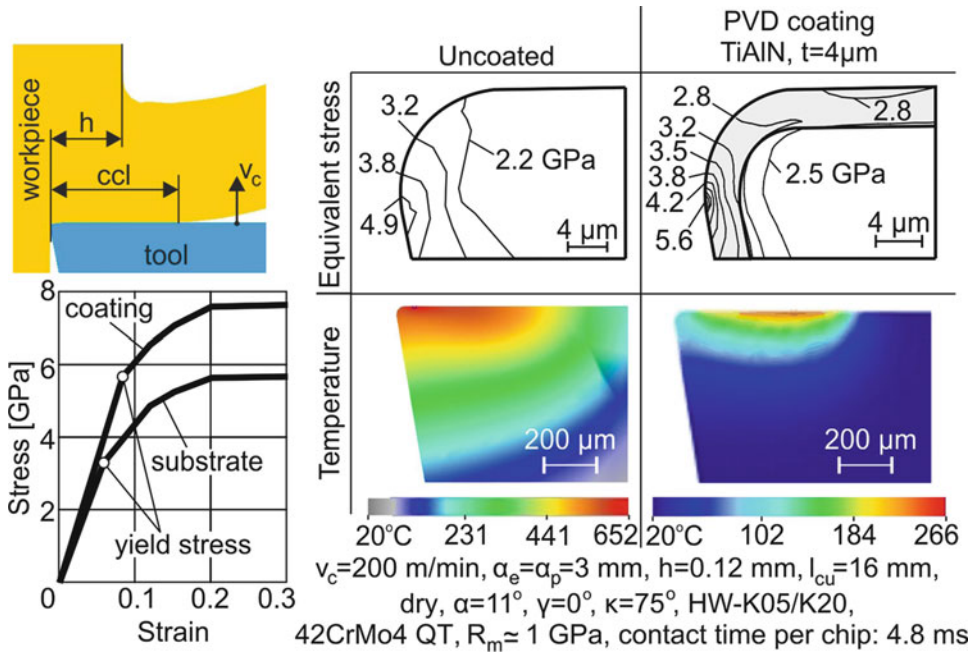
Coated Tools Technical and Thermal Loads During Cutting

The elevated cutting performance of coated tools can be also explained by the mechanical and thermal loads acting on the cutting edge during the material removal. In an example of milling hardened steel, the maximum equivalent stress in the coating determined by finite element method

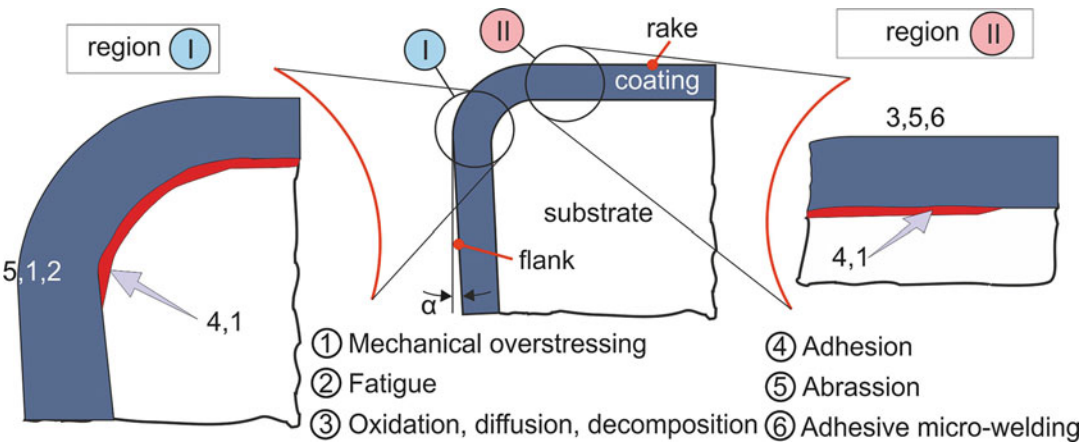
(FEM) calculations reaches 5.6 GPa on the cutting-edge roundness close to the flank, remaining below the film yield stress of 5.9 GPa (see Fig. 4) (Bouzakis et al. 2008b). Additionally, the substrate is less stressed (max. equivalent stress ≈ 3 GPa) compared to the uncoated tool (4.9 GPa). In the uncoated tool, the stress of 4.9 GPa exceeds its yield strength of ca. 3.2 GPa, thus leading to cutting-edge micro-breakages and accelerating the wear growth. The maximum temperature in the coated insert amounts to ca. 266°C , at a tool–chip contact time of 4.8 ms. In the case of an uncoated tool, a comparatively higher amount of the total cutting energy is conducted into the tool, leading to a maximum temperature of up to 652°C , thus affecting its cutting performance. In interrupted cutting, depending on the tool–workpiece contact time, the maximum tool temperature is commonly lower than the corresponding steady-state temperature of continuous material removal processes.

Wear Development on Coated Tools

The wear mechanisms of coated tools in cutting vary from application to application, and the ones dominating in steel milling are displayed in Fig. 5 (Bouzakis et al. 2013). Mechanical overstressing as well as the exceeding of the fatigue strength during material removal leads to microchipping of the coating mainly at the transient cutting-edge



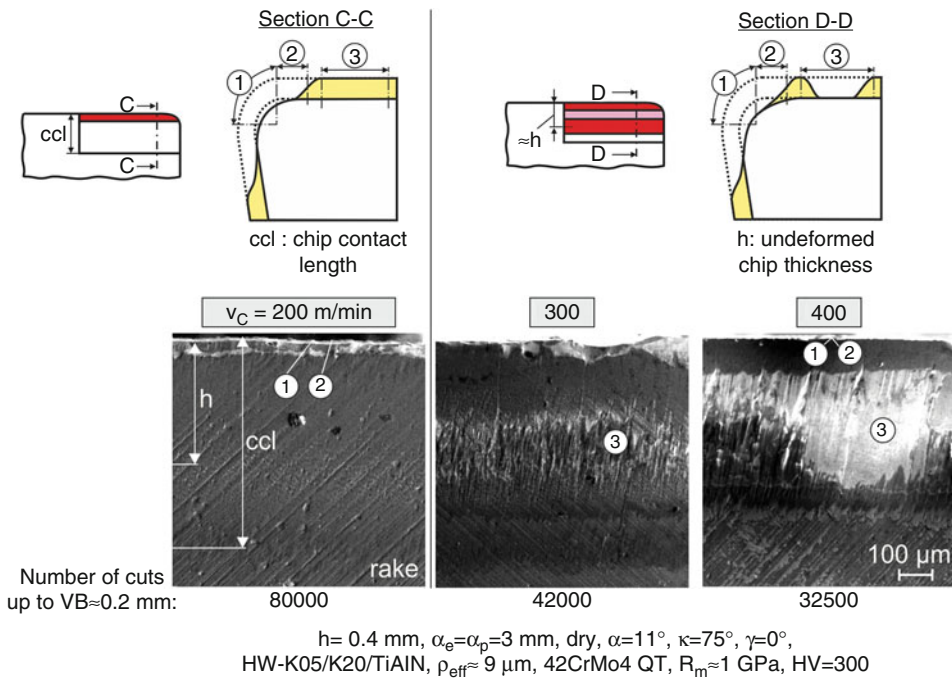
Coated Tools, Fig. 4 Decrease of mechanical and thermal loads of cemented carbide tools by the application of PVD coatings



Coated Tools, Fig. 5 Developed wear mechanisms in coated cutting tools

region from the flank to the tool rake (region I). The development of this wear phenomenon increases the width of the flank wear land at low cutting velocities, without any significant wear on the tool rake, and causes tool failure. Moreover, depending on the temperature developed and coating composition, oxidation and diffusion mechanisms develop at higher cutting velocities, mainly

on the tool rake face (region II). High cutting temperatures may also lead to coating decomposition (Alling et al. 2009). Due to these mechanisms, a deterioration of the coating’s mechanical properties occurs, which accelerates its abrasive wear. Furthermore, the film adhesion quality significantly affects coating wear, since inadequate interlocking of the coating with the substrate



Coated Tools, Fig. 6 Coating failure at a flank wear of 0.2 mm, investigated by electron micrographs, at various cutting speeds

increases the developing stresses (Bouzakis et al. 2011b). These mechanisms appear in the cutting wedge region I and lead to film fracture and rapid tool wear. Finally, adhesive micro-welding leading to micro-peeling can occur at low cutting speeds, in part, as a result of common elements between workpiece and coating materials.

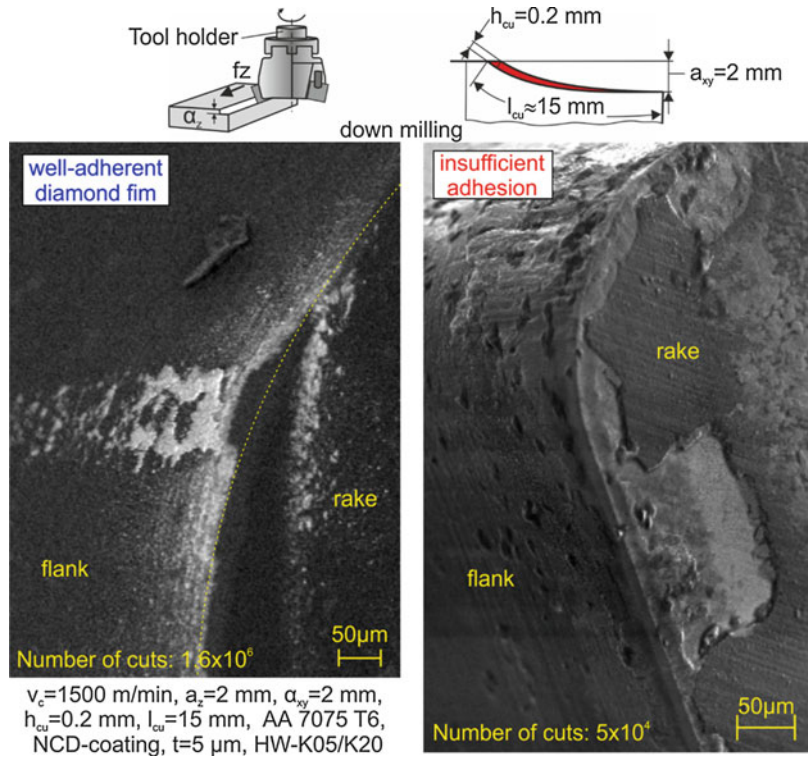
The wear mechanisms are significantly affected by the applied cutting speed. As it is shown at the upper part of Fig. 6, at the cutting speed of 200 m/min, coating fatigue fracture at the rounded transient region of the flank to the cutting edge develops, restricting the tool life. At elevated cutting speeds, in the present case over 300 m/min, besides the aforementioned mechanically overstressed flank region, tribo-oxidation along with increased abrasion develops. These mechanisms appear on the rake face close to the cutting edge and are predominant in limiting tool performance. The electron micrographs of the tool rake face shown at the bottom of the figure exhibit the aforementioned coating wear mechanisms. On one hand, in the frame of these

investigations, the width of flank wear land VB up to a value of 0.2 mm is evenly distributed along the cutting edge. On the other hand, a coating failure appears at the indicated wedge locations 1 and 2, but the wear extent and the number of the achieved cuts vary, depending on the cutting speed.

The film adhesion crucially affects the wear development of a diamond-coated tool. The diamond film adhesion can be assessed employing methodologies described in Skordaris et al. (2016). Characteristic SEM micrographs exhibiting the wear evolution on the NCD-coated tools possessing improved adhesion or insufficient adhesion after 1.6×10^6 or 5×10^4 cuts, respectively, in milling AA7075 T6, are shown in Fig. 7. Coating detachment in a restricted region of the tool rake also develops even in cases of well-adherent diamond-coated tools, when the shear strength of the coating interface is exceeded, among others, due to film thickness decrease on the cutting-edge roundness because of wear (Skordaris et al. 2016).

Coated Tools,

Fig. 7 Characteristic SEM micrographs of worn NCD-coated tools with different adhesion qualities after various numbers of cuts



Coated Tools' Material and Functional Properties Determination

The cutting performance of coated tools can be significantly improved by tailoring the coating properties to application-specific requirements. For achieving this target, a thorough understanding of the coated tools wear mechanisms is required. Since CVD and PVD thin films are very hard and brittle materials, properties such as fatigue, toughness, residual stresses, and adhesion along with tribological and dimensional ones play a pivotal role in cutting with coated tools. To quantify these parameters, experimental-analytical test procedures have been developed. These provide information concerning material and functional properties of the film and its substrate as well as the actual coated tool geometry. In Fig. 8 methods for determining material, dimensional, and functional data of coated tools are displayed. Combinations of these procedures jointly with FEM-supported computations contribute to the explanation of the cutting tool films' failure mechanisms, thus restricting the experimental cost for optimizing

cutting conditions. Characteristic examples will be introduced in the following sections.

Several test procedures are applied for determining material, dimensional, and functional properties of coated tools. Moreover, experimental in combination with FEM-supported techniques are used for assessing the performance of coated tools. Some of these procedures are significant for cutting tools and will be briefly described:

- *Strength properties and hardness at various temperatures:* The determination of the coating strength properties and hardness is conducted by nanoindentations at ambient and elevated temperatures. With this technique, in situ measurements are conducted in a wide range of temperatures, enabling an accurate estimation of coating properties. Based on FEM simulations of the indentation procedure, experimental results may be evaluated and coating stress-strain curves as well as hardness at various temperatures are determined (Bouzakis et al. 2005a).

PROPERTIES		TEST METHODS																		
		EDX	SEM	XRD	TEM	...	NI	...	NIT	IT	ITMFS	BC	WLS	IIT	S	NS	RC	DiF	OX	TRM
Material	Structure	✓	✓	✓	✓															
	Residual stresses			✓																
	Mechanical properties						✓													
	Hardness						✓													
	Brittleness								✓											
	Fatigue									✓										
	Fatigue at high strain rates										✓									
Dimensional	Thickness										✓									
	Thickness distribution on the cutting edge											✓								
Functional	Friction																			✓
	Adhesion												✓	✓	✓	✓				
	Diffusion																	✓		
	Chemical stability																			✓

SEM: Scanning Electron Microscope
 EDX: Energy-dispersive X-ray spectroscopy
 TEM: Transmission Electron Microscopy
 XRD: X-ray Diffraction
 NI: NanoIndentations
 NIT: Nano-Impact Test
 IT: Impact Test
 ITMFS: Impact Test with Modulated Force Signal
 BC: Ball Cratering Test
 WLS: White light scanning 3D measurements
 IIT: Inclined Impact Test
 S: Scratch test
 NS: Nano-scratch test
 RC: Rockwell C
 DiF: DiFusion test
 OX: Oxidation test
 TRM: TRiBoMeter

Coated Tools, Fig. 8 Characteristic methods for determining coating material, dimensional, and functional properties

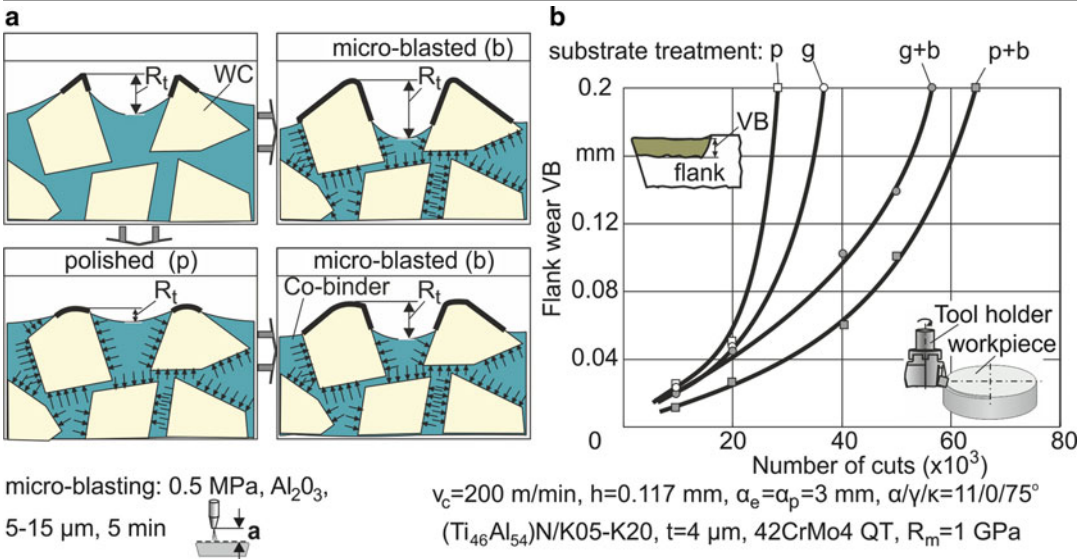
- Fatigue strength at various temperatures and impact force signals:* Coated tools’ film failures commonly develop during cutting, due to fatigue problems. The films’ fatigue properties at ambient and elevated temperatures are determined by perpendicular impact tests, employing appropriate devices (Knotek et al. 1992; Bouzakis et al. 2001, 2010a, 2012). In these experiments, the impact force signal (force and duration) is pivotal for coating failure. Moreover, the possibility to calculate the developed cutting temperature field allows the correlation between the coating impact resistance and the tool wear at various cutting speeds and cutting-edge entry impact durations (Bouzakis et al. 2007, 2013).
- Coating adhesion:* The film adhesion can be qualitatively assessed by Rockwell and scratch test methods. These test procedures do not always yield reliable results, due to limitations of the test procedures (Bouzakis et al. 2011a). The evolution of the inclined impact test renders possible the accurate and

quantitative coating adhesion evaluation (Bouzakis et al. 2010b).

Enhancement of Coating Adhesion

Prior to coating deposition, cemented carbide cutting tool substrates are mechanically treated via various methods for improving the film adhesion. As a side effect of these treatments, different surface topographies are generated (Toenshoff et al. 1997).

Typical mechanical pretreatments of cemented carbide tools are presented in Fig. 9a. The applied processes are grinding (G) or grinding with subsequent polishing (P) for achieving a medium or a low roughness, respectively. Furthermore, microblasting (mb) is conducted in all the examined cases. After polishing and microblasting, the exposed WC carbides are better embedded in the binding material, compared to ground and microblasted substrates. Thus the effective film adhesion is enhanced, and a cutting performance increase is realized. Milling tests validate these models (see Fig. 9b). The coated



Coated Tools, Fig. 9 Effect of substrate's microblasting on (a) its microstructure and (b) coated tools' cutting performance

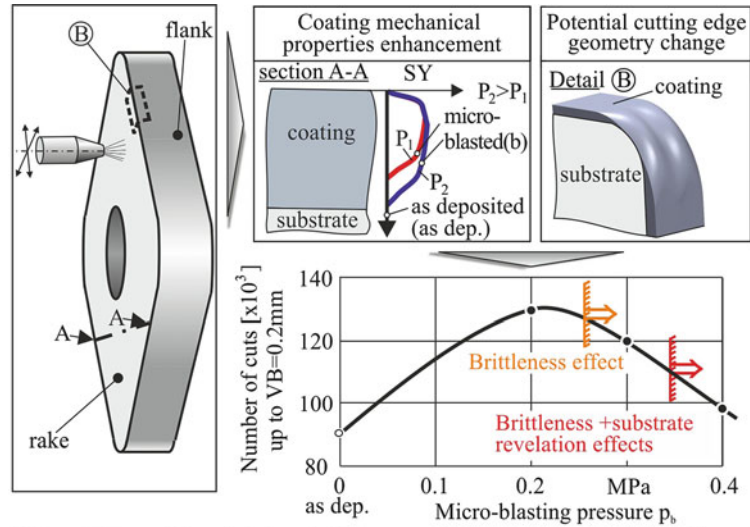
inserts with ground and microblasted substrates reach a tool life of approximately 55×10^3 cuts, at a flank wear width of 0.2 mm. Moreover, the results exhibit a further wear resistance growth, by polishing and subsequent substrate microblasting. Inserts with polished or ground substrates managed to cut ca. 28×10^3 and 35×10^3 times, respectively, up to the same flank wear width. The wear resistance improvement is evident, when coated inserts with polished and microblasted substrates are used (Bouzakis et al. 2005b).

Further ways for improving the coating adhesion are via deposition of thin adhesive interlayers between substrate and coating (Bouzakis et al. 2010b) and through surface nitriding, prior to the PVD film deposition (Erkens et al. 2011).

Improvement of Coated Tools Cutting Performance

Microblasting on PVD-coated tool surfaces may be an efficient method for improving the cutting performance. Through microblasting on coated cemented carbide inserts, it is possible to enhance film strength properties and thus the tool cutting performance. On one hand, microblasting induces residual compressive stresses into the film

structure, resulting to coating hardness increase (Bouzakis et al. 2009). On the other hand, the film becomes more brittle (Bouzakis et al. 2011b). As blasting materials, aluminum oxide (Al_2O_3) with sharp-edged grains or ZrO_2 with smooth surfaces is commonly used. The blasting grains are transferred by compressed air (dry) or combination of compressed air with water (wet) and can cause coating's material deformations (strengthening effect), as well as material removal (abrasive effect). This is qualitatively demonstrated in Fig. 10. The residual compressive stresses, which are simultaneously induced into the film structure, lead to an increase in coating hardness and strength properties. Microblasting parameters such as pressure, time, abrasive grains' size, and quality affect the coated tool's cutting performance. According to experimental and computational results, by microblasting pressure augmentation, an enlargement of the plastically deformed film region into its depth takes place. Although an increased microblasting pressure is beneficial for enhancing the coating hardness, this can cause the substrate revelation as well as increased film brittleness, and in this way, a deterioration of the tool life may occur, as it is shown in the diagram at the bottom of Fig. 10

Coated Tools,**Fig. 10** Effect of microblasting on coated tools' properties and cutting performance

42CrMo4 QT, $v_c=200$ m/min, $h_{cu}=0.12$ mm, $a_{xy}=3$ mm, $a_z=3$ mm, $\alpha=11^\circ$, $\gamma=0^\circ$, $\kappa=72.5^\circ$
 Wet micro-blasting: Al_2O_3 , $d_g=10$ μm , wet, $t_b=4$ s, $a=10$ mm
 Substrate: HW-K05/K20, Coating: $Ti_{46}Al_{54}N$, $t=3.5$ μm

(Klocke et al. 2009; Bouzakis et al. 2011b). According to these results, microblasted tools at a pressure of 0.2 MPa exhibited the best cutting performance, reaching a tool life of approximately 130,000 cuts. A slight tool life reduction at 120,000 cuts up to the same flank wear of 0.2 mm was encountered at a pressure of 0.3 MPa. Hence, over this critical microblasting pressure, which depends on the microblasting conditions, the higher microblasting pressure increases the film brittleness. In this way, the coated tool wear resistance is also deteriorated. At the higher microblasting pressure of 0.4 MPa, the cutting performance is additionally restricted by substrate revelation effects.

Reconditioning of PVD-Coated Tools of Complex Geometry

In contrast to simple cutting inserts, solid tools such as twist drills, milling cutters, gear hobs, gear-shaping wheel cutters, and broaching tools have to be reconditioned after achieving the wear limit, due to their elevated cost compared to one-use cutting inserts. The potential of reconditioning worn-coated cemented carbide and high-speed steel tools through sequential electrochemical

coating removal, tooth rake regrinding, microblasting, and PVD recoating has a wide industrial importance. However, the effect of all these procedures on the substrate mechanical properties, on the edge sharpness, and on the cutting performance, especially of cemented carbide tools, must be given due consideration. The mechanical properties of the cemented carbide substrate may deteriorate after the first film deposition (Denkena and Breidenstein 2010) and may further degrade, albeit to a lesser extent in further recoating steps. As such, a deterioration in the cementing of carbide grains by the cobalt binder may arise leading to cutting-edge chipping, which in turn reduces cutting performance and process reliability. The appropriate control of procedures such as macro- and microblasting enhances the cutting performance after tool reconditioning and improves the productivity when using cemented carbide tools (Bouzakis et al. 2008b; Klocke et al. 2009).

Key Applications

The application of coatings is currently a "must" on the vast majority of cutting tools. This is particularly true where high-speed and high-performance cutting is required or in the

machining of difficult-to-cut materials. For the majority of industrial applications, the use of coated tools is widespread and absolutely necessary for realizing satisfactory productivity and tool life.

High-Performance Cutting (HPC) and High-Speed Cutting (HSC)

The objective of high-performance cutting is the shortening of machining times by applying increased cutting speeds and/or feed rates with due consideration of tool wear and the surface quality of the generated workpiece. High-performance cutting applications place high demands on the properties of PVD coatings in terms of wear resistance, thermal stability, and oxidation resistance and hardness at elevated temperatures. Al-, Ti-, and Si-containing coatings such as AlTiN, AlCrN, and TiSiN on cemented carbide tools generally provide high performance in metal cutting applications.

Machining of Difficult-to-Cut Materials

Difficult-to-cut materials are characterized by low machinability, which prescribes the application of convenient tool and coating materials as well as machining conditions, for guaranteeing a satisfactory tool life. Characteristic materials with low machinability are aerospace alloys, e.g., titanium or nickel alloys. Aerospace alloys possess high strength, work hardening, and dynamic shear strength at ambient and elevated temperatures and are characterized by low thermal diffusivity and chemical reactivity with tool materials, associated with increased tool cutting loads and temperatures, as well as with extreme abrasion. For such demands, despite the trend to use uncoated tools, the application of single and multilayer TiAlSiN and CrAlN coatings containing alternatively Zr or Y dopants on cemented carbide tools can provide a superior cutting performance (Bouzakis et al. 2008a; Klocke et al. 2010).

Cross-References

► [Physical Vapor Deposition \(PVD\)](#)

References

- Alling B, Oden M, Hultman L, Abrikosov IA (2009) Pressure enhancement of the isostructural cubic decomposition in $Ti_{1-x}Al_xN$. *Appl Phys Lett* 95:18. art. no. 181906
- Bobzin K, Bagcivan N, Immich P, Bolz S, Alami J, Cremer R (2009) Advantages of nanocomposite coatings deposited by high power pulse magnetron sputtering technology. *J Mater Process Technol* 209(1):165–170
- Bobzin K, Bagcivan N, Reinholdt A, Ewering M (2010) Thermal stability of $\gamma-Al_2O_3$ coatings for challenging cutting operations. *Surf Coat Technol* 205(5):1444–1448
- Bohlmark J, Blomqvist H, Landälv L, Amerioun S, Ahlgren M (2011) Evaluation of arc evaporated coatings on rounded surfaces and sharp edges. *Mater Sci Forum* 681:145–150
- Bouzakis K-D, Michailidis N, Lontos A, Siganos A, Hadjiyiannis S, Giannopoulos G, Maliaris G, Erkens G (2001) Characterization of cohesion, adhesion and creep-properties of dynamically loaded coatings through the impact tester. *Z Metallkd Mater Res Adv Tech* 92(10):1180–1185
- Bouzakis K-D, Michailidis N, Anastopoulos N, Skordaris G, Hadjiyiannis S, Kombogiannis S, Erkens G, Rambadt S, Wirth I, Cremer R (2002) Increasing of the milling performance of cemented carbide coated inserts, by the deposition of a crystalline PVD Al_2O_3 top layer. In: *Proceedings of the 3rd international conference coatings in manufacturing engineering*, pp 137–147
- Bouzakis K-D, Michailidis N, Skordaris G (2005a) Hardness determination by means of a FEM-supported simulation of nanoindentation and applications in thin hard coatings. *Surf Coat Technol* 200:867–871
- Bouzakis K-D, Skordaris G, Michailidis N, Asimakopoulos A, Erkens G (2005b) Effect on PVD coated cemented carbide inserts cutting performance of micro-blasting and lapping of their substrates. *Surf Coat Technol* 200:128–132
- Bouzakis K-D, Mirisidis I, Michailidis N, Lili E, Sampris A, Erkens G, Cremer R (2007) Wear of tools coated with various PVD films: correlation with impact test results by means of FEM simulations. *Plasma Process Polym* 4(3):301–310
- Bouzakis K-D, Michailidis N, Gerardis S, Katirtzoglou G, Lili E, Pappa M, Brizuela M, Garcia-Luis A, Cremer R (2008a) Correlation of the impact resistance of variously doped CrAlN PVD coatings with their cutting performance in milling aerospace alloys. *Surf Coat Technol* 203(5–6):781–785
- Bouzakis K-D, Lili E, Michailidis N, Friderikos O (2008b) Manufacturing of cylindrical gears by generating cutting processes: a critical synthesis of analysis methods. *CIRP Ann Manuf Technol* 57(2):676–696
- Bouzakis K-D, Skordaris G, Klocke F, Bouzakis E (2009) A FEM-based analytical-experimental method for

- determining strength properties gradation in coatings after micro-blasting. *Surf Coat Technol* 203(19): 2946–2953
- Bouzakis K-D, Batsiolas M, Malliaris G, Pappa M, Bouzakis E, Skordaris G (2010a) New methods for characterizing coating properties at ambient and elevated temperatures. *Key Eng Mater* 438:107–114
- Bouzakis K-D, Makrimalakis S, Katirtzoglou G, Skordaris G, Gerardis S, Bouzakis E, Leyendecker T, Bolz S, Koelker W (2010b) Adaption of graded Cr/CrN-interlayer thickness to cemented carbide substrates' roughness for improving the adhesion of HPPMS PVD films and the cutting performance. *Surf Coat Technol* 205(5):1564–1570
- Bouzakis K-D, Michailidis N, Bouzakis E, Katirtzoglou G, Makrimalakis S, Gerardis S, Pappa M, Klocke F, Schalaster R, Gorgels C (2011a) Cutting performance of coated tools with various adhesion strength quantified by inclined impact tests. *CIRP Ann Manuf Technol* 60(1):105–108
- Bouzakis K-D, Bouzakis E, Skordaris G, Makrimalakis S, Tsouknidas A, Katirtzoglou G, Gerardis S (2011b) Optimization of wet micro-blasting on PVD films with various grain materials for improving the coated tools' cutting performance. *CIRP Ann Manuf Technol* 60(1):587–590
- Bouzakis K-D, Maliaris G, Makrimalakis S (2012) Strain rate effect on the fatigue failure of thin PVD coatings: an investigation by a novel impact tester with adjustable repetitive force. *Int J Fatigue* 44:89–97
- Bouzakis K. D., Makrimalakis S., Skordaris G., Bouzakis E., Kombogiannis S., Katirtzoglou G., Maliaris G., (2013) Coated tools' performance in up and down milling stainless steel, explained by film mechanical and fatigue properties. *Wear* 303:546–559
- Denkena B, Breidenstein B (2010) Pre PVD-coating processes and their effect on substrate residual stress in carbide cutting tools. *Key Eng Mater* 438:17–22
- Endrino JL, Derflinger V (2005) The influence of alloying elements on the phase stability and mechanical properties of AlCrN coatings. *Surf Coat Technol* 200: 988–992
- Erkens G (2007) New approaches to plasma enhanced sputtering of advanced hard coatings. *Surf Coat Technol* 201:4806–4812
- Erkens G, Vetter J, Mueller J, Brinke T, Fromme M, Mohnfeld A (2011) Plasma-assisted surface coating: processes, methods, systems and applications. Verlag Moderne Industrie, Landsberg am Lech
- Flink A, M'Saoubi R, Giuliani F, Sjöln J, Larsson T, Persson P, Johansson MP, Hultman L (2009) Microstructural characterization of the tool-chip interface enabled by focused ion beam and analytical electron microscopy. *Wear* 266:1237–1240
- Haubner R, Kalss W (2010) Diamond deposition on hardmetal substrates: comparison of substrate pretreatments and industrial applications. *Int J Refract Met Hard Mater* 28(4):475–483
- Klocke F, Krieg T (1999) Coated tools for metal cutting: features and applications. *CIRP Ann* 48(2):1–11
- Klocke F, Gorgels C, Bouzakis E, Stuckenberg A (2009) Tool life increase of coated carbide tools by micro blasting. *Prod Eng* 3(4–5):453–459
- Klocke F, Michailidis N, Bouzakis KD, Witty M, Gerardis S, Lili E, Pappa M (2010) Investigation of coated tools' cutting performance in milling Ti₆Al₄V and its correlation to the temperature dependent impact resistance of the film. *Prod Eng Res Dev* 4(5):509–514
- Knotek O, Bosserhoff B, Schrey A, Leyendecker T, Lemmer O, Esser S (1992) A new technique for testing the impact load of thin films: the coating impact test. *Surf Coat Technol* 54–55:102–107
- López de Lacalle LN, Lamikiz A, Fernández J, Azokona I (2010) Cutting tools for hard machining. In: Davim P (ed) *Hard machining*. Springer, London
- Quinto DT (1988) Mechanical property and structure relationships in hard coatings for cutting tools. *J Vac Sci Technol A* 6:2149–2157
- Shimada S, Fuji Y, Tsujino J, Yamazaki I (2010) Thermal plasma CVD and wear resistance of double layered Ti-Si-B-C/Ti-B-C coatings on WC-Co cutting tools with various roughness. *Surf Coat Technol* 204(11): 1715–1721
- Skordaris G, Bouzakis K-D, Charalampous P, Kotsanis T, Bouzakis E, Lemmer O (2016) Effect of structure and residual stresses of diamond coated cemented carbide tools on the film adhesion and developed wear mechanisms in milling. *CIRP Ann*. <https://doi.org/10.1016/j.cirp.2016.04.007>
- Toenshoff HK (2011) Cutting, fundamentals. In: Hans Kurt (H.-K. Toenshoff) (eds) *Encyclopedia of production engineering*. Springer, Heidelberg
- Toenshoff HK, Blawit C, Rie KT, Gebauer A (1997) Effects of surface properties on coating adhesion and wear behaviour of PACVD-coated cermets in interrupted cutting. *Surf Coat Technol* 97(1–3):224–231
- Uhlmann E, Koenig J (2009) CVD diamond coatings on geometrically complex cutting tools. *CIRP Ann Manuf Technol* 58:65–68

Cocreation

- ▶ [Emergent Synthesis](#)

Codevelopment of Manufacturing (Production) Systems

- ▶ [Coevolution of Manufacturing Systems](#)

Coevolution of Manufacturing Systems

Tullio Tolio¹, Hoda A. ElMaraghy² and Anna Valente³

¹ITIA Institute of Industrial Technologies and Automation, CNR National Research Council, Milan, Italy

²Canada Research Chair in Manufacturing Systems, Intelligent Manufacturing Systems Centre, University of Windsor, Windsor, ON, Canada

³ISTePS, Institute of Systems and Technologies for Sustainable Production, SUPSI- University of Applied Sciences and Arts of Italian Switzerland, Manno, Italy

Synonyms

[Codevelopment of manufacturing \(production\) systems](#)

Definition

The coevolution paradigm refers to the joint design, development, and management of products, processes, and production systems throughout their life cycles. These three entities are defined in the following consistent with the CIRP Dictionary of Production Engineering:

- *Product* is the output of the transformation made by a production system during execution of a process.
- *Process* is the set of basic operations and logical procedures executed by the manufacturing (production) system to carry out a transformation resulting in obtaining a product.
- *Production (manufacturing) system* is the set of resources, control logics, and management policies that allow performing a transformation to obtain a product by executing a process.

Theory and Application

Introduction

Manufacturing is challenged worldwide by complex economic, sociopolitical, and technological dynamics having tremendous impact on strategies followed by manufacturing enterprises and their behavior in the market and, consequently, on the research priorities of the scientific community. Many external drivers modify the way products, processes, and systems are designed and exploited, among them the introduction of new materials, technologies, services, and communications, in addition to the constant pressure on costs and the attention paid to sustainability requirements (Tolio et al. 2010).

Products are increasingly becoming more complex involving both the physical product enhanced by services which are proposed to the end users by carefully designed communication plans. Physical products are characterized by innovative materials and more complex shapes that ensure the achievement of very high technological and functional performance over time. The realization of such advanced product solutions relies on the development of very innovative technologies, the efficiency of which in terms of productivity, costs, and environmental impacts is significantly improved compared to traditional technologies. New solutions of products and technologies concurrently require radically new production system solution.

The “coevolution” concept embraces such a challenge by representing the ability to manage strategically and operationally the concurrent design, implementation, and management of products, processes, and production systems to gain competitive advantage from the resulting market and regulatory dynamics (Tolio et al. 2010).

History

The features and complexities of the coevolution of product, process, and systems attracted over time a significant interest from the scientific and industrial communities. This inspired in 2006 the creation of an international working group within CIRP Academy entitled SPECIES – robuSt

Production system Evolution Considering Integrated Evolution Scenarios – whose primary objective was to investigate the different aspects related to the coevolution of products, processes, and production systems. The working group represented the first occasion where discussions, case studies, and best practices in the field of coevolution have been shared between scientific and industrial colleagues. Even after the end of the SPECIES working group, the research in the field of coevolution still represents a flourishing ongoing activity laying the foundation for new promising research opportunities in manufacturing.

The following subsections will outline the main features of the coevolution approach along with the related research challenges and future steps.

Coevolution Enablers

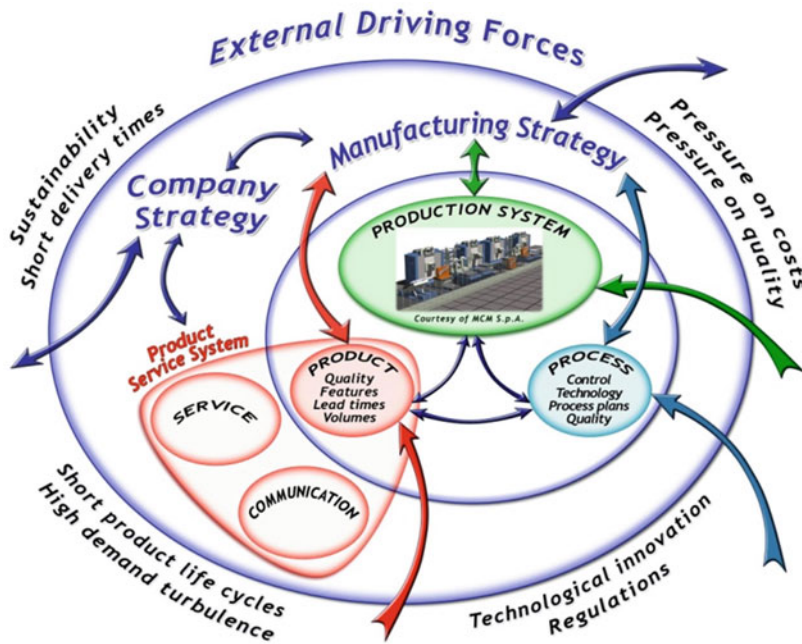
As a result of the dynamic manufacturing scenario, the production requirements such as responsiveness and flexibility are evolving into new production enablers such as cognitive adaptability, changeability, self-diagnosis, self-resilience, self-improving environment paradigms, and co-creation (Wiendahl et al. 2007; Ueda et al. 2009; Zhang and van Luttervelt 2011). The procedures to trigger system configuration modification by using existing system coevolution enablers can be classified as reactive and proactive. Reactive procedures trigger the production system modification after a change in one of the other two entities has been observed (product and process), while proactive procedures trigger a modification of the system when performance improvement is required. An example of a reactive procedure to properly address the coevolution of production systems and products is based on the reusability principle that – applied to manufacturing systems – represents their capability to be repeatedly utilized from one generation of products to another after the initial use (Ko et al. 2005). This approach considers production systems that have the modularity to be organized into many different configurations (e.g., serial, parallel, or hybrid) each one characterized by different levels of quality, throughput, responsiveness, and costs. When planning for the

coevolution of products and production systems, it is necessary to select the configuration that maximizes reuse of the machines and resources in the system from one product generation to another. Together with these new enablers, new approaches and tools have been developed (ElMaraghy et al. 2008; AlGeddawy and ElMaraghy 2010). ElMaraghy et al. (2008) introduced new coevolution hypotheses and their proofs which are inspired by the coevolution between species in nature and applied them to the evolution and coevolution of products and manufacturing systems. The study showed that association and symbiosis in manufacturing may take one of two forms: (1) disruptive, when new manufacturing paradigms, materials, and technologies are introduced, and (2) gradual, where small modifications in product design are handled by small incremental changes in manufacturing systems. This new concept was applied to many real products and systems coevolution (ElMaraghy and AlGeddawy, 2012). The inherently complex dynamics of change propagation that companies are continuously pursuing by shaping their corporate strategy and combining external needs to the internal requirements of efficiency, productivity, and cost-effectiveness impacts all levels of the organization, as illustrated in Fig. 1.

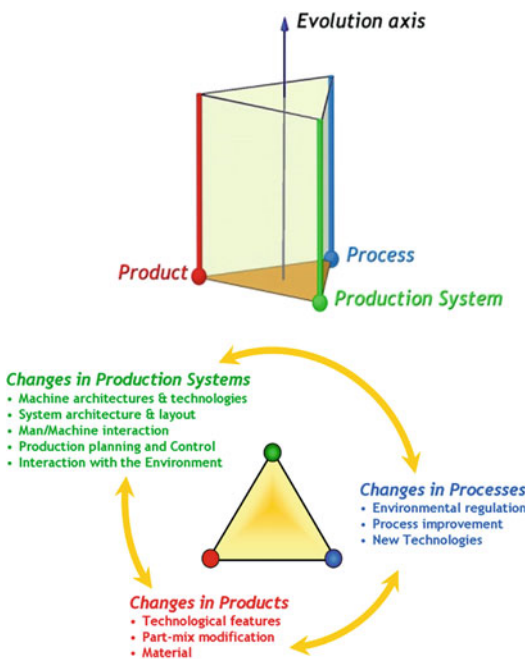
Within the coevolution concept, this process is conceived as dynamic over time in order to accomplish the changes of the production requirements across the product, process, and system life cycles from their design to their end-of-life. This necessitates avoiding myopic vision and approaches focused only on products, technologies, or equipment that could lead to lower performance and partially exploited production solutions.

The Coevolution Approach

The coevolution paradigm embraces the very strong correlation between products, technologies, and manufacturing equipment over time. It specifically involves the repeated configuration of product, process, and production system over time together with their concurrent management and optimization, to profitably face and proactively shape the market dynamics (Fig. 2).



Coevolution of Manufacturing Systems, Fig. 1 Manufacturing dynamics

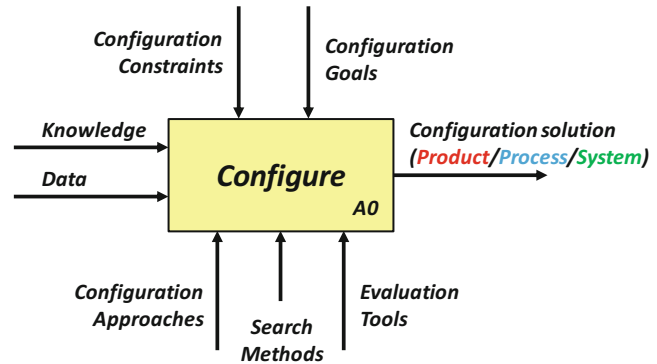


Coevolution of Manufacturing Systems, Fig. 2 The coevolution paradigm

The coevolution paradigm refers to a model that delimits a space where coevolution management approaches, tools, and problems can be mapped, by following a number of logical rules and a metrics. For the sake of graphical clarity, in the diagram (Fig. 2), different colors are associated with products (red), processes (blue), and equipment/production systems (green). The vertical axis represents the evolution axis. At any level of the evolution axis, the triangular cross section represents the integration space among the three entities.

This coevolution model has a number of uses. From the research perspective, it can support the classification of the present state of the art related to coevolution of products, processes, and production systems together with the identification of research areas that are poorly addressed but represent potential for future activities. From the industrial perspective, the model enables the framing of approaches supporting coevolution that are suitable to address and solve the specific problems of companies. It also supports the

Coevolution of Manufacturing Systems, Fig. 3 IDEF0 model for the “Configuration” activity



formalization of different industrial problems, considering the impact of the market and the company’s organization together with the achievement of company strategy targets.

The coevolution paradigm involves a deep understanding of the dynamics of products, processes, and production systems. Figure 3 outlines the high-level formulation of the product-process-system joint configuration problem constituting the basis upon which the specific product, process, and system configuration activities can be derived. Thus, this general approach can be implemented differently with the specific production requirements and objectives for each company. Several examples of the configuration problem application are outlined in Tolio et al. (2010).

The input of the activity (Fig. 3, horizontal arrow entering the activity box from the left) is “information,” which includes knowledge and data. Knowledge denotes the basic set of rules known to the individual who performs the activity, whereas data define a specific instance. The output (Fig. 3, horizontal arrow exiting the activity box from left to right) of the activity “configure” is a configuration solution, characterized by a detailed and complete set of logical and physical descriptions. The mechanisms are the methods used to perform the activity (Fig. 3, vertical arrow entering the activity box from the bottom). For the activity “configure,” these methods and tools consist of configuration approaches, search methods, and evaluation tools. The configuration approaches support the problem formulation and systemization, thus driving the way a specific

configuration activity is carried out. They include very heterogeneous approaches dealing with the production aspects such as concurrent engineering together with approaches referring to organization aspects where also the market dynamics are incorporated. Search methods facilitate the selection of the most suitable solutions. They can be based on mathematical programming, expert systems, gradient methods, genetic algorithms, simulated annealing, and other soft-computing techniques. Evaluation tools are used to estimate and quantify some performance measures related to one particular configuration solution. In this way, alternative solutions can be compared based on common performance indexes. They can be either analytical, simulation, or digital tools. For example, simulation tools can support the simulation of the product (e.g., FEM and dynamic simulation), the physical process (e.g., process planning simulation), or the system simulation (e.g., discrete event simulation), while the virtual mock-up of the product, process, and system can be an example of digital tool. Constraints (Fig. 3, vertical arrows entering the activity box from the top) represent the set of rules limiting extension of the configuration space. The configuration goals define the set of criteria according to which different configuration alternatives are compared.

A configuration approach is defined as the entire procedure followed to jointly configure the product, process, and production system. Indeed, product, process, and system must all be designed to carry out a production transformation. The ways of handling the configuration approach can

range from tightly integrated to sequential configuration strategies. An example of a unique and integrated approach concerns the collaborative configuration where the product, process, and production system are collaboratively configured, considering the knowledge available about all the objects by a multidisciplinary team. An example of a sequence of isolated configuration methodologies considers as a first step the product configuration using only product data and knowledge, followed by the process configuration where product and technologies data and knowledge are used to end-up with the system configuration that is developed on the basis of product and process data together with information about the physical equipment.

The coevolution model enables the evaluation of the comprehensive configuration approach by analyzing both the integration and the evolution level. The level of integration is defined as the ability of a configuration approach to provide product-process-system configuration solutions taking into account the product, process, and production system data as well as knowledge. The level of integration is related to the input information used to carry out the configuration activity. The level of evolution is defined as the capability of a configuration approach to provide configuration solutions considering uncertain information about future evolution of one or more configuration entity. Uncertainty usually affects constraints, goals, or the input information of the configuration activity.

Benefits of Applying Coevolution Strategies

In the field of coevolution, a number of works deal with the analysis and application of the coevolution paradigm with regard to specific industrial problems with the support of companies operating across different sectors and industries (e.g., automotive, aerospace, equipment production, component manufacturing) as well as embracing different cultures and countries. An overview can be found in Tolio et al. (2010). Coevolution of products and systems has been applied in many areas: it was applied to predicting and synthesizing of new products and manufacturing systems (AlGeddawy and ElMaraghy 2012) and their coevolution (AlGeddawy and ElMaraghy 2011).

The major benefits related to the implementation of the coevolution paradigm are listed in the following:

- The coevolution paradigm has the power to comprehensively embrace the industrial dynamics leading to a more efficient management of products, processes, and production systems joint evolutions.
- The coevolution paradigm enables the evaluation of the optimization actions across several levels of the factory.
- Managing coevolution can be economically beneficial both for technology users and providers. Industrial companies are experiencing a trend toward increased investments in their ability to drive coevolution.
- The coevolution paradigm would lead industries to mature the practice of identifying and mapping their own capabilities in terms of products, technologies, and equipment. As a consequence, on the one hand, products can be (re) designed and upgraded with the knowledge of the actual and potential manufacturing technologies and systems capabilities. On the other hand, the development of machine tools and production systems can result from a structured analysis of the technological requirements of co-evolving products, processes, and systems.
- The coevolution paradigm would support a conscious control of the industrial evolving dynamics. Manufacturers would maximize their systems' current and future adaptability to frequent products changes, while product designers would be challenged to utilize all available and forecasted manufacturing capabilities before introducing features that require significant changes of those capabilities.

Challenges

The adoption of the coevolution paradigm outlines a number of *challenges for the scientific and industrial communities* which are briefly listed in the following:

- The joint analysis of product, process, and system data over time is severely limited by the existing software tools and configuration methodologies. Software tools and development

platforms lack the possibility to manage all-in-one multidisciplinary knowledge and information, while the existing configuration methodologies still cannot enable multiple configuration tasks (e.g., dealing with the product and the process at the same time).

- The structuring and systemization of the factory knowledge, data, and constraints necessary to apply the coevolution approach because of the high number of heterogeneous information along with a loosely coupled organization structure and the lack of multidisciplinary teams.
- The application of coevolution to new ways to manufacture increasingly complex products which often consist of components produced in several production sites.
- A radical chance of machine tool builder business strategies that would require the shift of the production from standard and rigid catalogue resources to instrumented goods and physical equipment characterized by high levels of modularity and reconfigurability in order to match the frequent evolution of production requirements.

Concurrently with the scientific and industrial challenges, the coevolution approach embraces various *research opportunities* for the future developments in manufacturing. Few examples are briefly outlined in the following:

- Investing in the knowledge management where the product, process, and system engineering knowledge would be merged with the knowledge about economic, sociopolitical, and strategic aspects. The number of different aspects to be considered within the configuration process as well as the reciprocal impact of one single decision on the manufacturing environment and the market will be only handled by multidisciplinary teams and researchers with an extremely broad know-how.
- Conceiving configuration processes where humans will have an instrumental role by enabling both the incorporation of human choices and policies in structured software environment and the human workers harmonious cooperation with physical devices operating in the shop-floor. This would allow the possibility

to enhance the configuration decisions with the human expertise, know-how, and capability to interpret, forecast, and evaluate the exogenous and endogenous production requirements.

- Achieving a persistent interaction among the various layers of the factory to ensure the achievement of more efficient configuration choices by drastically reducing the times and mistakes characterizing the communication and cooperation procedures across the company. An example pertains to the interaction between the corporate and manufacturing strategy during the configuration activity which is currently extremely vertical and loosely coupled resulting in decision processes starting from the corporate strategy and ending up on the shop-floor going through many inefficient iterations.
- The development of software platforms and frameworks conceived to support the manipulation of a large cluster of information and activities pertaining the product, process, and system life cycles in order to handle the multifaceted aspects characterizing the overall configuration problem together with the heterogeneous knowledge and cooperative communication infrastructure. The achievement of such a level of integration would require both the research effort and the proactive support of technology and ICT providers who would be asked to realize radically new solutions of open and interoperable software.
- The design and development of radically innovative configuration methodologies oriented to coevolution where the product-process-system integration and evolution features will be addressed by effective methods with efficient resolution times capable of dealing with large problems and frequently regenerating the configuration solution to face production changes.

Cross-References

- ▶ [Cladistics for Products and Manufacturing](#)
- ▶ [Changeable Manufacturing](#)
- ▶ [Life Cycle Engineering](#)
- ▶ [Manufacturing System](#)
- ▶ [Process](#)
- ▶ [Reconfigurable Manufacturing System](#)

References

- AlGeddawy T, ElMaraghy H (2010) Co-evolution hypotheses and model for manufacturing planning. *CIRP Ann Manuf Technol* 59(2):445–448
- AlGeddawy T, ElMaraghy HA (2011) A model for co-evolution in manufacturing based on biological analogy. *Int J Prod Res (IJPR)* 49(15):4415–4435
- AlGeddawy T, ElMaraghy H (2012) A co-evolution model for prediction and synthesis of new products and manufacturing systems. *ASME J Mech Des* 134(5) Art. no. 051008. <https://doi.org/10.1115/1.4006439>
- ElMaraghy H, AlGeddawy T (2012) Co-evolution of products and manufacturing capabilities and application in auto-parts assembly. *Flex Serv Manuf J (FSMJ)* 24(2):142–170. <https://doi.org/10.1007/s10696-011-9088-1>
- ElMaraghy H, AlGeddawy T, Azab A (2008) Modelling evolution in manufacturing: a biological analogy. *CIRP Ann Manuf Technol* 57(1):467–472
- Ko J, Hu SJ, Huang T (2005) Reusability assessment for manufacturing systems. *CIRP Ann Manuf Technol* 54(1):113–116
- Tolio T, Ceglarek D, ElMaraghy H, Fischer A, Hu SJ, Laperriere L, Newman ST, Vancza J (2010) SPE-CIES—co-evolution of products, processes and production systems. *CIRP Ann Manuf Technol* 59(2): 672–693
- Ueda K, Takenaka T, Vancza J, Monostori L (2009) Value creation and decision-making in sustainable society. *CIRP Ann Manuf Technol* 58(2):681–700
- Wiendahl H-P, ElMaraghy H, Nyhuis P, Zäh MF, Wiendahl H-H, Duffie N, Brieke M (2007) Changeable manufacturing – classification, design and operation. *CIRP Ann Manuf Technol* 56(2):783–809
- Zhang WJ, van Luttervelt CA (2011) Toward a resilient manufacturing system. *CIRP Ann Manuf Technol* 60(1):469–472

Coining

- [Embossing](#)

Cold Bulk Forming

- [Cold Forging](#)

Cold Extrusion

- [Cold Forging](#)

Cold Forging

Marion Merklein

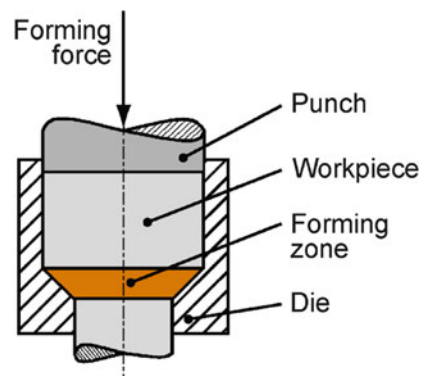
LFT, Institute of Manufacturing Technology, Friedrich-Alexander-Universität Erlangen-Nürnberg, Erlangen, Germany

Synonyms

[Cold bulk forming](#); [Cold extrusion](#); [Impact extrusion](#)

Definition

The term “cold forging” represents both a range of bulk forming processes done with workpieces at room temperature without an additional external heating and the resulting component made by cold forging. Metalworking by cold forging predominantly comprises cold extrusion processes. In an extrusion process, the cross-sectional area of a single workpiece is reduced by forcing it through an orifice with a punch, as shown in Fig. 1. In cold extrusion, the workpiece is initially at room temperature when supplied to the forming process (CIRP 1997).



Cold Forging, Fig. 1 Principle of cold forging exemplified by a forward rod extrusion process. (According to Schuler GmbH, Solid forming (Forging), 1998, p. 471, Fig. 5.1)

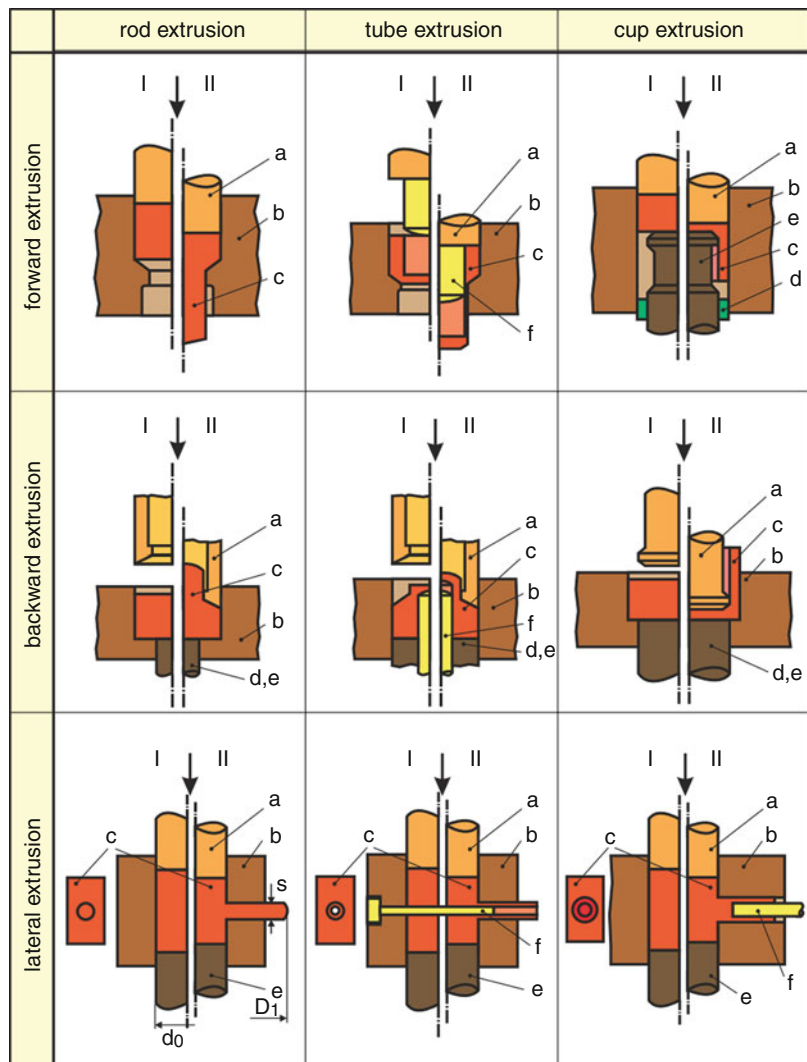
Theory and Application

Classification

Cold forging is a manufacturing process in the area of bulk forming. This implies the use of compact and commonly massive semi-finished parts. These billets are subjected to considerable changes in cross-sectional areas and wall thicknesses in all spatial directions (Lange 1985). A high fraction of cold forging processes are extrusion processes. These belong to the subgroup extrusion (DIN 8583-6 2003) within the group forming under compressive conditions (DIN 8583-1 2003). In an extrusion process, a punch

presses the workpiece through the die that forms the designated shape of the part. This class of forming processes is predominantly characterized by a multiaxial compressive stress condition, along with a multiaxial material flow. According to Lange (1985), extrusion processes can be classified by the flow direction of the workpiece material related to the tool movement direction (forward, backward, lateral) as well as the geometry of the extruded workpiece (solid, hollow, can). This leads to the nine basic process layouts shown in Fig. 2. The terms “rod,” “tube,” and cup extrusion in Fig. 2 correspond to solid, hollow, and can extrusion, respectively.

Cold Forging,
Fig. 2 Schematic representation of cold extrusion processes: *I* prior to forging; *II* after forging (BDC); *a* punch; *b* container; *c* workpiece; *d* ejector; *e* counterpunch; *f* mandrel. (With kind permission from Springer Science+Business Media: Metal Forming Handbook/Schuler, Solid forming (Forging), 1998, p. 434, Fig. 1.1)



Besides extrusion, further common bulk forming processes are upsetting and ironing. The former belongs to the group of free forming (DIN 8583-3 2003), the latter to the group of tensile-compressive forming (DIN 8584-2 2003). In addition, shafts may be formed by reducing, a variant of extrusion. Forged components often have an axially symmetric shape and are usually manufactured in several stages. Combinations of several basic processes in one stage are possible and even desirable to shorten process chains and to reduce forces. Compared to bar extrusion, which is used for the fabrication of continuous or semi-continuous parts to a great extent, cold forging is usually applied to manufacture discrete components (Schuler GmbH 1998).

Process Characteristics

Cold forging of metals has several remarkable advantages over hot forging or machining. Compared to hot forging, the most significant benefits are the increased geometrical accuracy as well as the high surface quality. Hence, the required machining allowances can be kept very low. This helps to increase the material utilization and to reduce processing steps like milling and grinding after forging. Some functional surfaces, such as splines or ball tracks for constant-velocity joints, even achieve net-shape quality after cold forging. Due to an increasing scarcity of resources and the demand for energy and cost savings, this aspect is gaining importance.

Cold forging also causes considerable work hardening of the workpiece material including a continuous grain orientation. This leads to an extended loadability and high fatigue resistance of the part, which is a significant advantage compared to machining. However, this benefit is diminished by a final heat treatment process, which involves a recrystallization of grain structure (Dahme et al. 2011).

Besides these advantages, there are some challenges and disadvantages the application of cold forging has to face. Compared to hot forging and machining, the low formability and restricted variety of shapes have to be considered. In addition, the high flow stress in cold

forging leads to high forming forces and high mechanical loading of the tool. The need for high-strength tools results in increased tool costs. Hence, cold forging is not profitable in small lot sizes. However, due to short cycle times and a low energy input per workpiece, it is suitable for an economic large quantity production of high-strength parts. Cold forging can also be applied after warm or hot forging stages for calibration purposes. In the majority of cases, cold forging is performed on force- and stroke-controlled presses.

Range of Parts and Workpiece Materials

A major amount of cold forging processes is applied in the automotive industry. This comprises a variety of chassis and steering components, for example knuckle joints, as well as transmission and drive line parts, such as transmission shafts, pinions, and constant-velocity joints. Another considerable application for cold forging is the manufacturing of various kinds of fasteners. Figure 3 shows the inner race for a constant-velocity joint, a component of an automotive drive line.

Steel is the prevailing workpiece material in cold forging. For low mechanical requirements, unalloyed or low-alloyed steels are in use. For higher demands, heat treatable steels are employed. Besides steel, aluminum materials and, for electrical engineering, copper is applied. To ensure a high



Cold Forging, Fig. 3 Inner race of a constant-velocity joint

formability, the billets are often prepared by a special heat treatment before forging. If the formability of the workpiece material is exceeded, an intermediate heat treatment between the forming stages is required. Due to the beneficial strain hardening, sufficient workpiece strength can be achieved without using high alloy steels depending on the application (Lange et al. 2008).

Tools

The high flow stress of the workpiece material, considerable changes in cross-sectional areas, and long sliding paths lead to high loading of cold forging tools concerning wear and fatigue. Occurring radial stresses in the die during the forming operation are critical with respect to fatigue and overload breaking. In order to prevent the die inserts from failure, reinforcement by one or more shrink rings in radial direction is required when an internal die pressure of about 1.000 N/mm^2 is exceeded. The layout of this radial prestressing system should reduce or entirely avoid tangential tensile stresses and strains in the die during the forging process. The die insert has to provide sufficient hardness to resist the prestressing as well as the internal process loads. High hardness also implies high wear resistance. The prestress condition is realized by an interference fit between die and the shrink rings (ICFG Document No. 14/02 2002).

If the required strength exceeds the limits of standard tool steels, powder metallurgical steels, cemented carbides, or even ceramics can be used as material for die inserts. However, cemented carbides and ceramics are highly sensitive to tensile strains. If very high radial prestress conditions have to be applied, strip wound containers with a core made of cemented carbide are applied. Axial tensile stresses in the die inserts have to be avoided as well. By dividing the die in lateral direction and applying an axial prestressing, tensile stresses can be avoided and tool life can be enhanced (ICFG Document No. 16/04 2004).

Lubrication and Coatings

The occurring load conditions in cold forging in terms of contact normal stresses and surface

enlargements make high demands on lubrication. To deal with these tough tribological conditions, the billets are usually bonderized whereby a phosphate coating represents the industrial standard. During the bonding process a zinc phosphate coating is formed on the workpiece surface. This is the base for the application of lubricants like molybdenum disulfide or soap and ensures an improved adhesion to the metal surface. Oil-based lubricants are used for processes with low strains and contact normal stresses (Lange et al. 2008). However, there are efforts to reduce the use of lubricants and to avoid bonderizing of coils and semi-finished parts for economic and ecological reasons.

To extend tool life by increased wear resistance, ceramic coatings can be used. Common coatings in cold forging are TiN and TiCN that are applied by Physical Vapor Deposition. Beyond single-layer coatings, multilayer coatings can be employed to effectively inhibit superficial crack initiation and propagation (Doege and Behrens 2007).

The friction factor resulting from a certain tribological system can be determined by means of the double cup extrusion test. The plastic strains and contact stresses in this test are similar to the conditions in cold forging. The friction factor is an important input value for numerical simulation.

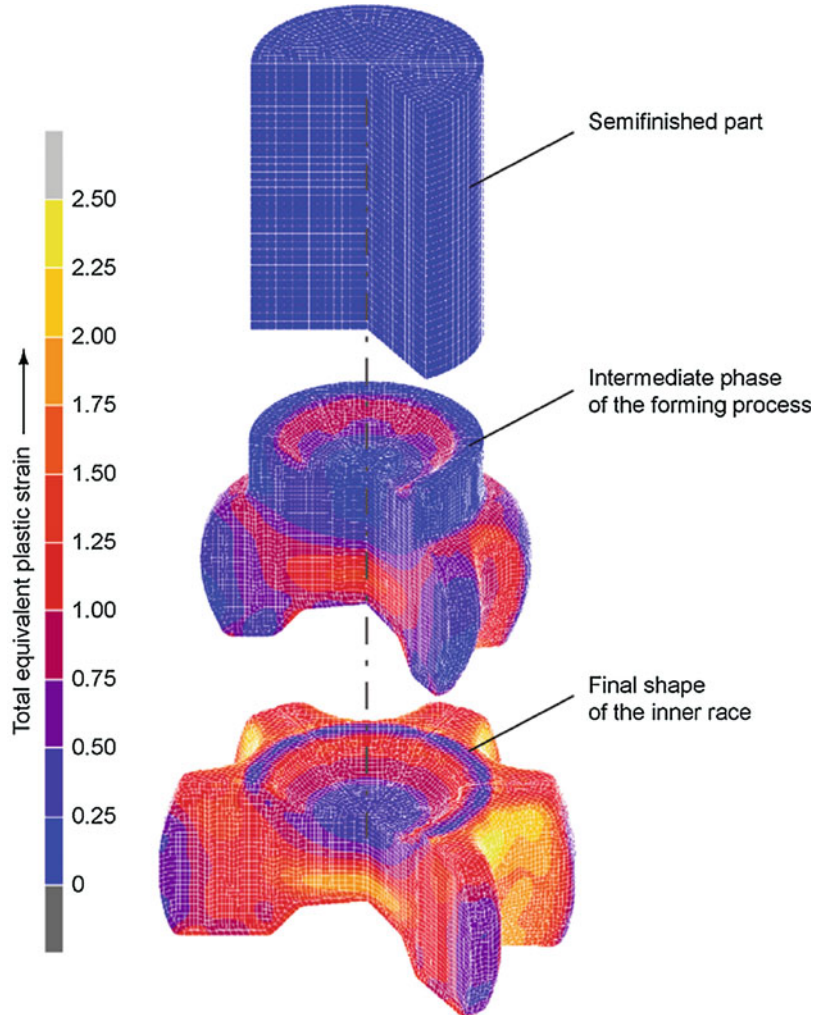
FE Simulation

FE simulation can serve as a valuable instrument to analyze the material flow and to determine the shape of single forging stages (Fig. 4).

In addition, FE simulation is applied to determine load-adapted tool layouts by modeling the die insert and the prestressing system. This helps to enhance tool life and to reduce tool failure by overload and fatigue. The commonly used procedure nowadays is a combined modeling of workpiece and tool, including the prestressing system for a 2D axial symmetric as well as a 3D representation of processes. However in order to reduce the great computational effort for a 3D representation, a decoupled approach with a separate investigation of material flow and tool loading is possible. Therefore the material flow of the forging process is simulated while assuming rigid behavior of the die insert

Cold Forging, Fig. 4

3D FE simulation of the cold forging process for the manufacturing of an inner race. Workpiece material: boron-manganese steel



and prestressing system. Subsequently, the determined process loads are applied to an elastic model of the tool to elaborate a load-adapted layout. Thus, the use of the FE simulation in the stage of tool and process design can ensure a reliable process and a resistant tool. This can lead to considerable cost and time savings (Lange et al. 2008).

Trends

The future developments in cold forging are influenced by ecological as well as economic challenges. Due to its distinct dependency on the automotive industry, ecological issues affect the cold forging industry in terms of the need for lightweight construction to a great extent. Hollow

parts, for example, can effectively contribute to weight saving. In addition, increased material utilization, net-shape parts, function integration, and efficient process chains enable material and energy savings during the manufacturing process. These trends also help to fulfill the economic challenges that are mainly characterized by an increasing cost and time pressure in the global competition. However, meeting these trends leads to increased tool loads and sophisticated tool and process layouts. Thus, novel solutions in tool design are required, including advanced FE analysis, materials, tool manufacturing and polishing, surface treatment and coating, and other factors influencing tool life and tool quality (Engel et al. 2011).

Cross-References

- ▶ [Finite Element Analysis](#)
- ▶ [Finite Element Method](#)
- ▶ [Forming Tools \(Die, Punch, Blank Holder\)](#)
- ▶ [Friction](#)
- ▶ [Hot Forging](#)
- ▶ [Residual Stress \(Forming\)](#)

References

- CIRP (Collège International pour la Recherche en Productique) (1997) Dictionary of production engineering, metal forming 1, 2nd edn. Springer, Berlin
- Dahme M, Hirschvogel M et al (2011) Forged components. Hirschvogel Holding GmbH, Denklingen
- DIN 8583-1:2003-09 (2003) Manufacturing processes forming under compressive conditions – part 1: general; classification, subdivision, terms and definitions. Beuth, Berlin
- DIN 8583-3:2003-09 (2003) Manufacturing processes forming under compressive conditions – part 3: free forming; classification, subdivision, terms and definitions. Beuth, Berlin
- DIN 8583-6:2003-09 (2003) Manufacturing processes forming under compressive conditions – part 6: extrusion; classification, subdivision, terms and definitions. Beuth, Berlin
- DIN 8584-2:2003-09 (2003) Manufacturing processes forming under combination of tensile and compressive conditions – part 2: drawing through constricted tool orifices; classification, subdivision, terms and definitions. Beuth, Berlin
- Doege E, Behrens B-A (2007) Handbuch Umformtechnik [Metal forming handbook]. Springer, Berlin (in German)
- Engel U, Groenbaek J, Hinsel C, Kroiß T, Meidert M, Neher R, Räuchle F, Schrader T (2011) Tooling solutions for challenges in cold forging. *UTF Sci* 2011(3):1–24
- ICFG/International Cold Forging Group, Meisenbach GmbH (2002) ICFG-Document No. 14/02: tool life & tool quality in cold forging – part 1: general aspects of tool life. Meisenbach, Bamberg
- ICFG/International Cold Forging Group, Meisenbach GmbH (2004) ICFG-Document No. 16/04: tool life & tool quality in cold forging, part 2: quality requirements for tool manufacturing. Meisenbach, Bamberg
- Lange K (1985) Handbook of metal forming. McGraw-Hill, New York
- Lange K, Kammerer M, Pöhlandt K, Schöck J (2008) Fließpressen: Wirtschaftliche Fertigung metallischer Präzisionswerkstücke [Extrusion: efficient production of metallic precision parts]. Springer, Berlin (in German)
- Schuler GmbH (1998) Metal forming handbook. Springer, Berlin

Cold Gas Dynamic

- ▶ [Cold Spray](#)

Cold Gas Dynamic Manufacturing

- ▶ [Cold Spray](#)

Cold Gas Spray

- ▶ [Cold Spray](#)

Cold Joining

- ▶ [Mechanical Joining](#)

Cold Spray

Rocco Lupoi
Department of Mechanical and Manufacturing Engineering, Parsons Building, Trinity College Dublin, The University of Dublin, Dublin, Ireland

Synonyms

[Cold gas dynamic](#); [Cold gas dynamic manufacturing](#); [Cold gas spray](#); [Kinetic spray](#); [Supersonic spray](#)

Definition

Cold spray (CS) is a solid-state additive process, whereby material layers are added onto substrates or more general engineering components through the acceleration of the feedstock material (in the

form of powder) up to supersonic speed in a converging–diverging nozzle. Melting temperatures in the process are typically not reached.

Theory and Application

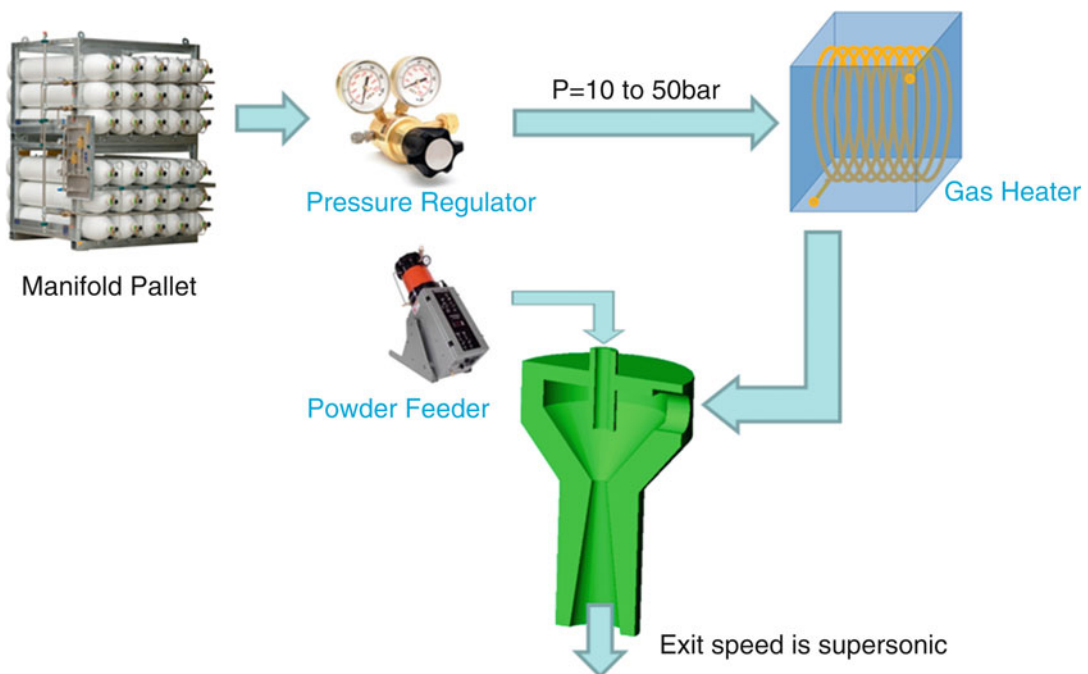
Introduction and Working Mechanism

In the 1980s, a group of scientists from the Institute of Theoretical and Applied Mechanics of the Siberian Branch of the Russian Academy of Sciences (ITAM of RAS) in Novosibirsk, Russia, conducted experimental and theoretical work on the interaction of a two-phase flow with the surface of immersed bodies. They used new gas dynamics diagnostic tools to study two-phase flow around bodies, which resulted in the discovery of some sort of “deposition phenomena.” The scientists had in fact observed thin copper layers deposited on the back walls of the wind tunnel they were using; soon after they realized the mechanism and formation of such was from a small amount of copper “dust” propelled at high

velocity on the walls. As many of the most successful inventions in engineering, also this one happened totally by chance.

A number of USSR patents followed to the initial discovery of the technology; however, in its modern form, cold spray (CS) was patented in 1994 in the USA by A.P. Alkhimov and A.N. Papyrin (Alkhimov et al. 1994).

Despite the simplistic working principles, CS is an efficient technology, whereby material is added to a general substrate in a solid-state manner; hence, melting temperatures are not crossed. As shown in Fig. 1, a supersonic converging–diverging nozzle is fed with a high-pressure gas (nitrogen or helium at pressures between 10 bar and 50 bar), which expands as it flows through the nozzle internal profile. Supersonic speed is therefore reached at the exit of the device ($M > 2$). At the same time, solid particles ($\sim 40 \mu\text{m}$ in size) are injected at the inlet of the nozzle. The generated fast jet stream can accelerate the particles up to velocities to cross 1000 m/s; upon impact against a substrate material, the



Cold Spray, Fig. 1 Cold spray working principles

particles will plastically deform and bond to it, hence the formation of a deposit. In most cases, the carrier gas is also preheated before entering the nozzle through a gas heater; this is to increase the carrier gas sonic speed, hence exit velocity.

In CS, each material is therefore characterized by a “critical speed.” Such is the minimum to be achieved at impact for the deposit to start forming. Strong materials (such as Ti and its alloys or WC–Co) have a high critical value; they will therefore require the use of helium to be processed (helium is a low-density gas with high sonic speed).

CS has a number of technical advantages over other methods that are based upon the partial or full melting of materials, such as laser cladding, high velocity oxygen fuel (HVOF), and plasma/flame spray (Champagne 2007):

The preservation of feedstock properties, no microstructural changes.

There is no heat-affected zone (HAZ) at the deposition interface.

Deposition rates (or build rates) can be very high.

Environmentally friendly relative to others due to the ambient temperature working conditions.

No theoretical limit in achievable deposition thickness.

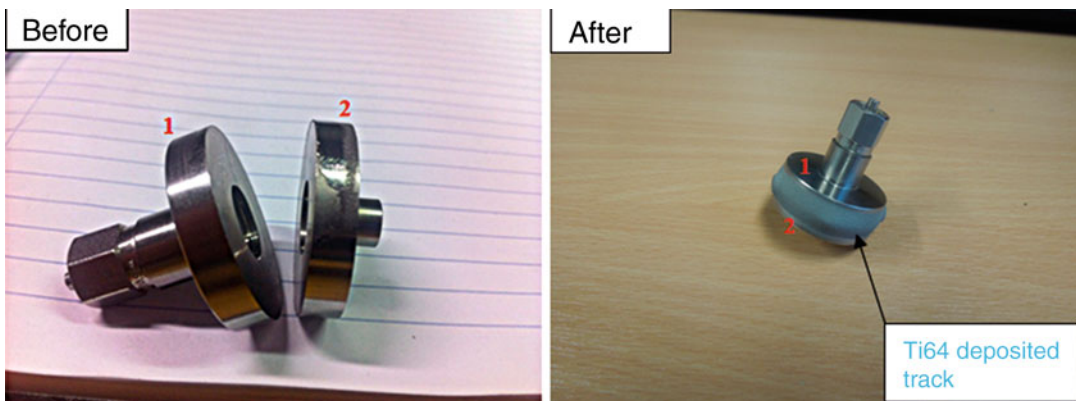
No thermal distortion and good bond strength.

Metallurgical compatibility feedstock/substrate is in theory not a requirement.

Since its invention and first implementations, CS has rapidly evolved at both European and global levels with a rather diverse field in terms of generated intellectual property (Irissou et al. 2008). A number of major companies have formed in across the globe, primarily coming from university spinouts and currently selling CS equipment. Research is very active in the field, with the main groups located in Ireland (Trinity College, Dublin), the UK (University of Cambridge, University of Nottingham, The Welding Institute (TWI)), France (School of Mines, Paris), and Germany (University of the Federal Armed Forces, Hamburg; European Aerospace Research Institute (EADS)). There are other key research facilities in Spain, the USA, Japan, Canada, Russia, South Africa, and Australia.

Examples of Applications

A vast variety of feedstock/substrate material combinations has so far been attempted with the process, with reasonably good results. The major advantage is its flexibility and absence of the thermal component; however, CS can be an expensive process to run. When helium is required, processing costs can become industrially not viable. This is the reason of why the vast majority of CS systems are currently installed in R&D facilities (such as universities or research institutes) and not in production lines. Research is active in this topic, therefore, in the proposition



Cold Spray, Fig. 2 Joining Ti64 components with CS (Courtesy of Trinity College Dublin and University of Twente)

and testing of new solutions so as to address the cost problem.

The list below provides some examples of recent applications, in relation to the deposition of:

- Hard-facing materials, such as WC–Co, onto steel (Dosta et al. 2013).
- Superalloys (Levasseur et al. 2012).

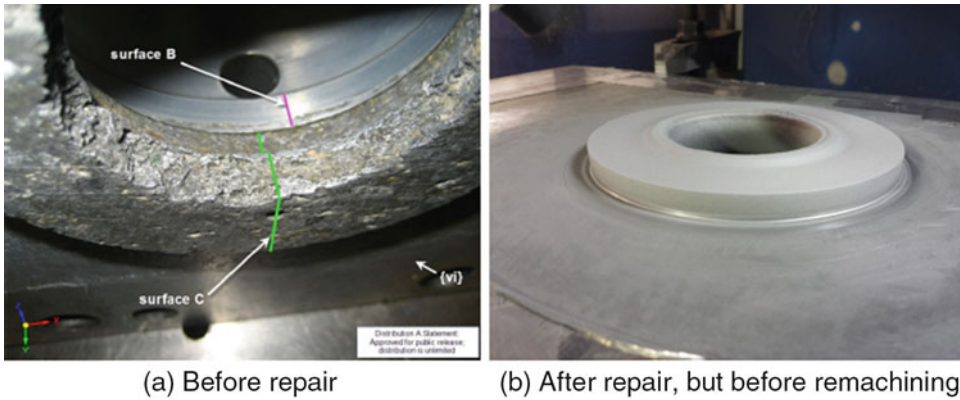
Reactive materials, such as Al/CuO mixtures (Bacciochini et al. 2013).

$M_{n+1}AX_n$ (MAX) phases (Gutzmann et al. 2012).

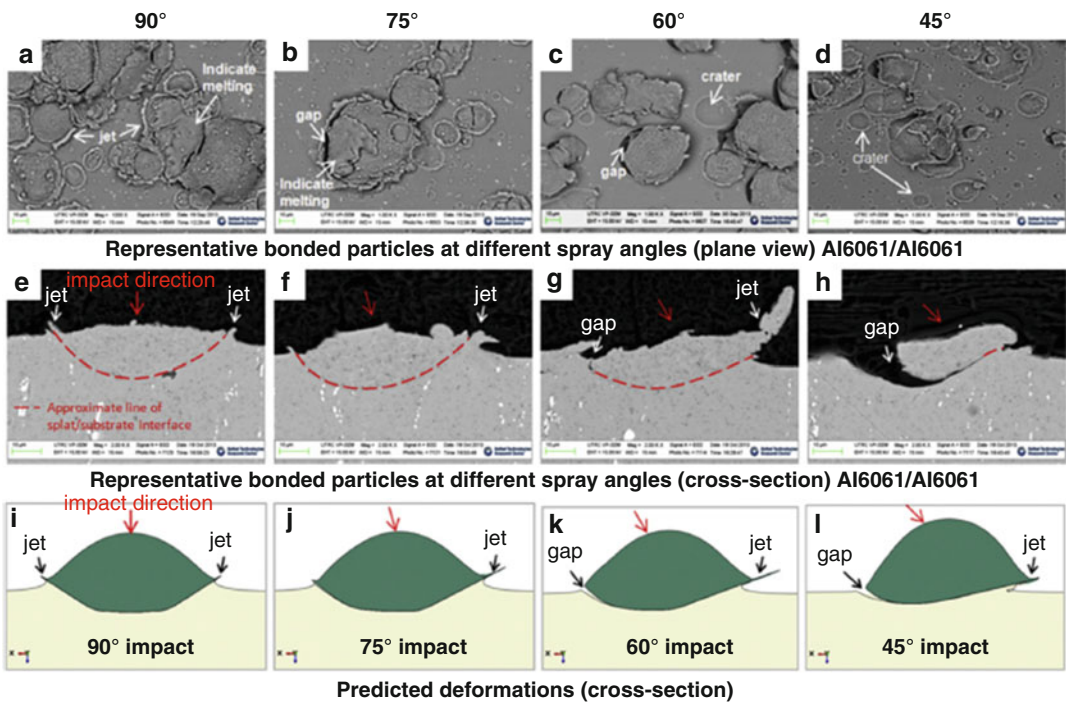
Tantalum (Trexler et al. 2012).

Diamond composites (Aldwell et al. 2016).

Recent work has also highlighted the potential for CS to be used for alternative



Cold Spray, Fig. 3 Repair of an actuator using CS (Widener et al. 2016)



Cold Spray, Fig. 4 Effect of particle impact angle on particle deformation and bond quality (Wang et al. 2015)

purposes, such as joining. As an example, Fig. 2 shows two axial-symmetric components (approximately 30 mm in outer diameter) made out of Ti64. They were joined through the application of a Ti64 track around the geometry using CS. This work is interesting due to the general unsuitability of Ti and its alloys to be welded using conventional thermal processes due to its high affinity to oxygen.

A common application area cited for CS is also the repair of corroded components, especially for the military and aerospace industry. This would involve the cleaning of corroded surfaces, followed by CS of material onto the damaged zone, and machining of the cold-sprayed material back to the pre-corrosion dimensions. The use of CS allows for the repair of components where hot weld deposition is not possible, such as magnesium or aluminum alloys, where traditional welding processes often yield poor results. Widener et al. reported porosity levels of 1.53% or below on a repaired actuator manufactured from 6061 which had been corroded in service. This actuator repair process is shown in Fig. 3.

An obvious extension of the use of CS for repair is the implementation of the process for the additive manufacture of new components, for now limited to Al and its alloys. CS was shown to be capable of forming Al6061 deposits with 96% of the bulk density and 92% of the bulk Young's modulus (Spencer et al. 2012). This process has been studied in a real-world application by Champagne et al. in 2015, who demonstrated the deposition of Al6061 onto magnesium substrates to allow friction stir welding to a sheet of the same material. Wang et al. (2015) have shown that the shear strength is up to 34.5 MPa for CS processed Al6061 onto an Al6061 substrate. Wang et al. also observed that the angle at which the cold-sprayed particle impacts the substrate has a large effect on the bond quality, as shown in Fig. 4.

Cross-References

► Additive Manufacturing Technologies

References

- Aldwell B, Yin S, McDonnell KA, Trimble D, Hussain T, Lupoi R (2016) A novel method for metal-diamond composite coating deposition with cold spray and formation mechanism. *Scr Mater* 115:10–13
- Alkhimov SP, Papyrin AN, Kosarev VF, Nesterovich NI, Shushpanov MM (1994) Gas-dynamic spraying method for applying a coating. Patent Nos: US5302414 A; DE69016433D1, DE69016433T2, EP0484533A1, EP0484533A4, EP0484533B1, WO1991019016 A1
- Bacciochini A, Radulescu MI, Yandouzi M, Maines G, Lee JJ, Jodoin B (2013) Reactive structural materials consolidated by cold spray: Al–CuO thermite. *Surf Coat Technol* 226:60–67
- Champagne VK (2007) The cold spray materials deposition process: fundamentals and applications. Woodhead Publishing, Sawston
- Champagne VK, West MK, Reza Rokni M, Curtis T, Champagne VK, McNally B, Kenneth V, Iii C, West MK, Rokni MR, Curtis T, Champagne V Jr (2015) Joining of cast ZE41A Mg to wrought 6061 Al by the cold spray process and friction stir welding. *J Therm Spray Technol* 25:143–159
- Dosta S, Couto M, Guilemany JM (2013) Cold spray deposition of a WC-25Co cermet onto Al7075-T6 and carbon steel substrates. *Acta Mater* 61(2): 643–652
- Gutzmann H, Gartner F, Höche D, Blawert C, Klassen T (2012) Cold spraying of Ti₂AlC MAX-phase coatings. *J Therm Spray Technol*. <https://doi.org/10.1007/s11666-012-9843-1>
- Irissou E, Legoux J-G, Ryabinin AN, Jodoin B, Moreau C (2008) Review on cold spray process and technology: part I-intellectual property. *J Therm Spray Technol* 17(4):495–516
- Levasseur D, Yue S, Brochu M (2012) Pressureless sintering of cold sprayed Inconel 718 deposit. *Mater Sci Eng A* 556:343–350
- Spencer K, Luzin V, Matthews N, Zhang M-X (2012) Residual stresses in cold spray Al coatings: the effect of alloying and of process parameters. *Surf Coat Technol* 206(19–20):4249–4255
- Trexler MD, Carter R, de Rosset WS, Gray D, Helfritsch DJ, Champagne VK (2012) Cold spray fabrication of refractory materials for gun barrel liner applications. *Mater Manuf Process* 27:820–824
- Wang X, Feng F, Klecka MA, Mordasky MD, Garofano JK, El-Wardany T, Nardi A, Champagne VK (2015) Characterization and modeling of the bonding process in cold spray additive manufacturing. *Addit Manuf* 8:149–162
- Widener CA, Carter MJ, Ozdemir OC, Hrabe RH, Hoiland B, Stamey TE, Champagne VK, Eden TJ (2016) Application of high-pressure cold spray for an internal bore repair of a navy valve actuator. *J Therm Spray Technol* 25(1):193–201

Combination

► Synthesis

Complex Geometry

► Freeform

Complexity in Manufacturing

Waguih H. ElMaraghy
 Mechanical, Automotive and Materials
 Engineering (MAME), University of Windsor,
 Windsor, ON, Canada

Synonyms

Complexness

Definition

The original Latin word “complexus” signifies “entwined” or “twisted together.” The Oxford Dictionary defines “complex” as something that is “made of (usually several) closely connected parts.” A system would be more complex if more parts or components exist and with more connections in between them (ElMaraghy et al. 2012).

Several different measures defining complexity have been proposed within the scientific disciplines. Such measures of complexity are generally context dependent. Colwell (2005) defines 32 complexity types in 12 different disciplines and domains such as projects, structural, technical, computational, functional, and operational complexity. Engineered system complexity is invariably multidimensional. A complex system usually consists of a large number of members, elements, or agents, which interact with one another and with the environment. They may generate new collective behavior, the

manifestation of which can be in one or more of the following domains: functional, structural, spatial, or temporal.

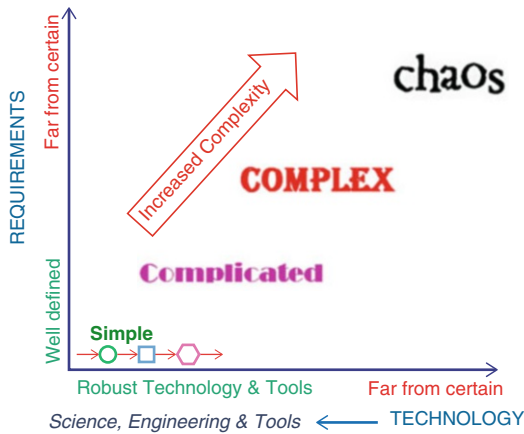
A complex system is an “open” system, in the thermodynamics sense, involving entropy principles as well as involving nonlinear interactions among its subsystems which can exhibit, under certain conditions, a degree of disorderly behavior. In particular, the future progression of events may become very sensitive to conditions at any given point of time and “chaotic behavior” may emerge.

Extended Definition

Complicatedness, Complexity, and Chaos

In simple terms for now, a simple system or artifact is easily knowable. A complicated system or product is not simple but is knowable, e.g., a car is a complicated product/system. A complex system is one where uncertainty exists. For instance, the development of a car is complex; it requires engineering business knowledge in several disciplines and collaborative work in teams. Details are not fully knowable to each development engineer. A complicated system could refer to a system having many parts, making it somewhat harder to understand, perhaps by virtue of its size, whereas complex refers to a system containing uncertainty during the development process or intrinsically in its design, the outcome not being fully predictable or controlled. Complexity may also be at the operational level such as during the manufacturing process itself. What is complicated is not necessarily complex and vice versa, and what is complicated for one person may be complex for another less knowledgeable individual or a group with less technological tools (Fig. 1). The word technology comes from Greek (*technologia*) meaning “art, skill, craft.” Technology is the knowledge, scientific methods, engineering techniques, and tools that help analyze, solve problems, and mitigate against the negative effects of complexity.

While researchers adopting the axiomatic complexity theory argue that engineers should constantly be working to reduce the complexity of engineered systems to make them more



Complexity in Manufacturing, Fig. 1 The spectrum of process complexity (EIMaraghy et al. 2012)

robust, others disagree with this approach and argue that the engineered system design should advocate complexity as a way to generate novelty and nurture creativity. Indeed, chaos and bifurcation theories have been proposed as means for qualitative, structural changes in mathematics and social sciences and creativity in engineering.

Sources of Complexity

Modern complex products or equipment may have many thousands of parts and take hundreds of manufacturing and assembly steps to be produced. Most complex products and equipment now incorporate not only mechanical and electrical components but also software, control modules, and human-machine interfaces. Some equipment are connected online to the World Wide Web and “the Internet of things” for real-time reporting and diagnostics. Although these additions have made equipment more versatile and dependable, significant complexity has been introduced to the product design.

The state of the art and the research literature in complexity are reviewed for the world of manufacturing from three perspectives: (i) complexity of engineering design and the product development process, (ii) complexity of manufacturing processes and systems, and (iii) complexity of the global supply chain and managing the entire business, as well as their intersections.

Perspectives on Complexity in Engineering

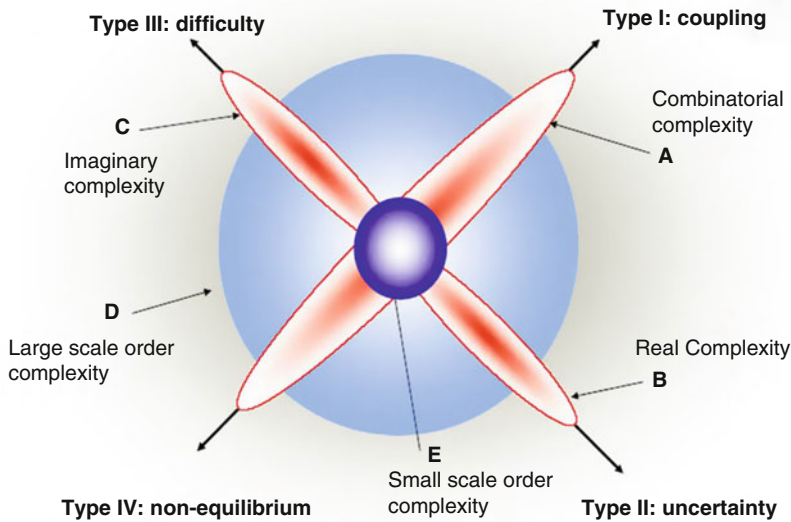
The research publications on complexity in engineering are divided into two groups: the first treats engineering complexity in the functional domain, e.g., the axiomatic design complexity theory, and the second treats complexity in the physical domain. The former (Suh 2005) promotes the idea that complexity must be defined in the functional domain as a measure of uncertainty in achieving a set of tasks defined by functional requirements. This complexity theory aims to reduce the complexity of any system by taking the following actions: (i) minimizing the number of dependencies, (ii) eliminating the time-independent real complexity and the time-independent imaginary complexity, and (iii) transforming a system with time-dependent combinatorial complexity into one with time-dependent periodic complexity by introducing functional periodicity and by reinitializing the system at the beginning of each period. This theory has been successfully applied in the design of engineered systems including in manufacturing.

Theory and Application

Engineering Complexity in the Functional Domain

The theory of complexity in the functional domain is based on the axiomatic design theory, which is useful when looking at design as the transformation from the functional requirements (FRs) to the design parameters (DPs) in the physical domain at the conceptual and embodiment design levels (EIMaraghy et al. 2012). In this complexity is defined as the measure of uncertainty in achieving the functional requirements of a system within their specified design range.

Kim (2004) illustrated the four causalities of complexity with respect to the design axioms (Fig. 2). Type I complexity is a result of heavy coupling of the functional requirements, which is a violation of the independence axiom. Time-independent complexity is a type II complexity and is a result of the information axiom violation, resulting in real complexity due to uncertainty. Time-independent imaginary complexity is a type



Complexity in Manufacturing, Fig. 2 Complexity in the functional domain – causality-based complexity radar chart (Kim 2004)

III complexity, or “difficulty,” which is a result of lack of understanding about the system. Type IV complexity is due to non-equilibrium. If an engineered system is at an equilibrium state with its surroundings, it is going to be stable until its equilibrium state is disturbed by the application of external energy. Some engineered systems are not at an equilibrium state at all times. However, they are stable if they possess a functional periodicity. For instance, modern physics such as quantum mechanics and superstring theory assumes the existence of a functional periodicity in natural matter such as atoms, electrons, and subatomic particles.

Time-dependent combinatorial complexity is a combined result of type I, II, and IV complexities. Time-dependent periodic complexity is a smaller-scale complexity.

According to this complexity theory, complexity of any system can be reduced by taking the following actions: (1) minimize the number of functional requirements (FRs), (2) eliminate the time-independent real complexity, (3) eliminate the time-independent imaginary complexity, and (4) transform a system with time-dependent combinatorial complexity into a system with time-dependent periodic complexity by introducing functional periodicity and by reinitializing the system at the beginning of each period. The importance of the functional periodicity in

reducing time-dependent combinatorial complexity is illustrated using several examples by Suh (2005). The main objective of this complexity theory is to reduce complexity while designing and operating engineering systems such as products and manufacturing systems so as to make the system robust, guarantee their long-term stability, make the system reliable, and minimize the cost.

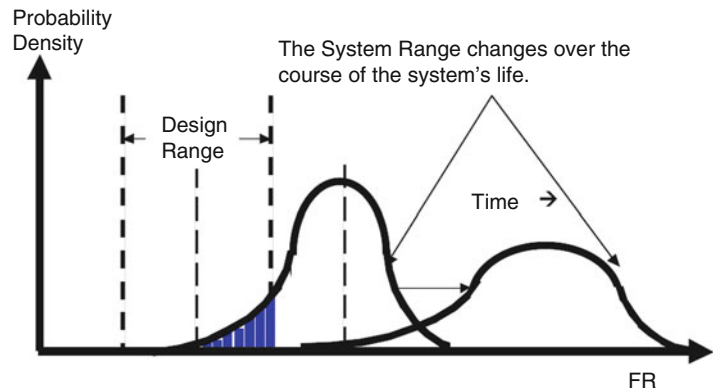
Real Complexity

There are two kinds of time-independent complexity: real and imaginary. Time-independent real complexity is defined as a measure of uncertainty when the probability of achieving the FR is less than 1.0 because the system range does not lie inside the design range. The real complexity arises for many different reasons: (i) coupling of FRs, (ii) decrease in the allowable tolerance due to the presence of coupling terms, (iii) lack of robustness (increase in entropy), (vi) wrong choice of DPs, or (v) wrong decomposition of FRs and DPs. To eliminate the real complexity, we must come up with a design that satisfies the independence axiom in which the FRs are maintained independent and then make the design robust so that the system range is always in the design range.

In design and manufacturing of mechanical parts, it is commonly assumed that a system with a large number of parts is more complicated

Complexity in Manufacturing,

Fig. 3 The spectrum of process complexity (Suh 2005)



than that with smaller number of parts. This assumption is true only if the interface between the interconnected parts adds additional uncertainty in satisfying the FRs. However, the mere presence of many interconnected parts does not necessarily make a system more complex, if the interconnected parts do not add any additional uncertainty.

Imaginary Complexity

Imaginary complexity is defined as uncertainty that is not real uncertainty but arises because of the designer's lack of knowledge and understanding of a specific design itself. Even when the design is a good design, consistent with both the independence axiom and the information axiom, imaginary uncertainty can exist when we are ignorant of what we have. An example is the combination lock which is easy to open once we know the sequence of numbers we have to activate it, but in the absence of the information on the combination, it would appear to be complex (Suh 2005).

The time-independent imaginary complexity and time-dependent periodic complexity can occur only when we must satisfy many FRs at the same time, whereas the time-independent real complexity and the time-dependent combinatorial complexity can exist regardless of the number of FRs that must be satisfied at the same time.

Time-Dependent Complexity

Time-dependent complexity occurs because future events affect the system in unpredictable ways. Often this results in a time-varying system range, i.e., the system range moves away from the design range (change in "information content" or

entropy) as shown in Fig. 3. Ideally, the design range should be much below the system range to avoid this type of complexity.

There are two types of time-dependent complexity, which are defined as follows: (i) the periodic complexity is defined as the complexity that only exists in a finite time period, resulting in a finite and limited number of probable combinations, and (ii) the combinatorial complexity is defined as the complexity that increases as a function of time due to a continued expansion in the number of possible combinations with time, which may eventually lead to a chaotic state or a system failure. To reduce combinatorial complexity, we have to devise a means of preventing the system range from moving out of the design range (Suh 2005).

Application in Multidiscipline Complexity of Engineered Systems

Multidisciplinarity (Tomiyama et al. 2007) causes problems that were nonexistent when products were mono-disciplinary, because multidisciplinarity significantly increases not only the complexity of products but also that of the product development process. Complexity resulting from multidisciplinarity is different from other types of complexity such as computational complexity and uncertainty complexity, because it results from how our knowledge itself is formulated. Simpler design problems can be first decomposed into simpler mono-disciplinary subproblems with the classic divide-and-conquer strategy. These mono-disciplinary problems can be easily attacked and

solutions for the entire problem can be synthesized. In contrast, multidisciplinary problems cannot be solved in a straightforward manner. When a design problem involves multiple domains, unless there is a uniform theory that can attack the problem as a whole, we are forced to use a set of theories, each of which is valid only in one domain. While in principle these theories are independent from each other, they can have intrinsic interactions for a variety of reasons. These interactions among theories indicate the existence of cross-disciplinary problems. The complexity involving multiple disciplines is explained by examining the structure of knowledge represented by relationships among theories. Tomiyama et al. (2007) identified “complexity by design” and “intrinsic complexity of multidisciplinary.” Due to size (computational complexity) and multidisciplinary, we apply the “divide-and-conquer” approach. However, due to very high “functional density,” the approach can fail because it is almost impossible to decompose the whole system (particularly with high functional density) into subsystems that have the least interactions among them. Often, systems designers are surprised by “unpredicted” interactions that are hard to solve, somewhat similar to the “imaginary complexity” in the functional complexity theory. This type of “no-fault” failure has been on the increase in many complex multidisciplinary

products and deserves more attention from designers and industrial enterprises. A detailed example application in the design and operation of an AGV (automatic guided vehicle) system is discussed in EIMaraghy et al. (2012).

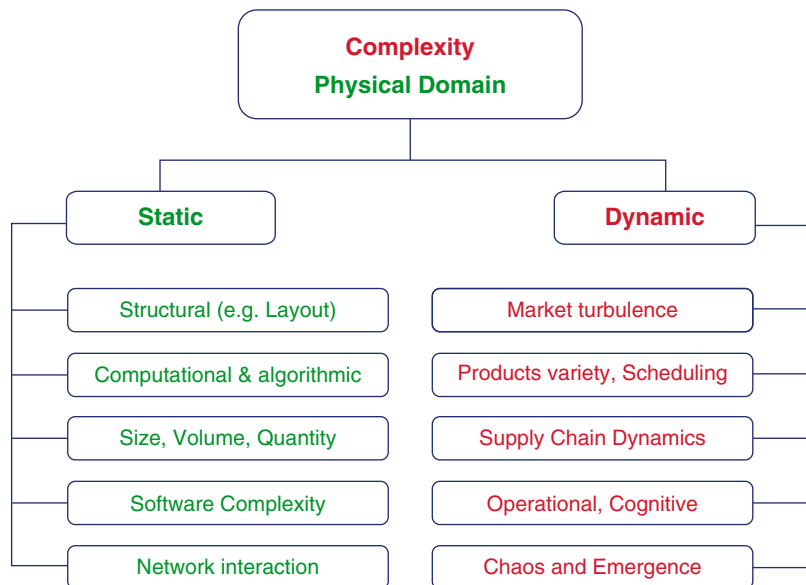
Engineering Complexity in the Physical and Operational Domains

Complexity in the physical and the operational domains is represented by models that capture the three elements of complexity: absolute quantity of information, diversity of information, and information content (effort). Figure 4 shows the classification of the various types of complexity in the physical domain (EIMaraghy et al. 2012).

EIMaraghy and Urbanic (2004) developed metrics and applications for product, process, and operational complexity. In these metrics, an important factor is considered: the human operators and their perception of the tasks’ complexity (cognitive complexity). The complexity of manufacturing systems, products, processes, and operations is related to the information to be processed in the system, including the physical and the cognitive aspects as illustrated in Fig. 5. Increasing system size and variety leads to more information and higher complexity.

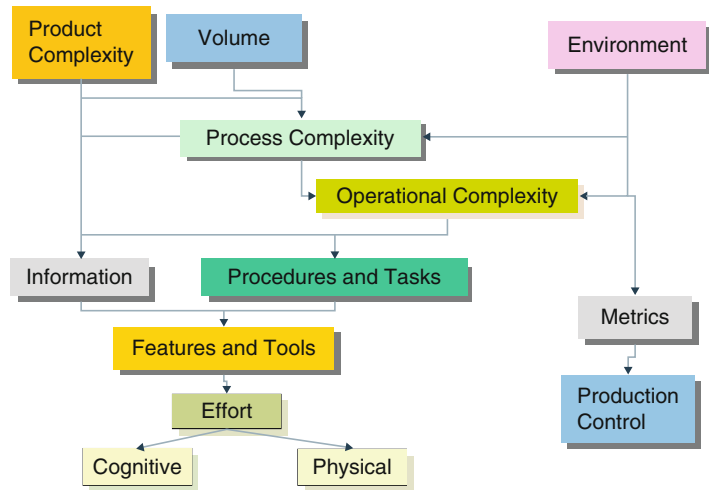
Complexity in Manufacturing,

Fig. 4 Classification of engineering design and manufacturing complexity in the physical domain (EIMaraghy et al. 2012)



Complexity in Manufacturing,

Fig. 5 Physical and cognitive complexity (EIMaraghy and Urbanic 2004)



Another application using both functional and physical complexity theories was presented by Kim (1999). He found that in lean manufacturing, the system complexity, which is affected by increased product variety, is much less than in an equivalent mass production system. He proposed a series of system complexity metrics based on a complexity model developed using systems theory. These measures are (1) relationships between system components (number of flow paths, number of crossings in the flow paths, total travel distance by a part, and number of combinations of product and machine assignments) and (2) number of elementary system components. These metrics include a mix of structure (static time-independent) and operation (dynamic and time-dependent) factors. No suggestion regarding their relative importance or how they may be combined into one system complexity metrics was offered.

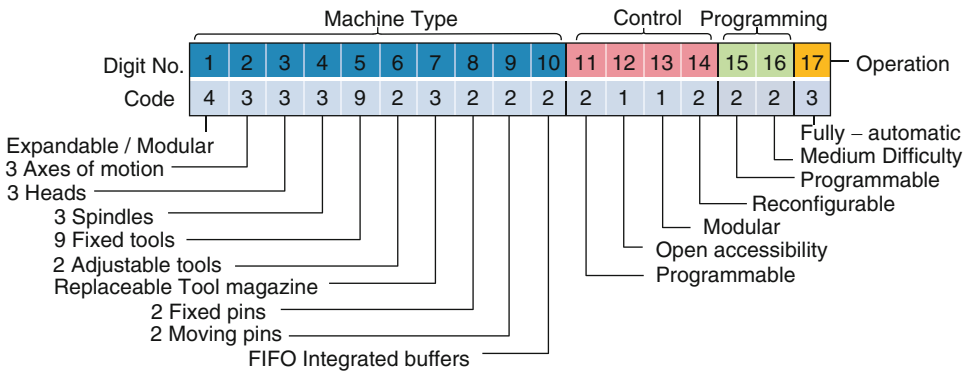
Engineering Complexity Using Heuristics and Indices

Kuzgunkaya and EIMaraghy (2006) introduced a metric to measure the structural complexity of manufacturing systems based on the complexity inherent in the structure of its components: machines, buffers, and Material Handling Systems (MHS). It includes quantity of information (using the entropy) and diversity of information. Classification and coding systems were originally

developed for manufactured parts. However, equivalent coding and classification systems for manufacturing systems did not exist until the development of the structural classification and coding system (SCC) by EIMaraghy (2006) to classify the various types of equipment in a manufacturing system, such as machines, buffers, and transporters, as well as their layout. They used this classification code to assess the structural complexity of manufacturing systems configurations. The original equipment has been extended (EIMaraghy et al. 2010) to include the assembly-specific structural features of typical equipment used in products assembly systems. It accounts for the number, diversity, and information content within each class of the assembly system modules caused by the assembled products variety. The chain-type structure of the SCC coding scheme facilitated its extension (Fig. 6). The code characterizes the complexity of the various equipment within the assembly system such as machines, transporters, buffers, feeders, and handling equipment. Equipment controls, programming, operation, power source, and sensors are common fields.

Graph and Network Complexity Theories

Topological complexity is used by the graph and network theories. The complexity of such structures can be described by symmetry-based measures



Complexity in Manufacturing, Fig. 6 Structural classification and coding system (SCC) (EIMaraghy 2006)

frequently applying the concept of entropy or by other measures including average- or normalized-edge complexity, subgraph count, overall connectivity, total walk count, and others based on adjacency and distance (EIMaraghy et al. 2012).

Computational and Information Complexity

Computational complexity is measured by the quantity of computational resources (e.g., time, storage, program, communication) which is required for solving a particular task. Here, the Turing machines are used as a fundamental tool for analyzing algorithms and combinatorial optimization problems. The complexity of a structure is defined in the Kolmogorov’s complexity (Li and Vitányi 2008) as its minimal description length, e.g., by a program on a universal Turing machine. Some other complexity measures, e.g., time complexity, space complexity, and, for distributed systems, communication complexity, are associated with algorithms (EIMaraghy et al. 2012).

Computational complexity comes from the number of elements (subsystems, components, or parts). This complexity becomes problematic, when the number of elements (N) grows, because the same algorithm that was able to solve a problem for a smaller N cannot solve one for a larger N’ in a reasonable time (or with using reasonable memory). For example, assume every element in

a system has a direct relationship with all other elements. The computational complexity in terms of the number of relationships in this case is $O(N(N - 1)) = O(N^2)$, which is called polynomial complexity ($O(N^a)$, in which a is a positive constant). Practically, it is well known that computational complexity grows very quickly, when the complexity is $O(a^N)$ (exponential), $O(N!)$ (factorial), or $O(NN)$ (double exponential). These are called non-polynomial (NP) complexity as opposed to polynomial cases (P). Some NP complexity classes (NP-complete or NP-hard) are known to be difficult or even impossible to manage and solve. In manufacturing, NP-complete problems can be found, for instance, in production planning problems and logistics problems.

Cross-References

- ▶ Logistics
- ▶ Manufacturing System
- ▶ Production Planning
- ▶ System

References

Colwell B (2005) Complexity in design. *IEEE Comput* 38(10):10–12

EIMaraghy H (2006) A complexity code for manufacturing systems. In: *ASME international conference on manufacturing science & engineering (MSEC)*.

American Society of Mechanical Engineers, Ypsilanti, pp 625–634

- EIMaraghy W, Urbanic R (2004) Assessment of manufacturing operational complexity. *CIRP Ann Manuf Technol* 53(1):401–406
- EIMaraghy H, Samy SN, Espinoza V (2010) A classification code for assembly systems. In: 3rd CIRP conference on assembly technologies and systems, CATS2010. Trondheim, Norway, pp 145–150
- EIMaraghy W, EIMaraghy H, Tomiyama T, Monostori L (2012) Complexity in engineering design and manufacturing. *CIRP Ann Manuf Technol* 61(2): 793–814
- Kim Y-S (1999) A system complexity approach for the integration of product development and production system design. Master of Science, Massachusetts Institute of Technology
- Kim S-G (2004) Axiomatic design of multi-scale systems. In: Proceedings of international conference on axiomatic design ICAD2004, 3rd international conference on axiomatic design, 21–24 June 2004, Seoul, Korea
- Kuzgunkaya O, EIMaraghy H (2006) Assessing the structural complexity of manufacturing systems configurations. *Int J Flex Manuf Syst* 18(2):145–171
- Li M, Vitányi P (2008) An introduction to Kolmogorov complexity and its applications, 3rd edn. Springer, New York
- Suh NP (2005) Complexity in engineering. *CIRP Ann Manuf Technol* 54(2):581–598
- Tomiyama T, D’Amelio V, Urbanic J, EIMaraghy W (2007) Complexity of multi-disciplinary design. *CIRP Ann Manuf Technol* 56(1):185–188

Complexity Theory

- ▶ [Axiomatic Design](#)

Complexness

- ▶ [Complexity in Manufacturing](#)

Component Feeding

- ▶ [Feeding](#)

Composite Materials

Dirk Biermann

Institut für Spanende Fertigung, Technische Universität Dortmund, Dortmund, Germany

Synonyms

[Composites](#)

Definition

Composite materials are made from at least two materials with substantially different mechanical properties. The mechanical properties of the composite material are different from the constituent materials.

There are three types of composite materials:

Ceramic matrix composites (CMC) consisting of fibers embedded in a ceramic matrix.

Metal matrix composites (MMC) consisting of fibers embedded in a metal ceramic matrix.

Fiber-reinforced plastics (FRP) made of a polymer matrix reinforced with fibers.

Theory and Application

Ceramic Matrix Composites (CMC)

Applications

Originally, requirements in aerospace applications played a decisive role in developing ceramic matrix composites. Selection criteria for materials in power plants, heat shield systems for space shuttles and rockets, were a desperate temperature resistance and good characteristics considering its mass. In practice, one of the first CMCs used was the carbon-fiber-reinforced carbons (C/C). Especially in the high temperature range, these materials illustrate the state of technology and are assembled among others in brake discs, rocket nozzles, and forming tools (Krenkel 2003). CMCs are also used in slide bearings of

pumps in order to improve the wear and corrosion resistance.

Properties

The fibers typically consist of carbon (C), silicon carbide (SiC), alumina (Al_2O_3), or mullite ($\text{Al}_2\text{O}_3\text{-SiO}_2$). For the matrix components, alumina, zirconium oxide, and silicon carbide are most commonly used. The terminology of CMC usually follows the principle “type of fiber/type of matrix.” C/SiC stands for a carbon-fiber-reinforced silicon carbide. Today, the most important CMCs are C/C, C/C-SiC, C/SiC, and SiC/SiC. In some cases, the term is preceded with the abbreviation of the manufacturing process.

Due to their material structure, including strong bonds, CMCs show many characteristics that make these ceramics suitable and attractive for engineering applications. In comparison to unreinforced ceramics, which fracture easily, CMCs possess considerable improved fracture toughness. In addition to that, they can be characterized by high temperature and corrosion resistance, resistance to chemical degradation, wear resistance, high hardness and stiffness, and low density. As negative properties of CMCs, the high brittleness and fast crack extension can be mentioned. As a result of these characteristics, CMCs can only be efficiently machined using tools with diamond abrasive grains.

Machining of CMCs

Although components can be manufactured near-net-shape, post-processing is required as a result of shrinkage or material expansion after the infiltration process. The machining process is dominated by brittle fracture, despite a macroscopic quasi-ductile behavior of the compound (Malkin and Hwang 1996). Ceramic and non-ceramic phases of the CMC with strongly different mechanical properties lead to varying engagement conditions. Abrasive cutting processes can be regarded as the most cost-effective method to machine CMCs (Weinert and Jansen 2008). For inserting drill holes, diamond abrasive points with an electroplated, brazed, or sintered bond can be used (Biermann et al. 2009). These tools can as well be applied for pocket and circular routing and groove machining.

Metal Matrix Composites (MMC)

Application

The field of aeronautics, the automobile industry, and also in many areas of the engineering, the demand for lightweight components leads to the adaptation of materials having a very low specific weight. Light metal alloys are not often used because they have some drawbacks such as a low stiffness, high thermal expansion coefficient, and low wear resistance. However, the combinations of the alloys with other materials can improve the mechanical as well as their thermal properties.

Properties

Important distinguishing properties of the composite materials are the shape of the reinforcement phase, such as long fibers, short fibers, and particle. Concerning the mechanical properties, the best results are achieved by long-fiber reinforcements. Since they are not economically feasible because of their complex manufacturing process, it is preferred to use short-fiber or particle reinforcements. They do not have the same resistance as the long-fiber reinforcement, but the potential gain of stiffness, resistance to wear, and other property improvement are usually sufficient and acceptable.

Machining of MMCs

For the industrial use of these composite materials, the processing of these materials in particular is of great importance. Here, the machining shown as problematically, with occurrence of extremely high tools wear. This is caused due to the high hardness and the resulting abrasive effect of the ceramic reinforcement (Chen 1992; Tomac and Tønessen 1992).

For turning of ceramic fiber-supported aluminum alloy, cemented carbides or polycrystalline diamond (PCD) is suitable. Here, PCD leads to much lower wear values and determines a much lower roughness, compared to coated cemented carbide (Weinert and König 1993). In the cutting process, the micro-contact between the SiC-reinforced particles and the cutting edge can produce temperatures that are far above the melting point of aluminum (Teti 2002).

While drilling, PCD-tipped drill bits are best suited in comparison to the carbide tools, depending on the type of fiber, 20–100 times longer life possible. The tool wear occurs in the form of a cutting edge rounding. A wear increase comes with increasing fiber volume fraction, increasing cutting speed, and the use of coolant.

Grinding with diamond wheels can achieve smaller deposits than that with ceramic grinding wheels. The best surface quality can be achieved with the combination of diamond- and CBN (Cubic Boron Nitride)-grinding wheels. The generated surfaces will be strongly influenced by the adhesion of the wheels to material.

For ultra-precision machining of ceramic fiber-reinforced aluminum, single point diamond tools are the best suited. While processing, very low surface roughness can be achieved. The surface quality depends on the orientation of the fibers from the cutting direction (Yuan et al. 1993).

Fiber-Reinforced Plastics (FRP)

Application

In various engineering applications ranging from aerospace, civil engineering, wind energy, and various consumer products to sports goods, the core issue is to minimize the overall weight of a part or its assembly in order to improve its service performance as well as its efficiency (Jain and Yang 1993). FRPs satisfy this objective with their superior strength-to-weight ratio, stiffness, good damping and corrosion resistance, and low coefficient of thermal expansion (Faraz 2011).

Properties

FRPs are essentially formed by the combination of two or more materials to tap physical, chemical, and mechanical properties that are almost superior to those of its individual constituents. The principal components include fiber reinforcement and a thermoset or thermoplastic matrix or binder. The fibers, usually fiberglass, carbon, or aramid, provide most of the stiffness and strength, and the matrix material, usually epoxy, vinylester, or polyester thermosetting plastic, binds the fibers together in position.

An individual structural glass fiber is both stiff and strong in tension and compression, that is,

along its axis. Although it might be assumed that the fiber is weak in compression, it is actually only the long aspect ratio of the fiber which makes it seem so, that is, because a typical fiber is long and narrow, it buckles easily. On the other hand, the glass fiber is unstiff and unstrong in shear, that is, across its axis. Therefore, if a collection of fibers is arranged permanently in a preferred direction within a material and the fibers are prevented from buckling in compression, then that material will become preferentially strong in that direction.

Furthermore, by laying multiple layers of fiber on top of one another, with each layer oriented in various preferred directions, the stiffness and strength properties of the overall material can be controlled in an efficient manner. With chopped strand mat, this directionality is essentially an entire two-dimensional plane; with woven fabrics or unidirectional layers, directionality of stiffness and strength can be more precisely controlled within the plane (Smallman and Bishop 1999).

Machining of FRPs

Although composites are generally fabricated on moulds, but nevertheless, there is often a need to conduct some additional machining operations which should be precise in nature. For instance, trimming of the edges of the cured FRP component needs to be performed to guarantee the shape as well as dimensional accuracy and stability, that otherwise, may not be controlled through simple curing process within itself (König et al. 1990).

Various cutting and machining techniques are being utilized both in industrial practice as well as in research. They, namely, include milling, turning, abrasive water-jet machining, ultrasonic machining, laser beam cutting, sawing, edge trimming, and drilling (Faraz 2011).

It is noteworthy here that almost all of the researchers do have a consensus that the comprehensive knowledge as well as experience, which has been well acquired in case of drilling of metals and other conventional engineering materials, cannot simply or directly be applied to the drilling of FRPs. This is mainly because of their very strong, inherent material inhomogeneity and anisotropy. Furthermore, it is also commonly known that owing to the extremely abrasive nature of their fiber content, FRPs exhibit totally

different drilling results and characteristics, when compared to that of the drilling of common metals and their alloys. Their main classification could be, on the one hand, as cutting tool related, while, on the other hand, it could be concerning the workpiece quality. The former classifications, that is, tool-related problems, are excessive and rapid tool wear due to abrasion of aggressive fiber content of FRPs. And the latter ones mainly include part edge/surface and hole quality defects, namely, hole entry and exit delamination, edge chipping, fiber pullouts, fiber-bundle pullouts, spalling, macroscopic pitting, matrix burning, thermal residual stresses and material cracking, etc. (Teti 2002; Faraz 2011).

Delamination

In research as well as there in industry, delamination during drilling FRP is recognized as one of the most critical problems. As defined by various researchers, it is an interlaminar or inter-ply failure phenomenon or behavior. When occurred at the topmost surface ply around the drilled hole periphery, it is called “peel-up delamination” or simply hole entry delamination of the composite workpiece. In addition, this interlaminar shearing of the last ply at the bottommost surface of the FRP composite material is usually more severe and is generally called “push-out delamination” or in simple words hole exit delamination. Delamination can be introduced by three mechanisms: peeling up of the topmost layer, pushing out of the bottommost layer, and an additional cause, called thermal stress mode.

The phenomenon of hole entry delamination occurs due to the action of cutting force that acts in the peripheral direction. As the name suggests itself, a peeling force is generated due to the slope of the rake face of a drill cutting edge, which separates the top-ply of the composite workpiece being drilled. Moreover push-out delamination occurs as the drill reaches the bottommost laminate-ply, where the uncut thickness reduces considerably and the resulting resistance to deformation is also reduced. The loading (thrust force) exceeds the interlaminar bonding strength, thus resulting into hole exit or push-out delamination. The drill chisel edge, which is quasi-stationary and gives rise to the indentation effect

during drilling, is supposed to be the major responsible for the said hole exit damage. To summarize, hole exit delamination is proposed to be occurring mainly due to drilling thrust force. It is also noteworthy here that many researchers have acknowledged the peel-up type of delamination (hole entry side) as not much significant as that observed around the hole exit periphery. In their opinion, the exit delamination that reduces the strength and stiffness of the cured FRP parts severely affects their performance and efficiency, especially, under the applied external loads (Teti 2002; Faraz et al. 2009; Faraz 2011).

Cross-References

- ▶ [Cutting Edge Geometry](#)
- ▶ [Drilling](#)
- ▶ [Water-Jet Cutting](#)

References

- Biermann D, Jansen T, Feldhoff M (2009) Machining of carbon fibre-reinforced silicon-carbide composites. *Adv Mater Res* 59:51–54
- Chen P (1992) High performance machining of SiC-whisker-reinforced aluminum composite by self-propelled rotary tools. *Ann CIRP* 41(2):59–62
- Faraz A (2011) Experimental study on delamination mechanical loads and tool wear in drilling of woven composite laminates. Vulkan Verlag, Essen
- Faraz A, Biermann D, Weinert D (2009) Cutting edge rounding: an innovative tool wear criterion in drilling CFRP composite laminates. *Int J Mach Tools Manuf* 49(15):1185–1196
- Jain S, Yang DCH (1993) Effects of federate and chisel edge on delamination in composites drilling. *J Eng Ind Trans ASME* 115(4):394–405
- König W, Cronjäger L, Spur G, Tönshoff HK, Vigneau M, Zdeblick WJ (1990) Machining of new materials. *Ann CIRP* 39(2):673–681
- Krenkel W (2003) *Keramische Verbundwerkstoffe* [Ceramic composites]. Wiley-VCH, Weinheim (in German)
- Malkin S, Hwang TW (1996) Grinding mechanisms for ceramics. *CIRP Ann Manuf Technol* 45(2):569–580
- Smallman RE, Bishop RJ (1999) *Modern physical metallurgy and materials engineering*, 6th edn. Butterworth-Heinemann, Oxford
- Teti R (2002) Machining of composite materials. *CIRP Ann Manuf Technol* 51(2):611–634
- Tomac N, Tønnessen K (1992) Machinability of particulate aluminum matrix composites. *Ann CIRP* 41(1):55–58

- Weinert K, Jansen T (2008) Machining aspects for the drilling of C/C-SiC. In: Krenkel W (ed) Ceramic matrix composites. Wiley-VCH, Weinheim, pp 287–301
- Weinert K, König W (1993) A consideration of tool wear mechanism when machining metal matrix composites (MMC). *Ann CIRP* 42(1):95–98
- Yuan ZJ, Geng I, Dong S (1993) Ultraprecision machining of SiCw/Al composites. *Ann CIRP* 42(1):107–109

Composites

- ▶ [Composite Materials](#)

Computational Intelligence

- ▶ [Artificial Intelligence](#)

Computed Axial Tomography (CAT)

- ▶ [Computed Tomography](#)

Computed Tomography

Simone Carmignato
Department of Management and Engineering,
University of Padua, Vicenza, Italy

Synonyms

[Computed axial tomography \(CAT\)](#); [Computer-aided tomography \(CAT\)](#); [Computerized tomographic imaging](#); [Computerized tomography](#); [Computerized transverse axial scanning](#); [X-ray computed tomography](#)

Definition

X-ray computed tomography, or simply computed tomography (CT), is an imaging method using

X-ray transmission and computer algorithms to reconstruct two-dimensional (2D) images of an object, representing object's slices, or three-dimensional (3D) representations of the object's structure, including inner geometries.

In this context, the term “tomography” refers to nondestructive imaging of sections. The term derives from two Greek words: *tomos*, meaning “section,” and *graphein*, meaning “to write.”

Although the term “computed tomography” is very general and could refer even to tomographic techniques not using X-rays, in practice it usually refers to the computation of tomographic images by X-ray transmission. The term “X-ray computed tomography” is more specific.

Theory and Application

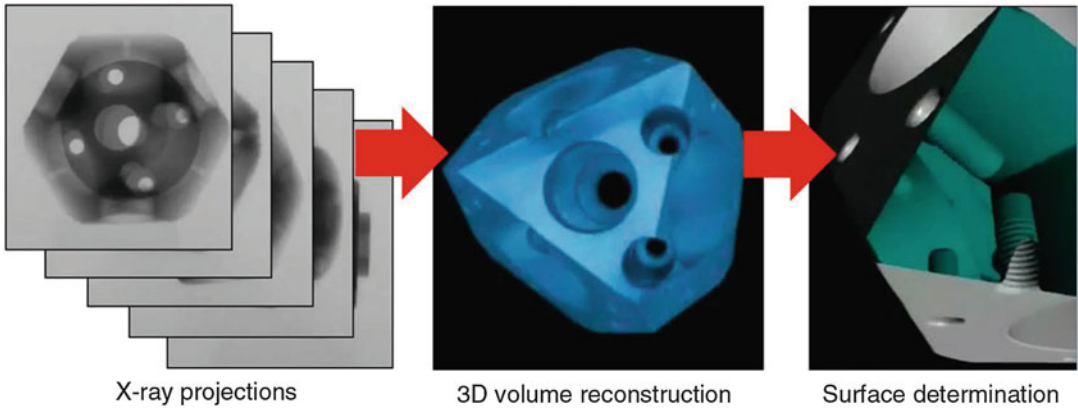
Introduction

Unlike conventional radiography, computed tomography goes far beyond the collection of radiographic projections. The fundamental limitation of conventional radiography is that the three-dimensional volume of an object is compressed along the direction of X-ray to a two-dimensional radiographic projection, in which all the underlying object's structures are superimposed, which results in significantly reduced visibility of the object. A recognition of this limitation led to the development of computed tomography, which allows the object's slices and volume reconstruction from X-ray projections (Morgan 1983). Figure 1 illustrates the progression of CT data, from X-ray projections, to 3D volume reconstruction, and to surface determination.

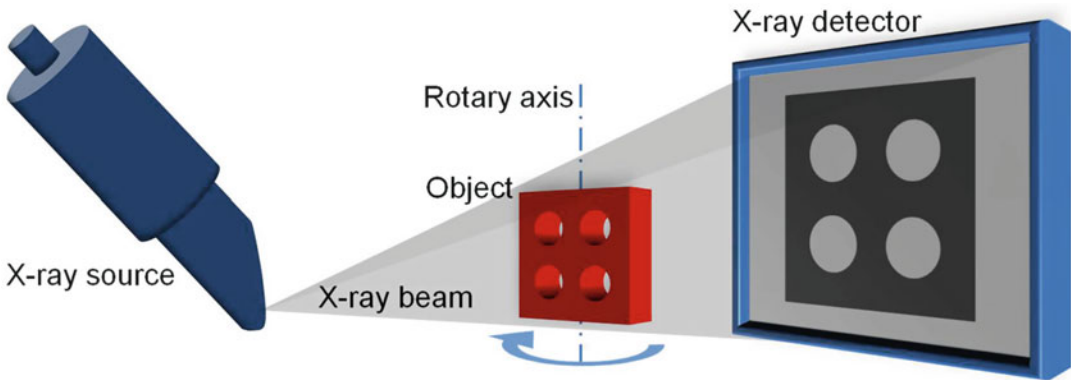
History of CT

Early X-ray Tomography Techniques

The idea of determining the inside structure of an object from multiple X-ray images taken from various angulations goes back to the first decades of the twentieth century. Before the advent of computed tomography, other techniques were developed for displaying internal sections using

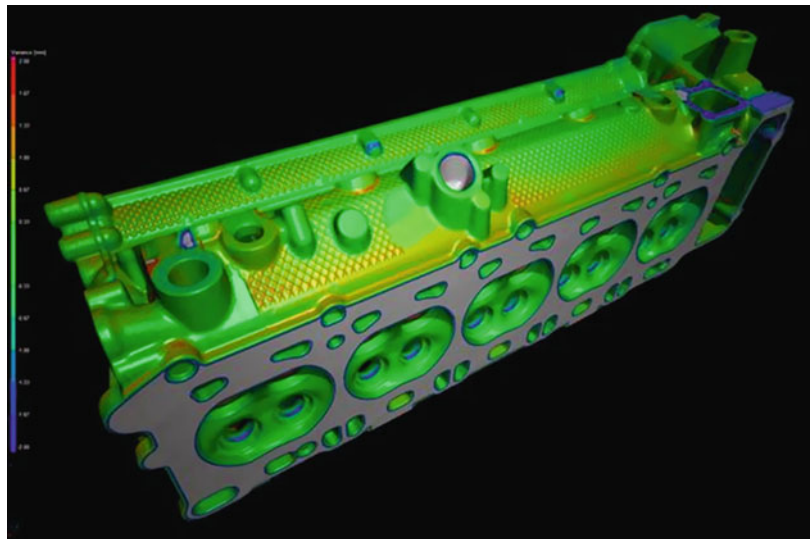


Computed Tomography, Fig. 1 CT process chain, from X-ray projections to 3D volume reconstruction and to surface determination



Computed Tomography, Fig. 2 Schematic representation of a CT scanner

Computed Tomography, Fig. 3 Dimensional quality control of a cylinder head: comparison of CT measurement data to nominal CAD data (Courtesy of Volume Graphics GmbH)



X-rays. These techniques are often referred to as “conventional tomography,” or “stratigraphy” or “noncomputed tomography” (Hsieh 2009). As early as 1921, one of the pioneers of conventional tomography, André Bocage, conceived a device to blur out structures above and below a section of interest (Bocage 1921). Few years later, Alessandro Vallebona developed the tomographic technique called “stratigraphy” (Vallebona 1930). Although these early tomographic techniques were somewhat successful in producing images

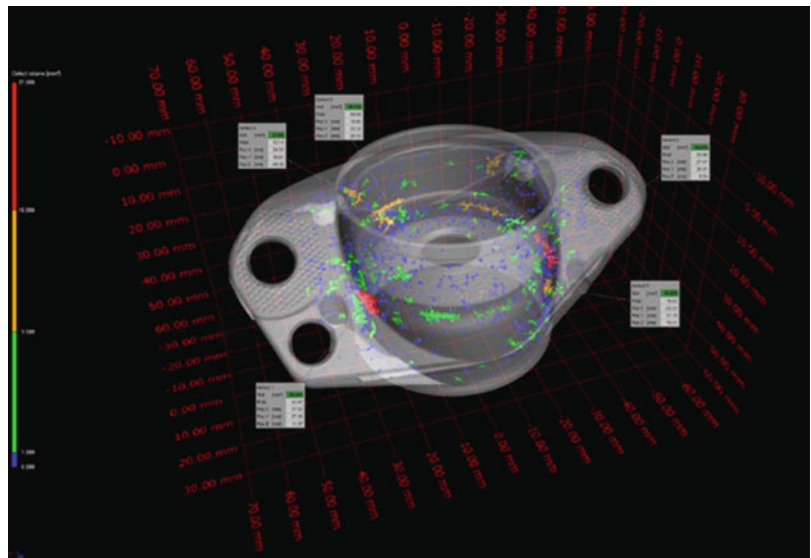
of an object’s internal plane, they could not completely eliminate superimposition of other structures outside the imaging plane. This drawback, combined with the large X-ray dose to the patient, limited the use of conventional tomography in clinical applications.

Development of Computed Tomography

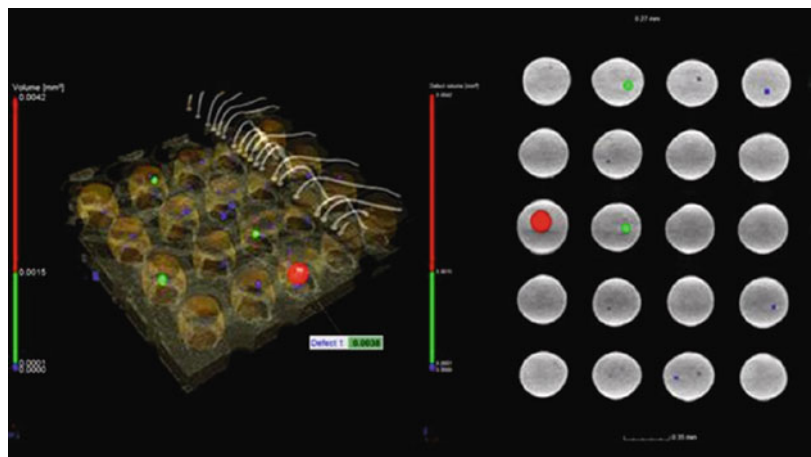
The mathematical model for reconstructing an object from multiple projections dates back to 1917, when Johann Radon demonstrated



Computed Tomography, Fig. 4 Porosity and inclusion analysis of castings (Courtesy of Volume Graphics GmbH)



Computed Tomography, Fig. 5 Quality control of solder points and bonding wires of a ball grid array (BGA) used for microchips (Courtesy of Volume Graphics GmbH)



mathematically that an object could be replicated from an infinite set of its projections (Hsieh 2009). This concept was applied only many years later. The Nobel Prize winners Allan M. Cormack and Godfrey N. Hounsfield made substantial contributions to the development of computed tomography (Cormack 1979; Hounsfield 1979). The first clinical CT scan on a patient took place on 1st October 1971 using a prototype scanner developed by Hounsfield. Since the 1970s, CT have rapidly become a fundamental imaging technique in medical practice (Kalender 2006).

Industrial CT Scanning

Industrial application of CT scanning became frequent since the 1980s, especially for material analysis and nondestructive testing (Kruth et al. 2011). The use for dimensional metrology purposes was not yet possible at that time, since the attainable measurement uncertainty was in the range of few hundreds of millimeters. As hardware and software have progressed reaching submicron resolution, the metrological performances of industrial CT systems have continuously improved, and measurement uncertainty of few micrometers has become possible (Carmignato 2012). The first commercial coordinate measuring system using a CT sensor was presented in 2005 (Kruth et al. 2011). Current challenges in CT dimensional metrology are establishment of measurement traceability and proper uncertainty evaluation (De Chiffre et al. 2014).

Principles of CT

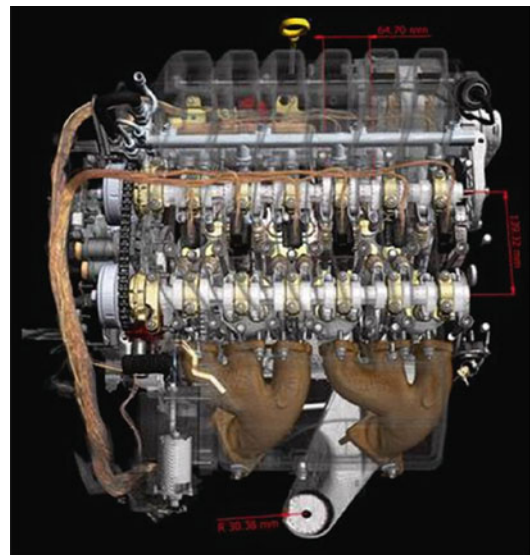
Fundamentals

Computed tomography uses the ability of X-rays to penetrate objects. As schematically represented in Fig. 2, the radiation produced by an X-ray source passes through the scanned object to reach the X-ray detector. On the way through the object, X-rays are attenuated, and the amount of attenuation depends on the length traveled in the absorbing material, the type of material (i.e., attenuation coefficient), and the energy of the

X-rays. The attenuation is measured by the X-ray detector, which captures the projection image resulting from the transmitted X-rays. Projection images are taken from different angular positions of the object, using a rotary axis (see Fig. 2). The mathematical reconstruction of 2D slices and 3D volume model out of the acquired projection images is usually done by “filtered back projection” (Kak and Slaney 1988). When a 3D volume reconstruction is obtained, the 3D model is constituted by a set of voxels (volumetric pixels), where the gray value associated to each voxel is a measure for the absorptivity of the material. Subsequently, the voxel data can be post-processed to detect the object’s surface by a threshold process (i.e., segmentation) (Hsieh 2009).

Types of CT Scanners

Industrial CT scanners are fundamentally different from clinical scanners. Although both types of scanners need to take X-ray projections from several angulations as discussed above, in industrial CT scanners the object is rotated in the beam path produced by a stationary X-ray source, while in clinical CT the X-ray unit (source and detector)

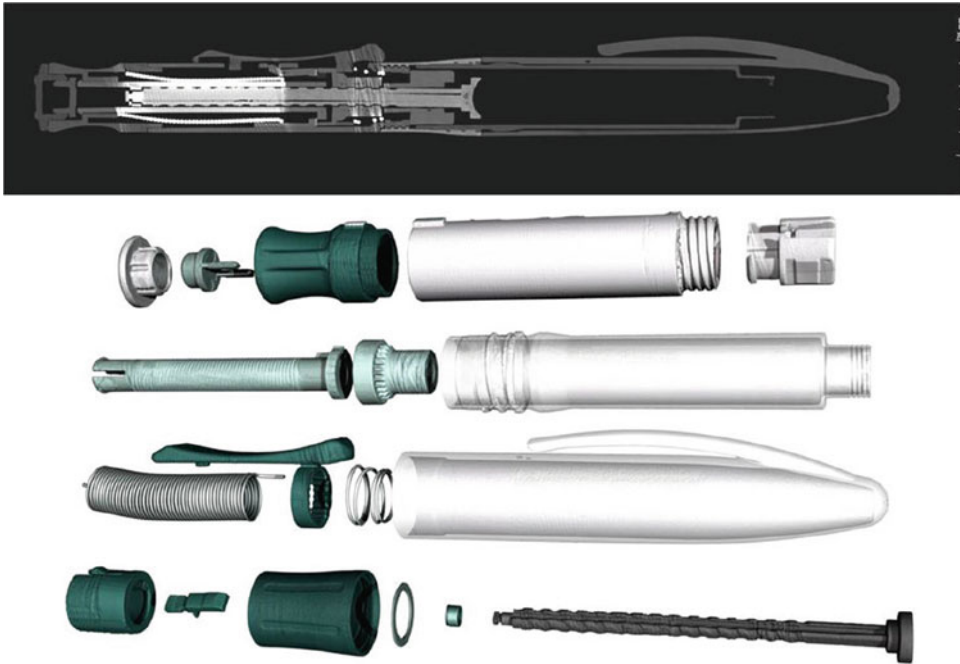


Computed Tomography, Fig. 6 Volume rendering resulting from CT scan of a complete VR6 3.6 liters car engine (Courtesy of Volume Graphics GmbH)

rotates around a stationary patient. In addition, since the radiation exposure of the object being scanned is normally not a problem in industrial CT, greater radiation intensities can typically be used than those applied in clinical CT. Also, because resolution and accuracy requirements are different, scanning parameters usually

differ significantly in industrial and clinical CT scanners.

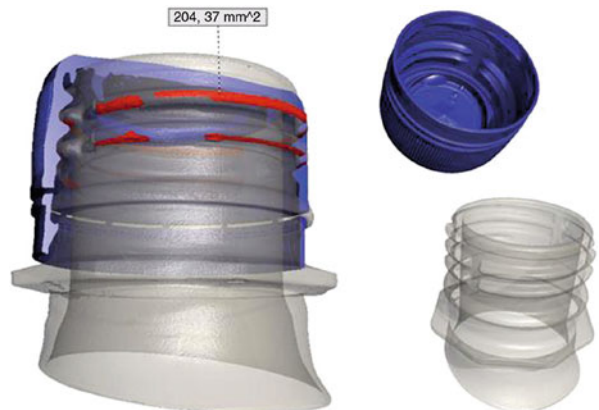
Another important distinction between different types of CT scanners is based on the X-ray detector. Depending on the type of detector used, CT scanners may be able to detect only one or multiple slices per revolution. X-ray detectors



Computed Tomography, Fig. 7 Inspection of assembled insulin injector. The CT scan allowed testing the operability and production quality of sample parts before going into serial production (initial sample inspection

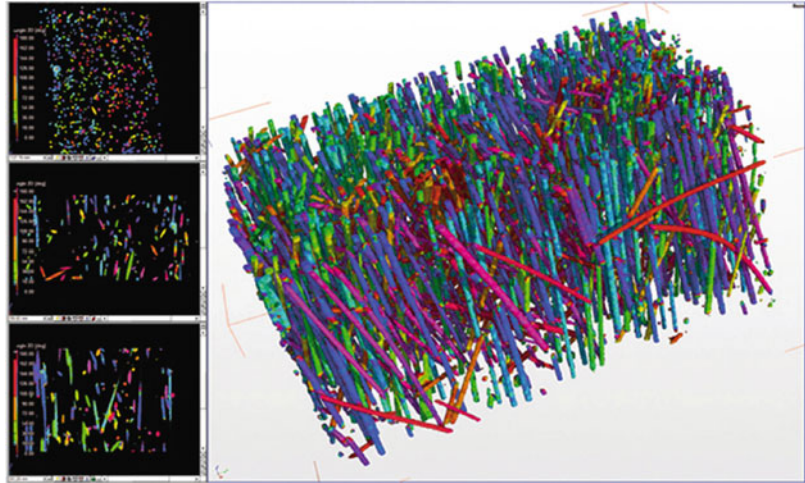
report), with typical tolerances of $\pm 50 \mu\text{m}$ and more than 300 inspection features per part (Courtesy of Volume Graphics GmbH)

Computed Tomography, Fig. 8 Measurement of the contact area between bottleneck and cap within the thread of a plastic bottle (Courtesy of Volume Graphics GmbH)



Computed Tomography,

Fig. 9 Fiber orientation analysis of composite materials. Different colors correspond to different orientations (Courtesy of Volume Graphics GmbH)



used nowadays are either flat panel detectors (consisting of a 2D array of pixels) or straight or curved line detectors (consisting of a 1D array of pixels). While 2D detectors determine faster scanning because multiple slices are measured during one revolution, 1D line detectors may yield superior reconstruction accuracy and resist higher X-ray energies, allowing thicker objects to be scanned (Kruth et al. 2011).

CT scanners can also be classified based on their X-ray source. For common X-ray tubes, the dimension of the X-ray spot is essential to obtain sharp images. Microfocus sources have spot diameters ranging typically from few to 1,000 μm . Today, nanofocus spots of less than or around 1 μm diameter are achievable with X-ray photon energies up to 250 keV. Besides the common X-ray tubes based on an electron gun, more expensive linear accelerator X-ray sources can be used for industrial scanning of large and high absorbing parts. In exceptional cases, large synchrotron radiation facilities are also used to generate X-rays for scientific CT applications (Kruth et al. 2011).

Industrial Applications

Industrial CT scanning is used in many manufacturing areas, from quality control of large castings to inspection of micro-components. Some of the key applications are nondestructive testing, failure analysis, assembly analysis,

reverse engineering, and dimensional metrology. Figures 3, 4, 5, 6, 7, 8, and 9 show examples of industrial applications. The number of applications and number of installed scanners in industry are growing rapidly (De Chiffre et al. 2014).

Advantages

Industrial CT scanning benefits from several advantages over traditional 3D measurement techniques such as coordinate measuring machines. Some of the main advantages are:

- Nondestructive inspection of internal features
- Simultaneous material analysis and dimensional quality control
- Measurement of components in assembled state
- Measurement of interfaces in multi-material components
- Holistic measurement of the entire workpiece obtaining dense volumetric data
- Fast inspection and reverse engineering of complex geometrical features
- Noncontact measurement, without probing and clamping stresses to the part
- Inspection of complex and internal features produced by additive manufacturing
- In-depth realistic visualization of the object's details

Cross-References

- ▶ [Coordinate Measuring Machine](#)
- ▶ [In-Process Inspection](#)
- ▶ [Inspection \(Assembly\)](#)
- ▶ [Inspection \(Precision Engineering and Metrology\)](#)
- ▶ [Metrology](#)
- ▶ [Reverse Engineering](#)

References

- Bocage AEM (1921) Procédé et dispositifs de radiographie sur plaque en mouvement [Moving plate radiography process]. French Patent No. 536,464 (in French)
- Carmignato S (2012) Accuracy of industrial computed tomography measurements: experimental results from an international comparison. *CIRP Ann Manuf Technol* 61(1):491–494
- Cormack AM (1979) Early two-dimensional reconstruction and recent topics stemming from it. Nobel prize lecture. http://nobelprize.org/nobel_prizes/medicine/laureates/1979/cormack-lecture.pdf. Accessed 2 Feb 2016
- De Chiffre L, Carmignato S, Kruth J-P, Schmitt R, Weckenmann A (2014) Industrial applications of computed tomography. *CIRP Ann Manuf Technol* 63(2):655–677
- Hounsfield GN (1979) Computed medical imaging. Nobel prize lecture. http://nobelprize.org/nobel_prizes/medicine/laureates/1979/hounsfield-lecture.pdf. Accessed 2 Feb 2016
- Hsieh J (2009) *Computed tomography: principles, design, artifacts, and recent advances*, 2nd edn. Wiley, Hoboken
- Kak AC, Slaney M (1988) *Principles of computerized tomographic imaging*. IEEE Press, New York
- Kalender WA (2006) *Computed tomography: fundamentals, system technology, image quality, applications*, 2nd edn. Wiley, New York
- Kruth J-P, Bartscher M, Carmignato S, Schmitt R, De Chiffre L, Weckenmann A (2011) Computed tomography for dimensional metrology. *CIRP Ann Manuf Technol* 60(2):821–842
- Morgan CL (1983) *Basic principles of computed tomography*. University Park Press, Baltimore
- Vallebona A (1930) Una modalità di tecnica per la dissociazione radiografica delle ombre applicata allo studio del cranio [A technical method for the radiographic dissociation of the shadows applied to study of the skull]. *Radiol Med* 17:1090–1097 (in Italian)

Computer Numerical Control

Yusuf Altintas

Faculty of Applied Science, Department
Mechanical Engineering/MAL- Manufacturing
Automation Laboratory, University of British
Columbia, Vancouver, BC, Canada

Synonyms

[CNC](#); [Feed drives](#); [Interpolation](#); [Servo control](#); [Trajectory generation](#)

Definition

Computer numerical control (CNC) means the digital control of machine tool units that consist of series of integrated mechanical actuators, electrical or electrohydraulic servomotors, power amplifiers, position and velocity sensors, and a dedicated computer running under a real-time operating system.

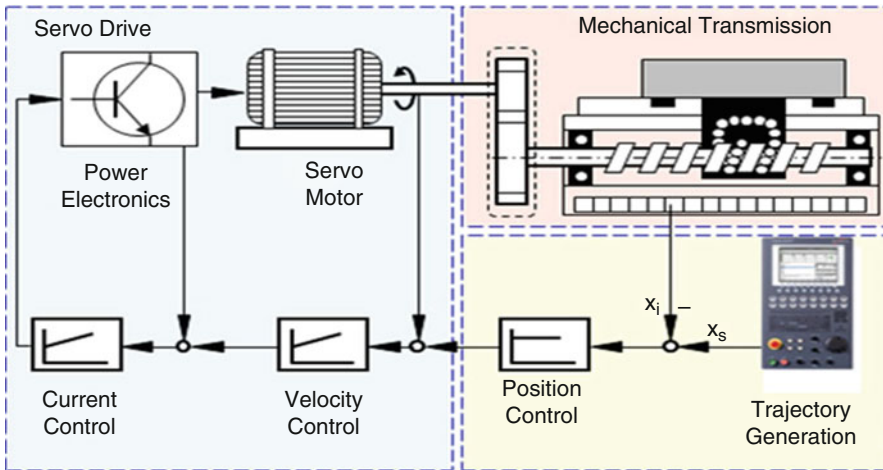
Theory and Application

Introduction

CNC systems control the moving units of a machine tool. The moving units are classified under feed and spindle drives, and auxiliary components such as tool and pallet changers, coolant pumps, and chip conveyors. Feed and spindle drives require smooth position, speed, and acceleration control which are carried out by the trajectory generation and digital control algorithms executed in fixed time intervals by dedicated computers. The auxiliary units are activated by programmable logical controllers (PLCs) that operate on the basis of ON/OFF logic (Altintas 2000).

Feed Drive System

Physical components of a feed drive system are shown in Fig. 1. The trajectory commands are generated in the CNC system and sent to a digital



Computer Numerical Control, Fig. 1 Physical components of feed drive (Altintas et al. 2011)

control law executed in real time, typically at 1 ms or less time intervals.

The digital control law is executed in the CNC computer and sent to amplifier of servomotor if it is an analog drive (Koren and Lo 1992). Position commands are sent to the embedded computers which execute the control law in digital drives (Pritschow et al. 2001). The discrete position commands generated in constant control intervals are typically few micrometers per millisecond, and they are converted into voltage and current by power amplifiers of the motors. The current on the armature of the motor creates a torque, which is used to accelerate the inertia of the mechanical drive, to overcome disturbance loads contributed by the friction and cutting process (Altintas 2012). Analog current controller uses the current sensor feedback to compensate the disturbance loads acting on the drive. The table is either driven by a ball screw drive mechanism or linear drive mechanism as shown in Fig. 2. The position of the rotary or linear motors is measured by encoders attached to the motor shaft or on the linear guides, respectively (Pritschow 1998). The velocity is usually measured by taking the digital derivative of encoder measurements. High-order interpolating circuits are used to improve the accuracy and to filter the jitter in encoder measurements (Altintas et al. 2011).

Trajectory Generation Algorithm

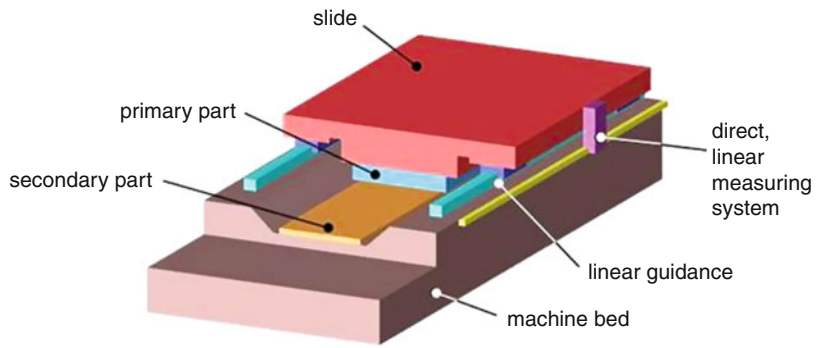
The position commands to each drive on the machine tool are generated as shown in Fig. 3.

Numerical control (NC) program is generated from the computer-aided design (CAD) model of the part using computer-aided manufacturing (CAM) systems. CAM system creates cutter location (CL) file that contains machine tool kinematics independent motion commands. CL file is converted to an NC program by a machine tool specific postprocessor. NC program is loaded to the CNC of the machine tool, parsed, and tool path geometry is interpreted as interconnected linear, circular, and spline interpolators. Trajectory generation algorithm of the CNC reads the feed speed (dS/dt) command and generates spatial displacement commands ($S(t)$) as a function of machine tool's acceleration (d^2S/dt^2) and jerk (d^3S/dt^3) limits at control intervals (i.e., $T = 1$ ms). A jerk limited spatial displacement command is expressed by a cubic function of time (t) as follows:

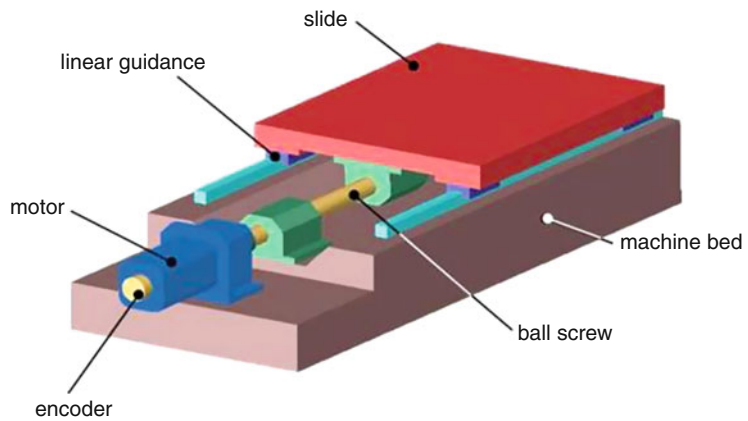
$$S(t) = C_3t^3 + C_2t^2 + C_1t + C_0 \quad (1)$$

where the parameters (C) are evaluated from the feed, acceleration, and jerk limits of the machine tool. The spatial displacement command is divided into acceleration, constant velocity, and deceleration time zones in discrete time intervals (T),

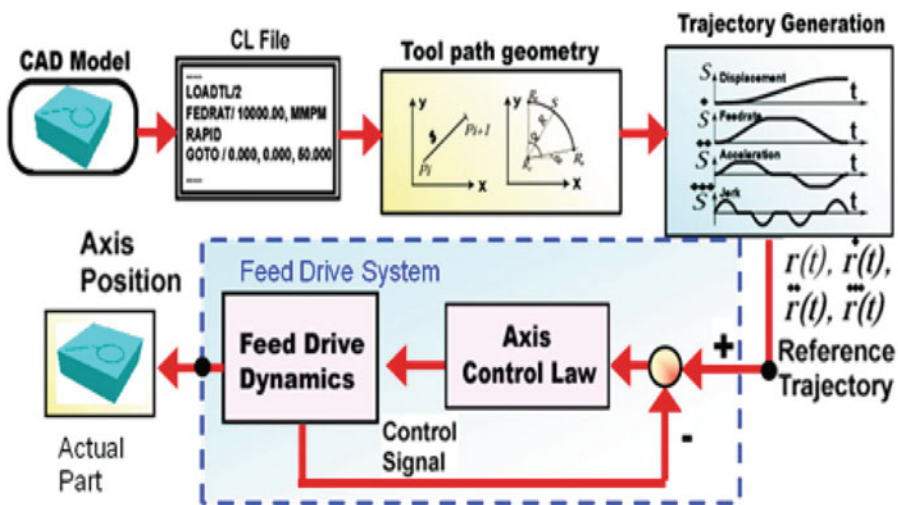
Computer Numerical Control, Fig. 2 Linear and ball screw drives used in CNC machines (Altintas et al. 2011)



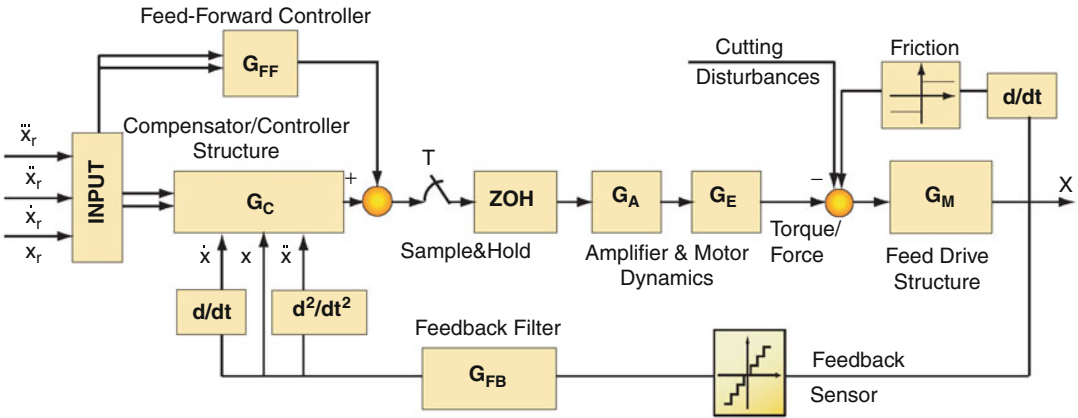
Linear motor



Ball screw



Computer Numerical Control, Fig. 3 Command generation and machine tool control in a CNC system (Altintas et al. 2011)



Computer Numerical Control, Fig. 4 Block diagram of a feed drive control system (Pritschow 1998)

and decoupled to individual feed drives (x_r, y_r, z_r) by the interpolator and kinematics of the machine tool. The discrete position command for each axis is generated as follows:

$$r(kT) = \{x_r(kT) \quad y_r(kT) \quad z_r(kT)\}^T \quad (2)$$

where k is the discrete time counter (Altintas 2012). The decoupled position commands (x_r, y_r, z_r) are sent to individual axes control algorithms at each discrete interval.

Axis Control System

The trajectory generation algorithm sends discrete time-stamped position commands to individual feed drive control units as shown in Fig. 4. The first (dx_r/dt), second (d^2x_r/dt^2), and third (d^3x_r/dt^3) derivatives of the discrete position commands inherently carry axis velocity, acceleration, and jerk commands imposed by the trajectory generation algorithm. The position commands (x_r) are terminated by the trajectory generation once the total position command is reached. The actual position (x) is measured by the encoder and subtracted from the position command (x_r) to find the instantaneous position error. The position error is processed by a digital servo controller (G_C) at each control interval (T). Feedforward controller is usually used to compensate Coulomb friction losses, which are time invariant along the drive stroke. The resulting control command is

converted to analog voltage by a sample and hold device and sent to the power amplifier (G_A) of the servomotor. The electrical winding of the motor (G_E) creates torque in rotary drives and force in linear drives. Some of the torque is spent by the cutting and friction loads, and the remaining is spent to accelerate the inertia of the drive reflected at the motor (G_M). This cycle of position measurement, error generation, control law computation, and analog command generation is executed at each time interval (T) until the drive reaches to the commanded position (Altintas et al. 2011).

Cross-References

- ▶ [Actuator](#)
- ▶ [Computer-Aided Manufacturing](#)
- ▶ [Control](#)
- ▶ [Machine Tool](#)
- ▶ [Mechatronics](#)
- ▶ [Sensor \(Machines\)](#)
- ▶ [Servo System](#)

References

- Altintas Y (2012) Manufacturing automation. 2nd Edition, Cambridge University Press, Cambridge
- Altintas Y, Verl A, Brecher C, Uriarte L, Pritschow G (2011) Machine tool feed drives. Ann CIRP 60(2): 779–796

- Koren Y, Lo CC (1992) Advanced controllers for feed drives. *Ann CIRP* 41(2):689–698
- Pritschow G (1998) A comparison of linear and conventional electromechanical drives. *Ann CIRP* 47(2):541–547
- Pritschow G, Altintas Y, Jovane F, Koren Y, Mitsuishi M, Takata S, Van Brussel H, Weck M, Yamazaki K (2001) Open controller architecture: past, present and future. *Ann CIRP* 50(2):446–463

Computer-Aided Design

Eric Lutters

Faculty of Engineering Technology, Department of Design, Production and Management, University of Twente, Enschede, The Netherlands

Synonyms

CAD

Definition

Computer-aided design (CAD) is the use of a wide range of computer-based tools that assist engineers, architects, and other design professionals in their design activities. It is the main geometry authoring tool within the product life cycle management process and involves both software and sometimes special-purpose hardware. Current packages range from 2D vector-based drafting systems to 3D parametric surface and solid design modelers.

Theory and Application

CAD is used in a variety of ways within engineering companies. At its simplest level, it is a 2D wireframe package that is used to create engineering drawings. This has, however, over the last decades, been overtaken by 3D parametric feature-based modeling. Component forms are created either using freeform surface modeling or solid modeling or a hybrid of the two. These individual components are then assembled into a 3D representation of the final product; this is called bottom-up design.

These assembly models can be used to perform analysis to assess if the components can be assembled and fit together as well as for simulating the dynamics of the product. For example, finite element analysis (FEA) can also be performed on the components and assemblies to assess their strength; alternatively, e.g., acoustic simulation or flow simulations are possible.

Over the last few years, methods and technology have been developed to do top-down design within CAD. This involves starting with a layout diagram of the product, which is broken down into subsystems with ever-increasing detail until the level of single components is reached, with geometry in each level being associative with the level above. Detailed design of the individual components is then completed before building up the final product assembly. In future approaches, this so-called in-context modeling will become increasingly important.

Traditionally, 3D models were used to generate 2D technical drawings; this is, however, being replaced by direct transfer of the data to computer-aided manufacturing (CAM), computer numerical control (CNC), rapid prototyping, and product visualization systems, with nongeometric information being communicated to downstream processes with the aid of PMI (Stroud and Nagy 2011).

Types of CAD Systems

In more or less chronological order, the following types of CAD systems have been developed (Horváth et al.):

- *Two-Dimensional CAD*

Two-dimensional CAD is the most primitive CAD modeling technique. It only creates geometry entities on a 2D plane. The basic 2D geometry entities are points, lines, arcs, circles, and splines. Two-dimensional CAD can only present the part model in a plane view. It is possible to use three plane views to describe a part. Commonly, the three plane views used are the top, front, and side views.

- *Wireframe CAD Model*

A wireframe model represents an object by defining its edges with a series of lines and curves. The term “wireframe” is derived from the fact that one may imagine a wire that is bent

to follow the object's edges to generate the model. The basic constructing elements of wireframe models are points, lines, arcs and circles, conics, and curves. Wireframe modeling systems are capable of constructing three-dimensional representations and have considerably enhanced interactive procedures. Three-dimensional wireframe models are frequently ambiguous in interpreting the entity representation.

- *Surface CAD Model*

A surface model defines the surface skin of the part, including the edges and each surface. Models show not only the edges of surfaces but also the shapes. A surface actually is the mathematical representation of a part's skin. It has no thickness or volume. To create a surface model, usually wireframe entities are constructed that are connected appropriately with the proper surfacing technique. Examples include ruled, loft, coons, revolved, draft, and swept surfaces.

- *Solid CAD Modeling*

A solid model fully describes the shape, size, and volume of the object. It provides a complete set of geometric data about the object for further applications. These may include mass properties calculation, kinematic analysis, stress analysis, and manufacturing. Solid modeling uses a feature-based concept that a part is geometrically composed of a combination of several identifiable features, such as blocks, holes, and slots to model parts.

CAD/CAD Interfacing

The exchange of CAD data became an important topic in the late 1970s. By that time, there were already many different CAD systems on the market. The first version of the Initial Graphics Exchange Specification (IGES) standard was released in 1979. It marginally supported the exchange of 2D drawings, usually mutilating their structure and, because of that, making them of limited use for further processing on a different CAD system. It was recognized that although the IGES standard was developed further to keep in pace with the developments in geometrical modeling, it was still insufficient for the exchange of complete product model structures.

The German automotive industry developed some CAD interfacing standards like VDA-FS for the exchange of surfaces and VDA-PS for the neutral interfacing of application programs. The latter formed the basis for DIN and later on CEN/CENELEC standards which allow to develop portable standard part catalogues for CAD systems. The catalogues are based on CAD parametric programs and files with standardized part data. Standards are developed so that parametric programs and data files can be developed independently of any specific CAD system and may easily be interfaced to most of the commercial CAD systems.

Feature-based modeling generates an additional problem with respect to interfacing. The most important dilemma of feature-based modeling is that many different methods can be used for the synthesizing of parts from features. This implies that the number of possible features is virtually infinite. It has become clear that features must be user adaptable and that the feature library must be extendable. However, this will complicate the exchange of product models between different design systems as well as between those systems and other application programs.

Future

Despite all of the spectacular achievements to date, CAD still has far to go in terms of performance, simplicity, connectivity, and intelligence (Kim; Piegl). Using CAD will change in a number of ways. The following list represents a non-exhaustive number of aspects that will change in future CAD systems:

- Performance that is related to actual requirements by the user.
- Reliability, both in kernels and in user experience.
- Disappearing "CAD overhead," thus focusing more on design intent.
- CAD becomes more service-oriented (i.e., cloud) than seat-based (and version-based).
- Data management will become an inherent and integral part of every CAD operation.
- CAD will become more device-independent.

- CAD will continue to become more of an engineering tool than a design tool.
- Solutions for CAD-CAM interfaces will become more flexible and less vendor-specific.

Cross-References

- ▶ [Product Life Cycle Management](#)

References

- Horváth I, Lee K, Patrikalakis NM (eds) Computer-aided design. Elsevier, Amsterdam
- Kim T (ed) International Journal of CAD/CAM
- Piegl LA (ed) Computer-aided design and applications. CAD Solutions LLC
- Stroud I, Nagy H (2011) Solid modelling and CAD systems: how to survive a CAD system. Springer, London

Computer-Aided Industry

- ▶ [Computer-Integrated Manufacturing](#)

Computer-Aided Manufacturing

Dimitris Mourtzis, Sotiris Makris and George Chryssolouris
 Laboratory for Manufacturing Systems and Automation (LMS), Department of Mechanical Engineering and Aeronautics, University of Patras, Patras, Greece

Synonyms

[CAM](#); [Computer-assisted manufacturing](#)

Definition

Computer-aided manufacturing (CAM) can be defined as the effective utilization of computers in manufacturing (Groover 1987).

Extended Definition

Computer-aided manufacturing (CAM) can be defined as the use of computer systems to plan, manage, and control the operations of a manufacturing plant through either direct or indirect computer interface with the plant's production resources. In other words, the use of computer system in nondesign activities but in the manufacturing process is called CAM (Elanchezhian et al. 2007).

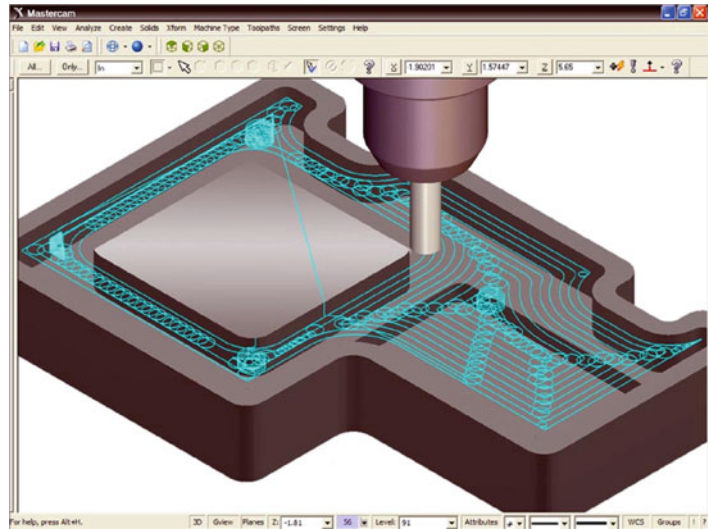
Theory and Application

History

Historically, CAD/CAM systems firstly appeared in ancient Egypt and Greece, as graphics communication used by the engineers. Later on, Leonardo Da Vinci developed techniques such as cross-hatching and isometric views. The invention of computers and xerography made possible the creation of graphics and visualization (Zeid 1991). Practically, the history of computer-aided manufacturing begins in the early 1950s, when the first Numerical Control (NC) machines were designed aiming to substitute the requirements for highly skilled human machine operators (Chang et al. 2006). At the same time another invention, namely, the digital computer, assisted the development of Numerical Control (NC) and provided the means for the creation of ▶ [robots](#), ▶ [computer-aided design](#) (CAD), computer-aided manufacturing (CAM), ▶ [flexible manufacturing systems](#) (FMS), computer-aided process planning (CAPP), as well as product lifecycle management. The utilization of CAM software systems began in large automotive and aerospace industries in 1950. During the late 1950s, Automatically Programmed Tools (APTs) were developed and in 1959, General Motors (GM) began to explore the potential of interactive graphics. GM developed a historically significant system called DAC-1 (Design Augmented by Computer) in 1964. This program became a key element during the design process of GM's cars and trucks. The decade of 1970 can be characterized as the golden era of computer drafting and the beginning of ad

Computer-Aided Manufacturing,

Fig. 1 Example of an up-to-date CAM software workspace



hoc instrumental design applications (Zeid 1991). Among the first CAD/CAM systems was UNISURF that was developed by Pierre Bézier in 1971 for the Renault industry for automotive body design and tooling (Bézier 1989). In 1979, the IGES (Initial Graphics Exchange Specification) was introduced as a communication file structure, aiming to enable data exchange among CAD/CAM and other systems. Other notable standards that were developed in the same period include (Zeid 1991):

- Graphic Kernel System (GKS). ANSI and ISO standard that interfaces the application program with the graphics support package
- Programmer's Hierarchical Interactive Graphics System (PHIGS) that supports high function workstations and their related CAD/CAM applications
- Virtual Device Metafile (VDI) that describes the functions needed to describe a picture.
- North American Presentation Level Protocol Syntax (NAPLPS) that describes text and graphics in the form of sequences of bytes in ASCII code

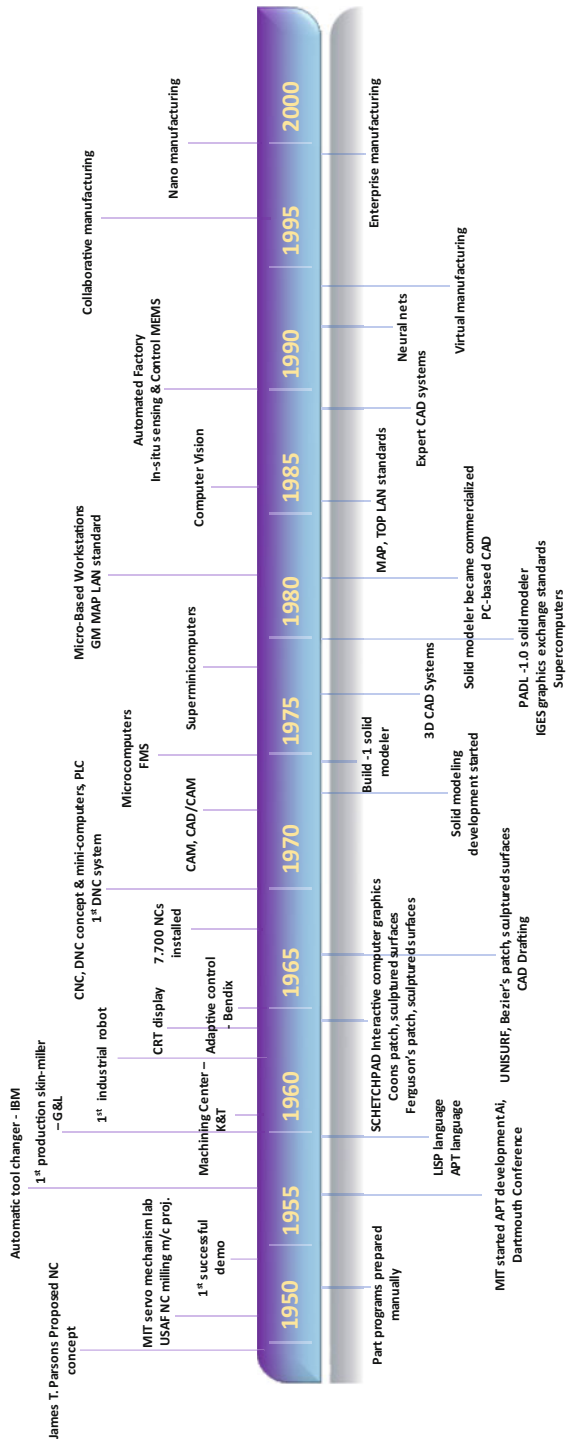
The evolution of virtual manufacturing has led to the creation of work-cell simulation tools that

are capable of developing, simulating, and validating manufacturing processes. Moreover, off-line programming of multidevice robotic and automated processes (virtual commissioning) offer optimization functionalities, from the concept to the implementation phase. At the 2000s, commercial CAM suites (Fig. 1) provided complete solutions to Product Lifecycle Management (PLM) in multiple stages of the production, i.e., conceptualization, design (► CAD), manufacturing (CAM), and engineering (CAE). A great number of ► CAD tools exist today that provide functionalities of CAM/CAE (Chryssolouris 2006) (Fig. 2).

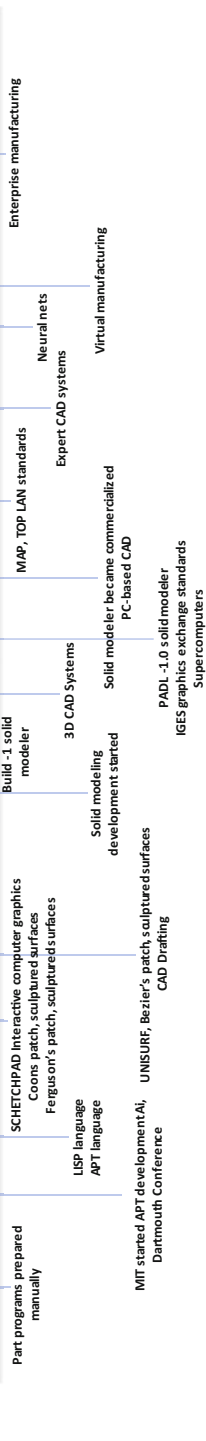
Strategic Role of CAM

According to Lee-Post 2003, the application and the adoption of CAM systems in manufacturing has a number of advantages enabling the manufacturing companies to develop and enhance their existing capabilities and achieve among others, greater and more accurate supervision of the production, increased flexibility and reduced time to market, increased product variety, and capability to deliver small lot sizes.

HARDWARE



SOFTWARE



Computer-Aided Manufacturing, Fig. 2 Evolution of CAD/CAM and related technologies

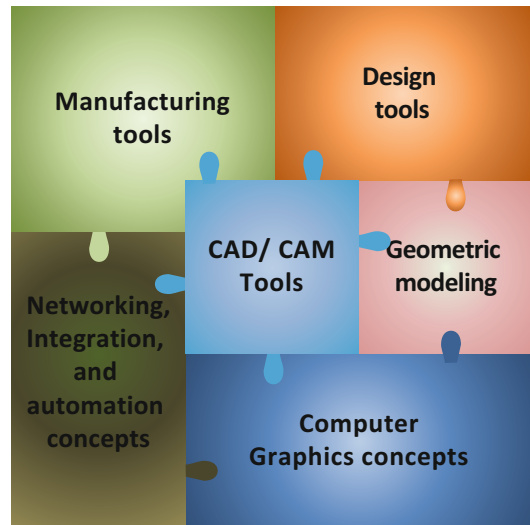


Application of CAM in the Production

Following the design of the part through computer-aided design (► [CAD](#)) software and its analysis through computer-aided engineering (CAE) software, computer-aided manufacturing (CAM) connects product design with manufacturing. CAM systems enable the control and the operation of equipment on the shop floor, such as ► [robots](#), controllers, machine tools, and machining centers (Lee-Post 2003). CAM technologies comprise NC machines, expert systems, machine vision, ► [robots](#), lasers, and ► [FMS](#) technologies used alongside computer hardware, databases, and communication technologies. CAM systems are tightly connected with ► [CAD](#) systems. As CAM does not offer model editing abilities, there is a need to combine CAM software with a CAD system, supporting the user to add or edit the drawing of the part to be manufactured (Seames 2002). As industrial design becomes more complex, developing algorithms for tool paths optimization for free-form surfaces becomes important (Lazoglu et al. 2009). The ► [CAD](#) databases must reflect the manufacturing requirements, such as tolerances and features. The part drawings must be designed bearing in mind CAM requirements. As modern manufacturing systems require synchronization among ► [robots](#), vision systems, manufacturing cells, material handling systems, and others, CAM systems offer high coordination between the interconnected systems in order to tackle the challenging shop-floor tasks. The role of CAD/CAM systems in the production can be depicted as the intersection of five sets: design tools, manufacturing tools, geometric modeling, computer graphics concepts, and networking concepts (Fig. 3).

Moreover, CAM technology enables the linkage between the three-dimensional (3D) model and its production, supporting in that way mass production as well as increased flexibility (Yeung 2003).

The data exchange between CAM, ► [CAD](#), and ► [CAPP](#) is a dynamic procedure and takes place through various production stages. Data

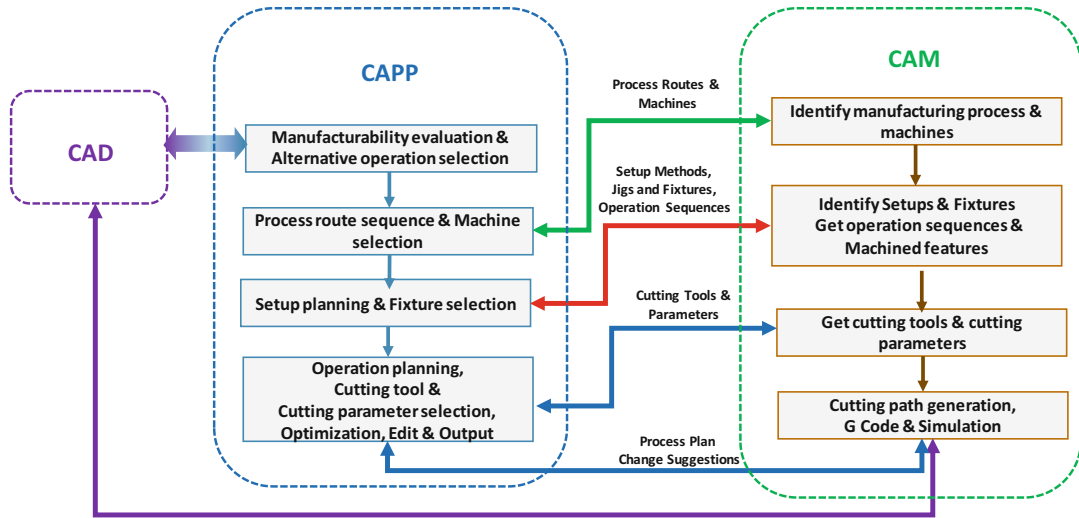


Computer-Aided Manufacturing, Fig. 3 CAD/CAM and their constituents

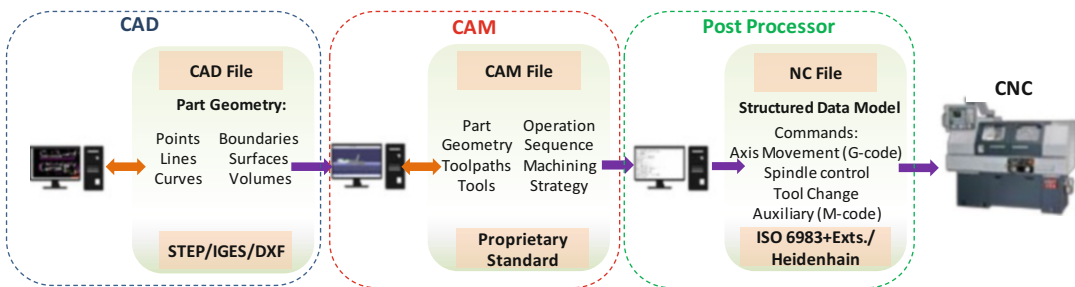
generated from CAM regarding the process and the manufacturing machine requirements need to be combined with ► [CAPP](#) generated information regarding process routes sequence and machine assignments. Moreover, reports regarding setup methods, fixtures, and operations sequences between function of setup planning and fixture selection in ► [CAPP](#) and function of identifying setups, fixtures, getting operation sequences, and machined features in CAM are transmitted.

Bringing it all together, an approach concerning process plan is created that includes change suggestions between the function of operation planning, cutting tool selection, cutting parameter selection, optimization, edit and output in ► [CAPP](#), the function of generating cutting path, ► [CNC](#) code, and the CAM simulation (Ming et al. 2008). In Fig. 4, the connection of CAM systems with ► [CAPP](#) and ► [CAD](#) is depicted.

The mechanical drawing files from ► [CAD](#) applications are required from the CAM system in order for a part to be manufactured. The ► [CAD](#) drawing geometry information is transferred to the CAM system, in order to generate the tool paths in the form of the NC code required by the manufacturing machines.



Computer-Aided Manufacturing, Fig. 4 The collaboration between CAM, CAPP, and CAD systems. (Adapted by Ming et al. 2008)



Computer-Aided Manufacturing, Fig. 5 Manufacturing information flow in the state-of-the-art CAD/CAM/CNC chain. (Adapted by Newman et al. 2008)

Numerical Control (NC) and CAM

Numerical control refers to a system that includes hardware and software to control machine tools and other production equipment via numerical input (Lee-Post 2003). NC utilizes a code that consists of letters, numbers, and special characters to give operation orders to a manufacturing machine. In 1947, during a US Air Force funded project, John Parson of the Parsons Group introduced the idea of using three-axis curvature data to control machine tool motion for the production

of aircraft components, setting the ground for NC. In 1951, MIT (Massachusetts Institute of Technology), in USA, took the project’s developments one step further, developing the first NC machine (Seames 2002). MIT has not only developed the first NC machine but also the first universal programming language for NC. This language gradually became the G-Code. The evolution of computers led to the creation of Computer Numerical Control (► CNC) in the 1970s.

The difference in NC and ► CNC lies in the controller technology. While NC functions need

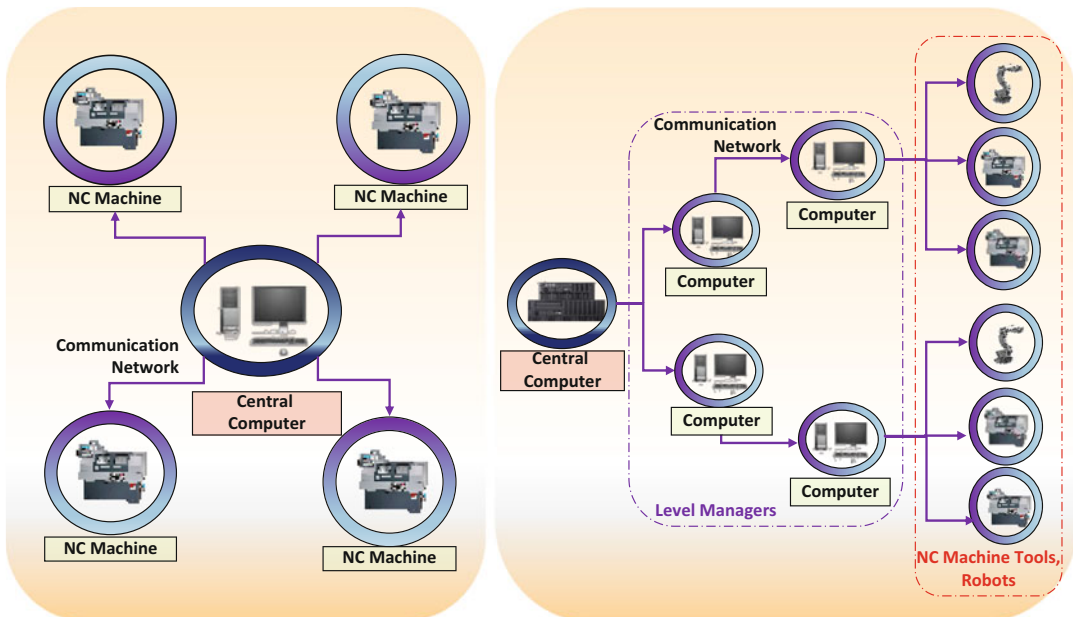
to be designed and implemented in hardware circuits, ▶ CNC functions can be implemented in CAM software. The whole process has been standardized in the ISO 6893 standard, formalizing G&M codes used in early NC and modern CNC machines (International Standards Organization 2009). The codes were originally stored in magnetic tapes, the most common of which was 1/4 in. computer grade cassette tape, until the Electronics Industries Association (EIA) standardized the tape format and coding (Seames 2002). To further formalize the process and ensure seamless data interoperability between different software packages and machines, the STEP standard has been developed and formalized into ISO10303 (International Standards Organization 1994) and evolved later to ISO14649 (International Standards Organization 2003) and ISO10303-AP238 (International Standards Organization 2007) commonly known as STEP-NC.

The main difference between the STEP-NC and the G-, M-Code is that the first describes “what to do,” thus the targeted end product, while the second “how to do,” including the

instructions of movements for the CNC machine tools (Xu 2009). The STEP-NC describes tasks that are based on the machining features so that the part program provides the shop-floor with higher-level information. As cyber-physical systems and cloud computing are expected to play a major role in the future of manufacturing, STEP-NC may become the champion standard (Toquica et al. 2018).

The steps from the original CAD of the part to the CNC code are depicted in Fig. 5.

An evolution of CNC that has been more recently introduced is the Direct Numerical Control (DNC). DNC involves a computer that acts as a partial or full controller to one or more NC machines. Further to that, improvements in the field led to the creation of Distributed Numerical Control. In order to support the gathering and storing of upstream and downstream shop-floor information, several ▶ CNC machines are linked together inside a network. In Fig. 6, the differences in the architectures of Direct and Distributed Numerical Control are presented.



Computer-Aided Manufacturing, Fig. 6 Direct numerical control (left) and distributed numerical control (right)

Flexible Manufacturing Systems (FMS) and CAM

A flexible manufacturing system (► FMS) is a reprogrammable manufacturing system capable of producing a variety of products (Chryssolouris 2006). The components that constitute an ► FMS are characterized by high adaptability, capable of meeting a wide variety of processing requirements. Therefore, automatic systems such as CNC turning/machining centers and robotic workstations are commonly found in such a system (Chryssolouris 2006). CAM systems, NC, and robotics offer reprogramming capabilities at the machine level with minimum setup time. As smart systems become embedded in machine controllers, a new level of process-related information is created, increasing the number of decision points, and thus the flexibility (Xu 2017).

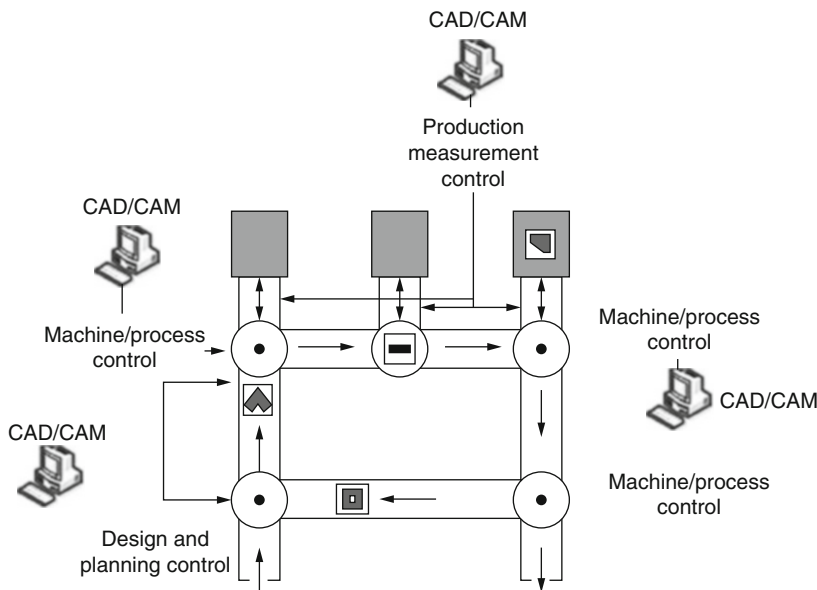
An ► FMS (Fig. 7) comprises the following features:

- Interchangeable and/or specific machining units
- Various workpieces within a component range
- Usually free component selection

The main challenge in the installation of an ► FMS lies in the control of the complex network of equipment and shop-floor activities of such a system. State-of-the-art CAM systems offer a set of features that make feasible the implementation of ► FMS in modern manufacturing systems.

CAM Software

CAM software can be divided into 2D and 3D applications. The main difference between these two applications is that the 2D, based on the received 2D drawing, calculates the tool path and the movements taking place on the Z axis, while the 3D applications generate the tools paths based on the 3D model. Moreover, CAM software systems can be categorized as high-end systems and simple ones. The simple programs provide limited functionalities and as a result are low-cost solutions. The high-end CAM systems are capable of supporting advanced machining of 4 and 5 –axis machines, optimization for high-speed machining, and multiple options of machining strategies among others.



Computer-Aided Manufacturing, Fig. 7 FMS with integrated CAD/CAM systems



CAM Software Survey

Software vendors are currently developing integrated CAD/CAM systems, further enhancing the capabilities of today's CAM applications. Table 1 gives a glimpse of the status of CAM technology by presenting some of the most popular CAD/CAM systems.

The solutions provided by the leading CAD/CAM vendors offer high-end features,

like parametric modeling for solid shapes, 2.5 to 5 axis machining tool path generation, networking and collaborative design features, postprocessing capabilities, resequencing of operations, simulation and optimization of NURBS interpolation and generative machining and assisted manufacturing that captures manufacturing and process know-how and automates repetitive NC functions.

Computer-Aided Manufacturing, Table 1 Commercial CAD/CAM suites

CAD/CAM suite	Vendor	Features
CimatronE	3D systems http://www.cimatron.com/Main/homepage.aspx?FolderID=5&lang=en	Solid modeling capabilities range from wireframe and surfaces to parametric solids 2.5 to 5-axis milling, drilling, turning, punching, and wire EDM tools paths generation
VERICUT	CGTech www.cgtech.com	Multiaxis milling, drilling, and turning Optimizes NC tool paths automatically Simulates and optimizes NURBS interpolation
Mastercam	CNC Software www.mastercam.com	Intel-based 2.5-axis milling and drilling package 5-axis positioning and lathe operation handling Creates CAD geometry and wire EDM
CATIA	Dassault Systèmes www.catia.com	Generative machining and assisted manufacturing that captures manufacturing and process know-how and automates repetitive NC functions Networking and collaborative design feature
CADDS 5	PTC www.ptc.com	2-, 2.5-, 3-, 5-axis machining
SolidCAM	SolidCAM www.solidcam.com	3D high-speed machining, Indexial multiaxis machining
GibbsCAM	3D Systems www.gibbscam.com	2- to 5-axis milling, multitask machining, Swiss-style machining and wire EDM
hyperMILL	OPEN MIND www.openmind-tech.com	5-axis simultaneous machining and 3D plane level machining and optimizations for 3D milling
POWERMILL	Autodesk http://www.autodesk.com/products/powermill/overview	Multiaxis machining Object linking and embedding for design and modeling
ALPHACAM	Vero Software www.alphacam.com	Parallel and flat area 3d machining Adaptive feed rate support for Z contour roughing Editable spline/polyline tool paths
Tebis CAM	Tebis www.tebis.com	2.5-axis machining Creation of collision-safe tool paths for 5-side complete machining Neutral and control-specific postprocessing
Surfcam	Vero Software www.surfcam.com	Machines undercut in one setup Parametric design capabilities Creates optimized tool paths according to user-defined tolerances
NX CAM	Siemens www.plm.automation.siemens.com	High definition 3D technology PMI-driven feature-based machining Synchronized point distribution

CAM and High-End Market Share in 2016

For 2016, Mastercam was the market leader in High-End Market Share. Among the main changes are that HSMWorks remains second, but their share has fallen from 17% to 14% (Fig. 8). Last year's third player was OneCNC with 6% market share, but they have fallen to number 10. SolidCAM is holding steadily to fifth place, where they were last year, though their share is up from 5% to 7%.

Future of CAM Systems

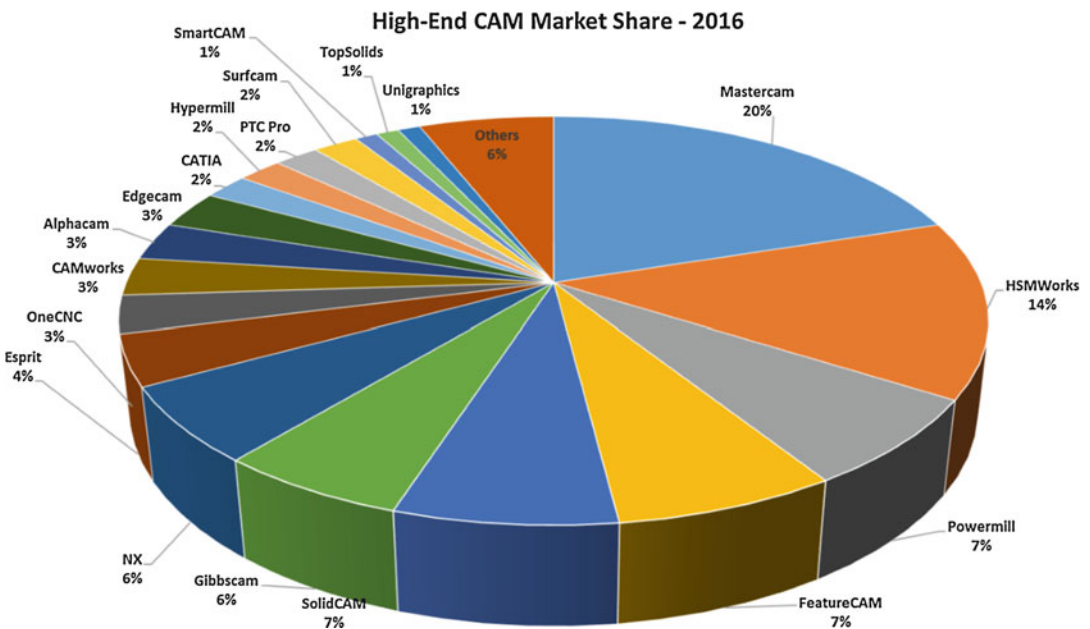
The manufacturing environment is characterized by ever-changing dynamics and evolution. The production process is based more and more on virtual simulations and networking features not only in factory level but also in global level. Among the main needs are: effective coordination, collaboration, and communication throughout the aspects of production, from humans to machines. Moreover, Artificial Intelligence (AI) will allow the development of smart tools. The exploitation of AI in the CAM systems will

offer automatic optimization of NC tool paths and benefit from knowledge-based systems. Furthermore, self-evolving and self-adjustable ▶ robots are upcoming concepts that will entail advantages towards a more economic application of CAM systems. Smart robots are evolving due to the low cost of their design and implementation. As a result, smart robots of low cost are used in production to assembly parts or to package produced products, among other tasks (Lee-Post 2003).

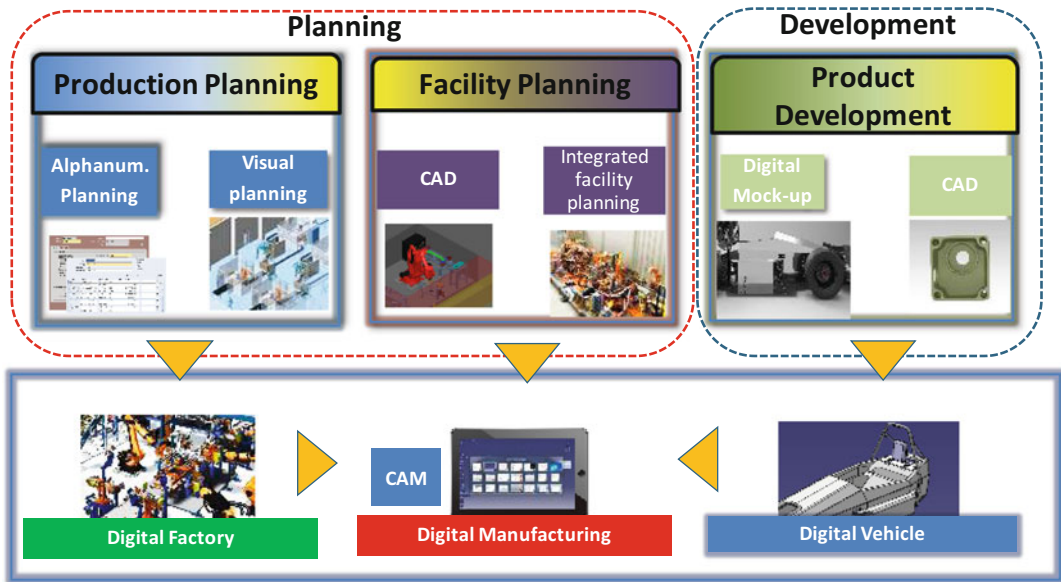
Digital Manufacturing and CAM

The future and the evolution of CAD/CAM systems is highly influenced by the evolution of manufacturing systems in general. The transition from mass production to ▶ mass customization and global manufacturing (Mourtzis et al. 2013), which is performed with the support of the key enabling technologies, greatly influences the CAD/CAM systems (Fig. 9).

In addition to the above, moving towards digital manufacturing or digitalized manufacturing, which incorporates technologies like 3D printing, virtual and augmented reality technologies, as



Computer-Aided Manufacturing, Fig. 8 High-End Market Share (adapted from CNCCookBook CAM Survey 2016)



Computer-Aided Manufacturing, Fig. 9 CAD/CAM and digital factory

well as cloud, will transform the state-of-the-art CAD/CAM systems into effective and advanced ones. The implementation of digital manufacturing is relying on state-of-the-art CAD/CAM and ► **CAPP** systems and their evolution (Chryssolouris et al. 2008).

Virtual Commissioning and CAM

Virtual commissioning will play an important role in addressing the need to reduce the complexity of the production systems and the need for short ramp-up time. In the Virtual commissioning approach, virtual prototypes are used for the commissioning of control software in parallel with the manufacture and assembly of the particular production system (Reinhart and Wunsch 2007). Virtual commissioning is a current trend in automotive assembly lines, capable of efficiently handling the complexity of the assembly systems, highly reducing the system's ramp-up time, and a shortening the product's time to market (Makris et al. 2012), through advanced CAD/CAM software (Fig. 10).

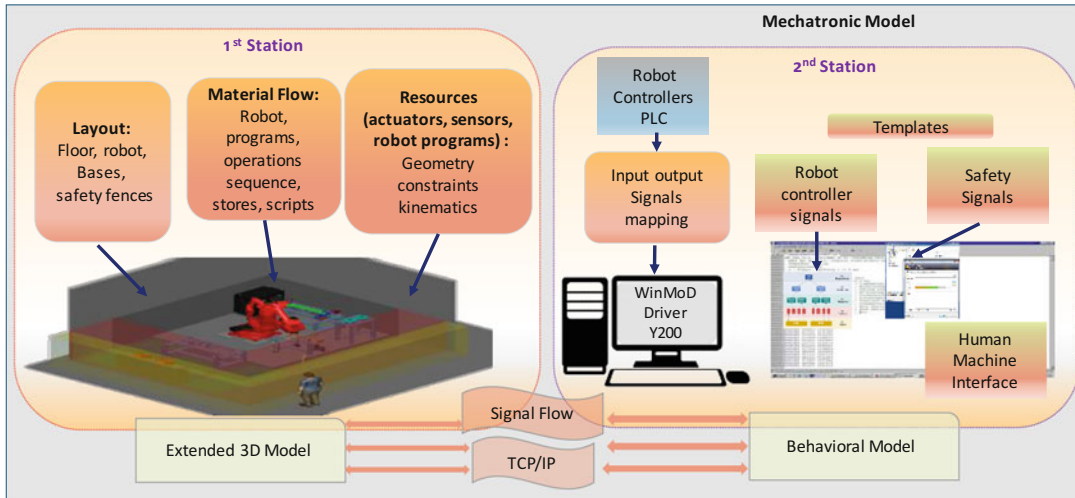
Cloud Manufacturing and CAM

Cloud technology will support the digital manufacturing and will enable effective

communication and collaboration (Xu 2012). Moving from production-oriented to service-oriented manufacturing and inspired by cloud computing, cloud manufacturing seems to offer an attractive and natural solution. Through cloud manufacturing, distributed and interoperable manufacturing platforms that will integrate CAD/CAM/CAPP/CNC applications will be offered (Xu 2012) (Mourtzis et al. 2016). Examples of such platforms have been developed in 2007 (Newman and Nassehi 2007). Known developments in cloud-based CAM include Autodesk's CAM 360 announced in 2014, as well as Esprit by DP technology.

3D Printing: Additive Manufacturing and CAM

Moreover, the growing interest in ► **additive manufacturing** will introduce new innovative hybrid approaches in CAM systems, as new hybrid additive-subtractive machining systems have come and will be further introduced onto the market (Siemens PLM Software 2015). Complex part geometries and process planning of hybrid operations will necessitate advanced CAM software to facilitate their operation effectively (Flynn et al. 2016).



Computer-Aided Manufacturing, Fig. 10 An example of virtual commissioning from an assembly cell with advanced robotic systems. (Adapted by Makris et al. 2012)



Computer-Aided Manufacturing, Fig. 11 Mass customization will influence both CAD/CAM systems

Mass Customization and CAM

Finally, the trend of mass customization will further influence the CAD/CAM systems, requiring a systematic information modeling for CAM planning. This information modeling will enable efficient and accurate CAM operations, by retrieving data from various sources inside and outside the

industry in order to address the need for customized and personalized products (Fig. 11). Feature combination, combined features manufacturing strategies, manufacturing resources capabilities and availability, as well as knowledge from manufacturing databases will constitute the main data retrieved from several sources (Yao et al. 2007).

Cross-References

- ▶ Additive Manufacturing Technologies
- ▶ Computer Numerical Control
- ▶ Computer-Aided Design
- ▶ Computer-Aided Process Planning
- ▶ Computer-Integrated Manufacturing
- ▶ Flexible Manufacturing Systems
- ▶ Mass Customization
- ▶ Robot

References

- ALPHACAM. www.alphacam.com. Date of Access: 25 June 2018
- Autodesk, POWERMILL. <http://www.autodesk.com/products/powermill/overview>. Date of Access: 25 June 2018
- Bézier P (1989) First steps of CAD. *Comput-Aided Des* 21(5):259–261
- CGTech VERICUT. www.cgtech.com. Date of Access: 25 June 2018
- Chang T-C, Wysk RA, Wang H-P (2006) *Computer-aided manufacturing*, 3rd edn. Prentice-Hall, Upper Saddle River
- Chryssolouris G (2006) *Manufacturing systems: theory and practice*, 2nd edn. Springer, New York
- Chryssolouris G, Mavrikios D, Papakostas N, Mourtzis D, Michalos G, Georgoulis K (2008) Digital manufacturing: history, perspectives, and outlook. *Proc Inst Mech Eng Part B: J Eng Manuf* 223(5):451–462. <https://doi.org/10.1243/09544054JEM1241>
- Cimatron E. <https://www.3dsystems.com/software/cimatron>. Date of Access: 25 June 2018
- CNCCookBook CAM Survey 2016. <http://blog.cnccookbook.com/2017/01/03/results-2016-cnccookbook-cam-survey/>. Date of Access: 25 June 2018
- Dassault Systèmes. CATIA. <https://www.3ds.com/products-services/catia/>. Date of Access: 25 June 2018
- Elanchezhian C, Selwyn TS, Sundar GS (2007) *Computer-aided manufacturing*, 2nd edn. Laxmi Publications, New Delhi
- Flynn J, Shokrani A, Newman S, Dhokia V (2016) Hybrid additive and subtractive machine tools – research and industrial developments. *Int J Mach Tool Manu* 101: 79–101
- GibbsCAM. www.gibbscam.com. [Date of Access: 25 June 2018]
- Groover MP (1987) *Automation production systems and computer-aided manufacturing*, 1st edn. Prentice-Hall, Englewood Cliffs
- ISO 10303-1 standard (1994) *Industrial automation systems and integration – product data representation and exchange, part 1: overview and fundamental principles*. Beuth, Berlin
- ISO 10303-238 standard (2007) *Industrial automation systems and integration – product data representation and exchange, part 238: application protocol: application interpreted model for computerized numerical controllers*. Beuth, Berlin
- ISO 14649-1 (2003) *Industrial automation systems and integration – physical device control; data model for computerized numerical controllers, part 1: overview and fundamental principles*. Beuth, Berlin
- ISO 6893-1 standard (2009) *Numerical control of machines-program format and definition of address words, Part 1: data format for positioning, line motion and contouring control systems*. Beuth, Berlin
- Lazoglu I, Manav C, Murtezaoglu Y (2009) Tool path optimisation for free form surface machining. *CIRP Ann Manuf Technol* 58(1):101–104
- Lee-Post A (2003) *Computer-aided manufacturing. Encyclopedia of information systems vol 1*. Elsevier Science, pp 187–203. Amsterdam, Netherlands. <https://doi.org/10.1016/B0-12-227240-4/00012-5>
- Makris S, Michalos G, Chryssolouris G (2012) Virtual commissioning of an assembly cell with cooperating robots, *Adv Decis Sci* 2012:1–11. Article ID 428060. <https://doi.org/10.1155/2012/428060>
- Mastercam. www.mastercam.com [Date of Access: 25 June 2018]
- Ming XG, Yan JQ, Wang XH, Li SN, Lu WF, Peng QJ, Ma YS (2008) Collaborative process planning and manufacturing in product lifecycle management. *Comput Ind* 59(2–3):154–166
- Mourtzis D, Doukas M, Psarommatas F (2013) Design and operation of manufacturing networks for mass customisation. *CIRP Ann Manuf Technol* 62(1): 467–470
- Mourtzis D, Vlachou E, Xanthopoulos N, Givehchi M, Wang L (2016) Cloud-based- adaptive process planning considering availability and capabilities of machine tools. *J Manuf Syst* 39:1–8. <https://doi.org/10.1016/j.jmsy.2016.01.003>
- Newman ST, Nassehi A (2007) Universal manufacturing platform for CNC machining. *CIRP Ann Manuf Technol* 56(1):459–462
- Newman ST, Nassehi A, Xu XW, Rosso Jr RS, Wang L, Yusof Y, Ali L, Liu R, Zheng LY, Kumar S, Vichare P (2008) Strategic advantages of interoperability for global manufacturing using CNC technology. *Robot Comput Integr Manuf* 24(6):699–708
- NX CAM. Siemens. <https://www.plm.automation.siemens.com/global/en/products/manufacturing-planning/cam-software.html>. Date of Access: 25 June 2018
- OPEN MIND. hyperMILL. www.openmind-tech.com. Date of Access: 25 June 2018
- PTC. www.ptc.com. Date of Access: 25 June 2018
- Reinhart G, Wunsch G (2007) Economic application of virtual commissioning to mechatronic production systems. *Prod Eng* 1(4):371–379
- Seames WS (2002) *Computer numerical control. Concepts and programming*, 4th edn. Delmar, Albany
- Siemens PLM Software (2015) *NX Hybrid Additive Manufacturing: Transforming component design and manufacturing*. <http://majentaplms.com/wp-content/uploads/NX-hybrid-additive-manufacturing.pdf>. Date of access: 17 May 2017

- SolidCAM. www.solidcam.com. Date of Access: 25 June 2018
- Surfcam Vero Software. www.surfcam.com. Date of Access: 25 June 2018
- Tebis CAM. Tebis. www.tebis.com. Date of Access: 25 June 2018
- Toquica JS, Alvares AJ, Bonnard R (2018) A STEP-NC compliant robotic machining platform for advanced manufacturing. *Int J Adv Manuf Technol* 95:3839–3854
- Xu X (2009) Integrating advanced computer-aided design, manufacturing, and numerical control: principles and implementations. Information Science Reference, IGI Global, London
- Xu X (2012) From cloud computing to cloud manufacturing. *Robot Comput Integr Manuf* 28(1):75–86
- Xu X (2017) Machine tool 4.0 for the new era of manufacturing. *Int J Adv Manuf Technol* 92:1893–1900
- Yao S, Han X, Yang Y, Rong Y, Huang SH, Yen DW, Zhang G (2007) Computer-aided manufacturing planning for mass customization: part 3, information modeling. *Int J Adv Manuf Technol* 32:218–228. <https://doi.org/10.1007/s00170-005-0329-x>
- Yeung MK (2003) Intelligent process-planning system or optimal CNC programming – a step towards complete automation of CNC programming. *Integr Manuf Syst* 14(7):593–598
- Zeid I (1991) CAD/CAM theory and practice. McGraw-Hill, New York

Computer-Aided Process Planning

- Hoda A. ElMaraghy^{1,2} and Aydin Nassehi³
- ¹Intelligent Manufacturing Systems Center, University of Windsor, Windsor, ON, Canada
- ²Canada Research Chair in Manufacturing Systems, Intelligent Manufacturing Systems Centre, University of Windsor, Windsor, ON, Canada
- ³Department of Mechanical Engineering, University of Bristol, Bristol, UK

Synonyms

CAPP

Definition

Process planning, in the manufacturing context, is the determination of processes and resources

needed for completing any of the manufacturing processes required for converting raw materials into a final product to satisfy the design requirements and intent and respect the geometric and technological constraints. Process planning is the link between product design and manufacturing (Scallan 2003). At the “macrolevel,” the sequence of operations and the selection of appropriate resources are the main concerns, whereas at the “micro” process planning level, the focus is on defining parameters of each operation, determining the time it takes to perform that operation, and selecting tools and fixtures as needed (ElMaraghy 1993). Computer-aided process planning (CAPP) is the application of computer software to assist in these activities.

Theory and Application

Theory and Methodologies

Process planning techniques can also be classified into variant and generative. Variant (retrieval-based) process planning techniques that rely on a master template of a composite part are predicated on a predefined part/part family with some commonality in geometry or manufacturing processing. Upon retrieving a similar part, by visual inspection or using a coding and classification system, modifications are made to the process plan to suit the new part and its features. However, while this approach is fast, it results in less than optimal process plans. Generative process planning generates process plans from scratch for each part using rule- and knowledge-based systems, heuristics, and problem-specific algorithms. It requires full understanding and mathematical models of the processes and sufficient knowledge about its behavior, influencing factors, and constraints. Therefore, truly generative systems are not yet a reality with few exceptions and hybrid/semi-generative approaches have been developed (Azab and ElMaraghy 2007a). Computerized process planning involves mathematical formulation of an optimization problem which seeks to minimize some cost function such as total process time and maximize resources utilization subject to several technological constraints, the

most important of which are the precedence constraints. Such models aim to establish the best operation sequence and resources required for each at the macrolevel or the specific values of operations parameters at the detailed micro-level. The challenges include knowledge representation schemes, heuristics, and optimization algorithms such as classical optimization algorithms, the traveling salesperson formulation and solution, precedence representation using graph, neural nets, expert systems, etc. (Azab and ElMaraghy 2007b). The trade-off is often between the complexity of the models, the solution time, and quality of the resulting process plan and its production cost implications.

Hierarchy of Process Planning

Process planning and its outcomes can be divided into several levels according to the fidelity and the granularity of the activities (ElMaraghy 1993). Generic process planning is used to refer to the highest level of process planning where the overall production strategy and process type are selected from the pool of available and feasible technologies. Macro process planning encompasses routing and nonlinear planning activities where alternate sets of resources that are capable of realizing production goals are identified. Detailed planning is at a lower level where the sequence of operations on a single resource is determined. Finally, at the lowest level, micro process planning comprises all activities undertaken to select appropriate operational parameters. The four levels of process planning are shown in

Table 1. While in large manufacturing enterprises, these levels are clearly identifiable, in smaller manufacturing operations, the boundaries are very fuzzy and the planners often work on different levels at the same time.

Common Process Planning Approaches

There are two principal approaches for process planning: manual process planning and computer-aided process planning. There has been some research in creating fully automated process planning systems, but these efforts have been largely abandoned due to challenges, both technical and philosophical; it is often argued that the best approach is to present viable alternatives to a human expert planner.

Manual Process Planning

A significant portion of process planning is still done manually. Here, the quality of the process plan is reliant on the knowledge of the expert planner about the product, the resources, and the available processes. Development of such knowledge is time consuming and expensive, and as such computer-aided process planning systems were introduced to move the knowledge from the expert planner to a computer-based system (Alting and Zhang 1989).

Computer-Aided Process Planning (CAPP)

Computer-aided process planning systems rely on a computerized knowledge base to provide support for the expert process planner. Through their use in process planning, it is possible to raise the

Computer-Aided Process Planning, Table 1 Levels of process planning (Adapted from ElMaraghy 1993)

Process planning level	Main focus of planning at this level	Level of detail	Planning output at this level
Generic planning	Selecting technology and rapid process planning	Very low	Manufacturing technologies and processes, conceptual plans, and DFX analysis results
Macro planning	Multi-domain	Low	Routings, nonlinear plans, alternate resources
Detailed planning	Single domain, single process	Detailed	Detailed process plans (sequence, tools, resources, fixtures, etc.)
Micro planning	Optimal conditions and machine instructions	Very detailed	Process/Operation parameters, time, cost, etc., NC codes

productivity, reduce the cost, increase the consistency, and lower the skill requirements for the expert process planner. Two major methods are used for CAPP: generative CAPP and variant CAPP (Marri et al. 1998).

Generative CAPP In this approach, decision rules, optimization algorithms (Azab and ElMaraghy 2007b) or artificial intelligence in its various forms – i.e., intelligent agents (Nassehi et al. 2009; Shen et al. 2006), evolutionary algorithms (Li et al. 2010), etc. – are used to make planning decisions. These systems essentially simulate the decision process of a human expert. In realization of these systems, the two principal challenges – representation of the manufacturing domain knowledge and the inference mechanism – are still under research (Xu et al. 2011).

Variant CAPP In this approach, an existing process plan is retrieved and modified for use with a new product similar to the one for which the original process plan was prepared; process plans are often prepared for part families that have significant similarities.

Reconfigurable Process Planning (RPP) RPP was first introduced by Azab and ElMaraghy (2007a). It is a hybrid generative/retrieval approach which develops a process plan for a new part, some features of which are not within the boundaries of the existing part families or its composite part and master plan, i.e., the new part belongs to an evolving parts family (ElMaraghy 2007). The master plan is modified to meet the requirements of the new part and its features. Portions of the process plan, corresponding to

the removed/added features (and their manufacturing operations), are generated and optimally positioned, similar to genetic mutation, within the overall process plan. An innovative mathematical formulation using 0–1 integer programming is used for reconfiguring process plans and minimizing the cost of disruption on the shop floor.

Process Planning Activities

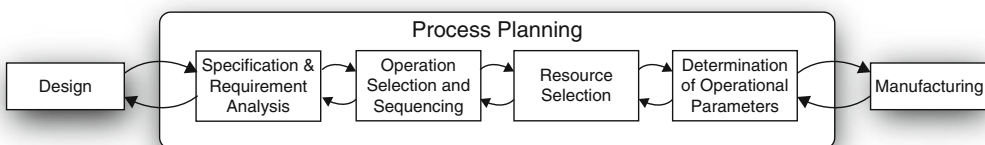
In the broadest sense, process planning is the consolidation of planning activities that allow manufacturing of the products to commence after their design specifications have been established. In this broad definition, process planning involves a wide variety of activities as shown in Fig. 1:

- Component specification and requirement analysis
- Operation selection and sequencing
- Resource selection
- Determination of appropriate operational parameters

It is noteworthy that, in general, these activities are not carried out in a sequential manner and usually there are many iterations necessary until process planning is completed and the manufacturing of the product commences.

Component Specification and Requirement Analysis

The first set of activities in process planning is concerned with analyzing the design requirements to identify the features that should be manufactured. When manufacturing a product,



Computer-Aided Process Planning, Fig. 1 Overall view of process planning activities (Adapted from Xu 2009)

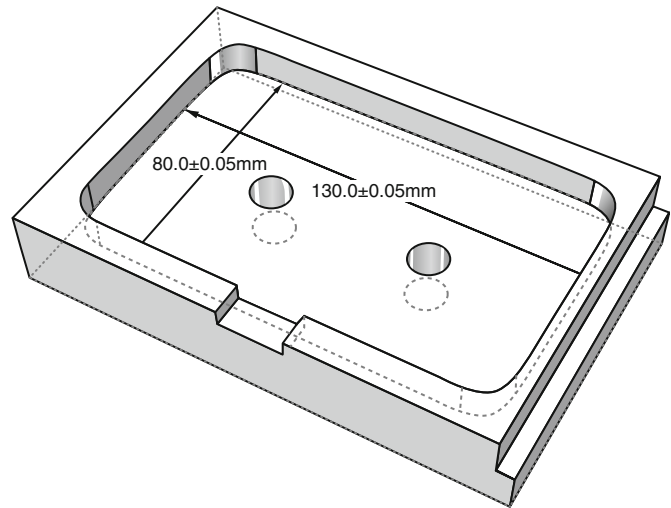
this activity manifests as identification of manufacturing features and associating the required tolerances with these features. For example, the features and the tolerances in the 3D drawing in Fig. 2 are identified as shown in Fig. 3.

Operation Selection and Sequencing

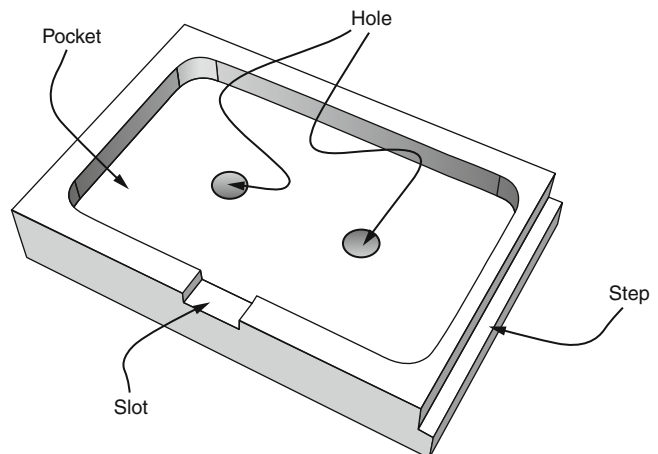
After the identification of features, it is necessary to determine the appropriate types of manufacturing operations and their sequence to create the features according to the required specifications. The operations required for producing a feature can vary depending on the desired accuracy and precision. For example, a simple drilling operation would suffice for

machining a hole with low tolerance and moderate surface roughness requirements whereas machining the same hole with finer surface finish and tighter tolerances shall require the use of drilling operation followed by a reaming operation. In most cases, there are several ways to produce a design. Constraints emerging from accessibility or setup requirements, or indeed limitations of resources, often necessitate certain features to be manufactured in certain orders. For example, in order to produce the part in Fig. 4, it is necessary to machine pocket 1 in order to access pocket 2 and consequently, machine pocket 2 has to be finished before pocket 3 can be machined.

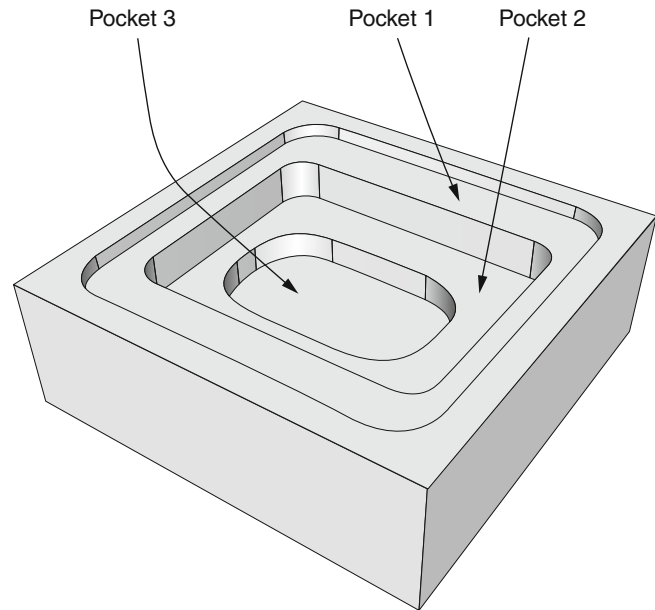
Computer-Aided Process Planning, Fig. 2 3D CAD drawing of a simple part



Computer-Aided Process Planning, Fig. 3 Manufacturing features identified on the component



Computer-Aided Process Planning, Fig. 4 A simple milled part with three pockets



In addition, the desired quantity of the product or the service will also affect the selection and sequencing of operations. For example, a sequence of operations that is optimal for machining a metal component on a 3-axis vertical machining center in a batch of 10 will not be optimal for producing the same component on a 4-axis horizontal machining center in batches of 1000. It is necessary to establish criteria for comparison of operation sequences; usually, these include the quality of the produced product and the efficiency with which it is produced.

Resource Selection

In conjunction with the selection of the manufacturing operations and their sequence, it is essential to select the appropriate resource required to produce the desired product. The nature of required resources varies widely depending on the nature of the product, the available technologies, the desired quantity, and so forth. Some of the resource selection activities that are often undertaken within the remit of process planning for manufacturing metal products are: selection of materials and workpieces; selection of machine tools; selection of cutting tools; and, selection of auxiliary devices.

Selection of Materials and Raw Workpiece In the manufacturing of products, the selection of the appropriate raw workpiece from which the component is made is an essential element of process planning. The selection of the workpiece comprises of determination of attributes such as shape, size, and material.

Selection of Machine Tools Machine tools are fundamental resources in manufacturing of products and it is therefore imperative to select the appropriate devices to meet product requirements. The selection of machine tools is generally influenced by workpiece-related factors, machine tool-related factors, and production-related factors. Workpiece-related factors such as the material or the size of the raw work piece have implications for the possibility of machining the components on a specific machine. The machine tool-related factors comprise of the technological, i.e., the capability of the machine to carry out the required types of operation (e.g., turning or grinding), tools that can be used on a machine and auxiliary devices (i.e., tool changing arms and loading and unloading robots and fixtures) that can be utilized together with the machine tool. Production-related factors are fundamentally related to the unit cost of production, the quality

of the produced components, and the lead time for the production.

Selection of Cutting Tools Machining is realized by controller motion of cutting tools in relation to the workpiece. An appropriate selection of cutting tools is therefore a major part of process planning. The tools are chosen with regard to the attributes of the workpiece and product features as well as to the machine tools and operations that have been selected for production.

Selection of Auxiliary Devices In addition to the machine tool and cutting tools, several auxiliary devices are often necessary to accomplish production goals. Work-holding devices such as jigs and fixtures, clamps and chucks, loading and unloading equipment are classified among these devices. Furthermore, inspection equipment such as on-machine probes and coordinate measuring machines (CMM) that are used to guarantee the dimensional accuracy of the produced parts are also categorized as auxiliary production equipment. In process planning, it is necessary to identify the auxiliary devices that are required to achieve the production goals and meet the quality requirements of the part.

Determination of Appropriate Operational Parameters

Once the production resources have been selected, it is necessary to select the appropriate values for controllable parameters in manufacturing operations. In product manufacturing scenarios, parameters such as cutting speed, feed, and depth of cut or width of cut need to be selected for each feature. In provision of services, parameters are more context sensitive. For example, in providing a helpdesk to technically support a software system, the number of personnel is a parameter that needs to be chosen. Various models are used for the selection of operational parameters including the minimum cost models that seek to minimize the overall resource cost of the operation, maximum production rate models that aim to realize the highest possible throughput, and lead time-oriented models that strive to lower the production's time to market.

Process Planning Application Domains

Process planning is required and applied to just about any manufacturing process or operation in many domains including metal removal, additive manufacturing (Jin et al. 2013), assembly, bulk and sheet metal forming, inspection, robot manipulation and processing tasks, etc.

Process Planning for Combined Processes

While process planning of single processes is a well-recognized problem, process planning for combination of processes whether simultaneous in the case of hybrid processes (Lauwers et al. 2014) or sequential in the case of additive/subtractive combinations (Nassehi et al. 2011) is still under research. There are many challenges due to the much larger solution space that results from combining processes, requiring changes, extensions, and enhancements of the traditional process planning methods. Iterative methods (Newman et al. 2015) and micro process planning for a limited subset of processes (Luo et al. 2013) have been investigated, but this is a beginning, and more challenges require further research.

Cross-References

- ▶ [Design Methodology](#)
- ▶ [Machine Tool](#)
- ▶ [Planning](#)

References

- Alting L, Zhang H (1989) Computer-aided process planning: the state-of-the-art survey. *Int J Prod Res* 27(4): 553–585
- Azab A, ElMaraghy H (2007a) Mathematical modeling for reconfigurable process planning. *CIRP Ann Manuf Technol* 56(1):467–472
- Azab A, ElMaraghy H (2007b) A novel QAP mathematical programming formulation for process planning in reconfigurable manufacturing. In: *Proceedings of the 4th international CIRP sponsored conference on digital enterprise technology (DET'07)*. Bath, pp 259–268
- ElMaraghy H (1993) Evolution and future perspectives of CAPP. *CIRP Ann Manuf Technol* 42(2):739–751

- ElMaraghy H (2007) Reconfigurable process plans for responsive manufacturing systems. In: Cunha PF, Maropoulos PG (eds) *Digital enterprise technology: perspectives & future challenges*, Springer, pp 35–44
- Jin GQ, Li WD, Gao L (2013) An adaptive process planning approach of rapid prototyping and manufacturing. *Robot Comput Integr Manuf* 29(1):23–28
- Lauwers B, Klocke F, Klink A, Tekkaya AE, Neugebauer R, McIntosh D (2014) Hybrid processes in manufacturing. *CIRP Ann Manuf Technol* 63(2):561–583
- Li X, Gao L, Shao X, Zhang C, Wang C (2010) Mathematical modeling and evolutionary algorithm-based approach for integrated process planning and scheduling. *Comput Oper Res* 37(4):656–667
- Luo X, Li Y, Frank MC (2013) A finishing cutter selection algorithm for additive/subtractive rapid pattern manufacturing. *Int J Adv Manuf Technol* 69: 2041–2053
- Marri H, Gunasekaran A, Grieve R (1998) Computer-aided process planning: a state of art. *Int J Adv Manuf Technol* 14(4):261–268
- Nassehi A, Newman ST, Allen RD (2009) The application of multi-agent systems for STEP-NC computer aided process planning of prismatic components. *Int J Mach Tools Manuf* 46(5):559–574
- Nassehi A, Newman ST, Dhokia V, Zhu Z, Asrai RI (2011) Using formal methods to model hybrid manufacturing processes. In: *Proceedings of the 4th international CIRP conference on changeable, agile, reconfigurable and virtual production (CARV2011)*, Montreal, Canada, pp 52–56
- Newman ST, Zhu Z, Dhokia V, Shokrani A (2015) Process planning for additive and subtractive manufacturing technologies. *CIRP Ann Manuf Technol* 64(1): 467–470
- Scallan P (2003) *Process planning: the design/manufacture interface*. Butterworth-Heinemann, Oxford
- Shen W, Wang L, Hao Q (2006) Agent-based distributed manufacturing process planning and scheduling: a state-of-the-art survey. *IEEE Trans Syst Man Cybern Part C Appl Rev* 36(4):563–577
- Xu X (2009) *Integrating advanced computer-aided design, manufacturing, and numerical control: principles and implementations*. Hershey Information Science Reference-Imprint of IGI Publishing
- Xu X, Wang L, Newman ST (2011) Computer-aided process planning—a critical review of recent developments and future trends. *Int J Comput Integr Manuf* 24(1): 1–31

Computer-Aided Tomography (CAT)

- [Computed Tomography](#)

Computer-Assisted Manufacturing

- [Computer-Aided Manufacturing](#)

Computer-Integrated Manufacturing

Gisela Lanza and Steven Peters

Institute of Production Science (wbk), Karlsruhe Institute of Technology (KIT), Karlsruhe, Germany

Synonyms

[CIM](#); [Computer-aided industry](#)

Definition

Computer-integrated manufacturing (CIM) is an approach to integrate production-related information and control entire production processes, automated lines, plants, and networks by using computers and a common database (please compare: Abramovici and Schulte 2004; Kalpakjian and Schmid 2006; Laplante 2005). Moreover, managerial philosophies improve organizational and personnel efficiency (Alavudeen and Venkateshwaran 2008).

Theory and Application

Introduction

Computer-integrated manufacturing (CIM) coexists of two components. Both hard- and software components of computer systems are considered to be indispensable for the enhancement of manufacturing (Kabitzsch et al. 2001). Thereby, each individual island of automation uses the full capabilities of digital computers while computer-integrated manufacturing comprises the integration and consolidation of these island solutions

(Alavudeen and Venkateshwaran 2008). Besides their overarching integration through software applications and the support of a common database, islands of automation also adopt hard- and software components themselves (Andersin 1993). The main methodologies of the CIM approach are computer-aided design (CAD) and computer-aided manufacturing (CAM), which are essential to reduce throughput times in the organization. Other considerable components of the CIM are computer-aided process planning (CAPP), computer numerical control machine tools (CNC), direct numerical control machine tools (DNC), flexible machining systems (FMS), computer-aided testing (CAT), automated storage and retrieval systems (ASRS), and automated guided vehicles (AGV). CAD and CAM are often considered to be one CAD/CAM integrating tool between design and manufacturing (Madsen et al. 2002).

History

Approached by the US Air Force, the Massachusetts Institute of Technology (MIT) is credited with pioneering the development of both CAD and CAM (Radhakrishnan and Subramanian 2007). However, the computer technology in the late 1940s and 1950s could not meet the requirements of sophisticated control systems, drives, and programming techniques. Over the next decades, major innovations in the computer industry evolved. In 1952, the MIT developed the numerical control (NC) (Reintjes 1991). By the mid-1960s, mainframe computers were used to operate these numerical control machines which were then called DNC (Reilly 2003). Subsequently, computer technology progressed and numerical control became soft wired. This then led to the development of CNC in the late 1960s.

Although the precise terminology was only introduced 8 years later, the concept of computer-integrated manufacturing was first introduced by Joseph Harrington in 1973. Harrington emphasized the importance of information integration in the fields of production. Furthermore, Harrington identified potential synergies between the so-called island solutions (CAD/CAM, DNC, CNC), which were applied

individually without any kind of integration through computer control or digital information. By tying these “pieces of puzzles” (Harrington 1973) together, Harrington’s goal was to utilize potential synergies as effectively and efficiently as possible. In the early 1980s, the idea of computer-integrated manufacturing was promoted by several machine tool manufacturers and the “Computer and Automated Systems Association” (CASA) of the “Society of Manufacturing Engineers” (SME) of the United States of America (http://202.114.32.200:8080/courseware/208405/20840511/context/Text/EC14_3.htm). At that time, the same association, the CASA/SME, also developed the so-called CIM wheel. Referring to the approach of computer-integrated manufacturing, the CIM wheel attempts to provide a holistic view of the company based on an integrated system architecture with a common database and information resource management and communication (Alavudeen and Venkateshwaran 2008). With the overall goal of a continuous computer-aided information processing based on a cross-functional database (Abramovici and Schulte 2004), corporate functions such as factory automation or production planning were included in the integrated system architecture of the CIM wheel. Today, the manufacturing enterprise wheel, which developed from the CIM wheel, also includes administrative tasks such as operational management, human resources, or finance (Alavudeen and Venkateshwaran 2008).

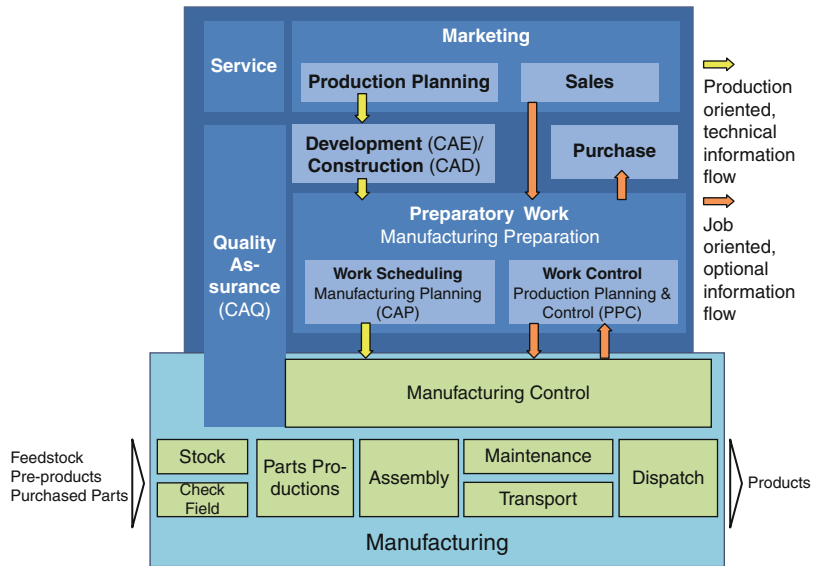
CIM Today

Modern computer-integrated manufacturing not only comprises the islands of automation but basically involves the integration of all activities of an organization (Alavudeen and Venkateshwaran 2008). To obtain the full potential of computer integration, all elements of manufacturing and all associated corporate support functions have to be integrated, permitting the data transfer throughout the enterprise (Radhakrishnan and Subramanian 2007; Gausemeier et al. 2009, compare Fig. 1).

Enterprise resource planning (ERP) systems support the processing of orders and all related business operation (Gausemeier 2008). ERP

Computer-Integrated Manufacturing,

Fig. 1 Overview of CIM components and workflow (Gausemeier et al. 2009)



systems are used to effectively plan and control all resources needed for the procurement, manufacturing, and the distribution of customer orders (Greef and Ghoshal 2004). Therefore, these software systems comprise all needed functions for purchasing, logistics, invoicing, and billing activities. They also include production planning and control (PPC) systems as well as automated order entry modules (Glenn 2008). Sometimes all divisions of a company are linked to an ERP system (Alavudeen and Venkateshwaran 2008). Software solutions are also used for analysis, simulation, and communication (Radhakrishnan and Subramanyan 2007). Intranet applications, for example, support internal communication, improve knowledge transfer throughout the organization, and thereby improve quality and avoid inefficient loops.

Solutions like computer-aided design and computer-aided manufacturing support an integrated design phase of new products, and product life cycle management enables a holistic perspective on data management during whole life cycles of products.

Hardware solutions in the context of CIM comprise CNC machines, automated conveyance, DNC/FMS systems, robotics, storage devices, sensors, inspection machines, condition monitoring, computerized work centers,

CAD/CAM modules, bar code readers, etc. (compare Radhakrishnan and Subramanyan 2007). Manufacturing-related functions are required to be changeable in order to react on a volatile environment. To ensure this goal, research has to be done on decentralized approaches as well as optimization, simulation, and scheduling activities. In recent future, a new dimension of CIM could be enabled by fast Internet connections available at any time all over the world and the so-called cyber-physical systems (http://www.acatech.de/fileadmin/user_upload/Baumstruktur_nach_Website/Acatech/root/de/Material_fuer_Sonderseiten/Industrie_4.0/Final_report_Industrie_4.0_accessible.pdf). CPS have the potential to enable a highly productive and flexible “smart factory” with socio-technical interaction and communication.

Cross-References

- ▶ [Changeable Manufacturing](#)
- ▶ [Computer Numerical Control](#)
- ▶ [Computer-Aided Design](#)
- ▶ [Computer-Aided Manufacturing](#)
- ▶ [Computer-Aided Process Planning](#)
- ▶ [ERP Enterprise Resource Planning](#)
- ▶ [Flexible Manufacturing System](#)
- ▶ [Optimization in Manufacturing](#)

- ▶ [Production Planning](#)
- ▶ [Scheduling](#)
- ▶ [Simulation of Manufacturing Systems](#)

References

- Abramovici M, Schulte S (2004) PLM, logische fortsetzung der PDM-ansätze oder neuauflage des CIM-debakels? [Is PLM a logical consequence of PDM-approaches or a remake of the CIM-debacle?] In: VDI-Berichte 1819, I²P 2004 (Tagungsband) – Integrierte Informationsverarbeitung in der Produktentstehung, Stuttgart, 12–13 Oct 2004 (in German)
- Alavudeen A, Venkateshwaran N (2008) Computer integrated manufacturing. Prentice Hall, Englewood Cliffs
- Andersin H (1993) The development of modern manufacturing automation. In: Pau L-F, Paul L, Willums J-O (eds) Manufacturing automation at the crossroads: standardization in CIM software. Ios Press, Amsterdam, pp 19–32 (Chap 3)
- Gausemeier J (2008) Computer integrated manufacturing, Enzyklopädie der Wirtschaftsinformatik [Encyclopedia of business informatics]. <http://www.enzyklopaedie-der-wirtschaftsinformatik.de/> (in German)
- Gausemeier J, Plass C, Wenzelmann C (2009) Zukunftsorientierte Unternehmensgestaltung: Strategien, Geschäftsprozesse und IT-systeme für die Produktion von morgen [Future-oriented shaping of enterprises: strategies, business processes and IT systems for tomorrow's production]. Carl Hanser Verlag, Munich, in German
- Glenn G (2008) Enterprise resource planning 100 success stories: 100 most asked questions—the missing ERP software, systems, solutions, applications and implementations guide. Lighting Source UK, London
- Greef G, Ghoshal R (2004) Practical E-manufacturing and supply chain management. Elsevier, Amsterdam
- Harrington J (1973) Computer integrated manufacturing. RE Krieger, Malabar
- Kabitzsch K, Kotte G, Vasyutynskyy V (2001) Classification method for fault diagnosis in networked CIM systems. In: 10th IFAC symposium on information control problems in manufacturing INCOM 2001, Vienna, Sep 2001
- Kalpakjian S, Schmid S (2006) Manufacturing engineering and technology, 5th edn. Prentice Hall, Englewood Cliffs
- Laplante P (2005) Comprehensive dictionary of electrical engineering, 2nd edn. CRC Press, Boca Raton
- Madsen DA, Folkestad J, Schertz KA, Shumaker TM, Stark C, Turpin JL (2002) Engineering drawing and design, 3rd edn. Delmar-Thomson Learning, Albany
- Radhakrishnan P, Subramanian S (2007) CAD/CAM/CIM, 3rd edn. New Age International, New Delhi
- Reilly ED (ed) (2003) Concise encyclopedia of computer science. Wiley, Hoboken
- Reintjes JF (1991) Numerical control: making a new technology. Oxford University Press, New York

Computerized Tomographic Imaging

- ▶ [Computed Tomography](#)

Computerized Tomography

- ▶ [Computed Tomography](#)

Computerized Transverse Axial Scanning

- ▶ [Computed Tomography](#)

Conceptual Design

Francois Christophe¹, Eric Coatanéa² and Alain Bernard³

¹Department of Computer Science, University of Helsinki, Helsinki, Finland

²Department of Mechanical Engineering and Industrial Systems, Tampere University of Technology, Tampere, Finland

³IRCCyN UMR CNRS 6597 – System Engineering – Products, Performances, Perceptions, Ecole Centrale de Nantes, Nantes, France

Synonyms

[Early design](#)

Definition

This is a combination of tasks starting with the product design definition and modeling by using precise and neutral concepts coming from needs or ideas. This is followed by the generation of design concepts taking the

different phases of the physical life cycle into account and ended by the evaluation of proposed design concepts. The analysis of the adequacy of the design concepts with the formalized needs ends these tasks. A design concept defines and describes the principles and engineering features of a system, machine, or component which is feasible and which has the potential to fulfill all the essential design requirements (Thompson 1999).

The definition selected here is the definition commonly accepted in engineering design and is different from the vision of industrial designers. The early design phase is the first phase of a design process integrating other stages such as embodiment design, detail design, production, integration, test and validation (Pahl and Beitz 2003).

Presentation of the Activity

Conceptual design is the initial activity of the engineering design process according to the traditional decomposition found in several engineering design textbooks (Pahl and Beitz 2003).

The conceptual design activity encompasses activities such as the refinement of the design problem, the evaluation and comparison, and selection of the concepts created to answer to the design problem.

Conceptual design as a process contains the following subprocesses:

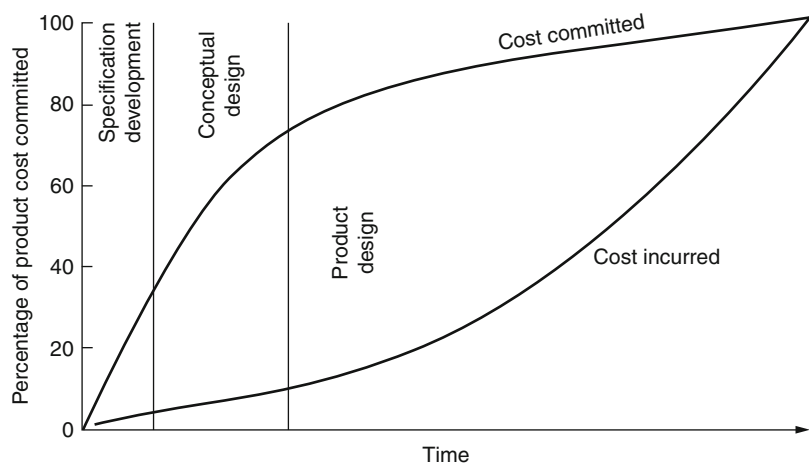
- Requirements engineering (environment and problem analysis)
- Generation of concepts (synthesis)
- Evaluation and Comparison of concepts (adequacy and performance analysis)

This activity is considered to be of the highest importance in engineering design as the decisions made during conceptual design constrain the entire engineering design process. Therefore, the above-described process should not be seen as linear, but as a complex activity involving several contributors from different disciplines. Cost being only one of the performance variables of the product being conceived, Fig. 1 presents the importance of conceptual design within the entire design activity: 75% of the manufacturing cost is committed when final conceptual decisions are made.

According to the recursive logic of design (Zeng and Yao 2009), at most stages of (conceptual) design, an evaluation operation will be determined only after a (partial) design solution is generated, which will in turn trigger a new synthesis operation. As a result, design is a non-linear process where a small change in the initial design problem may give rise to significant differences in the final design solutions, among which creative design solutions may exist. According to the recursive vision of the design process, both functions and structure are participating in the

Conceptual Design,

Fig. 1 Manufacturing cost commitment during design (Hsu and Woon 1998)



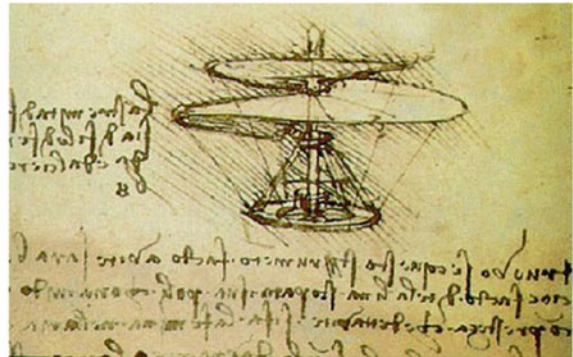
design process and cannot be separated; in the same way, it is very difficult to see what is coming first, the function or the structure, because both of these concepts require the presence of the other in order to be thought.

Theory and Application

History

The design activity is deeply embedded in the human nature. Design activity has been at the center of the interaction of human with its environment since the beginning. Famous examples of concrete design artifacts or design concepts can be traced already in the Greek texts with the Eolipyle (pneumatic device) of Heron of Alexandria (first Century AC) (see Fig. 2 left), as well as in the concepts of “helicopter” and “plane” from Leonardo da Vinci (1452–1519) (see Fig. 2 right). A step forward for the design activity was

the pioneering attempt to formalize the process made by Franz Reuleaux (1829–1905), which strongly influenced the American Society of Mechanical Engineers as well as the German engineering community. Since the 1950s, design methods’ development has emerged as an active field of research and, in return, has also influenced practitioners and companies. The impulse for this change of paradigm related to design activity is due to a converging movement driven both by an initial phase of globalization of the economic system which has forced companies developing products integrating more differentiation and innovation as well as a consequence of the development of the first computers that have initiated the Cybernetics science (Herbert Wiener). Following this latest movement, it has appeared necessary to better understand the human process of designing. Herbert Simon established in 1969 the foundations for a science of design (Simon 1969). This attempt to



Conceptual Design, Fig. 2 Eolipyle (pneumatic device) from Heron of Alexandria and concepts of helicopter and plane by Leonardo Da Vinci

understand the foundations of the design activity have still to be associated was a ground work for analytic, partially formalizable, and teachable methods about the design process.

Later, methodologies for applying systematically a clearly defined process to design problems appeared during the 1980s (Hubka 1982; Pahl and Beitz 2003; French 1985; Pugh 1991). These systematic approaches form a consensus on the concepts used in different parts of the design process; even if the terms used by each author may differ, their meaning remains rather similar, i.e., analysis of the needs, design specification, and design requirements. Such methodology enabled the appearance of computer-aided design applications.

Nowadays, due to the application of design paradigms coming from computer science and information technology (e.g., Object-Oriented Modeling, Agent-based design), the conceptual design of technical systems can be achieved by considering mostly interactions between the system and its environment (Zeng 2004; Meinadier 1997). This paradigm is relevant to model-driven engineering and is probably going to enable a better use of computers at the stage of conceptual design.

Process Clarification

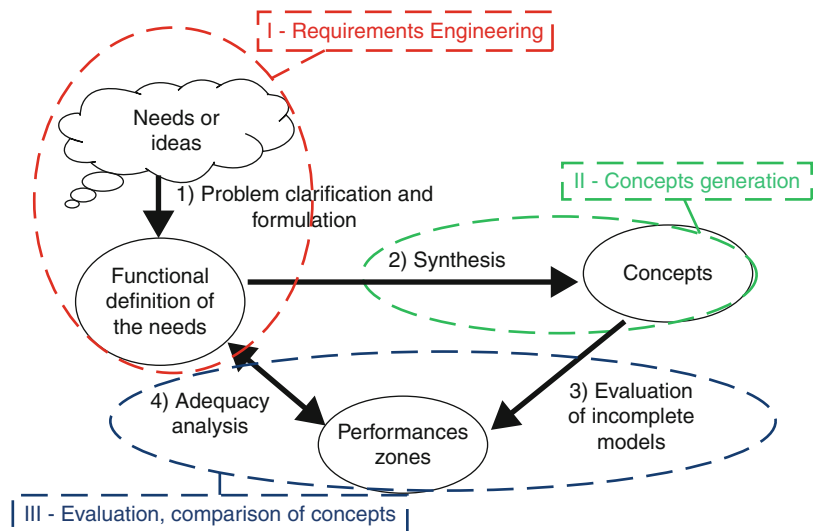
As presented in the definition, conceptual design is mainly composed of three subprocesses: requirements engineering, concepts generation, and evaluation and comparison of concepts. Figure 3 presents these subprocesses and their interactions. It is important to note that this representation does not account for the precedence of processes as, in fact, these subprocesses can be operated concurrently and the conceptual design process itself can be regarded as a long-term iterative process. This paragraph presents these subprocesses of conceptual design in more detail.

Requirements Engineering and Design Specification

The discipline of requirements engineering has recently emerged from Systems and Software Engineering (Hull et al. 2011). This term is used to reconcile the different terminologies from the literature. Requirements engineering contains three major disciplines, namely: requirements definition, requirements management, and acceptance testing. Regarding conceptual design, one focuses mostly on the requirements definition part. However, issues, such as change management, traceability, and status tracking, which

Conceptual Design,

Fig. 3 The conceptual design process (Adapted from Coatanéa (2005) and Yannou (2000))



belong to requirement management, remain of great importance in order to keep track of the history of the product's different versions.

Requirements definition is usually decomposed into: elicitation, analysis, representation (i.e., modeling), and validation.

Generation of Concepts

Functional Analysis A functional analysis is usually conducted in the beginning of the concept generation. This analysis works as the interface between requirements and their realization. It used to focus only on the part of requirements expressing what the final product should do. The concept of function is often represented as a black box containing a verb of action, inputs, and outputs. Such analysis consists of an abstraction layer in order to consider mainly the use of a product and what the product should do in order to be functioning. This abstraction avoids designers from considering how they will realize the product too early during the design process and, therefore, helps them to explore more widely the possible solutions for a product, the design space.

Functional analysis is proposed in different methodologies such as the APTE method (le Méthode APTE[®]: APplication des Techniques d'Enterprise(fr.) or Application of Corporation Methods (en.), APTE 2013), Value Analysis, or Pahl and Beitz's Systematic Design. Each of these methodologies provides tools and representations of what the product does in interaction with its environment. These methodologies are similar and all pursue the same goal of exploring the design space. Similarly, methodologies proposing brainstorm sessions and use cases address also the analysis of functionalities of a product. Nevertheless, methodologies issued from Value Analysis (APTE 2013) propose a more normative and systematic approach toward the generation of concepts.

The deliverables of a functional analysis should contain graphical descriptions or models of the functional architecture of the product, and a representation of the flow of matter, energy, or information between the different technical

functions composing the product (Block-Flow diagram). A functional architecture is usually in the form of a hierarchical tree showing how the service functions of a product were broken down into technical functions necessary to fulfill such service. A Block-Flow diagram usually represents functions considered at the same level of the architecture and focuses on the interactions and exchanges between these parts.

Analysis of Contradictions G.S. Altshuller (1984) distinguished between the following three types of contradictions: administrative contradictions, technical contradictions, and physical contradictions. The two last types are of interest in this definition.

Technical contradictions: An action is simultaneously useful and harmful or it causes Useful Function(s) and Harmful Function(s).

Physical contradictions: The physical contradiction implies inconsistent requirements to a physical condition of the same element of a Technical System (TS) or operation of a Technological Process (TP). For example, we want that an insulator in semiconductor chips has low dielectric constant k in order to reduce parasitic capacities and we want that insulator in semiconductor chips has high dielectric constant k in order to store information better.

Physical contradictions as well as technical contradictions are usually crystallized during the problem analysis. Sometimes technical contradictions can be obtained by analysis techniques such as in the Root Cause Analysis framework or Goldratt's Theory of Constraints (Wilson et al. 1993).

Theory of Inventive Problem Solving: TRIZ (Russian Acronym for TIPS) Synthesis in Conceptual design is related to creativity. Probably, the most relevant work in terms of creativity and inventive design was proposed by Altshuller with TRIZ (Altshuller 1984). The two main ideas of TRIZ are the following:

- Many problems faced by engineers contain elements that have already been solved in a different context and industrial field.

- Patterns of technological change can be predicted and applied to any situation to determine the successful next steps in technological change.

TRIZ is the theory of innovation applied in a systematic manner. The main idea behind this theory is that inventions could be organized and generalized by function. Therefore, generalizing the design problem in a functional manner could enable finding the essential physical principles which will solve the problem. TRIZ provides principles and rules to find general solutions to a specific problem. Nevertheless, this process of specialization is strongly context dependent, and it is not possible to automate it. Therefore, scientists have developed many other conceptual design models adapted to a specific domain of product development, e.g., electronics, mechanics.

Evaluation and Comparison of Concepts

In this phase of conceptual design, mainly three concepts are considered of importance: evaluation, verification and validation.

Evaluation The evaluation of concepts corresponds to grading concepts according to performance objectives established during the Requirements Engineering process. This phase has many commonalities with an optimization problem. Indeed, as the objectives defined in requirements might be correlated and contradictory, evaluating globally the fitness of a concept to a design problem is harder than summing up the scores of this concept on each of the required objectives.

Similarly, comparing multiple concepts according to requirements is a multi-criteria and multi-objective optimization problem because the stocks and flows of energy, material and information might be completely different and of various orders of magnitude from one concept to another (Coatanéa et al. 2008).

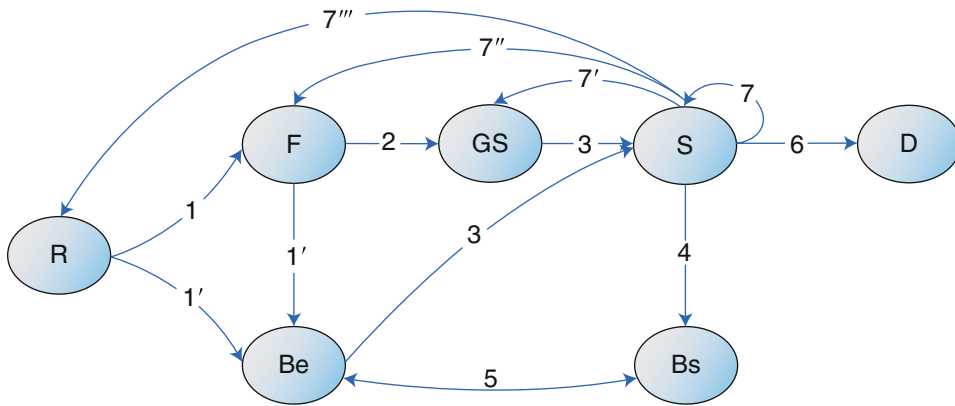
Verification Verification corresponds to the formal examination of the possible states of a concept of solution. This phase is used to verify that

no situation would end up in a blockage of the system resulting in its malfunctioning. This phase is particularly difficult to approach during conceptual design as descriptions of a concept are still fuzzy due to few known physical parameters and the orders of magnitude of their values. However, there are recent attempts to formalize the behavior of concepts with, for example, state representation (Blondet et al. 2015) or with the representation of physical parameters interactions in the form of a directed graph (Coatanéa et al. 2014).

Validation This phase corresponds to the final stage in the process evaluation with a presentation of the selected concept to customers and users. Such validation usually deals with early simulations and demonstration of functioning of this concept. The objective at that stage is to acquire acceptance of this prototype by users and customers. Therefore, it inherently includes aspects related with capturing users' emotions and cultural reactions to the design.

Knowledge Representation of Conceptual Design

This paragraph presents the knowledge required in conceptual design for building computer applications which support that activity. Even though other representations of conceptual design or the design activity in general exist, for instance, the C-K or Concept-Knowledge theory (Hatchuel and Weil 2009), the model presented in Fig. 4 uses the most commonly used concepts during the conceptual design activity, such as requirements, function, behavior, and structure (Christophe et al. 2010). This model was adapted from Gero's initial FBS or Function-Behavior-Structure model (Gero 1990) and follows a long tradition of models for the knowledge representation in design (Umeda and Tomiyama 1997; Labrousse and Bernard 2008). Table 1 presents a view of the interactions between the concepts of requirement, function, behaviors (expected or structural) generic structure, structure, and detail design.



Conceptual Design, Fig. 4 The RFBS model of conceptual design (Christophe et al. 2010)

Conceptual Design, Table 1 Processes of conceptual design as flows between R, F, B, and S (Christophe et al. 2010)

Representation stages	Processes of conceptual design	Reformulation processes
R is the set of constraints and performance criteria required by the system	1. Requirement analysis: transforms the design problem, expressed in requirements (R), into functions (F) that the system should provide	7'''. Reformulation type 4: addresses changes in the design state space in terms of requirement variables or their ranges of values (this reformulation involves discussion with the client to find an agreement)
F represents a set of functions, the necessary knowledge in order to be able to explain what the system should do according to requirements, thus F is derived from R	1'. Problem formulation: (Gero's process 1) transforms the design problem, expressed in function (F) and requirements (R), into behavior (Be) that is expected to enable this function to work with the performance criteria set by the requirements	7''. Reformulation type 3: (Gero's process 8) addresses changes in the design state space in terms of function variables or their ranges of values (this reformulation induces automatic changes in the expected behavior)
Be is the expected behavior of the system, specifically the set of variables showing how the system should work. Be is set according to requirements and functions	2. Pre-synthesis: transforms the functional architecture of the system (F) into a generic structure (GS) using abstract organs	
GS is the representation of generic structure, specifically abstract classes encapsulating function and their intrinsic attributes. GS is derived from F	3. Synthesis: (Gero's process 2) specializes GS according to the expected behavior (Be) into a solution structure (S) that is intended to exhibit this desired behavior	7'. Reformulation type 2: addresses changes in the design state space in terms of abstract organs or generic structure variables or their ranges of values
S is the set of classes representing the physical structure of the system, S specializes GS according to Be	4. Analysis: (Gero's process 3) derives the "actual" behavior (Bs) from the synthesized structure (S)	7. Reformulation type 1: (Gero's process 6) addresses changes in the design state space in terms of structure variables or their ranges of values
Bs is the set of variables enabling the representation of the effective behavior of the system, e.g., its "actual" behavior	5. Evaluation: (Gero's process 4) compares the behavior derived from structure (Bs) with the expected behavior to prepare the decision if the design solution is to be accepted	
D represents the transfer of the models to the next stage of design: detailed design	6. Detailing: prepares all drawn models for the detailed design phase (from work classes into technology involvement)	

Cross-References

- ▶ [Engineering Design](#)
- ▶ [Product Development](#)

References

- Altshuller G (1984) Creativity as an exact science: the theory of the solution of inventive problems (trans: Williams A). Gordon & Breach Science, Amsterdam
- APTE (2013) <http://www.methode-apte.com>. Accessed 26 June 2013
- Blondet G, Le Duigou J, Boudaud N, Belkadi F, Bernard A (2015) Simulation data management for design of experiments: concepts and specifications, Proceedings of CAD'15, pp 291–296. <https://doi.org/10.14733/cadconfp.2015.291-296>
- Christophe F, Bernard A, Coatanéa E (2010) RFBS: a model for knowledge representation of conceptual design. CIRP Ann Manuf Technol 59(1):155–158. <https://doi.org/10.1016/j.cirp.2010.03.105>
- Coatanéa E (2005) Conceptual modelling of life cycle design: a modelling and evaluation method based on analogies and dimensionless numbers. Doctoral Dissertation, Helsinki University of Technology
- Coatanéa E, Alizon F, Christophe F, Yannou B (2008) Selecting technology alternatives for product families through technological coverage and functional verification, ASME 2008 IDETC, New York, 3–6 Aug
- Coatanéa E, Nonsiri S, Christophe F, Mokammel F (2014) Graph based representation and analyses for conceptual stages, 2014 IDETC, Buffalo, 17–20 Aug
- French MJ (1985) Conceptual design for engineers, 2nd edn. The Design Council, London
- Gero JS (1990) Design prototypes: a knowledge representation schema for design. AI Mag 11(4):26–36
- Hatchuel A, Weil B (2009) C-K design theory: an advanced formulation. Armand Res Eng Des 19:181–192
- Hsu W, Woon IMY (1998) Current research in the conceptual design of mechanical products. Comput Aided Des 30(5):377–389
- Hubka V (1982) Principles of engineering design, 1st English edn (trans and ed: Eder WE). Butterworth Scientific Press, London
- Hull E, Jackson K, Dick J (2011) Requirements engineering, 2nd edn. Springer, London
- Labrousse M, Bernard A (2008) FBS-PPRE, an enterprise knowledge lifecycle model. In: Bernard A, Tichkiewetich S (eds) Methods and tools for effective knowledge life-cycle management. Springer, Berlin, pp 285–305
- Meinadier J-P (1997) L'intégration de systèmes [Systems integration]. Presses Universitaires de France, Paris (in French)
- Pahl G, Beitz W (2003) Engineering design: a systematic approach 2nd edn (trans and ed: Wallace K). Springer, London
- Pugh S (1991) Total design: integrated methods for successful product engineering. Addison-Wesley, Wokingham
- Simon HA (1969) The sciences of the artificial. MIT Press, Cambridge
- Thompson G (1999) Improving maintainability and reliability through design. Professional Engineering Publishing, London
- Umeda Y, Tomiyama T (1997) Functional reasoning in design, AI in design. IEEE Expert 12(2):42–48
- Wilson PF, Dell ID, Anderson GF (1993) Root cause analysis: a tool for total quality management. ASQC Quality Press, Milwaukee
- Yannou B (2000) Préconception de Produits [Product preliminary design]. Memoire d'habilitation a diriger des recherches. Discipline: mécanique. Institut Nationale Polytechnique de Grenoble (INPG) (in French)
- Zeng Y (2004) Environment-based formulation of design problem. Trans SDPS J Integr Des Process Sci 8(4): 45–63
- Zeng Y, Yao S (2009) Understanding design activities through computer simulation. Adv Eng Inform 23(3):294–308

Condition Monitoring

- ▶ [Grinding Monitoring](#)

Constraints

- ▶ [Requirement Specification](#)

Construct

- ▶ [Engineering Design](#)

Construction

- ▶ [Assembly](#)

Control

Burak Sencer
College of Engineering, Oregon State University,
Corvallis, OR, USA

Synonyms

Control system; Drive control; Sliding mode control

Definition

This essay presents feed drive control systems used in modern CNC machine tools. Considering the rigid body motion of the feed drive, widely used control algorithms such as P-PI and PID control are being introduced. At last, the sliding mode control algorithm is presented, and its performance against the conventional PID control is shown.

Theory

In general context, a control system is a device to manage, command, or regulate the behavior of another device or a system. In CNC machine tool systems, the objective of the control system is to

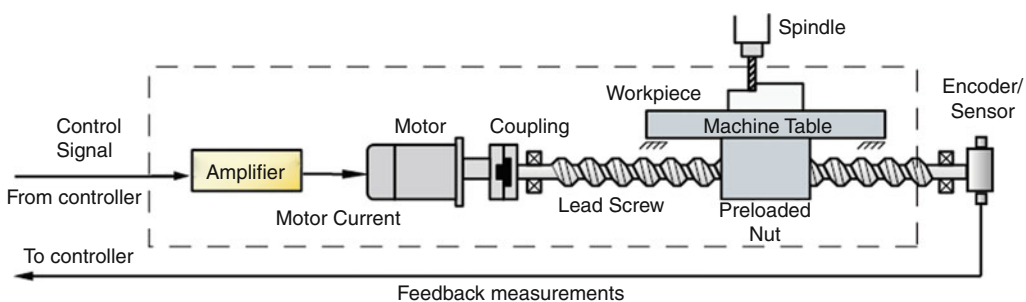
regulate the actual position of the feed drive to follow the reference motion trajectory programmed by the user. Hence, the control law on a machine tool tries to minimize deviation of the drive position $x_m(t)$ from the commanded position $x_r(t)$.

$$e(t) = x_r(t) - x_m(t) \quad (1)$$

Dynamic Model of Feed Drive

Considering a widely used ball screw feed drive design, the system consists of a current amplifier, servomotor, lead screw coupling mechanism, ball screw with preloaded nut, table carrying workpiece, guide friction, and feedback sensors (Erkorkmaz and Altintas 2001; Altintas et al. 2011; Frey et al. 2012). Figure 1 shows the overall structure.

Focusing only on the rigid body motion of the mechanism (Altintas et al. 2011; Sencer and Altintas 2011), the model parameters can be identified as J [kgm^2] as the total inertia and B [kgm^2/s] as the viscous friction. Motor and the amplifier are assumed to operate within their linear range, where u [V] is the control voltage command to the current amplifier modeled by a gain factor, K_a [A/V], and the corresponding torque delivered to the drive is obtained by multiplying the current with the motor torque constant K_t [A/V], and r_g [mm/rad] is transmission gain of the ball screw.



Control, Fig. 1 Feed drive mechanism with a lead screw drive

Closed-Loop Feed Drive Dynamics Model

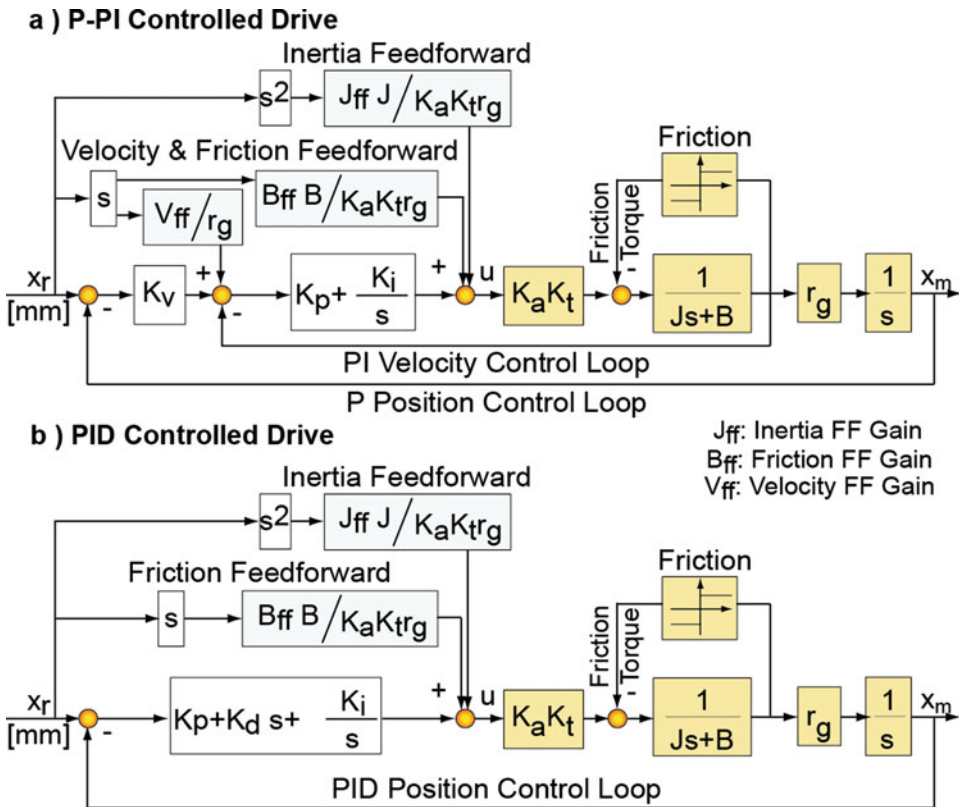
Commonly Used Control Algorithms

Utilizing the rigid body dynamics of the feed drive system, the most commonly used position control structures in CNC drive systems are shown in Fig. 2. In the P-PI controller scheme (Fig. 2a), the velocity loop is closed using proportional-integral (PI) control by adjusting the gains K_p , K_i , and the position loop is closed by a proportional controller, K_r . The well-known PID (Szabat and Orłowska-Kowalska 2007; Franklin et al. 2002) controller scheme is shown in Fig. 2b. The position loop is directly closed with the gains K_p , K_i , K_d . In both controller schemes, feed-forward compensation of axis dynamics is applied to widen the servo tracking bandwidth

where V_{ff} , B_{ff} , J_{ff} are the respective gains. Hence, the closed-loop transfer function between the commanded and the actual axis position can be presented in the general form of:

$$x(s) = \underbrace{\frac{b_0 s^2 + b_1 s + b_2 + a_3 \frac{1}{s}}{s^2 + a_1 s + a_2 + a_3 \frac{1}{s}}}_{G_{\text{track}}(s)} \cdot x_r(s) - \underbrace{\frac{d(s)}{s^2 + a_1 s + a_2 + a_3 \frac{1}{s}}}_{G_{\text{dist}}(s)} \quad (2)$$

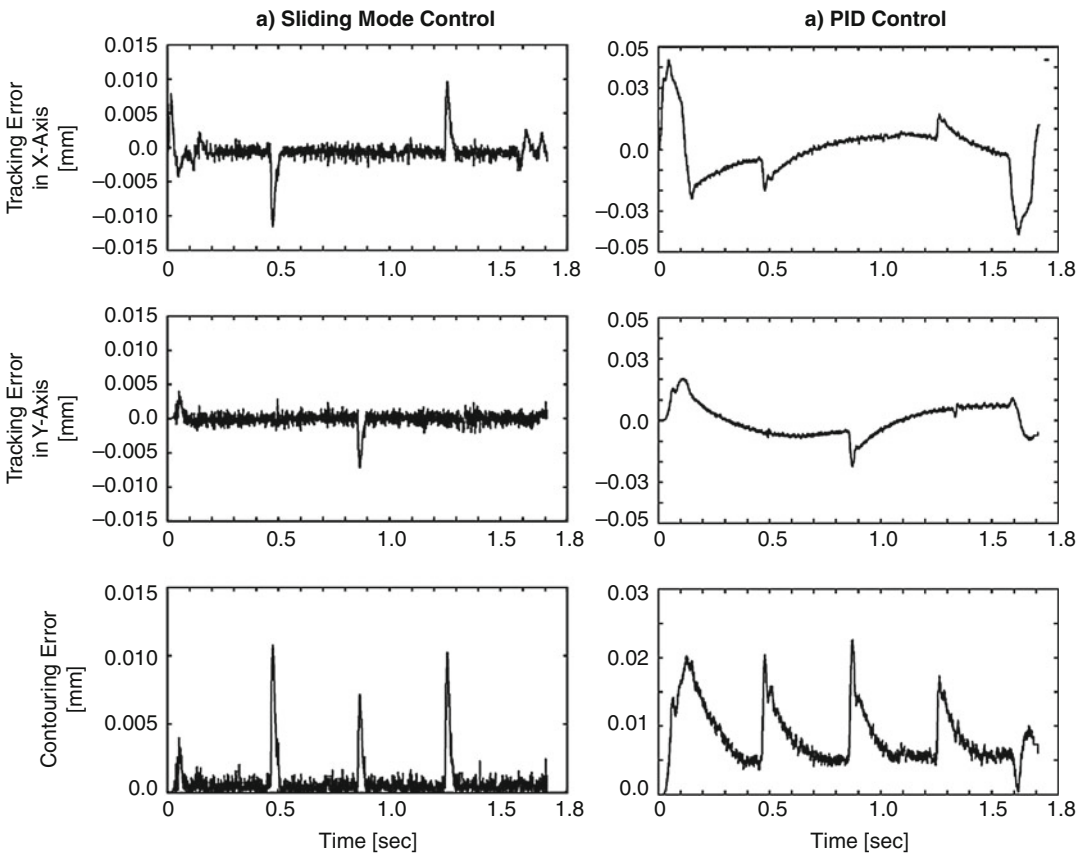
where $G_{\text{track}}(s)$ and $G_{\text{dist}}(s)$ are the equivalent tracking and disturbance transfer functions



Control, Fig. 2 Closed-loop feed drive block diagram

Control, Table 1 Summary of control parameters for PID and SMC

PID control		X-axis	Y-axis
Proportional gain, K_p	[Volt/mm]	70	70
Integral gain, K_i	[Volt/(mm · s)]	800	800
Differentiation gain, K_d	[Volt/(mm/s)]	0.30	0.30
Sliding mode control (SMC)		X-axis	Y-axis
Sliding surface bandwidth, λ	[rad/s]	200	200
Feedback gain, K_s	[Volt/(mm/s)]	0.30	0.30
Disturbance adaptation gain, ρ	[Volt/mm]	30	30



Control, Fig. 3 Circle test performance comparison of PID and SMC control

(Erkorkmaz and Altintas 2001; Sencer and Altintas 2011). $d(s)$ is the external disturbances. Including the feed-forward terms, the closed-loop drive model parameters presented in Eq. 2 can be derived for the P-PI structure as:

$$\left. \begin{aligned}
 a_1 &= \frac{B + K_a K_p K_t}{J}, a_2 = \frac{K_a K_p K_v K_t r_g + K_a K_i K_t}{J}, \\
 a_3 &= \frac{K_a K_i K_t K_v r_g}{J}, b_0 = I_{ff}, b_1 = \frac{B B_{ff} + K_a K_p K_t V_{ff}}{J}, \\
 b_2 &= \frac{K_a K_p K_v K_t r_g + K_a K_i K_t V_{ff}}{J}, d = \frac{d_c r_g}{J}
 \end{aligned} \right\} \quad (3)$$

Sliding Mode Control Algorithm

In contrast to the conventionally used P-PI and PID control algorithms, a more robust sliding mode control algorithm has been introduced to improve the tracking performance of the drives (Altintas et al. 2000; Kamalzadeh and Erkorkmaz 2007). The control law of rigid body-based sliding mode controller (SMC) for high-speed feed drives is given as follows (Altintas et al. 2000):

$$u_c^{\text{SMC}}(k) = J_e \cdot [\lambda \cdot (\dot{x}_r(k) - \dot{x}_m(k)) + \ddot{x}_r(k)] + B_e \cdot \dot{x}_m(k) + K_S \cdot S(k) + \hat{d}(k) \quad (4)$$

where

$$\begin{cases} S(k) = \lambda \cdot [x_r(k) - x_m(k)] + [\dot{x}_r(k) - \dot{x}_m(k)] \\ \hat{d}(k) \approx \rho \cdot \left\{ \lambda \cdot \left[\frac{T_s \cdot z}{z-1} \cdot x_r(k) - \frac{T_s \cdot z}{z-1} \cdot x_m(k) \right] + [x_r(k) - x_m(k)] \right\} \\ J_e = \frac{J}{K_a \cdot K_t \cdot r_g}; \quad \& \quad B_e = \frac{B}{K_a \cdot K_t \cdot r_g}; \end{cases} \quad (5)$$

S is a sliding surface function and \hat{d} is the axis disturbance estimated using simple observer for adaptation. The control parameters that need to be tuned are sliding surface bandwidth λ [rad/s], feedback gain K_S [Volt/(mm/s)], and disturbance adaptation gain ρ [Volt/mm]. λ is assumed to be fixed and it is determined according to the achievable bandwidth of the drive, and the two control parameters (K_S and ρ) are considered in the auto-tuning of SMC.

Standard two-dimensional circular test is used to compare the contouring performance of both controllers. The circle is traveled at a feed rate of 200 [mm/s], and the control gains are given in Table 1 (Yeung et al. 2006).

The experimental results are presented in Fig. 3. It clearly indicates that a well-tuned sliding mode controller (SMC) gives significantly less contouring and tracking errors as compared to a standard PID controller.

References

- Altintas Y, Erkorkmaz K, Zhu W-H (2000) Sliding mode controller design for high speed drives. *Ann CIRP* 49(1):265–270
- Altintas Y, Verl A, Brecher C, Uriarte L, Pritschow G (2011) Machine tool feed drives. *CIRP Ann Manuf Technol* 60(2):779–796
- Erkorkmaz K, Altintas Y (2001) High speed CNC system design: Part II – modeling and identification of feed drives. *Int J Mach Tools Manuf* 41(10):1487–1509
- Franklin GF et al (2002) Feedback control of dynamic systems, 4th edn. Prentice Hall, Upper Saddle River. ISBN 0-13-032393-4
- Frey S, Dadalau A, Verl A (2012) Expedient modeling of ball screw feed drives. *Prod Eng* 6(2):205–211
- Kamalzadeh A, Erkorkmaz K (2007) Accurate tracking controller design for high-speed drives. *Int J Mach Tools Manuf* 47(9):1393–1400
- Sencer B, Altintas Y (2011) Identification of 5-axis machine tools feed drive systems for contouring simulation. *Int J Autom Technol* 5(3):377–385
- Szabat K, Orłowska-Kowalska T (2007) Vibration suppression in a two-mass drive system using PI speed controller and additional feedbacks – comparative study. *IEEE Trans Ind Electron* 54(2):1193–1206
- Yeung C-H, Altintas Y, Erkorkmaz K (2006) Virtual CNC system – Part I: system architecture. *Int J Mach Tools Manuf* 46(10):1107–1123

Control System

- ▶ Control

Coolant

- ▶ Cutting Fluid

Cooling Lubricants

- ▶ Grinding Fluids

Cooperative Engineering

Jan-Fabian Meis

Verein der Freunde und Förderer des Instituts für Werkzeugmaschinen und Betriebswissenschaften der TU München (iwb e.V.), Garching, Germany

Synonyms

[Integrated product development](#); [Simultaneous engineering](#)

Definition

Cooperative engineering describes an approach which aims to develop products and support production structures and processes within disciplines parallel and with strong interaction between all stakeholders.

Theory and Application

Overview

Sequential development of products within specific areas as well as insufficient communication between departments combined with increased product complexity has led to an increased time-to-market. Simultaneous engineering and concurrent engineering have emerged as development concepts in the early 1960s (Lawson and Karandikar 1994; Kusiak 1992). The benefit of strong integration of all stakeholders involved in product development process as well as the parallelization of activities has promised significant improvements in development time and development cost. Primary approach is the overlap and parallelization of activities which traditionally were performed in sequential order. Additionally, all elements of the product life cycle from development to disposal are regarded during early design stages.

While approaches differ in specific details, the main concept focusses on enabling the development of structures and processes based

on preliminary data, simulation, and prototypes. Even though all disciplines of a company can be involved, most applications focus on integrating production development with the product development process. Strong emphasis is laid on integrating the customer expectations along the complete development process (Pokojski et al. 2010).

Simultaneous Engineering Versus Concurrent Engineering Versus Integrated Product Development

Specific concepts for cooperative engineering have evolved during the last decades. Simultaneous engineering, concurrent engineering, as well as integrated product development are most commonly used (Ehrlenspiel and Meerkamm 2013). While early promoters of the concepts held fierce arguments of their approach over the other, contemporary understanding accepts the approaches as synonyms being summarized in the category of cooperative engineering (CE).

Collaboration engineering is the research discipline which evaluates principles of collaboration and design processes and organizations to foster collaboration. Computer-based collaboration work as a focus area addresses specifically how cooperation in engineering can be enhanced through information technology. Recent literature is ambiguous concerning the terminology. While some authors regard collaboration engineering as the summarizing term for the principles of cooperative engineering, others regard it as the underlying research area.

Goals of Cooperative Engineering

Initially SE was described as an organizational strategy which focuses on the integration of all development and production departments as well as the customer. Based on parallelized planning of products and production processes, key elements of product design can be identified earlier in the development process. Shorter design iterations based on early feedback from all involved stakeholders lead to increased product quality and reduced development times and costs as the

primary results of successful CE implementations. Two main changes can be identified from traditional, sequential approaches.

Parallelization of Processes

Development processes of the different stakeholder are parallelized. This approach focusses on starting processes earlier based on preliminary data. Production departments may start production development based on rough concept decisions and increase the level of planning as product development proceeds. This approach focusses on early information transfer from development departments toward other stakeholders (Backhouse and Brookes 1996).

Increased Communication

Development activities of all stakeholders are synchronized, and results are discussed in cross-functional teams. This approach focusses on creating shorter feedback loops between development processes of different stakeholders. Concepts for parts, for example, are immediately evaluated with regard to their production process, and feedback is given toward the development process. This approach concentrates on the information transfer between stakeholders and toward the development process.

CE employs both approaches to parallelization as well as increased communication (Ehrlenspiel and Meerkmann 2013; Loureiro and Curran 2007), to improve the development process. This leads to longer concept phases compared to conventional, sequential approaches but to a shorter overall development time. To realize the potentials of CE, two main approaches must be taken:

1. Reduction of total production costs in early stages
2. Avoidance of costly changes in late stages

Elements of Cooperative Engineering

Cross-Functional Teams

Cross-functional teams (CFT) integrate experts from different disciplines like product development, cost controlling, purchasing, and

production development. Each team takes a holistic approach for a certain product function or component including all aspects from design to production.

Interdisciplinary work relies heavily on supporting infrastructure like collaboration and simulation software. Successful implementations do not only introduce CFT as organizational units but also physically locate team members outside their original departments.

Incremental Information Sharing

Product development is accelerated by sharing incomplete and preliminary information with involved team members. Thereby, process steps which were conducted in sequential order may be started earlier leading to the desired decrease in the time-to-market. Calculations and simulations are of significant importance, and successful implementations of CE focus largely on support through information technology.

Two aspects of information can be distinguished in the context of CE. Incremental sharing involves the early transfer of fixed and validated information in small packages. Technical specifications for a product may be transferred to manufacturing departments for each part individually as soon as they are defined. This transfer principle poses additional requirements on the organization as numerous interactions between departments have to be managed as opposed to few design transfer events. The second aspect involves exchange of preliminary information which is not fully confirmed at the time of transfer. Results of a simulation are transferred to other departments even though physical evaluation of a prototype has not been fully performed. This aspect requires precise information and requirement tracking throughout the organization. Transparency concerning the state of each information artefact has to be ensured, to allow for adequate decision-making processes for each recipient.

Increased product complexity requires approaches as modularization and systems engineering to reduce the impact of insufficient or false information on parallel processes which are based on incremental information (Loureiro and Curran 2007).

Integrated Project Management

CE requires all projects along the development process to be managed simultaneously. While central project management functions are required for a successful CE implementation, project management has to be performed by cross-functional teams and other involved units. This requires appropriate training for all employees involved as well as clearly defined project management methods (Sohlenius 1992).

Concurrent Product Realization

Product development tasks are divided into sub-systems and components which can be developed and tested and to an increased extent be produced independently of the main system. Especially the later stages of the development process including production development are special to CE activities. This enables strong parallelization of the tasks leading to significantly lower total development times (Ehrlenspiel and Meerkamm 2013).

Methods of Cooperative Engineering

Despite of the nature of CE as an organizational strategy, methods have been identified which foster a successful implementation (Ehrlenspiel and Meerkamm 2013).

Management by Objectives

CE and development in cross-functional teams requires independent decision-making within those teams. All members have to be aligned to common development targets. Singular alignment toward department goals may not lead to optimal results in holistic context. Leadership by targets needs to support the alignment of employees toward those goals (Backhouse and Brookes 1996).

Integration of Customer

Frontloading of development activities requires early integration of customers to evaluate preliminary designs. This is not only limited to engineering decisions but also extended to production properties defined by production processes.

CE engineering aims at acquiring stakeholder requirements as early as possible and reviewing all design artefacts frequently. Total quality management (TQM) on the basis of quality function deployment (QFD) has been traditional methods which have been extended to fully cover production and additionally business processes. Those methods are extended by lead user approaches as well as early prototype evaluations by customers (Ehrlenspiel and Meerkamm 2013).

Requirements Management

Formalized management of requirements creates the base for efficient product development. Requirements engineering (RE) originated from the sector of software development has been widely adopted for product development processes. Integration of stakeholder requirements has gained increased importance for CE processes. New approaches have enabled additional stakeholders to articulate their requirements allowing SE teams to develop optimal solutions based on formalized criteria.

Simulation and Virtual Reality

Following the overarching goal perform changes to the product designs as early as possible, methods which allow the identification based on preliminary development results are of great importance to CE. Those include all forms of simulation as well as virtual reality (VR). Physical mock-ups and experiments are currently still common methods to evaluate development results for all stakeholders. Software-based simulations have gained increased potential and in combination with powerful virtual reality approaches foster the communication within the SE teams.

Rapid prototyping has gained significant importance in CE with the advent of additive manufacturing. Physical models of development artefacts are commonly used to evaluate their compliance with stakeholder requirements. Despite the visualization of properties virtually, physical prototypes for products but also for production processes foster the common understanding within SE teams.

Information and Data Management

Increased complexity of products has led to an increased amount of data generated during the development process. Close cooperation between departments based on preliminary or partial development results requires efficient management of data. All development efforts from idea generation to production planning must be based on a singular data basis. CE requires clear indicators for each development artefact which allows members involved in the project to know whether they are working on fixed or preliminary data. Efficient data management in the context of CE does not only require appropriate software systems but also well-defined product and process architectures.

Successful implementations of CE in industry focus on uninterrupted tool chains from computer-aided design (CAD) to computer-aided manufacturing (CAM) as well as traceability through all stages. Propagation of changes from design to other stakeholders and their results can be identified by applying methods of system engineering and a powerful IT infrastructure (Skalak 2002).

Qualification and Mind-Set

CE is particularly successful if team members manage to exchange their knowledge efficiently. This requires education and continuous training for systemic development methods.

Team members must have a broad understanding of all processes within their department to integrate all requirements into the development process. Job rotation may support this broad knowledge.

Cost Controlling

Immediate targets and cost evaluations are necessary for sound concept evaluations within the cross-functional teams. Therefore, methods and structures for target costing as well as cost controlling are essential to CE. Due to the nature of CE, cost controlling does not only include the costs created during the development process but also costs which are directly or indirectly defined by development artefacts.

Quality Management Functions

During CE development activities, quality management functions become integrated elements for all cross-functional teams. Total quality management and quality function deployment as well as reengineering are core elements of CE. Additionally, failure mode and effect analysis (FMEA) is used frequently due to its multi-disciplinary nature. In addition to the traditional product-centered FMEA, process FMEAs are mandatory elements of CE development activities.

Introduction of frequent review meetings as well as quality circles has been implemented in most CE development processes.

Organizational Structure

Cooperative engineering requires the transition from functional organizations to product-orientated structures in the form of matrices. Workers assigned to a specific product development project report to the project manager instead of the department. In order to accelerate decision-making processes, flat hierarchical structures as well as efficient delegation of competencies are required for cooperative engineering.

Local Integration

Despite the increased relevance of digital and online communications as well as virtual reality integration, a strong interaction between involved actors across all departments is ensured by local integration. Work areas are shared by project-specific cross-functional teams and allow for an early evaluation of product and process prototypes. Development centers have to be designed as fully integrated work zones.

Software Support

Fragmented software environments along the development were present at the advent of CE. In recent past, closed CAD–CAM interaction and universal data formats have reduced problems and inefficiencies during CE activities. Especially view-based approaches which allow different team members to access master data from their perspective significantly support the work in CFT (Lamghabbar et al. 2004). Current software aims

to present an increasing support for agile communication and project management.

Shortcomings and Challenges

CE has been introduced by major companies around the world, and significant benefits have been reported. However, current implementations still face some major challenges. Early reports of problems primarily stated insufficient software support as a lack of computation power of information systems. Recent sources state missing data models and data structures as well as technologies to manage the increased amount of data as current IT problems. Communication within teams including the holistic evaluation of design alternatives is still regarded as highly critical without optimal generic approaches.

Cross-References

- ▶ [Computer-Aided Design](#)
- ▶ [Computer-Aided Manufacturing](#)
- ▶ [Virtual Reality](#)

References

- Backhouse J, Brookes N (1996) *Concurrent engineering: what works where: what's working where*. Gower Publishing, Hampshire
- Ehrlenspiel K, Meerkamm H (2013) *Integrierte Produktentwicklung. Denkläufe, Methodeneinsatz, Zusammenarbeit*. [Integrated product development. Processes, methods, collaboration]. Hanser Verlag, München (in German)
- Kusiak A (1992) *Concurrent engineering: automation, tools, and techniques*. Wiley, New York
- Lamghabbar A, Yacout S, Ouali MS (2004) Concurrent optimization of the design and manufacturing stages of product development. *Int J Prod Res* 42:4495–4512
- Lawson M, Karandikar HM (1994) A survey of concurrent engineering. *Concurr Eng: Res Appl* 2:1–6
- Loureiro G, Curran R (2007) *Complex systems concurrent engineering: collaboration, technology innovation and sustainability*. Springer, London
- Pokojski J, Fukuda S, Salwiński J (2010) *New world situation: new directions in concurrent engineering*. Springer, London
- Skalak S (2002) *Implementing concurrent engineering in small companies*. Marcel Dekker, New York
- Sohlenius G (1992) Concurrent engineering. *CIRP Ann Manuf Technol* 41(2):645–655

Coordinate Measuring Machine

Enrico Savio

Department of Industrial Engineering, University of Padova, Padova, Italy

Definition

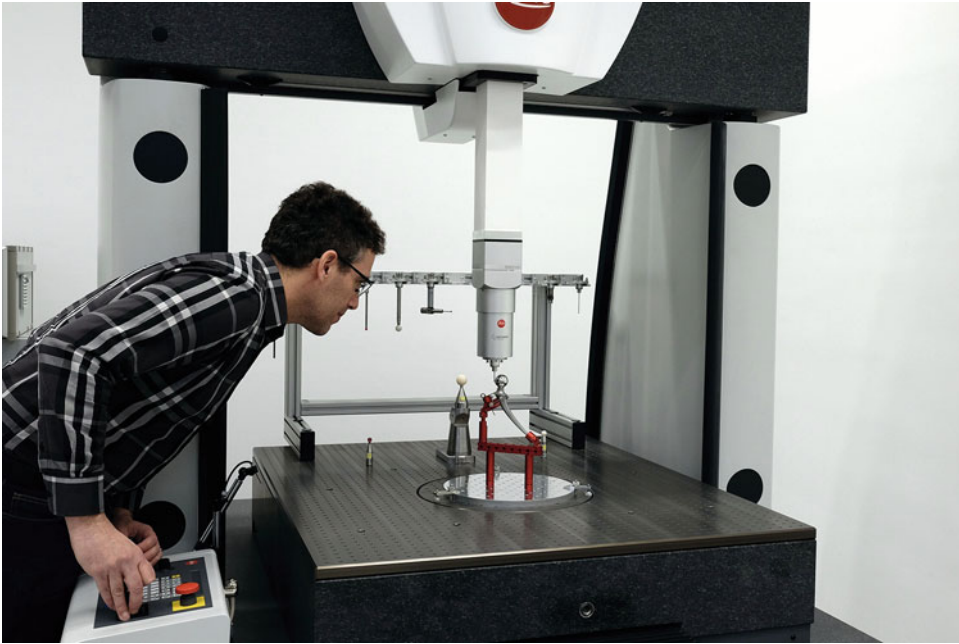
A coordinate measuring machine (CMM) is a measuring device with the capability to determine spatial coordinates of points that are probed on the surface of a workpiece (ISO 10360–1:2000), by means of a probing system that is moving in a defined measuring volume. The probing system can be contact or noncontact, with point acquisition rate depending on the measuring principle.

The term coordinate measuring system (CMS) is used to indicate all measuring devices having the capability to determine spatial coordinates on the surface of a workpiece. In addition to CMMs, examples are laser trackers, fringe projection systems, and computed tomography systems.

Theory and Application

Introduction

Coordinate measuring machines (CMMs) are the most important measuring systems for the measurement of workpieces in industry, because they are very flexible and allow the automated measurement of points in space with high accuracy, even on complex parts and surfaces. The probed spatial points are computed into substitute geometrical elements, enabling the evaluation of size and geometrical deviations of workpiece features within a short period of time and relatively low measuring uncertainty (Christoph and Neumann



Coordinate Measuring Machine, Fig. 1 Fixed-bridge CMM with contact probing system. (Source: NTB – Institute for Production Metrology, Materials and Optics, Buchs, Switzerland)

2004; Keferstein and Marxer 2015; Savio et al. 2007; Weckenmann 2011).

A CMM consists of the following main elements: mechanical assemblies, drives, length transducers, probing systems, and control unit. The measurement process is programmed step by step using a measuring software.

Architecture

The most common CMM designs are Cartesian, i.e., three components are moving along guideways perpendicular to one another, and can be described as follows (ISO 10360-1:2000; ISO 10360-2:2009; Hocken and Pereira 2011):

- a. Moving bridge: a stationary table supports the workpiece; the probing system is attached to the ram axis, which moves vertically in relation to a carriage that moves horizontally on the bridge. The bridge is supported on two legs, which descend on opposite sides of the stationary table, and moves horizontally. It is the most common in industry, has small to medium measuring volume, and medium to high accuracy.
- b. Fixed bridge: a moving table supports the workpiece, while the bridge is rigidly attached to the machine bed (Fig. 1). This design enables higher accuracy; therefore it is the preferred solution to achieve the smallest measuring uncertainty. Limitations are lower speed due to the larger moving mass, lower permissible workpiece weight, and larger footprint for the moving table.
- c. Cantilever: a stationary table supports the workpiece; the probing system is attached to the ram axis, which moves vertically in relation to a carriage that moves horizontally on a cantilever. It enables high accessibility on three sides and has low to medium accuracy.
- d. Horizontal arm: the probing system is attached to the ram axis, which moves horizontally in relation to a carriage that moves vertically on a column. The third displacement is horizontal by a moving column. It is limited in accuracy however has very good accessibility; therefore it is commonly used for the measurement of

large and heavy parts. Dual-arm designs allow best accessibility to all sides of large objects, e.g., car bodies.

- e. Gantry: the probing system is attached to the ram axis, which moves vertically in relation to a carriage that moves horizontally on a beam. The beam moves horizontally on two guide rails raised on either side above the machine base on which the workpiece is located. This design allows large measuring volume, excellent accessibility, and medium accuracy.

An example of non-Cartesian design is the articulated arm CMM: the probing system is attached to the end of two or more linkage arms connected by rotating joints with optical encoders to a base having a vertical rotating axis. It is operated manually and portable, with medium accuracy; therefore, it can be cost-effective in case of large parts.

The selection of the most suitable CMS for a certain measuring task is based on multiple aspects (Hocken and Pereira 2011; Savio 2012; Weckenmann 2011); the most important can be summarized as follows:

- Size and geometrical complexity of the part
- Target measurement uncertainty
- Single or repetitive measurement
- Production step (process control or final inspection)
- Economical aspects (initial investment, productivity, labor cost, etc.)

Probing Systems

The probing system designs can be grouped in:

- Tactile probing systems
- Optical probing systems

Tactile probing systems, mainly designed on inductive or capacitive principles, are usually equipped with changeable styluses. Common stylus tip geometries are sphere, cylinder, and spherical disk. The sphere is suitable in most cases for all kinds of surfaces. Cylindrical tips are used, e.g., for holes in flat sheet metals, where it is challenging to probe the edge correctly using a

spherical tip. When applied to boreholes or shafts, spherical disk geometries of the tip are a suitable solution. Most of the stylus tips are made of steel, artificial ruby, or ceramics.

Optical probing systems can be divided into distance sensors (e.g., laser triangulation sensors) and vision-based edge detection sensors (e.g., sensors based upon CCD cameras using image processing and edge detection). Being non-contact, they are preferred for the measurement of deformable parts, e.g., made of sheet metal, rubber, plastic, or features too small for contact probing (e.g., small holes or grooves). Optical probing systems can measure with high point density and speed. It is worth noting that the interaction of light with the surface, edges, and material of a workpiece is of a different nature than in contact probing and may result in higher measuring uncertainty (Carmignato et al. 2010; Keferstein and Marxer 2015; Schwenke et al. 2002; Weckenmann et al. 2004).

The integration of different probing systems on a single CMM (Fig. 2) offers the opportunity to combine the strengths of one with another, depending on the feature to be measured (Hocken and Pereira 2011).

Geometrical Error Compensation of CMMs

The accuracy of CMMs is affected by error sources that may cause a change in the geometry of the machine's components; consequently, the probing system position and orientation relative to the workpiece differ from the nominal position and orientation, resulting in a relative error. The magnitude of this error depends on the sensitivity of the machine's structural loop on various error sources (Schwenke et al. 2008).

When the single parts of a CMM are assembled, the mechanical axes show specific deviations and also deviations to each other. A Cartesian 3-axis CMM has a total of 21 deviations in all 3 axes:

- Length or position deviations in x-, y-, and z-direction: x_{px} , y_{py} , and z_{pz}
- Rotary deviations around the x-, y-, and z-direction: x_{rx} , x_{ry} , x_{rz} , y_{rx} , y_{ry} , y_{rz} , z_{rx} , z_{ry} , and z_{rz}



Coordinate Measuring Machine, Fig. 2 Fixed-bridge CMM equipped with contact and optical probing systems. (Source: NTB – Institute for Production Metrology, Materials and Optics, Buchs, Switzerland)

- Translatory/straightness deviations perpendicular to the x-, y-, and z-direction: xty, xtz, ytx, ytz, ztx, and zty
- Perpendicularity deviation between axes: xwy, xwz, and zwy

CMM accuracy is increased by mapping of these systematic deviations and appropriate compensation using software. These deviations are evaluated using direct measurements (e.g., laser interferometers, straightedges) or indirect measurements (e.g., 2D- and 3D-calibrated artefacts, multilateration).

This approach is also applied to specific effects of the probing systems. In contact probing, the mechanical bending caused by probing forces is compensated. This applies also to the size and form of the stylus tip (Hochen and Pereira 2011; Weckenmann 2011).

Acceptance and Reverification

The ISO 10360 series describes a number of widely accepted tests covering the most common aspects for CMMs equipped with tactile and optical probing systems.

Acceptance tests are to verify that the performance of a CMM is as stated by the manufacturer; they are also used for reverification, with frequency depending on use and conditions of the machine (ISO 10360-1:2000). The common approach is to perform measurements on calibrated material standards (e.g., gauge blocks, step gages, spheres, ball plates) or laser interferometers, preferred for large CMMs.

The performance of a CMM is mainly defined in terms of errors of indication and related maximum permissible error (MPE); a number of specialized tests have been designed with reference to the specific CMM types and probing systems:

- CMMs used for measuring linear dimensions (ISO 10360-2:2009)
- CMMs with a rotary table as the fourth axis (ISO 10360-3:2000)
- CMMs in scanning measuring mode (ISO 10360-4:2000)
- CMMs using single and multiple stylus contacting probing systems (ISO 10360-5:2010)
- CMMs equipped with imaging probing systems (ISO 10360-7:2011)
- CMMs with optical distance sensors (ISO 10360-8:2013)
- CMMs with multiple probing systems (ISO 10360-9:2013)
- Articulated arm CMMs using tactile probes and optionally optical distance sensors (ISO 10360-12:2016)

Traceability

The tests described in the ISO 10360 series of standards are delivering only a partial picture of the error sources of the complete measuring process, because the CMM itself is only one out of a number of contributors to the measuring uncertainty on workpieces. For instance, the influence of the measuring strategy can dominate the result, especially when in combination with significant

form errors on the part to be measured. When measuring using imaging probing systems, the interactions between type and intensity of illumination, part geometry, and material are also influencing the measurement result. Therefore, it is important to emphasize that traceability in the sense of the definition is not obtained by ISO 10360 tests only, in case of measuring task that are different from those described in the specific tests.

Task-specific uncertainty assessment is therefore required, and this is a challenging activity in case of CMM measurements. Different approaches have been proposed (Wilhelm et al. 2001), and the two most widely accepted are now described in the ISO 15530 series (ISO/TS 15530-1:2013) as follows.

Use of Calibrated Workpieces

The experimental approach described in ISO 15530-3:2011 consists in carrying out repeated measurements cycles on calibrated workpieces, respecting similarity conditions to the actual measurement task in terms of geometrical features, form deviations, roughness, material characteristics, measuring strategy, and probe configuration, as well as environmental conditions. The limitations of this approach method are related to its experimental nature: the time required, the need of artefacts with adequate stability and sufficiently small calibration uncertainty, and related costs.

Use of Computer Simulation

The assessment of uncertainty based on computer simulation of the measurement process (i.e., Monte Carlo method) was demonstrated to be feasible for CMMs (Trapet et al. 1999), and today different implementations are available in industry. ISO/TS 15530-4:2008 specifies requirements for the application of simulation-based uncertainty evaluating software to CMM measurements and gives informative descriptions of simulation techniques used for evaluating task-specific measurement uncertainty, along with advantages and disadvantages of various testing methods.

Cross-References

- ▶ [Accuracy](#)
- ▶ [Computed Tomography](#)

- ▶ [Inspection \(Precision Engineering and Metrology\)](#)
- ▶ [Measurement Uncertainty](#)
- ▶ [Reverse Engineering](#)
- ▶ [Traceability](#)

References

- Carmignato S, Voltan A, Savio E (2010) Metrological performance of optical coordinate measuring machines under industrial conditions. *CIRP Ann* 59(1):497–500. ISSN:0007–8506. <https://doi.org/10.1016/j.cirp.2010.03.128>
- Christoph R, Neumann HJ (2004) *Multisensor coordinate metrology: measurement of form, size and location in production and quality control*. Verlag Moderne Industrie, Landsberg
- Hocken RJ, Pereira PH (2011) *Coordinate measuring machines and systems*, 2nd edn. CRC Press, Boca Raton. ISBN:1574446525
- ISO 10360-1:2000 Geometrical product specifications (GPS) – acceptance and reverification tests for coordinate measuring machines (CMM) – part 1: vocabulary
- ISO 10360-2:2009 Geometrical product specifications (GPS) – acceptance and reverification tests for coordinate measuring machines (CMM) – part 2: CMMs used for measuring linear dimensions
- ISO 10360-3:2000 Geometrical product specifications (GPS) – acceptance and reverification tests for coordinate measuring machines (CMM) – part 3: CMMs with the axis of a rotary table as the fourth axis
- ISO 10360-4:2000 (Cor 1:2002) Geometrical product specifications (GPS) – acceptance and reverification tests for coordinate measuring machines (CMM) – part 4: CMMs used in scanning measuring mode
- ISO 10360-5:2010 Geometrical product specifications (GPS) – acceptance and reverification tests for coordinate measuring machines (CMM) – part 5: CMMs using single and multiple stylus contacting probing systems
- ISO 10360-7:2011 Geometrical product specifications (GPS) – acceptance and reverification tests for coordinate measuring machines (CMM) – part 7: CMMs equipped with imaging probing systems
- ISO 10360-8:2013 Geometrical product specifications (GPS) – acceptance and reverification tests for coordinate measuring systems (CMS) – part 8: CMMs with optical distance sensors
- ISO 10360-9:2013 Geometrical product specifications (GPS) – acceptance and reverification tests for coordinate measuring systems (CMS) – part 9: CMMs with multiple probing systems
- ISO 10360-12:2016 Geometrical product specifications (GPS) – acceptance and reverification tests for coordinate measuring systems (CMS) – part 12: articulated arm coordinate measurement machines (CMM)
- ISO/TS 15530-1:2013 Geometrical product specifications (GPS) – coordinate measuring machines (CMM):

technique for determining the uncertainty of measurement – part 1: overview and metrological characteristics

- ISO 15530-3:2011 Geometrical product specifications (GPS) – coordinate measuring machines (CMM): technique for determining the uncertainty of measurement – part 3: use of calibrated workpieces or measurement standards
- ISO/TS 15530-4:2008 Geometrical product specifications (GPS) – coordinate measuring machines (CMM): technique for determining the uncertainty of measurement – part 4: evaluating task-specific measurement uncertainty using simulation
- Keferstein CP, Marxer M (2015) *Fertigungsmesstechnik: praxisorientierte Grundlagen, moderne Messverfahren [Production metrology: fundamentals for practitioner, modern measurement methods]*, 8th edn. Springer, Wiesbaden (in German)
- Savio E (2012) A methodology for the quantification of value-adding by manufacturing metrology. *CIRP Ann* 61(1):503–506. ISSN:0007-8506. <https://doi.org/10.1016/j.cirp.2012.03.019>
- Savio E, De Chiffre L, Schmitt R (2007) Metrology of freeform shaped parts. *CIRP Ann Manuf Technol* 56(2):810–835
- Schwenke H, Neuschaefer-Rube U, Pfeifer T, Kunzmann H (2002) Optical methods for dimensional metrology in production engineering. *CIRP Ann Manuf Technol* 51(2):685–699
- Schwenke H, Knapp W, Haitjema H, Weckenmann A, Schmitt R, Delbressine F (2008) Geometric error measurement and compensation of machines-an update. *CIRP Ann Manuf Technol* 57:660–675
- Trapet E, Franke M, Härtig F, Schwenke H, Wäldele F, Cox M, Forbes A, Delbressine F, Schellekens P, Trenk M, Meyer H, Moritz G, Guth Th, Wanner N (1999) Traceability of coordinate measuring machines according to the method of the virtual measuring technique, PTB-F-35 PTB, Braunschweig. ISBN:3-89701-330-4
- Weckenmann A (2011) *Koordinatenmesstechnik: Flexible Strategien für funktions- und fertigungsgerechtes Prüfen: Flexible Messstrategien für Maß, Form und Lage*, 2nd edn. Carl Hanser Verlag, München (in German)
- Weckenmann A, Estler T, Peggs G, McMurtry D (2004) Probing systems in dimensional metrology. *CIRP Ann Manuf Technol* 53(2):657–684
- Wilhelm RG, Hocken R, Schwenke H (2001) Task specific uncertainty in coordinate measurement. *CIRP Ann Manuf Technol* 50(2):553–563

Coordinating

- ▶ [Planning](#)

Corporate Management

- ▶ [Management of Production Enterprises](#)

Corporate Social Responsibility

- ▶ [Sustainable Manufacturing](#)

Correctness

- ▶ [Precision](#)

Corrosion

Nikolaos Michailidis^{1,2} and Homero Castaneda³
¹Physical Metallurgy Laboratory (PML), Department of Mechanical Engineering, Aristotle University of Thessaloniki, Thessaloniki, Greece
²Center for Research and Development on Advanced Materials – CERDAM, Thessaloniki, Greece
³National Corrosion and Materials Reliability Laboratory, Texas A&M University, College Station, TX, USA

Synonyms

[Change of elemental and functional characteristics of the surface](#); [Surface degradation](#)

Definition

Corrosion is the degradation of the surface properties, most commonly appearing in metals and alloys, through a chemical and/or electrochemical interaction with the environment, converting matter into a more chemically stable form, such as oxide, hydroxide, or sulfide.

Theory and Application

Introduction

Corrosion is a surface-originated phenomenon, having though a strong impact on the service life of components and structures. Some of the major parameters affecting the corrosion performance of a surface are its inherent material properties and its potential to passivate, the type and aggressiveness of the environment, the operating temperature, the surface characteristics (roughness, texture, porosity), and the surface condition (manufacturing process, residual stresses) (Schulze et al. 2016; Stergioudi et al. 2016). In most of the used components, the presence of multi-effect features is complicating the prediction of the corrosion performance, i.e., materials with complex microstructure and multiple heat and mechanical treatments and manufacturing processes, exposed to severe corrosion environments and temperatures.

History and Economic Impact of Corrosion

Corrosion has been the endless war for several centuries since the use of the metallic structures when exposed to aggressive environment; during the pass of the years, the awareness and conscience of the natural phenomena has been addressed from intuition to macroscopic economic numbers (Johnson et al. 1987; McCafferty 2010). Materials performance and degradation in corrosive environments have been impacting the global economy when each country reports its losses in terms of the GNP.

An IMPACT report issued by NACE states that the cost of corrosion is estimated to be US 2.5 trillion or an equivalent of 3.4 GNP of the global impact in terms of corrosion (NACE 2017). This cost is directly related to the corrosion process occurring in different sectors and industries around the world. The awareness and best practices in corrosion control can help to reduce such cost between 15% and 35% annually.

In the USA the economic losses due to corrosion process have reached close to the global number of 3% GNP; this represents high impact in the US economy. The corrosion phenomenon impacts close to \$1 trillion per year on the

global economy to different industrial sectors. The awareness of corrosion phenomena has been increased through the years; however the economic, environmental, and health impact due to this process has not been reflected in the last decades. In 1998 the cost of corrosion in the USA was 298 billion dollars; only few years later in 2013, the cost increases to 1 trillion dollars. The number of people studying and understanding corrosion has increased; R&D efforts have been introduced for more awareness and diligence in this phenomenon. Corrosion is the degradation of the material due to the interaction with the environment; this latter puts a dynamic aspect in corrosion science and engineering, part of the reason is the new materials that have been developed, and a second reason is the continuous change in the environment with time. Different industrial sectors have placed corrosion as one of the key areas in their R&D centers to understand the degradation mechanisms due to the newest development in materials. The impact results in the society by the corrosion mechanisms have been helping the global economy by the validation of new materials, control and prevention of current materials exposed to harsh environments, and management of the assets based on corrosion mitigation, control, and repairing actions.

Forms of Corrosion

Uniform Corrosion

This form considers the continuous area dissolution of a material when anodes and cathodes are distributed homogeneously over the entire surface in contact with the electrolyte.

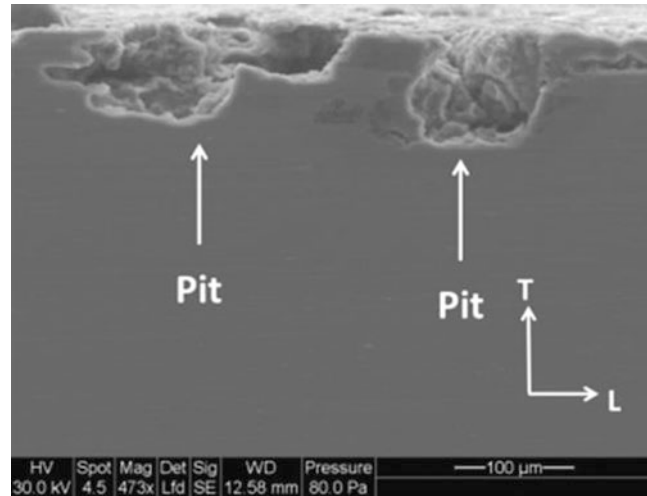
Galvanic Corrosion

Two dissimilar metallic materials are in electrical contact and exposed to electrolytic environment causing a potential difference between the metallic electrodes. The interfacial reactions anodic and cathodic are activated due to the energy (in terms of potential).

Pitting Corrosion

This localized form of degradation includes the generation of cavities, holes, from a smooth

Corrosion, Fig. 1 SEM cross section of an aluminum sample suffering from pitting corrosion after exposure in an acidic solution (Karayan 2015)



metallic surface when anodic sites act as dissolution sites in contact with cathodic sites in corrosive environments. The initial state of the pitting includes the initiation and later becomes the growth state (see characteristic example of Fig. 1).

Stress Corrosion/Corrosion Fatigue

The synergetic interaction between materials properties susceptibility, mechanical loads, and corrosive environment leads to electrochemical processes combining to crack initiation – and propagation mechanisms. Hence, the life expectancy of structural elements imposed to mechanical loadings and corrosion may be severely affected, leading to significant deviations from the designed one. When the mechanical load is static, we refer to stress corrosion, while when the load is cyclic, then corrosion fatigue takes place (Michailidis et al. 2014). Figure 2 shows the comparison of the performance of a NiTi shape memory alloy (SMA) imposed solely to cyclic mechanical loading versus combined with corrosion in a 3.5 wt% NaCl aqueous solution. Although NiTi is supposed to be super-passive, the combined action of cyclic mechanical load and corrosion yields to the half-life span.

Hydrogen Embrittlement

The permeation of hydrogen atoms within the metallic matrix due to incomplete formation of hydrogen molecule and integration in the

microstructure produces internal stresses and surface brittleness. Thus, crack growth is facilitated.

Crevice Corrosion

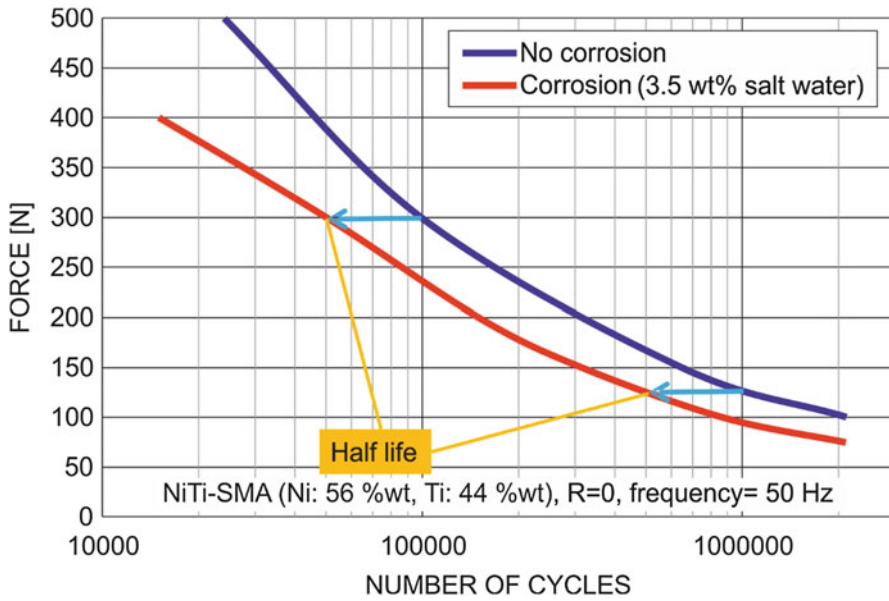
Original design in a metallic material when in operation conditions can form a cavity promoting a gradient within the cavity and the external part of the original cavity. The corrosion mechanism includes the synergic action of such naturally formed gradient with the corrosive environment.

Intergranular Corrosion

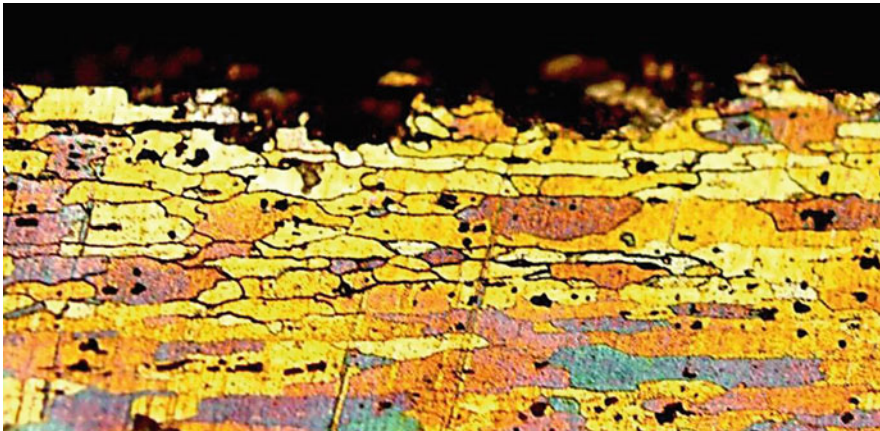
Intergranular corrosion is the result of the selective attack on the grain boundaries of a metal or alloy. The main cause of that is either the segregation of impurities at the grain boundaries or the depletion/enrichment of one or more of the alloying elements in the areas of the grain boundaries. A typical example of intergranular corrosion, leading to exfoliation of grains, is presented in Fig. 3, in the case of AA2024-T3, after 6 h exposed to NaCl/KNO₃/HNO₃ solution.

Filiform Corrosion

Filiform corrosion appears at the interface of coated metals in the form of threadlike filaments, leading to unwanted marks on the surface. Usually, this form of corrosion is not critical for the component performance but downgrades its surface quality. Figure 4 presents an example of the evolution of filiform corrosion of a



Corrosion, Fig. 2 Fatigue and corrosion-fatigue performance of NiTi SMA. (Source: PML)



Corrosion, Fig. 3 Intergranular (exfoliation type) corrosion of AA2024-T3, after 6 h in NaCl/KNO₃/HNO₃ solution. (Source: PML)

powder-coated aluminum alloy, exposed to relative humidity of 80% at 40 °C for 30, 60, and 90 days. The length of the threadlike filaments is increasing over the exposure time.

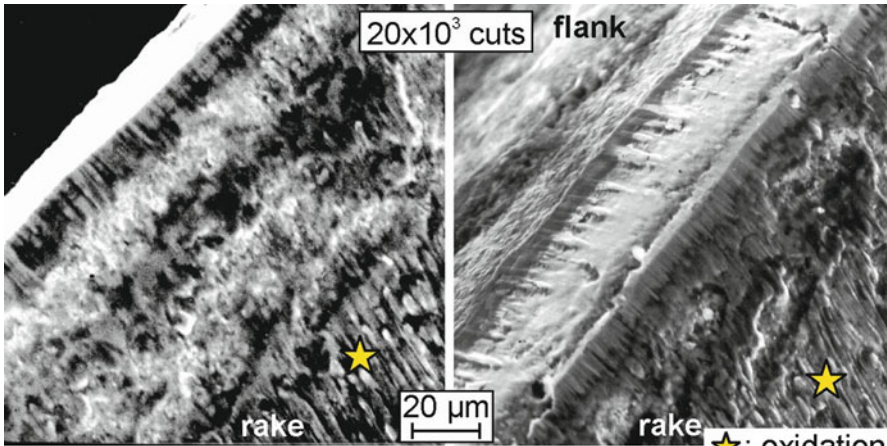
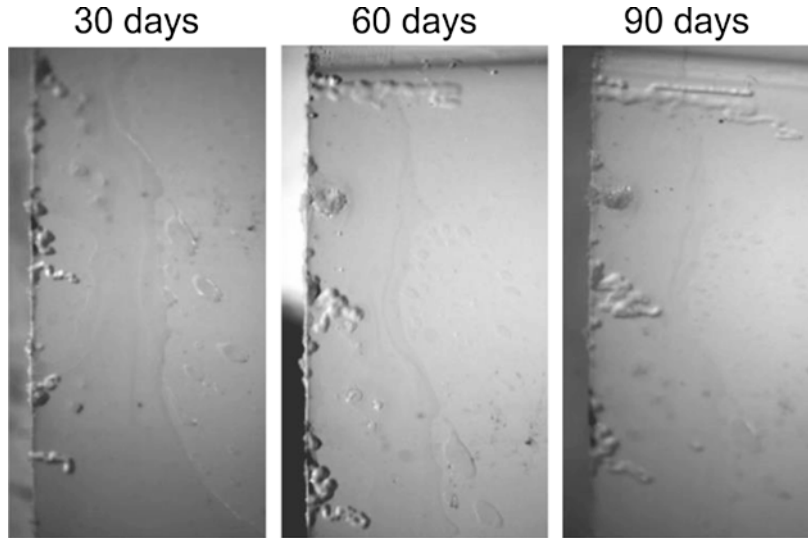
Fretting Corrosion

The relative motion of surfaces being in contact under mechanical loading in a corrosive

environment (atmosphere) is the combination of conditions that flourish fretting corrosion. The damage in this type of corrosion appears at the vicinity of the surfaces in the form of debris next to pits or grooves. Examples of fretting corrosion lie in mechanical joints like nails and screws/bolts imposed to vibrations or even in ball bearings.

Corrosion,

Fig. 4 Evolution of filiform corrosion after 30-, 60-, and 90-day exposure. (Source: PML)



★: oxidation
 Cutting velocity $v_c = 600$ m/min, Chip thickness $h = 0.2$ mm,
 Cutting depths $a_e = a_p = 3$ mm, Clearance angle $\alpha = 7^\circ$,
 Rake angle $\gamma = 0^\circ$, Orthogonal cutting, Coating (Ti,Al)N,
 Thickness $t = 3$ μm , Substrate K35, Workpiece 42CrMo4 QT

Corrosion, Fig. 5 Oxidation appearing on a coated tool in milling hardened steel at high cutting speeds (Bouzakis et al. 1999)

High-Temperature Corrosion

High-temperature corrosion is mostly manifested in the form of oxidation. Above a critical temperature, metals tend to oxidize, leading to scaling, loss of material, and changes in physical properties. This includes the aerospace, automotive, power, manufacturing, and chemical processing

industries. Especially in metal machining, oxidation is one of the major wear parameters at high cutting speeds, even when high-end coated tools are employed. Figure 5 shows the oxidation appearing on the rake of a (Ti,Al)N-coated cutting tool in milling 42CrMo4+QT at a cutting speed of 600 m/min (Bouzakis et al. 1999).

Microbiology Induced Corrosion

The presence of bioorganisms originate biofilm at the substrate/electrolyte interface where bioactivity occurs, producing charge transfer and mass transfer processes causing dissolution of metallic material. Figure 6 is indicative of the susceptibility of low carbon steel to bacteria.

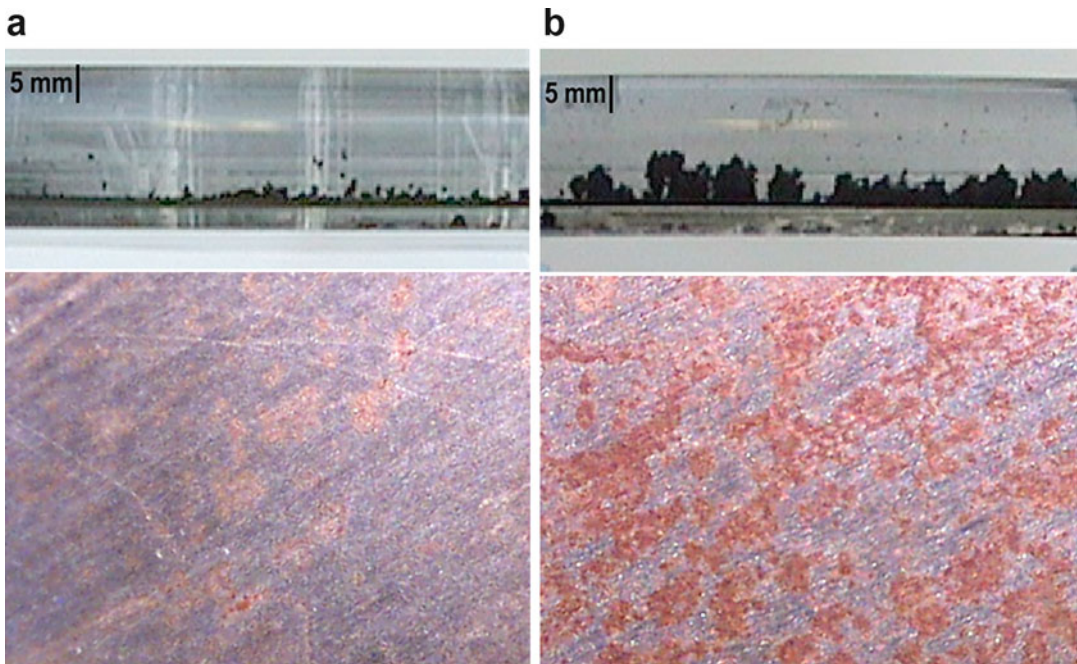
Corrosion Protection

An electrochemical cell consists of four different elements: anode, cathode, electrical path, and ionic path. Once the system is formed, naturally or by original design, corrosion is initiated. The anode and the cathode are exposed to the environment causing the anodic (metallic dissolution) and cathodic reactions (reduction). Corrosion is a galvanic cell generated thermodynamically by anodic and cathodic process; the mechanisms can be avoided if one of the elements is not in continuous contact forming the cell. There are different approaches for corrosion control and mitigation, called anodic protection and cathodic protection. The principle is to suppress or avoid either one of

the electrochemical reactions (Jones 1996). The anodic protection includes the chemical inhibitors; the cathodic protection covers the galvanic anodes, impressed current, and coatings. Finally, one classification that is unique in principle is the materials selection, mostly the anode in the electrochemical cell.

Inhibitors

The inhibitors are chemical species or compounds that act by following two different mechanisms that prevent corrosion. The first mechanism considers the influence in the mass transport by blocking the corrosive species going at the interface as a barrier layer avoiding the direct contact of such species, such as oxygen, chloride, and different ions with the metallic substrate; the name of these chemicals are filmic inhibitors. The second mechanism is the chemical reaction of corrosion precursors by the added chemical into the electrochemical cell formed to trap the aggressive species by transforming to a less hazard species.



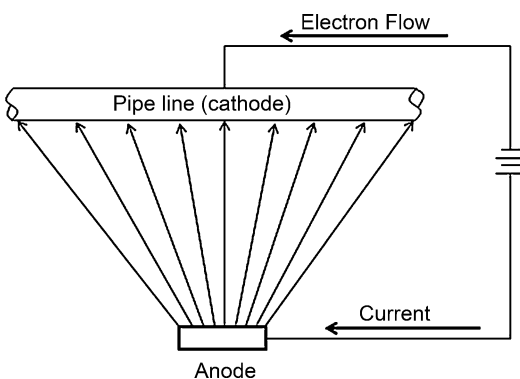
Corrosion, Fig. 6 Sulfate reduces bacteria for MIC on low carbon steel. (a) No bacteria, (b) with bacteria (Castaneda and Benetton 2008)

Cathodic Protection

Cathodic protection considers the reduction of potential difference created by the cathodic and anodic sites in one metallic structure when exposed to corrosion environment to zero gradient. There are two paths to achieve this; the first one is by creating an electrochemical cell, where the anode is the electrode used to drain the current to the cathode (metallic structure) to be protected by inducing a current to the system. The second mode for cathodic protection is by the formation of a galvanic cell thermodynamically activated by the formation of an electrochemical cell, named galvanic anodes. Both modes of protection are based on the current drain to the electrode that is going to be corroded, which is the cathode (Fig. 7).

Coatings

Coatings are the most used form of corrosion control; the principle is by the elimination of the interaction between the corrosive environments with the metallic substrate by adding a physical barrier between them. Different mechanisms have been developed to influence the dissolution mechanism of the anode by avoiding the anodic reaction. Different coating systems utilize anodic protection, inhibition protection, and cathodic protection principles (Uhlig and Revie 1985).



Corrosion, Fig. 7 Cathodic protection system (Revie 2015)

Corrosion in Industry

Oil and Gas

The oil companies are classified in three different business units: downstream, upstream, and transportation. Each unit owns different assets that are exposed in continuous harsh and extreme environmental conditions and could suffer aging by degradation. Metallic assets are exposed to harsh environments, among which temperature, pressure, and loads can influence corrosion or degradation kinetics. Upstream operations can add the sweet or sour corrosion to the extreme environment (Castaneda 2009). Lately, more exploration fields in this sector have increased the sulfur content and subsequently the H_2S in the oil content. Deeper waters to extract more oil increase the influence of parameters that catalyze or kinetically favor the corrosion mechanism. Different environment and range of the similar parameters produce the downstream operations. An electrochemical cell is formed during downstream due to the aqueous (water cut) content but also due to organic electrolytes influencing the corrosion mechanism. The metallic assets suffer from corrosion degradation due to a natural electrochemical cell formed at the interface metal/electrolyte in combination with parameters existing for operation conditions. Flow dynamics, loads, temperature, and pressure are parameters enhancing the kinetics of the corrosion process. Finally, the transportation unit in oil and gas relates all about systems that carry the oil and gas and subproducts. The most known transportation system is the pipeline; this later suffers from the aging, chemical, and electrochemical degradation with time (see Fig. 8). This transportation is included in the upstream and downstream operations.

Infrastructure

Corrosion in infrastructure has captured the attention of the entire world because the structures that connect communities, cities, and countries have been deteriorating due to the interaction with the environment and parameters that, while are used to maintain a continuous operation, may be a corrosion precursor in the short or long term, such as salts to deice the roads. The Department of Transportation (DOT) in the USA maintains



Corrosion, Fig. 8 Underground pipeline corrosion (original)

a large bridge inventory among the entire nation in addition to different pipelines, sewer, and other infrastructure systems. The electrolyte with corrosive precursors in the natural environment corrosion precursors such as oxygen, humidity, temperature, CO_2 , NO_x , and also the corrosion precursors used that affects the infrastructure systems are some examples of corrosion-induced damages to structural elements are one of the leading causes for damage to spend an enormous amount of annual budget for maintenance, repair, rehabilitation, and replacement.

Automotive

Automotive industry is expected to grow at a rate of 6.27% by the next decade. This grow will affect the design and characteristics of each automobile due to the more demanding environment conditions. Vehicles require coatings not only as aesthetic requirement but also as barrier environmental protection. Today, it can be assured that corrosion protection of almost all-automobile bodywork includes a multilayer coating system. New trends for corrosion and durability testing are leading to the simulation of more realistic conditions of the automobile parts exposed to daily conditions. With the new challenges of low CO_2 emissions to the environment, the automotive industry is targeting lightweight materials to

reduce the total weight of the vehicle, while the oil consumption becomes more cost-effective. This challenge put corrosion on the map; the materials selected such as aluminum and magnesium are more prone to corrosion, making this phenomenon important for this industry. The control and prevention actions for this industry have been mainly for coatings, this latter due to the corrosion nature in these systems.

Cross-References

- ▶ [Electroforming](#)
- ▶ [Electroplating](#)
- ▶ [Residual Stress \(Abrasive Processes\)](#)
- ▶ [Residual Stress \(Forming\)](#)
- ▶ [Roughness](#)
- ▶ [Surface texture](#)

References

- Bouzakis K-D, Vidakis N, Michailidis N, Leyendecker T, Erkens G, Fuss G (1999) Quantification of properties modification and cutting performance of $(\text{Ti}_{1-x}\text{Al}_x)\text{N}$ coatings at elevated temperatures. *Surf Coat Technol* 120–121:34–43
- Castaneda H (2009) The impact of sour environment in anodic dissolution of metallic structures used in the refinery industry. *Hydrocarb World* 4(20):1

- Castaneda H, Benetton X (2008) SRB-biofilm influence in active corrosion sites formed at the steel-electrolyte interface when exposed to artificial seawater conditions. *Corros Sci* 50(4):1169–1183
- Johnson J, Kiepusa R, Humphries D (1987) *Metals handbook*. ASM International, Metals Park
- Jones D (1996) *Principles and prevention of corrosion*. Prentice Hall, Upper Saddle River
- Karayan I (2015) Exfoliation corrosion susceptibility and mechanisms of Al-Li 2060 T8E30 aluminum lithium alloy in acidic media. PhD Thesis, University of Akron, p 175
- McCafferty E (2010) *Introduction to corrosion science*. Springer, New York
- Michailidis N, Stergioudi F, Maliaris G, Tsouknidas A (2014) Influence of galvanization on the corrosion fatigue performance of high-strength steel. *Surf Coat Technol* 259:456–464
- NACE Impact Report (2017) *International measures of prevention, applications and economics of corrosion technologies study*. Gretchen Jacobson
- Revie RW (2015) Chapter 20: External Corrosion of pipelines in soil. Oil and gas pipelines. *Integrity and Safety Handbook*, Winston Review, John Wiley and Sons
- Schulze V, Bleicher F, Groche P, Guo Y, Pyun Y (2016) Surface modification by machine hammer peening and burnishing. *CIRP Ann* 65(2):809–832
- Stergioudi F, Vogiatzis C, Pavlidou E, Skolianos S, Michailidis N (2016) Corrosion resistance of porous NiTi biomedical alloy in simulated body fluids. *Smart Mater Struct* 25(9):095024
- Uhlig H, Revie R (1985) *Corrosion and corrosion control*. Wiley, New York

Cost

Sotiris Makris, George Michalos and George Chryssolouris

Laboratory for Manufacturing Systems and Automation (LMS), Department of Mechanical Engineering and Aeronautics, University of Patras, Patras, Greece

Synonyms

Charge; Disbursement; Expenditure; Expense; Monetary value; Price

Definition

Cost is the amount of cash expended or other property transferred, the capital stock issued, the

services performed or a liability incurred, in consideration of the goods or services received or to be received (Belkaoui 1985).

However, there is no exact definition of the term “cost” since its interpretation would depend upon the nature of the business or industry and the context used. The use of the term “cost” without qualification may be misleading. Different costs arise for different purposes.

Theory and Application

Cost, together with flexibility, time, and quality are the main manufacturing attributes that should be considered during the manufacturing system design and operation (Chryssolouris 2006). In order for manufacturers to evaluate the effectiveness of their facilities and formulate their strategies and decision-making procedures, there is a need for methods that are able to quantify the exact cost numbers related to their manufacturing process (Alexopoulos et al. 2007). To this effect, a breakdown of costs and an identification of different cost types are usually followed.

Manufacturing Costs

The costs related to manufacturing encompass a number of different factors, which can be broadly classified into the following categories (Chryssolouris 2006):

- Equipment and facility costs. These include the costs of equipment necessary for the operation of manufacturing processes, the facilities used for housing the equipment, the factory infrastructure, etc.
- Materials. This category includes the cost of raw materials for the production of the product, and that of the system’s tools and auxiliary materials, such as coolants and lubricants.
- Labor. The direct labor required for the operation of both equipment and facilities.
- Energy required for the performance of the different processes. In some manufacturing industries, the cost of energy may be negligible, compared with other factors, while in other

industries it significantly contributes to the financial burden of the manufacturing system.

- Maintenance and training. This includes labor, spare parts, etc., which are required for the maintenance of the equipment, facilities, and systems, as well as the training necessary to accommodate new equipment and technology.
- Overhead. This is a part of the cost that is not directly attributable to the operation of the manufacturing system, but supports its infrastructure.
- The cost of capital, which may not be readily available within the manufacturing firm, and therefore, has to be borrowed under specific terms.

This classification provides a general framework of the way that cost issues can be addressed in the manufacturing environment by establishing a systematic way of measuring the cost performance of different solutions. Another classification considers the distinction between cost factors that are directly and indirectly related to the manufacturing or assembly process. Such a classification is presented in Fig. 1 (Michalos et al. 2008).

Cost Modelling and Accounting Techniques

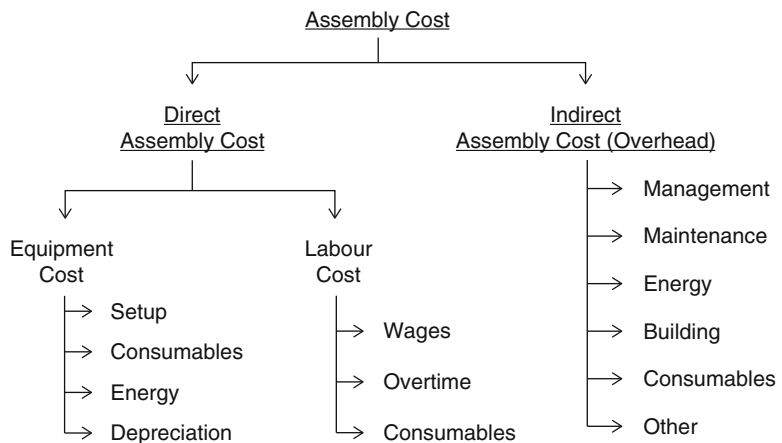
During the past decades, several attempts, ranging from very simple “rules of thumb” and activity-based cost models to complicated and specialized technical cost models, have been proposed for the

quantification of the assembly cost (Monteiro 2001). Other empirical methods include function costing and cost scaling methods, which involve the use of historical data for determining the cost of producing a certain part, with a given set of features (Esawi and Ashby 2003). An overview of the most relevant accounting techniques is presented hereafter:

Traditional cost accounting: This method considers three basic cost categories, namely, direct labour, raw material, and overhead costs. All costs that are not included in the first two categories are regarded as overhead costs. This is considered to be the main weakness of the method due to the fact that over the last years, the estimation of the overhead costs is becoming both significant and hard (Monteiro 2001).

Activity-based Costing (ABC): Due to the inability of traditional cost accounting to capture the actual cost of the process, new methods capable of considering lower level information, regarding the manufacturing processes, were sought. This led to the generation of the Activity-based Costing (ABC) techniques, which break down even further the costs at activity level, thus providing estimates of the cost per unit of the activity’s output. Activity-based costing (ABC) considers that almost all activities taking place within a firm support the production, marketing, and delivery of goods and services.

Cost, Fig. 1 Assembly cost factors



Technical Cost Modelling (TCM) was developed by the Massachusetts Institute of Technology and is a method mainly focusing on the manufacturing cost, breaking it into its constituent elements, and estimating them separately. TCM provides a model that uses empirical data, regression analysis, theoretical formulae, and the knowledge of experts. TCM allows the direct link and investigation of the interaction between manufacturing cost and process parameters through engineering and physical principles, underlying the process under examination (Monteiro 2001). TCM can provide a much more detailed estimation of the manufacturing cost, but it is weak at capturing the indirect and overhead costs. This favours the use of TCM for the evaluation of competing production technologies.

Function based cost estimating (FUCE) aspires to improve the communication between cost estimators with commercial (CE-C) and engineering (CE-E) backgrounds. The approach enables the communication of the functional requirements of CE-C as the basis of cost estimation, where CE-E works at the detailed

design level, based on a previous similar product family for data collection and development of cost estimates. The two activities are then integrated through function-attribute-product parameter mapping (Roy et al. 2008).

Resource-based modelling is another approach that assesses the resources of materials, energy, capital, time, and information, associated with manufacturing applications. The basic advantage is that it is applicable to all processes (since they all consume the basic resources) and therefore, it provides a measure for the comparison of the relative costs of processes (Esawi and Ashby 2003).

Techno-economical Model Example

The techno-economical models enable the scientific execution of the decision-making process. This paragraph provides an example of a techno-economical model in the case of a Machining (Turning) operation (Eq. 1):

Techno economical model for a turning operation

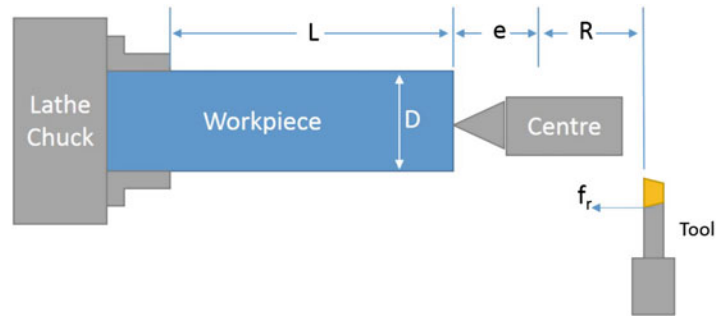
$$\text{Cost per Workpiece} = \left[\begin{matrix} \text{Machine} \\ \text{Rate} \end{matrix} + \begin{matrix} \text{Labor} \\ \text{Rate} \end{matrix} + \begin{matrix} \text{Overhead} \\ \text{Rate} \end{matrix} \right] \times \underbrace{\left[\begin{matrix} \text{Feeding} \\ \text{Time} \end{matrix} + \begin{matrix} \text{Rapid} \\ \text{Feeding} \\ \text{Time} \end{matrix} + \begin{matrix} \text{Portion of} \\ \text{tool insert} \\ \text{replacement} \\ \text{time per} \\ \text{workpiece} \end{matrix} \right]}_{\text{Operating Time per Workpiece}} + \frac{1}{\text{No. of workpieces bet. tool insert changes}} \times \left[\begin{matrix} \text{Cost} \\ \text{per} \\ \text{tool} \\ \text{insert} \end{matrix} \right] \tag{1}$$

Factors contributing to the cost per workpiece include machine, labour, and overhead rates. The contribution of these factors is proportional to the operating time, which comprises the feeding time for material removal, rapid movement time for tool positioning, and tool replacement time (Fig. 2). The tool is a replaceable insert, whose cost is another factor contributing to the cost per workpiece. This “techno-economical” model can be derived from the mechanics and geometry of the turning process. In turning, material is

removed from a workpiece, rotating about an axis of symmetry by a cutting tool or insert, which travels in the axial and radial workpiece directions.

The decision variables of the process are two typical parameters of machining, namely the feed rate f_r [mm/rev], usually expressed as length per revolution, and the Cutting Speed v [m/min]. These decision variables are mapped into the manufacturing attribute “cost”, expressed in [\$/piece] by a techno-economical model as follows:

Cost, Fig. 2 Turning process representation



Mathematical formulation of the techno-economical model

$$C = M[T_F + T_{RF} + T_{IR}] + \frac{1}{N_{IR}}[C_I] \quad (2)$$

Where:

$$T_F = \frac{D(L + e)}{318f_r v}$$

$$T_{RF} = \frac{R}{r}$$

$$T_{IR} = \frac{DL_{td}}{318f_r v T}$$

$$\frac{1}{N_{IR}} = \frac{DL}{318f_r v T}$$

Where:

C is the cost of turning one workpiece [\$]

f_r is the feed per revolution [mm]

v is the cutting speed of the insert along the workpiece surface [m/min]

M is the machine + labour + overhead cost on lathe [\$ / min]

T_F is the feeding time per workpiece [min]

T_{RF} is the rapid feeding time per workpiece [min]

T_{IR} is the insert replacement time per workpiece, assuming that the insert replacement time is distributed evenly over the workpieces [min]

N_{IR} is the number of workpieces between insert changes

C_I is the cost per insert [\$]

D is the diameter of the workpiece [mm]

L is the length of the workpiece [mm]

e is the extra travel at feed rate f_r [mm]

R is the total rapid traverse distance for one part [mm]

r is the rapid traverse rate [mm/min]

t_d is the insert replacement time [min]

T is the tool life [min]

For a given workpiece, the insert material, the feed rate and the machining cost [\$/piece] primarily constitute a function of the cutting speed v . As the cutting speed increases, the material removal rate increases, thereby reducing the machining cost by allowing more pieces to be made per unit time. However, the machining cost also depends, among other things, on tool wear; inserts, creating costs both in terms of acquiring new ones and time lost from production, have to be replaced periodically. As the cutting speed increases further, the wear of the tool also increases, leading to higher tooling costs and more frequent tool replacements; this, in turn, increases the cost per piece.

Product Cost Estimation

According to the life cycle theory, the majority of product costs occur during the manufacturing phase, however, most of these costs are mainly determined in the design phase. The possibility to influence the costs during the design phase is much higher than in the other phases. Therefore, good cost estimation techniques are required (Chryssolouris 2006). Within literature, there is a common classification of cost estimation methods in quantitative and qualitative techniques (Chryssolouris et al. 2008).

Quantitative approaches, based on a detailed analysis of the product design and the manufacturing processes, demand a lot of information (Niazi et al. 2006). In parametric techniques, the cost is expressed as an analytical function of constituent variables, based on statistical methods.

In contrast to quantitative techniques, the qualitative methods seem to be more effective for cost estimation, during the design phase, since they neither require detailed information of the product design nor the manufacturing processes. Case Based Reasoning (CBR), decision support techniques, regression analysis and Artificial Neural Networks (ANNs), are mainly based on a comparison between the new product and the past products in order to provide a first draft cost estimation. Artificial Neural Networks (ANNs) have also been used in product cost estimation. ANNs are trained by utilizing data from past products for the evaluation of the cost of a new product (Cavalieri et al. 2004). Moreover, rule-based approaches, fuzzy algorithms and case-based reasoning (CBR) have been employed for the estimation of the process time and cost (Shehab and Abdalla 2001).

Cross-References

- ▶ [Decision-Making](#)
- ▶ [Factory](#)
- ▶ [Life Cycle Cost](#)
- ▶ [Maintenance](#)
- ▶ [Manufacturing](#)
- ▶ [Manufacturing System](#)
- ▶ [Neural Network](#)
- ▶ [Process](#)
- ▶ [Production](#)
- ▶ [Quality](#)

References

- Alexopoulos K, Mourtzis D, Papakostas N, Chryssolouris G (2007) DESYMA – assessing flexibility for the lifecycle of manufacturing systems. *Int J Prod Res* 45(7):1683–1694
- Belkaoui A (1985) *Accounting theory*. Harcourt Brace Jovanovich, New York
- Cavalieri S, Maccarrone P, Pinto R (2004) Parametric vs. neural network models for the estimation of production costs: A case study in the automotive industry. *Int J of Prod Economics* 91:165–177

- Chryssolouris G (2006) *Manufacturing systems: theory and practice*, 2nd edn. Springer, New York
- Chryssolouris G, Papakostas N, Mavrikios D (2008) A perspective on manufacturing strategy: produce more with less. *CIRP J Manuf Sci Technol* 1(1):45–52
- Esawi AMK, Ashby MF (2003) Cost estimates to guide pre-selection of processes. *Mater Des* 24(8):605–616
- Michalos G, Makris S, Chryssolouris G (2008) An approach to automotive assembly cost modelling. In: 2nd CIRP conference on assembly technologies and systems – CATS2008, University of Windsor, Toronto, 21–23 Sept 2008
- Monteiro AJM (2001) *Production cost modelling for the automotive industry*. Thesis from Universidade Técnica de Lisboa, Instituto Superior Técnico
- Niazi A, Dai JS, Balabani S, Seneviratne L (2006) Product cost estimation: technique classification and methodology review. *J Manuf Sci Eng* 128(2):563–575
- Roy R, Souchoroukov P, Griggs T (2008) Function-based cost estimating. *Int J Prod Res* 46(10):2621–2650
- Shehab EM, Abdalla HS (2001) Manufacturing cost modelling for concurrent product development. *Robot Comput Integr Manuf* 17(4):341–353

Crack Forming

- ▶ [Crack Initiation](#)

Crack Initiation

Fengzhou Fang^{1,2} and Min Lai¹

¹State Key Laboratory of Precision Measuring Technology and Instruments, Centre of MicroNano Manufacturing Technology, Tianjin University, Tianjin, China

²Centre of MicroNano Manufacturing Technology (MNMT-Dublin), University College Dublin, Dublin, Ireland

Synonyms

[Crack forming](#); [Crack nucleation](#)

Definition

Crack initiation is the formation process of a crack, including the incubation period and the embryonic stage.

Theory and Application

Introduction

Fracture failure is one of the biggest threats to the structures in the engineering materials. The fracture process of materials consists of the crack initiation, crack propagation, and final parting. Apparently, the crack plays an important role in the fracture of materials. The cracks can be produced in the process of manufacturing, assembly, and service, which are the interaction results of the material microstructures, loading condition, and environment. Generally, the performance of structures would be adversely affected by the existence of cracks. For example, the cracks in the laser crystal would reduce its laser-induced damage threshold (LIDT), the cracks in the bearing structure are likely to shorten its service life, and the cracks on the optical surface would affect its performance. Therefore, the crack initiation should be avoided or reduced as much as possible in the manufacturing of materials. Taking silicon, for instance, brittle materials easily crack during machining. However, the super smooth surface without cracks can be achieved by optimizing the process conditions and technological parameters (Fang and Venkatesh 1998).

There are many kinds of classification basis for cracks. The cracks can be classified as opening-mode cracks (mode I), sliding-mode cracks (mode II), and tearing-mode cracks (mode III), as shown in Fig. 1. A cracked body can be loaded in any one of these modes or their combinations (Anderson 2005). The cracks can also be classified as surface cracks,

embedding cracks, and through cracks according to their locations in the material. Based on the mode of crack propagation and the relative failure characteristics in the static loading, there are transgranular brittle cracks, transgranular ductile cracks, intergranular brittle cracks, and intergranular ductile cracks. Considering the physical cause for the formation of cracks, the cracks consist of weld cracks, fatigue cracks, hydrogen embrittlement cracks, stress corrosion cracks, creep cracks, and so on. On the basis of relative size to the microstructure of materials, the crack can be classified as macroscopic cracks, mesoscopic cracks, and microscopic cracks. The crack initiation is mainly involved with the microscopic cracks.

Mechanism of Crack Initiation

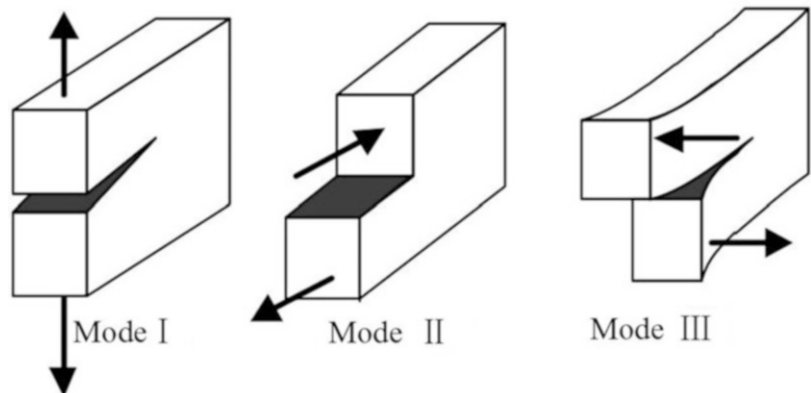
The various microstructural features of materials have fundamental important influence on the mechanism and process of crack initiation. Taking the complex metallic alloy, for example, the microstructural features (not all of which would be present in a particular material) such as dislocation, slip line, precipitate, grain boundary, and second phase would have different effects on the formation process and propagation path of the crack and then on the fracture path (Janssen et al. 2004), as shown in Fig. 2.

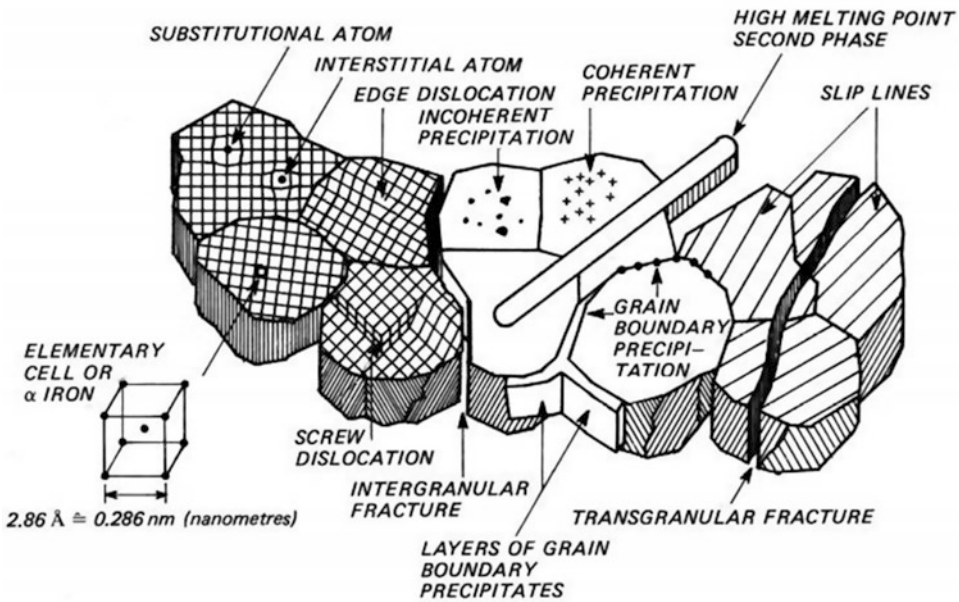
Brittle Crack

The abrupt brittle fracture is very dangerous for material structures. Based on the type of fracture path, there are transgranular fracture and

Crack Initiation,

Fig. 1 Three kinds of cracks according to the loading





Crack Initiation, Fig. 2 Schematic of microstructural features in metallic materials (Reprinted from Janssen et al. 2004, pp. 285, with permission)

intergranular fracture, which correspond to transgranular brittle cracks and intergranular brittle cracks, respectively.

Under static loading, transgranular brittle crack usually propagates along the cleavage plane of the grain. When the material undergoes localized plastic deformation, the materials would respond to the applied loading by separation along the cleavage plane instead by continued plastic deformation if the dislocation motion is hindered for some reason (e.g., dislocation pileup). There are several cleavage crack initiation models based on the dislocation theory, such as Stroh's dislocation piling-up model (Stroh 1957), Cottrell's dislocation reaction model (Cottrell 1958), and Smith's model (Smith 1966). The stress criterion for crack initiation is that the local stress reaches the cleavage fracture stress of material, which is relevant to the grain size and surface energy. The smaller dimensions of grain and higher surface energy usually indicate the greater cleavage fracture stress. In addition, how easily the transgranular brittle cracks initiate and propagate is also related to the lattice resistance to the dislocation motion (Peierls-Nabarro force). The smaller the

Peierls-Nabarro force is, the more easily the dislocations are emitted from the crack tip, which would induce the crack tip blunting, and almost no cleavage crack initiation and propagation would happen, such as the single crystal with FCC or HCP structure. The greater the Peierls-Nabarro force is, the more easily the cleavage fracture occurs, such as covalent bond crystal and ionic crystal. In addition, the grain boundary, sub-boundary, phase boundary, and nonmetallic inclusion would block the motion of dislocation, inducing the dislocation pileup and then the crack initiation and propagation.

The grain boundary of metallic materials is usually thought to be conducive to the material strengthening because of the greater grain-boundary bonding than that inside the grain. However, when the embrittling elements and particles and precipitates segregate along the grain boundaries at certain levels, the grain-boundary bonding would be weakened and leads to the reduction of local effective fracture energy, resulting in the decrease of impact toughness and fracture toughness of materials. As a result, the propagation path of brittle crack changes from the cleavage plane to

the grain boundary, forming the intergranular brittle crack. The critical value depends on the yield strength, grain size, and microstructure of materials. Moreover, the high-temperature environment and the hydrogen embrittlement would also weaken the grain boundary and induce intergranular brittle cracks.

Ductile Crack

Ductile fracture is one of the main failure models for metallic materials, the obvious plastic deformation occurs in materials before fracture. There are transgranular ductile cracks and intergranular ductile cracks according to the propagation path of cracks.

Under static loading, transgranular ductile cracks mainly relate to the second-phase particles and nonmetallic inclusions. The forming process of transgranular ductile cracks is described as follows: the debonding at the boundary of the second-phase particles or the nonmetallic inclusions, or particles themselves cracking at the high-strain zones, causes the nucleation of microvoid, which grows around the particles in the promotion of plastic strain and hydrostatic stress. As the local stress increases, the interactions of microvoids or the microvoids and microcracks initiate the internal necking, inducing microvoid coalescence

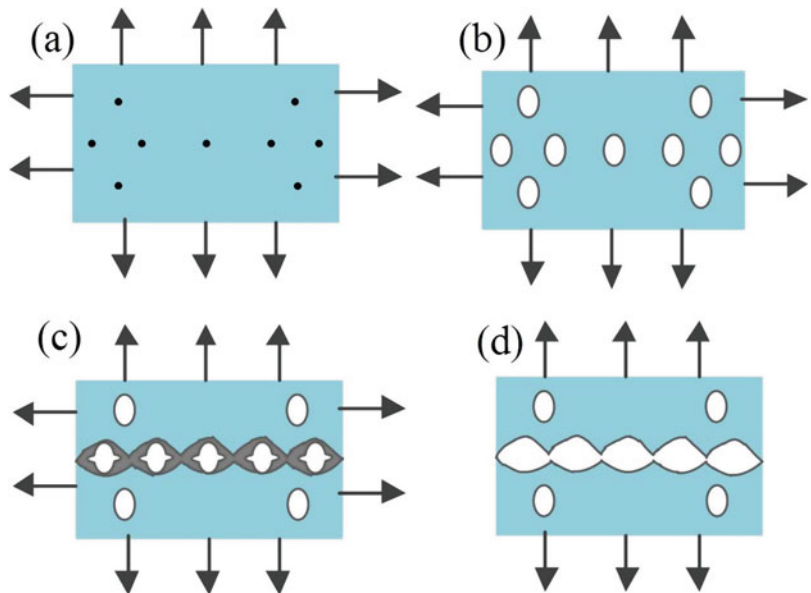
and crack propagation as well as the eventual formation of a continuous fracture surfaces. A schematic of void nucleation, growth, and coalescence in ductile metals is given in Fig. 3. Figure 4 shows the scanning electron microscope (SEM) images of damage during an in situ tensile test of copper; the microvoids/cavities nucleate by interfacial decohesion of inclusions and coalesce along shear directions.

The micro-mechanism of intergranular ductile crack initiation is also related to the growth and coalescence of microvoids in the boundaries of second-phase particles and inclusions. There are two reasons for the crack propagation along the grain boundaries, one is that the impurity segregation and precipitation at the grain boundaries cause the reduction of grain-boundary energy and make it the propagation path of ductile cracks, and the other is that the high-temperature environment weakens the grain boundary and then the grain-boundary sliding resulting from the long-time loading promotes the initiation and propagation of ductile cracks.

Fatigue Crack

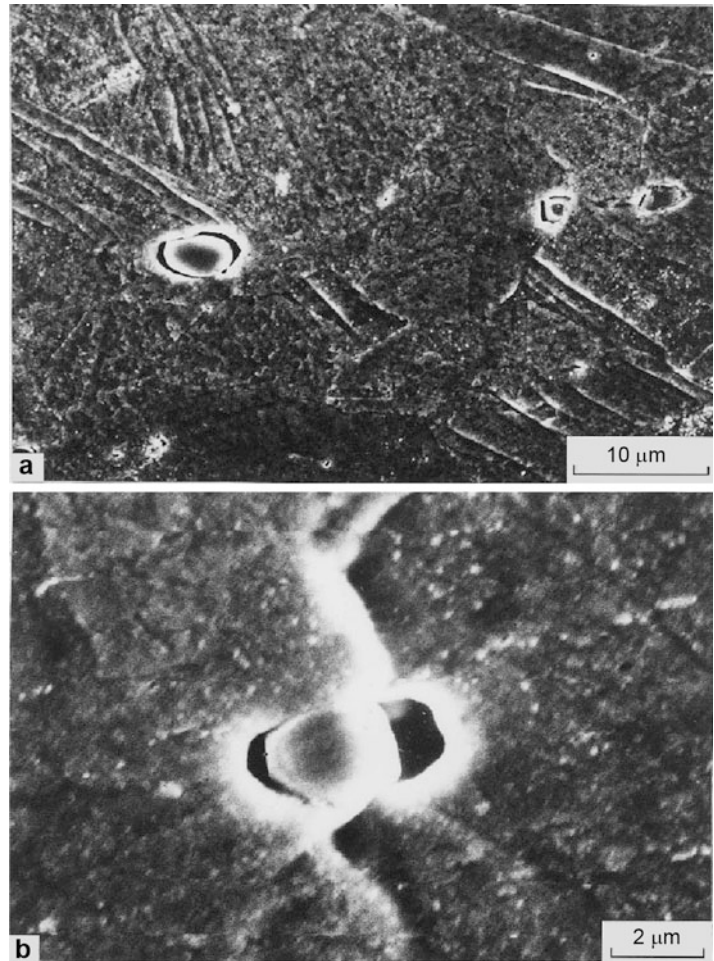
Fatigue crack occurs in the cyclic loading. More than 80 percent of practical structure failures appear in the form of fatigue failure, which have

Crack Initiation,
Fig. 3 Schematic of void nucleation, growth, and coalescence in ductile metals: (a) inclusions in materials; (b) microvoid nucleation and growth; (c) internal necking by strain localization; (d) microvoid coalescence and fracture



Crack Initiation,

Fig. 4 SEM micrographs of damage during an in situ tensile test: (a) complete decohesion of the interface; (b) coalescence along shear directions (Reprinted from Pardoen et al. 1998, with permission from Elsevier)



caused many catastrophic accidents and is now generally recognized as a significant problem. The fatigue failures usually happen in the condition of repeated loading far below the static strength or even the yield strength and without obvious macroscopic plastic deformation previously.

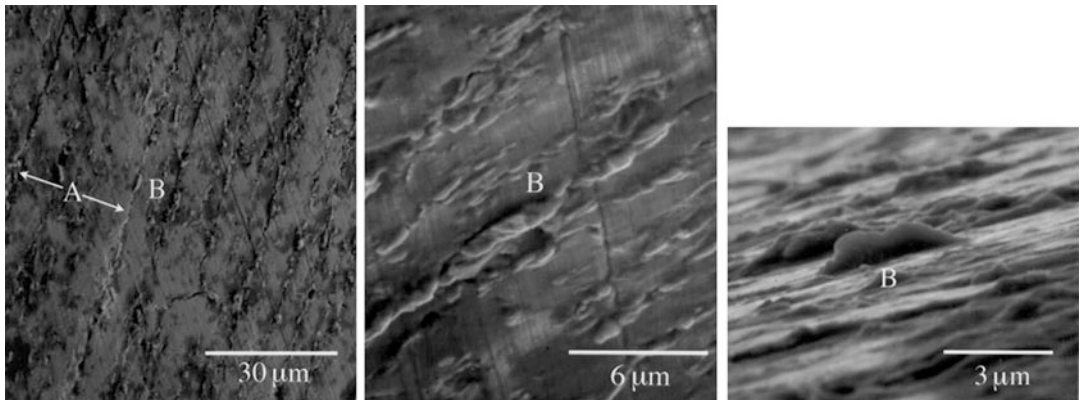
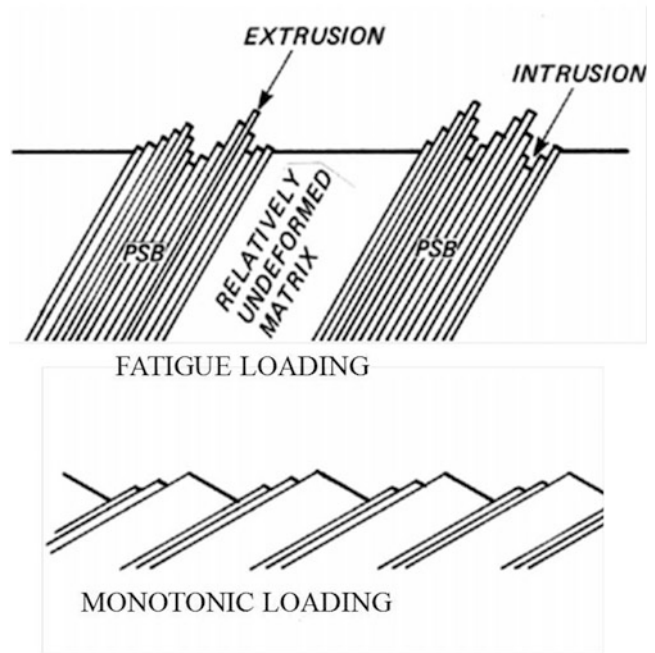
The fatigue life until failure consists of macroscopic crack initiation period and macroscopic crack growth period. The fatigue crack initiation period includes the microcrack nucleation and microcrack growth. The initiation period is supposed to be completed when microcrack growth is no longer depending on the material surface conditions (Schijve 2009).

Fatigue cracks usually initiate at the inclusion, grain boundary, twin boundary, the inhomogeneous region, and the stress concentration region

of materials, deriving from the nonuniform local cyclic plastic deformation, which is the result of cyclic slip. Under fatigue loading, the surface material tends to deform by cyclic slip, the concentration of which is called the persistent slip band (PSB). A large number of random and irreversible cyclic slip deformations in PSBs form the slip steps, intrusions, and extrusions on the surface, inducing the formation of stress concentration region and benefitting to the fatigue microcrack initiation. Figure 5 shows the slip distributions during fatigue and monotonic loading. The parallel microcracks or extrusions were observed by SEM on the surface of Cu after some cyclic deformation, which associated with the persistent slip band (PSB) activity, as shown in Fig. 6. For homogeneous metallic materials, PSBs generally appear on

Crack Initiation,

Fig. 5 Illustration of slip distribution during fatigue and monotonic loading. (Reprinted from Janssen et al. 2004, pp. 304, with permission)



Crack Initiation, Fig. 6 SEM images show surface features typically associated with persistent slip band activity. Microcracks (a) and extrusions (b) are typical for fatigued samples but surprising in a metal with such a fine starting

microstructure. The scratches run parallel to the loading axis of the sample (Reprinted from Agnew et al. 1999, with permission from Springer)

the free surface. For heterogeneous material, fatigue crack often initiated at inclusions, resulting from the interaction of slip band and inclusion. The fatigue crack initiation at a notch or some other geometric discontinuity is promoted by the inhomogeneous stress distribution.

There are three kinds of nucleation site for fatigue crack. The first one is the slip band; these

fatigue cracks are commonly seen in many ductile pure metals, single-phase alloys, and high-strength alloys with nonprecipitation strengthening in the condition of high-cycle fatigue with slight higher stress than fatigue limit. The second one is the grain boundary, which is common in high-strain fatigue or in high-temperature environment or in hydrogen embrittlement. The third one is the inclusion or

second-phase particle; these fatigue cracks usually form in commercial alloys.

In practice, the micron-scale crack nucleation at slip band and grain boundary, or the roughening of fatigue specimen surface, is defined as the initiation period of fatigue crack in the view of physics and material science. From an engineering perspective, the resolution limit of nondestructive testing equipment is thought as the critical dimension of crack initiation.

Environmental Influence on Crack Initiation

The service environment including the temperature, medium, surrounding atmosphere, and so on, together with the stress, would have a strong influence on both crack initiation and crack growth of structural components.

In an aggressive environment, the chemical reaction between the material and corrosive medium would promote the initiation and propagation of cracks in static loading, inducing the failure in low stress level, which is called the stress corrosion. The combination of corrosion and cyclic loading would accelerate the initiation and propagation of fatigue cracks.

In smelting, machining, and service process of metallic materials, the invasive hydrogen atoms diffuse and migrate with dislocations in the material; the local enrichment of hydrogen (usually at defect locations such as phase boundary, grain boundary, microcrack, and microvoid) gives a rise to the decrease of atomic bonding nearby, promoting the crack initiation. This phenomenon is known as the hydrogen embrittlement.

At high temperature, the materials usually evolve by diffusion, aging, dislocation recombine, recrystallization, and so on. The microstructure of material comes to change, showing up as the time-dependent plastic deformation of material at a constant stress, and this process is called creep. High temperature would weaken the grain boundary, with assistance from stress, creep cavities, or wedge cracks which easily initiate and grow at grain boundary (Wilkinson and Vitek 1982).

Detection of Cracks

In engineering, the common nondestructive testing methods for cracks mainly include various

types such as the visual testing (VT), penetrant testing (PT), magnetic particle testing (MT), radiographic testing (RT), ultrasonic testing (UT), eddy current testing (ET), thermal infrared testing (TIR), and acoustic emission testing (AE) (Hellier 2003). Since each method has its own advantages and limitations, the appropriate method or the combination should be chosen according to the actual situation. The microstructure of crack is usually analyzed by optical microscope, scanning electron microscope, and transmission electron microscope. However, the monitoring of the crack initiation is very difficult; it generally needs to design the detection scheme flexibly according to the situation. For example, microcracks on the monocrystalline silicon surface occurred during nanoindentation can be examined by absorbed energy (Fang et al. 2007).

Cross-References

- ▶ Deformation
- ▶ Ploughing
- ▶ Surface Integrity

References

- Agnew SR, Vinogradov AY, Hashimoto S, Weertman JR (1999) Overview of fatigue performance of Cu processed by severe plastic deformation. *J Electron Mater* 28(9):1038–1044
- Anderson TL (2005) *Fracture mechanics: fundamentals and applications*, 3rd edn. CRC Press, Florida
- Cottell AH (1958) Theory of brittle fracture in steel and similar metals. *Trans Metall Soc AIME* 212:192–203
- Fang FZ, Venkatesh VC (1998) Diamond cutting of silicon with nanometric finish. *CIRP Ann Manuf Technol* 47:45–49
- Fang FZ, Liu Y, Pei QX (2007) Method of examining surface cracks on monocrystalline silicon. *Key Eng Mater* 364–366:902–924
- Hellier CJ (2003) *Handbook of nondestructive evaluation*. McGraw-Hill, New York
- Janssen M, Zuidema J, Wanhill R (2004) *Fracture mechanics*, 2nd edn. Spon Press, London/New York
- Pardoen T, Doghri I, Delannay F (1998) Experimental and numerical comparison of void growth models and void coalescence criteria for the prediction of ductile fracture in copper bars. *Acta Mater* 46(2):541–552
- Schijve J (2009) *Fatigue of structure and materials*, 2nd edn. Springer, Dordrecht

- Smith E (1966) The nucleation and growth in cleavage microcracks in mild steel. In: Proceedings of the conference on the physical basis of yield and fracture. Inst Phys Soc. Oxford, pp 36–46
- Stroh AN (1957) A theory of the fracture of metals. Adv Phys 6:418–465
- Wilkinson DS, Vitek V (1982) The propagation of cracks by cavitation: a general theory. Acta Mater 30:1723–1732

Crack Nucleation

- ▶ [Crack Initiation](#)

Cradle-to-Cradle Assessment

- ▶ [Life Cycle Assessment](#)

Create

- ▶ [Engineering Design](#)

Creation

- ▶ [Synthesis](#)

Creep Feed Grinding

Eckart Uhlmann
Fraunhofer Institute for Production Systems and Design Technology, Berlin, Germany

Synonyms

[Creep grinding](#); [Deep grinding](#)

Definition

Various standards define creep feed grinding as a peripheral grinding process with a relatively large

depth of cut a_c and accordingly low feed rate v_f (ISO 3002-5 1989; VDI 3390 2014; VDI 3391 2016). Commonly, surface grinding is referred to as creep feed grinding when depth of cut $a_c \geq 0.1$ mm and a feed rate $v_f \leq 3,000$ mm/min are applied. In contrast, pendulum grinding can be characterized by varying a_c and v_f opposingly; hence, a relatively high feed rate v_f and low depth of cut a_c are applied. For a better understanding of creep feed grinding, comparisons will be drawn between both mentioned grinding strategies in the following.

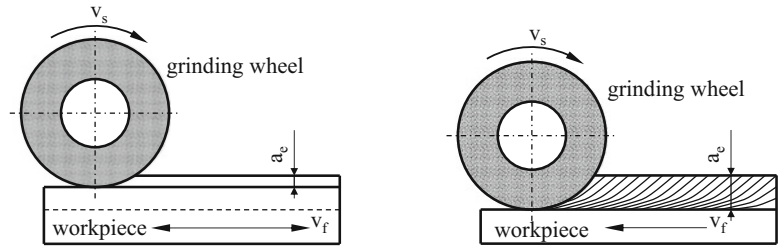
Theory and Applications

Creep feed grinding is a special grinding strategy where considerable material removal rates and high surface qualities are attained along with quite low grinding wheel wear. It was applied in the early 1950s for the first time and led to an extensive development of machines, grinding tools, and grinding technology in order to fully exploit the potential of this grinding process (Uhlmann 1994). Through creep-feed grinding, the total stock removal is being cut in only one or a few passes. In comparison, the depth of cut a_c in pendulum grinding with equal specific material removal rates Q'_w is in the range of a few hundredths of a millimeter, and the feed rate is in a scope of several meters per minute. The speed ratio $q = v_g/v_f$ is greater by the factor of 100–1,000 for creep-feed grinding compared to pendulum grinding. Figure 1 depicts the two process variants pendulum grinding and creep feed grinding and compares characteristic process parameters. Creep feed grinding can be used for both surface grinding and cylindrical grinding. The feed motion may be radial to the workpiece as in the case of cylindrical plunge grinding, or it may be axial as in the case of cylindrical traverse grinding or peal grinding (Klocke and König 2005).

A negative profile of the grinding wheel is reproduced into the workpiece by creep feed grinding. Mostly the time of one finishing run equals the total machining time; thus, the auxiliary process time in creep feed grinding is considerably lower as in the case of pendulum grinding.

Creep Feed Grinding,

Fig. 1 Comparison of pendulum grinding and creep feed grinding (Based on Marinescu et al. 2007)



Pendulum grinding		Creep feed grinding
0.001 - 0.05	Depth of cut a_c (mm)	0.1 - 30
100 - 500	Feed rate v_f (mm/s)	0.1 - 40
40 - 400	Speed ratio q (-)	3,000 - 300,000
1.4 - 4.5	Geometrical contact l_g (mm)*	14 - 110
Function of infeed	Number of grinding passes	Usually one

* radius of the grinding wheel $r = 200$ mm

Creep Feed Grinding,

Fig. 2 Differences between pendulum grinding and creep feed grinding (Based on guideline VDI 3390 2014 with reprint courtesy of the German Association of German Engineers (Verein Deutscher Ingenieure e. V.))

Pendulum grinding		Creep feed grinding
High	Feedrate	Low
Low	Infeed	High
High	Number of tool passes	One (or a few)
Larger	Average chip thickness	Smaller
Smaller	Average chip length	Larger
Lower	Grinding temperature	Higher
Lower	Grinding forces	Higher
Larger	Surface roughness	Smaller
Smaller	Total wear on the grinding wheel	Larger

The geometrical contact length l_g between workpiece and grinding wheel rises with increasing depth of cut a_c , whereby the transport of coolant into the grinding contact zone and the removal of grinding chips are impeded. As this causes friction and heat, porous grinding wheels with low hardness and an effective coolant supply might be applied. Furthermore, up-grinding, where the vectors of the cutting and the feed motion have opposite directions, is also a way to allow coolant to access the contact zone faster, and especially the grains contacting the final product surface are optimally cooled.

The advantages of creep-feed grinding over pendulum grinding are higher workpiece surface qualities and lower grinding wheel wear since a considerably higher speed ratio q and depth of cut a_c lead to a smaller average chip thickness and hence to a lower surface roughness: The larger contact area between tool and workpiece results in a higher number of active cutting edges compared to pendulum grinding. Creep feed grinding is used industrially especially for the manufacturing of precise profiles, as guideways and clamping profiles for turbine blades. Figure 2 lists the differences between pendulum grinding and creep feed grinding (Heisel et al. 2014).

High-Performance Creep Feed Grinding

The development of the creep feed grinding process toward higher material removal rates Q'_w led to the term high-performance creep feed grinding. Firstly, high-speed grinding was developed by increasing grinding wheel circumferential speed v_s . Later on, with an additional increase of the feed rate v_f high-performance creep feed grinding provided even higher material removal rates Q'_w and hence the opportunity of shorter primary process times. Figure 3 categorizes the mentioned creep feed grinding processes depending on grinding wheel circumferential speed v_s and depth of cut a_e .

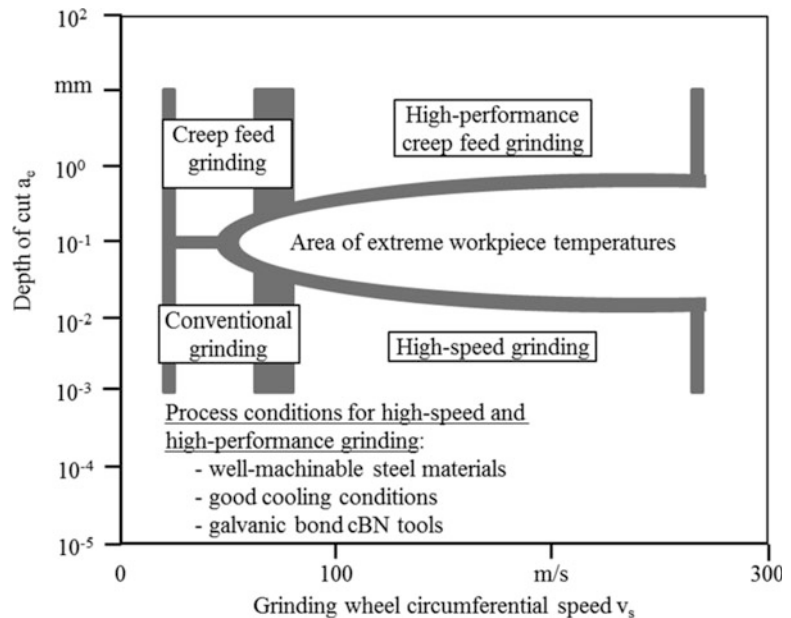
Machines used for high-performance creep-feed grinding require more demanding features due to higher grinding forces and temperatures compared to conventional creep feed grinding (Marinescu et al. 2007):

- Superior stiff structural design or rigid concrete construction
- Resilient guiding elements
- Potent spindle drives and mountings
- User-friendly cooling system and lubricant
- Adjusted grinding tools and dressing gear
- Efficient control equipment

For grinding wheel circumferential speeds $v_s \geq 100$ m/s, special grinding wheels have to be engaged. Only few corundum grinding wheels can be used at grinding wheel circumferential speeds v_s up to 125 m/s. Metallic bond cBN grinding wheels allow extremely high grinding wheel circumferential speeds $v_s \geq 100$ m/s. To acquire high removal rates Q'_w , high grinding wheel circumferential speeds v_s and feed rates v_f are necessary. The enlargement of the feed rate v_f and hence a larger specific material removal rate Q'_w lead to a rise of temperature in the contact zone between the workpiece and the grinding tool. Nevertheless, a high contact zone temperature does not inevitably lead to a high temperature in the generated workpiece surface, as, e.g., the local contact time is shorter with increasing feed rates v_f . The impact of an increased grinding wheel circumferential speed v_s can be summarized as follows: Less grinding forces and tool wear lead to higher surface qualities due to smaller chip dimensions. On the other side the temperature in the contact zone between the grinding wheel and the workpiece increases with higher grinding wheel circumferential speeds v_s (Tawakoli 1990).

Creep Feed Grinding,

Fig. 3 Categorizing variants of creep feed grinding depending on the grinding wheel circumferential speed v_s and depth of cut a_e (Based on Werner and Tawakoli 1988)



Creep Feed Grinding with Continuous Dressing

Creep feed grinding makes it possible to reduce machining times through a significant increase in material removal rates. CBN and diamond grinding wheels can be used as well as conventional grinding wheels. There are particular advantages of combining creep feed grinding with continuous dressing (CD) when conventional grinding wheels are used. Conventional grinding wheels are dressed continuously during the grinding process with a diamond profile roller which has at least the width of the grinding wheel. As a result, the profile of the grinding wheel is constantly regenerated, and new sharp cutting grains get engaged in the grinding process. Hereby, high profile accuracy along with high material removal rates can be achieved (Pearu and Howes 1979; Saljé 1984). Due to the continuous feed motion, the grinding wheel diameter is constantly reduced as a result of the dressing process. To achieve a plane and parallel workpiece surface during creep feed grinding, the diameter reduction of the grinding wheel must be compensated. Thus a precise control of the spindle and dressing roller feed is inevitable (Uhlig et al. 1982). When conventional creep feed grinding is applied, the achievable specific material removal rate depends very much on the material removal as the grinding wheel's sharpness drops as a result of wear. Therefore the maximum achievable material removal is considerably reduced. In contrast, material removal in CD grinding only depends on the grinding wheel's volume which can be dressed.

Creep Feed Grinding with Continuous In-Process Sharpening

In order to maintain the cutting ability of the grinding wheel during grinding, continuous in-process sharpening (CIS) was developed to be applied in pendulum grinding and creep feed grinding of ceramics (Tio 1990; Uhlmann 1994). The aim of CIS is to ensure low and constant grinding forces as well as small and constant surface roughness values along with uniform grinding wheel wear. Through the sharpening process, an optimal constant protrusion of the abrasive grain is obtained. Thus, a balance between reduction of grain protrusion by

grinding and increase of grain protrusion by sharpening is established. By implementing CIS it is possible to control grinding forces, wear mechanisms, and surface qualities to the greatest possible extent. Based on vast technological investigations, Uhlmann (1994) developed a process model for practically oriented process dimensioning of creep-feed grinding for high-strength ceramics with CIS. Only few grinding experiments are needed to obtain the optimal operating point for any grinding process.

Cross-References

- ▶ Grinding
- ▶ Grinding Machines
- ▶ Grinding Monitoring
- ▶ Grinding Parameters
- ▶ Grinding Tool Structuring
- ▶ Grinding Wheel

References

- Heisel U, Klocke F, Uhlmann E, Spur G (2014) Handbuch Spanen [Handbook Chip Removal], 2nd edn. Hanser, Munich. (in German)
- ISO 3002-5 (1989) Grundgrößen beim Spanen und Schleifen, Teil 5: Grundbegriffe für Schleifverfahren mit Schleifscheiben [Basic quantities in cutting and grinding, Part 5: Basic terminology for grinding processes using grinding wheels]. Beuth, Berlin. (in English or French)
- Klocke F, König W (2005) Fertigungsverfahren 2, Schleifen, Honen, Läppen [Production Methods 2: Grinding, Honing, Lapping], 4th edn. Springer, Berlin/Heidelberg. (in German)
- Marinescu ID, Hitchiner M, Uhlmann E, Rowe WB, Inasaki I (2007) Handbook of machining with grinding wheels. CRC/Taylor & Francis Group, Boca Raton
- Pearu TRA, Howes TD (1979) The application of continuous dressing in creep feed grinding. In: Proceedings of the 20th MTDR2, 1999
- Saljé E (1984) Abrichten während des Schleifens, Grundlagen, Leistungssteigerungen, Wirtschaftlichkeit [Dressing during the grinding process, basics, increase in performance, efficiency]. 4. Feinbearbeitungskolloquium, Braunschweig. (in German)
- Tawakoli T (1990) Hochleistungs-Flachschleifen, Technologie, Verfahrensplanung und wirtschaftlicher Einsatz [High performance creep feed grinding, technology, process planning and economical use]. VDI-Verlag GmbH, Düsseldorf. (in German)
- Tio TH (1990) Pendelplanschleifen nichtoxidischer Keramiken [Pendulum grinding of non-oxide

- ceramics]. Dissertation, Technical University of Berlin. (Produktionstechnik – Berlin 80) Hanser Fachbuchverlag, Munich (in German)
- Uhlig U, Redeker W, Bleich R (1982) Profilschleifen mit kontinuierlichem Abrichten [Profile grinding with continuous dressing]. *Werkstatttechnik* 72(6):313–317. (in German)
- Uhlmann EG (1994) Tiefschleifen hochfester keramischer Werkstoffe [Creep feed grinding of high-strength ceramics]. Dissertation, Technical University of Berlin. Hanser (Produktionstechnik – Berlin 129) Fachbuchverlag, Munich. (in German)
- VDI 3390 (2014) Tiefschleifen [Creep feed grinding]. Beuth, Berlin. (in English or German)
- VDI 3391 (2016) Pendel-Planschleifen und Pendel-Profilschleifen mit Umfangsschleifscheiben [Pendulum surface and pendulum profile grinding with peripheral grinding wheels]. Beuth, Berlin. (in English or German)
- Werner G, Tawakoli T (1988) Fortschritte beim HEDG-Verfahren mit CBN-Schleifscheiben [Progress in high efficiency deep grinding (HEDG) with cubic boron nitride]. *Ind Diamanten Rundsch* 22(1):17–24. (in German)

Creep Grinding

- ▶ [Creep Feed Grinding](#)
- ▶ [High-Performance Dry Grinding](#)

Cropping

- ▶ [Billet Shearing](#)

Cross Wedge Rolling

Bernd-Arno Behrens
Institute of Forming Technology and Machines,
Leibniz Universität Hannover, Garbsen, Germany

Synonyms

[Flashless](#); [Forming](#); [Preforming](#)

Definition

Cross wedge rolling is a forming process for reshaping circular cylindrical billets to plastic

rotationally symmetrical workpieces with variable diameter in axial direction using two oppositely moving wedge-shaped tools. While in cross rolling the rolled material is passed through two or more rolls to reduce the overall thickness of the parts, in cross wedge rolling, the wedges of the tools lead to an unequal mass distribution along the main axis. It is mostly used for preforming, but also some shafts are formed entirely by cross wedge rolling. Depending on the tool geometry, three different process variants can be distinguished:

- Cross wedge rolling with convex curved tools rotating in the same direction
- Cross wedge rolling with a fixed concave tool and a rotating convex tool
- Cross wedge rolling with two flat wedge tools linearly moving in opposite directions

The geometry and arrangement of the tools of the three different process variations for cross wedge rolling are shown in Fig. 1 (Lange 1988, Chapter 4.3.2.2).

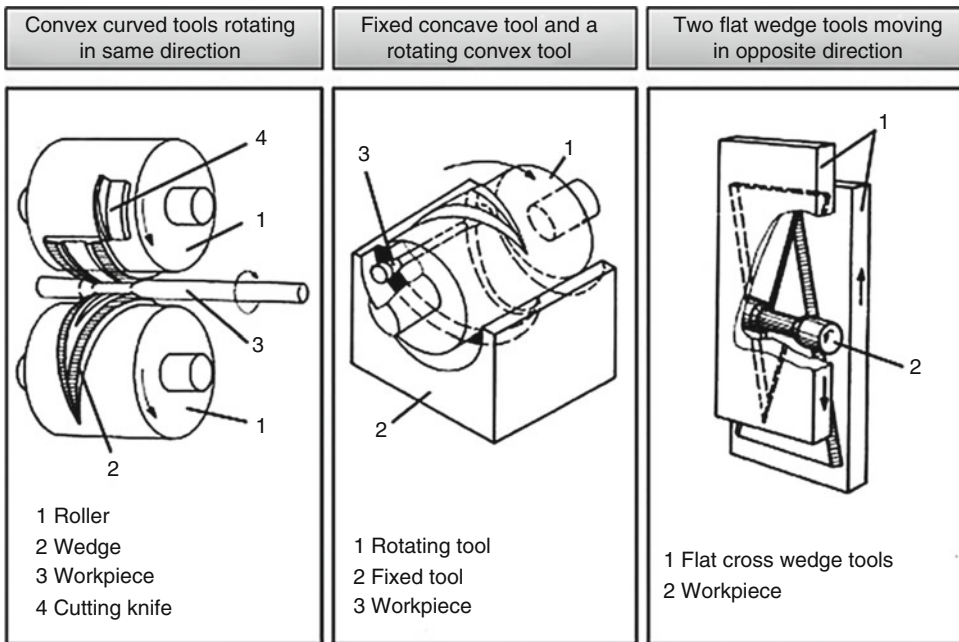
Theory and Application

Advantages of Cross Wedge Rolling

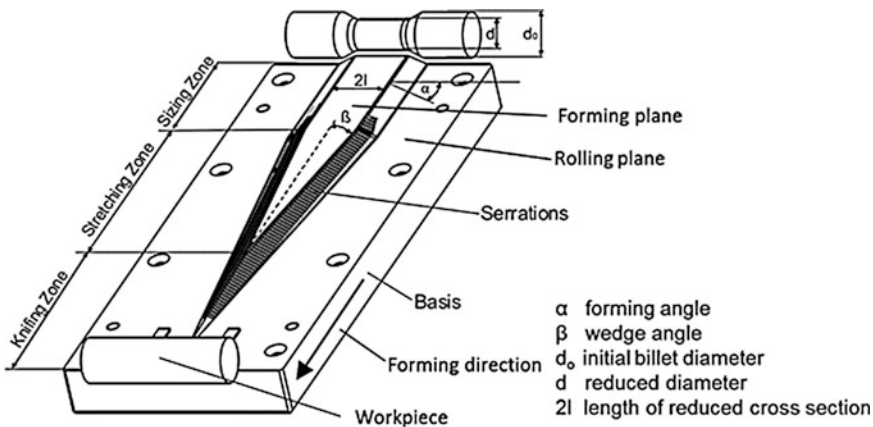
The main advantages of the cross wedge rolling technology in comparison with other preforming technologies are:

- High productivity
- Material utilization of up to 100%
- Low operating costs
- Less energy consumption
- Better product quality (compared to machining or casting)
- Very high cross-sectional reduction with high angles
- High geometrical tolerances
- Easy tool and machine concept

Although the cross wedge rolling technology has a lot of advantages, it has not been widely accepted throughout the forging community. One of the main reasons is the complexity of cross wedge rolling tools and process design. The tool



Cross Wedge Rolling, Fig. 1 Process variants for cross wedge rolling according to Lange (1988) (Reprinted with permission of Springer)



Cross Wedge Rolling, Fig. 2 Flat cross wedge tool and corresponding workpiece

design is difficult because of potential failure mechanisms that can be encountered during cross wedge rolling processes. The risk of faulty manufactured parts increases even more for cross wedge rolling parts with complex shapes.

Geometrical Parameters of Cross Wedge Rolling Tools and Billets

Cross wedge rolling tools, round or flat wedge tool design, are divided into different forming zones, the knifing zone, guiding zone, stretching

zone, and sizing zone (Li et al. 2002). Most tools are designed with only three zones (see Fig. 2); in this case, the guiding zone, between knifing and stretching zone, is eliminated (Pater 2010). This reduces the tool length without reducing workpiece quality.

Regardless of process variants, the geometrical parameters of cross wedge tools are the forming angle α , the wedge angle β , the workpiece diameter d_o , the reduced diameter d , and the reduced cross-sectional length $2l$. The angle α is located

between the rolling plane and the forming plane. The angle β is situated between the rolling direction and the shoulder plane and defines the forming progress during the rolling process. An important rolling parameter is the cross-sectional reduction ΔA . If the cross-sectional reduction is too high ($\Delta A > 70\%$), two or more reduction steps are necessary, and if the cross-sectional reduction is too low ($\Delta A < 20\%$), a rolling process cannot be established.

The shoulder angle α , the wedge angle β , and the cross-sectional reduction ΔA are the most important parameters for the design of the different forming zones. The form and length of the different forming zones and therefore the dimension of the cross wedge rolling tool depend mostly on these parameters.

In the first zone – the knifing zone – a V-shaped cut is centered upon the billet. Within the subsequent stretching zone, the central cut is dilated to a designated value, and the billet is stretched in longitudinal direction. Within the final sizing zone, the billet is, at least once, rotated around its longitudinal axis. Only minimal forming is done in this zone in which the wedge sides are parallel, and tolerances are adjusted (Doege and Behrens 2010). The serrations on the wedge sides in the knifing and stretching zone are necessary to enable a rotation of the billet. In cross wedge rolling operations, the serrations increase the friction so that the billet rotates during the process. The use of lubrication in cross wedge rolling would be counterproductive

since it would interfere with the rotating of the billet. The serrations can leave marks on the workpiece; therefore, the serrations end in the sizing zone, so that eventual marks can be removed.

Process Parameters in Cross Wedge Rolling

The main process parameters are billet temperature, tool temperature, and rolling speed. The billet temperature depends on the material used, like in forging. Tool heating is used to reduce manufacturing tolerances. Due to the heat transfer, the hot billets heat up the tools, causing them to expand during the forming process and resulting in different end geometries. Furthermore, heated tools are needed to avoid a cooling of the billet. Especially for parts with complex shapes, cooling is a challenge due to the long contact time between billet and tool. Various heating concepts can be taken into consideration for tool heating in cross wedge rolling: gas fired, infrared radiation, laser, or induction. A temperature reduction impairs the formability of forged parts and therefore increases the risk of defectively manufactured parts. The rolling speed affects the rolling quality of the billet. The lower the rolling speed, the lower is the risk of improperly formed workpieces.

The geometrical and process parameters have to be in a specific size range in order to enable a functional rolling process. Depending on the chosen parameter values, the tendency toward workpiece failure can rise and fall (see Fig. 3).

Cross Wedge Rolling,

Fig. 3 Influence of process and geometrical parameters on cross wedge rolling defects

Parameter	Range	Tendency	Roll-force	Improperly formed workpiece	Surface defects	Internal defects
Forming angle α [°]	15 - 45	→ 15°	↑	↓	↑	↑
		→ 45°	↓	↑	↓↑	↓
Wedge angle β [°]	3 - 15	→ 3°	↓	↓	-	↓
		→ 15°	↑	↑	-	↑
Cross section reduction ΔA [%]	20 - 70	→ 20 %	↓	↓	↓	↓
		→ 70 %	↑	↑	↑	↑
Rolling speed v [m/s]	0,1 - 4,0	→ 0,1 m/s	↓	↓	-	-
		→ 4,0 m/s	↑	↑		
Edge rounding [°]	5 - 25	→ 5 mm	↑	-	↑	-
		→ 25 mm	↓		↓	

Defects in Cross Wedge Rolling

Johnson and Mamalis (1977) distinguish between three categories of failure mechanisms: improperly formed workpiece cross section, surface defects, and internal defects (see Fig. 4).

Li et al. have investigated defects occurring in cross wedge rolling (Li and Lovell 2008). Improperly formed cross sections are characterized by compression of the workpiece without distributed material at its axis (see Fig. 4a). If the workpiece has excessive slip, it fails to rotate, basically preventing the rolling process which leads to an improperly formed cross section by merely compressing the workpiece. To ensure the interfacial friction forces in all zones of the cross wedge rolling tool is one of the main challenges in the development of a new cross wedge rolling process.

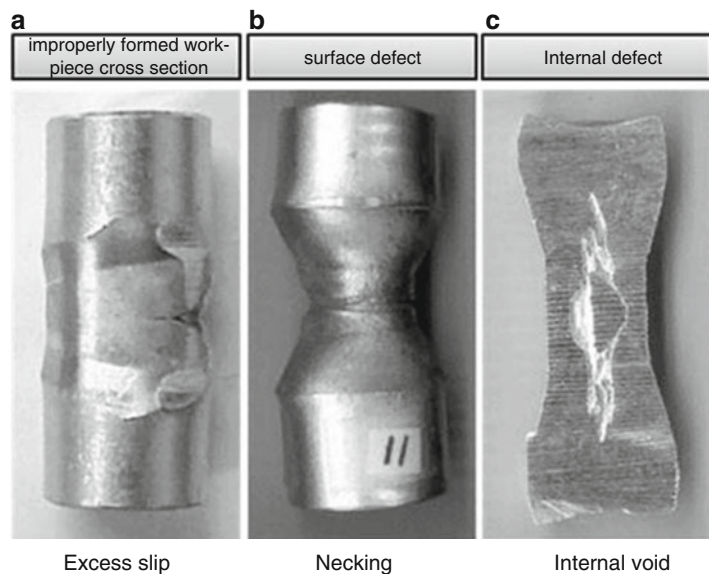
The second defect of cross wedge rolled parts is the surface defect (see Fig. 4b) occurring due to the CWR tool design, e.g., the serrations of the wedges. The wedge can leave marks on the reduced part. The serrations are machined onto the surface of cross wedge rolling wedges. These serrations can leave marks on the surface of the cross wedge rolling parts. Parts with surface defects cannot be used in further processing since the defects reduce the mechanical properties of the parts so that they do no longer meet the

surface requirements. Another possible surface defect is the final size of the cross wedge rolling parts. Especially for flash-reduced final forming processes, the cross wedge rolling parts have to be in a small range of tolerances. The production of cross wedge rolling parts with small tolerances depends on the roll gap between the wedges. The roll gap changes during cross wedge rolling processes due to the heating of the tools by the high billet temperatures.

Internal defects (see Fig. 4c) are cavities along the longitudinal axis in the workpiece. Especially for mechanical products with high loads and high requirements on the microstructure, these cavities are a problem, since they are weak points in the cross wedge rolling parts. Under high loads, the parts are likely to fail at this point. The development of cavities during rolling processes is also known as the Mannesmann effect. The Mannesmann effect occurs due to a combination of mechanical and thermal loads on the part during rolling processes. Alternating tensile and pressure loads are the main reason for the Mannesmann effect. Depending on the temperature of the billet, these loads exceed the formability of the part, so the cavities are formed. The Mannesmann effect is therefore a consequence of the chosen process parameters and is especially critical for complex parts due to the high strain rate.

Cross Wedge Rolling,

Fig. 4 Failure mechanisms in cross wedge rolling (Li and Lovell 2008) (Reprinted with permission of Springer)





Cross Wedge Rolling, Fig. 5 Examples for cross wedge rolled parts (Reprinted courtesy of Officina Meccanica Sestese (OMS) S.p.A., www.oms-spa.it)

Cross Wedge Rolling Workpiece Materials

Nearly all metallic materials can be processed by cross wedge rolling. With the correct process design, even brittle materials can be rolled without defects due to high tensile stress (Lange 1988, Chapter 4). Industrially manufactured rolled parts mainly consist of steel, e.g., 42CrMo4 and 38MnVS6. State of the art is rolling at a temperature between 1.050 and 1.250 °C, the so-called hot forging. Latest research projects have shown that cross wedge rolling is also possible in warm forging, at temperatures between 650 and 950 °C (Kache et al. 2011).

The use of aluminum alloys like EN AW-6082 and EN AW-7075 is less common. One major problem in rolling aluminum is adhesion. While rolling aluminum parts, the material of the billet has the tendency to stick to the surface of the tools. The experience in rolling titanium and other valuable materials is very low due to the complex process design and tool layout. Acceptable tool geometries (e.g., forming, wedge angle) depend on the rolled material.

Cross Wedge Rolling Workpiece Examples

See Fig. 5.

References

Doege E, Behrens B-A (2010) Handbuch Umformtechnik: Grundlagen, Technologien, Maschinen [Metal forming handbook: fundamentals, technologies, machines], 2nd edn. Springer, Berlin/Heidelberg. (in German)

Johnson W, Mamalis AG (1977) A survey of some physical defects arising in metal working processes. In: Proceedings of the 17th international MTDR conference, Birmingham, 20–24 Sept 1976. Macmillan, London, pp 607–621

Kache H, Groß D, Nickel R (2011) Pioneering a new forming concept. Forging Penton Media 20(4):20–23

Lange K (1988) Umformtechnik band 2: Massivumformung [Metal forming. Bd. 2: forging], Chapter 4. Springer, Berlin u.a. (in German)

Li Q, Lovell M (2008) Cross wedge rolling failure mechanisms and industrial application. Int J Adv Manuf Technol 37(3–4):265–278

Li Q, Lovell MR, Slaughter W, Tagavi K (2002) Investigation of the morphology of internal defects in cross wedge rolling. J Mater Process Technol 125–126:248–257

Pater Z (2010) Development of cross-wedge-rolling: theory and technology. In: Steel research international, Proceedings of the 13th international conference on metal forming, Toyohashi, 19–22 Sept 2010. Verlag Stahleisen, Düsseldorf, pp 346–349

Cubic Boron Nitride

► [Cutting of Inconel and Nickel Base Materials](#)

Cubic Boron Nitride (CBN)

► [Superabrasives](#)

Cut Ability

► [Machinability](#)

Cutting

► [Shear Cutting](#)

Cutting Edge Geometry

Jens Köhler

ProWerk GmbH, Wedemark/Hannover, Germany

Synonyms

Chamfer; Honed cutting edges; Macro geometry; Micro geometry; Rounded cutting edge

Definition

The cutting edge geometry is the geometry of the cutting wedge in the orthogonal cut of the tool. It has to be divided in the cutting edge micro geometry and macro geometry. The macro geometry is described by the rake, clearance, and wedge angle. The micro geometry is described by the cutting edge rounding and the chamfer geometry. The cutting edge geometry has a big influence on the machining forces, the chip formation, and the tool wear.

Theory and Application

Introduction

Besides the process parameters and tool coatings, the cutting edge geometry shows a major impact on the chip formation, machining forces, and tool wear. The right choice of the cutting edge geometry enables a higher productivity, workpiece quality, and a reduced tool wear (Byrne et al. 2003). The cutting edge geometry is the geometry of the cutting wedge in the orthogonal cut (ISO 3002-1 1982). The cutting edge macro geometry is described via the rake angle γ , clearance angle α , and wedge angle β . The sum of these angles is 90° . The choice of the angle values depends on the process and the workpiece material, whereby the rake angle can be positive or negative (Tönshoff and Denkena 2004). However, besides the process parameters, the cutting edge macro geometry has

a big influence on the chip formation process (Shaw 1984). For example, a change of the clearance angle by -1° leads to an increase of the cutting force of 1–2%. Furthermore, the tool wear is influenced by the cutting edge geometry. The wedge angle determines the stability of the cutting edge and though the resistance against tool breakage. The clearance angle affects the friction between tool and workpiece and though the flank wear of the tool.

Current research focuses mainly on the cutting edge micro geometry (Denkena et al. 2011). The micro geometry describes the wedge geometry within a distance of up to $150\ \mu\text{m}$ from the ideal cutting edge. The main geometry features are the cutting edge rounding and the chamfer geometry on the rake and the clearance face. In the following, these geometry features are described and their main impact on the process variables is shown.

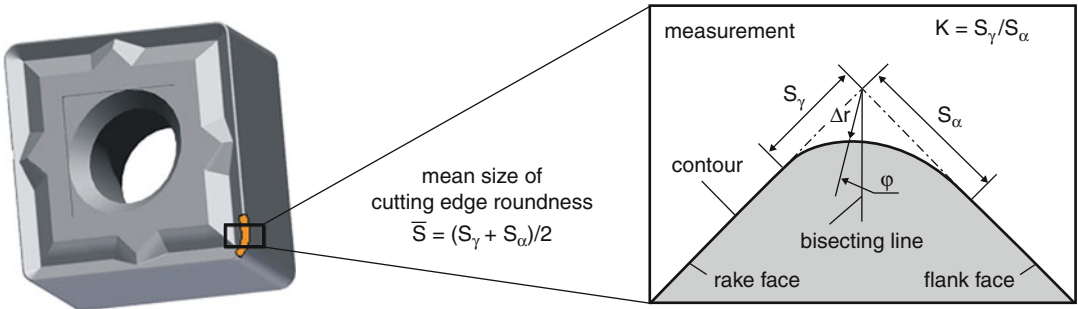
Cutting Edge Rounding

Geometry

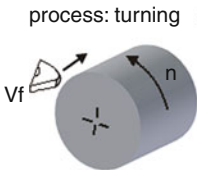
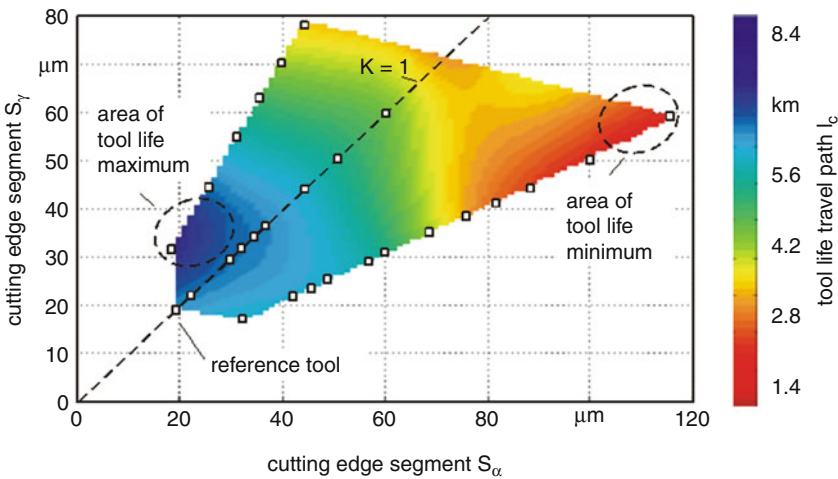
Conventionally, the cutting edge rounding has been described by the cutting edge radius or hone geometry (Stephenson and Agapiou 2006). However, current research shows that a single radius is not appropriate to describe the micro geometry. Due to the manufacturing process (e.g., abrasive blasting, brushing, magnetic finishing), the rounding at the cutting edge is irregular and has to be described by further parameters. One approach is shown in Fig. 1.

This approach enables the differentiation of three shapes. If the geometry is symmetrical, the mean size of the cutting edge roundness can be used for the description. In this case, the form factor K is equal to 1. A form factor higher than 1 indicates a slope toward the rake face, and a form factor smaller than 1 a slope toward the flank face. For these asymmetrical geometries, the parameters S_α and S_γ describe the size of the cutting edge rounding.

The size and the shape of the honed cutting edge geometry have a big impact on the tool life. For this reason, tool life maps have been



Cutting Edge Geometry, Fig. 1 Cutting edge micro geometry



process: turning

process parameters:
 $V_c = 200 \text{ m/min}$
 $f = 0.25 \text{ mm}$
 $a_p = 1.5 \text{ mm}$
 cutting fluid: none

Workpiece: AISI1045
 tool substrate: KMF
 coating: TiN/ALOX
 cutting tool: SNGA 120408

tool life criterion:
 $VB_B = 200 \text{ }\mu\text{m}$
 cutting edge breakage

α	β	γ	ϵ	κ	λ
6°	90°	-6°	90°	75°	0°

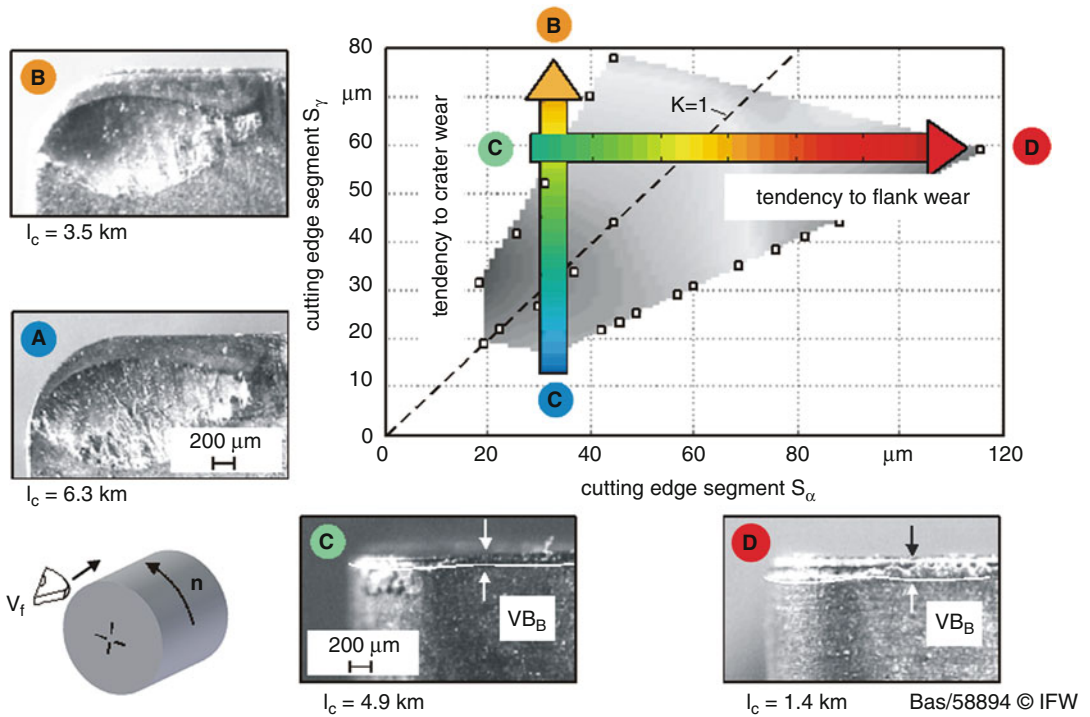
Bas/58894 © IFW

Cutting Edge Geometry, Fig. 2 Tool life map for varying cutting edge roundings

developed. These maps show the tool life travel path for different shapes and sizes of cutting edge micro geometry. Figure 2 shows such a tool life map for an external turning operation of AISI1045 steel. It can be seen that the tool life travel path is reduced by a factor of 4 for a big rounding with a slope toward the clearance face. On the other hand, the tool life travel path can be doubled by small rounding with a slope toward the rake face.

The main reason for this effect is the change in the tool wear mechanism (Fig. 3). Increasing

the cutting edge segment S_γ leads to an increase of the crater wear, while a rising cutting edge segment S_α leads to an increase of the flank wear. This effect can be used when the wear mechanism of a sharp ground cutting edge is known. When crater wear is dominant, the rounding should have a high cutting edge segment S_α and a small cutting edge segment S_γ . When flank wear is the dominant wear mechanism, small cutting edge segments S_α should be applied.



Cutting Edge Geometry, Fig. 3 Tool wear mechanisms for changing cutting edge rounding

The described effect could be observed for the machining of different materials. Furthermore, investigations with interrupted cut have been carried out. In this case, a breakage of the cutting edge is dominant. For this reason, high values for the cutting edge segments are favorable (see Fig. 4).

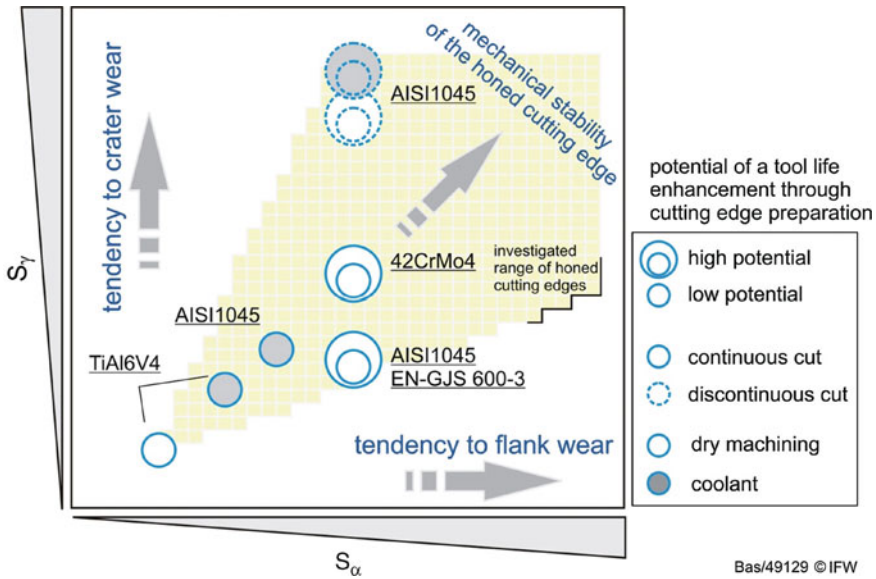
Another effect that occurs when honed cutting edges are applied is an increase of the process reliability (Fig. 5). When nonconditioned tools are used, sporadic tool breakage may occur. However, when honed cutting edges are applied, the tool wear can be higher than for sharp ground tools, but the sporadic tool breakage can be avoided.

Apart from the tool wear, the chip formation as well as the cutting forces is influenced by the cutting edge rounding. Figure 6 shows the machining force F_z with regard to the cutting edge rounding. An increase of the parameters S_α and S_γ leads at all to increasing machining forces. However, the impact of the cutting edge segment

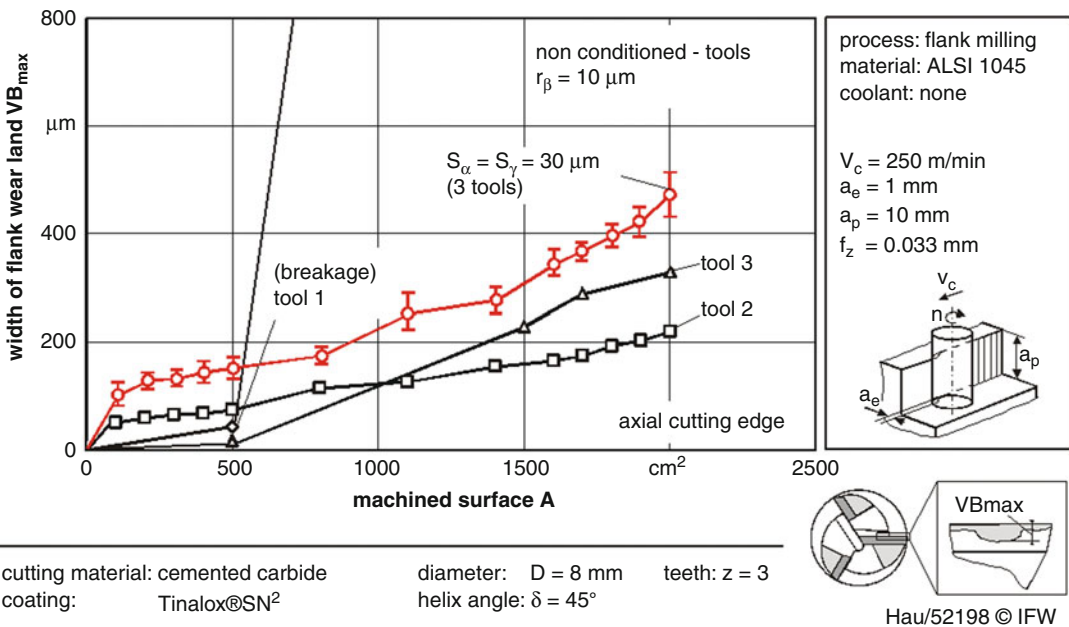
S_α on the machining force is much higher than the influence of the cutting edge segment S_γ . When S_α and S_γ are increased together, the influence on the forces is comparable to the single influence of S_α . This is mainly due to the higher friction at the clearance face.

A further analysis of the machining forces, according to Ernst and Merchant, shows that the friction angle is also influenced by the cutting edge rounding. This means that a higher cutting edge segment S_α leads to a higher machining force at all, but mainly the passive force is increased.

As it can be seen from the exemplarily presented results, the cutting edge rounding is a very important factor regarding the development of new tool geometries. However, dependent on the workpiece material as well as the tool macro geometry and process parameters, tailored micro geometries are needed. Applying the right rounding may result in an increase of the tool life by a factor of 2, and applying the wrong geometry may result in a strongly decreased tool wear.



Cutting Edge Geometry, Fig. 4 Favorable micro geometries for different workpiece materials

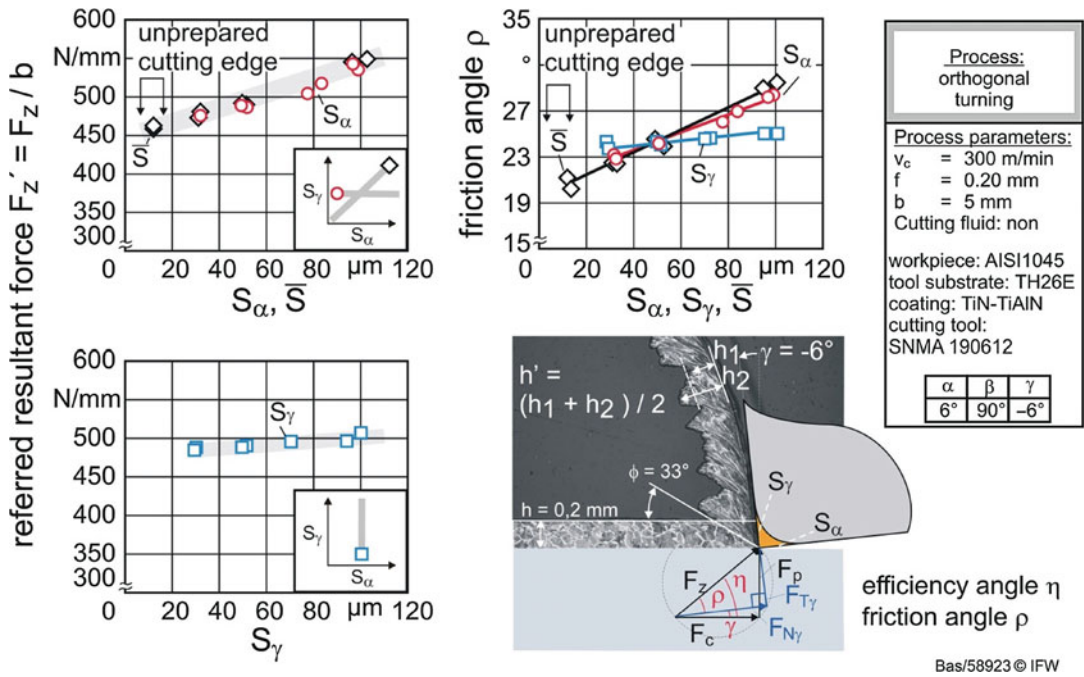


Cutting Edge Geometry, Fig. 5 Influence of the cutting edge preparation on process reliability

Chamfer Geometry

Besides the cutting edge rounding, also chamfer geometries have a high impact on the machining process. Chamfers can be applied at the rake face or at the clearance face for different reasons.

Chamfers at the clearance face are mainly applied for influencing the process stability. Due to the reduced clearance angle, a damping effect occurs, which allows, e.g., the application of higher depth of cut in milling operations. The effects on the



Cutting Edge Geometry, Fig. 6 Forces for different cutting edge roundings

process stability are described in (Altintas and Weck 2004).

Chamfers on the rake face of the cutting tools (chamfer lengths of 100–300 μm and chamfer angle of 10–30°) are applied for two main reasons. The first is an increase of the stability of the cutting wedge. A higher chamfer angle leads to a higher wedge angle and to a decreased effective rake angle of the tool (Stephenson and Agapiou 2006). However, for several machining operations, especially when ceramics or CBN as tool material is applied, the higher wedge angle is necessary to avoid a sudden tool breakage. The second effect is a result of the highly negative effective rake angle (Tönshoff et al. 2000). The negative rake angle leads to a higher friction and to higher temperatures in the chip formation zone. This can be helpful, when hard materials, e.g., hardened steels, are machined. The higher temperatures in front of the tool path result in a thermal softening of the workpiece material. This leads to a better machinability of the material and to reduced machining forces and load on the tool.

Cross-References

- ▶ Cutting, Fundamentals
- ▶ Machinability

References

Altintas Y, Weck M (2004) Chatter stability of metal cutting and grinding. *CIRP Ann Manuf Technol* 53(2):619–642

Byrne G, Dornfeld D, Denkena B (2003) Advancing cutting technology. *CIRP Ann Manuf Technol* 52(2):483–507

Denkena B, Lucas A, Bassett E (2011) Effects of the cutting edge microgeometry on tool wear and its thermo-mechanical load. *CIRP Ann Manuf Technol* 60(1):73–76

ISO 3002-1 (1982) Basic quantities in cutting and grinding (part 1): geometry of the active part of cutting tools: general terms, reference systems, tool and working angles, chip breakers

Shaw MC (1984) *Metal cutting principles*. Oxford University Press, Oxford, UK

Stephenson DA, Agapiou JS (2006) *Metal cutting: theory and practice*, 2nd edn. Taylor & Francis Group, London

Tönshoff HK, Denkena B (2004) *Spanen: Grundlagen [cutting: basics]*, 2nd edn. Springer, Berlin

Tönshoff HK, Arendt C, Ben Amor R (2000) Cutting of hardened steel. *CIRP Ann Manuf Technol* 49(2):547–566

Cutting Edge Influence on Machining Titanium Alloy

Konrad Wegener

Institut für Werkzeugmaschinen und Fertigung (IWF), ETH Zürich, Zürich, Switzerland

Definition

The performance of machining titanium can be enhanced by using cutting tools with rounded cutting edges at adapted cutting speed and feed. The rounded cutting edges influence the active force components including plowing forces and tool face friction, which are especially important in machining titanium alloy as Ti-6Al-4V. Methods to correctly determine the cutting edge radius are prerequisite for this analysis as well as methods to prepare cutting edge geometry in a controlled way.

The state of the art is mainly described in Wyen and Wegener (2010) as well as in Wyen et al. (2012).

Theory and Application

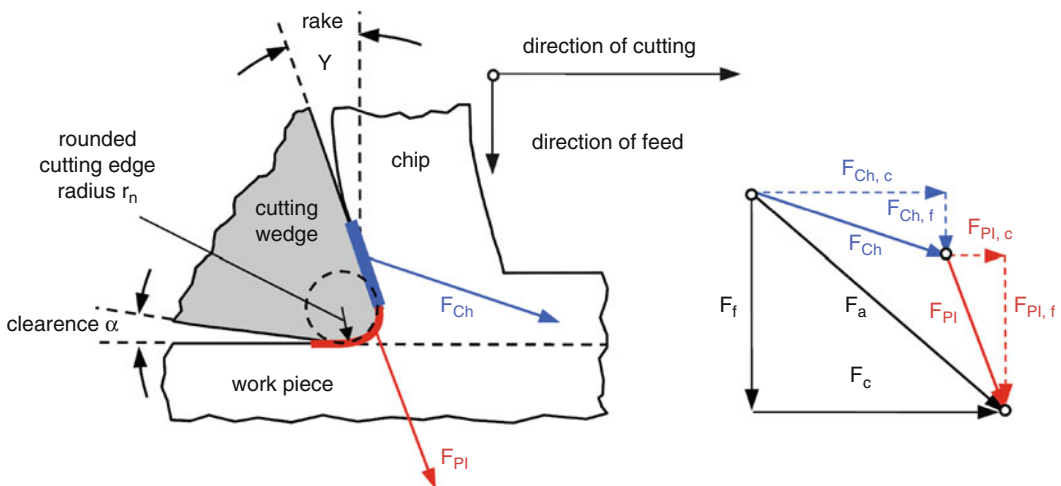
Introduction

Titanium is classified as a difficult-to-machine material. Its mechanical and chemical properties cause

high wear on cutting edges. By preparing cutting edges with defined rounding, initial crack formation can be reduced, the mechanical strength of a cutting edge can be improved, and the load on the cutting edge is changed. Different researchers prove an enhancement of the tool life when using cutting tools with rounded cutting edges (Bouzakis et al. 2002; Rech et al. 2005; Denkena et al. 2008). The optimal cutting edge radius for a machining process depends on the work material and tool material including its coating and machining conditions.

Generally, total forces recorded in a cutting process are the sum of forces acting on the tool flank and its cutting edge, as well as on the face. The force acting directly on the cutting edge is called plowing force F_{PI} ; see Fig. 1. It originates from elastic and plastic deformation of the work material around the cutting edge. The plowing force is also referred to as parasitic force or zero-feed force (Albrecht 1960; Stevenson 1998; Guo and Chou 2004). In literature, different methodologies exist to reveal the plowing force (Albrecht 1960; Stevenson 1998). Its determination and separation from the total forces allows a better understanding of tool wear and shearing process and enables the determination of actual coefficients of friction in a cutting process.

The analysis of these forces in machining titanium alloy needs to be done for different cutting edge radius r_n , cutting speed v_c , and feeds f .



Cutting Edge Influence on Machining Titanium Alloy, Fig. 1 Separation of active force F_a into plowing force F_{PI} and chip forming force F_{Ch} and into components in feed and cutting direction (Albrecht 1960)

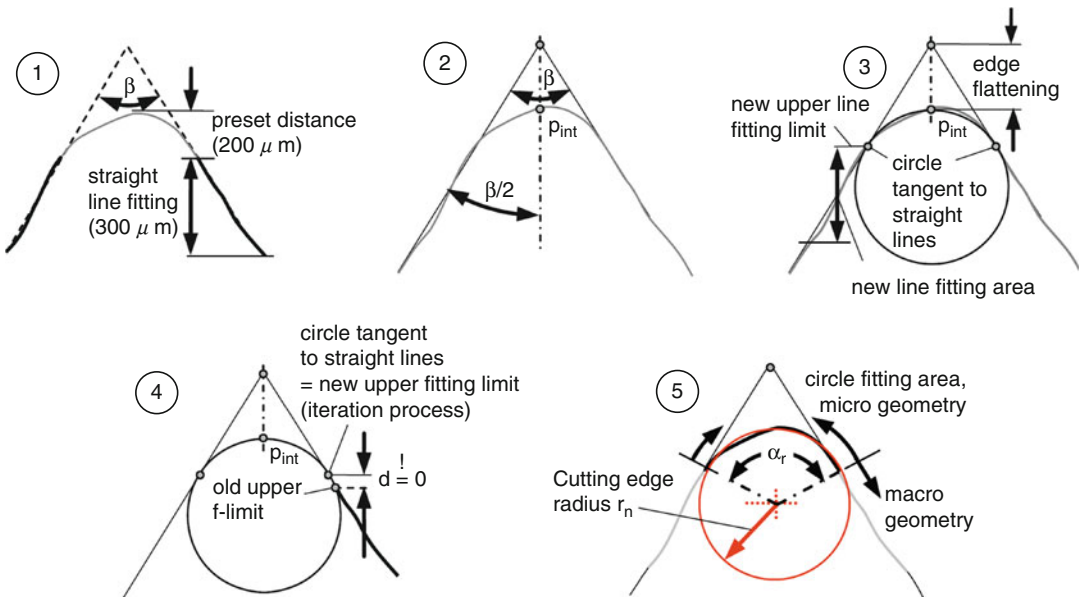
Cutting Edge Characterization

As essential precondition, such analysis needs precise cutting edge preparation and characterization method featuring high repeatability. Currently available characterization methods for rounded cutting edges are often found to be not repeatable. A recent survey (Denkena 2008) comparing the cutting edge radius measurement at different institutions shows significant deviations in the determined radii. No international standard yet exists that defines how the microgeometry of a cutting edge profile has to be described. The characterization of a rounded cutting edge by its radius is mentioned in DIN 6582 (1988–2002). Unfortunately, no details are given about how the area for a circle fitting is to be chosen or what fitting procedure is to be used. This missing detail is a major drawback in the application of this method. Thus, results may differ depending on measurement uncertainty, user, fitting area, and procedure used for the fitting. Other attempts for the characterization of rounded cutting edges (Denkena et al. 2002; Cortés Rodríguez 2009) exist. However, in some cases their significance and applicability is

strongly influenced by the uncertainty factors mentioned, too, and the same characterization method may produce different results for the characterization of a cutting edge.

In general, the uncertainty of a circle fitting depends on uncertainty of the individual points, the number of points, and the area chosen for the fitting. To reduce uncertainties in the characterization, C. F. Wyen (Wyen et al. 2011) developed an algorithm that defines its fitting area iteratively as a function of edge flattening and wedge angle β of the cutting edge. By making the fitting area user independent, the repeatability increases. As one uncertainty driver – definition of cutting area – is eliminated, the resulting characterization uncertainty is reduced. The steps described by C. F. Wyen are illustrated in Fig. 2.

Following this algorithm a circle fitting is achieved that gives a unique solution for the characterization of a rounded cutting edge by its radius r_n independent from starting values. To characterize the asymmetry of a rounding, further parameters have to be used, e.g., distances between cutting edge profile and an auxiliary horizontal straight line left and right to the wedge angle bisector.



Cutting Edge Influence on Machining Titanium Alloy, Fig. 2 Steps to characterize the rounding of a cutting edge profile by a Gaussian fitted circle with a unique solution

Cutting Edge Influence on Machining Titanium Alloy

Influence of Rounded Cutting Edge Radius r_n on Forces and Coefficient of Friction μ

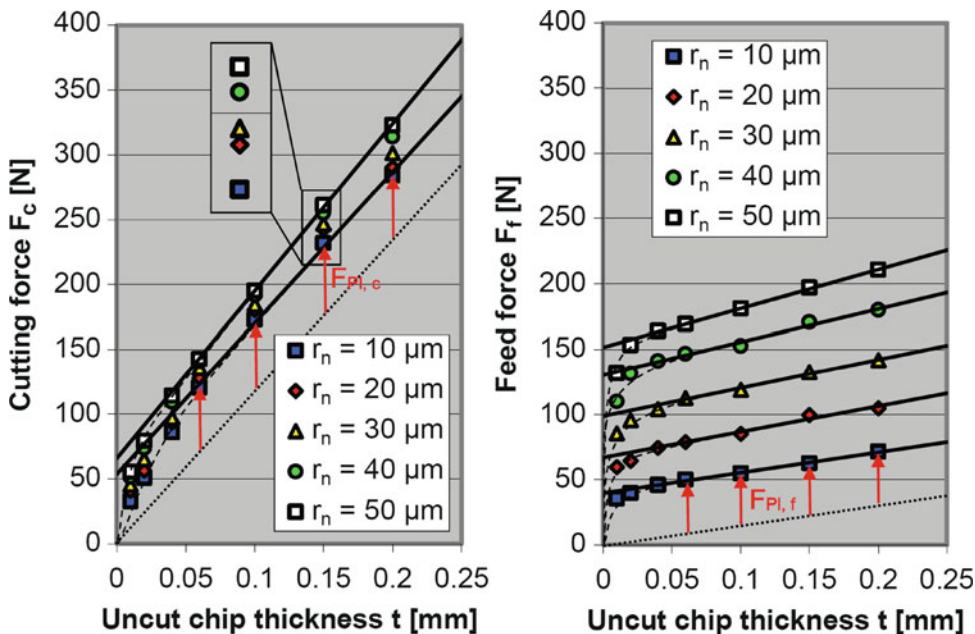
For different uncut chip thicknesses t , Fig. 3 represents the cutting forces F_c and feed forces F_f in orthogonal turning of Ti–Al6–V4 using rounded cutting edges with different radii r_n . The force values are standardized to a cutting width of $b = 1$ mm. As can be seen, both force components increase when raising the cutting edge radius. The cutting force is less sensitive to a change in cutting edge radius than the feed force. The influence of uncut chip thickness t is non-linear for small values of t , also indicated by the dashed lines in Fig. 3. For larger values of uncut chip thickness, the relation between forces and uncut chip thickness can be linearly approximated (full straight lines in Fig. 3).

The plowing force components $F_{Pl, c}$ and $F_{Pl, f}$ from this data can be determined by the same approach as reported in Albrecht (1960). The approach is based on the assumption that (1) the

total force in a cutting process increases linearly with increasing feed, provided that the zone of the cutting edge, which is influenced by the plowing force, is fully engaged, (2) the plowing force F_{Pl} does not change with increasing feed, and (3) the coefficient of friction μ on the tool–chip interface is independent of the uncut chip thickness. Force values can then be extrapolated to an uncut chip thickness of $t = 0$. The resulting force is the plowing force F_{Pl} .

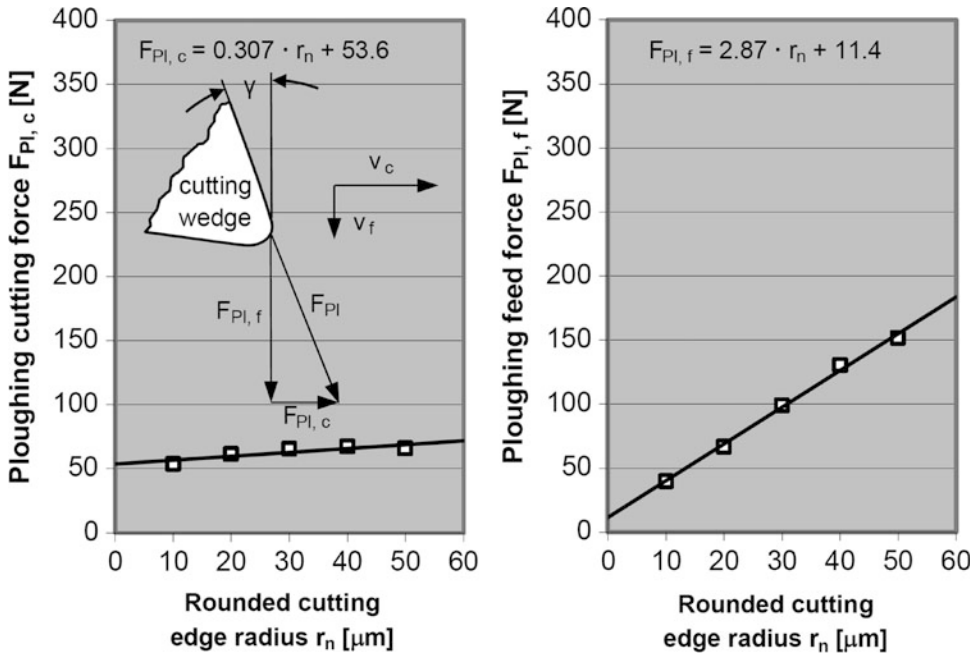
To ensure that no data is used for the extrapolation, which is still influenced by a changing plowing force (which is the case for large ratios of r_n/t), force values of cutting tests with an uncut chip thickness t above 0.06 mm were considered only. The extrapolated values of the plowing force components in the direction of cutting $F_{Pl, c}$ and in the direction of feed motion $F_{Pl, f}$ are represented in Fig. 4 for the cutting edge radii tested.

For plowing cutting force and plowing feed force values $F_{Pl, c}$ and $F_{Pl, f}$, a linear fitting was accomplished. The different slope of these two functions implies that the direction of plowing force changes with increasing cutting edge radius.



Cutting Edge Influence on Machining Titanium Alloy, Fig. 3 Experimentally determined cutting forces F_c and feed forces F_f for turning Ti–Al6–V4 with different

cutting edge radii r_n at different uncut chip thicknesses t : data is standardized to a cutting width of $b = 1$ mm ($v_c = 70$ m/min)



Cutting Edge Influence on Machining Titanium Alloy, Fig. 4 Influence of cutting edge radius r_n on plowing force components in the direction of cutting

(left) and direction of feed motion (right): forces are standardized to a cutting width of $b = 1 \text{ mm}$ ($v_c = 70 \text{ m/min}$)

The extrapolated forces for a perfectly sharp tool (cutting edge radius $r_n = 0$) are not zero. Titanium possesses a low Young’s modulus which can cause excessive deflection of the surface being machined, leading to a spring back of material behind the cutting edge. Interpreting the plowing force data, such a material deflection also occurs for ideal sharp tools in machining titanium.

By knowing the direction and magnitude of the plowing force F_{pl} , it is now possible to determine the average coefficients of friction μ on the tool–chip interface by subtraction of the plowing force from the total force F . As a result direction and magnitude of the force acting on the face, the chip forming force F_{Ch} , can be deduced. According to Fig. 1, the coefficient of friction μ on the face can be determined by

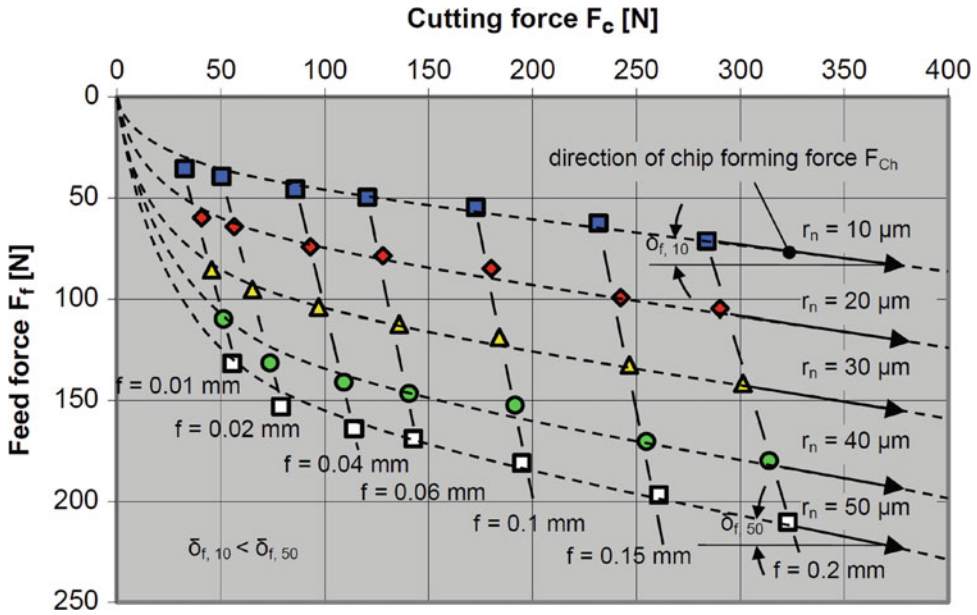
$$\mu = \frac{\sin \gamma \cdot F_{Ch,c} + \cos \gamma \cdot F_{Ch,f}}{\cos \gamma \cdot F_{Ch,c} + \sin \gamma \cdot F_{Ch,f}} \quad (1)$$

The direction of the chip forming force F_{Ch} can also be deduced from the slope of the measured

curves given in Fig. 5, which shows the recorded feed forces against cutting forces at different feeds f using different cutting edge radii r_n . The direction of the chip forming force F_{Ch} and thus the friction on the tool face correspond to the slope of that part of the curve, where the curvature approaches zero. It can be noticed that the slope rises with increasing cutting edge radius ($\delta_{f, 10} < \delta_{f, 50}$). Thus, the coefficient of friction on the tool–chip interface is apparently dependent on the cutting edge radius in machining Ti–Al6–V4. The calculated coefficients of frictions, using Eq. 1, are presented in Table 1 for the different cutting edge radii.

Influence of Cutting Speed v_c on Plowing Force F_{pl} and on Coefficient of Friction μ

The influence of cutting speeds v_c of 10, 30, 70, and 110 m/min at different cutting edge radii r_n of 10 and 40 μm using feeds f of 0.06 and 0.1 mm on the active force values and their components is shown in Fig. 6.



Cutting Edge Influence on Machining Titanium Alloy, Fig. 5 Influence of cutting edge radius r_n and feed f on cutting forces F_c and feed forces F_f for turning

Ti–Al6–V4, standardized to a cutting width of $b = 1$ mm ($v_c = 70$ m/min): angle δ indicates slope of straight part of curve

Cutting Edge Influence on Machining Titanium Alloy, Table 1 Experimentally determined average coefficients of friction μ on tool face for machining Ti–Al6–V4 with different cutting edge radii, $v_c = 70$ m/min, rake $\gamma = 10$

Cutting edge radius r_n (μm)	10	20	30	40	50
Coefficient of friction μ	0.32	0.35	0.37	0.39	0.42

The influence of the cutting speed on the force components and thus on the active force is nonlinear. While cutting forces tend to decrease with increasing cutting speed for the machining parameters tested, feed forces behave differently depending on the cutting edge radius. With increasing cutting speed, feed forces increase when using cutting edge radii of 40 μm , and they decline for cutting edge radii of 10 μm . This interdependency might be caused by opposite effects of cutting speed on deformation resistance and thermal softening in a cutting process.

For cutting edge radii of $r_n = 10$ μm , $r_n = 20$ μm , and $r_n = 40$ μm , plowing forces for cutting speeds of 10, 30, 70, and 110 m/min are shown in

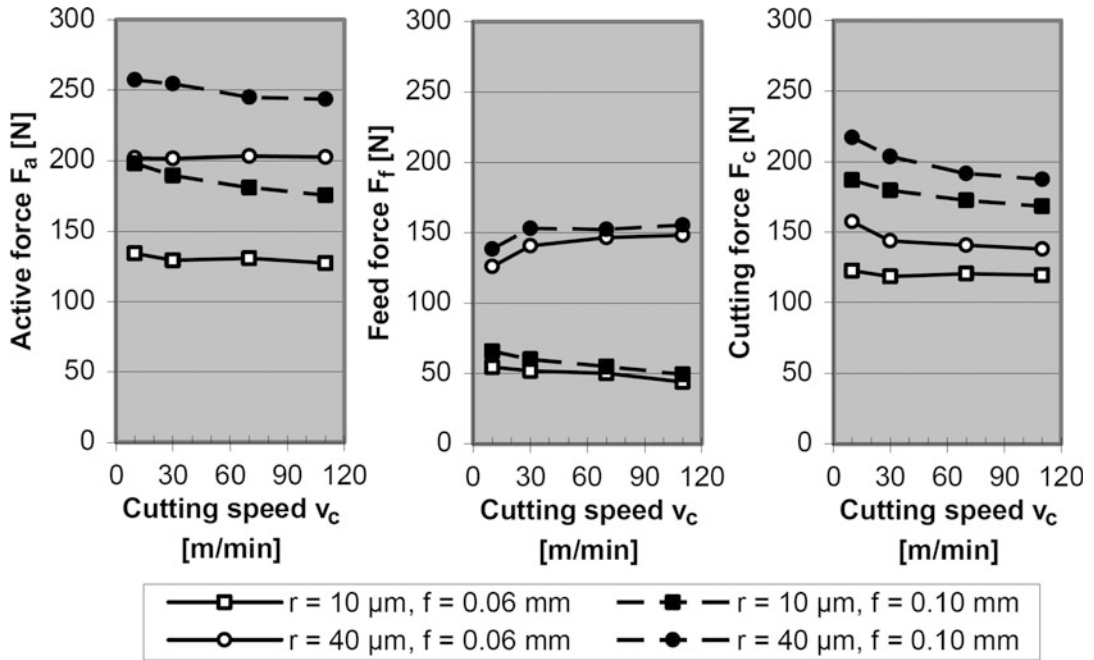
Fig. 7. No uniform influence of the cutting speed can be recognized. Forces are spread within a range of 30 N or less, dependent on the cutting edge radius. The calculated coefficients of friction on the tool–chip interface for machining at different cutting speeds are given in Table 2.

The data indicate that there is an influence of cutting speed and cutting edge radius on friction. A large cutting edge radius causes a large deformation of material in front of the cutting edge. More energy is needed for the plus of deformation. Thus, temperatures increase. The same result is caused by an increasing cutting speed and is a possible explanation for the increase in friction. The increase in friction with increasing temperature is in agreement with high-temperature tribotests.

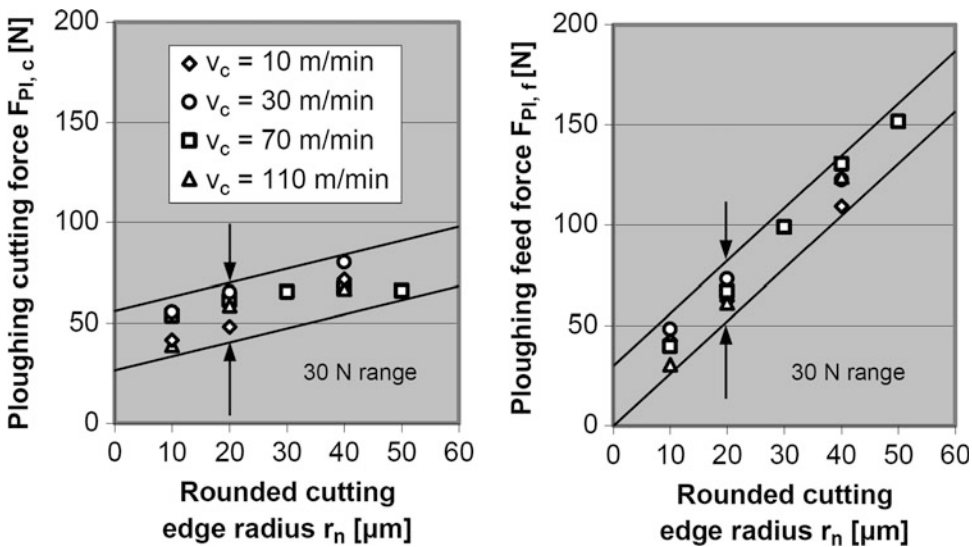
Influence of Cutting Edge Radius on Surface Integrity

Residual Stress

Residual stress is generally caused by mechanical and thermal loads.



Cutting Edge Influence on Machining Titanium Alloy, Fig. 6 Influence of cutting speed v_c on forces in turning Ti-Al6-V4 with different feeds f and different cutting edge radii r_n , standardized to a cutting width of $b = 1 \text{ mm}$



Cutting Edge Influence on Machining Titanium Alloy, Fig. 7 Influence of cutting edge radius on plowing force in turning Ti-Al6-V4 at different cutting speeds: forces are standardized to a cutting width of $b = 1 \text{ mm}$

It is thus the force which also directly influences the surface being generated. With increasing cutting edge radius, especially the feed force

component of the plowing force increases. This indicates that an additional material deformation in front of the cutting edge, respectively between

Cutting Edge Influence on Machining Titanium Alloy, Table 2 Experimentally determined average coefficients of friction μ on tool face for machining Ti–Al6–V4 with different cutting edge radii at different cutting speeds v_c , rake $\gamma = 10$

Cutting edge radius r_n (μm)	10	20	40
$v_c = 10$ m/min	0.34	0.35	0.38
$v_c = 30$ m/min	0.32	0.37	0.37
$v_c = 110$ m/min	0.34	0.49	0.49

the cutting edge and surface being generated, occurs, which consequently generates compressive stresses. Hence, an increase in mechanical deformation and thus compressive residual stress with increasing cutting edge radius can be expected for processes both up and down milling. Compressive residual stresses are favorable as they improve workpiece fatigue strength and resistance to stress corrosion cracking.

In up milling, the uncut chip thickness increases within the cut. Before chip formation occurs, a friction and material compression process starts, inducing elastic–plastic deformation into the workpiece surface. The larger the cutting edge radius, the higher are the forces on the surface to be generated. At cutting edge entry, the edge temperature is assumed to be low. The generated surface is thus expected to be mostly influenced by mechanical-induced compression processes.

In down milling, however, the tool exit condition is characterized by a continuously decreasing chip thickness until no cutting action occurs due to underrunning the minimum chip thickness. The properties of the generated surface are mainly determined by the separation processes involved in chip formation. Moreover, tool temperature in down milling can be expected to have a higher effect on residual stress as the edge which is in contact with the new surface is heated up by the foregoing cutting action.

Figure 8 shows the results of residual stress measurements on surfaces generated in up milling (left) and down milling (right) with different cutting edge radii. The angle φ denotes the measurement direction in residual stress analysis. An angle of $\varphi = 0^\circ$ denotes measurements in the direction of cutting, whereas $\varphi = 90^\circ$ stands for

measurements orthogonal to the direction of cutting. The directions of feed and cutting speed were parallel to each other at tool entry and exit.

Polished reference samples showed an average residual stress of $\sigma = 12$ N/mm². Both up and down milling induce residual stresses of compressive type. The compressive stresses measured in the direction orthogonal to the cutting velocity are generally higher than those determined in the direction of cutting.

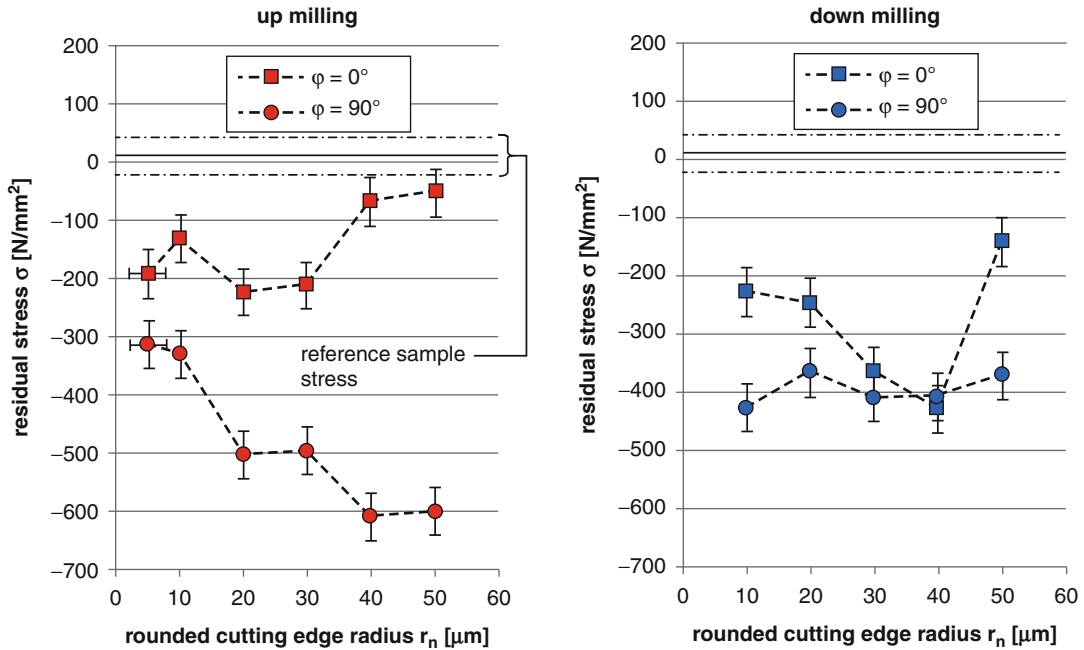
In up milling, the maximum induced residual compressive stresses on the surface increase with increasing cutting edge radius from around $\sigma = -310$ N/mm² when using a non-rounded cutting edge ($r_n \approx 6 \pm 2$ μm) to approximately $\sigma = -600$ N/mm² when machining with edges rounded to a radius of $r_n = 50 \pm 1$ μm . Including measurement uncertainty, the scattering of residual stresses averages ± 32 N/mm² for machined surfaces.

In down milling, the maximum detected compressive stresses react less sensitive to a change in cutting edge radius. Compressive stresses on the surface remain roughly at an average value of $\sigma = -400$ N/mm². This behavior might be caused by opposite effects of mechanical and thermal load when using rounded cutting edges. The mechanical deformation increases with increasing cutting edge radius, causing a specific elastic–plastic deformation on the machined surface.

At the same time, process temperatures increase, which shift the surface stress toward the tensile direction. Especially in the machining of titanium, known for its poor thermal conductivity that causes high temperatures which effect only small subsurface areas, this effect might be more strongly pronounced than for other metals. However, in up milling, this effect is assumed to have only little influence as a cooled down cutting edge is entering the workpiece. No explanation can be given for the strong variation of the residual stress measured in the direction of cutting ($\varphi = 0^\circ$).

Microhardness

Hardness is the measure for the resistance of a material against plastic deformation caused by an



Cutting Edge Influence on Machining Titanium Alloy, Fig. 8 Residual stress up milling and down milling measured on Ti-6Al-4 V surfaces machined with different cutting edge radii r_n

indenter. Hardness measurements are generally suited for cross-checking the results of residual stress measurements. The higher the compressive stress, the larger is typically the resistance against plastic deformation. The opposite is the case for residual tensile stresses.

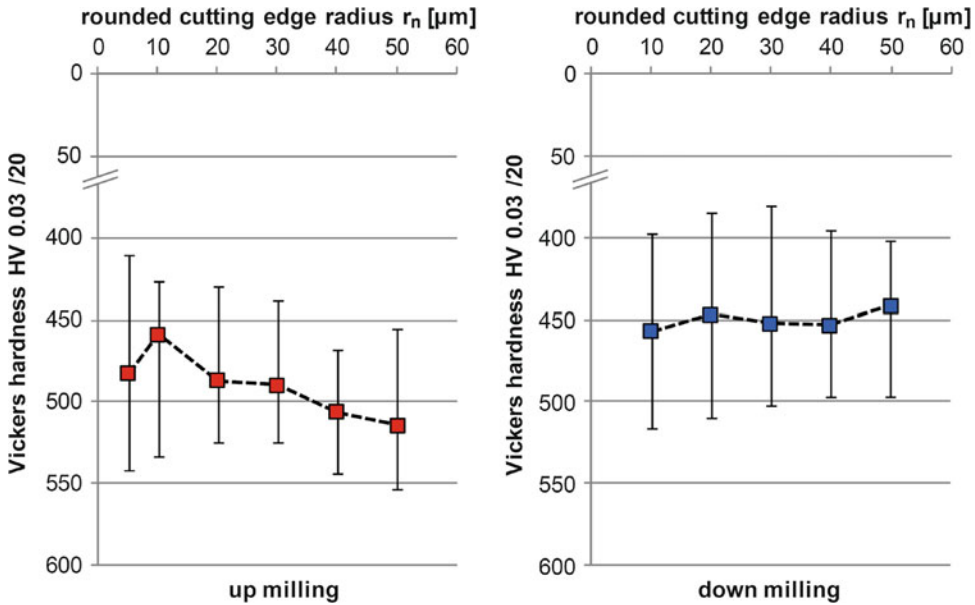
Figure 9 shows Vickers hardness measurements carried out on the identical surfaces as used for the residual stress measurements. At an indentation time of $t_i = 20$ s, an indentation force of $F = 300$ mN was used. The results are depicted in. Each data point is the average of at least nine measurements randomly distributed over the generated surface. The polished reference surface has an average hardness of roughly HV420. As expected from the residual stress measurements, the hardness values of milled surfaces are generally higher. The average slope of hardness values against cutting edge radius is in agreement with the maximum compressive residual stresses from the X-ray diffraction measurements in Fig. 8. On the surfaces that were machined by up milling, hardness increases slightly with increasing cutting edge radius,

whereas no significant influence of cutting edge radius on hardness was detected on the down-milled surfaces. Thus, rounded cutting edges have a positive influence on residual compressive stresses, with a more significant effect in up milling than in down milling.

Surface and Near-Surface Characterization

The effect of the cutting edge radius on surface finish was analyzed using scanning electron microscopy. Figure 10 shows images of surfaces generated by up and down milling. Horizontal traces are caused by notchedness of the edge, whereas vertical marks are caused by the tool feed. Independent of process kinematics, feed marks become more pronounced at larger cutting edge radii.

In up milling, the following mechanism is assumed: the feed marks result from elastic material deflections that occur when the cutting edge enters the cut and successive separation of material at the point when minimum chip thickness is reached. A similar mechanism is proposed in down milling: while cutting, material is



Cutting Edge Influence on Machining Titanium Alloy, Fig. 9 Results of microhardness measurements on Ti-6-Al-4 V surfaces machined with different cutting edge radii r_n

continuously being separated from the workpiece surface until the minimum chip thickness is reached.

Surface Roughness

With a tool diameter of $d = 25$ mm and a feed per tooth of $f_z = 0.08$ mm, the following theoretical kinematic roughness values are expected:

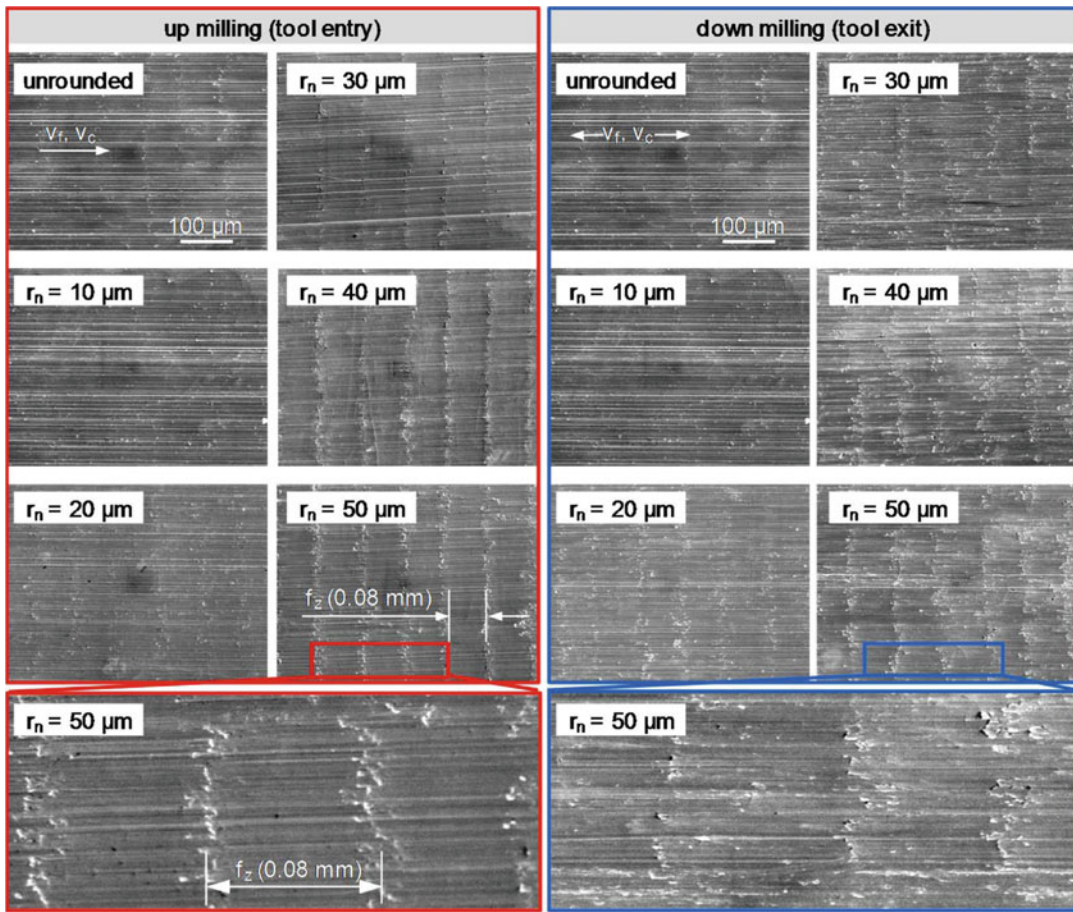
$$Rz_t = 0.064 \text{ mm}, Ra_t = .0164 \text{ mm}$$

The experimentally determined kinematic surface roughness values Ra and Rz are depicted in Fig. 11. Each data point is the average value of nine individual measurements carried out on the surfaces of two different workpieces. The values of Ra and Rz generally lie above the theoretical surface values. For both up- and down-milled surfaces, roughness is minimal when using a rounded cutting edge radius of $r_n = 30 \mu\text{m}$. Moreover, the roughness is not in agreement with the visual surface appearance given in Fig. 10, from which an increase in roughness would be expected with increasing edge

radius for both up- and down-milled surfaces. The reason of this difference is that the theoretical kinematic stiffness does not consider cutting edge radius.

Influence of Cutting Edge Radius on Burr Formation

Machining burrs are generally classified by the cutting edge concerned and the mechanism of their formation. The size of burr is a function of the material properties, the effective cutting edge radius, and the pressure at the effective radius and flank of the tool. The pressure and thus the tendency to form burr are especially high on materials with low thermal conductivity and low Young’s modulus. Both are properties that titanium (Fig. 12) depicts surfaces and resulting burr in milling titanium with different cutting edge radii. The left side shows surfaces generated by up milling. The right side shows down-milled surfaces. Burr formation occurs on both top and



Cutting Edge Influence on Machining Titanium Alloy, Fig. 10 SEM images of surfaces machined with different cutting edge radii r_n

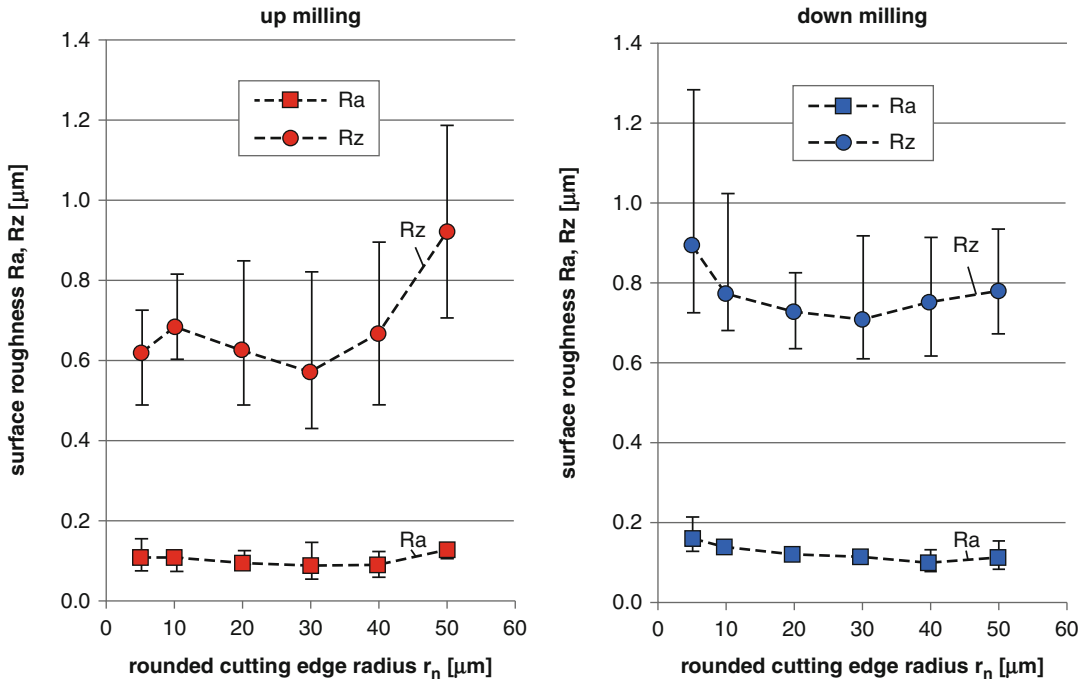
bottom edges as the surfaces were generated in free orthogonal milling.

The burr produced in up milling is frayed (ruptured type). This results from the repeated entrance of the cutting edge into the workpiece. Every time the cutting edge enters the cut, new material is bulged at the free surfaces, pushing out the burr from the previous cut. On the one hand, this leads to an increase in burr height. On the other hand, it causes a partial separation of burr from the machined edge. Below a certain cutting edge radius, it can be assumed that burr of the previous cut is partly removed by the successive cut. With increasing cutting edge radius, however,

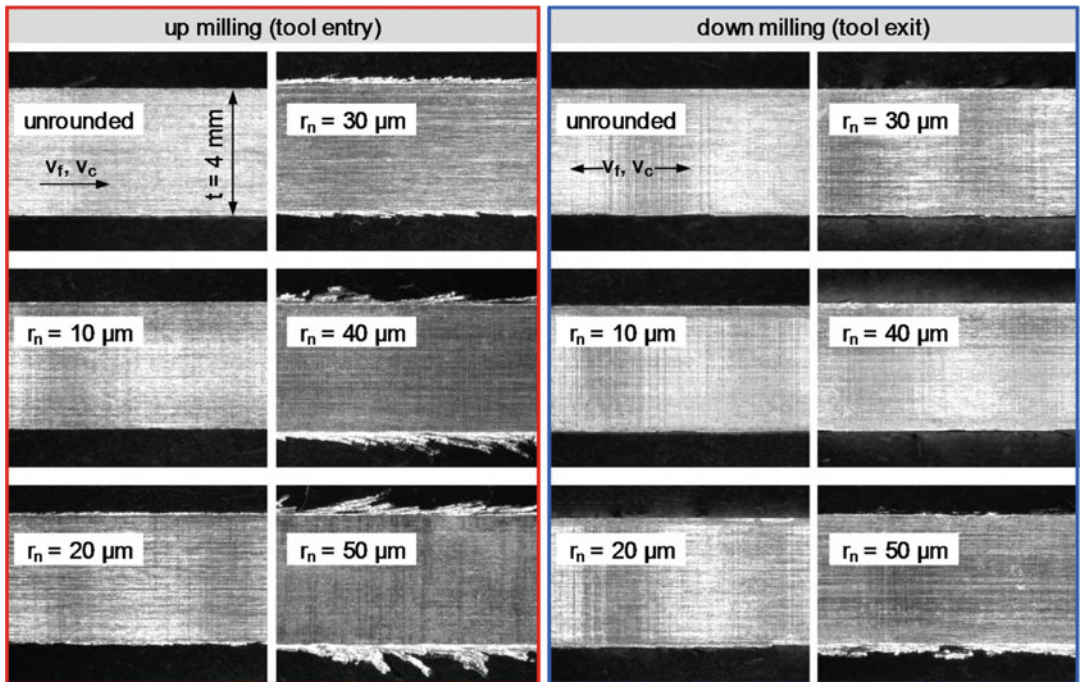
the burr formed at the beginning of chip formation is not removed by a successive cut, but only pushed away, leading to burr with long fringes. Especially for cutting edge radii of $r_n = 40 \mu\text{m}$ or larger, this effect seems to take place.

In down milling, no significant burr formation was observed for cutting edge radii of $r_n = 10 \mu\text{m}$ or smaller. As expected, burr formation increased when the cutting edge radius became larger. The burr formation is generally much more pronounced in up milling than in down milling.

Nevertheless, an increase of burr with increasing cutting edge radius was also observed in down milling. Thus, the increase in burr with increasing



Cutting Edge Influence on Machining Titanium Alloy, Fig. 11 Roughness up milling and down milling measurements on Ti-6Al-4 V surfaces machined with different cutting edge radii r_n



Cutting Edge Influence on Machining Titanium Alloy, Fig. 12 Burr formation when milling Ti-6Al-4 V with different cutting edge radii r_n , ($v_c = 70$ m/min, $f_z = 0.08$ mm, $a_e = d = 25$ mm)

cutting edge radius is generally in agreement with the measurement results of residual stress of machined surfaces.

References

- Albrecht P (1960) New developments in the theory of metal cutting process, part. 1: the ploughing process in metal cutting. *ASME J Eng Ind* 82(4):348–357
- Bouzakis KD, Michailidis N, Skordaris G, Kombogiannis S, Hadjiyiannis S, Efstathiou K, Erkens G, Rambadt S, Wirth I (2002) Effect of the cutting edge radius and its manufacturing procedure on the milling performance of PVD coated cemented carbide inserts. *Ann CIRP* 51(1):61–64
- Cortés Rodríguez CJ (2009) Cutting edge preparation of precision tools by applying micro-abrasive jet machining and brushing. Dissertation, Kassel University Press, Kassel
- Denkena B (2008) CIRP STC-C minutes. Annex A, Aug. 2008
- Denkena B, Friemuth T, Fedorenko S, Gropp M (2002) An der Schneidewird das Geld verdient: Neue Parameter zur Charakterisierung der Schneidengeometrien an Zerspanwerkzeugen [The money is earned at the cutting edge: new parameters to characterize the cutting edge geometry]. *Fertigung Sonderausgabe Werkzeuge* 12:24–26 (in German)
- Denkena B, De Leon L, Köhler J (2008) In der Verrundungliegt das Leistungspotential [The performance lies in the radius of the cutting edge]. *WB Werkstatt + Betrieb* 10:20–23 (in German)
- DIN 6582 (1988–2002) Begriffe der Zerspantechnik; Ergänzende Begriffe am Werkzeug, am Schneidkeil und an der Schneide [Terminology of cutting; additional terms for the tool, wedge and the cutting edge]. German Institute for Standardization, Berlin (in German)
- Guo YB, Chou YK (2004) The determination of ploughing force and its influence on material properties in metal cutting. *J Mater Process Technol* 148(3):368–375
- Rech J, Yenb YC, Schaffé MJ, Hamdia H, Altanb T, Bouzakisd KD (2005) Influence of cutting edge radius on the wear resistance of PM-HSS milling inserts. *Wear* 259(7–12):1168–1178
- Stevenson R (1998) The measurement of parasitic forces in orthogonal cutting. *Int J Mach Tools Manuf* 38(1–2): 113–130
- Wyen CF, Wegener K (2010) Influence of cutting edge radius on cutting forces in machining titanium. *CIRP Ann Manuf Technol* 59(1):93–96
- Wyen CF, Knapp W, Wegener K (2011) A new method for the characterisation of rounded cutting edges. *Int J Adv Manuf Technol* 59(9–12):899–914
- Wyen CF, Jäger D, Wegener K (2012) Influence of cutting edge radius on surface integrity and burr formation in milling titanium. *Int J Adv Manuf Technol* 67(1–4): 589–599

Cutting Fluid

Toshiaki Wakabayashi
Faculty of Engineering, Kagawa University,
Takamatsu, Kagawa, Japan

Synonyms

Coolant; Cutting lubricant; Cutting oil; Metal-working fluid; Water-based cutting fluid; Water-miscible cutting fluid

Definition

Cutting fluids, or coolants, are media used to facilitate machining operations. Their function is mainly resulted from the action to cool and lubricate the vicinity of cutting zones. The term “coolant” is often employed if the cooling action of the media is more important, whereas the term “cutting fluid” applies to rather general cases.

Theory and Application

Action Mechanism of Cutting Fluids

Cutting fluids and coolants are used in order to elongate tool life by restraining tool wear, to reduce cutting resistance, to provide a fine surface finish, and to improve machining accuracy. At higher cutting speeds, since the tool suffers from wear because of sufficiently raised temperature to cause thermal softening, their cooling action is more important. As cutting speed lowers, their lubricating properties become more prominent, easing the chip removal at the tool rake face. However, a distinction between high and low cutting speeds is rather ambiguous, and actually in most cases, both cooling and lubrication are to some extent performed by cutting fluids (Shaw 1984).

Cooling is readily understood to be the ability to remove heat generated during cutting. Regarding the lubricating action, investigations showed that the application of a lubricant to the contact

between the chip and the tool induced a steeper interfacial shear stress gradient, leading to a lowered frictional force at the rake face and a smaller radius of chip curl. This result is closely related to the other experimental evidence suggesting that cutting lubricants decrease the frictional force on the tool rake face by reducing the chip-tool contact length (DeChiffre 1981).

Access of Cutting Fluids to the Chip-Tool Interface

Provided that a cutting fluid acts as a lubricant at the chip-tool interface, the problem is the mode of its access to this boundary. In all cases, the fluid must penetrate down the interface in a direction opposed to the motion of the chip flow. There had been argument about the approach of the fluids through the chip-tool, and hence, the access from the sides of the tool or from the flank face was thought to be important.

Some intimate sticking also exists between the chip and the tool near the cutting edge, so that no liquid lubricant is probably able to gain access to this sticking region. However, the distribution of the normal stress on the rake face over the chip-tool contact area can be divided into the portion of very high stress near the cutting edge and the remainder of decreasing stress near the part where the chip and the tool separate. It is therefore possible that a potential fluid may penetrate into this latter area of the chip-tool contact. Further, cutting fluids in vapor phase, rather than liquid, can penetrate deeper and faster through a network of interconnecting micro-capillaries existing at least over a portion of the chip-tool contact area (Williams 1977).

Another mode of the penetration has been proposed as diffusion of a lubricant to the chip-tool interface through the plastically deforming material within the primary shear zone, but the existence of such bulk diffusion through the chip is still under controversy.

Gaseous Lubrication

If cutting fluids can approach the vicinity of a cutting point in a vapor phase, even in the case

of dry cutting, some gas, mainly oxygen, in the air should probably influence the cutting phenomena. From this point of view, cutting of ferrous materials was carried out in a vacuum chamber, and the results demonstrated a lower cutting force in oxygen than in vacuum. This fact emphasized the role of gaseous oxygen in preventing gross adhesion between the chip and the tool. In machining of aluminum and copper, on the contrary, the cutting force was lower in the absence of oxygen than in its presence.

Such distinctive effects of oxygen on individual materials can be explained by a difference between the shear strength of the material and that of its oxide, and these results reinforce the importance of the action of cutting lubricants in gaseous phase. In practical cutting, therefore, if a fluid can satisfactorily act as a lubricant, it may probably evaporate due to high cutting temperature and readily penetrate, against the chip flow motion, to some extent deep through a network of micro-capillaries existing between the tool and the chip.

Additives for Lubrication in Cutting

Since the metal cutting process is accomplished under such severe conditions that boundary lubrication predominates, most cutting fluids involve boundary lubrication additives, such as oiliness agents or extreme-pressure (EP) additives which can avoid metallic contact between sliding surfaces of solids. The boundary lubrication additives embrace numerous chemicals and various compositions which can form a lubricating film possessing a high load-carrying capacity at the interface under very severe frictional conditions. While oiliness agents are categorized as those which make such film by means of chemical adsorption on metal surfaces, EP additives provide the film by reaction with the metal at the interface.

The lubricating ability of an adsorbed film delivered from an oiliness agent is strongly influenced by the adsorption potential and the structure of the film. The high load-carrying

capacity of oiliness agents is commonly considered to necessitate their molecule having a strong polar group at one end and a linear structure of a long carbon chain. Polar groups, such as $-\text{OH}$, $-\text{COOH}$, and $-\text{COOC}-$, are typical examples which enable the molecule to adsorb chemically, rather than physically, on the metal surface. For this reason, alcohols, fatty acids, and esters with a long linear carbon chain are usually added into cutting fluids as an oiliness agent.

Under such severer frictional conditions that raised temperature destroys the lubricating film provided by oiliness agents, EP additives replace the role as an effective lubricant. The considerably high load-carrying capacity of these additives could be due to the lubricating film of an inorganic metal compound formed by reaction of the additive with the metal under extremely high pressure and temperature. In metal cutting operations, compounds containing chlorine, sulfur, or phosphorus perform as an effective EP additive. In particular, organic chlorides are well known as a successful heavy-duty EP additive: they react with the metal surface and form some lubricating film of a metallic chloride whose shear stress is lower than that of the base metal.

Key Applications

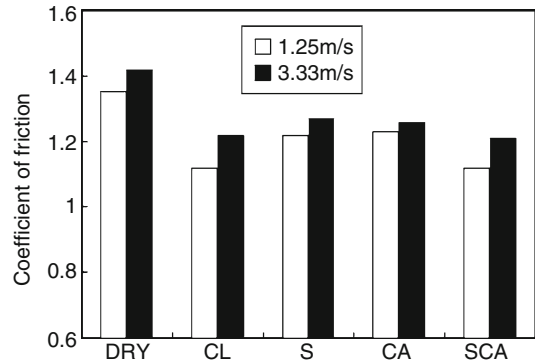
Replacements for Chlorinated EP Additives

Recent concern about environmental issues regarding cutting fluids has raised the problem of using lubricants containing chlorinated chemical compounds because chlorine causes serious air pollution in connection with dioxin emission when they are disposed by incineration. At the moment, the most practicable replacement for chlorinated EP additives would be the combination of organosulfur compounds and overbased sulfonates.

Under the cutting conditions shown in Table 1, the effects of this combination on the cutting performance were examined by turning. Figure 1 illustrates the typical results of the measured coefficient of friction on the tool rake face for various

Cutting Fluid, Table 1 Cutting conditions of turning

Workpiece	JIS S45C steel (corresponding to AISI 1045)
Cutting speed	1.25, 3.33 m/s
Depth of cut	0.5 mm
Feed	0.1 mm/rev
Tool materials	Cermet



Cutting Fluid, Fig. 1 Results of turning test

Cutting Fluid, Table 2 Sample oils containing EP additives

EP additives	Name of sample oils			
	CL	S	CA	SCA
Chlorinated paraffin mass %	10	—	—	—
Polysulfide mass %	—	10	—	10
Calcium sulfonate mass %	—	—	10	5
Chlorine content mass %	5.0	—	—	—
Sulfur content mass %	—	3.2	—	3.2
Calcium content mass %	—	—	1.6	0.8

cutting oils listed in Table 2. As seen in this figure, chlorinated paraffin is more effective in reducing the coefficient of friction than single polysulfide or calcium sulfonate. However, the sample oil containing both polysulfide and calcium sulfonate shows almost the same coefficient of friction as that provided by chlorinated paraffin. It is

therefore evident that the combination of polysulfide and calcium sulfonate can synergistically improve the cutting performance.

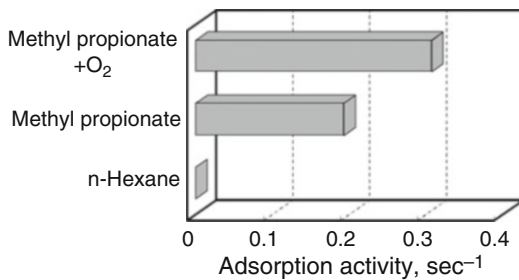
Synthetic Esters as an Optimal Lubricant for MQL Machining

Minimal quantity lubrication (MQL) machining supplies a cutting lubricant as oil mist particles to the cutting zone with a compressed carrier gas. The oil particles provide lubrication, and the compressed gas, normally air, partly provides cooling. The amount of lubricant supply in MQL is typically only several tens of milliliters per hour and is very small compared with the conventional flood coolant supply of generally several tens of thousands of milliliters per hour. Nevertheless, MQL machining provides suitable cutting performance in a number of practical applications. Hence, MQL machining can considerably reduce the

consumption of cutting fluids, leading to environmentally friendly manufacturing operations (Weinert et al. 2004). Under the circumstances, fully synthetic biodegradable polyol esters have been developed as an optimal lubricant for MQL machining (Suda et al. 2002).

Perhaps, in the case of MQL machining, compared with coolants in the case of flood fluid supply, small particles of the lubricant should evaporate extremely easily, so that the gaseous lubrication is most likely expected in MQL machining. In addition, since the lubricity of an ester usually depends on a metal soap film formed by some strong chemical adsorption onto the sliding surfaces, there is the possibility that the lubricating action of MQL machining esters is related to their adsorption phenomena on the freshly cut metal surface.

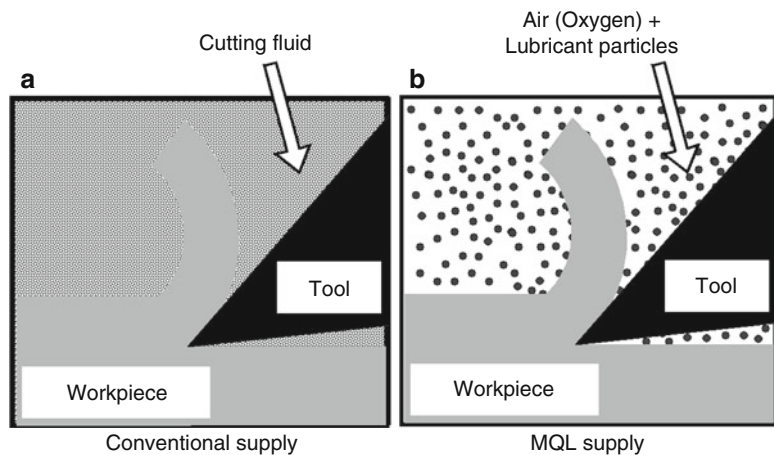
Using a controlled atmosphere machining apparatus, therefore, the adsorption activity of methyl propionate as a model ester on a freshly cut steel surface was measured in comparison with *n*-hexane as a model hydrocarbon (Wakabayashi et al. 2006). Figure 2 presents the results, demonstrating that methyl propionate shows relatively high adsorption activity, whereas *n*-hexane shows no significant adsorption. This is the expected result because hydrocarbons have no polar group to be adsorbed by the metal surface. It is considerably interesting that the adsorption activity of methyl propionate is increased if



Cutting Fluid, Fig. 2 Values of measured adsorption activity

Cutting Fluid,

Fig. 3 Schematic illustration of the difference between (a) conventional supply and (b) MQL supply



Conventional supply

MQL supply

oxygen is present, suggesting that oxygen can enhance the adsorption ability of ester. This situation may possibly be very similar to the behavior of a lubricant in MQL machining because, even near the cutting point, the lubricant particles are surrounded by a large amount of air containing oxygen.

Figure 3 illustrates schematically the difference between (a) the conventional flood supply and (b) the MQL supply, in this sense. In MQL cutting, the adsorption ability of the lubricant ester is supposed to be intensified by atmospheric oxygen, leading to the formation of a robust and tribologically effective lubricating film. The practical cutting performance in MQL machining of steels was in good accordance with the above adsorption behavior of the ester and atmospheric gases. On the contrary, the cutting performance for machining of aluminum improved with lower oxygen concentration in the gas, presumably because of the aluminum oxide (alumina) formation: alumina is extremely hard and its machining is difficult.

Cross-References

► [Cutting, Fundamentals](#)

References

- DeChiffre L (1981) Lubrication in cutting – critical review and experiments with restricted contact tool. *ASLE Trans* 24(3):340–344
- Shaw MC (1984) *Metal cutting principles*, 2nd edn. Clarendon Press, Oxford
- Suda S, Yokota H, Inasaki I, Wakabayashi T (2002) A synthetic ester as an optimal cutting fluid for minimal quantity lubrication machining. *CIRP Ann Manuf Technol* 51(1):95–98
- Wakabayashi T, Inasaki I, Suda S (2006) Tribological action and optimal performance: research activities regarding MQL machining fluids. *J Mach Sci Technol* 10(1):59–85
- Weinert K, Inasaki I, Sutherland JW, Wakabayashi T (2004) Dry machining and minimum quantity lubrication. *CIRP Ann Manuf Technol* 53(2):511–537
- Williams JA (1977) The action of lubricants in metal cutting. *J Mech Eng Sci* 19(5):202–212

Cutting Force Modeling

Karla P. Monroy Vazquez¹, Claudio Giardini² and Elisabetta Ceretti³

¹Engineering Group in Product, Process and Production, University of Girona, Girona, Spain

²Department of Engineering, University of Bergamo, Bergamo, Italy

³Department of Mechanical and Industrial Engineering, University of Brescia, Brescia, Italy

Synonyms

[Cutting forces model](#); [Shear stress modeling](#)

Definition

Cutting Force	Is a force that is generated by the cutting tool as it machines the workpiece. It can be divided into primary and secondary cutting forces.
Primary Cutting Force	Is a cutting force that is directly generated by the relative motion of the cutting tool with respect to the workpiece during machining. It occurs in the same direction as cutting tool movement.
Secondary Cutting Force	Is a cutting force that is generated in response to primary cutting forces, for example, vibrations during the machining.
Cutting Forces Modeling	The mathematical representation of a machining process in order to study the effects of varying process parameters on the cutting forces.

Theory and Application

Machining is a process of chip formation. Although the final purpose is to obtain a determined form and shape from the cutting of the

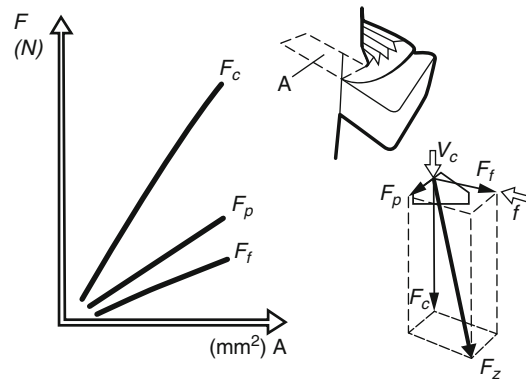
material, this has to be done by creating defined chips. Thus machining is a process in which the components of the process are in such form that the external forces applied can cause the fracture of the chips. This fracture can be caused by the combination of bending stresses: tensile stress and shear stress. Cutting is a process of extensive stresses and plastic deformations. The high compressive and frictional contact stresses on the tool face result in a substantial cutting force.

Knowledge of the cutting forces is essential to make a proper design of the cutting tools, of the fixtures used to hold the workpiece and cutting tool, for the calculation of the machine tool power, and for the selection of the cutting conditions to avoid an excessive distortion of the workpiece. Cutting force is also one of the most important parameters in the machining operation, as the power consumed by the machine to take out the process is always a factor to be optimized. In spite of their importance, it is one of the least understood operation parameters of a machining operation. In the following, the most important theoretical cutting forces modeling available in the literature will be presented for the most common cutting operations: turning, milling, and drilling (Van Luttervelt et al. 1998).

Mechanics of Cutting

In any machining operation, the unit product of the material removal is called chip. The thickness of the chip is always more than the layer of the metal removed. This is due to plastic deformation of the metal during the cutting process. The separation of the chip from the workpiece takes place by shearing. Frictional forces being generated at the cutting edge result in heat and tool wear.

In the actual cutting of the metal, the tool deforms some of the material and then separates it through plastic deformation. This elastic and plastic deformation of the metal takes place as it approaches and exceeds the yield strength of the material as it moves past the tool face. In this deformation, large forces are produced. For its convenient analysis and resolution of the resultant cutting force F acting on a tool, it is divided into three components (Fig. 1) (Black et al. 1996):



Cutting Force Modeling, Fig. 1 Cutting force components

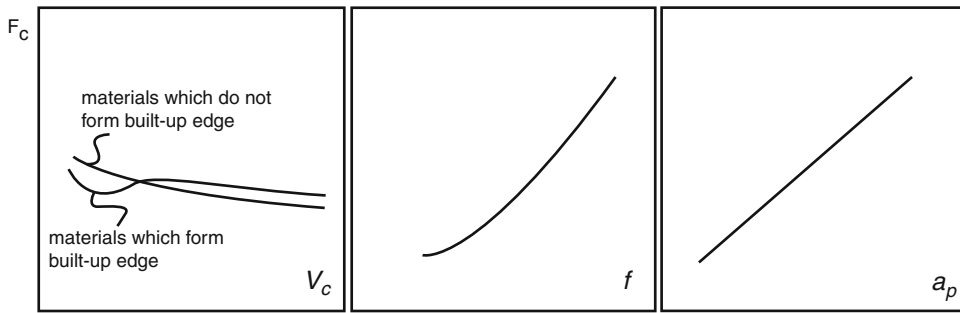
1. The tangential force F_c
2. The axial force F_f
3. The radial force F_p

The radial cutting force component (F_p) is directed at right angles to the tangential force from the cutting point. The axial cutting force (F_f) is directed along the feed of the tool, axially along the direction of machining of the component. This is an important force factor in drilling operations. The cutting ability of the drill geometry will considerably influence the size of the force needed and as a rule the axial feed force requirement rises with the diameter of the drill (Black et al. 1996).

The cutting force value is primarily affected by the following:

- Cutting conditions: cutting speed v_c , feed f , and depth of cut ap (Fig. 2)
- Cutting tool geometry (tool orthogonal rake angle)
- Properties of work material

The simplest way to control cutting forces is to change the cutting conditions. The cutting speed v_c does not change significantly the cutting force F_c . Increasing the cutting speed slightly reduces the cutting force. The decrease in force varies with the type and condition of material and the range of



Cutting Force Modeling, Fig. 2 Cutting forces as a function of cutting parameters

the cutting speed. The dependence is more complex in the low speed range for materials, which tend to form a built-up edge. When the built-up edge disappears at high cutting speeds, the dependence is essentially the same as this for materials, which do not form a built-up edge at all. For most workpiece materials, increasing the cutting speed leads to lower cutting forces. The higher temperature in the flow zone and reduced contact area contribute toward this effect (Black et al. 1996).

Feed changes significantly the cutting force. The dependence is nonlinear because of the so-called size effect at low feeds. Depth of cut also changes significantly the cutting force, but the dependence now is linear (Marinov 2010). All three components increase in size with increasing chip cross section, the most tangential one of all. For rough turning, a typical relationship might be for $F_c:F_p:F_f$ 4:2:1. The tangential cutting force is twice as large as the radial and four times that of the axial force (Fig. 1). In drilling, the relationship would be quite different and highly dependent upon the feed rate (Black et al. 1996). These dependences also can be seen on Fig. 2.

From the above, it can be concluded that the most effective method of force control is to change the depth of cut and feed. If for some reasons change of the cutting conditions is not justified, it can be controlled by the geometry of the rake angle (Marinov 2010). Especially, the entering angle will determine the size of the two force components. Their relationship becomes especially important when deflection of tool with large overhang or a slender workpiece is a factor as regards accuracy and vibration tendencies. The

rake angle also influences the size of the radial cutting force component. Positive rake angles mean lower cutting forces in general, but at the same time will increase the possibility of tool breakage (Black et al. 1996).

As it may be expected, the size relationship between the force components varies considerably with the type of machining operation. The tangential force often dominates in milling and turning operations, especially in power requirements. The radial force is of particular interest in boring operations and the axial, feed force in drilling. The size of the radial cutting force is dependent upon the entering angle used and the nose radius. A 90° entering angle and small nose radius will minimize the radial cutting force component, which strives to deflect the tool and gives rise to vibrations. Vibration tendency is one consequence of the cutting forces, as well as tool or workpiece deflection (Black et al. 1996).

Friction force also comes partly into the process as the material is forced onto the tool at great pressure and high temperature. The pressure depends upon the shear yield strength of the workpiece material and the area of the shear plane.

Cutting forces can be either measured in the real machining process or predicted in the machining process design. Cutting forces are measured by means of a special device called tool force dynamometer mounted on the machine tool. But there are other several possibilities available for cutting force prediction, for approximate calculations of sufficient accuracy for all practical purposes, with the so-called specific cutting force and by more advanced options for cutting force

prediction based on analytical or numerical modeling of metal cutting. Due to the complex nature of the cutting process, the modeling is typically divided by cutting conditions: generally orthogonal cutting conditions because of its ease, although solutions for the oblique cutting or three-dimensional cutting are accessible.

In order to simplify the analysis of the state of the art in force modeling, the study will be divided by cutting type based on the inclination in the cutting edge: orthogonal and oblique cutting.

Orthogonal Cutting

In order to understand the complex process of oblique cutting, the tool geometry is simplified from the three-dimensional (oblique) geometry, which typifies most processes, to a two-dimensional (orthogonal) geometry. Although the majority of the machining processes are tridimensional, the orthogonal model is an aid for the study of the basic cutting mechanisms. For understanding the forces acting on a tool, we will analyze the case of orthogonal cutting shown in Fig. 3 where it can be observed that the tool approaches to the workpiece with its cutting edge parallel to the uncut surface. Thus, tool approach angle and cutting edge inclination are zero, as shown in Fig. 4 (Bawa 2004).

Several forces can be defined relative to the orthogonal cutting model. Based on these forces, shear stress, coefficient of friction, and certain relationships can be defined (Groover 2010).

For the purpose of modeling chip formation, assume the relationships among the various forces (established by Merchant 1944) with the following assumptions:

- (i) The tool is perfectly sharp and there is no contact along the clearance face.
- (ii) The shear surface is a plane extending upward from the cutting edge.
- (iii) The cutting edge is a straight line, extending perpendicular to the direction of motion and generates a plane surface as the work moves past it.
- (iv) The chip does not flow to either side.
- (v) The depth of cut is constant.
- (vi) The width of the tool is greater than that of the workpiece.
- (vii) The work moves relative to the tool with uniform speed.
- (viii) A continuous chip is produced with no built-up edge.
- (ix) Planar strain conditions exist, that is, the width of the chip remains equal to the width of the workpiece.
- (x) The chip is assumed to shear continuously across a plane AB, on which the shear stress reached the value of the shear flow stress.

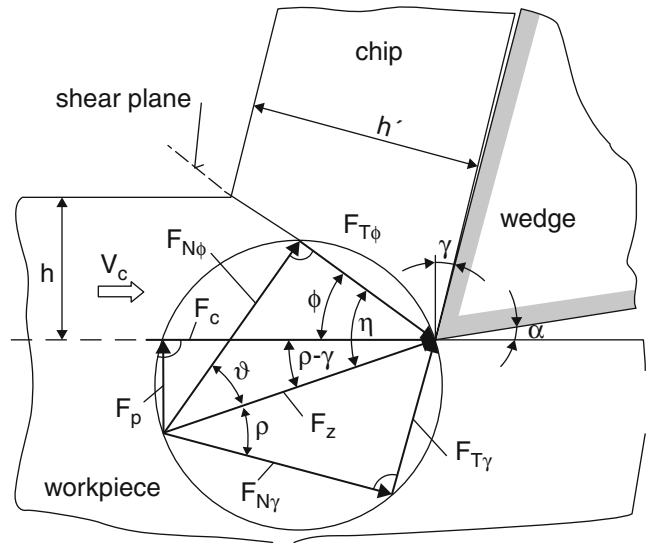
In an orthogonal cutting, the total cutting force F can be conveniently and simply resolved into two components in the horizontal and vertical directions. If the force and force components are plotted at the tool point instead of at their actual points of application along the shear plane and tool face, we obtain a convenient and compact diagram (Fig. 4) (Merchant 1944). The two basic components of the resultant Fz are Fc and $Fp \cdot Fc$, the force acting in the direction of the tool travel. It shows the amount of work required to move the cutting tool through a given distance. Force Fp does not work, but both components produce deflection in the workpiece and the cutting tool when it is in operation. The whole system is based on the assumption that chip is a body in stable equilibrium under the action of forces (Bawa 2004).

The forces applied against the chip by the tool can be separated into two mutually perpendicular components: friction force ($FT\gamma$) and normal force ($FN\gamma$) of friction. $FT\gamma$ represents the frictional resistance encountered by the chip as it slides over the face of the tool. $FN\gamma$ is the normal force to friction which is perpendicular to the friction force. The ratio of $FT\gamma$ to $FN\gamma$ is known as the coefficient friction between the tool and the chip and is represented by μ . The coefficient of friction between the chip and the tool is equal to the tangent of angle ρ as shown in Fig. 3 (Bawa 2004).

The relationships between the force components seen on Fig. 3 can be indicated in the following manner (Bawa 2004):

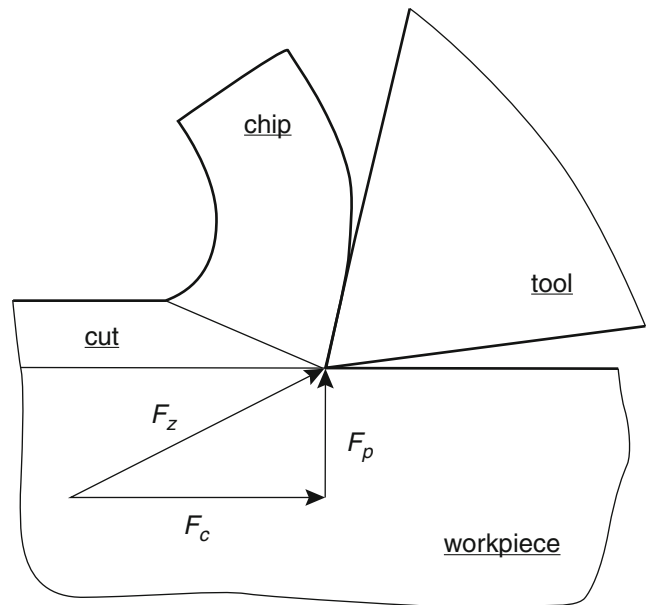
Cutting Force Modeling,

Fig. 3 Forces acting in orthogonal cutting with a continuous chip



Cutting Force Modeling,

Fig. 4 Total cutting force components



$$F_T(\phi) = F_c \cdot \cos(\phi) - F_p \cdot \sin(\phi) \quad (1)$$

$$F_Z = F_c \cdot \sin(\phi) + F_p \cdot \cos(\phi) \quad (2)$$

$$F_{N\gamma} = F_c \cdot \cos(\gamma) - F_p \cdot \sin(\gamma) \quad (3)$$

Mathematically, the coefficient of friction (μ) is

$$\mu = \frac{F_{T\gamma}}{F_{N\gamma}} = \frac{F_p + F_c \cdot \tan(\gamma)}{F_c - F_p \cdot \tan(\gamma)} \quad (4)$$

where

- γ = rake angle
- Φ = shear plane angle

The frictional force ($F_{T\gamma}$) is the actual force resisting the sliding of the chip over the tool face. Mathematically, the force of friction is (Bawa 2004):

$$F_T \gamma = F_c \cdot \sin(\gamma) + F_p \cdot \cos(\gamma) [N] \quad (5) \quad \text{where}$$

The total work done for cutting a material is equal to the sum of the work done in shearing the material plus work done in overcoming friction (Bawa 2004).

In addition to the tool forces acting on the chip, there are two force components applied by the workpiece on the chip: shear force and normal force to shear, shown in Fig. 3. $FT\Phi$ represents the shearing force and is the force required to shear the material on the shear plane. $FN\Phi$ acts normal to the shearing plane. It results in compressive stresses being applied to the shear plane. The mean shearing stress acting on the shear plane is equal to the mean strength of the metal subjected to cutting action. So based on the shear force, we can define the shear stress (τ) that acts along the shear plane between the workpiece and the chip (Groover 2010):

$$\tau = \frac{F_T \phi}{A} [N] \quad (6)$$

where A = area of the shear plane.

This shear plane area can be calculated as (Groover 2010)

$$A_S = \frac{t_1 \cdot w}{\sin(\phi)} \quad (7)$$

h = chip thickness before the cut
 w = width of cut

The shear stress in the equation represents the level of stress required to perform the machining operation. Therefore, this stress is equal to the shear strength of the work material under the conditions at which cutting occurs (Groover 2010).

The orthogonal cutting is just a particular case of the oblique cutting. Most of the metal cutting operations in industry are oblique cutting operations and the majority of the tools are supposed to be oblique. The fundamental difference in the analysis of cutting will be presented.

Oblique Cutting

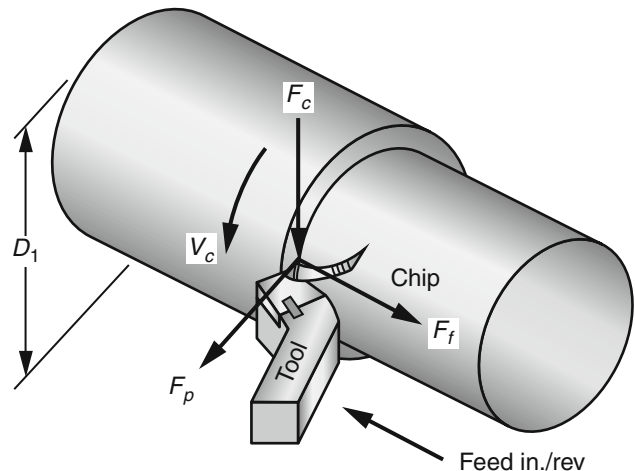
All of the processes such as turning, sawing, grinding, milling, shaping, planning, broaching, and drilling are examples of oblique or three-force cutting. The cutting force system in a conventional, oblique-chip formation process is shown schematically in Fig. 5.

Oblique cutting has three components:

1. F_c : Primary cutting force acting in the direction of the cutting velocity vector. This force is generally the largest force and accounts for 99% of the power required by the process.

Cutting Force Modeling,

Fig. 5 Oblique machining components of forces acting on the tool



2. F_f : Feed force acting in the direction of the tool feed. This force is usually about 50% of F_c but accounts for only a small percentage of the power required because feed rates are usually small compared to cutting speeds.
3. F_p : Radial or thrust force acting perpendicular to the machined surface. This force is typically about 50% of F_f and contributes very little to power requirements because velocity in the radial direction is negligible.

The relationships in oblique cutting forces shown in Fig. 6 illustrate the general relationship between these forces with speed, feed, and depth cut. Note that these figures cannot be used to determine forces for a specific process.

In oblique cutting, the resultant force F_z can be calculated as

$$F_z = \sqrt{F_c^2 + F_f^2 + F_p^2} \tag{8}$$

In which the primary cutting force F_c can be assessed by the proportional relation that experimentally can be observed with the area of the chip and can be given by.

$$F_c = k_c \cdot A [N] \tag{9}$$

where

k_c = Cutting pressure [N/mm²]

A = Area of the chip section = $f \cdot a_p$ [mm²]

After calculating the primary cutting force, the power (P) can be obtained by the scalar product of the force and cutting speed as

$$P = \overline{F_z} \times \overline{V} = F_f \cdot v_f + F_p \cdot v_p + F_c \cdot v_c [W] \tag{10}$$

where we know $v_p = 0$, then

$$P = F_f \cdot v_f + F_c \cdot v_c \tag{11}$$

where v_f is the feed rate in mm/min and v_c the cutting speed in m/min.

Furthermore,

$$v_f \ll v_c \text{ and } F_f < F_c$$

Therefore,

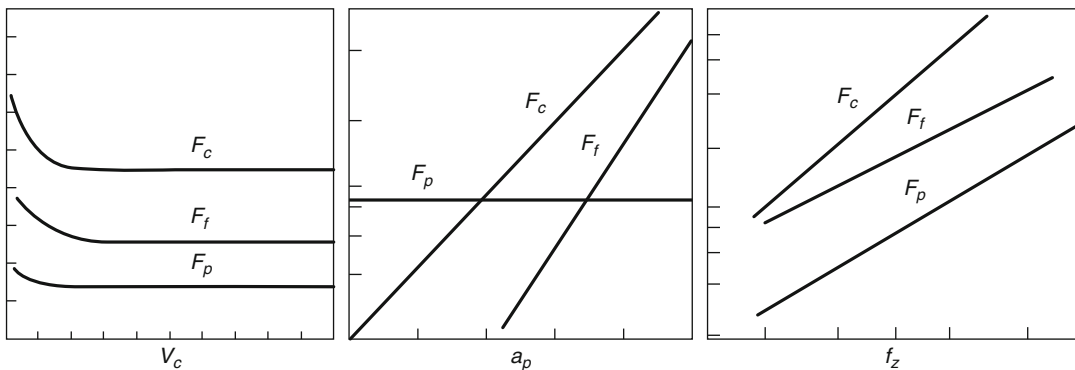
$$P = F_c \cdot v_c [W] \tag{12}$$

Remembering that

$$v_c = \frac{\pi \cdot D \cdot n}{1,000} \text{ [m/min]} \tag{13}$$

$$n = \frac{v_c \cdot 1,000}{\pi \cdot D} \text{ [rpm]} \tag{14}$$

$$v_f = f \cdot n \text{ [mm/min]} \tag{15}$$



Cutting Force Modeling, Fig. 6 Relationship between cutting forces in oblique cutting: the forces vary by speed, depth of cut, and feed

where

n = Spindle speed [rpm]
 f = Feed per revolution [mm/rev]

In case of tools with more than one cutting edge, like milling, v_f must be calculated as

$$v_f = f_z \cdot n \cdot Z \quad [\text{mm/min}],$$

where

f_z = Feed per tooth [mm/tooth]
 Z = Number of teeth

Another approach to calculate approximately the main cutting force is the exploit of a very useful parameter called unit, or specific pressure, which is defined as:

$$u = \frac{F_c \cdot 60,000}{Q} \quad [N/\text{mm}^2] \quad (16)$$

where Q = Material removal rate is given by

$$Q = 1,000 \cdot v_c \cdot f \cdot a_p \quad [\text{mm}^3/\text{min}] \quad (17)$$

where

v_c = cutting speed [m/min]
 f = feed per pass [mm/pass]
 a_p = depth of cut [mm]

The parameter u permits to roughly estimate the primary cutting force F_c according to

$$F_c = \frac{u \cdot \text{MRR}}{v_t} \quad [N] \quad (18)$$

This type of estimate of the major force F_c is useful in the analysis of deflection and vibration problems in machining and in the proper design of work holding devices, because these devices must be able to resist movement and deflection of the part during the process. In general, increasing the speed, the feed, or the depth of cut will increase the power requirement. Doubling the speed doubles the power directly. Doubling the feed or the

depth of cut doubles the cutting force F_c . However, speed has a strong effect on tool life because most of the input energy is converted into heat, which raises the temperature of the chip, the work, and the tool, to the latter's detriment.

The values for specific pressure u are normally obtained through orthogonal metal-cutting experiments. Specific pressure is related to and correlates well with shear stress τ_s for a given metal. The unit power is sensitive to material properties (e.g., hardness), rake angle, depth of cut, and feed, whereas τ_s is sensitive to material properties only. Specific power can be used to estimate the motor power required to perform a machining operation for a given material.

The power required for cutting (power at spindle).

$$P = F_c \cdot v_c \quad (19)$$

$$P = F_c \cdot v_c / 60 \quad [W] \quad (20)$$

For the motor power, the u values are multiplied by the approximate Q for the process. The motor power, P_{motor} is then

$$P_{\text{motor}} = \frac{u \cdot Q \cdot \text{CF}}{60,000 \cdot \eta} \quad [W] \quad (21)$$

where E is the efficiency of the machine which accounts the power needed to overcome friction and inertia in the machine and drive moving parts. Usually, 80% is used. Correction factors (CFs) may also be used to account for variations in cutting speed, feed, and rake angle, usually a tool wear correction factor of 1.25 used to account for the fact that dull tools use more power than sharp tools.

Note

In Eqs. 9 and 18, two different approaches in cutting force calculation are presented and the parameters kc and u are introduced. Considering Eq. 9, kc is the ratio between the cutting force and the removed chip area and some authors refer to cutting pressure. According to these authors, kc depends on the chip area and the $kc\theta$ parameter, specific cutting pressure, is introduced as reported

in Eq. 23 in the following paragraph. Other authors refer to the u parameter that, according to Eq. 16, is a specific cutting energy. Taking into account the Q expression in Eq. 17, it is evident that kc and u are referring to the same physical quantity (18).

Cutting Forces Modeling by Process

Cutting force is the most fundamental, and in many cases the most significant parameter in machining operations. In the main manufacturing processes like turning, milling, and drilling, they can cause part and tool deflections which may result in tolerance violations.

Force modeling and simulation have the potential for improving cutting tool designs and

selecting optimum conditions, especially in advanced applications. Force modeling in metal cutting is also important for a multitude of purposes, including thermal analysis, tool life estimation, chatter prediction, and tool condition monitoring. Numerous approaches have been proposed to model metal cutting forces with various degrees of success.

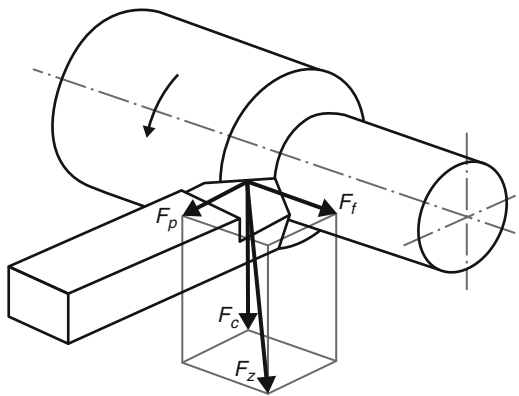
Turning

All the relations reported in orthogonal cutting condition can be also be applied in oblique conditions (according to Merchant), since the relevant section of the secondary cutting edge to the cut is too small compared to that of the main cutting edge, and the curvature of the machined surface is not excessively large. This is the case of turning an element with a diameter not too small, with a large depth with respect to the feed.

In a turning process, the resultant cutting force can be decomposed into three components (Fig. 7): feed force (F_f), radial force (F_p), and tangential force (F_c). The value of these components not only depends on the workpiece material, the tool geometry, and the cutting parameters, but also on the cutting angle and the area of the chip section.

The performance of the cutting force components as a function of the registration angle (κ) can be observed in Fig. 8.

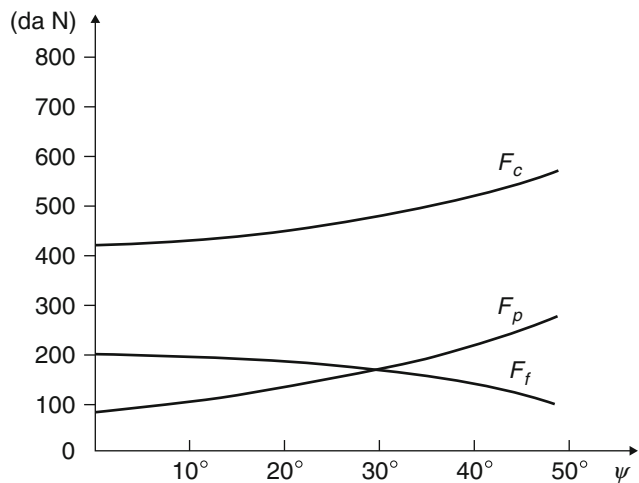
The tangential force in turning is the application of the main cutting force previously



Cutting Force Modeling, Fig. 7 Force components in turning

Cutting Force Modeling,

Fig. 8 Performance of cutting force components in function of registration angle. Material: UNI-C50
 $\lambda = 0^\circ; \gamma = 10^\circ; \alpha = 6$



explained in the oblique cutting section. The relationship between the tangential force and the area of the chip section is given by (Santochi and Giusti 2000)

$$F_z = K_s \cdot S \quad [N] \quad (22)$$

where

$$k_c = \text{Cutting pressure [N/mm}^2\text{]} \\ A = \text{Area of the chip section} = f \cdot ap \text{ [mm}^2\text{]}$$

The cutting pressure k_c , previously defined by the tangential force F_c and the chip area, is given according to Kronenberg by the relation:

$$k_c = \frac{k_{c0}}{A^{1/n}} \quad (23)$$

where n is a positive constant that depends only on the workpiece material (Table 1), while k_{c0} is the specific cutting pressure, where the cutting pressure corresponds to a unit cross section of the chip ($A = 1 \text{ mm}^2$). The value of k_{c0} depends on the workpiece material, rake angle, tool material, lubricant, etc.; the most common values are given on the Table 2 (Santochi and Giusti 2000).

Cutting Force Modeling, Table 1 Values of the constant $1/n$ according to Kronenberg

Steels	Irons	Brass	Aluminum alloys
0.197	0.137	0.255	0.060

Cutting Force Modeling, Table 2 Values of specific cutting pressure (k_{c0})

Material	Brinell hardness HB [N/mm ²]	Specific cutting pressure k_{c0} [N/mm ²]
Brass	80–120	70–90
Bronze	60–70	80
Aluminum alloys	65–70	55
Lightweight alloys	50–60	25

Kronenberg proposes for the steels:

$$k_c = 2.4 \cdot R_m^{0.454} \cdot \beta^{0.666} \quad [N/\text{mm}^2] \quad (24)$$

where R_m [N/mm²] is the tensile strength and β is the cutting angle of the tool ($\beta = 90^\circ - \gamma - \alpha$) and for the iron it is proposed:

$$k_c = 0.9 \cdot \text{HB}^{0.4} \cdot \beta^{0.666} \quad [N/\text{mm}^2] \quad (25)$$

where HB [N/mm²] is the Brinell hardness of the iron. For other materials, it can be used with their correspondent values of HB.

Then the Eq. 21 can be written as

$$F_c = k_c \cdot A^{1-1/n} \quad [N] \quad (26)$$

The relation (25) highlights that the cutting force increases when the chip section increases, but less than proportionally, maintaining all the other conditions. This is explained because the tangential force depends linearly from the depth of cut in orthogonal cutting, and approximately linear in constrained cutting conditions, if the radius between the main cutting edge and the secondary cutting edge is smaller than the depth of cut.

In regard to the feed, the F_c grows less rapidly than ap , when the feeds are not too high, as a result disturbing forces arise caused by the presence of a fillet radius between the tool rake face and the tool flank, the friction present at the tool flank and built-up edge.

These considerations explain the decreasing of the cutting pressure with the increment in the chip section as shown in Eq. 22.

It can be concluded with a following relation:

$$F_c = k_c \cdot f^s \cdot a_p^x \quad [N] \quad (27)$$

Thereby, resulting in

$$k_{c0} = \frac{F_c}{f \cdot a_p} = k_c \cdot f^{s-1} \cdot a_p^{x-1} \quad [N] \quad (28)$$

This takes into consideration, separately, the depth and the feed, fitting better than the one

proposed by Kronenberg, which involves only the chip section. As mentioned above, it assigns to x a value of 1, while the feed exponent has a value very close to 0.825.

Some researchers have proposed to introduce in Eq. 27, a correction factor that takes into account the influence of the angle of the main cutting edge:

$$F_c = k_c \cdot f^s \cdot a_p \cdot \left(\frac{\cos(45^\circ)}{\cos(90^\circ - k)} \right) \quad [N] \quad (29)$$

where the exponent z is assigned a value of 0.18. After the tangential force is calculated, the power (P) can be obtained by the scalar product of the force and cutting speed as

$$P = F_z \cdot v_t \quad [W] \quad (30)$$

Milling

Milling is a very commonly used manufacturing process in industry due to its versatility to generate complex shapes in variety of materials at high quality. Despite the developments, the process performance is still limited, and the full capability of the available hardware and software cannot be realized due to the limitations set by the process. The mills are tools with sharp teeth placed on diverse surfaces (cylindrical, flat, conical, in shape, etc.), each tooth, with its tool rake face and flank cutting edge, is comparable to a single cutting tool characterized by the rake angle, cutting edge angle, and clearance angle required for proper chip removal. The edge may be straight or helical, the latter being preferable for a more gradual cut.

The mode of chip breaking in machining is more complex than those for turning, since there is the presence of several teeth and the discontinuity in the chip formation. To analyze the problem it can be considered the simplest case of milling a flat surface, as the others are a combination of the two methods described. It can be done in two modes:

- Peripheral or end milling: in this case, the axis of rotation of the cutter is parallel to the worked surface.

- Face milling: in this case, the axis of rotation of the cutter is normal to the machined surface and each tooth removes variable chip thickness ranging from the entry point.

In both cases of milling, the resultant cutting force (F_z) on a tooth can be decomposed into two components, parallel and perpendicular to the direction of feed. The evaluation of cutting forces and power consumption is not easy to do in milling operations, given the complex shape of cutters and chip. For most applications it can be considered satisfactory, and the calculated values with the approximate method are described below.

End Milling Force Modeling Referring to Fig. 9 (Groover 2010), the chip thickness varies radially between two extreme values, zero and the value of (t_{\max}). The $F_{c \max}$ maximum tangential force on a tooth, in the simplified straight edge and with circular arc of contact, can be assessed as follows:

$$t_{\max} = f_z \cdot \sin(\phi) \quad (31)$$

where f_z is the feed per tooth, from the relation

$$v_f = f_z \cdot n \cdot Z \quad (32)$$

where

$$f_z = \frac{v_f}{n \cdot Z} \quad t_{\max} = \frac{v_f}{n \cdot Z} \cdot \sin(\phi) \quad (33)$$

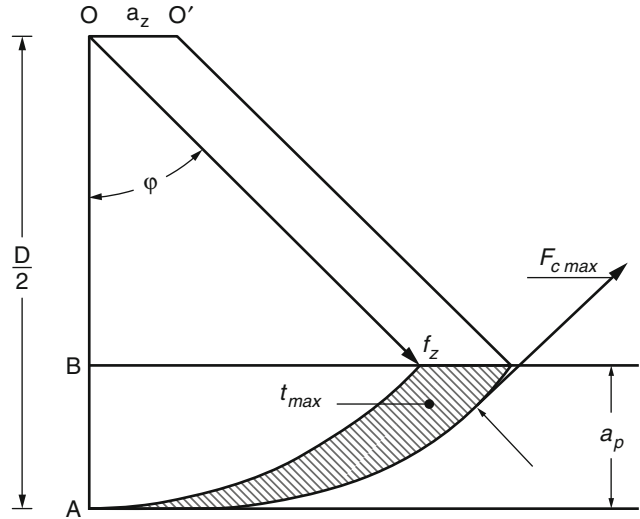
From Fig. 9 we obtain

$$\overline{OB} = \frac{D}{2} - a_p = \frac{D}{2} \cdot \cos(\phi) \quad (34)$$

D is the cutter diameter and a_p the depth of cut. Then

$$\cos(\phi) = \left(\frac{D}{2} - a_p \right) \cdot \frac{2}{D} = 1 - \frac{2 \cdot a_p}{D} \quad (35)$$

$$\begin{aligned} \sin(\phi) &= \sqrt{1 - (\cos(\phi))^2} = \sqrt{1 - \left(1 - \frac{2 \cdot a_p}{D}\right)^2} \\ &= \sqrt{\frac{4 \cdot a_p}{D} - \frac{4 \cdot a_p^2}{D^2}} = 2 \cdot \sqrt{\frac{a_p}{D} \cdot \left(1 - \frac{a_p}{D}\right)} \end{aligned} \quad (36)$$

Cutting Force Modeling,**Fig. 9** Form of the chip removed in end milling process

Since

$$1 - \frac{p}{D} \approx 1 \quad (p \ll D) \quad (37)$$

we have

$$\sin(\phi) \approx 2 \cdot \sqrt{\frac{a_p}{D}} \quad (38)$$

Therefore

$$t_{\max} = \frac{2 \cdot v_f}{n \cdot Z} \cdot \sqrt{\frac{a_p}{D}} \quad (39)$$

The maximum section of the chip is

$$A_{\max} = t_{\max} \cdot l$$

where l is the width of milling.

The maximum force ($F_{c \max}$) is expressed as follows:

$$F_{c \max} = k_c \cdot A_{\max} \quad (40)$$

where k_c cutting pressure is expressed in N/mm^2 .

Substituting we have

$$F_{c \max} = k_c \cdot l \cdot \frac{2 \cdot v_f}{n \cdot Z} \cdot \sqrt{\frac{a_p}{D}} \quad [N] \quad (41)$$

The maximum power is then.

$$P_{\max} = \frac{F_{c \max} \cdot v_c}{60 \cdot 1,000} \quad [\text{kW}] \quad (42)$$

The average values of force $F_{c \text{ avg}}$ and power consumption $P_{\text{ avg}}$ are a first approximation to half of their maximum values, because the average chip thickness is approximately equal to half the maximum thickness. So it can be said that

$$F_{c \text{ avg}} = \frac{F_{c \max}}{2} \quad (43)$$

$$P_{\text{ avg}} = \frac{P_{\max}}{2} \quad (44)$$

The power required for movement can be considered approximately equal to 15% of the cutoff. The knowledge of the maximum power consumption is useful for the selection of cutting parameters based on the machine on which you are working, while the average value is useful for evaluation of power consumption and thus the cost of processing.

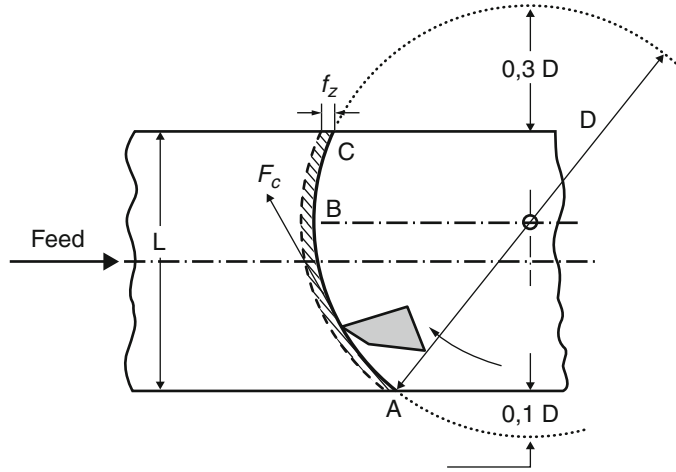
Face Milling Force Modeling

In this case, the tangential component F_c (Fig. 10) can be expressed as follows (Groover 2010):

$$F_c = k_t \cdot Z_i \cdot A \quad [N] \quad (45)$$

Cutting Force Modeling,

Fig. 10 Force components diagram in face milling process



where Z_i is the average number of working teeth in the mill. Z_i can be described as a function of the number of teeth Z of the cutter by the following relation:

$$Z_i = \frac{Z}{2 \cdot \pi} \cdot \phi \quad (46)$$

Assuming constant the chip section, A can be calculated as

$$A = a_p \cdot f_z \quad [\text{mm}^2] \quad (47)$$

where a_p is the depth of cut and f_z the feed per tooth. Then

$$F_c = k_c \cdot Z_i \cdot a_p \cdot f_z \quad [\text{N}] \quad (48)$$

And therefore, the power (P) consumption is

$$p = \frac{F_c \cdot v_c}{60 \cdot 1,000} \quad [\text{kW}] \quad (49)$$

Drilling

Drilling is one of the most important operations for metal removal, since, in quantitative terms, is the most frequent in the production of mechanical components. The drilling operation is the most common and is used to obtain a cylindrical hole with a quality equivalent to a roughing: Indeed, the tolerances on the diameter of the hole, its roundness, and surface finish are quite poor. The

easiest way to do this is a classic helicoidal drill, whose geometry is shown in Fig. 11 (Groover 2010).

The forces acting on the helicoidal drill can be originated from the following:

- The cutting edge
- The compression and the central cutting edge
- The friction of the two edges
- The lateral friction

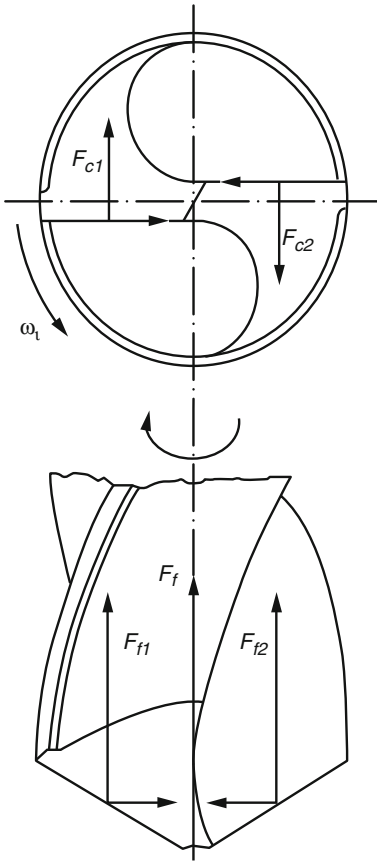
The cutting force for each cutting edge can be broken down as follows:

- Axial direction (F_{f1} , F_{f2}) component in the middle of the cutting edge which is along the axis of the tool and gives rise to the penetrating power (feed).
- Tangential direction (F_{c1} , F_{c2}) component that generates the cutting torque.

The estimation of the torque and power in drilling can be done as follows. The cutting section can be expressed as.

$$A = f \cdot \frac{D}{4} \quad (50)$$

where f is the feed in mm/rev and D is the diameter of the tool in mm. The relation for the calculation of the torque C and power P is based on the cutting pressure k_c in N/mm^2 (taken from oblique cutting relations) and the angular speed ω in rad^{-1} .



Cutting Force Modeling, Fig. 11 Forces in drilling

The cutting force (on a cutting edge) is given by

$$F_{c1} = F_{c2} = k_c \cdot A = k_c \cdot \frac{f \cdot D}{4} \quad [N] \quad (51)$$

The torque is given by

$$M_c = 2 \cdot F_{c1} \cdot \frac{D}{4,000} \quad [N \cdot m] \quad (52)$$

Substituting we have

$$\begin{aligned} M_c &= 2 \cdot \frac{k_c \cdot f \cdot D}{4} \cdot \frac{D}{4,000} \\ &= k_c \cdot \frac{f \cdot D^2}{8,000} \quad [N \cdot m] \end{aligned} \quad (53)$$

The power absorbed by the drilling is specified by

$$P = \frac{M_c \cdot \omega}{1,000} \quad [\text{kW}] \quad (54)$$

Remembering that

$$\omega = \frac{2 \cdot \pi \cdot n}{60} \quad [\text{rad}^{-1}] \quad (55)$$

where n is the spindle speed in rpm.

New Trends in Force Modeling

In the last years, finite element methods have been developed for simulating a variety of manufacturing processes such as metal forming and cutting.

Attempts to apply finite element techniques to machining have been made by many researchers. In these studies, we can distinguish basic differences due to the different approaches used by researchers. In particular, we can quote several finite element models used in the study of cutting processes:

- Eulerian model
- Lagrangian explicit model
- Lagrangian implicit model

The Eulerian Model

First examples for the application of this model to cutting processes can be found in the work of Strenkowski and Carroll (1985).

In particular, these authors have developed a viscoplastic model for the study of the steady state in orthogonal cutting. The finite element mesh defines a control volume through which the workpiece material flows through. The advantages of the Eulerian model consist of its simplicity in steady-state simulation and good computational velocity for predicting tool forces, chip geometries, and the residual plastic zone in the workpiece. The main limitations refer to the need of knowing the boundaries of the chip-free surface in advance.

The Lagrangian Explicit Model

In the Lagrangian explicit model, the equations of motions of each mass node are integrated directly and explicitly.

The original geometry of workpiece and tool are modeled, and the contact between two different surfaces and the friction influence in the area of contact between chip and tool are considered by the software.

The advantages of the Lagrangian explicit model are that they are able to handle large deformations, thermal effects, friction influence, and segmented chipping. The major disadvantages of this model are related to the need of implementing fracture criteria.

The Lagrangian Implicit Model

The Lagrangian implicit model was also used to study cutting processes. In this model, the workpiece is represented by a thermo-elastic-plastic material. The FEM codes consider the contact between solid bodies, different friction models, and chip separation criteria.

During the simulation, the tool is incrementally advanced into the undeformed workpiece. A deformation zone is formed depending on the tool advancement.

The advantages of the Lagrangian implicit model are the possibility to simulate all cutting stages, that is, indentation, incipient cutting and steady state, to handle chip segmentation, and to predict cutting forces with reasonable accuracy.

The main disadvantages are related with the long computational time for the simulation of a cutting process and for reaching the thermo-mechanical steady state.

In the last decade, these models have been developed and improved and efficient commercial solutions for 2-D and 3-D cutting process simulations are now available (Ceretti et al. 2008).

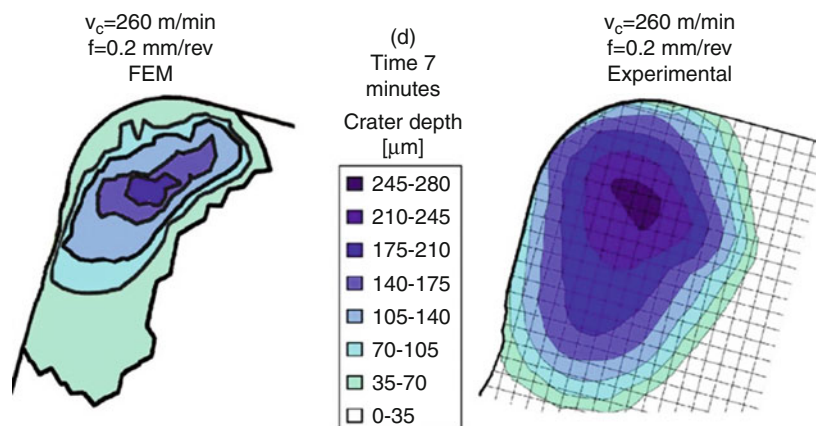
The input of finite element codes refers to the following:

- Workpiece and tool geometry and mesh
- Workpiece and tool material properties (flow stress as a function of stress, strain, strain rate and temperature, and coating properties)
- Thermal properties of materials and heat exchange coefficients
- Boundary conditions (workpiece and tool constraints)
- Friction at the tool workpiece interface
- Process parameters (cutting speed, feed, and depth of cut)

With such models, it is possible to identify the cutting forces, stress, strain rate, and temperature distributions in the tool and workpiece, to test the tool geometries and materials, to identify the best process parameters to obtain a segmented chip flow or a better surface roughness, and to evaluate the effect of tool wear on the machining process. As an example, Fig. 12 shows the results of four different machining processes: orthogonal cutting, oblique cutting, face milling, and drilling.

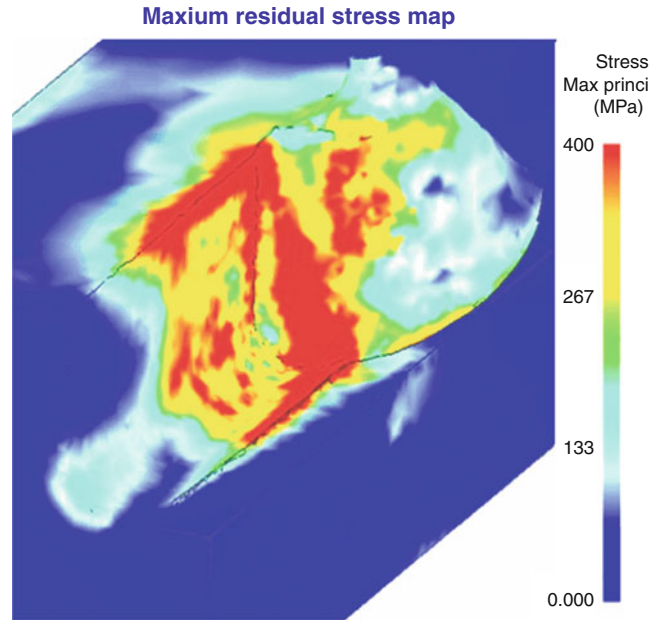
Thanks to these information it is possible to optimize the cutting process parameters in order to reduce tool wear, cutting forces, or cutting power

Cutting Force Modeling,
Fig. 12 FEM output of orthogonal cutting, oblique cutting, face milling, and drilling operations



Cutting Force Modeling,

Fig. 13 Tool wear simulation and residual stress distribution in orthogonal cutting



or to improve the surface finishing and residual stresses distribution as shown in Fig. 13.

Cross-References

- ▶ [Chatter Prediction](#)
- ▶ [Chip-Forms, Chip Breakability, and Chip Control](#)
- ▶ [Cutting Fluid](#)
- ▶ [Cutting Temperature](#)
- ▶ [Cutting, Fundamentals](#)
- ▶ [Geometric Modeling of Machining](#)

References

- Bawa HS (2004) Manufacturing processes I. Tata McGraw-Hill (TMH) Education, Noida
- Black SC, Chiles V, Lissaman AJ, Martin SJ (1996) Principles of engineering manufacture, 3rd edn. Butterworth-Heinemann, Oxford
- Ceretti E, Attanasio A, Giardini C, Filice L, Rizzuti S, Umbrello D (2008) Evaluation of accuracy in 2D and 3D simulation of orthogonal cutting processes. In: Proceedings of 11th CIRP Conference on modeling of machining operations, Gaithersburg, 16–17 Sept 2008, p 63
- Groover MP (2010) Fundamentals of modern manufacturing: materials, processes, and systems, 4th edn. Wiley, Hoboken

Marinov V (2010) Manufacturing technology. Lecture notes. Eastern Mediterranean University – Mechanical Engineering Department, pp 71–73. http://me.emu.edu.tr/me364/ME364_cutting_forces.pdf. Accessed 22 Jan 2013

Merchant ME (1944) Basic mechanics of metal cutting processes. ASME Trans J Appl Mech 11:168–175

Santochi M, Giusti F (2000) Tecnologia meccanica e studi di fabbricazione [Mechanical technology and manufacturing fundamentals]. Casa Editrice Ambrosiana, Rozzano. (in Italian)

Strenkowski JS, Carroll JT (1985) A finite element model of orthogonal metal cutting. Trans ASME J Eng Ind 107(4):349–354

Van Luttervelt CA, Childs T, Jawahir IS, Klocke F, Venuvinod PK (1998) The state of the art in modelling of machining processes. Ann CIRP 47(2):587

Cutting Forces

- ▶ [Machinability of Aluminum and Magnesium Alloys](#)

Cutting Forces Model

- ▶ [Cutting Force Modeling](#)

Cutting Lubricant

- ▶ [Cutting Fluid](#)
-

Cutting of Carbon Steel

- ▶ [Machinability of Carbon Steel](#)
-

Cutting of Fiber-Reinforced Plastics

- ▶ [Machinability of Carbon-Fiber-Reinforced and GLARE Materials](#)
-

Cutting of High-Alloyed Steel and Stainless Steel

- ▶ [Machinability of High-Alloyed Steel and Stainless Steel](#)
-

Cutting of Inconel and Nickel Base Materials

Eckart Uhlmann
Fraunhofer Institute for Production Systems and Design Technology, Berlin, Germany

Synonyms

[Cemented Carbides](#); [Ceramics](#); [Cubic Boron Nitride](#)

Definition

Nickel base materials have outstanding resistance to thermal, mechanical, and corrosive stresses. They include up to 15 elements with a portion of

more than 50% in weight and are able to resist long-term stresses up to a homologous temperature, which is the ratio between the temperature load and the melting temperature, of approximately 0.85 (Buergerl 2006). Nickel base materials are used in gas turbines, jet engines, space vehicles, and many more modern applications with extreme conditions.

However, due to the outstanding capabilities the material is hard to machine (Donachie and Donachie 2002). To understand the machinability of nickel base materials the following characteristics are essential (Wiemann 2006):

- Toughness stays stable with the temperature.
- Strain hardening is common.
- The structure includes hard and abrasive carbides.
- Poor heat conductivity leads to high temperatures in the cutting process.
- Diffusive wear appears for most cutting materials due to chemical affinities.
- Built-up edges and cold fusing of workpiece material and tool appear during cutting process.

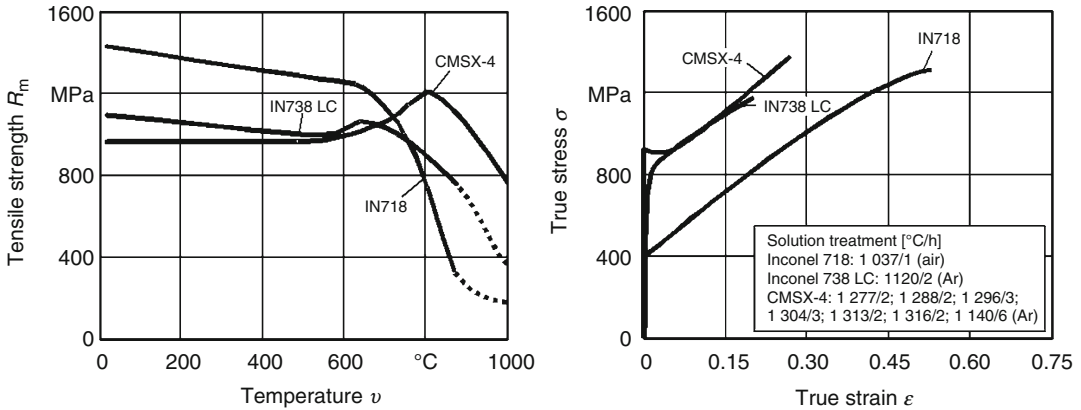
Table 1 shows the chemical composition of three alloys: Inconel 718, Inconel 738 LC, and CMSX-4. The interdependence of the tensile strength and the temperature is shown in Fig. 1.

Theory and Application

In the past decades, high-speed steel and cemented carbide cutting tools have dominated the cutting of nickel base materials and are still widely used. For intermitted cutting operations like milling, tapping, and broaching, high-speed steel is usually employed, whereas for continuous cutting mainly cemented carbide is used (Ezugwu et al. 1999). Figure 2 shows the results of tool life tests for machining different alloys with coated cemented carbide tools. A significant reduction of tool life with increasing cutting velocity can be observed. Therefore, milling of nickel base materials with cemented carbide is applicable only at a

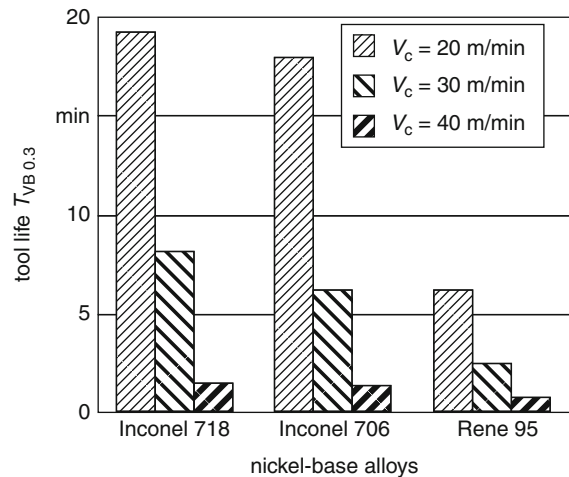
Cutting of Inconel and Nickel Base Materials, Table 1 Chemical composition of selected nickel base materials in wt-% (Donachie and Donachie 2002)

	Fe	Cr	Co	Mo	W	Ta	Nb	Al	Ti	Re	C	B	Zr	Hf	Ni
IN718	18.5	19	—	3	—	—	5.1	0.5	0.95	—	0.05	0.004	—	—	~52
IN738LC	—	16	8.5	1.7	2.6	1.7	0.9	3.4	3.4	—	0.11	0.01	0.05	—	~61
CMSX-4	—	6.5	9	0.6	6	6.5	—	5.6	1	3	—	—	—	0.1	~61



Cutting of Inconel and Nickel Base Materials, Fig. 1 Tensile strength in dependence of temperature and true stress in dependence on true strain of selected nickel base materials (Wiemann 2006)

Process:	Down-milling		
Cutting Mat.:	TiN-TiCN-K10		
Diameter:	$D_c = 50$ mm		
Width of cut:	$a_e = 30$ mm		
Depth of cut:	$a_p = 1$ mm		
Feed per tooth:	$f_z = 88$ μ m		
Coolant:	Emulsion 5 %		
Tool code:	R24512T3EML		
α_0	γ_0	κ_r	r_ϵ
20°	23°	45°	1.5 mm



Cutting of Inconel and Nickel Base Materials, Fig. 2 Tool life of cemented carbide in dependence of cutting velocity for different workpiece materials (Uhlmann and Wiemann 2004)

relatively low cutting velocity (Uhlmann and Wiemann 2004).

An alternative to cemented carbide are boron nitride and ceramics. Due to their properties, significant higher cutting velocities can be applied. Boron

nitride tools show good results for turning of nickel base materials. A tool life travel path of 3,000 m is reported for cutting Inconel 718 with coolant and a cutting velocity of 300 m/min (Gerschwiler 2002). In direct comparison with TiAlN-coated cemented

carbide tools, cubic boron nitride had a 100% longer tool life at a cutting velocity of 50 m/min (Uhlmann et al. 2009).

Plain oxide ceramics do not enable economical machining of nickel base materials, due to their poor resistance to thermal shock and low fracture toughness. Alumina oxide with titanium-carbide, so-called mixed ceramics, was successful applied with cutting velocities up to 500 m/min for turning operations (Wiemann 2006).

SiC-whisker-reinforced aluminum oxide ceramics have been developed especially for the machining of nickel base materials (Wei and Becher 1985). This ceramic cutting material allows cutting speeds between 200 and 750 m/min (Ezugwu et al. 1999). For milling 30 times higher, material removal rates were achieved with SiC-whisker-reinforced aluminum oxide compared to cemented carbide (Uhlmann and Wiemann 2004). Tool life travel path of SiC-whisker-reinforced aluminum oxide increases up to 70% by using high-pressure coolant supply with 15 MPa for turning Inconel 718. Further increase to 20.3 MPa show a negative impact (Ezugwu et al. 2005).

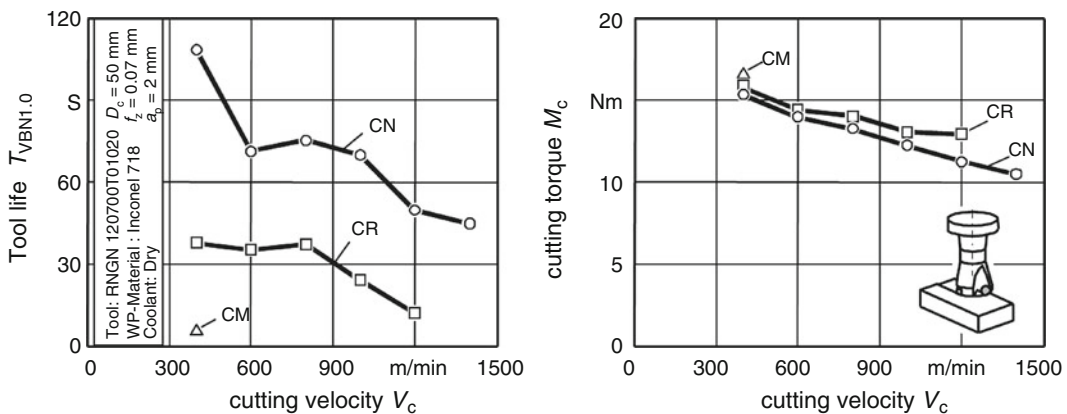
SiAlON is an alloy of silicon nitride and aluminum oxide and has proven to be the best performing ceramic cutting material for high-speed milling of nickel base materials. Cutting velocities up to 1400 m/min were employed without significant disruptions on the cutting edge

(Wiemann 2006). The positive influence of high-pressure cooling was confirmed for turning operations with SiAlON. Combining conventional cooling and 20 MPa high-pressure cooling reduced flank wear and increased tool life (Vagnorius and Sørby 2011).

Figure 3 shows tool life and cutting torque while milling Inconel 718 with three different ceramics: aluminum oxide with titanium-carbide (CM), SiC-whisker-reinforced aluminum oxide (CR) and SiAlON (CN).

Ceramic inserts are available with different types of normal clearance angle. In general, these are the positive (P) and neutral (N) geometry. The positive geometry has a clearance angle $\alpha_0 = 11^\circ$ and a wedge angle $\beta_0 = 79^\circ$. The neutral geometry has no clearance angle and has a wedge angle of 90° . In the tool holder, the inserts are arranged with an additional tool cutting edge inclination. Examinations on milling of Inconel 625 have shown that the neutral geometry reaches almost twice the tool lifetime compared to the positive (Rodrigues and Hassui 2008).

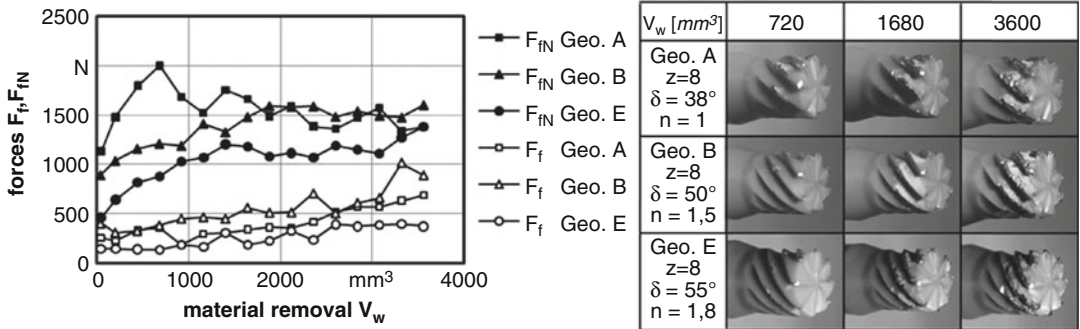
The potentials of ceramic cutting materials are, until now, restricted to applications where ceramic-indexable inserts can be employed. Performance of machining smaller geometrical features, which need tool diameters below 12 mm, is still tied to the limitations of high-speed steel and cemented carbide tools. To transfer the performance of modern ceramic cutting materials into this field of



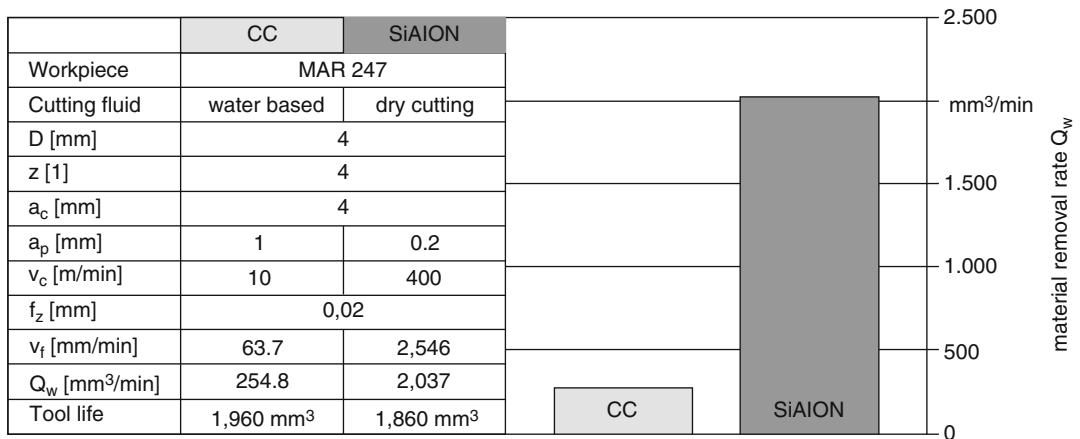
Cutting of Inconel and Nickel Base Materials, Fig. 3 Tool life and cutting torque of ceramic cutting materials while high speed machining of Inconel 718 (Wiemann 2006)

Cutting of Inconel and Nickel Base Materials, Table 2 Parameters for machining trails with monolithic ceramic milling cutters (Uhlmann and Wacinski 2010)

v_c [m/min]	f_z [mm]	a_c [mm]	a_p [mm]	D [mm]	Z [1]	N [1/min]	v_f [mm/min]	Q_w [cm ³ /min]	Workpiece material	Cutting material
600	0.05	0.2	4	8	8	23,873	9550	7.64	MAR 247	SiAlON



Cutting of Inconel and Nickel Base Materials, Fig. 4 Cutting forces and built-up edges for monolithic ceramic milling cutters with diameter of 8 mm (Uhlmann and Wacinski 2010)



Cutting of Inconel and Nickel Base Materials, Fig. 5 Benchmark of CC tool and ceramic milling cutters with 4 mm diameter (Source: Fraunhofer IPK)

applications, the development of monolithic ceramic milling cutters is essential. Regarding the fundamentally different material properties of ceramics, high-speed steel and cemented carbide, the transfer of typical tool geometries is disputable (Uhlmann and Wacinski 2010).

An obvious coefficient for peripheral milling is the so-called axial degree of uniformity denominated by “n”, which is the ratio between the projected length of cutting edge and the pitch. Since the significant influence of “n” on the

performance of peripheral milling of materials hard to machine was verified (Gey 2003), the design of monolithic ceramic milling cutters was based on it. Table 2 shows the parameters for machining test of the developed milling cutters. The experiments have shown that complex geometries can be used for monolithic ceramic cutters and result in lower process forces, Fig. 4 (Uhlmann and Wacinski 2010).

The direct benchmark of cemented carbide tools and monolithic ceramic milling cutters has shown a

material removal rate eight times higher. Figure 5 shows the process parameters used for the comparison of both cutting materials for groove-milling in the nickelbase material MAR 247.

Modern ceramic cutting materials like SiAlON have proven to push the limits of material removal rates for cutting of nickel base materials. Economical calculations have shown that the substitution of cemented carbide tool by SiAlON enables a machining cost reduction of 28% (Wiemann 2006).

Cross-References

- ▶ [Cemented Carbides](#)
- ▶ [Ceramic Cutting Tools](#)
- ▶ [Cutting, Fundamentals](#)
- ▶ [High Speed Cutting](#)
- ▶ [Superhard Tools](#)

References

- Buergel R (2006) Handbuch hochtemperaturwerkstofftechnik [Handbook of high-temperature alloys], 3rd edn. Vieweg & Sohn Verlag, Wiesbaden (in German)
- Donachie M, Donachie S (2002) Superalloys: a technical guide, 2nd edn. ASM International, Materials Park
- Ezugwu EO, Wang ZM, Machado AR (1999) The machinability of nickel-based alloys: a review. *J Mater Process Technol* 86:1–16
- Ezugwu EO, Bonney J, Fadare DA, Sales WF (2005) Machining of nickel-base, Inconel 718, alloy with ceramic tool under finishing conditions with various coolant supply pressures. In: Dobrzanski L (ed) *Journals of Materials Processing Technology*, pp 162–163
- Gerschwiler K (2002) Drehen und Fräsen von Nickelbasislegierungen [Turning and milling of nickel-base alloys]. In: Klocke F (ed) *Tagungsband "Perspektiven der Zerspantechnik: Entwicklung und Integration der Fertigungsprozesse von morgen"* [Proceedings "Material Removal Technology Perspectives: Development and Integration of Future Production Processes"]. WZL der RWTH Aachen University, pp 183–197 (in German)
- Gey C (2003) Prozessauslegung für das Flankenfräsen von Titan [Process parameters for shoulder milling of titanium]. VDI Verlag, Düsseldorf (in German). *Fortschritt-Berichte VDI* 2(625)
- Rodrigues MA, Hassui A (2008) An investigation into the high speed milling of the nickel base alloy Inconel 625 with ceramic cutting tools. In: Byrne G, O'Donnell G (eds) *Proceedings of the 3rd international CIRP high performance cutting conference*, Dublin, Ireland
- Uhlmann E, Wacinski M (2010) Development and test of monolithic ceramic end milling cutters for high speed machining of nickel-based alloys. In: Aoyama T, Takeuchi Y (eds) *Proceedings of the HPC2010, 4th CIRP international conference on high performance cutting*, Gifu
- Uhlmann E, Wiemann E (2004) High-speed milling and high-performance milling of nickel-base alloys. *International Conference on High Speed Machining*, Nanjing
- Uhlmann E, Oyanedel Fuentes JA, Keunecke M (2009) Machining of high performance workpiece materials with CBN coated cutting tools. *Thin Solid Films* 518(5):1451–1454
- Vagnorius Z, Sørby K (2011) Effect of high-pressure cooling on life of SiAlON tools in machining of Inconel 718. *Int J Adv Manuf Technol* 54(1):83–92
- Wei GC, Becher PF (1985) Development of SiC-reinforce ceramics. *Ceram Bull* 64(2):298–304
- Wiemann E (2006) Hochleistungsfräsen von superlegierungen [High-performance cutting of superalloys]. In: Uhlmann E (ed) *Berichte aus dem produktionstechnischen zentrum Berlin*. Fraunhofer IRB Verlag, Berlin (in German)

Cutting Oil

- ▶ [Cutting Fluid](#)

Cutting Property

- ▶ [Machinability](#)

Cutting Temperature

Takashi Ueda
Department of Mechanical Science and Engineering, Nagoya University, Nagoya, Aichi, Japan

Synonyms

[Metal cutting temperature](#); [Temperature in machining](#); [Temperature in metal cutting](#)

Definition

During the cutting of metal, the temperature of the interaction area of the cutting tool and workpiece

becomes high. The temperature affects not only the rate of wear of the cutting tool but also the integrity of workpiece surface such as residual stress, hardness, and surface roughness. The cutting temperature is one of the very important factors to investigate the mechanism of cutting process.

Theory and Application

Heat Generation in Cutting

The cutting energy E_0 consumed in cutting process is expressed by the following equation:

$$\begin{aligned}
 E_o &= \frac{F_c v_c}{J} \\
 &= k_c Q_w \\
 &= k_c A v_c
 \end{aligned}
 \tag{1}$$

where F_c is the cutting force, v_c is the cutting speed, J is the mechanical equivalent of heat, k_c is the specific cutting energy, Q_w is the metal removal rate, and A is the chip cross section. E_0

is used to make a plastic deformation of work material as well as heat due to friction between the cutting tool and workpiece, and more than 95% of E_0 is converted to heat. As a result, the temperature of the interaction area of the cutting tool and workpiece becomes high. The conversion of energy to heat is performed in the following areas:

1. Primary shear zone
2. Secondary shear zone at rake face
3. Secondary shear zone at flank face

The chip formation in orthogonal cutting is shown in Fig. 1. “1” designates the primary shear zone, “2” the secondary shear zone at rake face, and “4” secondary shear zone at flank face.

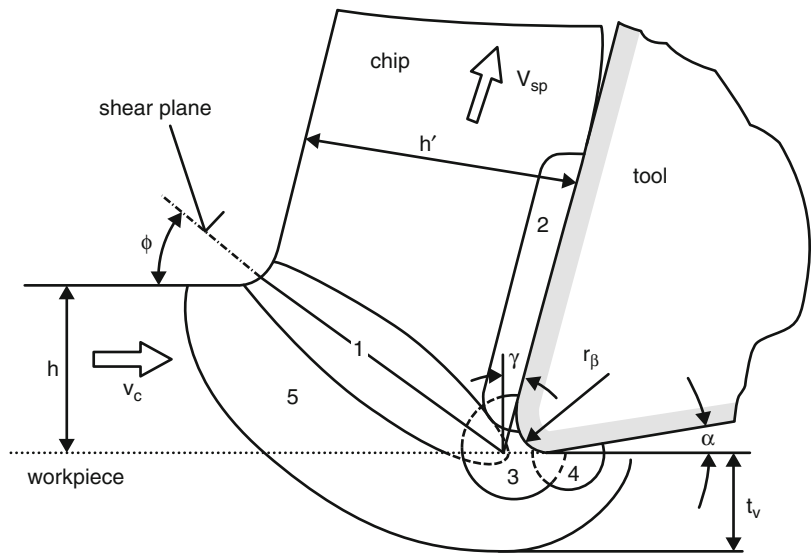
Therefore, E_0 is expressed as follows:

$$E_0 = E_1 + E_2 + E_3
 \tag{2}$$

where E_1 is the energy generated in area “1,” E_2 is the energy in area “2,” and E_3 is the energy at area “4.”

Cutting Temperature,

Fig. 1 Chip formation in orthogonal cutting (This figure is used in section C of CIRPedia under “Cutting, Fundamentals” Fig. 6)



- | | |
|---------------------------------------|----------------------------|
| 1 : primary shear zone | γ : rake angle |
| 2 : secondary shear zone at rake face | α : clearance angle |
| 3 : seperative zone | ϕ : shear angle |
| 4 : secondary shear zone at flank | t_v : deformation depth |
| 5 : preliminary deformation zone | |

(a) Case when the friction at flank face is ignored

It is possible to ignore the tool wear at flank face when the new cutting tool is used. Then the heat source E_3 at secondary shear zone (at flank face) need not be considered. Then the Eq. 2 can be expressed by:

$$E_0 = E_1 + E_2 \tag{3}$$

In Fig. 2, the shear speed v_s is expressed as follows:

$$v_s = \frac{v_c \cos \gamma}{\cos(\phi - \gamma)} \tag{4}$$

and the following relationship holds among the cutting forces.

$$F_s = F_c \cos \phi - F_p \sin \phi \tag{5}$$

where ϕ is the shear angle, v_c is the cutting speed, F_s is the shear force, F_c is the cutting force, and F_p is the thrust force (passive force).

Therefore, the energy E_1 generated at shear plane is expressed by:

$$E_1 = \frac{F_s v_s}{J} = (F_c \cos \phi - F_p \sin \phi) \frac{v_c \cos \gamma}{J \cos(\phi - \gamma)} \tag{6}$$

Let us consider the energy E_2 generated at the rake face:

$$v_{sp} = \frac{v_c \sin \phi}{\cos(\phi - \gamma)} \tag{7}$$

$$F = F_c \sin \gamma + F_p \cos \gamma \tag{8}$$

Therefore, E_2 is expressed by:

$$E_2 = \frac{F v_{sp}}{J} \tag{9}$$

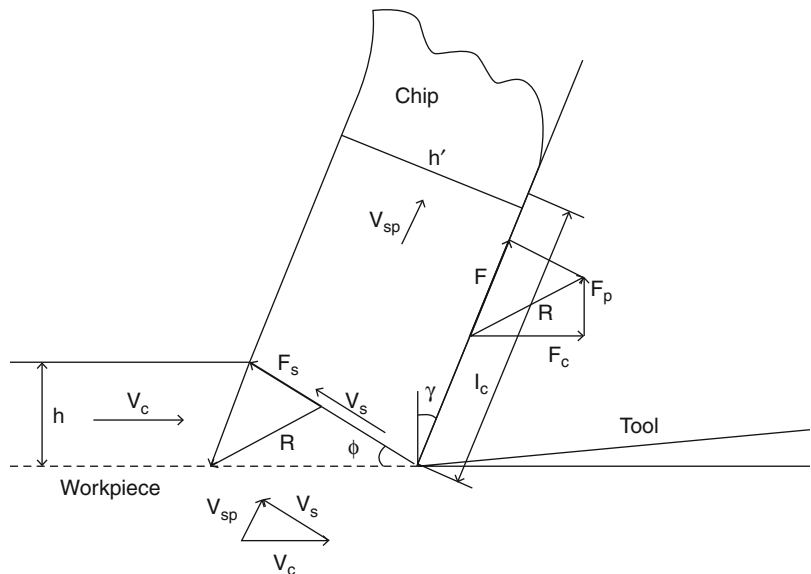
where F is the friction force at rake face and v_{sp} is the chip exit speed on rake face.

Consequently,

$$E_2 = (F_c \sin \gamma + F_p \cos \gamma) \frac{v_c \sin \phi}{J \cos(\phi - \gamma)} \tag{10}$$

Cutting Temperature,

Fig. 2 Model of cutting process in orthogonal cutting



When h designates the undeformed chip thickness and h' the chip thickness, then the chip thickness ratio λ_h is expressed by

$$\lambda_h = h/h' \quad (11)$$

so that the shear angle ϕ is given by:

$$\tan \phi = \frac{\lambda_h \cos \gamma}{1 - \lambda_h \sin \gamma} \quad (12)$$

The values of factors F_c , F_p , h , h' , ϕ , and v_c used in Eqs. 6 and 10 can be determined through the experiments. Substituting these quantities into Eqs. 6 and 10, the heat generated in cutting is calculated.

Since the area of shear plane is $(bh/\sin \phi)$ and the contact area between chip and rake face is (bl_c) , where b is cutting width and l_c is contact length between chip and rake face and assuming that the heat is generated in these faces uniformly, the energies e_1 and e_2 generated per unit time and unit area in these faces are given by the following equations:

$$e_1 = E_1 \sin \phi / bh \quad (13)$$

$$e_2 = E_2 / bl_c \quad (14)$$

(b) Case when the tool wear is not ignored

As the tool wear develops during the cutting operation, the friction between the workpiece

surface and the tool flank increases and the heat generated in the area "4" in Fig. 1 becomes more and more pronounced. Consequently, the temperature at flank face rises and the influence of the temperature on the surface layer of workpiece becomes significant. The temperature is closely related to the integrity of workpiece surface such as residual stress, hardness, and surface roughness. The width of the wear at flank face is sometimes used as the criteria of tool life. In Eq. 1, the specific cutting energy k_c increases with the tool wear so that the cutting energy E_0 increases and, as a result, the temperature of cutting edge rises (Boothroyd 1981; Shaw 1984; Oxley 1989; Childs et al. 2000).

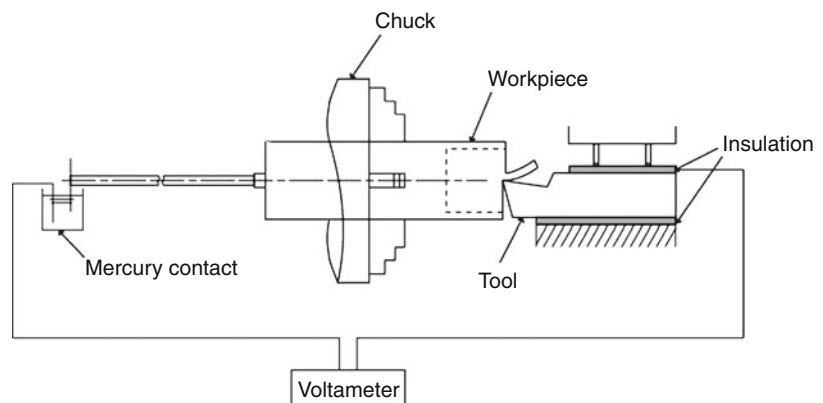
Temperature Measurement Method

Tool–Work Thermocouple Method

Thermocouples are most commonly used sensor for measuring cutting temperature. The tool–work thermocouple technique is applied to measure the mean temperature over the entire contact area between the tool and the work. The basic configuration of experiment setup is shown in Fig. 3. This method is based on the fact that an e.m.f. is generated at the interface of two different metals when the temperature of the junction changes. The figure is to measure the tool temperature during a turning operation. The tool–work junction constitutes the hot junction, while the cold junction remains at room temperature, and the e.m.f. is generated depending on the temperature difference between these two

Cutting Temperature,

Fig. 3 Tool–work thermocouple circuit in turning



junctions. This method measures the mean temperature over the entire contact area between work (chip) and tool (including the flank face). It cannot distinctly measure the temperature difference between work (chip) and rake face from that between work and flank face. However, this measuring technique is used conveniently because it is relatively simple to apply (Childs et al. 2000).

Thermocouple embedded in cutting tool has also been used to measure the distribution of cutting temperature in it. Temperature distribution at the tool edge can be measured by a fine insulated platinum wire embedded in the tool. The Pt wire constitutes the thermocouple with the chip (Shaw 1984; Childs et al. 2000).

Radiation Method

Two-Color Pyrometer with Optical Fiber

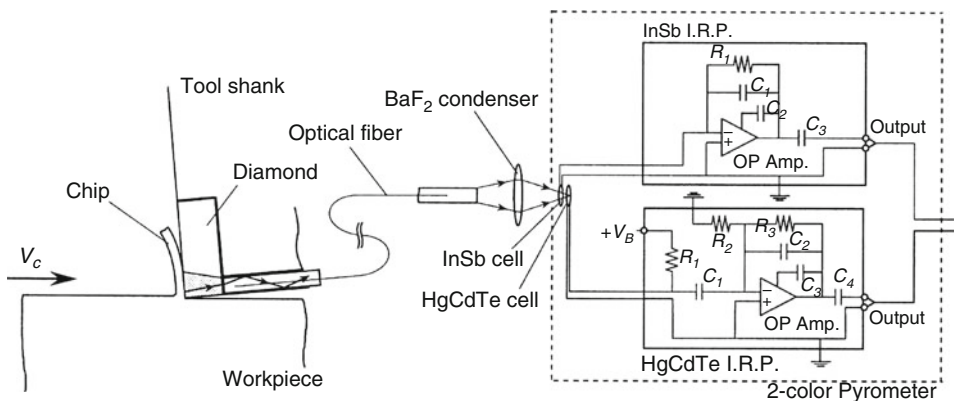
(a) Temperature on Rake Face in Turning

>In Fig. 4, the temperature on the rake face of a single crystal diamond tool is measured using an infrared radiation pyrometer. In the pyrometer, the infrared rays radiated from the contact area between the chip and the rake face of the diamond tool, are accepted by a chalcogenide fiber and led to a two-color detector consisting of InSb and HgCdTe detectors. The infrared energy is converted to an electric signal by the detectors

and the temperature is determined by the ratio of these two signals. Figure 5 shows the output wave when a work material of copper is cut at a cutting speed of 726 m/min. From the figure, it can be seen that the average temperature during cutting is approximately 214 °C (Ueda et al. 1998).

(b) Temperature on Flank Face in Turning

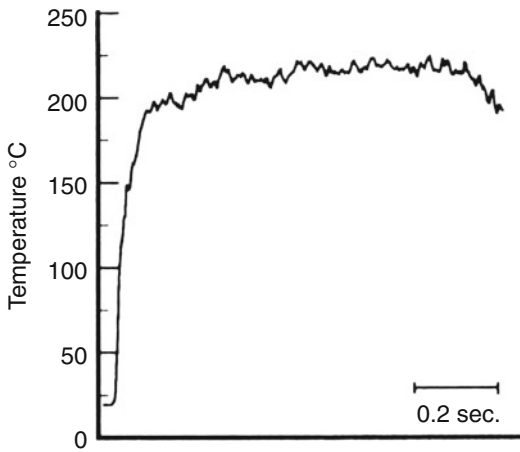
A schematic illustration of the experimental setup is shown in Fig. 6. A cylindrical workpiece is gripped by a chuck of lathe. Chalcogenide glass fiber-A is embedded in the workpiece and the incidence face of the fiber is inserted into a small hole which extends to the outer surface of the cylindrical workpiece. The incidence face of optical fiber-A which rotates with the workpiece accepts the infrared rays radiated from the flank face of the tool tip when the incidence face of fiber-A passes through the tool tip during the cutting operation. The infrared rays accepted by optical fiber-A are emitted at the other face. The infrared rays are accepted by fiber-B which is fixed at the pyrometer and led to the two-color detector. These two optical fibers are connected with the noncontact fiber coupler. The infrared energy is converted to electric signals by the two-color detector. Taking the ratio of these two output voltages, the temperature can be obtained (Ueda et al. 2008).



Cutting Temperature, Fig. 4 Two-color pyrometer with an optical fiber in diamond turning

(c) Temperature on Flank Face in End Milling

The temperature on the flank face during cutting is measured. Figure 7 shows the experimental setup. It is very difficult to measure the temperature of end milling cutter accurately when it is rotating at a high speed. The frequency characteristics of the pyrometer are crucially important

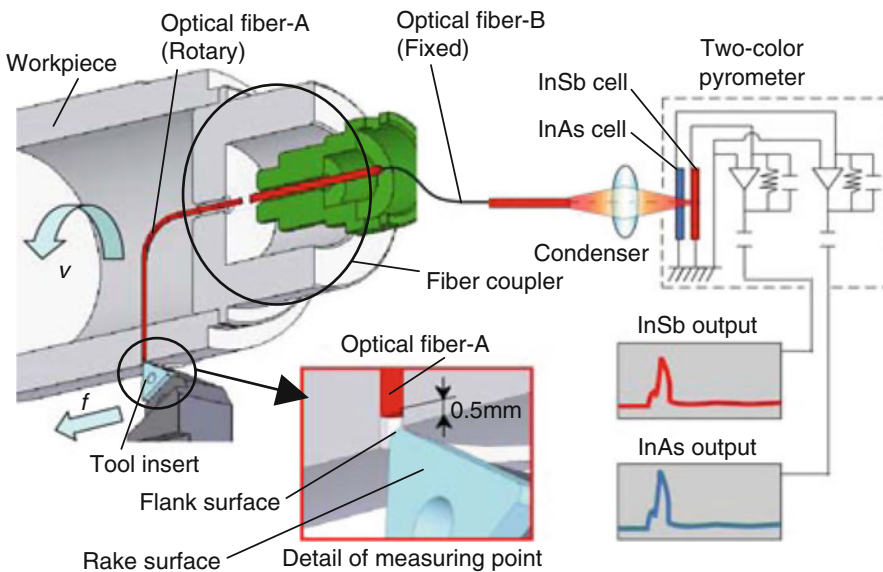


Cutting Temperature, Fig. 5 Cutting temperature in diamond turning (Work: Copper, Cutting tool: Single crystal diamond, Cutting speed: 726 m/min, Depth of cut: 10 μm)

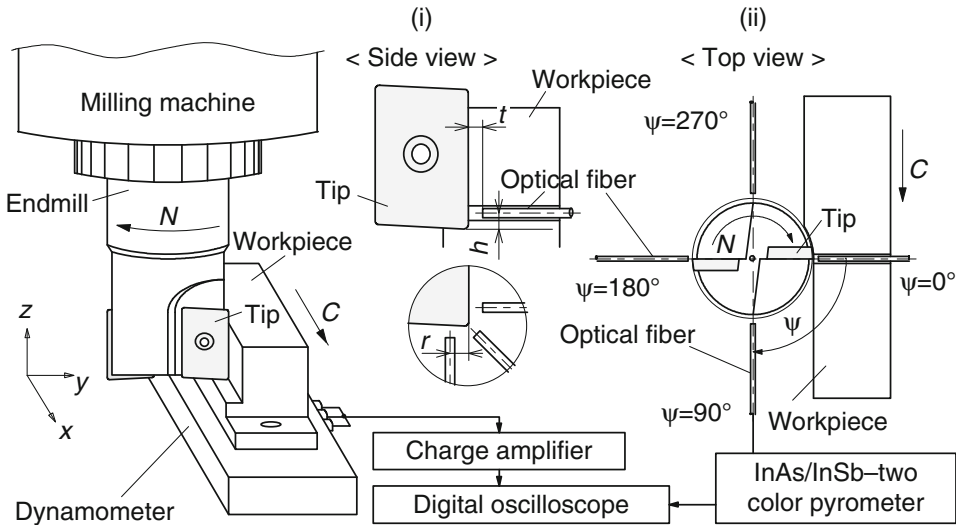
because they determine the limit of rotating speed to which this method is applied. Figure 8 shows the frequency characteristics of the pyrometer in Fig. 7. The pyrometer has a flat response to about 400 kHz. This pyrometer can be applied to measure the temperature when the end milling cutter is rotating at up to 50,000 rpm (Ueda et al. 2001).

In Fig. 7, the workpiece has a hole which extends to the tool-workpiece contact area. An optical fiber is inserted into the fine hole from the outer surface. The optical fiber can accept the infrared energy radiated from the flank face of the cutting tool when it passes above the hole. The temperature on the flank face of the cutting tool is measured at various intervals after cutting. The point where the cutting edge has just finished cutting is indicated by $\Psi = 0^\circ$ and the rotating angle is assigned based on this point. The optical fiber is set at $\Psi = 0^\circ, 90^\circ, 180^\circ,$ and 270° . It accepts the infrared rays radiated from the tool flank face when the cutting tool passes over the incidence face of the optical fiber.

Figure 9 shows the tool temperature on the flank face while the cutting tool revolves. During one cycle of intermittent cutting, the cutting edge cools almost linearly from 730 to 580 °C and is heated to 730 °C by the cutting process. The

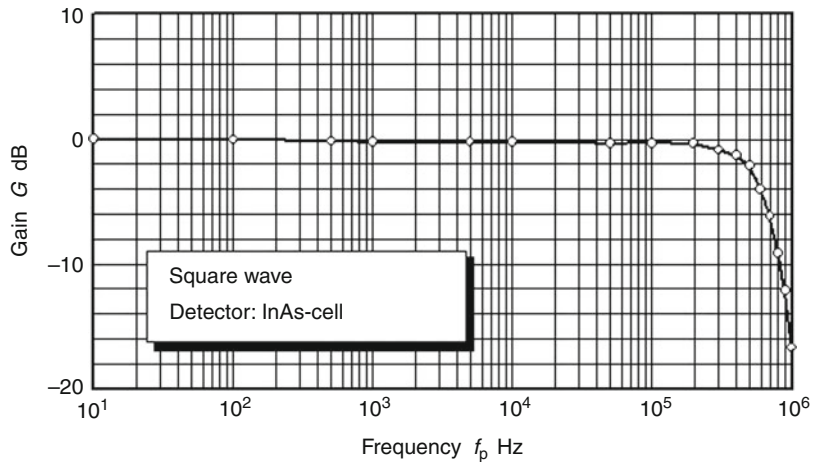


Cutting Temperature, Fig. 6 Two-color pyrometer with a fiber coupler in turning



Cutting Temperature, Fig. 7 Temperature measurement in end milling

Cutting Temperature, Fig. 8 Frequency characteristics of I.R.P



cutting tool, therefore, undergoes a thermal shock of 150 °C with every revolution.

The temperature on the rake face in end milling can be measured using the same equipment shown in Fig. 6 (Ueda et al. 2008).

Thermal Photograph The temperature distribution in workpiece, chip, and cutting tool under a constant cutting condition can be measured by taking an infrared photograph. Figure 10 shows the temperature distribution during orthogonal cutting. The workpiece is preheated at 611 °C before cutting in order to improve the sensitivity of the

infrared film. The workpiece (chip) is heated when passing through the primary deformation zone and secondary deformation zone, and the maximum temperature appears along the tool face some distance from the cutting edge (Boothroyd 1981).

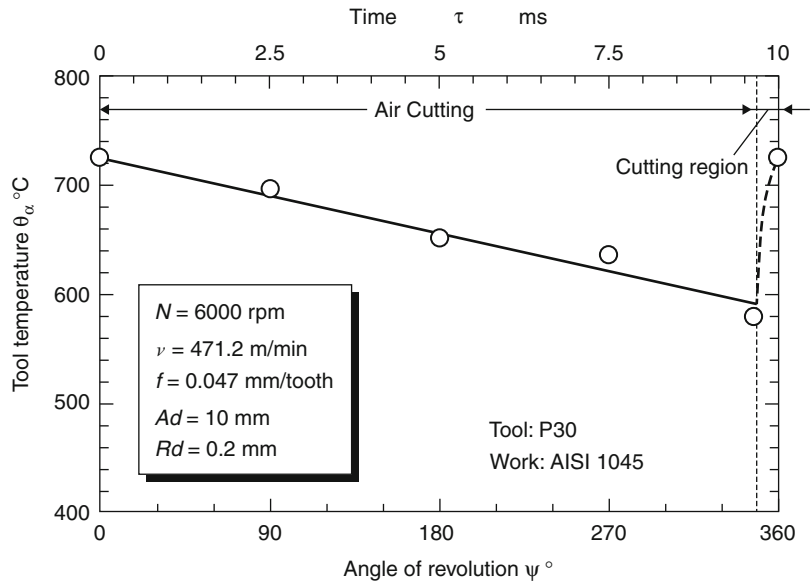
Recently, instead of thermal photograph, IR-CCD camera is used to measure the temperature distribution in cutting (Davies et al. 2007).

Influence of Cutting Conditions on Tool Temperature

It is important to understand the influence of cutting conditions such as cutting speed, depth of cut,

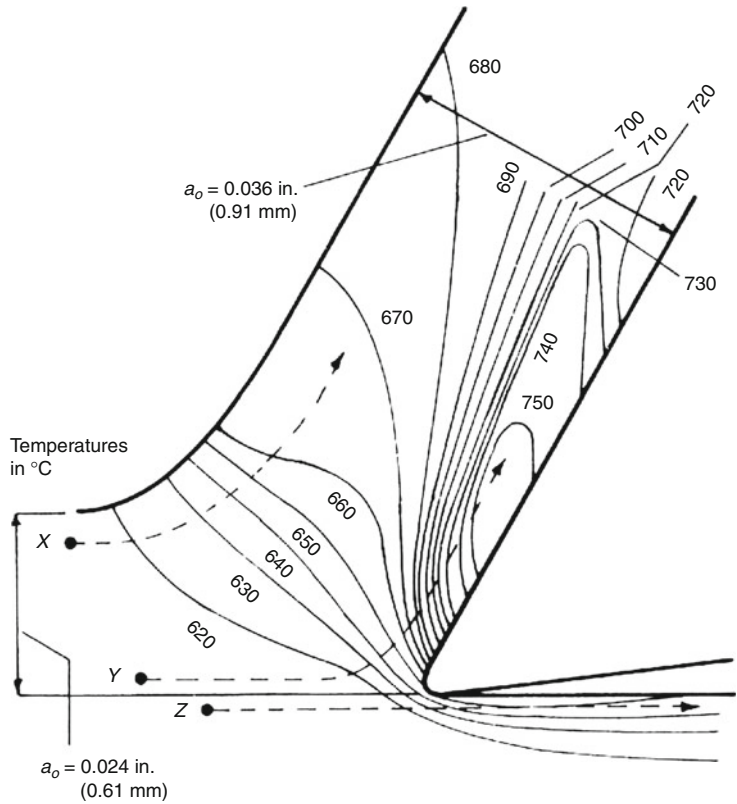
Cutting Temperature,

Fig. 9 Temperature history at flank face during one cycle in end milling



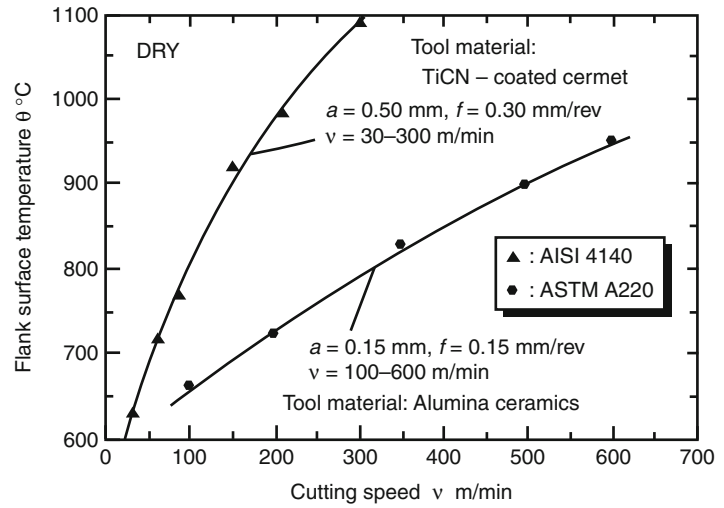
Cutting Temperature,

Fig. 10 Temperature distribution during orthogonal cutting (Work: Free-cutting mild steel, Cutting speed: 75 f/min, Width of cut: 0.25 in, Workpiece temperature: 611 $^{\circ}\text{C}$)



Cutting Temperature,

Fig. 11 Influence of cutting speed on tool temperature in turning



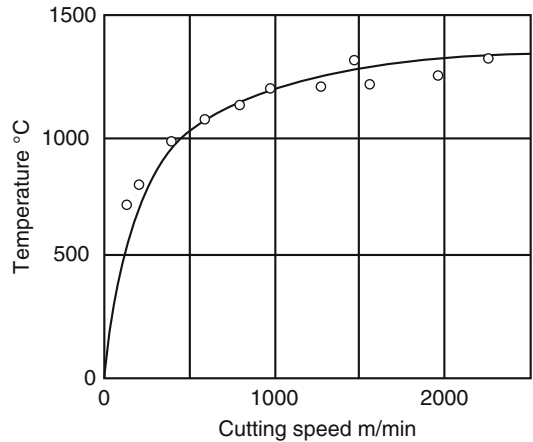
and feed rate on tool temperature. Kronenberg (1966) proposed the following empirical equation by measuring the tool temperature using a tool-work thermocouple method:

$$T = \frac{C_0 k_c v_c^{0.44} A^{0.22}}{K^{0.44} (\rho c)^{0.56}} = C_1 v_c^{0.44} A^{0.22} \quad (15)$$

where C_0, C_1 are constants, k_c is the specific cutting energy, A is the chip cross section, K is the thermal conductivity, ρ is the specific mass, and c is the specific heat. Equation 15 enables us to estimate the influence of each cutting condition on the tool temperature.

Influence of Cutting Speed

Equation 15 predicts that the tool temperature increases with the increase of cutting speed. Figure 11 shows the tool temperature in turning of chromium-molybdenum steel AISI 4140 and cast iron ASTM A220 (Ueda et al. 2008). The tool temperature increases with the increase of cutting speed. Especially, the tool temperature rise in turning of AISI 4140 is marked. This result raises us a question: What is the maximum temperature attained as the cutting speed is further increased? Figure 12 shows the cutting tool-workpiece interface temperature which is measured using a two-color pyrometer. As a cutting tool, a conical tool of translucent alumina is used and the workpiece is a carbon steel. The temperature shows the tendency to

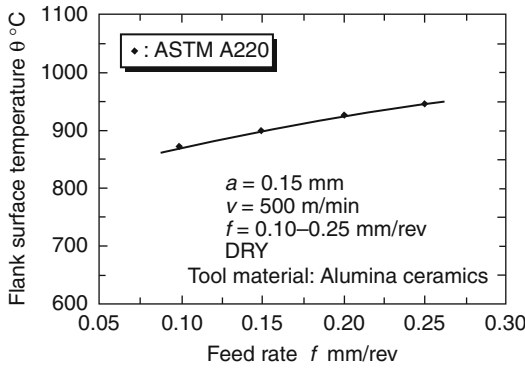


Cutting Temperature, Fig. 12 Tool-work interface temperature (Work: AISI 1055, Cutting tool: Al_2O_3 , Depth of cut: $30 \mu\text{m}$)

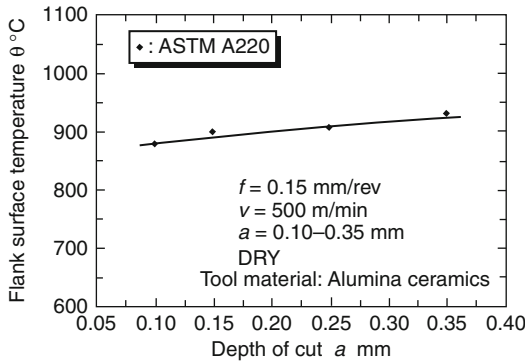
saturate at about $1,400 \text{ }^{\circ}\text{C}$, which is close to the melting point of the carbon steel (Ueda et al. 1995).

Influence of Depth of Cut and Feed Rate

In Eq. 1, the area of cross section $A (=fh)$ is larger for a larger depth of cut h and a higher feed rate f . Therefore, the cutting energy E_0 increases as a function of these factors. Figures 13 and 14 show the influence of depth of cut and feed rate on tool temperature. From these figures, the influence of depth of cut and feed rate on tool temperature is small compared to that of cutting speed. It



Cutting Temperature, Fig. 13 Influence of feed rate on tool temperature in turning



Cutting Temperature, Fig. 14 Influence of depth of cut on tool temperature in turning

is because a large part of the heat generated in cutting is removed by the chip. Consequently, the effects of depth of cut and feed rate on tool temperature are not as large as the effect of the cutting speed (Ueda et al. 2008). Equation 15 also explains the same tendency.

Influence of Work Hardness

The influence of work hardness on the tool temperature is shown in Fig. 15. There is a close relationship between the temperature on the flank face and the hardness of the work material. The highest temperature is attained for AISI52100 (700HV1) which has the greatest hardness among these materials. The temperature for AISI1045 (210HV1) is the lowest, even though severe cutting conditions are adopted (Ueda et al. 1999).

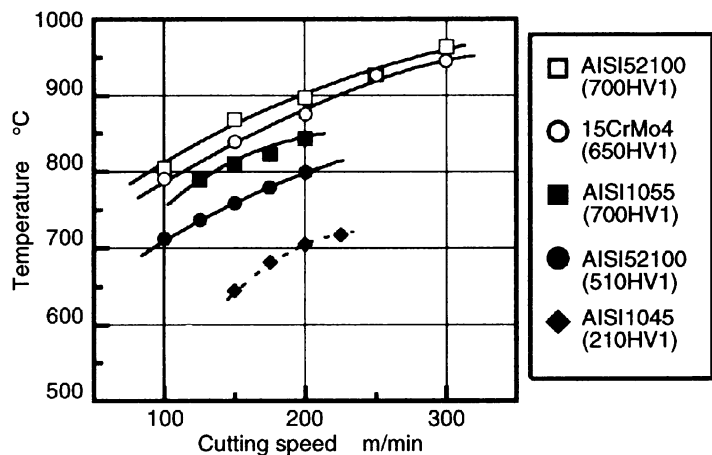
Influence of Thermal Conductivity of Cutting Tool

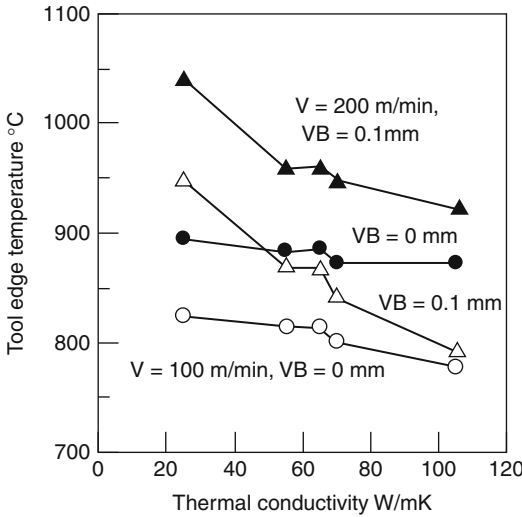
Figure 16 shows the relationship between the thermal conductivity of cutting inserts and the tool temperature on flank face. The thermal conductivity of the tool is varied by changing the content of CBN. From figure, it is found that the tool temperature decreases with an increase in thermal conductivity of tool (Tanaka et al. 2009).

Influence of Cutting Fluid and Oil Mist

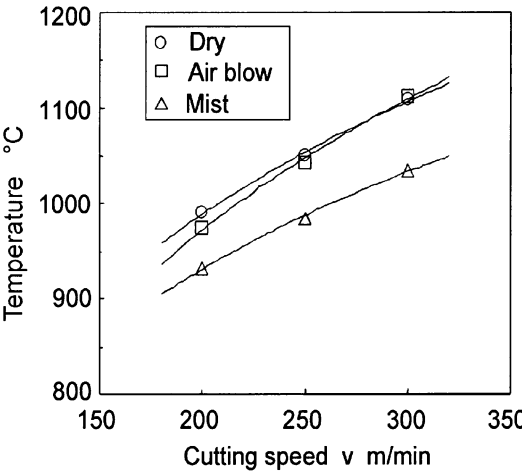
The influence of coolant on the temperature of the tool–chip interface is generally small in turning. The temperature in wet cutting is lowered only by about

Cutting Temperature, Fig. 15 Influence of work hardness on tool temperature (CBN tool, Depth of cut: 0.1 mm, Feed rate: 0.1 mm/rev, (For AISI1045, 0.8 mm, 0.15 mm/rev))





Cutting Temperature, Fig. 16 Influence of thermal conductivity of cutting tool on tool temperature (VB: width of flank wear, CBN tools are used mainly)



Cutting Temperature, Fig. 17 Influence of oil mist on tool temperature in intermittent cutting (Work: AISI1045, Cutting tool: HIP-Al₂O₃, Radial depth of cut: 0.2 mm, Axial depth of cut: 10 mm, Feed per tooth: 0.05 mm/tooth)

50 °C compared to the temperature in dry cutting. At high cutting speeds, the cutting fluid would not penetrate the tool–chip interface, since the contact pressure of the interface is very high and the cutting process operates very fast (Mahfudz et al. 2002).

Figure 17 shows the comparison of tool temperatures in dry, air-blow, and oil-mist cuttings during intermittent cutting. There is little

difference between the temperatures of dry and air-blow cutting. The temperature in the oil-mist cutting at a cutting speed of 300 m/min is lower by 70 °C than that in the case of the other cuttings. In end milling, the oil mist has more pronounced effect on cutting performances than the one in turning (Ueda et al. 2006).

Analytical Method

There are analytical methods to obtain the cutting temperature. Here, two typical methods are introduced, one derived by Carslaw and Jaeger (1967) and the other with FEM (Finite Element Method).

Figure 18 shows “Idealized diagram of shear-plane moving heat source” which was used by Shaw to drive the shear-plane temperature rise. Here the chip may be considered as a perfect insulator if the total heat flux through the interface is equal to the heat flux flowing into the work-piece, $(1 - R_1)q_1$, where $q_1 (= e_1$ given by Eq. 13) is the heat flux which flows from the shear zone. The detail of theory by M.C. Shaw can be found in his book (Shaw 1984).

The Finite Element Method is a very powerful and convenient tool to obtain temperature fields accounting for the variable material properties in the analysis. Figure 19 shows a two-dimensional model for FEM analysis. For calculation, the temperature on the rake face of a diamond tool is calculated. Two-dimensional heat conduction can be expressed by the equation:

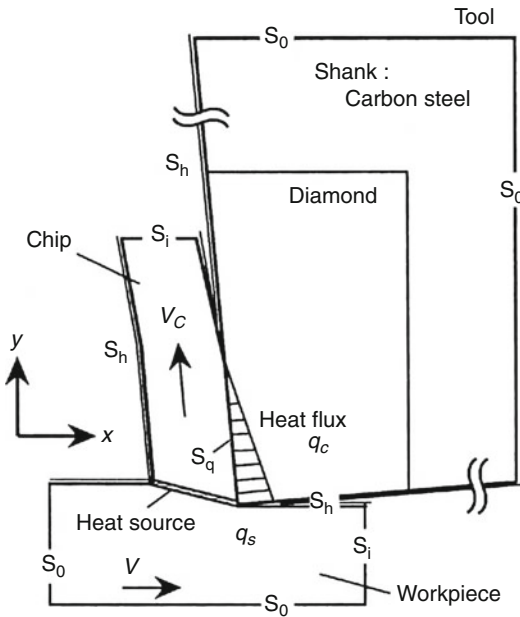
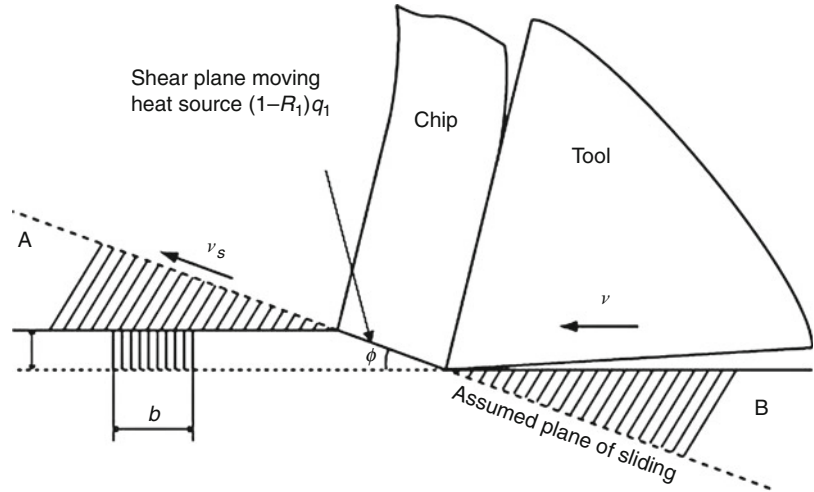
$$k \left(\frac{\partial^2 T}{\partial x^2} + \frac{\partial^2 T}{\partial y^2} \right) - \rho c \left(v_x \frac{\partial T}{\partial x} + v_y \frac{\partial T}{\partial y} \right) + q_s = 0 \tag{16}$$

where k is the thermal conductivity, ρ is the density, c is the specific heat, and T_0 is the room temperature.

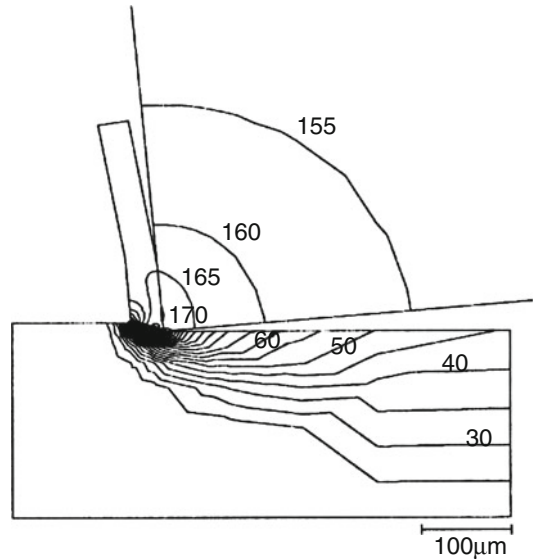
Then, boundary conditions are as follows:

$$\begin{aligned} T &= T_0 & |S_0 \\ -k \frac{\partial T}{\partial n} &= q_c & |S_q \\ -k \frac{\partial T}{\partial n} &= h(T - T_0) & |S_h \\ -k \frac{\partial T}{\partial n} &= 0 & |S_i \end{aligned} \tag{17}$$

Cutting Temperature, Fig. 18 Model of shear-plane moving heat source



Cutting Temperature, Fig. 19 FEM analysis model



Cutting Temperature, Fig. 20 Temperature distribution in tool and workpiece (Work: Al, Single crystal diamond tool, Cutting speed: 518 m/min, Depth of cut: 10 μm)

The temperature dependency of the thermal conductivity and the specific heat is considered. Figure 20 shows the calculated results of the temperature distribution in the tool and the workpiece. The average temperature at the contact area on rake face is 175 °C and the maximum temperature is 178 °C (Ueda et al. 1998).

Cross-References

- ▶ [Cutting Fluid](#)
- ▶ [Cutting Force Modeling](#)
- ▶ [Cutting, Fundamentals](#)
- ▶ [Machinability](#)
- ▶ [Tool Holder](#)

References

- Boothroyd G (1981) Fundamentals of metal machining and machine tools, International Student Edition. McGraw-Hill, New York, pp 92–106
- Carslaw HS, Jaeger JC (1967) Conduction of heat in solids. Oxford at the Clarendon Press, London, pp 50–91
- Childs T, Maekawa K, Obikawa T, Yamane Y (2000) Metal machining: theory and application. Arnold, London, p55, p147
- Davies MA, Ueda T, M'Saoubi R, Mullany B, Cooke AL (2007) On the measurement of temperature in material removal processes. *CIRP Ann* 56(2):581–604
- Kronenberg M (1966) Machining science and application. Pergamon Press, Oxford, p 53
- Mahfudz AH, Yamada K, Hosokawa A, Ueda T (2002) Investigation of temperature at tool-chip interface in turning using two-color pyrometer. *ASME, J Manuf Sci Eng* 124(5):200–207
- Oxley PLB (1989) The mechanics of machining: an analytical approach to assessing machinability. Ellis Horwood/Wiley & Sons, Chichester, pp 74–96
- Shaw MC (1984) Metal cutting principles. Clarendon, Oxford, pp 251–291
- Tanaka R, Morishita H, Yongchuan L, Hosokawa A, Ueda T, Furumoto T (2009) Cutting tool edge temperature in finishing hard turning of case hardened steel. *Key Eng Mater* 407–408:538–541
- Ueda T, Sato M, Sugita T, Nakayama K (1995) Thermal behaviour of cutting grain in grinding. *CIRP Ann* 44(1):325–328
- Ueda T, Sato M, Nakayama K (1998) The temperature of a single crystal diamond tool in turning. *CIRP Ann* 47(1):41–44
- Ueda T, Mahfudz AH, Yamada K, Nakayama K (1999) Temperature measurement of CBN tool in turning of high hardness steel. *CIRP Ann* 48(1):63–66
- Ueda T, Hosokawa H, Oda K, Yamada K (2001) Temperature on flank face of cutting tool in high speed milling. *CIRP Ann* 50(1):37–40
- Ueda T, Hosokawa A, Yamada K (2006) Effect of oil mist on tool temperature in cutting. *ASME, J Manuf Sci Eng* 128(2):130–135
- Ueda T, Sato M, Hosokawa A, Ozawa M (2008) Development of infrared radiation pyrometer with optical fibers: two-color pyrometer with non-contact fiber coupler. *CIRP Ann* 57(1):69–72

Cutting Tool

- ▶ [Self-Propelled Rotary Tool](#)

Cutting Tools

- ▶ [Superhard Tools](#)

Cutting, Fundamentals

Hans Kurt Toenshoff

Institute of Production Engineering and Machine Tools, Leibniz University Hannover, Garbsen, Germany

Synonyms

[Manufacturing by material removal](#); [Material removal processes](#); [Mechanical machining](#)

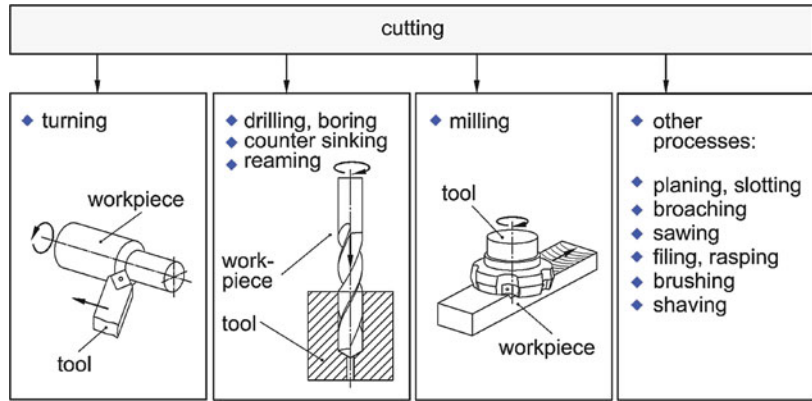
Definition

Cutting is manufacturing by removal of material ([DIN 8580](#); [CIRP Dictionary 2004](#)). Particles of material, the chips, are mechanically removed from the raw material or from an unfinished part by cutting edges of a tool. The tool has one or several cutting edges, which can be geometrically defined by number, shape, and position (cutting by geometrically defined cutting edges), whereas in abrasive processes the separation of chips takes place by numerous cutting edges which have to be statistically described and which are randomly distributed inside the tool (cutting by geometrically undefined cutting edges). [Figure 1](#) shows some cutting processes ([DIN 8589](#); [CIRP Dictionary 2004](#)).

History

The first systematic encyclopedic collection of manufacturing processes in Europe was written by K. Karmarsch (1837), describing the known methods and means of manufacturing. In 1873, Tresca had already investigated the mechanics of cutting on lead, iron, and other metals (Tresca 1873). For planning of iron, he found shearing

Cutting, Fundamentals,
Fig. 1 Cutting processes



as the dominant deformation resulting in a chip thickness ratio of 2–3. In 1907, F.W. Taylor published his fundamental work “On the Art of Cutting Metals.” He showed the strong dependency of tool life and cutting speed and was able to point out an economic optimization of the cutting process (Taylor 1907). The shearing process in front of the rake face was explained by V. Piispanen with the play card model (Piispanen 1937). Schwerd was the first to film high-speed cutting processes (Schwerd 1936). In 1944, Merchant published his “Basic Mechanics of Metal Processes,” which today is still seen as a milestone in the domain (Merchant 1944). The monograph of Shaw (1984) is another cornerstone in the history of the industrially important theory of cutting. In the recent past, many other scientists have worked in this field. A valuable knowledge pool is given in the CIRP Annals (CIRP Annals), especially in the keynote papers of STC Cutting (STC C).

Theory and Application

Cutting as a System

The cutting process may be seen as a system in which input operators go in and output operators come out. Process inputs are the cutting mode and the set variables, i.e., kinematic or geometric quantities controllable from the outside like speed, feed, or cutting depth; the properties of the workpiece relevant for the process like work

material or shape, of the tool as tool material; macro and micro properties of the active part of the tool and of the environment as the relevant machine properties or the coolant and lubrication.

Process interaction describes the actual process itself and summarizes those quantities which accompany the interaction of tool and workpiece real time as forces, power, and temperatures during interaction, vibrations of the mechanical structure, as well as stress and deformation in the working zone.

Process outputs denote the effects of the process concerning the workpiece, the tool, and the environment.

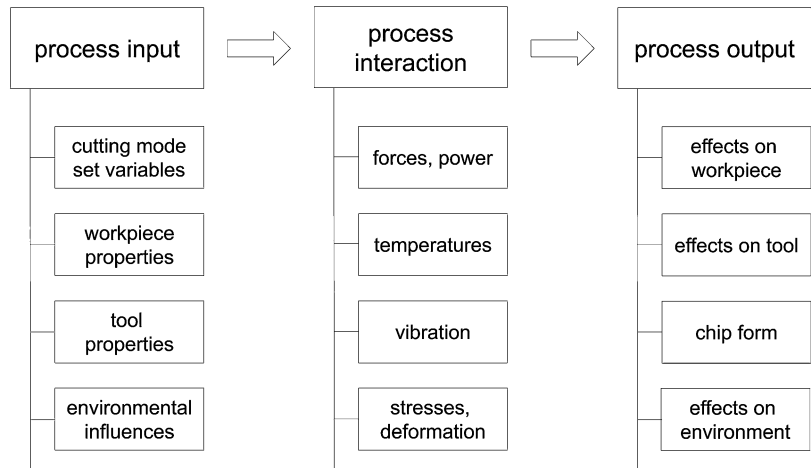
Following Figs. 2 and 3 show the basic structure of the field of cutting and the up-to-now-defined entries in the CIRP Encyclopedia of Production Engineering, section Cutting (see also the Cross-References below).

Kinematic and Geometric Parameters

The cutting processes are distinguished by the kind of tools and by the relative motion between the tool and the workpiece according to the cutting motion (cutting speed v_c), the feed motion (feed speed v_f), and the resulting effective motion (effective speed v_e) (Fig. 4).

The feed and cutting motion direction vectors fix the working plane. The angle between the two vectors is termed as the feed motion angle φ , while the angle between the effective direction and the cutting direction is termed as the effective direction angle η . The relationship

Cutting, Fundamentals,
Fig. 2 The cutting process
as a system



$$\tan \eta = \frac{\sin \varphi}{(v_c/v_f + \cos \varphi)}$$

applies to all cutting processes (Fig. 5).

With the cutting speed motion, the cross section of the undeformed chip A is removed from the workpiece (Fig. 6). The cross section A may be defined by the parameters depth of cut a_p and feed f , measured perpendicular to the working plane or by the undeformed chip parameters h (chip thickness) and b (chip width). These parameters are convertible by the cutting edge angle κ .

$$A = a_p \cdot f = h \cdot b \quad \text{with } h = f \sin \kappa \quad \text{and} \\ b = a_p / \sin \kappa$$

For processes in which the feed motion angle φ always measures 90° , i.e., turning, drilling, boring, and broaching, the material removal rate is

$$Q_w = A \cdot v_c$$

with A the chip cross section and v_c the cutting speed. For processes in which the feed motion angle φ is variable, i.e., milling, circular sawing, and drill-milling, the material removal rate is

$$Q_w = a_p \cdot a_e \cdot v_f$$

with a_p the depth of cut, a_e the width of cut, and v_f the feed speed.

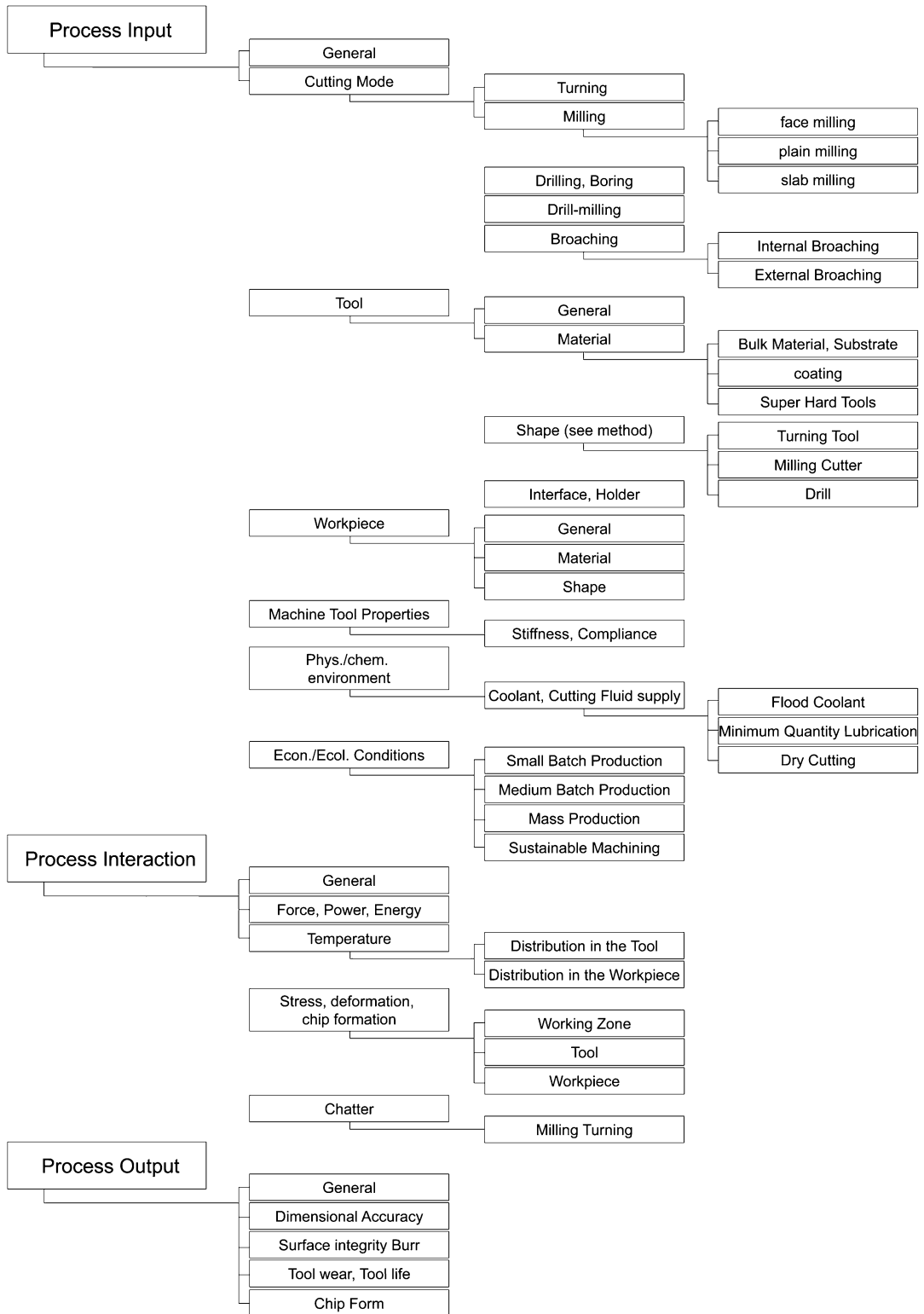
Chip Formation

The mechanical operation of cutting, the chip formation, can be described best referring to the orthogonal process (two-dimensional deformation) as shown in Fig. 7.

The cutting wedge is defined by the rake angle γ , the clearance angle α , the wedge angle β , and the edge radius r_β . The angles α , β and γ sum up to 90° . The penetration of the wedge causes elastic deformations, plastic deformations of the working material, and finally chip separation (chip removal). Figure 7 shows five zones of plastic deformation in continuous chip formation. The thickness of the material removed changes from the undeformed chip thickness h to the (deformed) chip thickness h' by passing through the deformation zones, resulting in the chip compression (upsetting) $\lambda_h = h'/h$. The shear angle Φ encloses the shear plane direction with the cutting speed vector.

Besides continuous or flowing chip formation, other kinds of chip formation may occur (Fig. 8):

- *Flowing chip formation* is a steady flow of material from the workpiece. The plastic deformation of the material is continuous. Periodic changes in the intensity of the deformation might occur. Preferably this happens at higher cutting speeds (see high-speed cutting, HSC). Lamellae are generated in the chip.



Cutting, Fundamentals, Fig. 3 Examples for the structural outline of the technological field “Cutting”

- *Shearing chip formation* occurs when the plastic formability of the material is exceeded in the shearing zone and locally concentrated shearing takes place. Shearing chip formation is found with negative rake angles, higher cutting speeds, larger chip thicknesses, and limited formability of the material.
- *Tearing (rupture) chip formation* occurs in materials with low formability, e.g., lamellar cast iron. The fracture interface between the chip and the generated surface on the workpiece is irregular.
- Forming of *built up edges* may occur when machining ductile, work hardening materials at low cutting speeds and sufficiently steady chip formation.

The chip formation process can be visualized by *quick stop devices*, by *micro cinematography* (for a video presentation, please see either a short version http://www.ifw.uni-hannover.de/fileadmin/IFW/07_Downloads/Warnecke-3.wmv or an extended version http://www.ifw.uni-hannover.de/fileadmin/IFW/07_Downloads/Warnecke-1.wmv) (Warnecke 1977; Warnecke and Inst.wis.Film 1988) or by *simulation*, e.g., FEM. Figure 9 shows a chip root gained by the quick stop method.



Shear Plane Model

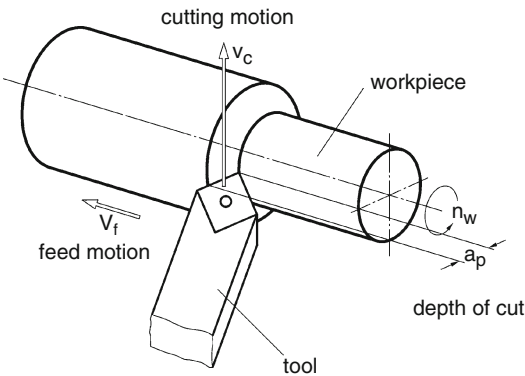
The shear plane model assumes that the plastic deformation of cutting takes place exclusively in a plane inclined against the cutting speed vector by the shear angle ϕ . The deformation is plain shear strain (card model of Piispanen 1937). Under the postulate of this model and two dimensional deformation (orthogonal cutting), the shear velocity v_ϕ can be determined

$$v_\phi = v_c \frac{\cos \gamma}{\cos (\phi - \gamma)}$$

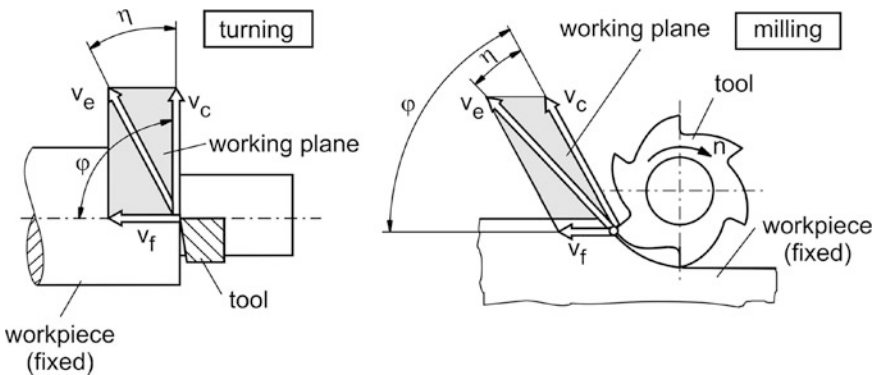
From the constancy of volume, which can be assumed with large plastic deformations, and two-dimensional deformation follows the chip thickness ratio λ_h

$$\lambda_h = \frac{\cos (\phi - \gamma)}{\sin \phi}$$

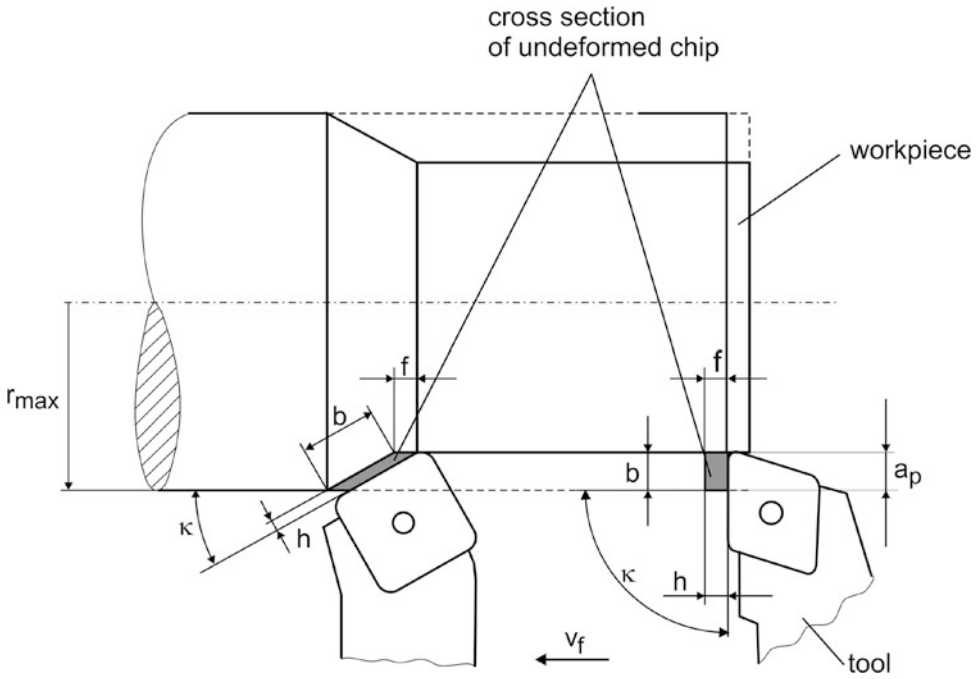
The shear strain γ_s (not to be mixed up with rake angle γ) therefore is (Fig. 10)



Cutting, Fundamentals, Fig. 4 Cutting and feed motion in turning

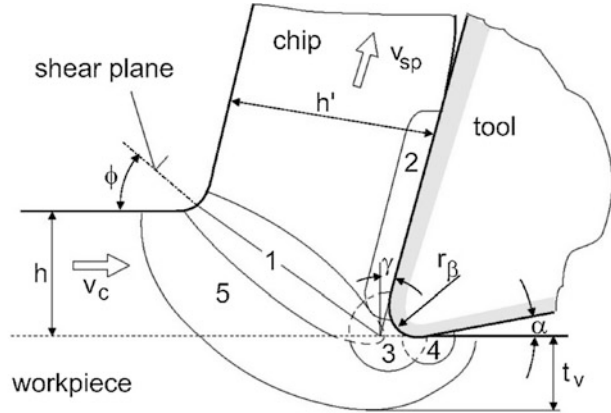


Cutting, Fundamentals, Fig. 5 Working plane



Cutting, Fundamentals, Fig. 6 Engagement parameters (turning)

Cutting, Fundamentals, Fig. 7 Chip formation, zones of deformation (acc. G. Warnecke)



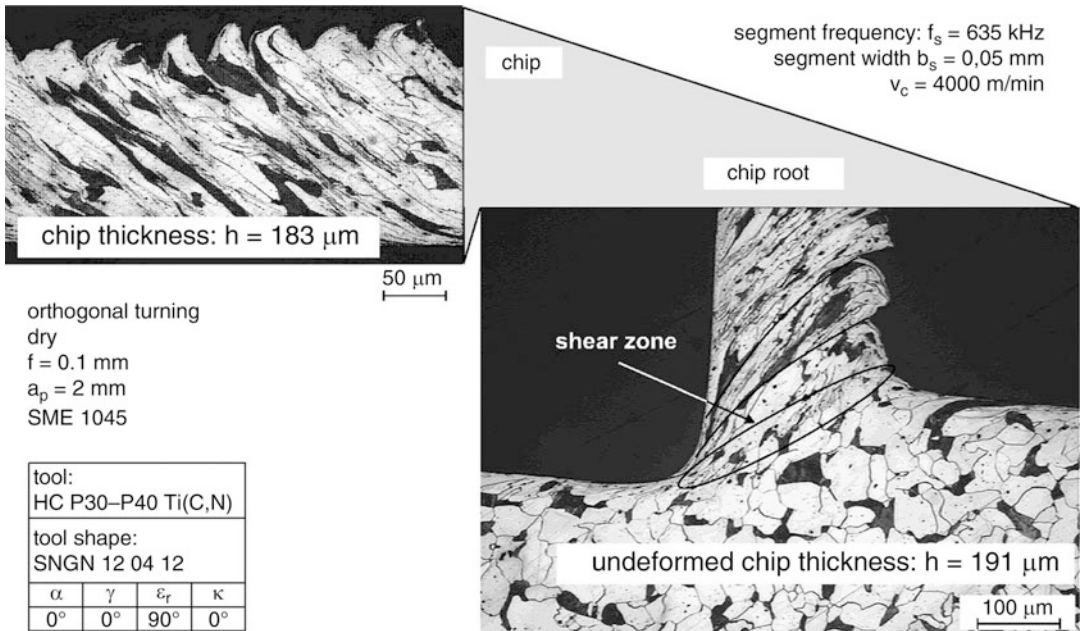
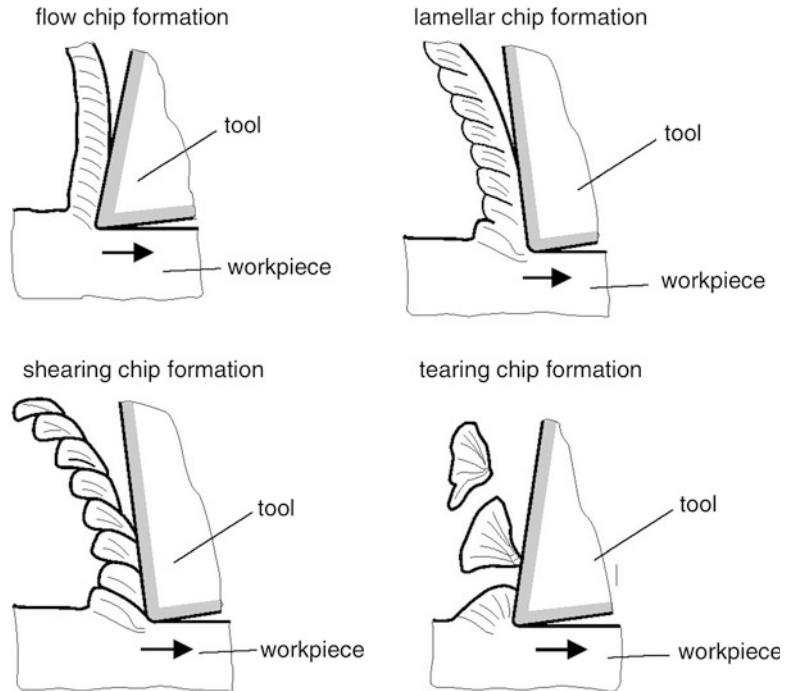
- | | |
|---------------------------------------|----------------------------|
| 1 : primary shear zone | γ : rake angle |
| 2 : secondary shear zone at rake face | α : clearance angle |
| 3 : separative zone | ϕ : shear angle |
| 4 : secondary shear zone at flank | t_v : deformation depth |
| 5 : preliminary deformation zone | |

$$\gamma_s = \tan(\phi - \gamma) + \frac{1}{\tan \phi}$$

The principal strains can be derived from there (Denkena and Toenshoff 2011) (Fig. 11).

The numeric simulation by finite element methods is based on two different approaches: the Euler formulation and the Lagrange formulation. In the Euler formulation, the knots are fixed; therefore, only stationary processes can be

Cutting, Fundamentals, Fig. 8 Kinds of chip formation



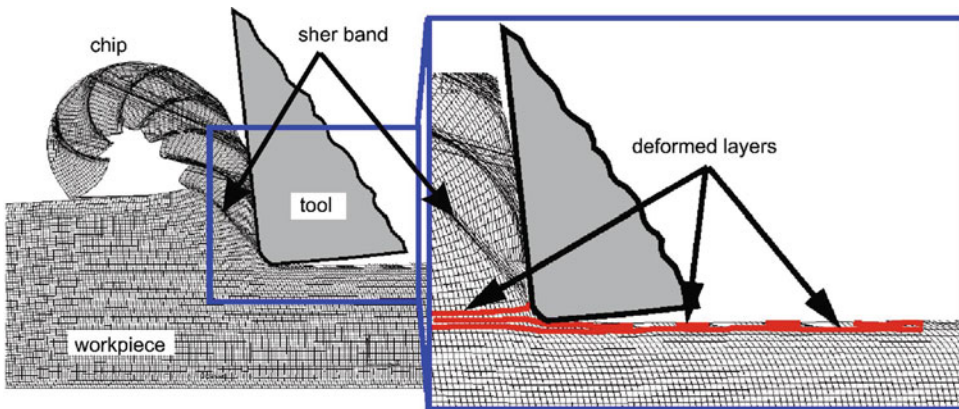
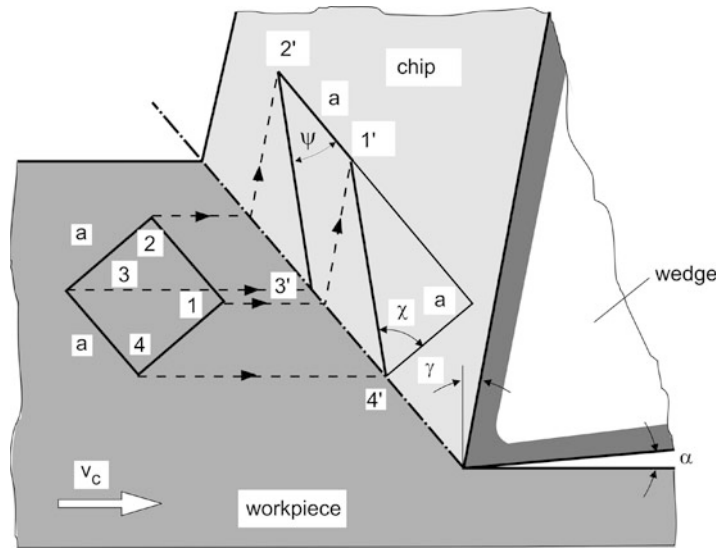
Cutting, Fundamentals, Fig. 9 Chip root from HSC (source: Ben Armor)

described. In the Lagrange formulation, the net flows and deforms with the work material. The net in front of the cutting tool is extremely deformed;

therefore, remeshing is necessary. The method needs separation criteria. It is able to simulate nonstationary deformations, loads, and thermal

Cutting, Fundamentals,

Fig. 10 Deformation for orthogonal cutting acc. shear plane model



Cutting, Fundamentals, Fig. 11 Simulation of segmented chip formation (FEM)

states. There are several customized programs which can be applied for the simulation of cutting processes, e.g., SFTC/Deform, MSC/Superform, and Abaqus.

- Empirical models using experimental data
- Analytical models based on elementary plastomechanics
- Finite element methods (FEM)

Power and Forces

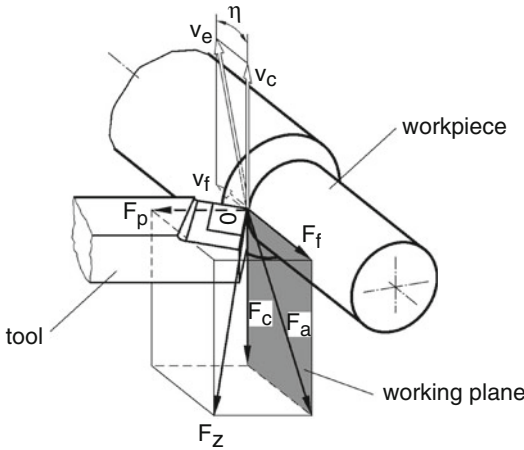
The resulting cutting force F_z is generally inclined directed in space. It is convenient to define components in a rectangular coordinate system according to the motions between tool and workpiece (Fig. 12), i.e., the cutting force F_c , the feed force F_f , and the passive force F_p .

To determine forces and the cutting process-related power, several approaches are applied:

Empirical models are used to determine forces and power with necessary accuracy in a limited domain of validity. An approach commonly applied is the Kienzle formula

$$F_{cfs,p} = k_{cfs,p1.1} \cdot b \cdot h_0 \left(\frac{h}{h_0}\right)^{1-m_{cfs,p}} \quad \text{and} \quad k_{cfs,p} = \frac{F_{cfs,p}}{A}$$

in which the parameters $k_{c,f,p}$ and the exponent $m_{c,f,p}$ are material-dependent constants. h_0 is a reference parameter usually assigned to $h_0 = 1 \text{ mm}$ (Kienzle 1952). Table 1 gives data experimentally obtained for different materials. The Kienzle formula was derived for turning processes with a large ratio of b/h , i.e., a slender rectangular undeformed chip cross section. For



Cutting, Fundamentals, Fig. 12 Components of the resultant force in turning (DIN 6584; CIRP Dictionary 2004)

curved cutting edges and milling processes, the approach of Friedrich may be favorable (Friedrich 1909; Engin and Altintas 1999).

$$F_{c,cN,p} = K_{c,cN,p} \cdot A + K_{e,cN,p} \cdot s \text{ and}$$

$$k_{c,cN,p} = \frac{F_{c,cN,p}}{A}$$

in which $F_{c,cN,p}$ are the force components in tangential (cutting), radial, and axial (passive) directions. K_c is the cutting coefficient, which implicates the shearing effect (dependent of the undeformed chip cross section A), and K_e is the edge coefficient which considers the friction between the cutting edge (length s) and the workpiece material.

The process-dependent cutting power P_c can be written as.

$$P_c = k_c \cdot Q_w$$

in which k_c is the specific (material removal related) energy. k_c can also be expressed by the cutting force

$$k_c = \frac{P_c}{Q_w} = \frac{F_c \cdot v_c}{A \cdot v_c} = \frac{F_c}{A}$$

and is therefore called the specific cutting force.

Cutting, Fundamentals, Table 1 Parameters of specific forces

workpiece material	parameter	Rm MPa	specific forces $k_{i,1}$ in MPa ($i = c, n, p$)					cutting tool material	
			$k_{c1,1}$	$1-m_c$	$k_{f1,1}$	$1-m_f$	$k_{p1,1}$		$1-m_p$
St 52-2		559	1499	0.71	351	0.30	274	0.51	P10
Ck 45 N		657	1659	0.79	521	0.51	309	0.60	P10
Ck 60		775	1686	0.78	285	0.28	259	0.59	P10
16 MnCr 5		500	1411	0.70	406	0.37	312	0.50	P10
100 Cr 6		624	1726	0.72	318	0.14	362	0.47	P10
GG-30		HB=206	899	0.59	170	0.09	164	0.30	K10
G-ALMg4SiMn*)		260	487	0.78					K10
X22CrNiMoNb1810**)		588	1397	0.76					K10

*) $V_c = 400 \text{ m/min } \gamma = 15^\circ$

**) $V_c = 100 \text{ m/min } \alpha = 8^\circ$

cutting speed : $V_c = 100 \text{ m/min}$
depth of cut : $ap = 3.0 \text{ mm}$

	α	γ	λ	ε	κ	r_e
steel	5°	6°	0°	90°	70°	0.8mm
cast iron	5°	2°	0°	90°	70°	0.8mm

Merchant has proposed an analytical approach elegantly applicable to determine the force components in orthogonal cutting (Merchant 1944). He assumes the shear plane model and Coulomb’s friction law. In Fig. 13, the force components are drawn in a Thales circle. F_z is the resulting force, F_c and F_p ; the normal and tangential force on the rake face $F_{N\gamma}$ and $F_{T\gamma}$ as well as the normal and tangential force on the shear plane $F_{N\phi}$ and $F_{T\phi}$ are perpendicular to each other. Assuming that the shear stress τ_ϕ in the shear plane is constant, the equation can be derived taking in consideration that the shear plane is directed as the maximum shear stress (extreme value).

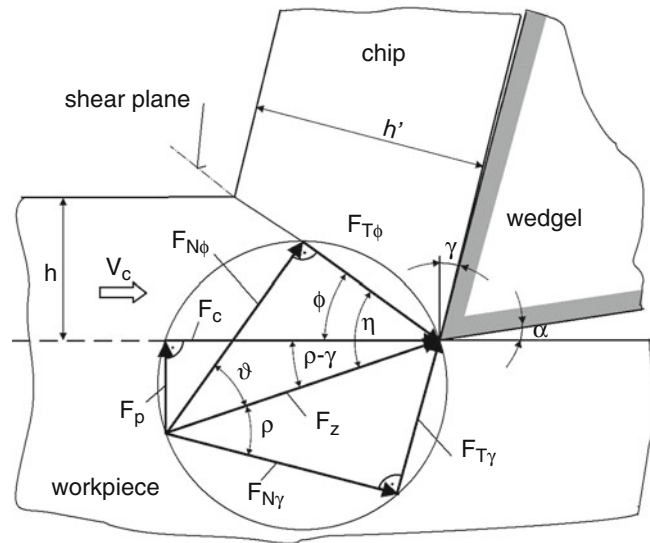
$$\tau_\phi = \frac{F_z}{b \cdot h} \cdot \cos(\phi - \rho - \gamma) \cdot \sin \phi$$

in which ρ is the friction angle. If three of the written variables are given ($\tau_\phi = \tau_{max}$ from metallurgical data, Φ via λ_h by measuring h and h' , and ρ from comparable incidents), the fourth can be determined.

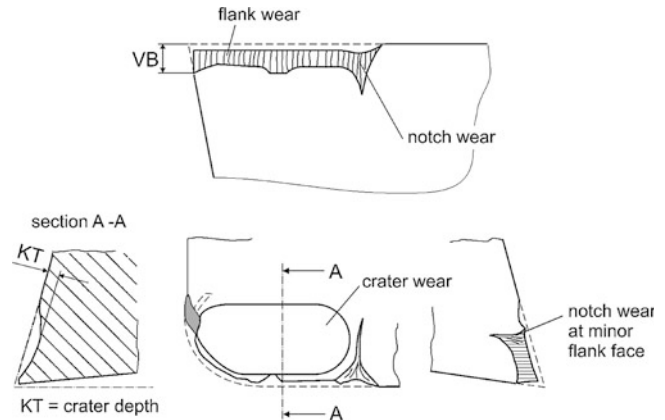
Wear and Tool Life

Cutting tools wear as a result of mechanical, thermal, and chemical loads (Klocke 2011). The main wear forms (phenomena) are shown in Fig. 14. The dominant input parameter for the development of

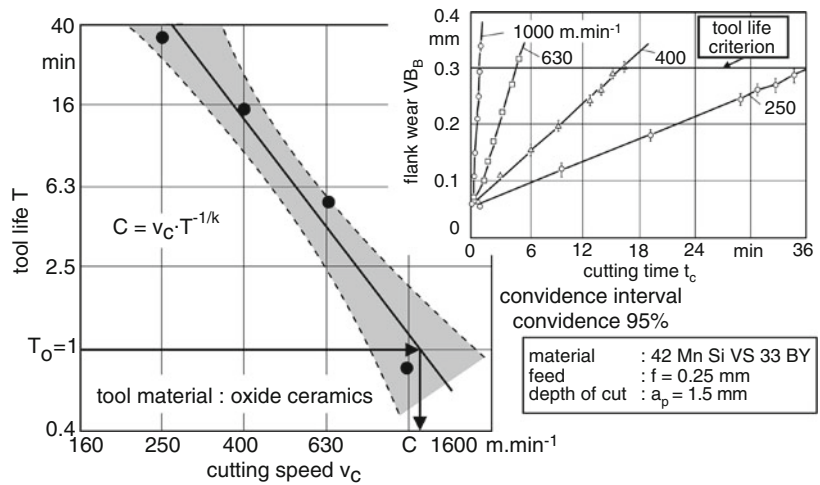
Cutting, Fundamentals,
Fig. 13 Composite force circle



Cutting, Fundamentals,
Fig. 14 Wear forms (ISO 3685)



Cutting, Fundamentals,
Fig. 15 Taylor tool life graph



wear is the cutting speed. Taylor (1907) already described the dependency between tool life and speed for a given tool life criterion (Fig. 15).

The dependency is

$$v_c = C \cdot \left(\frac{T}{T_0} \right)^{1/k}$$

in which C is the cutting speed resulting from $T_0 = 1$ min tool life. T is the tool life for the speed v_c . The material-dependent constants k and C may be found in the literature (Machinability Data Center 1980) (Fig. 15).

Cross-References

- ▶ Cutting Temperature
 - ▶ Diamond Machining
 - ▶ Drill Milling
 - ▶ Drilling
 - ▶ Fine Finishing of Holes
 - ▶ Gear Cutting
 - ▶ Geometric Modeling of Machining
 - ▶ Groove Milling
 - ▶ Hard Material Cutting
 - ▶ High Speed Cutting
 - ▶ Hybrid Cutting
 - ▶ Machinability
 - ▶ Micromachining
 - ▶ Milling of Titanium
 - ▶ Molecular Dynamics for Cutting Processes
 - ▶ Monitoring
 - ▶ Process Chain Design
 - ▶ Superhard Tools
 - ▶ Surface Integrity
 - ▶ Sustainability of Machining
 - ▶ Tool Holder
 - ▶ Ultraprecision Machining
 - ▶ Wear Mechanisms
- ▶ Adiabatic Shearing in Metal Machining
 - ▶ Broaching
 - ▶ Burr
 - ▶ Cemented Carbides
 - ▶ Ceramic Cutting Tools
 - ▶ Cermets
 - ▶ Chatter Prediction
 - ▶ Chip-Forms, Chip Breakability, and Chip Control
 - ▶ Coated Tools
 - ▶ Composite Materials
 - ▶ Cutting Edge Geometry
 - ▶ Cutting Fluid
 - ▶ Cutting Force Modeling
 - ▶ Cutting of Inconel and Nickel Base Materials

References

- CIRP Dictionary of Production Engineering II (2004) Material removal processes, vol 2, 1st edn. Springer, Berlin
- Denkena B, Toenshoff HK (2011) Spanen: Grundlagen [Cutting: fundamentals]. Springer, Berlin (in German)

- DIN 6584 (1982–1910) Begriffe der Zerspantechnik: Kräfte, Energie, Arbeit, Leistungen [Terms of the cutting technique: forces, energy, work, power]. Beuth Verlag, Berlin (in German)
- DIN 8580 (2003–2009) Fertigungsverfahren: Begriffe, Einteilung [Manufacturing processes: terms and definitions, division]. Beuth Verlag, Berlin (in German)
- DIN 8589-0 (2003–2009) Fertigungsverfahren Spanen, Teil 0: Allgemeines: Einordnung, Unterteilung, Begriffe [Manufacturing processes chip removal, part 0: general: classification, subdivision, terms and definitions]. Beuth Verlag, Berlin (in German)
- Engin S, Altintas Y (1999) Generalized modeling of milling mechanics and dynamics, part I: helical end mills. In: ASME international mechanical engineering congress and exposition symposium, machining science and technology. Nashville, 14–19 Nov 1999. Published by Manufacturing Automation Laboratories, Inc., Vancouver. Retrieved from http://www.malinc.com/pdf/GeneralTool_Endmill.pdf
- Friedrich H (1909) Ueber den Schnittwiderstand bei der Bearbeitung der Metalle durch Abheben von Spänen [About the cutting resistance at machining of metals by separation of chips]. Z VDI 58(23):860–866 (in German)
- ISO 3685 (1993–11) Tool-life testing with single-point turning tools. Beuth Verlag, Berlin
- Karmarsch K (1837) Grundriß der Mechanischen Technologie [Outline of the mechanical technology], vol 1. Helwingsche Hof-Buchhandlung, Hannover/Wien (in German)
- Kienzle O (1952) Die Bestimmung von Kräften und Leistungen an spanenden Werkzeugen und Werkzeugmaschinen [Determination of forces and power for cutting tools and machine tools]. ZVDI 94:299–305 (in German)
- Klocke F (2011) Manufacturing processes 1: cutting. Springer, Berlin
- Machinability Data Center (1980) Machining data handbook, 3rd edn. Metcut Research Associates Inc, Cincinnati
- Merchant ME (1944) Basic mechanics of metal cutting processes. J Appl Mech 66-A:168–175
- Piispanen V (1937) Lastunmuodostumisen Teoriaa [Chip forming theory]. Teknillien Aikakausleht i 27:315–ff (in Finnish)
- Schwerd F (1936) Filmaufnahmen des ablaufenden Spans bei üblichen und bei sehr hohen Geschwindigkeiten [Motion picture of chip flow at common and very high cutting speeds]. Z VDI 80:233–236, A 3+4
- Shaw MC (1984) Metal cutting principles. Clarendon, Oxford
- Taylor FW (1907) On the art of cutting metals (Trans). Am Soc Mech Eng 28:31–279
- Tresca M (1873) Mémoire sur le rabotage des métaux [Report on the machining of metals]. Bulletin de la Société d'Encouragement pour l'Industrie Nationale, pp 584–612, 655–683. Retrieved from <http://cnum.cnam.fr/CGI/gpage.cgi?p1=584&p3=BSPI.72%2F100%2F802%2F12%2F684> (in French)
- Warnecke G (1977) Manufacturing engineering transactions. In: 5th North American metalworking research conference proceedings, University of Massachusetts, 23–25 May, pp 229–236
- Warnecke G, Inst.wis.Film (1988) Zerspanen von Stahl Ck45 – Schnittvorgang im Feingefüge – Einfluss der Waermebehandlung [Cutting of steel Ck45 – cutting in the microstructure -influence of heat treatment]. Film E 2949 (German and English), available by TIB Hannover, Germany

Cyber-Physical Systems

Laszlo Monostori

Laboratory of Engineering and Management Intelligence, Research Institute for Computer Science and Control, Hungarian Academy of Sciences, Budapest, Hungary
Department of Manufacturing Science and Technology, Budapest University of Technology and Economics, Budapest, Hungary

Synonyms

[Smart systems](#)

Definition

Cyber-Physical Systems (CPS) are systems of collaborating computational entities which are in intensive connection with the surrounding physical world and its on-going processes, providing and using, at the same time, data-accessing and data-processing services available on the internet. With other words, CPS can be generally characterized as “physical and engineered systems whose operations are monitored, controlled, coordinated, and integrated by a computing and communicating core” (Rajkumar et al. 2010). The interaction between the physical and cyber elements is of key importance: “CPS is about the intersection, not the union, of the physical and the cyber. It is not sufficient to separately understand the physical components and the computational components. We must understand their interaction” (Lee and Seshia 2014).

Theory and Application

Origin, Short History

Most of the researchers originate CPS from the *embedded systems* (Park et al. 2012), which are defined as a computer system within some mechanical or electrical system to perform dedicated specific functions with real-time computing constraints. These embedded systems are characterized by tight integration and coordination between computation and physical processes. According to this conception, in CPS various embedded devices are networked to sense, monitor, and actuate physical elements in the real world.

The CPS notation can be traced back to 2006, when the first NSF Workshop on Cyber-Physical Systems was held in Austin, Texas, October 16–17. The following announcement can be read on the conference web page: “The research initiative on Cyber-Physical Systems seeks new scientific foundations and technologies to enable the rapid and reliable development and integration of computer- and information-centric physical and engineered systems. The goal of the initiative is to usher in a new generation of engineered systems that are highly dependable, efficiently produced, and capable of advanced performance in information, computation, communication, and control. ...Sensing and manipulation of the physical world occurs locally, while control and observability are enabled safely, securely, reliably and in real-time across a virtual network. This capability is referred to as *Globally Virtual, Locally Physical*” (N.N. 2006).

Application Fields

“The potential of CPS to change every aspect of life is enormous. Concepts such as autonomous cars, robotic surgery, intelligent buildings, smart electric grid, smart manufacturing, and implanted medical devices are just some of the practical examples that have already emerged” (N.N. 2013a).

The following main applications fields of CPS were identified by the CPS Vision Statement issued by the federal Networking and Information

Technology Research and Development (NITRD) CPS Senior Steering Group (N.N. 2012a):

- Agriculture
- Building controls
- Defense
- Energy response
- Energy
- Healthcare
- Manufacturing and industry
- Society
- Transportation

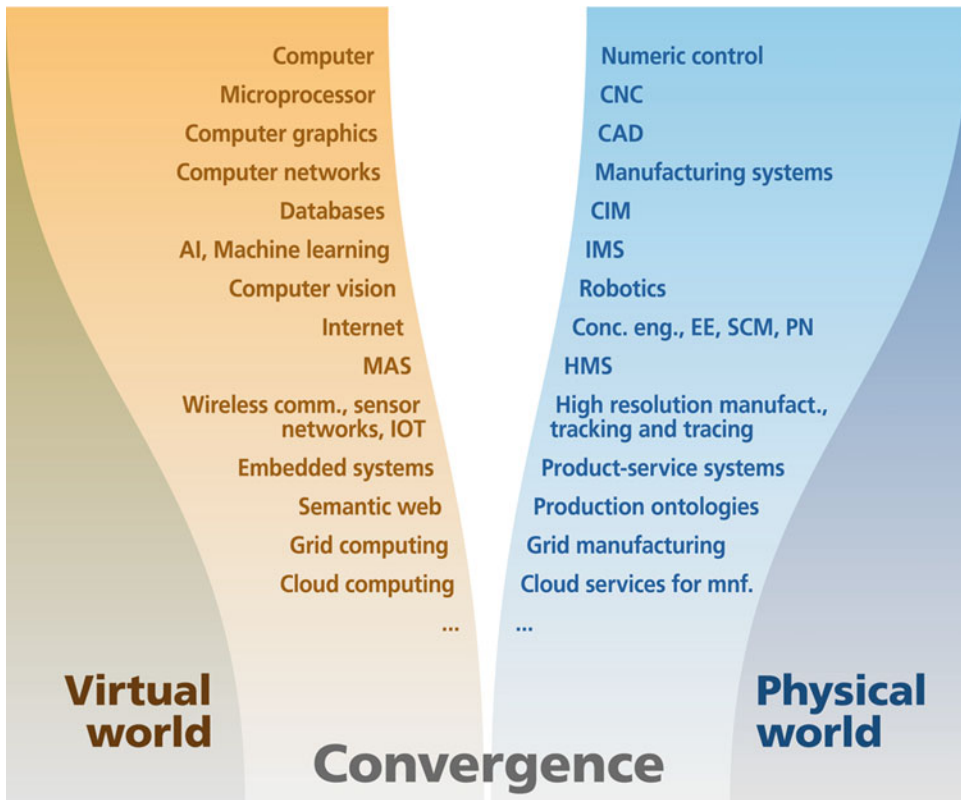
In the same mission statement, crosscutting challenges were also outlined that are essential to success in all sectors:

- Cybersecurity
- Economics
- Interoperability challenge
- Privacy
- Safety and reliability
- Socio-technical aspects of CPS

Cyber-Physical Production Systems (CPPS)

If we look through the development of computer science, information and communication technologies, and manufacturing science and technology, a parallel development can be observed (Fig. 1).

The development of computers led to the numerical control of machine tools and robots, the microprocessor constituted the heart of computer numerical control (CNC), and the application of computer graphics resulted in computer-aided design (CAD) systems. The development of manufacturing systems was unimaginable without computer networks. The data of computer-integrated manufacturing (CIM) systems were stored in databases. The then novel results of artificial intelligence (AI) and machine learning (ML) significantly contributed to the intelligent manufacturing systems (IMS). Computer vision algorithms were applied in robotics for recognizing the environment and the object to grasp. The internet revolutionized the cooperation of humans



Cyber-Physical Systems, Fig. 1 Interplay between CS, ICT, and MST (Monostori et al. 2016)

and systems (extended enterprises (EE), supply chain management (SCM), or production networks (PN)). Multi-agent systems were applied for realizing agent-based manufacturing and holonic manufacturing systems (HMS) (Van Brussel et al. 1998; Valckenaers and Van Brussel 2005; Monostori et al. 2006). Wireless communication, sensor networks, and internet of things (IOT) made the development of high resolution manufacturing systems possible (Schuh et al. 2007) and tracking and tracing solutions in production (Monostori et al. 2009). Embedded systems helped in realizing smart automation solutions and product-service systems, while the semantic web solutions supported the interoperability of systems by using ontologies. Grid computing led to grid manufacturing and, similarly, cloud computing to cloud services to manufacturing.

Summarizing, the results of CS and ICT undoubtedly contributed to the development in

production, but this was not a one-way street: the importance and highly complex nature of production gave newer and newer challenges for the representatives of other disciplines. As we look at this parallel, mutually inspiring developments, a kind of convergence can be observed, namely, between the virtual and physical worlds (Fig. 1).

Cyber-Physical Production Systems (CPPS), relying on the newest and foreseeable further developments of computer science (CS), information and communication technologies (ITC), and manufacturing science and technology (MST) may lead to the fourth Industrial Revolution, frequently noted as Industrie 4.0 (Kagermann et al. 2013). According to the Federal Ministry of Education and Research, Germany (BMBF): “Industry is on the threshold of the fourth industrial revolution. Driven by the Internet, the real and virtual worlds are growing closer and closer together to form the Internet of Things. Industrial

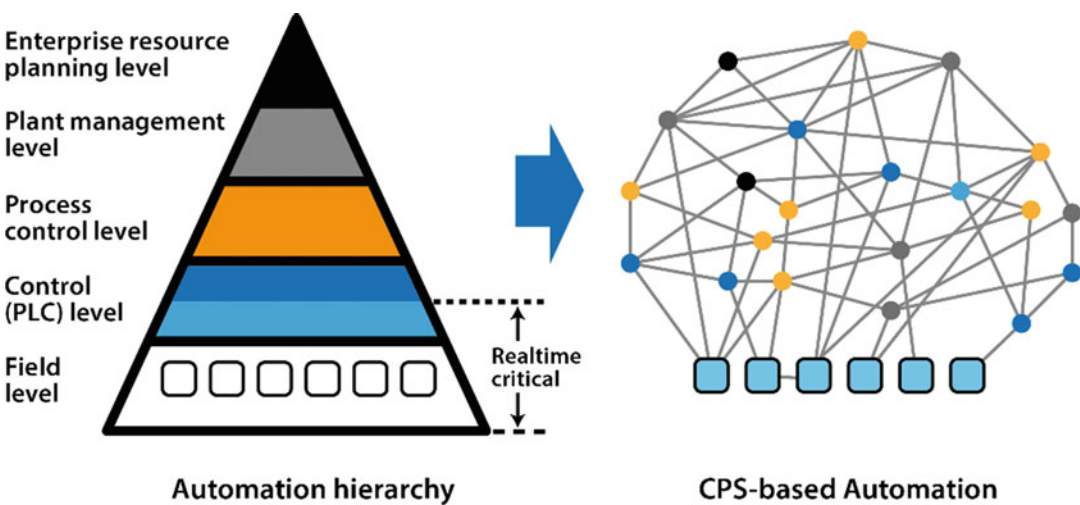
production of the future will be characterized by the strong individualization of products under the conditions of highly flexible (large series) production, the extensive integration of customers and business partners in business and value-added processes, and the linking of production and high-quality services leading to so-called hybrid products (Kagermann et al. 2013)”.

CPPS consist of autonomous and cooperative elements and subsystems that are getting into connection with each other in situation dependent ways, on and across all levels of production, from processes through machines up to production and logistics networks. Modelling their operation and also forecasting their emergent behavior raise a series of basic and application-oriented research tasks, not to mention the control of any levels of these systems. The fundamental question is how to explore the relations of autonomy, cooperation, optimization, and responsiveness. Integration of analytical and simulation-based approaches can be projected to become more significant than ever. One must face the challenges of operating sensor networks, handling big bulks of data, as well as the questions of information retrieval, representation, and interpretation, with special emphasis on security aspects. Novel modes of man-machine communication are to be realized in the course of establishing CPPS.

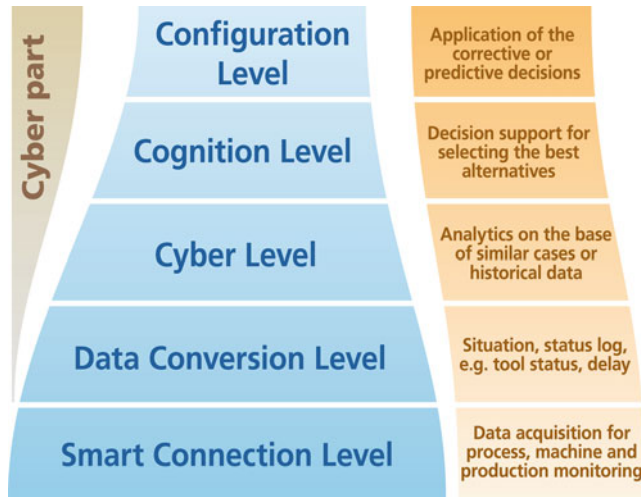
CPPS partly break with the traditional automation pyramid (left side of Fig. 2). The typical control and field levels still exist which includes common PLCs close to the technical processes to be able to provide the highest performance for critical control loops, while in the other, higher levels of the hierarchy a more decentralized way of functioning is characteristic in CPPS (right side of Fig. 2).

The general assumption, i.e., CPPS consists of two main functional components, is manifested in the right side of Fig. 2. The lower one is responsible for the advanced connectivity which ensures real-time data acquisition from the physical world and information feedback from the cyber space, while the higher level incorporates intelligent data management, analytics, and computational capabilities that constructs the cyber space.

The *5C architecture* introduced in Lee, et al. (2015) consists of five levels in a sequential workflow manner and illustrates how to construct a CPPS from the initial data acquisition, through analytics to the final value creation (Table 1). In the table some examples are also given from the field of process, machine, or system level monitoring. In a CPPS approach, the smart connection level (Level 1) manifests the physical space, while the configuration level (Level 5) realizes the feedback from the cyber space to the physical space.



Cyber-Physical Systems, Fig. 2 Decomposition of the automation hierarchy with distributed services (N.N. 2013b)

Cyber-Physical Systems, Table 1 5C architecture for implementation of CPPS. (After Lee et al. 2015)

The importance of CPPS is hard to underestimate. In the PCAST's Report to the President on Capturing Domestic Competitive Advantage in Advanced Manufacturing of July 2012, 18 recommendations were formulated (N.N. 2012b). In Recommendation No. 2 on Increase R&D Funding in Top Cross-Cutting Technologies, the first point was Advanced Sensing, Measurement, and Process Control (Including Cyber-Physical Systems).

In Germany CPPS play an especially favored central role, e.g., (Zühlke and Ollinger 2012; Spath et al. 2013; Schuh et al. 2013; Schmitt and Große Böckmann 2014; Bauernhansl et al. 2014; Michniewicz and Reinhart 2014). The strategic initiative Industrie 4.0 underlines the fact that "Germany has one of the most competitive manufacturing industries in the world and is a global leader in the manufacturing equipment sector" (Kagermann et al. 2013). The implementation of three features of Industrie 4.0 was targeted:

- Horizontal integration through value networks.
- End-to-end digital integration of engineering across the entire value chain.
- Vertical integration and networked manufacturing systems (Kagermann et al. 2013).

Expectations Towards CPS and CPPS

Expectations towards CPS are manifolds, sometimes over exaggerated:

- Robustness at every level
- Self-organization, self-maintenance, self-repair, generally, self-X
- Safety
- Remote diagnosis
- Real-time control
- Autonomous navigation
- Transparency
- Predictability
- Efficiency
- Model correctness

Through CPS, the development of new business models, new services are expected which may change many aspects of our life. The potential application fields are almost endless: air- and ground-traffic; discrete and continuous production systems; logistics; medical science, energy production, infrastructure surrounding us, entertainment, and we could keep on enumerating. Through cyber-physical approaches, they could result in smart cities,

production-, communication-, logistic- and energy systems; furthermore, they could contribute to creating new quality of life. In the latter case, we may either talk about cyber-physical society, which already includes human, social, cultural spheres as well, above the physical- and cyber spaces.

As to CPPS, many see the opportunity for the fourth industrial revolution in it (Kagermann et al. 2013). The first industrial revolution is contributed to the first mechanical loom, from 1764, the second to the Ford assembly belt from 1913, the third to the first PLC in 1968. It is envisioned that CPPS can bring a similar big jump as the above mentioned breakthrough inventions.

R&D Challenges

The expectations towards CPS and CPPS are versatile and enormous: robustness, autonomy, self-organization, self-maintenance, self-repair, transparency, predictability, efficiency, interoperability, global tracking and tracing, only to name a few. Though there are very important developments in cooperative control, multi-agent systems (MAS), complex adaptive systems (CAS), emergent systems, sensor networks, data mining, etc., even a partial fulfilment of these expectations would represent real challenges for the research community.

As to the main R&D challenges on the side of CS and ICT, we refer to the literature (Lee 2007, 2008; Poovendran 2010; Park et al. 2012; Borgia 2014), here only four fundamental ones with general importance are outlined:

- Appropriate handling of time in programming languages, operation systems, and computer networks.
- Development of computational dynamical systems theory. Namely, the behavior of the physical parts of the systems can be modelled, simulated and analyzed using methods from continuous systems theory, while the cyber part by computational systems theory (e.g., computability, complexity). Hybris solutions in this sense are required.

- Standardization in the CPS field. Standardization is of crucial importance and it necessitates wide range cooperation activities involving the main players of the ICT field. Without standardization only isolated CPS solutions can be developed.
- Security issues in the cyber-physical system era. CPS consists of various hardware and software parts working together. In addition to hardware and software security, operational issues are also required to be considered for safety and dependability reasons.

In the coming space only some of the R&D challenges are outlined from the much bigger set of research fields which are related to CPPS (Monostori 2014; Monostori et al. 2016).

- *Context-adaptive and (at least partially) autonomous systems.* Methods for comprehensive, continuous context awareness, for recognition, analysis and interpretation of plans and intentions of objects, systems and participating users, for model creation for application field and domain and for self-awareness in terms of knowledge about own situation, status, and options for action are to be developed.
- *Cooperative production systems.* New theoretical results are to be achieved and the development of efficient algorithms for consensus seeking, cooperative learning, and distributed detection is required.
- *Identification and prediction of dynamical systems.* The extension of the available identification and prediction methods is required, as well as development of new ones which can be applied under mild assumptions on the dynamical system, as well as the disturbance process.
- *Robust scheduling.* New results are to be achieved in handling production disturbances in the course of schedule execution.
- *Fusion of real and virtual systems.* The development of new structures and methods are required which support the fusion of the virtual and real subsystems in order to reach an intelligent production system which is robust in a changing, uncertain environment. Novel reference architectures and models of integrated

virtual and real production subsystems; the synchronization of the virtual and real modules of production systems and their role-specific interaction; and context-adaptive, resource-efficient shop floor control algorithms are needed.

- *Human-machine (including human-robot) symbiosis.* The development of a geometric data framework to fusion assembly features and sensor measurements and fast search algorithms to adapt and compensate dynamic changes in the real environment is required.

Without any questions, CPPS can be considered as an extremely important step in the development of manufacturing systems of cooperative and responsive nature (Váncza et al. 2011). However, in order to really come up at least to a portion of the partly exaggerated expectations, significant further R&D&I activities are needed.

The biological transformation in manufacturing, as defined by the authors “the use and integration of biological and bio-inspired principles, materials, functions, structures and resources for intelligent and sustainable manufacturing technologies and systems with the aim of achieving their full potential,” represents a new and ground-breaking frontier of digitalization and Industry 4.0 (Byrne et al. 2018). The cyber-physical-biological approaches, i.e., the use of biomimetic solutions in production structures in the cyber-physical era, can open up novel and highly promising ways for making some viable compromises between the seemingly contradictory issues of robustness, complexity, and efficiency.

Cross-References

- ▶ [Smart Products](#)
- ▶ [Smart Systems](#)

References

Bauernhansl T, ten Hompel M, Vogel-Hauser B (2014) Industrie 4.0 in Produktion, Automatisierung und Logistik – Anwendung – Technologien – Migration. Springer Vieweg, Wiesbaden

- Borgia E (2014) The internet of things vision: key features, applications and open issues. *Comput Commun* 54:1–31
- Byrne G, Dimitrov D, Monostori L, Teti R, van Houtem F, Wertheim R (2018) Biologicalisation: biological transformation in manufacturing. *CIRP J Manuf Sci Technol* 21:1–32
- Kagermann H, Wahlster W, Helbig J (2013) Securing the future of German manufacturing industry: recommendations for implementing the strategic initiative INDUSTRIE 4.0, Final report of the Industrie 4.0 Working Group, acatech
- Lee AL (2007) Computing foundations and practice for cyber physical systems: a preliminary report. Electrical Engineering and Computer Sciences, University at Berkeley, Technical Report No.:UCB/EECS-2007-2
- Lee AL (2008) Cyber physical systems: design Challenges. Electrical Engineering and Computer Sciences, University at Berkeley, Technical Report No.:UCB/EECS-2008-8
- Lee EA, Seshia SA (2014) Introduction to embedded systems – a cyber-physical approach, LeeSeshia.org., Edition 1.5. <http://LeeSeshia.org>
- Lee J, Bagheri B, Kao H-A (2015) A cyber-physical systems architecture for industry 4.0-based manufacturing systems. *Manuf Lett* 3:18–23
- Michniewicz J, Reinhart G (2014) Cyber-physical robotics – automated analysis, programming and configuration of robot cells based on cyber-physical systems. *Procedia Technol* 15:567–576
- Monostori L (2014) Cyber-physical production systems: roots, expectations and R&D challenges. *Procedia CIRP* 17:9–13
- Monostori L, Váncza J, Kumara SRT (2006) Agent-based systems for manufacturing. *CIRP Ann Manuf Technol* 55(2):697–720
- Monostori L, Kemény Z, Ilie-Zudor E, Szathmári M, Karnok D (2009) Increased transparency within and beyond organizational borders by novel identifier-based services for enterprises of different size. *CIRP Ann Manuf Technol* 58(1):417–420
- Monostori L, Kádár B, Bauernhansl T, Kondoh S, Kumara S, Reinhart G, Sauer O, Schuh G, Sihn W, Ueda K (2016) Cyber-physical systems in manufacturing. *CIRP Ann Manuf Technol* 65(2):621–641
- NN (2006) NSF Workshop on cber-physical systems. October 16–17, Austin, <http://varma.ece.cmu.edu/CPS/>
- NN (2012a) Cyber-Physical Systems, Networking and Information Technology Research and Development (NITRD) CPS Senior Steering Group. https://www.nitrd.gov/nitrdgroups/images/6/6a/Cyber_Physical_Systems_%28CPS%29_Vision_Statement.pdf
- NN (2012b) Report to the president on capturing domestic competitive advantage in advanced manufacturing. https://www.whitehouse.gov/sites/default/files/microsites/ostp/pcast_amp_steering_committee_report_final_july_27_2012.pdf
- NN (2013a) Strategic R&D opportunities for 21st century, Cyber-physical systems, connecting computer and information systems with the physical world. Report of the Steering Committee for Foundations and Innovation for Cyber-Physical Systems

- NN (2013b) Cyber-physical systems: Chancen und nutzen aus sicht der automation, Thesen und Handlungsfelder, VDI/VDE-Gesellschaft Mess und Automatisierungstechnik (GMA)
- Park K-J, Zheng R, Liu X (2012) Cyber-physical systems: milestones and research challenges. Editorial Comput Commun 36(1):1–7
- Poovendran R (2010) Cyber-physical systems: close encounters between two parallel worlds. Proc IEEE 98(8):1363–1366
- Rajkumar R, Lee I, Sha L, Stankovic J (2010) Cyber-physical systems: the next computing revolution. In: Proceedings of the design automation conference 13–18 June 2010, Anaheim, pp 731–736
- Schmitt R, Große Böckmann M (2014) Kollaborative cyber-physische Produktionssysteme: Ausbruch aus der Produktivitätsfalle. In: Brecher, C, Klocke, F., Schmitt, R., Schuh, G. (eds) Integrative Produktion – Industrie 4.0 – Aachener Perspektiven. Shaker Verlag, Aachen, pp 365–374
- Schuh G, Gottschalk S, Höhne T (2007) High resolution production management. CIRP Ann Manuf Technol 56(1):439–442
- Schuh G, Potente T, Wesch-Potente C, Hauptvogel A (2013) Sustainable increase of overhead productivity due to cyber-physical-systems. In: Proceedings of the 11th global conference on sustainable manufacturing, Berlin, 23–25 September, pp 332–335
- Spath D, Ganschar O, Gerlach S, Hämmerle M, Krause T, Schlund S (2013) Produktionsarbeit der Zukunft – Industrie 4.0. Fraunhofer Verlag, Stuttgart
- Valckenaers P, Van Brussel H (2005) Holonic manufacturing execution systems. CIRP Ann Manuf Technol 54(1):427–432
- Van Brussel H, Wyns J, Valckenaers P, Bongaerts L, Peeters P (1998) Reference architecture for holonic manufacturing systems: PROSA. Comput Ind 37: 255–274
- Váncza J, Monostori L, Lutters E, Kumara SR, Tseng M, Valckenaers P, Van Brussel H (2011) Cooperative, responsive manufacturing enterprises. CIRP Ann Manuf Technol 60(2):797–820
- Zühlke D, Ollinger L (2012) Agile automation systems based on cyber-physical systems and service-oriented architectures, advances in automation and robotics. Lecture Notes Elect Eng 122(1):567–574